ResearchOnline@JCU

This file is part of the following reference:

McKinna, Lachlan I.W. (2010*) Optical detection and quantification of Trichodesmium spp. within the Great Barrier Reef*. PhD thesis, James Cook University.

Access to this file is available from:

http://eprints.jcu.edu.au/29747/

The author has certified to JCU that they have made a reasonable effort to gain permission and acknowledge the owner of any third party copyright material included in this document. If you believe that this is not the case, please contact ResearchOnline@jcu.edu.au and quote **http://eprints.jcu.edu.au/29747/**

JAMES COOK UNIVERSITY AUSTRALIA

Optical Detection and Quantification of Trichodesmium spp. within the Great Barrier Reef

Thesis Submitted by:

Lachlan I.W. McKinna BSc. (Hons)

in November 2010

for the degree of Doctor of Philosophy

in the School of Engineering and Physical Sciences

James Cook University

Copyright © 2010 by Lachlan I.W. McKinna BSc. (Hons)
All rights reserved

In loving memory of

Nancy McKinna (1915 – 2009)

“Do just once what others say you can't do, and you will never pay attention to their limitations again.”

Captain James Cook

Explorer and Navigator (1728 – 1779)

“Both yesterday and today vast quantities of the sea Sawdust was seen; some of our people observd that on passing through a bed of it much larger than common they smelt an uncommon stink which they supposd to proceed from it.” 30 August 1770

Sir Joseph Banks

Naturalist (1743 – 1820)

Statement of Contribution of Others

Research Funding

Australian Postgraduate Award (stipend 3.5 years)	$ 73,000
AIMS@JCU Project Funding	$ 15,000
School of Engineering and Physical Sciences	$ 2000
Graduate Research School	$ 4600
The Oceanography Society Student Travel Grants	$ 1200
Great Barrier Reef Marine Park Authority	$ 1000
Australian Institute of Marine Science in-kind support	(NA)

Thesis Committee

Prof. Peter Ridd, School of Engineering and Physical Sciences, James Cook University

Prof. Miles Furnas, Australian Institute of Marine Science

Dr. Yvette Everingham, School of Engineering and Physical Sciences, James Cook University

Statistical and Analytical Assistance

Prof. Peter Ridd

Prof. Miles Furnas

Dr. Yvette Everingham

Mr. Matthew Slivkoff

Editorial Support

Prof. Peter Ridd

Prof. Miles Furnas

Acknowledgements

I would first and foremost like to thank my supervisor Prof. Miles Furnas. Miles, your knowledge regarding the Great Barrier Reef seems inexhaustible and your enthusiasm for developing new scientific gadgetry has been inspiring. To my second supervisor Prof. Peter Ridd, I wholeheartedly thank you for your assistance during this undertaking. Your passion for physics and scientific research has ingrained upon me. To my third supervisor Dr. Yvette Everingham, thank you for your guidance. You have greatly contributed to my skills as a scientist.

I would like to acknowledge the efforts of the external examiners who kindly reviewed my work. Your comments and feedback have improved the final form of this PhD thesis.

My sincere thanks are also extended to those who assisted during the field component of my PhD. The Masters and crew of the RV Lady Basten and RV Cape Ferguson were always willing to assist me in all aspects of *in situ* sampling, equipment maintenance and repair, and always seemed to have just the right spare part available somewhere in the hold. During AIMS research cruises I was fortunate to have worked with Irena Zagorskis, John Carelton, Britta Schaffelke, Dave McKinnon and many other fine marine scientists. I thank you all for your guidance, assistance and cheerful spirits which made long journeys at sea together memorable.

I am grateful to the James Cook University and Australian Institute of Marine Science academic and administrative staff for their support including Paula Rodger (JCU), Leanne Ashmead (JCU), Thomas Stieglitz (JCU), Ian and Anne Whittingham (JCU), Sue Bird (Graduate Research School), Barbara Pannach (Graduate Research School), Helene Marsh (Graduate Research School) and Michelle Heupel (AIMS@JCU). In addition, thank you to Michelle Devlin, Jon Brodie, Steve Lewis and Zoe Bainbridge of the Australian Centre for Tropical Freshwater Research for giving me the opportunity to work with your amazing team.

To Matt Slivkoff and Wojciech Klonowski of Curtin University, your extensive knowledge of marine optics and the DALEC instrument has been an important resource for me. In particular I thank Matt for our many conversations which have helped develop this thesis.

To my fellow PhD students with whom I have shared office spaces with over the past few years, Daniel Zamykal, Josh Davidson, Arnold Akem, Danny Cocks and

Severine Choukroun, I thank you for your comradeship. I also apologise for the never ceasing cascade of scientific papers that are always flowing from my desk onto the floor.

To my parents Ian and Carol McKinna, and my extended family, I thank you for your undivided love and support over these last few years and fostering my interest in learning from a young age. To my feline companion Hamish thanks for sitting up late at night with me whilst I have been madly typing. To you I say, “meow.” Finally, to my partner Jamie Coull, you have been my rock over these last few years and I love you dearly. Thank you so much for your never ceasing understanding and patience.

Abstract

The primary purpose of this PhD project was the development of suitable methods for the optical detection and quantification of the diazotrophic, marine cyanobacteria *Trichodesmium* within the Great Barrier Reef (GBR), Australia. Within the GBR, *Trichodesmium* is likely to contribute quantities of new-nitrogen of similar magnitude to that of rivers. However, due to uncertainties regarding the spatial and temporal abundance of *Trichodesmium*, there is an order of magnitude uncertainty associated with these nitrogen fixation estimates. Thus, improved methods for quantifying *Trichodesmium* within the GBR are essential. The key objectives of this PhD thesis were to:

- Study the bio-optical properties of *Trichodesmium*,
- Develop a binary flag for its detection using MODIS imagery and
- Examine hyperspectral radiometric data as a means of positively discriminating and quantifying *Trichodesmium*.

In addition, the bio-optical properties of a senescing surface aggregation of *Trichodesmium* were studied.

Within this PhD thesis, the bio-optical properties of *Trichodesmium* were studied primarily with discrete water samples analysed using a benchtop spectrophotometer. Particulate and coloured dissolved organic matter (CDOM) absorption coefficients were measured. From this research component, a relationship between the magnitude of the spectral absorption coefficient of *Trichodesmium* and chlorophyll-a (Chla) specific concentration was established. Results were comparable with those of the literature. The Chla-specific *Trichodesmium* absorption coefficients were later used as inputs for radiative transfer simulations with Hydrolight. *In situ* above-water hyperspectral radiometric measurements of *Trichodesmium* were also collected.

A *Trichodesmium*-specific binary classification algorithm was developed using quasi-250 m MODIS data. Above-water hyperspectral radiometric measurements of dense *Trichodesmium* surface aggregations (> 30 mg Chla m^{-3}) showed that the water leaving radiance at wavelengths greater than 700 nm were

much higher in magnitude (> 0.05 W m^{-2} sr^{-1}) relative to the visible wavelengths 400 - 700 nm (< 0.03 W m^{-2} sr^{-1}). This "red-edge" effect agreed with observations of others from the literature. The binary classification algorithm was based on three criteria. The first criteria relied on the difference in magnitude between the MODIS normalised water-leaving radiance (nLw) of band 2 (859 nm) and band 15 (678 nm). The magnitudes of the nLw of band 4 (555 nm) and band 1 (645 nm) relative to band 15 formed the second and third criteria respectively. The classification algorithm was tested on a small subset of 13 MODIS images with corresponding *Trichodesmium* sea-truths and yielded an 85 % accuracy. Fine scale features consistent with dense *Trichodesmium* surface aggregations such as eddy swirls and windrows were well represented within the algorithm results. The algorithm was also found to be robust in the presence of highly reflective, potentially confounding affects such as coral reefs, shallow bathymetry and riverine sediment plumes.

The suitability of the quasi-analytical algorithm (QAA) for inverting hyperspectral remote sensing reflectance, $R_{rs}(\lambda)$, and quantitatively discriminating *Trichodesmium* was examined. A technique combining the QAA and a similarity index measure (SIM) was developed using $R_{rs}(\lambda)$ data simulated for examples of Case 1 and Case 2 waters. Hydrolight radiative transfer software was used to model $R_{rs}(\lambda)$ with *Trichodesmium* Chla specific absorption inherent optical properties. The QAA was used to invert the simulated $R_{rs}(\lambda)$ spectra to yield an estimate of the phytoplankton absorption coefficient $a_{\phi}^{QAA}(\lambda)$. To ascertain the presence of *Trichodesmium*, seven SIM values were derived by comparing $a_{\phi}^{QAA}(\lambda)$ with a known *Trichodesmium* reference absorption spectrum $a_{tri}^{ref}(\lambda)$, and also with the absorption spectra of six other phytoplankton types. The results found that the SIM could discriminate *Trichodesmium* from the six other phytoplankton types for concentrations as low as 0.2 mg Chla m^{-3} and 3 mg Chla m^{-3} for the Case 1 and Case 2 scenarios considered. The QAA-SIM method was tested on along-transect $R_{rs}(\lambda)$ data collected within the GBR. Upon identifying the presence of *Trichodesmium*, the magnitude of $a_{\phi}^{QAA}(\lambda)$ was used to determine Chla concentration. The along-transect, QAA derived Chla values were validated with data from a Chla fluorometer within a

ship-board flow-through system. The predicted Chla values matched well with those fluorometrically measured yielding an R-squared value of 0.805.

Two distinct colour modes of *Trichodesmium* were sampled from a dense surface aggregation within the GBR. The two colour modes were denoted as: orange-brown (OB) and bright green (BG). The spectral particulate and coloured dissolved organic matter (CDOM) absorption coefficients were measured for the OB and BG samples. The absorption properties of the OB sample were consistent with those of *Trichodesmium* reported within literature. However, the absorption properties of the BG sample were significantly different to those of the OB sample. The particulate and dissolved absorption coefficients of the BG sample revealed that the water soluble red pigments phycourobilin (PUB) and phycoerythrobilin (PEB) had leached into the surrounding seawater. The results suggest that the BG samples were in the process of senescence. Hydrolight radiative transfer modelling was used to simulate the hyperspectral $R_{rs}(\lambda)$ of OB and BG colour modes. The results indicated that the $R_{rs}(\lambda)$ spectra of the OB sample was spectrally distinct from that of the BG sample. Thus, the potential to optically discriminate the physiological state of a *Trichodesmium* surface aggregation was established.

Publications Produced During the PhD Candidature

Publications

McKinna, L.I.W., Furnas, M.J. and P.V. Ridd, (2011), *A simple, binary classification algorithm for the detection of Trichodesmium spp. within the Great Barrier Reef using MODIS imagery*, Limnology and Oceanography: Methods, 9, 50-66.

McKinna, L. and Y. Everingham. (2011), *Seasonal Climate Prediction for the Australian Sugar Industry using Data Mining Techniques*, in: Data Mining, InTech, Vienna

Choukroun, S., Ridd, P.V., Brinkman, R. and **L.I.W. McKinna**, (2010). *On the surface circulation in the Western Coral Sea and residence times in the Great Barrier Reef*, Journal of Geophysical Research Oceans, Vol. 115, C06013.

Lembrechts, J., Humphrey, C., **McKinna, L.**, Gourge, O., Fabricius, K.E., Mehta. A.J., Lewis, S. and E. Wolanski.(2010). *Importance of wave-induced bed liquefaction in the fine sediment budget of Cleveland Bay, Great Barrier Reef*, Estuarine and Coastal Shelf Science, 89, 154—162.

Everingham, Y., Zamykal, D. and **L. McKinna** (2009), *Rain Forecaster - A Seasonal Climate Forecasting Tool*, Proceedings of the 31st Annual Australian Society of Sugar Cane Technologies, Ballina, May 2009.

Devlin, M., Schroeder, T., **McKinna, L.**, Brodie, J., Brando, V., Dekker, A. (In Press), *Monitoring and mapping of flood plumes in the Great Barrier Reef based on in-situ and remote sensing observations*, in: Advances in Environmental Remote Sensing to Monitor Global Changes, CRC Press, Boca Raton

Donald, D., Everingham, Y., **McKinna, L.** and D. Coomans. (2009), *Feature Selection in the Wavelet Domain: Adaptive Wavelets*, in: Comprehensive Chemometrics Vol. 3, Eds. Brown, S., Tauler, R. and B. Waalczak, pp. 649–667, Elsevier, Netherlands

McKinna, L.I.W., Furnas, M.J. and P.V. Ridd. (Submitted Manuscript), *Bio-optical properties of senescing Trichodesmium within the Great Barrier Reef*, Estuarine, Coastal and Shelf Science.

McKinna, L.I.W., Furnas, M.J., Ridd, P.V. and M. Slivkoff (In Prep), *Inversion of hyperspectral remote sensing reflectance for the quantitative detection of Trichodesmium within the Great Barrier Reef.*

McKinna, L.I.W., Furnas M.J. and P.V. Ridd (In Prep), *Two Decades of Remote Sensing Trichodesmium in the World's Oceans*

Devlin, M., **McKinna, L.**, Harkness, P., Schroeder, T., Waterhouse, J., Schaffelke, B., Brodie, J. (In Prep) *Mapping of water types in the GBR: A new approach to plume waters*, for Marine Pollution Bulletin.

Reports and Technical Documents:

Devlin, M., Harkness, P., **McKinna, L**. and J. Waterhouse (2010). *Mapping risk and exposure of Great Barrier Reef ecosystems to anthropogenic water quality: A review and synthesis of current status*. Report to the Great Barrier Reef Marine Park Authority August 2010, Australian Centre for Tropical Freshwater Research, Report Number 10/12.

Devlin, M., Waterhouse, J., **McKinna, L.** and S. Lewis. (2009), *Terrestrial Runoff in the Great Barrier Reef, Marine Monitoring Program (3.7.2b), Tully and Burdekin Case Studies*, Report to the Great Barrier Reef Marine Park ` Authority, Reef and Rainforest Research Centre.

McKinna, L.I.W. (2009), *SeaBird Electronics SBE 19plus CTD User Guide*, Australian Centre for Tropical Freshwater Research (ACTFR).

Presentations

McKinna, L.I.W., Furnas, M.J., Ridd, P.V. and M. Slivkoff. *Inversion of hyperspectral remote sensing reflectance for quantitative detection of Trichodesmium spp. Within the Great Barrier Reef*, Ocean Optics XX, Anchorage, September 27-October 1, 2010 (Extended Abstract).

Devlin, M., **McKinna, L.**, Harkness, P., Schroeder, T., Waterhouse, J., Schaffelke, B., Brodie, J. *Mapping of water types in the GBR: A new approach to plume waters*, Challenges in Environmental Sciences and Engineering CESE, Cairns, 26 September – 1 October, 2010.

Devlin, M., **McKinna, L.**, Schroeder, T., Schaffelke, B., Brando, V. and J. Brodie. *Riverine Plumes in the Great Barrier Reef: Mapping Extent and Composition using Remote Sensing Imagery*, Marine and Tropical Sciences Research Facility (MTSRF) Conference, Cairns, May 18 - 20, 2010.

McKinna, L.I.W., Furnas, M.J. and P.V. Ridd, *Detection of Trichodesmium* spp. *Surface Aggregations within the Great Barrier Reef using MODIS Imagery*, India-Australia Workshop on Ocean Colour Remote Sensing, Ahmedabad, March 18-19, 2010.

McKinna, L.I.W. and M. Devlin, *Riverine plumes in the Great Barrier Reef: Mapping the Plume Extent and Composition using Remote Sensing Imagery*, India-Australia Workshop on Ocean Colour Remote Sensing, Ahmedabad, March 18-19, 2010.

Furnas, M., Slivkoff, M., **McKinna, L.** and C. Steingberg, *The DALEC: Sea-level hyperspectral radiometry for ocean colour validation and underway spectral mapping*, India-Australia Workshop on Ocean Colour Remote Sensing, Ahmedabad, March 18-19, 2010

McKinna, L., Furnas, M. and Ridd, P. *Detection of Trichodesmium spp. surface aggregations within the Great Barrier Reef using MODIS imagery*, Ocean Sciences Meeting, Portland, February, 2010

McKinna, L., Nelson-White, G. and M. Devlin, *MODIS Satellite Imagery for Flood Plume Extent Mapping and Classification*, Surveying and Spatial Sciences Institute (SSSI) Northern Group Conference, Townsville, October 2009. (Invited Talk).

McKinna, L., Furnas, M., Ridd, P., Everingham, Y. and M. Slivkoff. *Hyperspectal Monitoring of Trichodesmium spp. within the Great Barrier Reef*, Ocean Optics XIX, Barga, October 2008.

Slivkoff, M., **McKinna, L.**, Furnas, M. and M. Lynch. *Inherent Optical Property Measurements and Modeling in the Great Barrier Reef World Heritage Area*, Ocean Optics XIX, Barga, October 2008.

Table of Contents

Abstract i
Publications iv
Reports and Technical Documents: v
Presentations vi
List of Figures xii
List of Tables xx
List of Common Symbols xxii
List of Abbreviations xxvi
1 General Introduction 1
Abstract 1
1.1 Trichodesmium spp. 2
1.2 Water Quality and the Great Barrier Reef 4
1.3 Ocean Colour Remote Sensing 6
1.4 Thesis Objectives and Outline 7
2 Two decades of ocean colour remote sensing *Trichodesmium* spp. in the World's oceans 9
Abstract 9
2.1 Introduction 10
2.1.1 Global Significance of *Trichodesmium* spp. 10
2.1.2 Ocean colour remote sensing 11
2.1.3 Purpose and Outline 12
2.2 Photography of *Trichodesmium* from Platforms in Orbit 13
2.3 Bio-optical properties of *Trichodesmium* spp. 15
2.3.1 Absorption 15
2.3.2 Backscattering 16
2.3.3 Remote Sensing Reflectance Spectrum 17
2.4 Satellite observations and Empirical Detection Algorithms 20
2.4.1 CZCS 20
2.4.2 SeaWiFS 29
2.4.3 OCM 38
2.4.4 MODIS 40
2.4.5 MERIS 42

2.5 Global Trichodesmium Algorithms 45
2.5.1 Adapted GSM01 Model 45
2.5.2 Adapted GSM01 Model Summary 48
2.6 Summary and Conclusion 49
2.7 Future Directions 53
3 A simple, binary classification algorithm for the detection of *Trichodesmium* spp. within the Great Barrier Reef using MODIS imagery. 55
Abstract 55
3.1 Introduction 56
3.2 Materials and Procedures 61
3.2.1 Trichodesmium surface aggregations within the Great Barrier Reef .. 61
3.2.2 Hyperspectral ship-borne above-water radiometry 63
3.2.3 Hyperspectral water-leaving radiance and remote-sensing reflectance data 66
3.2.4 MODIS high resolution imagery 69
3.2.5 Classification Algorithm 70
3.2.6 Comparison of MODIS and Hyperspectral Rrs 73
3.3 Model Assessment 75
3.3.1 Validation of Algorithm 75
3.3.2 Sensitivity Analysis 76
3.3.3 Confounding Effects 79
3.3.4 Application: The Capricorn Channel and Southern Great Barrier Reef 83
3.4 Discussion 85
4 Inversion of hyperspectral remote sensing reflectance for quantitative detection of *Trichodesmium* spp. within the Great Barrier Reef 89
Abstract 89
4.1 Introduction 91
4.2 Data 94
4.2.1 Discrete Water Samples 94
4.2.2 Above-water Hyperspectral Radiometry 96
4.2.3 Flow-through Chlorophyll-a Fluorometry 96
4.3 Methods 99
4.3.1 Hydrolight Modelling 99

4.3.2 The Quasi-Analytical Algorithm 102
4.3.3 Similarity Index Measure 103
4.4 Results and Discussion 108
4.4.1 Relationship between Chlorophyll-a Concentration and Absorption Coefficient Magnitude 108
4.4.2 Modelled R_{rs} 112
4.4.3 QAA Derived Phytoplankton Absorption Coefficient. 113
4.4.4 Discrimination using SIM values 113
4.4.5 Sensitivity of QAA-SIM to false-positive *Trichodesmium* detection 117
4.4.6 Inversion of Transect Rrs 119
4.5 Conclusion 125
5 Modelling the hyperspectral remote sensing reflectance signal of senescing *Trichodesmium* spp. 129
Abstract 129
5.1 Introduction 130
5.2 Data and Methods 133
5.3 Pigment Analysis 135
5.3.1 Absorption Coefficients 135
5.3.2 Radiative Transfer Modelling 136
5.4 Results and Discussion 138
5.4.1 Oceanographic Conditions 138
5.4.2 Discrete Pigment Samples 139
5.4.3 Particulate Pigment Absorption 140
5.4.4 Dissolved Pigment Absorption 142
5.4.5 Modelled Remote Sensing Reflectance 144
5.5 Discussion 146
5.6 Conclusion 152
6 Thesis Conclusions and Future Work 155
6.1.1 A Binary Classification Algorithm 155
6.1.2 Hyperspectral Inversion Algorithm 156
6.1.3 Bio-optical Properties of Senescing Trichodesmium 157
6.2 Overview and Implications 158
6.3 Future Work 159
6.3.1 Sampling Strategies and Bio-optical Properties 159

Thesis Appendices 162
Appendix 1: Look-up-table, LUT, of sky reflectance coefficients ρ 163
Appendix 2: FLNTU Linear Offsets 251
Appendix 3: The Quasi-Analytical Algorithm 253
Appendix 4: N-fixation Estimates from Derived *Trichodesmium* abundance 257
References 261

List of Figures

Chapter 1

Figure 1.1: Colonial forms of *Trichodesmium* spp. Samples taken from the Central Great Barrier Reef, April, 2007. ……...3

Figure 1.2: Examples of *Trichodesmium* surface aggregations, within the Great Barrier Reef, Australia. ……4

Figure 1.3: Estimated annual inputs of nitrogen into the Tully region of the GBR shelf (15°52'S – 16°55'S). Data source: Furnas and Mitchell (1996) ..…….....6

Chapter 2

Figure 2.1: Photographs captured from orbit of surface aggregations deemed to be *Trichodesmium* in the Capricorn Channel of the Great Barrier Reef, Australia. (a.) Image from the NASA Space Shuttle captured on November, 1983. Mission-Roll-Frame details: STS009-35-1622, centred on 23.5°S, 152.5°E. (b.) Image from the ISS captured on 27 November 2002. Mission-Roll-Frame details: ISS005-E-21570, centred on 24.3°S, 151.0°E. Images courtesy of the Image Science & Analysis Laboratory, NASA Johnson Space Center (http://eol.jsc.nasa.gov/), length scale data unavailable. …….14

Figure 2.2: *Trichodesmium* Chla-specific spectral absorption coefficient (solid line) (McKinna, unpublished data). Open circles represent the *Trichodesmium* Chla-specific backscattering coefficients measured at six wavelengths using a HOBI Labs Hydroscat 6 instrument (Dupouy et al. 2008a). The dashed line represents the spectral backscattering coefficients fitted according to Equation 2.1. …….....17

Figure 2.3: (a.) Normalised remote sensing reflectance spectrum of *Trichodesmium* measured by Dupouy et al. (2008a). (b) Normalised remote sensing reflectance of Dupouy et al. (2008) in blue compared with a reflectance spectra collected within this thesis red (see section 3.2.3). Note a vertical offset applied to separate the two spectra for interpretive purposes. ……...……19

Figure 2.4: (a.) Un-projected, quasi-true colour CZCS image captured over New Caledonia (bottom left, outlined in red) and the Vanuatu Archipelago (centre) in the south-western tropical Pacific Ocean. At the centre of the image (21°S, 168°E) is a mass of discoloured, green/yellow water which was attributed to *Trichodesmium* by Dupouy et al. (1988). White patches in the image are convective clouds. (b.) A projected, Chla pigment concentration (mg Chla m^{-3}) map of the CZCS scene, cloud and land appear black. …..…….....22

Figure 2.5: A quasi-true colour CZCS image of the Arabian Sea captured on 28 March 1979. The west coast of India is on the right had side of the image. A high suspended sediment load is evident extending from the Gulf of Khambhat (20°N, 72°E) (denoted +). Along the western continental shelf of India, bright green water was interpreted as high concentrations of *Trichodesmium*. The left side of this image shows highly reflective, milky coloured water which was potentially a coccolithophore bloom. ……..……24

Figure 2.6: CZCS image of the Arabian Sea from 28 March 1979. Sub-images a, b and c represents the normalised water leaving radiances at 443, 520 and 550 nm respectively. (d) CZCS map of Chla concentration. Regions containing *Trichodesmium* were assumed to be adjacent to the western Coast of India (right hand side of each sub-image). Black pixels correspond to land, cloud, or pixels with saturated radiances and/or algorithm failure. ……....25

Figure 2.7: CZCS Image of the west coast of Australia from 1 November 1980. (a.) A quasi-true colour image reveals bright green patches adjacent to the coastline around Barrow Island and the Dampier Archipelago. (b.) A Chla map of the region and (c.) the PPV map of *Trichodesmium* abundance shows high values around Barrow Island and the Dampier Archipelago as reported by Subramaniam and Carpenter (1994) and also offshore from Eighty Mile Beach…….27

Figure 2.8: A SeaWiFS image of the South Atlantic Bight on 30 October 1998. (a.) A quasi true colour image the, bright green colouration is evident off the coast of Cape Canaveral (denoted +). Little Bahamas Bank can be seen in the bottom right hand side. (b.) A Chla map of the region and (c.) the Subramanian et al. (2002) *Trichodesmium* classification scheme applied to the scene. The dashed red ellipse shows, the location of high concentrations of *Trichodesmium*, the solid red ellipse shows the top of Little Bahamas Bank. The white patches within images (b.) and (c.) correspond to clouds and atmospheric interference. ……..34

Figure 2.9: (a.) Quasi true colour MERIS image of the Great Barrier Reef captured on 5 October 2008. The yellow ellipse shows highly reflective brown streaks offshore from Shaolwater Bay. (b.) The corresponding MERIS MCI image, bright features correspond to brown streaks present in the true colour image and indicate high near-surface Chla concentrations. Note the MCI index also identifies highly reflective coral reef structures. …….....44

Chapter 3

Figure 3.1: (a) Map of the Great Barrier Reef region adjacent to the Northeast Australian Coastline with the Cairns and Mackay/Whitsunday study regions boxed in red. (b) A 17 km long southeast transect within the Cairns region on the 27 April, 2007 and (c) the northwest 38 km long transect within the Mackay/Whitsunday region on the 31 July 2008. …….....62

Figure 3.2: Photograph of the above-water, hyperspectral radiometer collecting data over *Trichodesmium* windrows along the Cairns Transect on the 27 April, 2007….....65

Figure 3.3: Hyperspectral, water-leaving radiances L_w for dense surface aggregations of *Trichodesmium* observed along (A.) the Cairns Transect and (B.) the Mackay/Whitsunday Transect. The corresponding hyperspectral, remote-sensing reflectance R_{rs} spectra for (C.) the Cairns Transect, and (D.) the Mackay/Whitsunday Transect. …….68

Figure 3.4: (a.) MODIS Aqua RGB true-colour image of the Cairns region captured on the 27 April, 2007. (b.) The result of the binary classification algorithm is plotted in red denoting regions of dense *Trichodesmium* surface aggregations. (c.) The result of criteria 1 alone (d.) The result of classification criteria 1 and 2, (e.) the result of classification criteria 1 and 3, and (f.) the result of classification criteria 2 and 3. Blue circles surround flagged pixels that are immediately adjacent to the coast……72

Figure 3.5: (a.) Four points α, β, γ and δ along the Cairns Transect were used to compare (b.) MODIS R_{rs} with (c.) hyperspectral above-water radiometer R_{rs}. Note that in (C.) the R_{rs} spectra for location β has been scaled by 10^{-1}. ……....74

Figure 3.6: Sensitivity analysis of the classification criteria nLw(859) > c_1 nLw(678), where c_1 = 0.001, 0.01, 0.1, 0.5,1, 5, 10, and 100 corresponding to (a.), (b.), (c.), (d.), (e.), (f.), (g.) and (h.). …….78

Figure 3.7: (a.) A true-colour RGB MODIS-Aqua image of the Whitsunday/Mackay region of the Great Barrier Reef from 27 January 2005. At the centre of the image is a river plume from the Pioneer and O'Connell Rivers and toward the top of the image is a high suspended sediment plume from the Burdekin River. Brown-red streaks are evident at the edge of the Pioneer/O'Connell River Plume and were identified as *Trichodesmium* spp. by Rohde et al. (2006). (b.) Results of the *Trichodesmium* binary classification algorithm plotted in red over the original true-colour RGB image…..……..……...82

Figure 3.8: (a.) A true-colour RGB MODIS-Aqua image of the Capricorn Channel region of the GBR captured on 17 October 2007. (b.) Results of the *Trichodesmium* binary classification algorithm plotted in red over the original true-colour RGB image……...84

Chapter 4

Figure 4.1: Photograph of floating *Trichodesmium* surface aggregations (brown discolourations) observed during the radiometric transect. Image capture at: 1440 hours, 3 October 2010. Location: 22°39'46''S, 151°04'21''E……...97

Figure 4.2: (a.) The Great Barrier Reef, Australia. The red square indicates the domain containing the transect. (b.) Zoom map of the transect location for which $R_{rs}(\lambda)$ and FLNTU Chla data were collected……98

Figure 4.3: (a.) *Trichodesmium* Chla specific absorption $a^{*}_{tri}(\lambda)$ and scattering $b^{*}_{tri}(\lambda)$ coefficients used within Hydrolight simulations. Open circles represent Hydroscat 6 measurements of $b^{*}_{tri}(\lambda)$ made by Dupouy et al. (2008a). (b.) *Trichodesmium* Chla specific CDOM absorption coefficient (McKinna, unpublished data)……101

Figure 4.4: Figure 4.4: Comparison of the normalised *Trichodesmium* (Tri) absorption coefficient with normalised absorption coefficients of (a.) Green Phytoplankton (PS), (b.) Generic Picoplankton, (c.) Generic Microplankton, (d.) Diatoms, (e.) *Prochlorococcus*, and (f.) *Synechococcus*. The shaded rectangle represents the spectral range of 520 – 580 nm.……..107

Figure 4.5: Spectral covariance matrix plot showing the spectral variability between the seven phytoplankton absorption spectra detailed in Table 4.1. Regions of highest variability occur between 520 – 580 nm and 660 – 680 nm.……108

Figure 4.6: (a.) Log-log plot of Chla concentration of *Trichodesmium* varying with absorption coefficient at 443 nm……...110

Figure 4.6 (b.) Unscaled plot of Chla concentration of *Trichodesmium* varying with absorption coefficient at 443 nm. The dashed line fitted according to Equation 4.4..……111

Figure 4.7: (a.) Modelled hyperspectral remote sensing reflectance for *Trichodesmium* in the Case 1 water scenario for Chla concentration increasing logarithmically from 0 – 100 mg m^{-3}. (b.) QAA-derived phytoplankton absorption coefficient $a^{QAA}_{\phi}(\lambda)$. (c.) Similarity index measures (SIM) computed using reference absorption spectra from the spectral library……...115

Figure 4.8: (a.) Modelled hyperspectral remote sensing reflectance for *Trichodesmium* in the Case 2 water scenario with Chla concentration increasing logarithmically from 0 – 100 mg m^{-3}. (b.) QAA-derived phytoplankton absorption coefficient $a_{\phi}^{QAA}(\lambda)$. (c.) Similarity index measures (SIM) computed using reference absorption spectra from the spectral library…….....116

Figure 4.9: (a.) (a.) Modelled hyperspectral remote sensing reflectance using Hydrolight Case 1 model with Chla concentration ranging from 0.1 – 100 mg m^{-3}. (b.) QAA-derived phytoplankton absorption coefficient $a_{\phi}^{QAA}(\lambda)$. (c.) Similarity index measures (SIM) computed using reference absorption spectra from the spectral library…….118

Figure 4.10: (a.) Along-transect remote sensing reflectance spectra $R_{rs}(\lambda)$ collected within the Great Barrier Reef on 3 October 2010. (b.) QAA-derived phytoplankton absorption coefficients [$a_{\phi}^{QAA}(\lambda)$ obtained by inverting each $R_{rs}(\lambda)$ spectra]……119

Figure 4.11: Along-transect similarity index measures (SIM) computed for each QAA derived $a_{\phi}^{QAA}(\lambda)$ spectra on 3 October 2010.……120

Figure 4.12: Sequence plot of Chla values measured using fluorometer in a flow-through system (green line), QAA derived Chla values (red line), NASA OC3 Chla algorithm (blue line) and NASA OC4 Chla algorithm (black line)……..122

Figure 4.13: Scatter plot of measured versus radiometrically predicted Chla concentration for the 3 October 2010 transect……...124

Chapter 5

Figure 5.1: (a.) A dense surface aggregation of *Trichodesmium* spp. encountered on 16 February 2009 within the Southern Great Barrier Reef, Australia. The photograph is looking in the aft direction over the starboard side of the RV Cape Ferguson. Two distinct colour modes of *Trichodesmium* were observed: orange/brown (OB) and bright

green (BG). Concentrations of OB and BG *Trichodesmium* colonies upon Whatman GF/F filters (Ø 25 mm) are shown in (b.) and (c.) respectively. [Image credit (a.): I. Zagorskis, Australian Institute of Marine Science (2009).] ……134

Figure 5.2: Vertical profile data collected using a SeaBird Electronics CTD instrument. (a.) Temperature (red) and salinity (dotted blue), (b.) optical backscattering (c.) Chla fluorescence, (d.) optical attenuation collected during a vertical profile beneath the *Trichodesmium* surface aggregation……..139

Figure 5.3: The normalised particulate absorption coefficient spectra for the OB and BG colour modes of *Trichodesmium*. The difference (DIFF) between the normalised OB and BG absorption spectra is plotted also…..……141

Figure 5.4: (a.) Measured CDOM spectral absorption coefficient for the OB *Trichodesmium* sample. (b.) Measured CDOM spectral absorption coefficient for the BG *Trichodesmium* sample. Note the scale of the y-axes on these plots differs.…….143

Figure 5.5: Spectra CDOM absorption coefficients $a_{gOB}(\lambda)$ and $a_{gBG}(\lambda)$ for the orange/brown (OB) and bright green (BG) colour modes of *Trichodesmium* respectively over the spectral range 400 – 700 nm.……....143

Figure 5.6: Hydrolight simulated remote sensing reflectance R_{rs} spectra for bright green (BG) and orange/brown (OB) colour modes of Trichodesmium. The grey and white boxes indicate the positions of the spectral bands of the MERIS and MODIS ocean colour sensors respectively. Dashed lines represent gradient between 490nm and 550nm……...…...145

Figure 5.7: The measured absorption coefficient of dissolved pigments sampled from beneath the BG colour mode of *Trichodesmium* is represented as blue circles. A fitted line created using a series of Gaussian basis functions is shown as a red line. The dashed lines represent the individual basis curves used to fit the data.……....148

Figure 5.8: Estimated total R_{rs} spectra for a pixel containing varying proportions of OB and BG *Trichodesmium* dictated by the mixing ratio, *c*, as defined in Equation 5.6. The grey and white boxes indicate the positions of the spectral bands of the MERIS and MODIS ocean colour sensors respectively……151

Appendix 2

Figure A2.1: Values of Chla concentration derived using a WETLabs FLNTU instrument plotted against *in situ* measurements……...251

Appendix 4

Figure A4.1: Plot of along-transect volumetric nitrogen fixation rate derived from *Trichodesmium* specific Chla concentration……..260

List of Tables

Chapter 2

Table 2.1: Chronologically ordered efforts to detect *Trichodesmium* using various satellite ocean colour sensors. Within this table, Y = yes, N= No. *Positive Discrimination – if the method was designed to be able to discriminate *Trichodesmium* from other marine constituents without user interpretation.……52

Chapter 3

Table 3.1: The mean absolute percentage error of four R_{rs} spectra derived with ρ varying as a function of sun-instrument viewing angle +/-30° either side of 135° only…….....65

Table 3.2: Time, dates and coordinates of *Trichodesmium* surface aggregations observed within the Great Barrier Reef for which the binary classification algorithm was applied. A positive match-up is denoted with a "+" and a negative match-up is denoted with "-" for each location.…….....77

Chapter 4

Table 4.1: Details of phytoplankton spectral absorption coefficient data used as reference spectra $a_{\phi}^{ref}(\lambda)$ for determination of similarity index measures SIM……105

Table 4.2: Similarity index measures (SIM) calculated over the spectral range 400 – 580 nm for seven difference reference phytoplankton absorption spectra $a_{\phi}^{ref}(\lambda)$…….106

Table 4.3: Similarity index measures (SIM) calculated over the spectral range 520 – 580 nm for seven difference reference phytoplankton absorption spectra $a_{\phi}^{ref}(\lambda)$ …….106

Appendix 4

Table A4.1: Values used for estimation of Chla-specific *Trichodesmium* N-fixation rate……...…..259

Table A4.2: Nitrogen inputs from rivers and *Trichodesmium* to the Great Barrier Reef……259

List of Common Symbols

Symbol	Units	Description
$a(\lambda)$	m^{-1}	Total spectral absorption coefficient
$a_{dg}(\lambda)$	m^{-1}	Coloured dissolved and detrital matter absorption coefficient
$a_{g}(\lambda)$	m^{-1}	Coloured dissolved organic matter absorption coefficient
$a_{gOB}(\lambda)$	m^{-1}	Coloured dissolved organic matter absorption coefficient of Orange-Brown (OB) *Trichodesmium*
$a_{gBG}(\lambda)$	m^{-1}	Coloured dissolved organic matter absorption coefficient of Bright Green (BG) *Trichodesmium*
$a_{nap}(\lambda)$	m^{-1}	Non-algal particulate matter absorption coefficient
$a_{p}(\lambda)$	m^{-1}	Particulate matter absorption coefficient
$a_{\phi}(\lambda)$	m^{-1}	Phytoplankton specific absorption coefficient
$a_{\phi}^{QAA}(\lambda)$	m^{-1}	QAA-derived phytoplankton absorption coefficient
$a_{\phi}^{ref}(\lambda)$	m^{-1}	Reference phytoplankton absorption coefficient
$a_{tri}(\lambda)$	m^{-1}	*Trichodesmium* specific absorption coefficient
$a_{tri}^{*}(\lambda)$	$m^{2}\ mg^{-1}$	Chlorophyll-specific *Trichodesmium* absorptioncoefficient
$a_{w}(\lambda)$	m^{-1}	Pure water absorption coefficient
$\mathbf{A_{ref}}$	$m^{-1}nm^{-4}$	Fourth derivative spectrum of $a_{\phi}^{ref}(\lambda)$
$\mathbf{A}_{\phi}$	$m^{-1}nm^{-4}$	Fourth derivative spectrum of $a_{\phi}^{QAA}(\lambda)$

A_f	m^2	Area of a Whatman GF/F filter
$b(\lambda)$	m^{-1}	Total scattering coefficient
$b_b(\lambda)$	m^{-1}	Total backscattering coefficient
$b_w(\lambda)$	m^{-1}	Pure water scattering coefficient
$b_{bw}(\lambda)$	m^{-1}	Pure water backscattering coefficient
$b_p(\lambda)$	m^{-1}	Particulate scattering coefficient
$b_{bp}(\lambda)$	m^{-1}	Particulate backscattering coefficient
$b_w(\lambda)$	m^{-1}	Pure water scattering coefficient
$b_{bw}(\lambda)$	m^{-1}	Pure water backscattering coefficient
$b_{tri}(\lambda)$	m^{-1}	*Trichodesmium* specific scattering coefficient
$b_{btri}(\lambda)$	m^{-1}	*Trichodesmium* specific backscattering coefficient
$b_p^*(\lambda)$	$m^2\ gm^{-1}$	Mass-specific particulate scattering coefficient
$b_{bp}^*(\lambda)$	$m^2\ gm^{-1}$	Mass-specific particulate backscattering coefficient
$b_{tri}^*(\lambda)$	$m^2\ mg^{-1}$	Chlorophyll-specific *Trichodesmium* scattering coefficient
$b_{btri}^*(\lambda)$	$m^2\ mg^{-1}$	Chlorophyll-specific *Trichodesmium* backscattering coefficient
$\tilde{b}_b$	Dimensionless	Backscattering ratio
β	Dimensionless	Pathlength amplification correction factor
$\tilde{\beta}$	sr^{-1}	Scattering phase function
Chla	$mg\ m^{-3}$	Chlorophyll-a
δ	dimensionless	Sky radiance correction coefficient
$E_d(\lambda)$	$W\ m^{-2}$	Downwelling irradiance
γ	dimensionless	The spectral power coefficient of the particulate backscattering coefficient

K_d	m^{-1}	Diffuse attenuation coefficient
K490	m^{-1}	Diffuse attenuation coefficient at 490 nm
l	m	pathlength
λ	nm	Wavelength
λ_0	nm	Reference wavelength
$L_{sky}(\lambda)$	W m^{-2} sr^{-1}	Sky radiance
$L_t(\lambda)$	W cm^{-2} sr^{-1}	Total upwelling radiance
$L_u(\lambda)$	W m^{-2} sr^{-1}	Upwelling radiance
$L_w(\lambda)$	W m^{-2} sr^{-1}	Water-leaving radiance
m		
$nLw(\lambda)$	W m^{-2} sr^{-1}	Normalised water-leaving radiance
$nLw^*(\lambda)$	dimensionless	Radiance anomaly spectrum for a given chlorophyll-a concentration
$nLw^*_{K490}(\lambda)$	dimensionless	Radiance anomaly spectrum for K490 for a given K490 value
$\langle nLw^{ref}(\lambda, Chla)\rangle$	W m^{-2} sr^{-1}	The average normalised water-leaving radiance for a given chlorophyll-a concentration
$\langle nLw^{ref}(\lambda, K490)\rangle$	W m^{-2} sr^{-1}	The average normalised water-leaving radiance for a given K490 value
π	dimensionless	Pi
S	nm^{-1}	Spectral slope parameter of CDOM
$r_{rs}(\lambda)$	sr^{-1}	Sub-surface remote sensing reflectance
$R_{rs}(\lambda)$	sr^{-1}	Above-water remote sensing reflectance
$R_{rsOB}(\lambda)$	sr^{-1}	Above-water remote sensing reflectance for Orange Brown (BG) *Trichodesmium*
$R_{rsBG}(\lambda)$	sr^{-1}	Above-water remote sensing reflectance for Bright Green (BG) *Trichodesmium*
$R_{rs}^{Case1}(\lambda)$	sr^{-1}	Above-water remote sensing reflectance for Case 1 simulations

$R_{rs}^{Case2}(\lambda)$	sr^{-1}	Above-water remote sensing reflectance for Case 2 simulations
$u(\lambda)$	dimensionless	Ratio of the backscattering coefficient to the sum of the absorption and backscattering coefficient $b_b/(a+b_b)$
V_f	m^3	Volume filtered through Whatman GF/F
ξ	dimensionless	$\xi = e^{S(443-431)}$
Z_d	m	Secchi disk depth
ζ	dimensionless	$\zeta = 0.74 + \frac{0.2}{0.8 + (r_{rs}(443)/r_{rs}(\lambda_0))}$

List of Abbreviations

Abbreviation	Meaning
AIMS	Australian Institute of Marine Science
ALI	Advanced Land Imager
AVHRR	Advanced Very High Resolution Radiometer
AVIRIS	Airborne Visible Infrared Imaging Spectroradiometer
BEAM	Basic ENVISAT Toolbox for (A)ASTR and MERIS
BG	Bright Green
CCD	Charge-coupled-device
CDM	Coloured dissolved and detrital matter
CDOM	Coloured dissolved organic matter
Chla	Chlorophyll-a
CTD	Conductivity-temperature-depth profile instrument
CZCS	Coastal Zone Color Scanner
DALEC	Dynamic Above-water L_u-E_d Collector
ESA	European Space Agency
ENVISAT	ENVIronmental SATellite
FAI	Floating Algae Index
GAC	Global-area-coverage
GSM01	Garver-Siegel-Maritorena semi-analytical ocean colour algorithm
HAB	Harmful algae bloom
EOS	Earth Observing Satellite
FLNTU	Combined chlorophyll fluorometer and nephelometric turbidity unit meter
GF/F	Glass fibre filter
HICO	Hyperspectral Imager for the Coastal Ocean

IOPs	Inherent Optical Properties
IOCCG	International Ocean Colour Coordinating Group
ISRO	Indian Space Research Organisation
JCU	James Cook University
K490	Diffuse attenuation coefficient at 490 nm
L0	Level-0
L2	Level-2
L3	Level-3
LAC	Local-area-coverage
MAAs	Microsporine-like Amino Acids
MCI	Maximum Chlorophyll Index
MERIS	Medium Resolution Imaging Spectroradiometer
merci	MERIS Catalogue and Inventory
MODIS	Moderate Resolution Imaging Spectroradiometer
N	Nitrogen
NAP	Non-algal Particulate Matter
NASA	National Aeronautical and Space Administration
NIR	Near-infrared
nLw	Normalised water-leaving radiance
OB	Orange-Brown
OD	Optical Density
OD_{NULL}	Optical Density null offset
OC3	NASA band-ratio chlorophyll-a retrieval algorithm 3
OC4	NASA band-ratio chlorophyll-a retrieval algorithm 3
OCM	Ocean Colour Monitor
Pa	Phaeophytin
PC	Phycocyanin
PEB	Phycoerythrobilin
PEC	Phycoeryrthocyanin
PSU	Practical salinity units

PUB	Phycourobilin
PPV	Protocol Pixel Value
RGB	Red-green-blue
QAA	Quasi-analytical Algorithm
RAS	Radiance Anomaly Spectrum
RV	Research Vessel
SeaWiFS	Sea-viewing Wide Field-of-View Sensor
SeaDAS	SeaWiFS Data Analysis System
SIM	Similarity Index Measure
SNR	Signal-to-Noise Ratio
SPOT	Satellite Pour l'Observation de le Terre
SWIR	Shortwave infrared
TOA	Top of atmosphere
UV	Ultra-violet
WFS	West Florida Shelf

1 General Introduction

Abstract

This PhD thesis examines optical remote sensing methods for the detection and quantification of the diazotrophic, marine cyanobacteria *Trichodesmium* spp. within the Great Barrier Reef (GBR), Australia. The main objective of this research was to develop new remote sensing methods applicable to the optically complex waters of the GBR. Outcomes from this research project may lead to an improvemed understanding of *Trichodesmium* abundance and hence, reduce uncertainties in estimates of *Trichodesmium* specific N-fixation. This chapter provides a general introduction to *Trichodesmium* spp. and its significance to the nitrogen budgets within the Great Barrier Reef region. Ocean colour remote sensing is introduced as a method for synoptic scale monitoring of *Trichodesmium*, and the objectives and outline of this thesis are also detailed.

1.1 Trichodesmium spp.

Trichodesmium is a genus of filamentous cyanobacteria, commonly found in clear, low-nutrient seawater throughout tropical and subtropical regions (Capone et al. 1997). Individual *Trichodesmium* occur as fine filaments known as trichomes which cluster together to form colonies of two distinct arrangements: (i) fusiform and (ii) radial (Capone et al. 1997). Fusiform (tuft) colonies are characterised by parallel alignment of trichomes whereas within radial (puff) colonies, trichomes arrange themselves radially to form small spherical clusters (see Figure 1.1). Colonies are often visible to the naked eye and can be up to 0.5 - 3 mm in length/radius (Carpenter and Romans 1991). *Trichodesmium* contain gas vesicles and can therefore regulate their buoyancy (Villareal and Carpenter 1990). *Trichodesmium* occur in the upper regions of the photic zone (depths < 50 m) however, population densities are highest in shallower regions between 20 and 40 m (Carpenter and Romans 1991; Capone et al. 1997). Under conditions of relaxed wind stress and reduced mixing, *Trichodesmium* often forms thick surface aggregations, also referred to as surface slicks or blooms which are orange/brown in appearance (Figure 1.2) (Capone et al. 1997). Such surface aggregations of *Trichodesmium* have been known to span as areas large as 52,000 km^2 (Carpenter and Capone 1992).

There are five described species of *Trichodesmium*: *T. contortum, T. hildebrandtii, T. tenue, T. thiebautii*, and *T. erythraeum* (Janson et al. 1995); of which the latter two species are common within the Great Barrier Reef (GBR), Australia (Furnas 1992). Each species of *Trichodesmium* are diazotrophic, and thus actively fix atmospheric nitrogen, N_2. Studies in the North Atlantic and North Pacific Oceans have shown that *Trichodesmium* is a regionally significant primary producer and introduces considerable quantities of new-N (Karl et al. 1997; Capone et al. 2005). Annual N-inputs due to *Trichodesmium* N-fixation are estimated to be at least 1.6×10^{12} mol N y^{-1} and 1.5×10^{12} mol N y^{-1} for the North Atlantic and North Pacific Oceans respectively (Capone et al. 2005; Mahaffey et al. 2005). These values represent approximately 40 – 59 % of the geochemically inferred N-fixation for these ocean basins (Mulholland 2007). In addition, it is important to note that visibly conspicuous surface aggregations of *Trichodesmium* contribute only in a minor way to the bulk of new-N introduced by the cyaonobacteria Furthermore, it should be noted that physiological and

environmental factors are known influence the prevalence of *Trichodesmium* and subsequent N-fixation (Hedge et al. 2008).

In addition, *Trichodesmium* has been responsible for fouling and closure of beaches within the GBR (Mancuso 2003). Mild symptoms, including skin irritation and nausea, have been reported for individuals who come in contact with dense surface aggregations of *Trichodesmium* (Falconer 2001). Thus, *Trichodesmium* has been listed as a harmful algae species within the Queensland Government Harmful Algal Blooms Operational Procedures (2004).

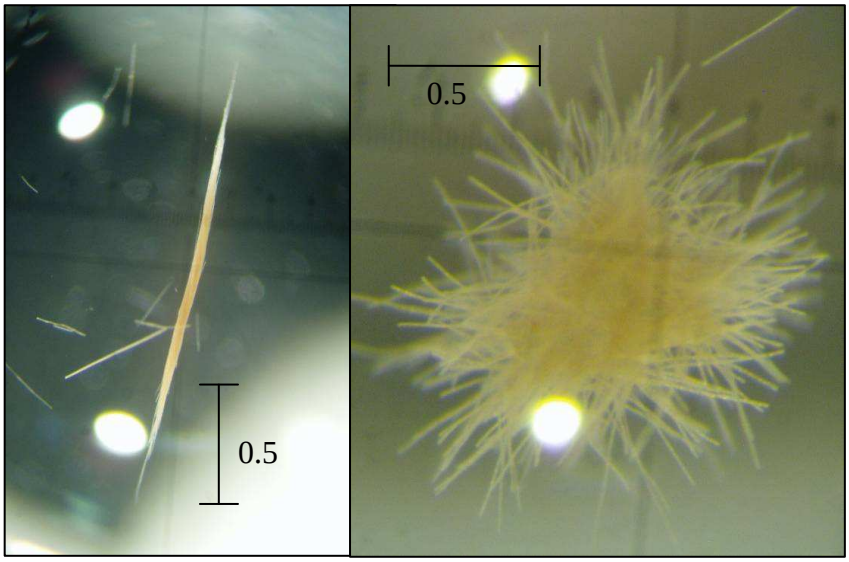

(a.)Fusiform (b.) Radial

Figure 1.1: Colonial forms of *Trichodesmium* spp. Samples taken from the Central Great Barrier Reef, April, 2007.

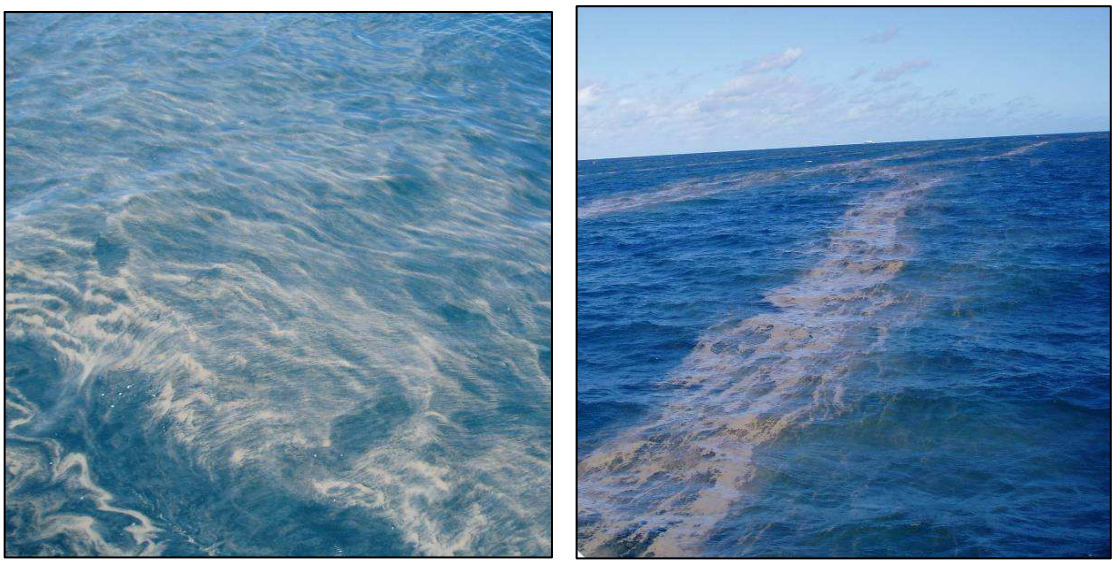

Figure 1.2: Examples of *Trichodesmium* surface aggregations, within the Great Barrier Reef, Australia.

1.2 Water Quality and the Great Barrier Reef

The GBR is a world heritage listed region located adjacent to the north-eastern coast of Australia. The GBR is the largest coral reef system on the Earth and extends approximately 2,600 km from a northern-most latitude of 9.2°S southward to a latitude of about 25°S (Wolanski 1994). Tourism, commercial fishing, and recreational activities within the GBR contribute an estimated $5.4 billion dollars to the Australian economy annually (GBRMPA 2005). In order to maintain economic and environmental integrity within the GBR, there are ongoing efforts to enact sustainable management practices in the region. There are several ecosystem stressors of concern within the GBR including: global climate variations, ocean-acidification, over-fishing, tropical cyclones and crown-of-thorns starfish (Hughes and Connell 1999; Mccook 1999; Bellwood et al. 2004; Berkelmans et al. 2004; Wei et al. 2009). There is presently concern regarding declining water quality within the GBR region (Brodie et al. 2008). Excess nitrogen, phosphorus, sediment and pesticides of terrestrial origin have been cited as of particular concern to the GBR ecosystem (Brodie et al. 2008). Consequently, the Australian Federal Government has invested 200 million Australian dollars to improve terrestrial, coastal and marine management practices, and implement ongoing water quality monitoring[†].

To assess water-quality trends within the GBR, accurate parameterisation of nutrient variability is essential (Moss et al. 2005). Many nutrient input mechanisms such as coastal runoff, rainfall, reefal fixation and upwelling are well understood or directly measurable, these are illustrated in Figure 1.3 (Furnas et al. 1995; Furnas and Mitchell 1996). However, there is still uncertainty regarding quantities of the nitrogen fixed by *Trichodesmium* (Furnas et al. 1995; Furnas and Mitchell 1996; Bell et al. 1999). These uncertainties are attributed to a limited understanding of the spatial and temporal abundances of *Trichodesmium* within the GBR (Furnas et al. 1995; Bell et al. 1999).

Thus, the ability to monitor and quantify *Trichodesmium* on appropriate spatial and temporal scales within the GBR is of great biogeochemical significance. With improved estimates of abundance, GBR regional uncertainties associated with *Trichodesmium* spp. N-fixation could likely be improved. Traditional *in situ* methods for quantifying *Trichodesmium* using bottle casts and/or phytoplankton net tows only provide localised estimates of population on a finite time scale. Furthermore, these discrete sampling methods are known to be highly variable in both space and time (Chang 2000). Thus, methods which can accurately monitor *Trichodesmium* on large spatial scales with higher temporal frequency are desirable. A method that can potentially produce quantitative synoptic scale maps of ocean parameters with near-daily resolution is satellite-based ocean colour remote sensing.

†Source: Department of Natural Resources and Management, Australian Government: http://www.nrm.gov.au/funding/2008/reef-rescue.html

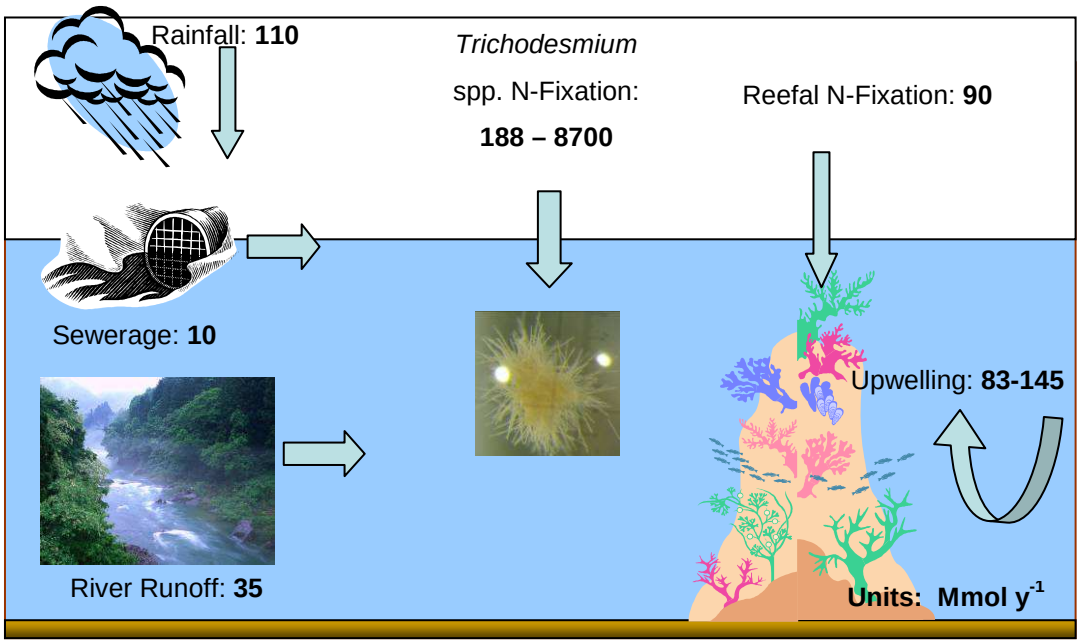

Figure 1.3: Estimated annual inputs of nitrogen into the Tully region of the GBR shelf (15°52'S – 16°55'S). Data source: Furnas and Mitchell (1996).

1.3 Ocean Colour Remote Sensing

When solar irradiance enters the aquatic environment, it interacts with optically active components within the water column. Optically active components within seawater are typically water molecules, non-algal particles, phytoplankton and dissolved and detrital matter (Kirk 1994). After a series of absorption and scattering processes, a fraction of the incident light is scattered back out of the water column. This water-leaving light has a spectral distribution or "colour" which is directly related to the optical properties of constituent matter within the water column (Mobley 1994). Thus, the study of "ocean colour" by space-borne imaging spectroradiometers can give synoptic scale, quantitative insight into marine constituent matter.

Presently there are several operational ocean colour satellites including: the Sea-viewing Wide Field-of-View Scanner (SeaWiFS), the Moderate Resolution Imaging Spectroradiometer (MODIS), and the Medium Resolution Imaging Spectroradiometer (MERIS). Each of these sensors is aboard the polar orbiting satellites: SeaStar (NASA), Terra and Aqua (NASA) and ENVISAT (ESA) respectively. Within the GBR, ocean colour remote sensing has been utilised for monitoring the water quality parameters of

chlorophyll-a (Chla) and total suspended minerals (TSM) (Brando et al. 2010). Ocean colour remote sensing techniques have also been used for the mapping of seasonal, river flood pulses within the GBR (Devlin and Schaffelke 2009; Brodie et al. 2010).

Several researches have examined ocean colour remote sensing as a means of detecting and quantifying *Trichodesmium* using the Coastal Zone Color Scanner (CZCS), SeaWiFS. MODIS and MERIS (Dupouy 1992; Subramaniam et al. 2002; Gower et al. 2008; Hu et al. 2010). However, there is currently scant literature which discusses regionally-specific algorithms for the detection and quantification of *Trichodesmium* within the GBR.

1.4 Thesis Objectives and Outline

This PhD thesis has been separated into self-contained chapters which all share the common theme of ocean colour remote sensing of *Trichodesmium* within the GBR. The primary objectives of this PhD thesis were to:

- Study the bio-optical properties of *Trichodesmium* spp. during a series of field campaigns within the GBR,
- Develop a categorical algorithm for the detection of dense surface aggregations of *Trichodesmium* within the GBR and,
- Develop a method to quantitatively detect *Trichodesmium* using hyperspectral above-water radiometric data

Each major chapter within this PhD thesis is in the form of a manuscript which is either in preparation, or has been submitted to scientific journals for peer review. Firstly, **Chapter 2** presents a comprehensive literature review of past research regarding remote sensing of *Trichodesmium* within the world's oceans. Historical advances in methodologies coinciding with the launch of new ocean colour sensors are detailed. In, addition limitations of contemporary algorithms and future directions are discussed.

Within **Chapter 3** a method for detection of dense surface aggregations of *Trichodesmium* using MODIS imagery is presented. The radiometric properties of *Trichodesmium* surface aggregations are detailed and a binary algorithm was developed using the 859 nm, near-infrared band of the MODIS ocean colour sensor. The algorithm was validated using *in situ* observations and its robustness was tested in the presence of potentially confounding effects.

A method to optically discriminate and quantify *Trichodesmium* using hyperspectral radiometric data is presented in **Chapter 4**. Within this chapter, hyperspectral above-water remote sensing reflectance spectra were measured *in situ* and also modelled using Hydrolight radiative transfer software. Hyperspectral above-water radiometric data was processed using the Quasi-analytical algorithm (QAA) and a similarity index measure (SIM) was used to discriminate *Trichodesmium* from other phytoplankton. The combined QAA-SIM method allowed a *Trichodesmium* specific Chla concentration to be derived. The potential of the QAA-SIM quantitative detection method for resolving regional variability of nitrogen fixation was also explored.

During field sampling within the GBR, two distinct colour modes of *Trichodesmium* were sampled from a dense surface aggregation. Observations suggested that the difference in colouration was due to pigment leaching associated with senescence. **Chapter 5** examines the absorption properties of both colour modes and uses radiative transfer simulations to model their respective remote sensing reflectance. The ability to determine the physiological state of a *Trichodesmium* using MODIS and MERIS is also discussed.

A summary of this PhD research is presented in **Chapter 6**. This section discusses the outcomes, implications, limitations and future directions of this work.

2 Two decades of ocean colour remote sensing *Trichodesmium* spp. in the World's oceans

Abstract

Earth observing, ocean colour remote sensing satellites provide the necessary platform for detection and monitoring of the N_2 fixing marine cyanobacterium *Trichodesmium*. Remote sensing of *Trichodesmium* spp. has been pursued particularly for the purposes of mapping variability in abundances. Such information is invaluable for global biogeochemical studies where an accurate quantification of atmospherically fixed nitrogen is essential. This chapter reviewed contemporary literature from the past two decades and discusses the development of *Trichodesmium*-specific remote sensing methods. How methods have been revised with improved parameterisation of bio-optical properties and new remote sensing technologies was also examined. Overall, the majority of *Trichodesmium* specific detection methods were found to be non-quantitative and developed primarily for mapping the occurrence of dense surface aggregations of the cyanobacteria. The ability to positively discriminate and quantify low concentrations of *Trichodesmium* dispersed within the water column has yet to be attained.

2.1 Introduction

2.1.1 Global Significance of *Trichodesmium* spp.

The pelagic, diazotrophic cyanobacteria *Trichodesmium* spp. is found in oligotrophic, warm (> 20 °C), tropical and sub-tropical marine waters (Capone et al. 1997). Waters inhabited by *Trichodesmium* are characterised as stable, with an upper mixed layer depth of around 100 m, with deep light penetration and low nutrients (Capone et al. 1997). *Trichodesmium* occur as single, filamentous trichomes which cluster together to form macroscopic radial or fusiform colonies with a length scale of about 0.5 –3 mm (Laroche and Brietbarth 2005). *Trichodesmium* can regulate their buoyancy due to the presence of gas vesicles and will often amass on the surface in dense aggregations (~10^6 trichomes L^{-1}) which are often referred to as "slicks", "surface blooms", or as "red tides" (Carpenter and Capone 1992). *Trichodesmium* surface aggregations appear as scum-like discolorations on the water surface and can range in colouration from green-yellow, to orange-brown to silvery-white in colour (Devassy et al. 1978). Surface aggregations of *Trichodesmium* form windrows and eddy swirls patterns and have been recorded to span areas as large as 50,000 km^2 (Kuchler and Jupp 1988).

Of global biogeochemical significance is *Trichodesmium's* ability to actively fix atmospheric nitrogen (Capone et al. 1997). Within tropical and sub-tropical oligotrophic oceanic waters, *Trichodesmium* has been identified as a significant contributor of new nitrogen (Karl et al. 1997; Capone et al. 2005). Mahaffey et al. (2005) estimated basin-scale amounts of geochemically inferred N_2 fixation due to *Trichodesmium* within oligotrophic waters. The results indicated that *Trichodesmium* was responsible for between 40 and 59 % of total N fixed for the North Atlantic and North Pacific respectively (Mahaffey et al. 2005). More specifically, estimates of annual N-input due to *Trichodesmium* N-fixation within the North Atlantic and North Pacific Oceans, range from 0.09 – 6.4 x 10^{12} mol N y^{-1} and 1.5 – 4.2 x 10^{12} mol N y^{-1} respectively (Mahaffey et al. 2005). Such quantitative estimates of global N-fixation due to *Trichodesmium* require accurate knowledge regarding the spatial distribution and abundance of the cyanobacteria. However, *in situ* oceanographic sampling only provides estimates of abundance on sparse spatial and temporal scales. This under-sampling means that there is a large degree of uncertainty in basin-scale estimates of

Trichodesmium abundance. As such, the tolerable range of environmental conditions deemed suitable for *Trichodesmium* growth are often used as a proxy for estimating its distribution (Laroche and Brietbarth 2005). Typically, criteria such as temperature, nutrient regimes and iron availability have been used to estimate *Trichodesmium* distribution (Laroche and Brietbarth 2005).

Within the discipline of biological oceanography, the use of ocean colour remote sensing has revolutionised the study of phytoplankton dynamics and hence primary productivity. Ocean colour remote sensing has become an important method for synoptic scale monitoring of phytoplankton within the ocean. Over the past two decades, ocean colour remote sensing has also provided a method for mapping the distribution of *Trichodesmium* in the world's oceans.

2.1.2 Ocean colour remote sensing

Ocean colour remote sensors measure the spectral characteristics of light leaving seawater within the visible part of the electromagnetic spectrum (400 – 700 nm). Solar irradiance that enters the water column interacts with constituent matter and a proportion of photons are scattered backward out of the water column. The spectral distribution and magnitude of light that is scattered out of the water column and towards space-borne ocean colour sensors can be used to optically characterise a body of water. Radiative transfer theory describes how the photons entering seawater interact with the medium via scattering and absorption with constituent matter. The optical constituents of seawater typically comprise: pure water, coloured dissolved organic matter (CDOM), non-algal particulate matter (NAP), and phytoplankton (Kirk 1994). The inherent optical properties (IOPs) of scattering and absorption dictate the underwater light field and the water-leaving radiance L_w signal. The L_w that exits the water column and is eventually detected by space-borne radiometers has a spectral distribution or "colour" which is dependent upon the IOPs and hence the optical properties of constituent matter.

Early use of ocean colour remote sensing data focused primarily upon mapping oceanic chlorophyll-a (Chla) pigment concentrations using simple empirical algorithms as a proxy of phytoplankton abundance (O'reilly et al. 1998). Such information regarding Chla has been of great significance to studies of global oceanic primary productivity (Longhurst et al. 1995; Antoine et al. 1996). Typically global ocean colour algorithms are only suitable for oceanic, Case 1 waters in which optical

constituents are deemed to covary with phytoplankton abundance. However, much effort has been placed upon developing methods for remote sensing optically complex, Case 2 waters. In addition, the development of physics-based inversion algorithms for retrieval of IOPs has also been pursued (IOCCG 2006). Ocean colour remote sensing products have been applied to a number of applications including: water quality monitoring in coastal zones, management of fisheries, detection of harmful algal blooms (HABs), and discriminating functional groups of phytoplankton (IOCCG 2008). Ocean colour remote sensing has also been studied as a means of detecting *Trichodesmium*.

2.1.3 Purpose and Outline

This chapter reviews the historical development and implementation of ocean colour remote sensing over the last two decades for detecting *Trichodesmium* abundance. The first part of this review briefly discusses photography of *Trichodesmium* surface aggregations made from space-borne platforms. The bio-optical properties of *Trichodesmium* are then discussed. An overview of previously developed satellite observations and retrieval algorithms will be then be presented. Some satellite imagery previously reported within literature have been reproduced using data accessed from NASA's Ocean Color Web (http://oceancolor.gsfc.nasa.gov/) and the MERIS Catalogue and Inventory (merci) website (http://merci-srv.eo.esa.int/merci/). Ocean colour imagery was processed using the SeaWiFS Data Analysis System (SeaDAS v6.0) (Baith et al. 2001) or the Basic ENVISAT Toolbox for (A)ASTR and MERIS (BEAM v4.5.2) (Brockmann 2003) for re-interpretation. This review aims to show how the structure and complexity of algorithms has evolved corresponding with the launch of newer ocean colour sensors over time. Each method will be presented, including the benefits and limitations of each. Thereafter, the potential for future remote sensing detection will be briefly discussed with regards to planned ocean colour remote sensing platforms yet to be launched. For coherence, methods discussed within this chapter are grouped under sub-headings of the remote sensing platform for which they were developed. This structuring approximately maintains chronological order.

2.2 Photography of *Trichodesmium* from Platforms in Orbit

Although this review is concerned primarily with ocean colour remote sensing, it is important to note that observations of *Trichodesmium* from other Earth orbiting platforms including NASA Space Shuttles and the International Space Station (ISS) have been made. These observations have provided spectacular images which have portrayed the distinct appearance of dense surface aggregations of *Trichodesmium* and have allowed a spatial measure of such events.

An image captured with a camera from the NASA Space Shuttle on 29 November 1983 revealed a large surface aggregation of phytoplankton within the Capricorn Channel (23.5°S, 152.5°E) of the southern Great Barrier Reef, Australia (Figure 2.1) (Kuchler and Jupp 1988). Strong circumstantial evidence suggested that the observed phenomenon was a large surface aggregation of *Trichodesmium*. Similarly, photographs from the ISS revealed large phytoplankton aggregations in the Capricorn Channel also deemed to be *Trichodesmium*. Although such photography provided valuable information regarding the spatial distribution of *Trichodesmium* surface aggregations, they provided little quantitative information regarding abundance. Unfortunately, space-borne photography is opportunistic and does not occur with a regular frequency suitable for monitoring seasonal fluctuations of *Trichodesmium* population. Moreover, photography from orbit offers little information regarding low concentrations of *Trichodesmium* which do not present in such a conspicuous manner as dense surface aggregations. To provide regular, large-scale spatial observations of *Trichodesmium*, ocean colour remote sensing is an ideal candidate.

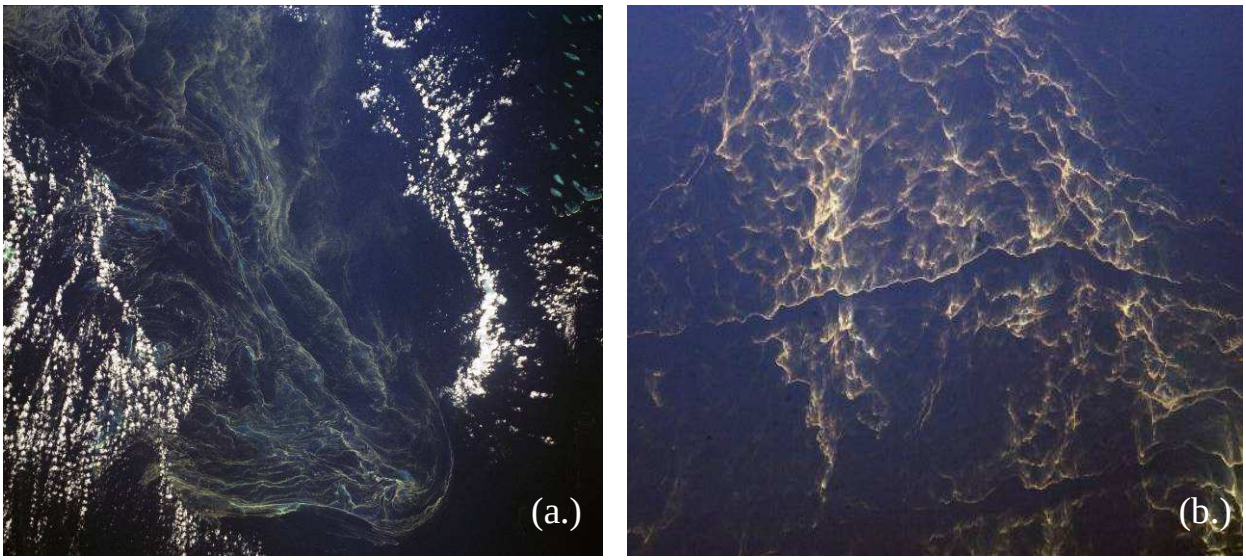

Figure 2.1: Photographs captured from orbit of surface aggregations deemed to be *Trichodesmium* in the Capricorn Channel of the Great Barrier Reef, Australia. (a.) Image from the NASA Space Shuttle captured on November, 1983. Mission-Roll-Frame details: STS009-35-1622, centred on 23.5°S, 152.5°E. (b.) Image from the ISS captured on 27 November 2002. Mission-Roll-Frame details: ISS005-E-21570, centred on 24.3°S, 151.0°E. Images courtesy of the Image Science & Analysis Laboratory, NASA Johnson Space Center (http://eol.jsc.nasa.gov/), length scale data unavailable.

2.3 Bio-optical properties of *Trichodesmium* spp.

The following section describes the absorption and scattering properties of *Trichodesmium* as well as its radiometric properties. Although the contents of this section do not explicitly refer to any particular ocean colour remote sensing algorithm, it is important to become familiar with the bio-optical properties of *Trichodesmium* as they have significantly influenced the development of detection methods (Subramaniam et al. 2002; Westberry et al. 2005).

2.3.1 Absorption

The spectral absorption properties of *Trichodesmium* have been examined by several authors (Fujita and Shimura 1974; Lewis et al. 1988; Borstad et al. 1992; Subramaniam et al. 1999a; Dupouy et al. 2008a). The pigment content of *Trichodesmium* comprises Chla, carotenoids and phycobilipigments resulting in a unique absorption spectrum (Subramaniam et al. 1999a). Early work conducted by Fujita and Shimura (1974) identified peaks in the absorption spectrum characteristic of phycoerythrin, phycocyanin, Chla and carotenoids. More recent studies of *Trichodesmium* absorption were conducted by Subramaniam et al. (1999a) and Dupouy et al. (2008a) who used the quantitative filter technique (QFT) to determine absorption coefficients (Mitchell 1990; Mitchell et al. 2003). Subramaniam et al. (1999a) determined the chlorophyll-specific absorption for *Trichodesmium* colonies over a spectral range of 400 - 750 nm and used a Gaussian decomposition method similar to that of Hoepffner and Sathyendranath (1991) to determine the contribution of individual absorbing pigments to the entire spectrum. The results of Subramaniam et al. (1999a) indicated that *Trichodesmium* exhibits distinct absorption peaks centred about 425 and 676 nm associated with Chla and peaks centred around 463, 496, 545, 578 and 621 nm corresponding to carotenoids, phycourobilin (PUB), phycoerythrobilin (PEB), phycoerythrocyanin (PEC), and phycocyanin (PC) respectively (see Figure 2.2).

Dupouy et al. (2008a) measured the absorption spectrum of *Trichodesmium erythraeum* colonies over 300 - 700 nm and yielded similar results to Subramaniam et al. (1999a). Within the absorption spectrum, Dupouy et al. (2008a) noted strong absorption peaks in the UV region centred about 330nm and 360nm. These were

previously identified by Subramaniam et al. (1999b) as due to microsporine-like amino acids (MAA's) and palythene respectively. These photoprotective agents are deemed necessary for *Trichodesmium* survival in a high light environment and have been reported to be present within the dissolved pigment pool surrounding *Trichodesmium* (Subramaniam et al. 1999a; Steinberg et al. 2004). Dupouy et al. (2008a) made hourly measurements of the absorption spectrum during daylight hours from 0900 – 1300 hrs. The results showed little variation between hourly measurements. Thus, the assumption of a constant shape for the spectral absorption coefficient was shown to be valid when parameterising forward and inverse *Trichodesmium*-specific models. Figure 2.2 details the Chla specific spectral absorption coefficient of *Trichodesmium* spp.

2.3.2 Backscattering

Optical backscattering of *Trichodesmium* was measured by Subramaniam et al. (1999b) and Dupouy et al. (2008a). Subramaniam et al. (2002) used a custom built instrument whereas Dupouy et al. (2008a) used a HobiLabs HydroScat 6 to measure *Trichodesmium* specific backscattering coefficients. Both investigations showed that the spectral backscattering coefficient of *Trichodesmium* exhibited wavelength dependence which was deemed to be a consequence of fluorescent emission and reabsorption of photons by accessory pigments (Subramaniam et al. 1999a; Subramaniam et al. 1999b; Dupouy et al. 2008a). However, Dupouy et al. (2008a) showed that the Chla specific spectral backscattering coefficient of *Trichodesmium* $b^*_{btri}(\lambda)$ could be fitted using the function

$$b^*_{btri}(\lambda) = b^*_{btri}(550)\left(\frac{550}{\lambda}\right)^{1.2} \qquad [2.1]$$

The Chla specific backscattering coefficient for *Trichodesmium* measured by Dupouy et al. (2008a) is shown in Figure 2.2.

The large magnitude of optical scattering exhibited by *Trichodesmium* has been discussed by several authors and is attributed to the presence of intercellular gas vesicles which give *Trichodesmium* a high refractive index relative to seawater (Subramaniam and Carpenter 1994). In addition, the backscattering ratio $\tilde{b}_b$ of *Trichodesmium* is estimated to have a value within the range of 0.018 - 0.028 (Borstad

et al. 1992; Dupouy et al. 2008a). This indicated that between 1.8 and 2.8 % of total light incident upon *Trichodesmium* is scattered in the backward direction. However, further studies of the scattering properties of *Trichodesmium* are warranted to further resolve backscattering and scattering coefficients and parameterise spectral dependencies in $\tilde{b}_b$.

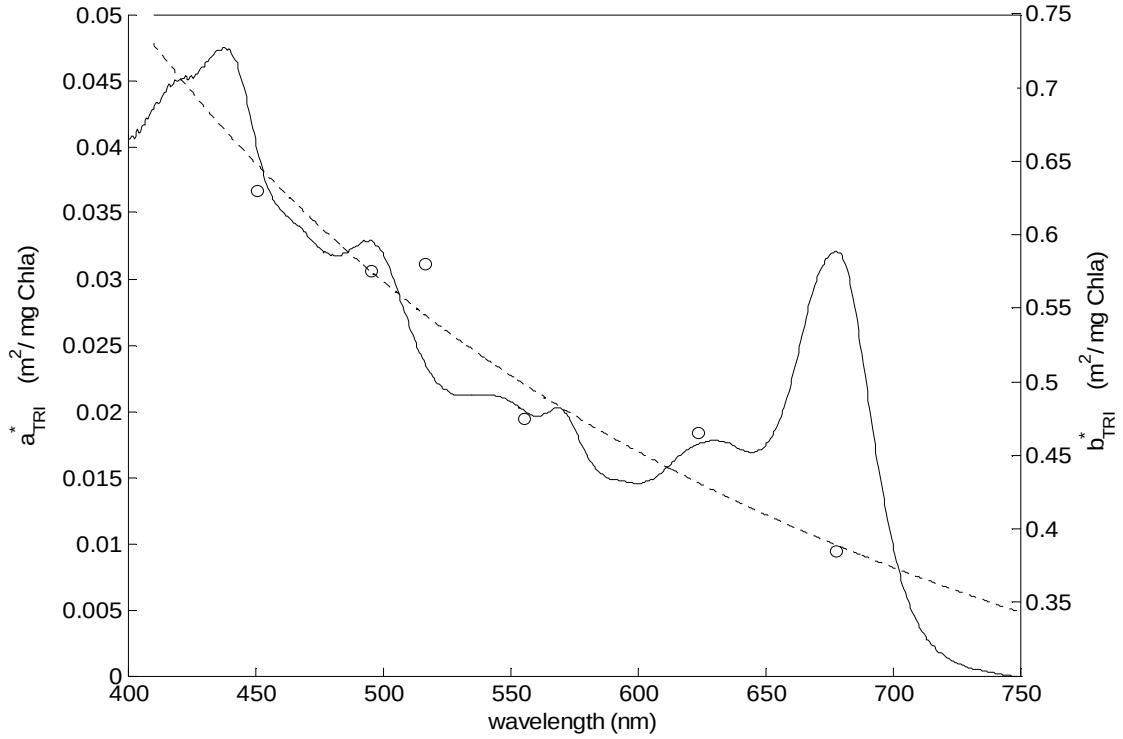

Figure 2.2: *Trichodesmium* Chla-specific spectral absorption coefficient (solid line) (McKinna, unpublished data). Open circles represent the *Trichodesmium* Chla-specific backscattering coefficients measured at six wavelengths using a HOBI Labs Hydroscat 6 instrument (Dupouy et al. 2008a). The dashed line represents the spectral backscattering coefficients fitted according to Equation 2.1.

2.3.3 Remote Sensing Reflectance Spectrum

A commonly measured radiometric quantity is the remote sensing reflectance, R_{rs}. The spectral above-water $R_{rs}(\lambda)$ may be defined as the ratio of the water-leaving radiance L_w to downwelling irradiance E_d just above the surface 0^+

$$R_{rs}(\lambda) = \frac{L_w^{0+}(\lambda)}{E_d^{0+}(\lambda)} \qquad [2.2]$$

The spectral distribution and magnitude of R_{rs} is dependent upon the IOPs of the water column and can be related using the quadratic relationship of Gordon et al. (1988)

$$R_{rs}(\lambda) = \sum_{i=1}^{2} g_i \left[\frac{b_b(\lambda)}{a(\lambda) + b_b(\lambda)} \right]^i \quad [2.3]$$

where g_1 and g_2 are constants (Gordon et al. 1988).

The R_{rs} of *Trichodesmium* was first reported by Borstad et al. (1989, 1992) and has been measured more recently by Dupouy et al. (2008a) and discussed by Hu et al. (2010). Modelled values of $R_{rs}(\lambda)$ for *Trichodesmium* were presented by Subramaniam et al. (1999b) and also by Westberry et al. (2005; 2006). A plot of the normalised *Trichodesmium* specific R_{rs} measured by Dupouy et al. (2008a) is shown in Figure 2.3a. The remote sensing reflectance measurement was made using an Ocean Optics spectroradiometer for a moderate concentration of *Trichodesmium* suspended in a Petri dish. A maximum reflectance peak was evident at 593 nm, with lesser peaks occurring at 524, 560 and 644 nm respectively. A broad peak was also present from 454 - 478 nm. The troughs within the spectra occurred at 438 and 667 nm corresponded to absorption by Chla. Additional troughs within the spectra occurred at 494, 546, 568 and 630 nm corresponding to absorption by PUB, PEB, PEC, PC respectively. Noteworthy was the presence of a red-edge reflectance feature. The red-edge feature was characterised by increased reflectance at wavelengths longer than 700 nm. A similar, red-edge effect was noted in the remote sensing reflectance spectra of *Trichodesmium* measured by Borstad et al. (1988) who suggested that this spectral feature could be useful for identifying surface aggregations of *Trichodesmium*.

A $R_{rs}(\lambda)$ spectrum of a dense surface aggregation of *Trichodesmium* was measured within this thesis using an above-water hyperspectral radiometer (see Chapter 3). This data is shown in Figure 2.3b relative to the measurement made by Dupouy et al. (2008a).

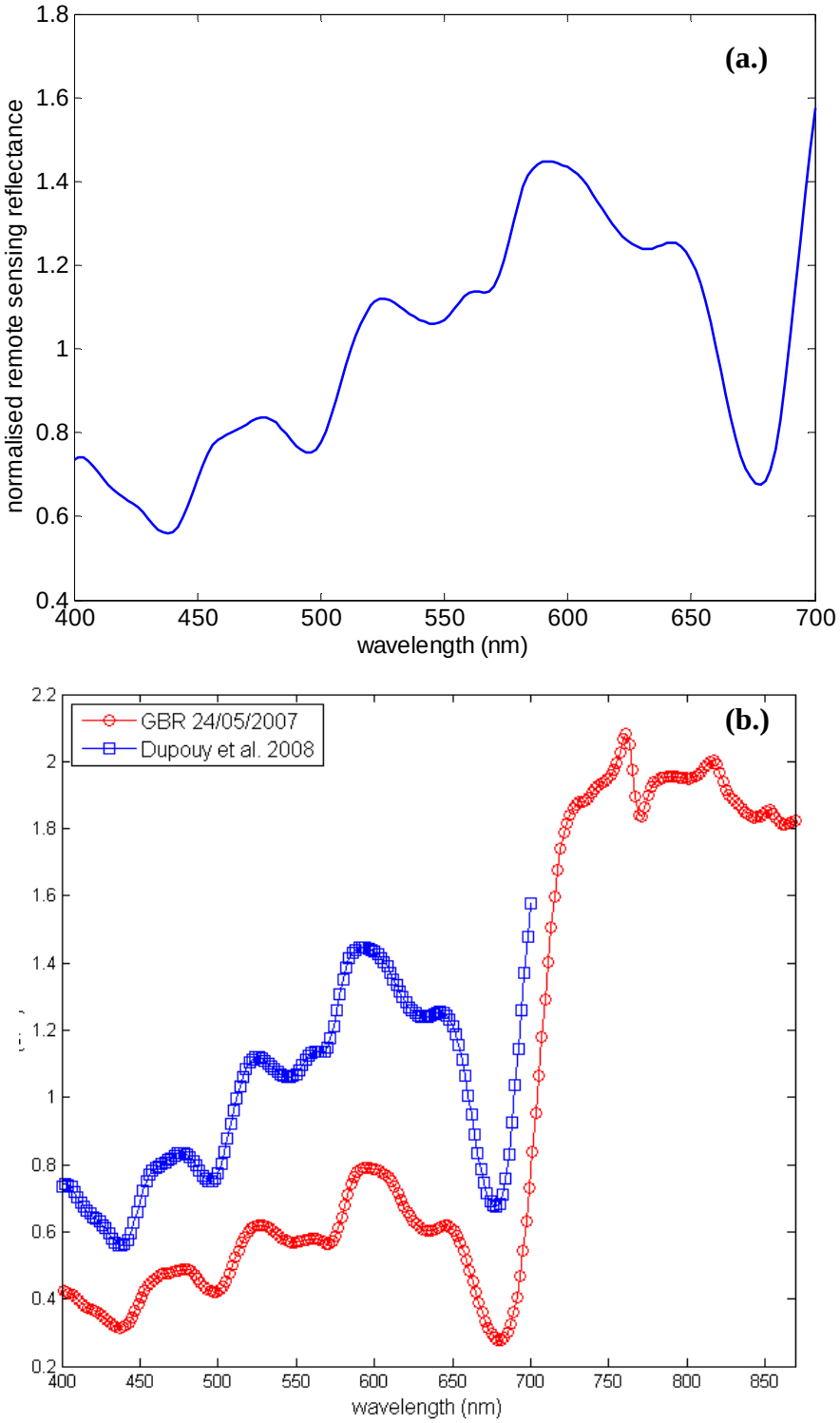

Figure 2.3: (a.) Normalised remote sensing reflectance spectrum of *Trichodesmium* measured by Dupouy et al. (2008a). (b) Normalised remote sensing reflectance of Dupouy et al. (2008) in blue compared with a reflectance spectra collected within this thesis red (see section 3.2.3). Note a vertical offset applied to separate the two spectra for interpretive purposes.

2.4 Satellite observations and Empirical Detection Algorithms

Over the past three decades there have been a number of satellite radiometers launched for the purpose of ocean colour monitoring. These instruments have progressively changed in design and capability providing more information about oceanic processes on a synoptic scale to researchers. In this section we will be focusing only on ocean colour remote sensing platforms that have been used for the detection of *Trichodesmium*.

2.4.1 CZCS

The Coastal Zone Colour Scanner (CZCS) was launched in October 1978 aboard the Nimbus-7 satellite and ceased operations in 1986 (Hovis et al. 1980; Kirk 1994). The CZCS detector had a 1 x 1 km pixel resolution and comprised four 20 nm width bands in the visible spectrum centred on 443, 520, 550, 670 nm for measurement of water-leaving radiances, L_w. The sensor also included a near-infrared (NIR) waveband (700 – 800 nm) and an infrared waveband (10.5 - 12.5 μm) for the purposes of land/cloud detection and temperature scanning respectively. The CZCS was specifically designed as a proof-of-concept instrument for remote sensing studies of marine constituents and was used by several researchers as a means of mapping *Trichodesmium* abundance.

CZCS images of Trichodesmium in the south western Pacific Ocean

One of the first CZCS-observed instances of *Trichodesmium* was captured on 4 January 1982. CZCS imagery indicated large areas of dark and yellow discoloured water in the region of New Caledonia and Vanuatu in the south-western tropical Pacific Ocean (see Figure 2.4) (Dupouy et al. 1988; Dupouy 1992). Typically, within this region mineral turbidity is uncommon and as such Dupouy et al. (1988) concluded that the discoloured phenomenon was due to high concentrations of phytoplankton. Based upon regional knowledge of phytoplankton ecology and merchant ship observations of “red tides” concurrent with the CZCS image, the discoloured water was attributed to an elevated abundance of *Trichodesmium* (Dupouy et al. 1988). Dupouy et al. (1988) examined the reflectance across all CZCS bands for two situations: (i) pixels within the dense *Trichodesmium* aggregation (>

20,000 trichomes L^{-1}), and (ii) pixels of oligotrophic, blue waters taken from a CZCS image of the Sargasso Sea. Pixels corresponding to high *Trichodesmium* abundance exhibited increased reflectance across all bands except band 1 (443 nm), which was lower in magnitude than blue Sargasso Sea pixels. This effect was likely due to high scattering of *Trichodesmium* detected by bands 2, 3 and 4 and strong absorption in the blue region by Chla resulting in reduced reflectance in band 1. The area covered by elevated Chla attributed to *Trichodesmium* was deemed to be 90,000 km^2 however, Dupouy (1992) remarked that only 10 per cent of this area consisted of bright linear patterns consistent with surface aggregations. Dupouy et al. (1988) thus presented the first quantitative estimate of *Trichodesmium* spatial extent using ocean colour imagery.

Discoloured waters around New Caledonia and Vanuatu were further examined by Dupouy (1992) by looking at a historical archive of all CZCS images from November 1978 – December 1984. This analysis allowed the seasonal variability of highly reflective features and regions of elevated Chla to be analysed. Bright elongated, streaky features were evident in the majority of Austral Summer images and were attributed to elevated abundances of *Trichodesmium*.

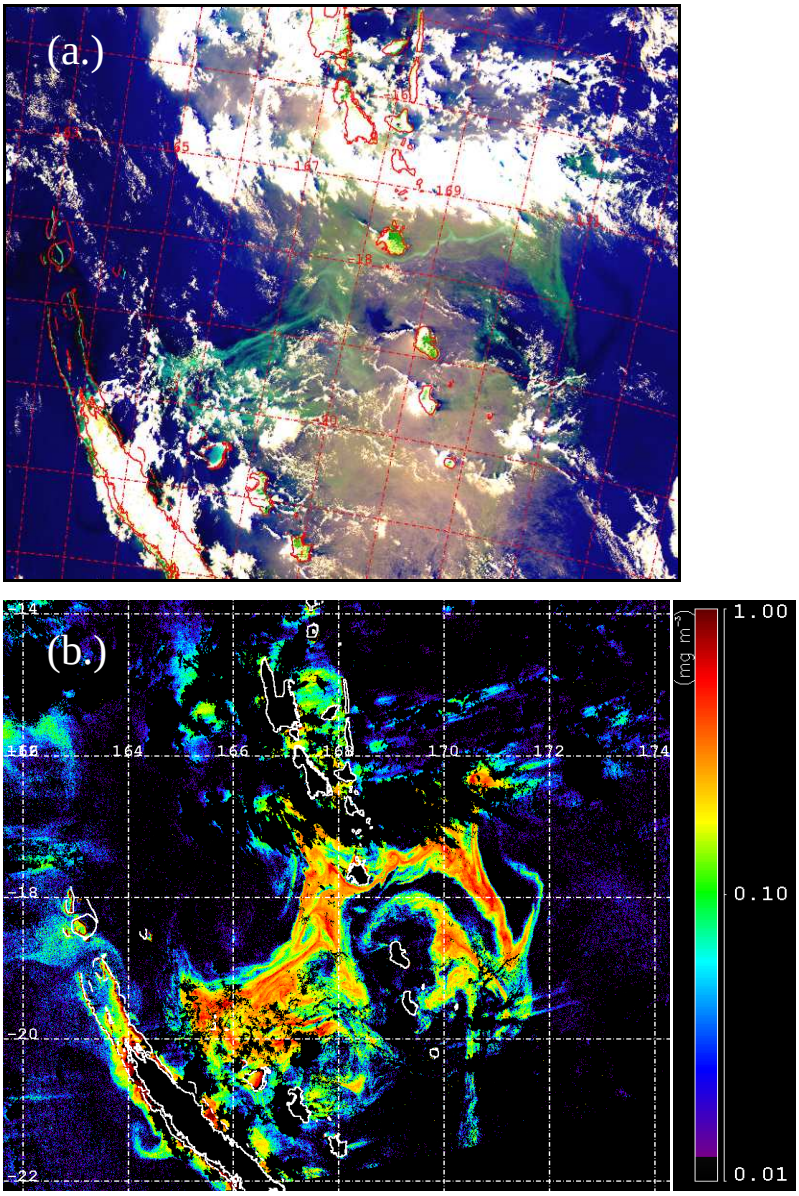

Figure 2.4: (a.) Un-projected, quasi-true colour CZCS image captured over New Caledonia (bottom left, outlined in red) and the Vanuatu Archipelago (centre) in the south-western tropical Pacific Ocean. At the centre of the image (21°S, 168°E) is a mass of discoloured, green/yellow water which was attributed to *Trichodesmium* by Dupouy et al. (1988). White patches in the image are convective clouds. (b.) A projected, Chla pigment concentration (mg Chla m^{-3}) map of the CZCS scene, cloud and land appear black.

CZCS images of Trichodesmium off the west coast of India

The presence of a large *Trichodesmium* surface aggregation off the west coast of India using the CZCS was examined by Borstad et al. (1992). Within this coastal region, dense *Trichodesmium* surface aggregations had previously been reported by Devassey et al. (1978) and the spatial features within the CZCS image were consistent with that of elevated *Trichodesmium* abundance. Borstad et al. (1992) reported the CZCS imagery had high L_w values for the 520nm and 550nm wavebands whilst the magnitude of L_w at 443nm was slightly reduced. These observations were consistent with those of Dupouy et al. (1988). The CZCS image described by Borstad et al. (1992) has been reproduced in Figures 2.5 and 2.6. These images lead Borstad et al. (1992) to surmise that high scattering particulate matter with high pigment concentrations were present adjacent to the Indian coastline. On the assumption that these highly reflective pixels adjacent to the Indian west coast were indeed *Trichodesmium*, Borstad et al. (1992) estimated the area occupied by the cyanobacteria to be approximately 20,000 km^2. However, the highly reflective features in the western Arabian Sea were deemed unlikely to be *Trichodesmium* (Figures 2.5 and 2.6). Borstad et al. (1992) suggested that these features may instead represent coccolithophores which are known to be common within the Arabian Sea (Guptha et al. 1995; Andruleit et al. 2003).

The CZCS image examined by Borstad et al. (1992) had no sea- truths and relied upon circumstantial evidence to infer that the high scattering, strongly absorbing features observed were *Trichodesmiuum*. Figure 2.6.d indicates regions of elevated concentrations of Chla (>1 μgL^{-1}) adjacent to the Indian coastline which may be indicative of *Trichodesmium* abundance. Unfortunately, parts of the west Indian coastline are also characterised by high concentrations of suspended sediment and coloured dissolved organic matter (CDOM) (Menon et al. 2005) which are known to confound CZCS Chla retrievals (Tassan 1988; Carder et al. 1989).

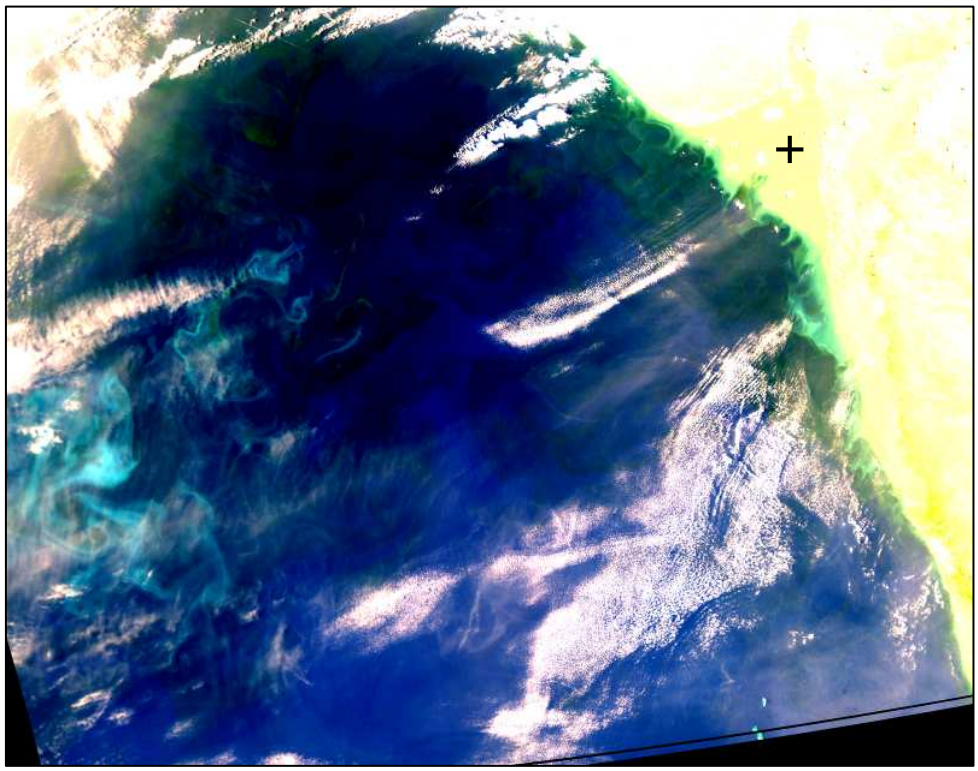

Figure 2.5: A quasi-true colour CZCS image of the Arabian Sea captured on 28 March 1979. The west coast of India is on the right had side of the image. A high suspended sediment load is evident extending from the Gulf of Khambhat (20°N, 72°E) (denoted +). Along the western continental shelf of India, bright green water was interpreted as high concentrations of *Trichodesmium*. The left side of this image shows highly reflective, milky coloured water which was potentially a coccolithophore bloom.

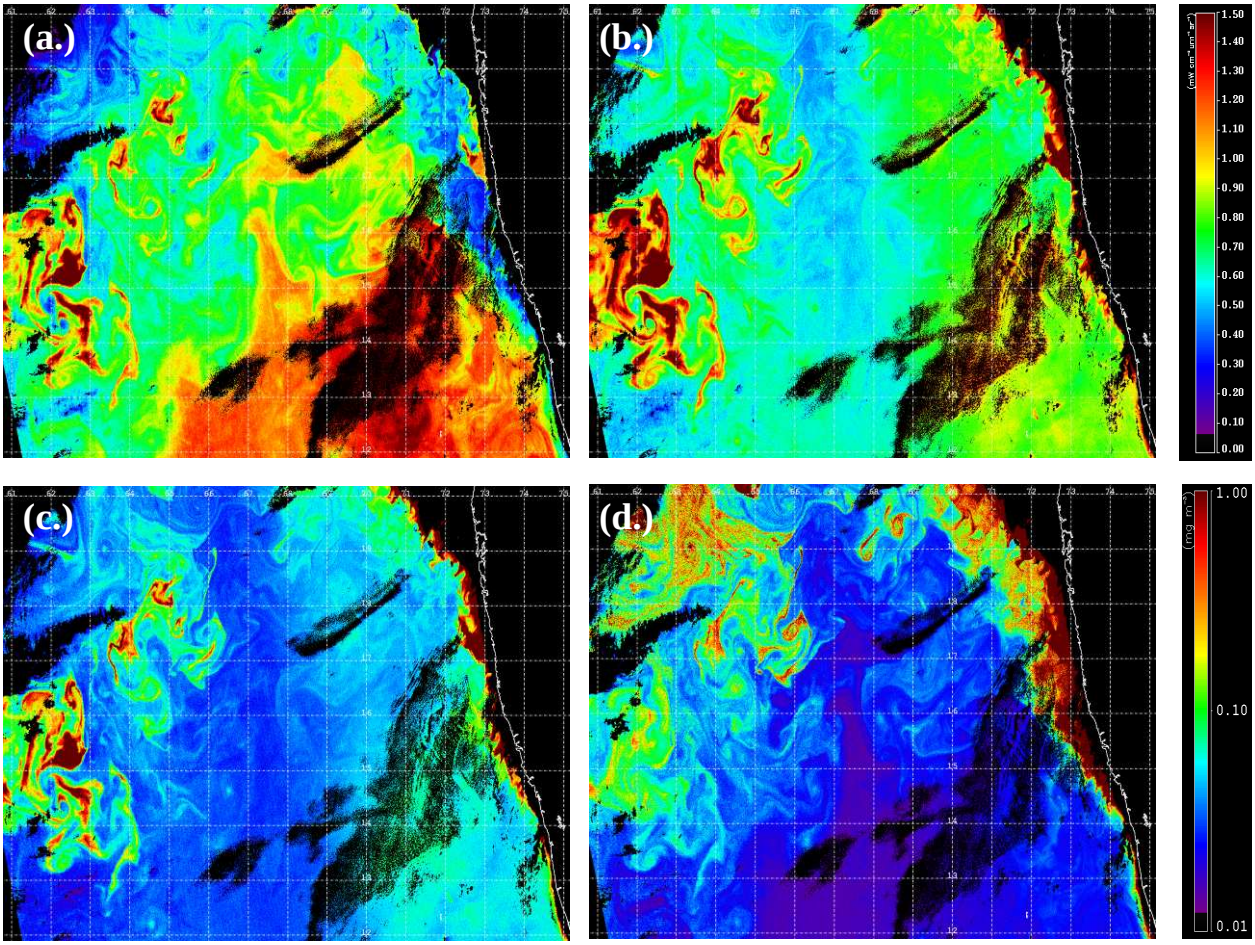

Figure 2.6: CZCS image of the Arabian Sea from 28 March 1979. Sub-images a, b and c represents the normalised water leaving radiances at 443, 520 and 550 nm respectively. (d) CZCS map of Chla concentration. Regions containing *Trichodesmium* were assumed to be adjacent to the western Coast of India (right hand side of each sub-image). Black pixels correspond to land, cloud, or pixels with saturated radiances and/or algorithm failure.

An empirical Trichodesmium detection method using CZCS

Subramanium and Carpenter (1994) developed the first empirical method for detection of *Trichodesmium* blooms using three CZCS L_w bands: 440, 520 and 550 nm and the derived Chla concentration. Unlike previous observations, the algorithm of Subramaniam and Carpenter (1994) provide an automated, unsupervised computational method for *Trichodesmium* detection using CZCS imagery. The empirical detection scheme presumed *Trichodesmium* would exhibit high reflectance across CZCS bands due to the presence of intercellular gas vacuoles with a slight reduction in reflectance at 550nm because of absorption by phycoerythrin. Notably, this was contrary to previous work by Borstad et al. (1992) who reported high reflectance across all bands, with a reduction at 443 nm for a presumed *Trichodesmium* bloom adjacent to the Indian coast (see section 2.4.1). Thus, an empirical classification scheme was developed which relied upon the difference between the 520 and 550 nm bands and the difference between the 440 and 550 nm bands. Through a series of empirical manipulations, a protocol pixel value (*PPV*) for *Trichodesmium* detection was derived

$$PPV = \left(m_2\right)^2 \left(m_3\right) Chla \qquad [2.4]$$

Where, $m_2 = \left[L_w\left(520\right) - L_w\left(550\right)\right] \times 30$ and $m_3 = \left[L_w\left(440\right) - L_w\left(550\right)\right] \times 110$

When the algorithm was applied, a high PPV identified the presence of a *Trichodesmium*. Subramaniam and Carpenter (1994) examined three CZCS images which had accompanying literature reports of dense *Trichodesmium* aggregations present at the time of satellite flyover. The algorithm worked well where dense concentrations of *Trichodesmium* were reported such as off the west coast of Australia (Figure 2.7) and within the Gulf of Thailand.

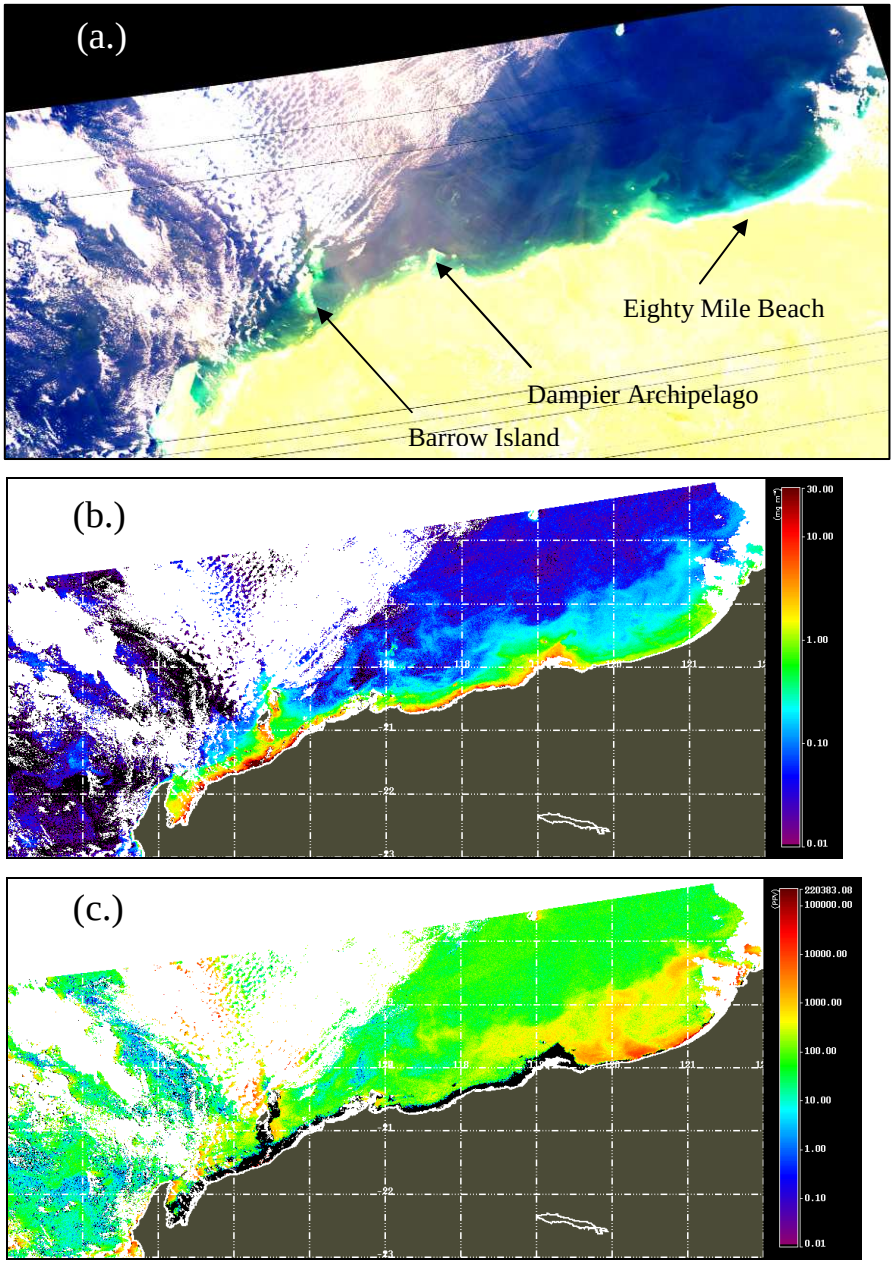

Figure 2.7: CZCS Image of the west coast of Australia from 1 November 1980. (a.) A quasi-true colour image reveals bright green patches adjacent to the coastline around Barrow Island and the Dampier Archipelago. (b.) A Chla map of the region and (c.) the PPV map of *Trichodesmium* abundance shows high values around Barrow Island and the Dampier Archipelago as reported by Subramaniam and Carpenter (1994) and also offshore from Eighty Mile Beach.

For a CZCS image of the Gulf Stream, *Trichodesmium* was in concentrations assumed too low for PPV detection (< 1 colony L^{-1}). The Gulf Stream CZCS image sea-truth observations reported that diatoms and dinoflagellates dominated the water column. Thus, the Gulf Stream CZCS image was used to justify the PPV as being robust against false-positive retrieval of these non-*Trichodesmium* phytoplankton groups. The study also examined if the PPV algorithm could be confounded by a highly reflective coccolithophore bloom within the English Channel where no *Trichodesmium* was present. When applying the PPV algorithm over the cocolithophore bloom, the centre of the bloom was successfully non-detected however, at the edges a bright ring was evident. Thus, Subramaniam and Carpenter (1994) conceded that the PPV algorithm was confounded in regions where the ratio of coccolithophore : Chla was low. It was noted that the PPV was robust to high suspended sediments and also shallow bathymetry. However, the PPV was not effective when the CZCS Chla product was invalid or failed.

2.4.1.1 CZCS Summary

The use of the CZCS scanner for the detection of *Trichodesmium* provided the first chance at synoptic scale mapping of the extent of the cyanobacteria. However, quantitative information regarding abundance had inherent uncertainties. Dupouy et al. (1988, 1992) mapped elevated Chla concentrations deemed to be associated with *Trichodesmium* using CZCS. However, the presence of *Trichodesmium* could only be inferred with supporting anecdotal evidence. Similarly, observations of *Trichodesmium* off the west coast of India using CZCS by Borstad et al. (1992) were inferred to be *Trichodesmium* based solely upon local knowledge of *Trichodesmium* variability. Only Subramaniam and Carpenter (1994) provided a method to discriminate *Trichodesmium* via the PPV algorithm. Within these studies, CZCS-retrieved Chla concentrations were used in all studies to infer *Trichodesmium* abundance. However, the efficiency of the CZCS Chla algorithm has been shown to be compromised in optically complex coastal waters (Tassan 1988). This is due to spectral contamination from high levels of CDOM and suspended minerals which adversely affect both the Chla algorithm and atmospheric correction of the CZCS (Tassan 1988; Carder et al. 1989).

To accurately quantify spatial distributions of *Trichodesmium* further research was required as well as improved ocean colour sensors. Although the CZCS provided almost a decade of ocean colour imagery, the need for additional spectral bands and improved atmospheric corrections was essential for the detection of *Trichodesmium*. This was outlined by Dupouy et al. (1992) and Subramanium and Carpenter (1994) who indicated that a waveband in the region of 490 – 495 nm would be useful for the detection of phycoerythrin pigments within *Trichodesmium*. No issues regarding CZCS atmospheric corrections over *Trichodesmium* blooms have been discussed within literature. Nonetheless, improved atmospheric corrections, *in situ* radiometric measurements and accurate parameterisation of the bio-optical properties were noted as necessary for improving ocean colour detection of *Trichodesmium* (Borstad et al. 1992; Dupouy 1992).

2.4.2 SeaWiFS

The launch of the Sea-viewing Wide Field of View Sensor (SeaWiFS) aboard the SeaStar satellite on August 1997 provided a much needed platform for ocean colour remote sensing after the CZCS ceased operations. SeaWiFS provided the user community with global continuous data capture and eight spectral bands. The whisk-broom scanner design also provided a larger swath width of 2800 km compared with 1566 km of the CZCS. Overall higher signal-to-noise-ratio (SNR) of spectral bands and improved atmospheric correction procedures were important design features of SeaWiFS. The SeaWiFS instrument undoubtedly provided a revolutionary platform for ocean colour science and consequently there has been much work done with SeaWiFS data for the detection of *Trichodesmium*.

The potential of SeaWiFS for sub-bloom Trichodesmium detection

The first discussion of SeaWiFS for the detection of *Trichodesmium* was published by Tassan (1995) prior to the launch of the SeaStar satellite. Tassan (1995) noted that the detection of thick, floating surface aggregations of *Trichodesmium* using remote sensing should be rather straightforward. However, the ability to detect *Trichodesmium* at low, "sub-bloom" concentrations was more challenging. Tassan (1995) conducted an exploratory analysis to assess the potential of SeaWiFS to detect *Trichodesmium* at low concentrations in Case 1 waters using simulated data. A three-

component optical model (Sathyendranath et al. 1989) was used to simulate subsurface reflectance for bands 1 - 6 of SeaWiFS. Two reflectance spectra were simulated for Case 1 waters: one containing *Trichodesmium* and a second containing other naturally occurring phytoplankton. Modelling was performed for increasing Chla concentrations over a logarithmic interval from 0.1 – 1 mg Chla m^{-3}. The study assumed that *Trichodesmium* was dispersed with trichomes not clustering into colonies, no photo-bleaching had occurred, and no mass accumulation on the surface was present.

Tassan (1995) compared the spectral absorption of *Trichodesmium* reported by Borstad et al. (1989) to that of naturally occurring phytoplankton from Hoepffner and Sathyendranath (1992). Tassan (1995) indicated that *Trichodesmium* exhibited absorption peaks at 494 and 541 nm associated with phycoerythrin; such features were not prominent within the naturally occurring phytoplankton absorption spectra. Thus, a *Trichodesmium* specific detection algorithm was proposed based upon the ratio of two Chla values derived using two separate retrieval algorithms: $C_{3,5}$ and $C_{2,3,5}$ respectively. The $C_{3,5}$ algorithm was based upon SeaWiFS bands 3 and 5 (490 and 555 nm) and designed to be insensitive to the spectral differences between *Trichodesmium* and other phytoplankton (Tassan 1995). This was attributed to a similarity between the slopes of the *Trichodesmium* and phytoplankton absorption between 510 and 550 nm (Tassan 1995). Conversely, the $C_{2,3,5}$ algorithm was based upon SeaWiFS bands 2, 3 and 5 (443, 490 and 555 nm) and was deemed to be sensitive to the presence of phycoerythrin in *Trichodesmium*. The ratio of $C_{3,5}$ to $C_{2,3,5}$ was found to approach unity for waters containing no *Trichodesmium*. However, as the concentration of *Trichodesmium* increased, the ratio of $C_{3,5}$ to $C_{2,3,5}$ was found to depart from unity monotonically with increasing *Trichodesmium*-specific Chla concentration.

The results of the modelling exercise showed that *Trichodesmium* may be discriminated at concentrations as low 0.1 - 0.3 mg Chla m^{-3}. However, Tassan (1995) conceded the model used in the study was over simplified. Furthermore, Tassan (1995) cited that with more experimental data, the method could be revised. Unfortunately, there is no record of the Tassan (1995) *Trichodesmium* algorithm being implemented with actual SeaWiFS data. Thus, a realistic evaluation of its performance cannot be commented upon.

Trichodesmium Chla enrichment in the south west Pacific Ocean

Trichodesmium abundance within the south western tropical Pacific Ocean was further examined by Dupouy et al. (2000) using SeaWiFS derived Chla data and sea-truth observations. Investigations of SeaWiFS data from the Austral Summer of 1998, revealed elevated Chla levels between New Caledonia and Vanuatu centred on 19°S, 165°E. This chlorophyll enrichment was estimated to have a spatial extent of about 300,000 km^2 and was very similar to CZCS observations described previously by Dupouy et al. (1988; 1992). Dupouy et al. (2000) examined a two year time series of SeaWiFS Chla data bounded between latitudes 20°S and 15°S and longitudes 152°E and 150°W over the period of September 1997 – April 1999. It was found that the regions of Chla enrichment were recurrent and lasted for up to 6 months. However, such regions were limited between 160°E and 175°E. Independent sea-truth observations by the French Naval base of New Caledonia reported large yellow surface meanders extending up to 100 nautical miles to the north and east of New Caledonia, suggesting that elevated Chla within SeaWiFS images were due to *Trichodesmium*. In addition, surveys of *Trichodesmium* abundance conducted during March-April 1998 to the East of New Caledonia provided further argument that recurrent Chla enrichment was due to fluctuations in *Trichodesmium* abundance. Dupouy et al. (2000) reiterated that in order to achieve accurate ocean colour remote sensing of *Trichodesmium*, a full understanding of the bio-optical properties of the cyanobacteria was required. Such studies of bio-optical properties were undertaken by Subramaniam et al. (1999a, 1999b) and Dupouy et al. (2008a).

A Trichodesmium specific classification scheme for SeaWiFS

Following studies involving the CZCS and investigations of bio-optical properties, Subramaniam et al. (2002) developed a classification scheme for the detection of *Trichodesmium* using five bands of SeaWiFS. The empirical classification scheme was developed to identify *Trichodesmium* in moderate abundance, having a Chla concentration between 0.5 - 3.0 mg Chla m^{-3}. The R_{rs} spectra of *Trichodesmium* and other phytoplankton were modelled at 412, 443, 490, 510 and 555 nm corresponding to SeaWiFS bands. Modelling of R_{rs} followed the

method of Subramaniam (1999b) whereby, R_{rs} is proportional to the ratio of the total backscattering coefficient b_b to the total absorption coefficient a

$$R_{rs} = 0.1079 \frac{b_b}{a}. \quad [2.5]$$

Values of R_{rs} were modelled for Chla concentrations ranging from 0.5 – 10 mg Chla m^{-3} and were converted to normalised water-leaving radiance (nLw) values by multiplying by the appropriated value of solar irradiance for a given wavelength (Subramaniam et al. 2002).

Sea-truth observations of *Trichodesmium* were made during a research cruise in South Atlantic Bight from 27 October – 13 November 1998. Surface concentrations of *Trichodesmium* were noted during this cruise and were used to confirm that highly reflective features visible in SeaWiFS imagery were *Trichodesmium* surface aggregations. The modelled nLw values were compared with SeaWiFS nLw values captured on 30 October 1998 over a region centred on 29.1°N, 80.2°W identified as containing *Trichodesmium*. From both modelled and SeaWiFS observed nLw data it was determined that in the presence of *Trichodesmium* values of nLw(490) were greagter than 1.3 mW cm^2 μm^{-1} sr^{-1}. In addition, nLw(490) values were greater in magnitude than nLw(412), nLw(443) and nLw(555). Modelled results also indicated that for *Trichodesmium*, the value of nLw(510) was always greater in magnitude than nLw(443). Thus, a spectral shape parameter [nLw(490) – nLw(443)]/[nLw(490) – nLw(555)] was determined. These three criteria were combined to develop a *Trichodesmium*-specific classification scheme. A pixel was classified as containing *Trichodesmium* if the following three criteria were met:

nLw(490) > 1.3 mW cm^2/μm/sr and nLw(490) > nLw(412), nLw(443), nLw(555)
nLw(510) > nLw(443), and
0.4 < [nLw(490) – nLw(443)]/[nLw(490) – nLw(555)] < 0.6

The classification scheme was tested on four SeaWiFS images of the South Atlantic Bight from 25, 28, 30 October 1998 and 1 November 1998. The results revealed spatial features consistent with those of a *Trichodesmium* surface aggregation (see Figure 2.8). The surface aggregations appeared reduced in intensity by 1 November,

at which stage sea-truth observations recorded *Trichodesmium* in the immediate vicinity.

It was noted that modelled values of nLw(555) were over-estimated, potentially due to over-exaggerated phycoerythrin fluorescence. Moreover, Subramaniam et al. (2002) noted that *Trichodesmium*-specific hyperspectral nLw features including peaks at 470 and 530 nm and reduced nLw near 510 nm could not be resolved using the five SeaWiFS bands. Potential confounding affects such as bottom reflectance in shallow water regions were eliminated by applying a bathymetry mask which removed pixels with water depths less than 30 m. However, the algorithm yielded a false-positive from the region of the Little Bahamas Bank which is a highly reflective feature (see Figure 2.8.c)

An adapted version of the Subramaniam et al. (2002) algorithm was incorporated into the SeaWiFS Data Analysis System (SEADAS) (Baith et al. 2001) software distributed by the Ocean Biology Processing Group, Goddard Space Flight Center (NASA). The algorithm was incorporated as a quality control flag to indicate if a level-2 ocean colour product was potentially contaminated by the presence of *Trichodesmium* (Hedge et al. 2008). Hedge et al. (2008) used the SEADAS *Trichodesmium* flag to study the occurrence of *Trichodesmium* in the Bay of Bengal using SeaWiFS image from 1997 to 2003. Although, this study did not focus on algorithm development, it demonstrated how a suitable *Trichodesmium* remote sensing could be applied in a useful way. The work of Hedge et al. (2008) successfully determined a month-by-month climatology of the spatial distribution of *Trichodesmium* which was then linked with information regarding sea surface temperature, nutrient regime and ocean currents. In addition, the study validated the algorithm successfully using SeaWiFS match-up scenes containing in situ observations of *Trichodesmium*. Furthermore, Hedge et al. (2008) found the algorithm did not yield false-positive retrievals for pixels which were known not to contain *Trichodesmium*.

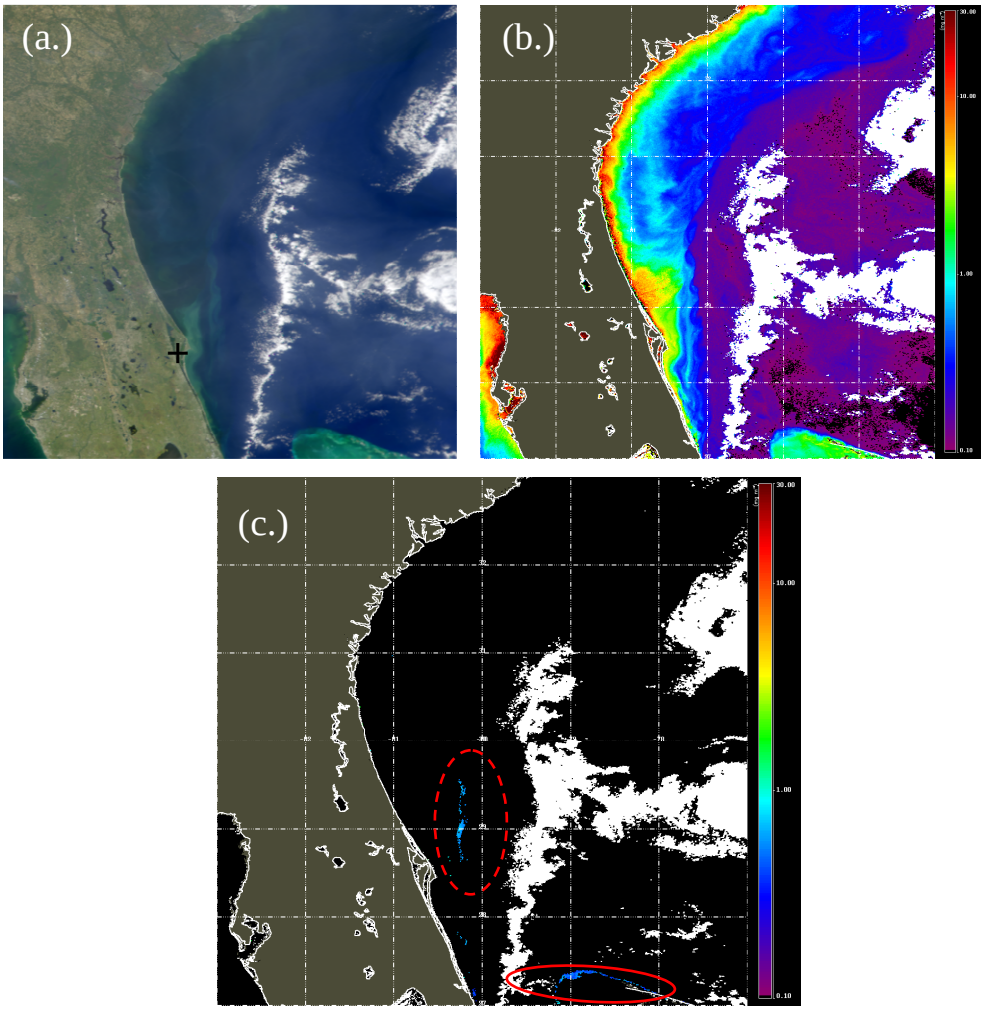

Figure 2.8: A SeaWiFS image of the South Atlantic Bight on 30 October 1998. (a.) A quasi true colour image the, bright green colouration is evident off the coast of Cape Canaveral (denoted +). Little Bahamas Bank can be seen in the bottom right hand side. (b.) A Chla map of the region and (c.) the Subramanian et al. (2002) *Trichodesmium* classification scheme applied to the scene. The dashed red ellipse shows, the location of high concentrations of *Trichodesmium*, the solid red ellipse shows the top of Little Bahamas Bank. The white patches within images (b.) and (c.) correspond to clouds and atmospheric interference.

Radiance Anomaly Spectrum: an adapted Physat algorithm

Dupouy et al. (2008b) further investigated remote sensing of *Trichodesmium* in the south-western tropical Pacific Ocean. Previously developed algorithms for the detection of *Trichodesmium* were identified as inappropriate within the southwest tropical Pacific Ocean. In particular, global algorithms failed to resolve well documented summer-time Chla maximums due to *Trichodesmium* (Dupouy et al. 2008b). Thus, Dupouy et al. (2008b) used an adapted version of the Physat algorithm (Alvain et al. 2005). The adapted Physat algorithm was implemented using eight years of SeaWiFS imagery with corresponding sea surface observations of *Trichodesmium* abundance acquired from the French Navy. Thus, the first comprehensive time series of *Trichodesmium* abundance within the south west Pacific Ocean was reported.

The Physat algorithm formulates specific water-leaving radiance nLw*(λ) for each wavelengths using the following equation Alvain et al. (2005)

$$nLw^*(\lambda) = nLw(\lambda) \Big/ \left\langle nLw^{ref}(\lambda, Chla) \right\rangle \qquad [2.6]$$

where, $\left\langle nLw^{ref}(\lambda, Chla) \right\rangle$ is the average *nLw*(λ) for a given Chla concentration. Thus a look-up-table (LUT) of $nLw^{ref}(\lambda)$ as a function of Chla concentration is required. The purpose of deriving the *nLw**(λ) parameter is to remove first order variability due to Chla concentration and preserve spectral variability in *nLw* due to non-Chla pigments (Alvain et al. 2005). This approach is regarded as being useful for discriminating phytoplankton (Alvain et al. 2005). Dupouy et al.(2008b) derived a value of *nLw**(λ) based upon the diffuse attenuation coefficient at 490 nm (K490) referred to as the radiance anomaly spectrum (RAS):

$$\text{RAS: } \mathrm{nLw}^*_{\mathrm{K490}}(\lambda) = \mathrm{nLw}(\lambda) \Big/ \left\langle \mathrm{nLw}^{\mathrm{ref}}(\lambda, K490) \right\rangle \qquad [2.7]$$

where, $\left\langle \mathrm{nLw}^{\mathrm{ref}}(\lambda, K490) \right\rangle$ is the average *nLw*(λ) for a given K490 value. Thus the corresponding Physat LUT was made up of $\mathrm{nLw}^*_{\mathrm{K490}}(\lambda)$ values as a function of K490. The perceived benefit of using K490 as apposed to Chla, was to reduce potential discontinuities associated within Chla algorithms (Dupouy et al. 2008b). These discontinuities were thought to be sourced from switching between three band ratios that occurs within the OC4 Chla algorithm (O'reilly et al. 1998; Dupouy et al.

2008b). Unfortunately, it was unclear what method Dupouy et al. (2008b) used to derive K490. Therefore, the specifics of the K490 algorithm cannot be further commented upon.

To determine the *Trichodesmium*-specific RAS spectral shape, empirical and statistical analyses of SeaWiFS imagery were performed using ten summer scenes of the tropical south-western Pacific (Dupouy et al. 2008b). Preliminary analysis of SeaWiFS imagery showed that pixels identified using the RAS Physat algorithm as containing *Trichodesmium* agreed with observations made by the French Navy. Furthermore, these pixels had little dependence upon Chla concentration. The adapted Physat algorithm was then applied to the entire series of SeaWiFS data from 1999 – 2004, and restricted to a spatial domain surrounding the tropical southwest Pacific (latitude: 5°S – 25°S; longitude: 150°E – 190°E). A time series plot showed a distinct seasonality in the percentage of pixels identified as containing *Trichodesmium*. An annual Austral summer maximum in *Trichodesmium* abundance was evident which represented between 0.2 - 0.5 % of all pixels in the domain during 1999 - 2004. Although the percentage cover of the summer *Trichodesmium* abundance identified with the RAS Physat algorithm were low, Dupouy et al. (2008b) noted that the results were higher than those derived using the method of Westberry et al. (2006) (see section 2.5).

Although the RAS Physat algorithm performed well in the south west Pacific Ocean, it remains uncertain if this approach is globally applicable. However, the work of Dupouy et al. (2008b) highlighted the benefits of having large volumes of *in situ* observations when developing a *Trichodesmium* specific algorithm.

2.4.2.1 SeaWiFS Summary

SeaWiFS provided a rich global data set for which several *Trichodesmium* detection methods were developed. All these algorithms were based upon level-2 (L2) derived products such as nLw, Chla concentration and K490. Thus, the aforementioned *Trichodesmium* specific SeaWiFS algorithms are only applicable where L2 products are valid. This becomes pertinent for dense concentrations of *Trichodesmium* which can hinder atmospheric correction or may be mistaken for clouds and masked out. This can lead to erroneous L2 products or in worse cases, L2 algorithm failure with flow-on effects to *Trichodesmium* specific retrieval algorithms.

Research using SeaWiFS imagery also identified highly scattering features such as coral reefs, sediments and bottom reflectance as possible sources of false positive retrieval. Thus, appropriate measures to eliminate potential confounding effects were introduced, including masking of shallow water pixels (< 30 m). Unfortunately, bathymetry masking precludes many coastal and shallow shelf seas from being analysed. For example, *Trichodesmium* is known to be common to the Great Barrier Reef (GBR), Australia . However, approximately half the GBR has bathymetry less than 30 m (Furnas 1992; Lewis 2001) and is thus excluded from analysis. Therefore, improved methods for identifying sources of false positive retrievals are warranted such that coastal waters can be analysed. However, upon solving this problem the dilemma of optically complex Case 2 waters remains. In Case 2 regions, *Trichodesmium* algorithms developed for oceanic Case 1 waters may no longer be applicable. Additional data such as latitude, wind speed, sea surface temperature (SST) and nutrient regimes may be used to geographically constrain algorithms to locations likely to contain *Trichodesmium* and reduce false positive retrievals (Westberry and Siegel 2006).

The spatial and spectral resolution of SeaWiFS was identified as a limiting factor upon the development of *Trichodesmium* specific algorithms. This issue of spatial patchiness was addressed by Subramaniam et al. (2002) who found that the *Trichodesmium* classification algorithm identified fewer than expected highly reflective SeaWiFS pixels. This was considered to be a consequence of the sub-pixel scale (< 1 km) of *Trichodesmium* surface aggregations. In effect, the spectral water-leaving signal from a 1 x 1 km SeaWiFS pixel was a combination of patches of *Trichodesmium* and the water in between. To resolve the issue of spectral smearing, future sensors with finer spatial resolutions are required. A benefit of SeaWiFS sensor design was the inclusion of a band at 490 nm which, as suggested by Subramaniam and Carpenter (1994), may have assisted in the detection of phycoerythrin pigments. However, a band corresponding to a characteristic *Trichodesmium* reflectance peak around 580 nm (see Figure 2.3) was not included in SeaWiFS.

Another important legacy of SeaWiFS was the production of extensive quality control and assurance documentation - The Ocean Optics Protocols for Satellite Ocean Colour Validation. These protocols were distributed for the purpose of providing guidelines to ensure accuracy and consistency when collecting *in situ* data

for algorithm development and validation. With respect to optical studies of *Trichodesmium*, the NASA Ocean Optics Protocols ensure that all future bio-optical and radiometric measurements of *Trichodesmium* are globally consistent.

2.4.3 OCM

The Ocean Colour Monitor (OCM) was an experimental sensor launched aboard the IRS-P4 satellite by the Indian Space Research Organisation (ISRO) in May 1999 (Suresh et al. 2006). The OCM provided a similar spectral band resolution to SeaWiFS, however the OCM differed in sensor design. The OCM design was that of a pushbroom linear array, having a swath width of 1420 km (Suresh et al. 2006) whereas SeaWiFS has a whiskbroom-type scanner with a swath width of 2800 km. The primary advantage of the OCM was its local area coverage (LAC) pixel resolution of 360 x 360 m compared to SeaWiFS LAC pixel resolution of 1 x 1 km (Suresh et al. 2006). Thus, the OCM held promises for resolving fine-scale spatial features such as surface aggregations of *Trichodesmium* which would be of sub-pixel scale for SeaWiFS. As such, the OCM was used to observe *Trichodesmium* along the Indian coastline and shelf waters.

During late April/early May 2002, Sarangi et al. (2004, 2005) observed highly reflective features thought to be surface aggregations of *Trichodesmium* along the Suruastra Coast of Gujarat, India using OCM false colour composite (FCC) imagery. Top of atmosphere (TOA) radiances from the OCM NIR band centred at 865 nm were also used to examine highly reflective surface features. The TOA 865 nm radiance imagery revealed fine scale spatial features such as spiral eddies, parallel bands and stripes (Sarangi et al. 2005). Such highly reflective spatial features were deemed consistent with *Trichodesmium*, and anecdotal sea-truth reports suggested the observed features were indeed *Trichodesmium*. Using the OCM TOA 865nm radiances, Sarangi et al. (2005) observed the development of a surface aggregation which spanned 200 km parallel to the Saurastra Coast with a width of 15 km and lasted for about 10 days. These observations complemented those of Borstad et al. (1992) made using the CZCS.

Desa et al. (2005) further examined OCM imagery of *Trichodesmium* abundance adjacent to the Indian coastline near Goa during April-May 2002. Within this investigation Desa et al. (2005) applied the *Trichodesmium* algorithm of Subramaniam et al. (2002) to OCM data. The method identified streaky patches

adjacent to the coastline with the longest being 74 km long. SeaWiFS imagery was also acquired during this period. The *Trichodesmium* classification algorithm of Subramaniam et al. (2002) was subsequently applied to both OCM and SeaWiFS imagery. Notably, SeaWiFS data resolved less spatial detail than OCM imagery and could not identify features located near to shore. This was likely due to the differences in sensor design between SeaWiFS and OCM. Particularly, pixel resolution was thought to be the limiting factor for resolving fine scale spatial patches of *Trichodesmium*. This was emphasised by Desa et al. (2005) who noted that an area observed by a single SeaWiFS 1 x 1 km pixel, would be represented by nearly nine OCM pixels. *In situ* sampling was also carried out by Desa et al. (2005) however, regions of *Trichodesmium* surface aggregations identified within the OCM imagery were not sampled. *In situ* sampling during OCM overpasses did however verify that regions abundant in *Trichodesmium* dispersed through the water column were not identified using the algorithm of Subramaniam et al. (2002).

2.4.3.1 Summary of OCM

The OCM provided a useful means for visualising spatial patterns of highly reflective features which were interpreted to be *Trichodesmium*. The 360 x 360 m pixel resolution of the OCM allowed fine scale, spatial patterns such as stripes and swirls to be resolved consistent with surface aggregations of *Trichodesmium*. However, as sea-truth observations were not available, these features could not be definitively classified as *Trichodesmium*. The issue of spatial patchiness hindering ocean colour detection of *Trichodesmium* was highlighted by Subramaniam et al. (2002) and seems to be illustrated well by the research of Desa et al. (2005).

Unfortunately quantitative values of Chla concentrations derived from OCM data in the presence of *Trichodesmium* proved to be problematic. Investigations comparing OCM derived products with *in situ* Chla data indicated that the empirical band ratio Chla algorithms OC2 and OC4 v4 were not suitable in regions of dense *Trichodesmium* surface aggregations (Chauhan et al. 2002). The results of Chauhan et al. (2002) indicated that Chla was consistently over-estimated. In addition, it has been shown that simple band ratio type algorithms are adversely affected within coastal Case 2 waters (IOCCG 2000). Thus, within optically complex coastal areas, other approaches such as physics-based, bio-optical inversion models are more appropriate (IOCCG 2000). In addition, the OCM was an experimental sensor and as

such, contained several inherent technical issues such as low signal-to-noise ratios for all spectral bands when compared to those of SeaWiFS. OCM imagery also was known to contain striping artefacts. However, investigations undertaken using the OCM highlighted the significance of spatial resolution when detecting *Trichodesmium* surface aggregations.

2.4.4 MODIS

The Moderate Resolution Imaging Spectroradiometer (MODIS) was launched aboard NASA's Earth Observing Satellites (EOS): Terra and Aqua. The Aqua satellite was launched in May 2002 with a MODIS sensor dedicated to ocean colour observations. MODIS is a whiskbroom sensor with a swath width of 2330 km and eigth spectral bands in the visible domain dedicated to ocean colour.

At present only one ocean colour algorithm has been developed for detection of *Trichodesmium* using MODIS. This algorithm is based on the floating algae index (FAI) of Hu (2009). The floating algae index exploits strong water leaving radiance values in the near-infra red (NIR) exhibited by near-surface phytoplankton, cyanobacteria and floating vegetation such as Sargassum (Hu 2009). The dedicated ocean colour bands of MODIS have a 1 x 1 km pixel resolution. However, non-ocean colour bands designed for land remote sensing purposes have finer spatial resolutions of either 500 x 500 m or 250 x 250 m resolution (Franz et al. 2006). Although the non-ocean colour bands have slightly lower signal-to-noise ratios, they have been shown to be useful for the purpose of ocean colour remote sensing (Miller and Mckee 2004; Franz et al. 2006).

Hu et al. (2009) found that high concentrations of floating algae within the marine environment have a strong water-leaving radiance signal at the 859 nm MODIS band. The 859 nm band of MODIS has a 250 x 250 m resolution and can thus resolve fine scale spatial structures of floating marine vegetation (Hu 2009). The FAI algorithm was defined as the magnitude of reflectance at the 859 nm band relative to a linear baseline interpolated between a red band (645 nm) and a shortwave infrared (1240 nm) band. Thus, the FAI algorithm gives positive values where there are high concentrations of floating vegetation.

The FAI algorithm was used to identify *Trichodesmium* in the southwest Florida Shelf within MODIS images captured on 21 August 2002, 17 September 2002, 22 May 2004 and 4 August 2007. The multi-band remote sensing reflectance

spectra were examined for those pixels with high FAI values. The MODIS spectral curvature followed a sawtooth pattern of high-low-high-low-high at 469-488-531-551-555 nm bands respectively. Sensitivity analysis identified that this spectral pattern was unlikely to be due to sensor calibration errors. Furthermore, this pattern complemented *in situ* hyperspectral remote sensing measurements of *Trichodesmium* surface aggregations measured in waters of the Florida Keys and also south of Puerto Rico (Navarro 1998; Hu et al. 2010). Thus, Hu et al. (2010) proposed that a two step approach could be used to detect *Trichodesmium* surface aggregations. First, waters with high FAI values are identified and secondly, the spectral curvature of the MODIS remote sensing reflectance is examined between 469 and 555 nm for a pattern consistent with that of *Trichodesmium*. The method was tested by examining the MODIS spectral reflectance curvatures over other floating algae (*Sargassum, Ulva prolifera and Microsytis aerugionosa*) that also give high FAI values. These floating algae did not exhibit the same spectral reflectance pattern as *Trichodesmium*. Thus, the unique spectral patterns observed in MODIS pixels over *Trichodesmium* were thought to be able to discriminate the cyanobacteria well.

2.4.4.1 FAI Summary

The FAI method was successfully applied for detecting *Trichodesmium* in the South Atlantic Bight and waters adjacent to the Saurastra Coast, India where the cyanobacteria has been observed previously using CZCS, SeaWiFS and OCM imagery respectively (Subramaniam et al. 2002; Sarangi et al. 2005). The spatial structure of these FAI features were consistent with those of *Trichodesmium* and included wind rows and eddy swirl patterns. However, these FAI images were not validated with sea-truth observations. In addition, the FAI method was limited in its ability to detect *Trichodesmium* unless a surface aggregation was present with strong NIR reflectance. Thus, sub-surface and dispersed concentrations of *Trichodesmium* can not be detected using the FAI algorithm, in which case other approaches must be applied. The FAI detection method also does not provided a quantitative measure of abundance and can only serve as a method for positively flagging MODIS pixels containing surface aggregations of *Trichodesmium*.

2.4.5 MERIS

The Medium Resolution Imaging Spectroradiometer (MERIS) aboard the European Space Agency (ESA) ENVISAT was launched in March 2002. MERIS provides nine spectral bands in the visible region at a LAC resolution of 300 x 300 m. The design of MERIS is that of a pushbroom sensor with five modules each containing a charge-couples-device (CCD) array which results in a swath width of 1150 km which is slightly less than that of MODIS. However, MERIS benefits from finer pixel resolution and slightly higher radiometric resolution.

At present, a dedicated *Trichodesmium*-specific retrieval algorithm has not been designed using MERIS. Nonetheless, the 709 nm band of MERIS is ideally suited for observing the red-edge reflectance feature of near-surface phytoplankton blooms and floating vegetation such as *Sargassum* (Borstad et al. 1992; Gower et al. 2006). To exploit this, Gower et al. (2005) developed the maximum chlorophyll index (MCI) which is analogous to the FAI. The MCI computes the height of the 709 nm band relative to a linear baseline interpolated between the 681 and 753 nm bands (Gower et al. 2005). To eliminate land, cloud, haze and sun glint, pixels with a top of atmosphere (TOA) radiance greater than 15 mW m^{-2} sr^{-1} nm^{-1} at 865 nm were ignored (Gower et al. 2008). A high, positive MCI value was deemed to be indicative of high concentrations of near-surface or floating phytoplankton (Gower et al. 2005; Gower et al. 2008). A major benefit of the MCI method is its use of TOA radiances. This negates the concern of poorly performing atmospheric corrections in optically complex waters.

Global 5 km resolution MCI composite imagery was published by Gower et al. (2008). A time series of a cyanobacterial bloom evolution within the Baltic Sea was presented as well as a "superbloom" of phytoplankton in the Weddell Sea, Antarctica (Gower et al. 2008). The global composite imagery also revealed strong MCI values within the Great Barrier Reef, Australia on 21 and 27 August 2006. The Blooms from Space website (http://www.bloomsfromspace.org/) presented a further example of MERIS MCI imagery within the Great Barrier Reef, Australia on 5 October 2008. Within these two images the positive MCI signals were likely due to dense surface aggregations of *Trichodesmium* however, no sea truth data was cited. Notably, the coral reef structures were also identified within the MCI image. The 5 October 2008 MCI image of the Great Barrier Reef has been reproduced in Figure 2.9.

2.4.5.1 MCI Summary

Although useful for mapping the spatial extent of high concentrations of phytoplankton biomass, the MCI at present cannot definitively discriminate *Trichodesmium* from other phytoplankton and floating vegetation such as *Sargassum* (Gower et al. 2006). Unlike the FAI method of Hu et al. (2010), the MCI approach does not consider spectral shape of the nLw signal for the purposes of identifying *Trichodesmium* specific features. In addition, the MCI does not provide a quantitative measure of biomass. Gower et al. (2008) stated that the radiance maximum at 709 nm is indicative of phytoplankton biomass in excess of 30 mg Chla m^{-3}. However, apart from this threshold value, the magnitude of MCI cannot be converted into quantitative units of Chla concentration.

The MCI approach also appears to yield false-positive retrievals in the presence of coral reef structures (see Figure 2.9) and benthic vegetation in shallow waters (Gower et al. 1999; Gower et al. 2005). This issue is pertinent to the tropical south-western tropical Pacific and Great Barrier Reef. Gower et al. (2006) showed that there was a discernable difference between the TOA water leaving radiance spectra of *Trichodesmium* and coral reefs. Thus it should be possible to derive a threshold value or spectral criteria to mask out coral reefs within MCI images.

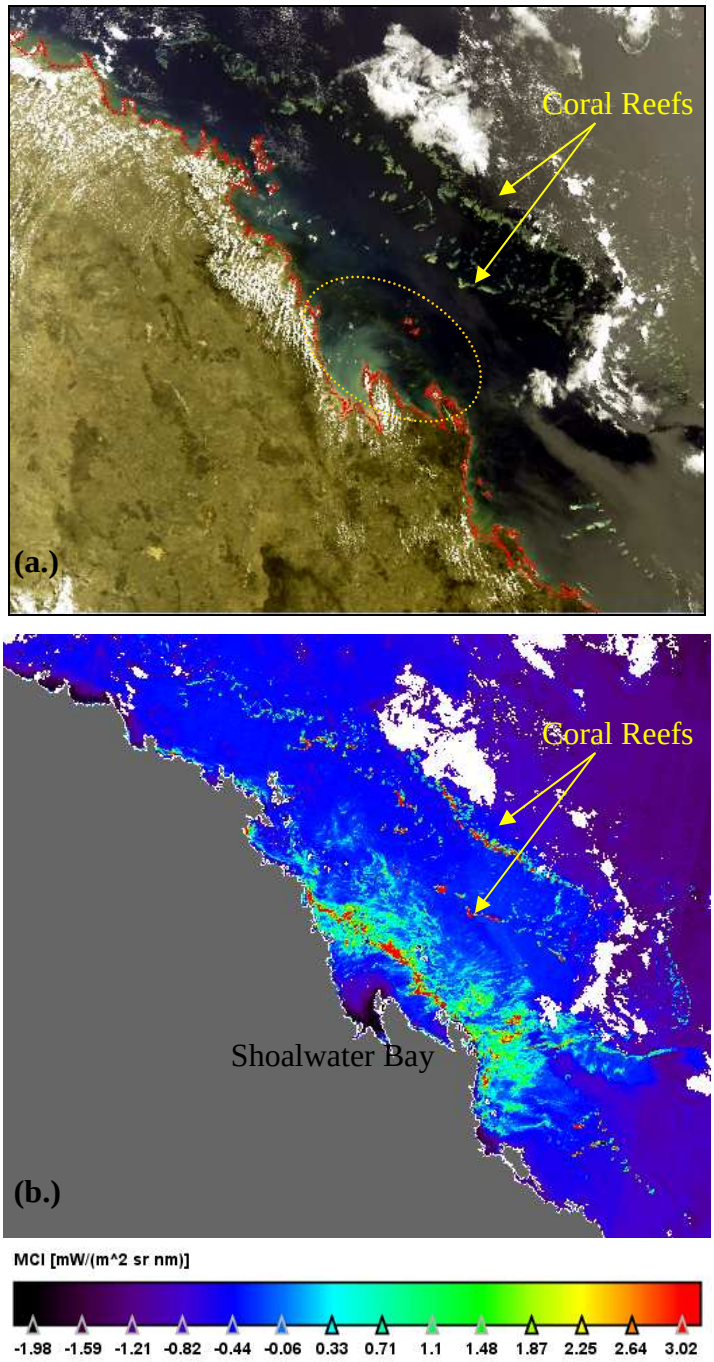

Figure 2.9: (a.) Quasi true colour MERIS image of the Great Barrier Reef captured on 5 October 2008. The yellow ellipse shows highly reflective brown streaks offshore from Shaolwater Bay. (b.) The corresponding MERIS MCI image, bright features correspond to brown streaks present in the true colour image and indicate high near-surface Chla concentrations. Note the MCI index also identifies highly reflective coral reef structures.

2.5 Global Trichodesmium Algorithms

The launch of ocean colour satellites with several spectral bands, such as SeaWiFS, MODIS and MERIS has provided an opportunity for researchers to develop physics-based ocean colour inversion algorithms. Such algorithms can determine an appropriate combination of IOPs that explain the observed water-leaving radiances. Such algorithms/models are based upon the physics of radiative transfer theory. Physics-based models aim to provide a "one-size-fits-all" approach so that accurate global retrievals are possible for Case 1 waters, and sometimes optically complex Case 2 waters.

2.5.1 Adapted GSM01 Model

The semi-analytical, Garver, Siegel and Maritorena (GSM01) ocean colour inversion algorithm (Maritorena et al. 2002) was adapted by Westberry and Siegel (2005) for the purpose of Chla-specific, quantitative detection of *Trichodesmium*. The GSM01 algorithm, utilised the empirical relationship between IOPs and R_{rs} of Gordon et al. (1988)

$$R_{rs}(\lambda) = \sum_{i=1}^{2} g_i \left[\frac{b_b(\lambda)}{a(\lambda) + b_b(\lambda)} \right]^i \qquad [2.8]$$

where g_1 and g_2 are constants (Gordon et al. 1988). The bulk IOPs of absorption, a, and backscattering, b_b, are the sum of the individual absorption and backscattering coefficients of constituents within the water column

$$a(\lambda) = a_w(\lambda) + a_\phi(\lambda) + a_{dg}(\lambda) + a_{tri}(\lambda) \qquad [2.9]$$

$$b_b(\lambda) = b_{b_w}(\lambda) + b_{bp}(\lambda) + b_{btri}(\lambda) \qquad [2.10]$$

where the subscripts w, ϕ, dg, p and tri refer to pure water, phytoplankton, coloured dissolved and detrital matter, particulate matter and *Trichodesmium* respectively (Kirk 1994; Westberry et al. 2005). The absorption and scattering coefficients of pure water are constants which are well defined within the literature (Smith and Baker 1981; Pope and Fry 1997).

The GSM01 algorithm determines the optimal set of IOP coefficients required to fit Equation 2.8 to an observed R_{rs} spectra (Maritorena et al. 2002). The standard GSM01 algorithm uses a pre-defined spectral shape for $a_\phi(\lambda)$ and does not consider

the backscattering coefficient of phytoplankton, $b_{b\phi}(\lambda)$ separately from the total particulate backscattering coefficient $b_{bp}(\lambda)$ (Maritorena et al. 2002). Furthermore, the magnitude of $a_{\phi}(\lambda)$ and $b_{bp}(\lambda)$ are both dependent upon Chla concentration,

$$a_{\phi}(\lambda) = Chla\ a^{*}_{\phi}(\lambda) \qquad [2.11]$$

$$b_{bp}(\lambda) = 0.416\ \text{Chla}^{0.766}\left[0.002 + 0.02\left(0.25\ \log\ \text{Chla}\right)\left(\frac{550}{\lambda}\right)\right], \qquad [2.12]$$

where, $a^{*}_{\phi}(\lambda)$ is the Chla specific phytoplankton absorption coefficient which had its spectral shape taken from Bricaud et al. (1995). The spectral shape of $a_{dg}(\lambda)$ is modelled using the equation

$$a_{dg}(\lambda) = a_{dg}(\lambda_0)e^{-S(\lambda-\lambda_0)}, \qquad [2.13]$$

where the reference wavelength, λ_0, is typically 443 nm and the spectral slope coefficient, *S*, ranges between 0.010 and 0.035 m^{-1}.

The adapted GSM01 model of Westberry and Siegel (2005) adds two IOP terms: the *Trichodesmium* chlorophyll specific absorption $a^{*}_{tri}(\lambda)$ and backscattering $b^{*}_{b\,tri}(\lambda)$ coefficients respectively taken from Subramaniam et al. (1999a, 1999b). Thus, the optimal solution of Equation 2.8 becomes one which explicitly contains *Trichodesmium* at some Chla-specific concentration (Westberry et al. 2005). The magnitude of $a^{*}_{tri}(\lambda)$ and $b^{*}_{b\,tri}(\lambda)$ are dependent upon the *Trichodesmium* concentration denoted Tri,

$$a_{tri}(\lambda) = C_1\ \text{Tri}\ a^{*}_{tri}(\lambda), \qquad [2.14]$$

$$b_{b\,tri}(\lambda) = C_2\ \text{Tri}\ b^{*}_{b\,tri}(\lambda), \qquad [2.15]$$

where, C_1 = 0.7097 and C_2 = 0.2864 were optimal coefficients determined during model tuning.

The Westberry and Siegel (2005) *Trichodesmium*-specific GSM01 algorithm was trained using 130 *in situ* radiometric measurements which were collected alongside quantitative measures of *Trichodesmium* abundance. These data were sampled from the Sargasso Sea, the tropical Atlantic Ocean, southwest Pacific Ocean and Arafura/Timor Sea. *Trichodesmium* concentrations within the data set ranged between 0 – 11,000 trichomes L^{-1} equivalent to a Chla concentration range of 0 – 0.80 mg Chla m^{-3} (Westberry et al. 2005). An independent validation data set was

constructed from 142 level-3 (L3) global area coverage (GAC) SeaWiFS images. Of these 142 L3 GAC images, 77 were overpasses corresponding with the *in situ* measurements previously mentioned, whilst the other 65 corresponded to *in situ* observations of *Trichodesmium* made without corresponding radiometric measurements (Westberry et al. 2005).

Initial inversion hind-casts showed poor predictive skill and as such an iterative approach was taken to tune the GSM01 free parameters C_1, C_2 and S. However, model tuning only marginally improved model performance yielding $R^2 = 0.3$ for observed versus predicted *Trichodesmium* abundance. Westberry and Siegel (2005) conceded that the adapted GSM01 had difficulties in quantitatively retrieving *Trichodesmium* abundance. Nevertheless, Westberry and Siegel (2005) showed that the adapted GSM01 could instead be used to discriminate the presence of *Trichodesmium* above an arbitrary "bloom" threshold value of 3200 trichomes L^{-1}. The algorithm was applied to the *in situ* radiometric data set (n = 130) and re-tuned. The results showed the algorithm could correctly identify 92 % of "bloom" observations and 84 % of "non-bloom" observations. When applied to the L3 GAC SeaWiFS validation set (n = 142), the adapted GSM01 algorithm was found to identify 76 % of "bloom" observations correctly and 71 % of "non-bloom" observations. False positive retrievals within the SeaWiFS validation set were 29 %, and higher than expected (Westberry et al. 2005). Thus, Westberry and Siegel (2005) suggested quality control filters be applied to SeaWiFS data to reduce false positive retrievals.

As an example, Westberry and Siegel (2005) applied the adapted GSM01 to an 8-day global composite SeaWiFS image (10 – 17 February 1998) at 0.25° resolution between the latitudes 35° S - 35° N. Within this test scene, 1.3 % of pixels were identified as containing *Trichodesmium* above the threshold value of 3200 trichomes L^{-1}. Regions identified within the SeaWiFS scene as having *Trichodesmium* present included the Indian Ocean, Arabian Sea, Gulf of Mexico, Caribbean Sea, and western Pacific Ocean. This result was supported by literature reports which have previously identified *Trichodesmium* as abundant within these regions (Janson et al. 1995; Capone et al. 1997; Capone et al. 1998; Mulholland et al. 2006; Neveux et al. 2006; Dupouy et al. 2008b).

A further examination of the adapted GSM01 method was performed by Westberry and Siegel (2006). A time series of 8-day, L3 GAC composites from

January 1998 to December 2003 was analysed to determine the global temporal frequency of *Trichodesmium*. Various filtering steps were implemented to remove single, isolated "bloom" pixels surrounded by "non-bloom" pixels. Regions of shallow water (< 100 m) and pixels with SST values less than 23.5 °C were disregarded. Additionally, the algorithm was only applied between latitudes of 45 °N – 45 °S. The results indicated that *Trichodesmium* "blooms" (> 3200 trichomes L^{-1}) were rare, occurring less than 5% of the time for most locations. In addition, approximately 30 % of the regions examined never experienced a *Trichodesmium* "bloom". Regions experiencing *Trichodesmium* "blooms" with the highest frequencies (~35 %) were the eastern equatorial Pacific Ocean and the Arabian Sea. A distinct seasonality of *Trichodesmium* "bloom" occurrence could be seen in the western Arabian Sea and eastern equatorial Pacific Ocean where the highest bloom frequencies occurred during the Austral spring and summer.

2.5.2 Adapted GSM01 Model Summary

The adapted GSM01 model of Westberry et al. (2005) provided the first physics-based, *Trichodesmium* specific inversion algorithm. The method was developed using *in situ* radiometric measurements collected alongside quantitative measures of *Trichodesmium* abundance. Unfortunately, the algorithm was unable to resolve *Trichodesmium* specific concentrations with desired accuracy. However, the algorithm was to be able to detect *Trichodesmium* above a "bloom" threshold of 3200 trichomes L^{-1}. Thus, the adapted GSM01 was shown to be useful as a method for detecting the presence/absence of *Trichodesmium* "blooms" using SeaWiFS imagery.

Westberry and Siegel (2006) used the adapted GSM01 to examine global distributions of *Trichodesmium* abundance. This exercise proved insightful and complemented previous estimates of *Trichodesmium* global abundance. In addition, global distribution data were used to estimate the annual global N-fixation by *Trichodesmium* blooms to be approximately 42 Tg N yr^{-1}. Based upon this estimate, *Trichodesmium* is responsible for approximately 36 % of the entire global pelagic N-fixation (~100 Tg N yr^{-1}). However, the method did not resolve *Trichodedsmium* abundance within the south-western Pacific Ocean as expected. Furthermore, due to quality control masking of shallow water (< 100 m), coastal regions and shallow shelf seas surrounding northern Australia and the west coast of India were ignored. These

regions are known to have significant abundances of *Trichodesmium* which are likely significant to regional N-budgets (Devassy et al. 1978; Revelante and Gilmartin 1982; Furnas 1992).

The retrieval of *Trichodesmium* specific Chla concentration was also investigated by Westberry and Siegel (2006). This was performed by identifying *Trichodesmium* "bloom" pixels using the adapted GSM01 model and calculating the Chla concentration for these locations using the standard SeaWiFS OC4 v4 Chla algorithm. The results suggested that the OC4 v4 Chla algorithm underestimated *Trichodesmium* specific Chla concentration by a factor of two. Underestimation of Chla concentration was deemed a consequence of pigment packaging and self shading (Westberry and Siegel 2006). This agrees with Subramaniam et al. (2002) who suggested that the packaging and self shading effects of *Trichodesmium* could result in underestimation of Chla by a factor of four. In addition, these results conflict with the research of Chauhan et al. (2002) who found that the standard SeaWiFS Chla algorithms (OC2 v 4 and OC4 v4) consistently over-estimated Chla concentrations for extremely dense surface aggregations of *Trichodesmium*. Thus, it is evident that standard band ratio-type Chla algorithms have great difficulty accurately resolving *Trichodesmium* abundance.

2.6 Summary and Conclusion

Over the past two decades, much effort has been placed upon the optical remote sensing of *Trichodesmium*, Table 2.1 summarises these efforts. Most efforts have focused upon detecting dense surface aggregations of *Trichodesmium*. Such dense surface aggregations exhibit strong NIR reflectance which makes them optically distinct from surrounding seawater. Although methods which flag the presence of *Trichodesmium* are useful for defining spatial distributions, they do not yield quantitative estimates of abundance. Furthermore, these methods, possibly with the exception of Hu et al. (2010), cannot definitively discriminate *Trichodesmium* from other forms of floating marine algae and vegetation. Such methods therefore require strong local knowledge of phytoplankton populations and benefit from regular local reports of *Trichodesmium* variability. Methods based on NIR reflectance also have not thoroughly explored potential confounding effects such as coral reefs and high concentrations of suspended sediment as outlined by Subramaniam et al. (2002).

In contrast, the adapted GSM01 algorithm of Westberry et al. (2005) provided a means for detecting *Trichodesmium* blooms (> 3200 trichomes L^{-1}) on a global basis. Although, the GSM01 algorithm performed well in open oceanic waters, it is known to under-perform in optically complex coastal waters (IOCCG 2006). Thus, when applying the adapted *Trichodesmium* specific algorithm for global analysis Westberry et al. (2006) applied a bathymetry mask excluding coastal pixels (< 100 m). Shelf waters within coastal India, northern Australia and the Gulf of Mexico are documented as having abundant *Trichodesmium* (Devassy et al. 1978; Furnas 1992; Mulholland et al. 2006; Neveux et al. 2006). However, bathymetry masks (< 100 m) exclude these shallow coastal regions from being processed by the Westberry et al. (2005) algorithm. For example, there have been no *Trichodesmium* specific ocean colour algorithms developed for the Great Barrier Reef, Australia. This optically complex region is known to have a significant *Trichodesmium* abundance (Revelante and Gilmartin 1982; Furnas 1992) and the quantification of *Trichodesmium* within this region would greatly improve estimates of N-fixation (Furnas et al. 1995; Bell et al. 1999).

Low pixel resolution of ocean colour sensors relative to patches of *Trichodesmium* has also been identified as a likely inhibitor of detection algorithms (Subramaniam et al. 2002; Desa et al. 2005). Studies using the 250 m bands of MODIS and the 360 m bands of the OCM were able to resolve *Trichodesmium* surface aggregations with a great degree of detail when compared to lower spatial resolution 1 km imagery of SeaWiFS (Desa et al. 2005; Hu et al. 2010). The consequences of this are significant, however, at present there is no consensus regarding what proportion of a pixel must be covered in order for it to be flagged as containing *Trichodesmium*. The consequences of the vertical distribution of *Trichodesmium* within the water column also have not been addressed specifically. Radiative transfer modelling studies have shown that the vertical distribution of cyanobacteria within the Baltic Sea can subtlety vary the water leaving radiance signal (Kutser et al. 2008). However, this is dependent not only upon vertical position but also Chla specific abundance. Further investigation into the influence of *Trichodesmium* spatial distribution upon its retrieval by ocean colour sensors is thus warranted.

Standard band ratio-type Chla algorithms have been shown to fail or perform poorly over *Trichodesmium* (Chauhan et al. 2002) and as such, previous methods that

have required Chla values as part of *Trichodesmium* detection algorithms may have intrinsic problems. Westberry et al. (2005) attempted to address this issue by adapting the GSM01 algorithm to be *Trichodesmium* specific, however, with limited success. Dupouy et al. (2008b) also attempted to avoid using Chla values by developing the RAS Physat algorithm with K490 values. One potential solution for quantifying *Trichodesmium* may be by adopting algorithms for retrieving phycocyanin (PC) concentration. Such algorithms have been developed using the 709 nm band of MERIS and used for quantifying cyanobacterial biomass in freshwater lakes (Simis et al. 2005a). However, such methods have not yet been explored for *Trichodesmium*. In order to develop and validate such algorithms, a shift toward routine quantification of *in situ* PC concentration is necessary.

Within remote sensing studies of *Trichodesmium* the term "bloom" is loosely used by most authors. In many cases the term "bloom" appears to be an arbitrary description of abundance used particularly to describe dense surface aggregation of *Trichodesmium* which can vary in concentration by up to an order of magnitude. The only formal definition of what constitutes a *Trichodesmium* bloom for the purposes of ocean colour remote sensing was outlined by Westberry et al. (2005) as concentrations exceeding 3200 trichomes L^{-1}. Within the Great Barrier Reef, Australia, dense surface aggregations of *Trichodesmium* can occur year-round (Furnas 1992). Such events are not necessarily associated with nutrient inputs or enhanced population growth and are likely associated with physical conditions such as relaxed wind stress, and a thinned mixed layer depth (Capone et al. 1997; Hood et al. 2004). Thus, the use of the term "bloom" when referring to *Trichodesmium* abundance requires further careful consideration.

Ocean Colour Sensor	Year	Location	Coastal Zone	Sea-truth	Positive Discrimination*	References
CZCS	1988; 1992	SW Tropical Pacific	N	No	N	Dupouy et al. (1988; 1992)
CZCS	1992	Western Indian Coast	Y	N	N	Borstad et al. (1992)
CZCS	1994	Western Australia	Y	Y	Y	Subramaniam and Carpenter (1994)
SeaWiFS	1995	Theoretical Study	-	-	-	Tassan (1995)
SeaWiFS	2000	SW Tropical Pacific	N	Y	N	Dupouy (2000)
SeaWiFS	2002	South Atlantic Bight	Y	Y	Y	Subramaniam et al. (2002)
SeaWiFS	2005	Global Dataset	Y	Y	Y	Westberry et al. (2005)
SeaWiFS	2006	Global Dataset	N	N	Y	Westberry et al. (2006)
SeaWiFS	2008	SW Tropical Pacific	N	Y	N	Dupouy (2008b)
OCM	2004; 2005	Western Indian Coast	Y	N	N	Sarangi et al. (2004); Sarangi et al. (2005)
OCM and SeaWiFS	2005	Western Indian Coast	Y	Y	N	Desa et al. (2005)
MERIS	2008	SE Australia	Y	N	N	Gower et al. (2008)
MODIS	2010	SW Florida Shelf	Y	N	Y	Hu et al. (2010)

Table 2.1: Chronologically ordered efforts to detect *Trichodesmium* using various satellite ocean colour sensors. Within this table, Y = yes, N= No.

*Positive Discrimination – if the method was designed to be able to discriminate *Trichodesmium* from other marine constituents without user interpretation.

2.7 Future Directions

At present MODIS and MERIS are nearing the end of their operational lifespans and are due to be replaced by new generation sensors. MODIS is to be replaced by the Visible Infrared Imaging Radiometer Suite (VIIRS), whereas MERIS is to be replaced by the Ocean and Land Colour Instrument (OCLI). Although these new sensors will have similar spectral resolution to their predecessors, they will have local area coverage (LAC) pixel resolutions of 300 – 400 m. Thus, these new sensors have the potential to resolve *Trichodesmium* patches that are presently of sub-pixel scales for current sensors. Unfortunately, a spectral band in the vicinity of 580 nm, potentially useful for the detection of *Trichodesmium*, does not appear to have been included in these new sensors.

Hyperspectral radiometric data would allow for the development of advanced *Trichodesmium* specific algorithms using the unique spectral bio-optical properties of the cyanobacteria. Research has shown that hyperspectral data can be inverted to detect harmful algae such as *Karenia brevis* (Craig et al. 2006) and presently *in situ* hyperspectral radiometric data is routinely collected using in-water and above-water sensors. Unfortunately, there are currently no operational hyperspectral ocean colour sensors aboard earth observing satellites. However, a proof-of-concept instrument called the Hyperspectral Imager for the Coastal Ocean (HICO) is at the moment aboard the International Space Station (Corson et al. 2008). HICO has a spectral range of 300 – 1000 nm with a resolution of 5 nm and provides pixels with a 100 x 100 m resolution (Corson et al. 2008). Unfortunately in its present state HICO has limited capture, irregular return time and a small scene size of 50 x 200 km. Nonetheless, the high degree of spectral information provided by HICO makes it an ideal candidate for developing and/or testing hyperspectral *Trichodesmium* specific algorithms.

Most contemporary algorithms have focused upon the detection of dense *Trichodesmium* surface aggregations. However, dispersed populations of *Trichodesmium* are more likely to be the norm. Thus, further efforts are required to resolve so called "sub-bloom" concentrations towards values of 0.1 – 1 mg Chla m^{-3} as envisioned by Tassan (1995). In addition, most algorithms, with the exception of

the adapted GSM01, are not mathematically parameterised to discriminate *Trichodesmium* from other phytoplankton in an efficient manner. Thus, further developments of ocean colour algorithms that directly incorporate the distinct bio-optical properties of the cyanobacteria are necessary.

Finally, additional *in situ* data collection which quantifies *Trichodesmium* abundance alongside its IOPs and radiometric properties is vital. Such data are essential for algorithm development and most importantly validation of algorithm performance.

3 A simple, binary classification algorithm for the detection of *Trichodesmium* spp. within the Great Barrier Reef using MODIS imagery.

This Chapter has been published in the peer reviewed journal Limnology and Oceanography: Methods

Abstract

A binary classification algorithm to detect the presence of high surface concentrations of the nitrogen fixing cyanobacterium *Trichodesmium* spp. was developed for high spatial resolution (250 m) imagery of the MODerate-resolution Imaging Spectroradiometer (MODIS). Above-water hyperspectral radiometric measurements of dense *Trichodesmium* surface aggregations (>10 mg Chla m^{-3}) showed that the water leaving radiance, L_w, at wavelengths greater than 700 nm were much higher in magnitude (>0.05 W $m^{-2}sr^{-1}$) relative to the visible wavelengths 400-700 nm (<0.03 W $m^{-2}sr^{-1}$). The binary classification algorithm is based on three criteria. The first criteria relied on the difference in magnitude between the MODIS normalised water-leaving radiance (nLw) at the 859 and 678 nm wavebands. The magnitude of the nLw at the 555 and 645 nm wavebands relative to nLw 678 nm waveband formed the second and third criteria respectively. The classification algorithm was tested on a small subset of 13 MODIS images with corresponding *Trichodesmium* sea-truths and yielded an 85 % accuracy. Fine scale features consistent with dense *Trichodesmium* surface aggregations such as eddy swirls and windrows appear to be well represented with the algorithm results. The algorithm was also found to be robust in the presence of highly reflective, potentially confounding effects.

3.1 Introduction

Trichodesmium spp. is a pelagic, colonial, cyanobacterium found throughout oligotrophic, tropical and sub-tropical waters of the world (Capone et al. 1997). The organism comprises individual thread-like Trichomes which bundle together to form colonies. *Trichodesmium* is known to form dense surface aggregations often called "red-tides" which are scum-like in appearance and range from silvery-white to yellow-green to orange-brown in colour (Devassy et al. 1978). *Trichodesmium* is common to the Great Barrier Reef (GBR) region adjacent to north-eastern Australia and surface aggregations of the cyanobacterium have been reported to span 52,000 km^2 within the Capricorn Channel (22°50'S, 152°50'E) (Kuchler and Jupp 1988; Furnas 1992). Surface aggregations of *Trichodesmium* are characterised by extremely high population densities (>10^6 Trichomes/L) which lie just beneath or on the water surface (Carpenter and Capone 1992). The use of the term "bloom" will be avoided in this paper and instead the term "surface aggregation" will be used. The reasoning for this terminology is that dense *Trichodesmium* surface aggregations appear year-round within the GBR and are not necessarily associated with nutrient input events or evidence of enhanced population growth (Furnas 1992). The mechanisms which cause the standing population of *Trichodesmium* to accumulate at the surface are thought to be related to extended periods of relaxed wind surface stress (Capone et al. 1997).

Trichodesmium is of biological, physical and biogeochemical significance. *Trichodesmium* colonies have been described as pelagic habitats in which many micro-organisms reside (O' Neil and Roman 1992). Also, nutrient release and grazing of *Trichodesmium* has been identified as of significance for oligotrophic regions. In dense concentrations, *Trichodesmium* has the potential to modify light penetration and ocean-atmosphere heat and gas exchanges (Capone et al. 1997). However it is the ability of *Trichodesmium* to actively fix atmospheric nitrogen (N_2) that is of great significance biogeochemically. *Trichodesmium* is considered an important source of new-nitrogen to the worlds oceans (Mulholland 2007). Within the GBR, it is estimated that the annual N-input associated with *Trichodesmium* N-fixation is at least similar in magnitude to that from river inputs (Furnas et al. 1995; Bell et al. 1999).

Bell et al. (1999) calculated *Trichodesmium* N-fixation rates for the GBR using three different methods. Method 1 estimated N-fixation based upon the average annual distribution of *Trichodesmium* from historical data of Revelente and Gilmartin (1982). Conversely, Method 2 considered the average concentration and duration of *Trichodesmium* surface aggregation events based on studies by Carpenter and Capone (1992) and data from Revelente and Gilmartin (1982). Method 3 assumed that all cellular nitrogen was due to N-fixation and determined the amount of new-N required to establish a surface aggregation of *Trichodesmium*. Bell et al. (1999) study found that the annual *Trichodesmium* N-input for the Northern GBR ranged between 900-3,700 t yr^{-1} compared with measured river N-inputs of about 10,000 t/year. Similarly for the Central GBR estimates of annual *Trichodesmium* N-input ranged from 12,000-30,000 t yr^{-1} compared with river N-inputs of about 20,000 t yr^{-1} (Bell et al. 1999).

Bell et al. (1999) stated that the total N-input due to *Trichodesmium* N-fixation would be best represented by combining estimates from methods 2 and 3 and part from Method 1. However, for Methods 1 and 2 to provide accurate N-fixation values, a better understanding of *Trichodesmium* population variability is required. Currently, only a small number of phytoplankton surveys detailing *Trichodesmium* abundance in the GBR region exist in literature (Marshall 1933; Revelante and Gilmartin 1982; Bell et al. 1999). Thus a more accurate assessment of the spatial and temporal abundance of *Trichodesmium* within the GBR is essential.

Mapping dense surface aggregations of *Trichodesmium* from orbit was discussed by Kuchler and Jupp (1988) who presented an image captured from a NASA Space Shuttle mission. The image showed a large phytoplankton bloom deemed to be *Trichodesmium erythraeum* in the Capricorn Channel region of the Southern GBR (22°30'S, 152°30'E). Borstad et al. (1992) discussed the potential development of *Trichodesmium*-specific algorithms for remote sensing satellites. Borstad et al. (1992) suggested the optical properties of absorption, scattering and fluorescence of *Trichodesmium* could be used to discriminate the cyanobacteria from other phytoplankton. Measurements of the absorption spectra of *Trichodesmium* have been made by several authors (Subramaniam et al. 1999a; Dupouy et al. 2008a). The results of these investigations have shown that *Trichodesmium* exhibits a unique absorption

spectrum due to the combination of chlorophyll-a (Chla), carotenoids, and the phycobilipigments: phycourobilin (PUB), phycoerythrobilin (PEB) phycoeryrthocyanin (PEC) and phycocyanin (PC) (Subramaniam et al. 1999a). The high optical scattering exhibited by *Trichodesmium* is due to the presence of intercellular gas vacuoles (Subramaniam et al. 1999b). The associated backscattering spectrum exhibits wavelength dependence which is determined to be a consequence of fluorescence and re-absorption (Subramaniam et al. 1999b; Dupouy et al. 2008a).

The mapping of surface aggregations of *Trichodesmium* using the Coastal Zone Colour Scanner (CZCS), the Satellite Pour l'Observation de la Terre (SPOT) and the Sea-viewing Wide Field-of-view Sensor (SeaWiFS) has been investigated (Dupouy et al. 1988; Dupouy 1992; Subramaniam and Carpenter 1994; Subramaniam et al. 2002). Dupouy et al. (1988) reported large regions of "discoloured" water associated with large phytoplankton blooms (~90,000 km^2) in the south-western Pacific Ocean around New Caledonia and Vanuatu. The discoloured surface features formed were deemed to be *Trichodesmium*, based upon strong circumstantial evidence, however, conclusive sea-truths were not available. Dupouy (1992) further examined *Trichodesmium* within the south-western Pacific using CZCS and SPOT images in the New Caledonian Archipelago. Subramaniam and Carpenter (1994) developed an empirical classification scheme to detect *Trichodesmium* using CZCS imagery. The algorithm of Subramaniam and Carpenter (1994) relied on high water leaving radiances in the 440, 520 and 550 nm wavebands due to high backscattering. It also considered absorption at 550 nm due to phycoerythrin. The algorithm was tested on a subset of CZCS images with known *Trichodesmium* presence and successfully detected surface streaks of *Trichodesmium* off north-western Australia (Subramaniam and Carpenter 1994). The increased spectral resolution of SeaWiFS imagery was investigated by Subramaniam et al. (2002) for detection of moderate concentrations of *Trichodesmium* (0.5-3.0 mg Chla m-3). The algorithm successfully detected *Trichodesmium* in the South Atlantic Bight along the south-east coast of the United States from 27 October - 7 November 1998 with a corresponding sea-truth observation. However, the Subramaniam et al (2002) algorithm was not tested for detecting extremely dense surface aggregations of *Trichodesmium*.

Subramaniam et al. (2002) discussed how highly reflective constituents such as high suspended sediment concentration, coral reefs and bottom reflectance in coastal regions may yield false-positive detection of *Trichodesmium* for a pixel. The classification scheme of Subramaniam et al. (2002) consequently masked out shallow water (>30 m) using bathymetric data in an attempt to reduce bottom reflectance and coral reef contamination. The issues raised by Subramaniam et al. (2002) are pertinent to the GBR where the depth is often less than 30 m, large coral reef structures are present and high suspended sediment loads are episodically common due to wind-driven resuspension and annual river flooding events (Wolanski 1994). During and after river flooding events within the GBR there are increased levels of suspended sediment, coloured dissolved and detrital matter (CDM) and increased phytoplankton biomass resulting from nutrient loads. The diverse water types of GBR coastal waters during such flood events also include *Trichodesmium* aggregations which have been recorded up to one metre in thickness on plume boundaries (Rohde et al. 2006). The presence of *Trichodesmium* alongside high sediment, high CDM and high-chlorophyll concentrations may present challenges in applying a *Trichodesmium*-specific remote sensing classification algorithm within the GBR.

The classification algorithm of Subramaniam et al. (2002) was examined by Desa et al. (2005) utilising both the Indian Space Research Organisation (ISRO) Ocean Colour Monitor (OCM) and SeaWiFS data. Desa et al. (2005) examined *Trichodesmium* surface aggregations in the Arabian Sea adjacent to the Indian coastline. Desa et al. (2005) noted better detectability of *Trichodesmium* with OCM imagery than with that of SeaWiFS. This was deemed to be a consequence of SeaWiFS having a lower spatial resolution than the OCM. SeaWiFS and the OCM have the same spectral resolution; however the pixel resolution of the OCM is 350 x 350 m compared with 1x1km pixel resolution of SeaWiFS. Thus, for a 1 x 1 km SeaWiFS pixel there are approximately 3 x 3 corresponding OCM pixels (Desa et al. 2005). Therefore, a lower spatial resolution sensor may limit the detectability of *Trichodesmium* distributions which have sub-pixel spatial scales. This was surmised by Subramaniam et al (2002) who noted that the number of highly reflective pixels corresponding to dense surface aggregations was much less than expected. This was considered to be a consequence of the sub-pixel scale

spatial variability of *Trichodesmium* surface aggregations which often appear as patchy, long streaks or windrows (Subramaniam et al. 2002). Each 1 x 1 km resolution SeaWiFS pixel represents a spectrally averaged combination of dense surface aggregations and the water in between, thus reducing the number of highly reflective pixels. To provide higher spatial and spectral resolution ocean colour remote sensing data, NASA's MODerate Resolution Imaging Spectroradiometer (MODIS) is preferable.

We present a simple, empirical method based upon information from above-water, hyperspectral radiometric data collected over dense surface aggregations of *Trichodesmium* spp. within the GBR. We examine the "red-edge" effect described by Borstad et al. (1992) in which *Trichodesmium* surface aggregates exhibit a low reflectance around 680 nm and high reflectance at wavelengths longer than 700 nm where pigment absorption is minimal. Strong reflectance in the near-infrared (NIR) is a feature exhibited by dense surface aggregations of other varieties of marine and freshwater cyanobacteria, and floating algal mats such as *Sargassum* (Gitelson et al. 1995; Kutser 2004; Gons et al. 2005; Gower et al. 2006; Reinart and Kutser 2006; Simis et al. 2007; Hu 2009). The strong NIR reflectance feature has been used for observing dense cyanobacterial concentrations, floating algal mats and harmful algal blooms (HABs) using both ocean colour and non-ocean colour sensors including: the Medium Resolution Imaging Spectroradiometer (MERIS), the MODerate Resolution Imaging Spectroradiometer (MODIS), Landsat, the Advanced Very High Resolution Radiometer (AVHRR), Hyperion and the Advanced Land Imager (ALI) (Galat and Verdin 1989; Kahru 1997; Svejkovsky and Shandley 2001; Ibelings et al. 2003; Kutser 2004; Stumpf and Tomlinson 2005; Gower et al. 2006; Reinart and Kutser 2006; Hu 2009). However, there is presently no such method developed for the detection of dense surface aggregations of *Trichodesmium* within the GBR based upon NIR reflectance characteristics.

A simple, binary classification algorithm to detect the presence or absence of a *Trichodesmium* surface aggregation using MODIS 250 x 250 m pixel resolution imagery is presented. The binary classification algorithm is validated using sea-surface observation to assess performance. The classification method is also tested for potential confounding effects using a MODIS image containing *Trichodesmium* in the presence of

high suspended sediments, high CDM, coral reefs and other phytoplankton. This is the first such *Trichodesmium*-specific satellite algorithm presented specifically for the GBR and the first to explore the use of MODIS 250 m resolution bands.

3.2 Materials and Procedures

3.2.1 Trichodesmium surface aggregations within the Great Barrier Reef

Field studies were conducted within GBR aboard the Australian Institute of Marine Science (AIMS) research vessels RV Cape Ferguson and RV Lady Basten. Above-water radiometric measurements were made along two transects over dense surface aggregations of *Trichodesmium*. On 27 April 2007 a 17 km south-east transect was traversed and is hereafter referred to as the "Cairns Transect" (Figure 3.1 b) On the 31 July 2008 a 38 km transect was traversed in a north-west direction and is hereafter referred to as the "Mackay/Whitsunday Transect" (Figure 3.1 c). Information from the hyperspectral radiometric data was then used to develop a *Trichodesmium*-specific binary classification algorithm for MODIS satellite imagery.

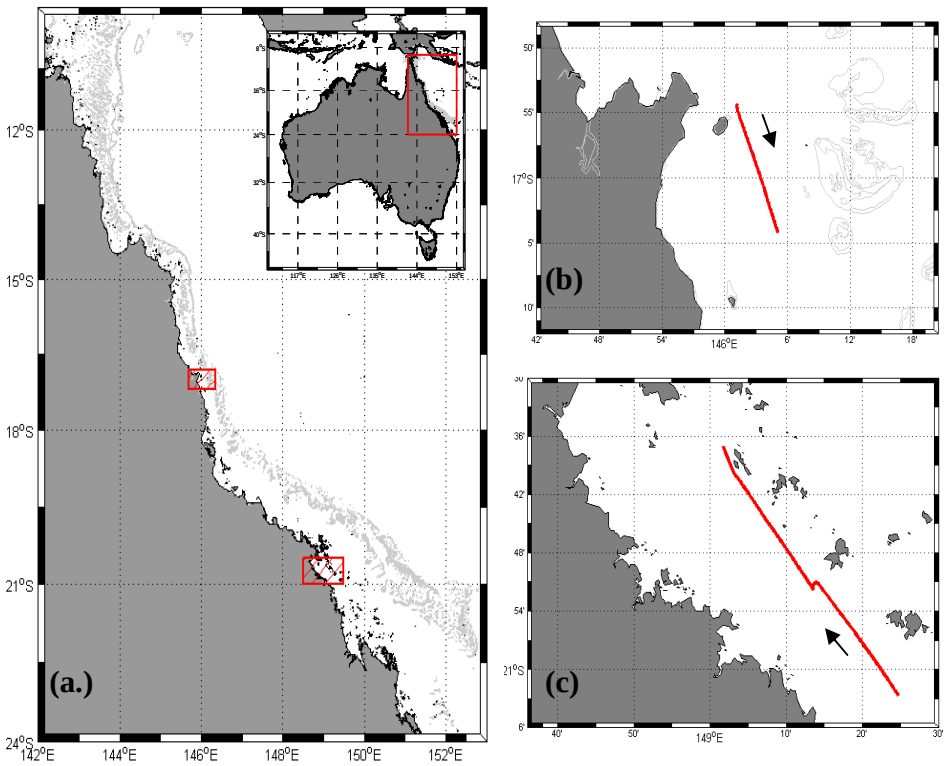

Figure 3.1: (a) Map of the Great Barrier Reef region adjacent to the Northeast Australian Coastline with the Cairns and Mackay/Whitsunday study regions boxed in red. (b) A 17 km long southeast transect within the Cairns region on the 27 April, 2007 and (c) the northwest 38 km long transect within the Mackay/Whitsunday region on the 31 July 2008.

3.2.2 Hyperspectral ship-borne above-water radiometry

There are few *in situ* radiometric field observations of *Trichodesmium* within the literature. Desa et al. (2005) used a vertical profiling, spectroradiometer to make multi-spectral, radiometric measurements of *Trichodesmium*. Desa et al. (2005) however, noted difficulties in obtaining radiometric measurements for a surface aggregation of *Trichodesmium*. This was because on immersion of the profiling instrument, the surface layer of *Trichodesmium* began to break up substantially. Thus, characterising the surface layer radiometrically was difficult. In this study, radiometric measurements were collected above *Trichodesmium* aggregations using a boom-mounted, above-water radiometer from the bow of the vessel. As a result of the boom mounting, the radiometer observed undisturbed water located ahead of the ships bow-wake. The above-water radiometer provided under-atmosphere data with a high spatial and spectral resolution.

During 12 February 2007 and again on 31 July 2008, radiometric measurements were made over dense surface aggregations of *Trichodesmium* (> 10 mg Chla m^{-3}) along the Cairns and Mackay/Whitsunday Transects respectively. Hyperspectral water-leaving radiance and remote sensing reflectance spectra were derived from the radiometric measurements made. The three-channel, above-water radiometer was comprised of three NIST-traceable calibrated spectrometers each with a 2 nm resolution over a 380 - 900 nm spectral range. The instrument simultaneously measured downwelling irradiance (E_d), upwelling radiance (L_u) and sky radiance (L_{sky}) at a given wavelength (λ) along a transect. Radiometric measurements were made during calm surface conditions with light winds to avoid whitecaps and reduce excessive sky radiance contamination. To maintain a stable orientation relative to the ship's pitch and roll, the radiometer was gimbal mounted.

The L_u spectrum collected at the detector was a combination of both water-leaving radiance, L_w, and a small fraction, ρ, of L_{sky} reflected from the surface (Mobley 1999). To derive the parameter of interest, L_w, the following equation was used,

$$L_w(\lambda) = L_u(\lambda) - \rho L_{sky}(\lambda) \qquad [\mathrm{W\,m^{-2}nm^{-1}sr^{-1}}] \qquad [3.1]$$

where ρ is the correction coefficient for sky radiance (Mobley 1999). The value of ρ is dependent on wind speed, solar zenith angle, cloud cover and viewing geometry (Mobley 1999) therefore, this ancillary data was recorded during transects. When calculating L_w, the ancillary data was used to select an appropriate value of ρ from a look-up-table (LUT) (Slivkoff et al. 2006). The ρ LUT was derived using Hydrolight radiative transfer simulation software (Slivkoff et al. 2006) which can be found in Appendix 1. The above-water remote-sensing reflectance was then calculated using Mobley's ad hoc formula (Mobley 1999)

$$R_{rs}(\lambda) = L_w(\lambda)/E_d(\lambda). \qquad [\mathrm{sr}^{-1}] \qquad [3.2]$$

The viewing angles of the L_u and L_{sky} sensors were set to 40° off nadir and 40° off zenith respectively in accordance with recommendations of the Ocean Optics Protocols for Satellite Ocean Colour Sensor Validation by Mueller et al. (2003). The azimuthal viewing angle of the radiometer relative to the sun was kept away from sunglint and ship shadow, and periodically centred close to an angle of 135° by adjusting the orientation of the instrument as ship heading and solar angles varied (Mueller et al. 2003; Slivkoff et al. 2006). Wind speed and solar zenith angle varied throughout the sampling days, this adds to approximately 5% uncertainty in the ρ value used at any particular time (Slivkoff, pers. comm). This 5% uncertainty on ρ can contribute up to 0.5% on the sea radiance at the worst case (Slivkoff, pers comm.). Often the relative sun-instrument azimuthal angle varied by approximately +/-30° during the course of measurements as a consequence of unavoidable sunglint or ship shadow. This variation in viewing geometry was considered to have a minimal effect on the derived R_{rs} values. To illustrate this, an R_{rs} spectrum was derived with fixed parameters for determining ρ except the sun-instrument viewing angle which was allowed to vary by +/-30°. Table 3.1 illustrates the mean absolute percentage error (MAPE) of four R_{rs} spectra derived for relative sun-instrument azimuthal viewing of 105, 120, 150 and 165° compared with a R_{rs} derived using the recommended 135°. Table 1 shows the MAPE in R_{rs} does not to exceed 0.03%. This indicates that varying the sun-instrument viewing angle +/-30° from 135° will impart only a minimal effect on the R_{rs} spectra.

Table 3.1: The mean absolute percentage error of four R_{rs} spectra derived with ρ varying as a function of sun-instrument viewing angle +/-30° either side of 135° only.

Relative Azimuthal Angle	MAPE
105°	0.027 %
120°	0.027 %
150°	0.024 %
165°	0.027%

Figure 3.2: Photograph of the above-water, hyperspectral radiometer collecting data over *Trichodesmium* windrows along the Cairns Transect on the 27 April, 2007.

3.2.3 Hyperspectral water-leaving radiance and remote-sensing reflectance data

Hyperspectral, above-water L_w and R_{rs} transect data recorded over *Trichodesmium* surface aggregations are shown in Figure 3.3. The most notable spectral feature of L_w and R_{rs} spectra is the red-edge effect where low reflectance occurs at 680 nm and higher reflectance occurs at wavelengths longer than 700 nm. The spectra shown in Fig 3A and Fig 3C exhibit behaviour consistent with the laboratory R_{rs} measurements performed in Petri dishes by Dupouy et al. (2008), and similar to those of Borstad et al. (1992) who concentrated *Trichodesmium* on GF/F filters. The L_w and R_{rs} spectra exhibit troughs due to strong Chl-a absorption at 437 and 680 nm, and absorption by PUB, PEB, PEC and PC at about 497, 547, 571 and 633 nm respectively. A small absorption dip appears at about 470nm and can be attributed to carotenoid pigments.

The L_w and R_{rs} spectra (Fig 3A, 3C) show notable peaks at about 460, 477, 527, 561, 593 and 647 nm, all of which are smaller than the reflectance peak exhibited at wavelengths longer than 700 nm. The peak at 593 nm agrees with observations by Borstad et al. (1992) and Dupouy et al. (2008). The small peak at 561 nm may be a consequence of PEB fluorescence which for *Trichodesmium thiebautti* occurs at 558±2 nm, and 558±2 nm with a shoulder at 681 nm for *T. erythraeum* (Neveux et al. 2006). Weak reflectance peaks around 565 and 660 nm corresponding to PEB and PC fluorescence were mentioned by Dupouy et al. (2008).

The above-water remote sensing reflectance spectra, R_{rs}, of *Trichodesmium* dominated waters was modelled by both Borstad et al. (1992) and Subramaniam et al. (1999b) using absorption, a, and backscattering, b_b, coefficients. Values of R_{rs} were calculated with the the following relationships

$$R_{rs}(\lambda) = k\left(\frac{b_b(\lambda)}{a(\lambda)}\right) \qquad [\mathrm{sr}^{-1}] \qquad [3.3]$$

Borstad et al.(1992) used k = 1076, whereas Subramaniam et al. (1999b) used k = 0.1079. In the investigation of Borstad et al. (1992), the spectral absorption coefficient of *Trichodesmium*, $a_{tri}(\lambda)$, was measured spectrophotometrically and the spectral backscattering coefficient, $b_{b\,tri}(\lambda)$ was estimated spectrophotometrically from a

sufficient amount of *Trichodesmium* deposited on a glass fibre filter. Values of $a_{tri}(\lambda)$ used by Subrmaniam et al. (1999b) were measured spectrophtometrically, whereas, $b_{b\,tri}(\lambda)$ was determined using a custom made instrument.

The modelled spectra of Subramaniam et al. (1999b) and Borstad (1992) showed high reflectance above 700nm and peaks at about 460, 560, 593 and 645 nm similar to results observed in this investigation and that of Dupouy et al. (2008). Conversely, the observed reflectance spectra of this investigation exhibit peaks at about 527 nm and troughs at 547 and 671 nm which are not present in the modelled spectra of Borstad et al. (1992) and Subramaniam et al. (1999b). The model of Borstad et al. (1992) included an approximation for solar-stimulated Chla fluorescence emission at 680 nm, whereas the model of Subramaniam et al. (1999b) did not. Furthermore, both models did not include solar-stimulated fluorescence emissions by the phycobilin-pigments. Because the absorption coefficients of *Trichodesmium* were well parameterised in both studies, these differences are most likely attributed to the parameterisation of backscattering and fluorescence in the reflectance models.

The measurements of remote sensing reflectance made using the hyperspectral, above-water radiometer are consistent with those measured carefully under laboratory conditions. Past efforts to capture the spectral signatures of floating surface aggregations of *Trichodesmium* in situ have proven difficult. Therefore, the ship-based, boom-mounted method has been identified as an excellent way to detect subtle changes in spectral reflectances along a horizontal transect.

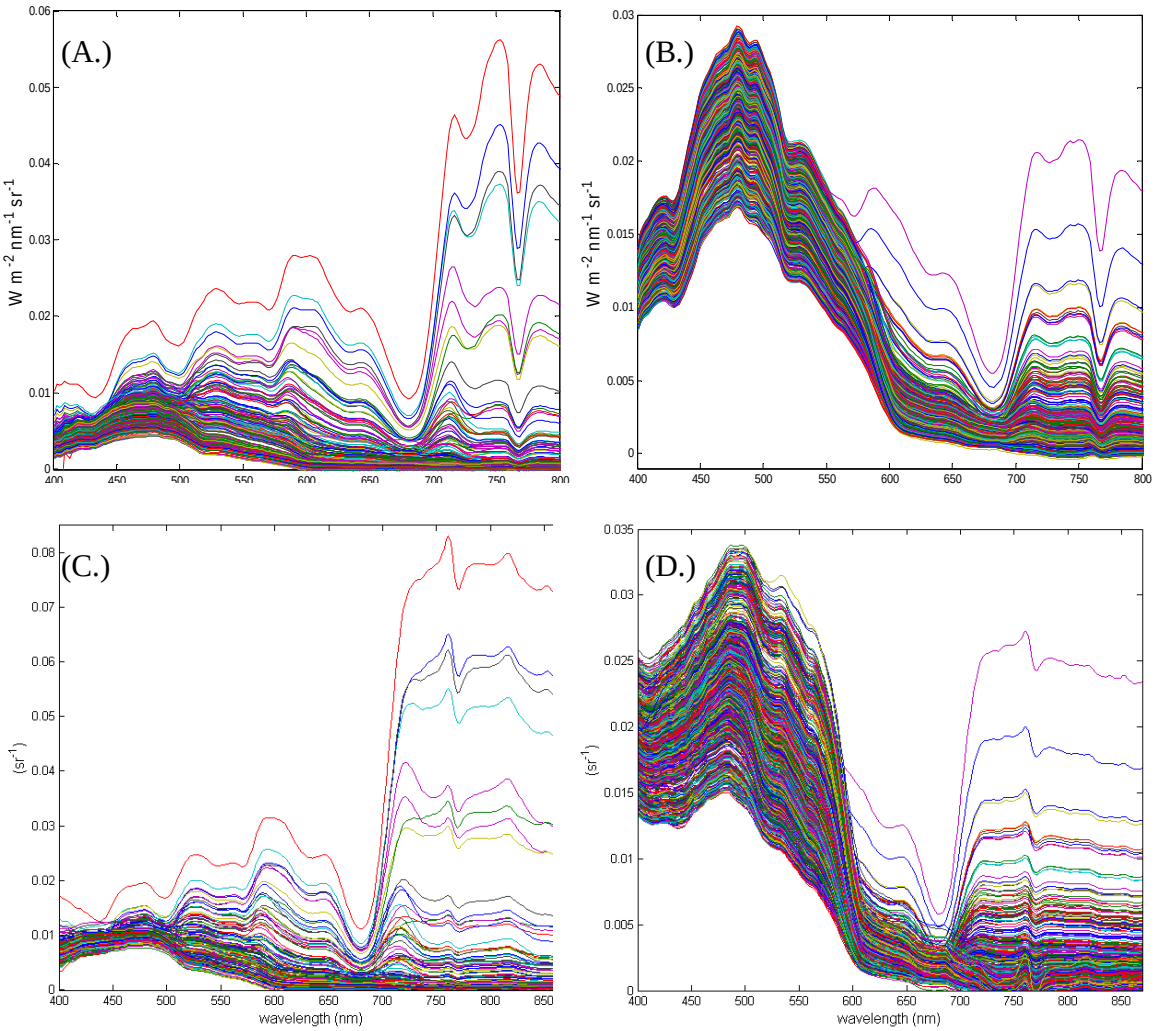

Figure 3.3: Hyperspectral, water-leaving radiances L_w for dense surface aggregations of *Trichodesmium* observed along (A.) the Cairns Transect and (B.) the Mackay/Whitsunday Transect. The corresponding hyperspectral, remote-sensing reflectance R_{rs} spectra for (C.) the Cairns Transect, and (D.) the Mackay/Whitsunday Transect.

3.2.4 MODIS high resolution imagery

High resolution (250 m), level-2 (L2), MODIS normalised water-leaving radiances (nLw) were derived from Level-0 (L0) data obtained from NASA's Ocean Color Web (http://oceancolor.gsfc.nasa.gov/). The SeaWiFS Data Analysis System (SeaDAS) (Baith et al. 2001) Multi-Sensor Level-1 to Level-2 (MSL12) code was used to process the 250 m resolution MODIS bands and then bi-linearly interpolate the 1 km and 500 m bands to provide a full set of bands with quasi-250 m resolution (Franz et al. 2006; Gumley et al. 2010). Of all the MODIS bands, only the 645 and 859 nm bands have a true spatial resolution of 250 m (Franz et al. 2006). Therefore, a derived L2 product must rely upon the 645 nm and/or 859nm bands to be truly considered a 250 m resolution product (Franz et al. 2006).

The standard method for atmospheric correction in SeaDAS is based upon the assumption that the NIR contribution to the water-leaving radiance spectrum is zero (Gordon and Wang 1994). However, in turbid coastal waters the NIR contribution is typically non-zero. Thus for turbid coastal regions the standard atmospheric correction does not perform well and underestimates the nLw values (Wang and Shi 2007). An atmospheric correction that is based upon the short-wave infrared (SWIR) has been shown to be suitable for coastal regions (Wang and Shi 2005). However the SWIR band of MODIS is characterised by a low signal-to-noise ratio which can introduce uncertainties (Wang and Shi 2007). Therefore it is recommended that SWIR be used only for turbid, coastal water pixels and the NIR method be used elsewhere. As such, an algorithm has been developed by Wang and Shi (2007) that can switch between the SWIR and NIR corrections by identifying pixels with non-zero NIR reflectance. The Wang and Shi (2007) NIR-SWIR atmospheric correction has been evaluated using the SeaWiFS Bio-optical Archive and Storage System (SeaBASS) global validation data set, (Wang et al. 2009). Wang et al (2009) derived L2 MODIS products (K490, Chl-a, nLw at 412,443, 488, 531, 551 and 667 nm) using the standard NIR, SWIR and combined NIR-SWIR atmospheric corrections. These results were then compared with corresponding *in situ* data from the SeaBASS data set. The results of the Wang et al. (2009) matchup analysis indicate that the combined NIR-SWIR switching algorithm

yields overall improved results. Therefore, the Wang and Shi (2007) NIR-SWIR switching algorithm has been used to derive L2 products in this study.

True-colour, red-green-blue (RGB) images were derived with SeaDAS using the 645, 555 and 469 nm wavebands. L2 processing masks were applied for contamination from land, cloud, stray light, glint and high total radiance. Pixels corresponding with large solar zenith and large sensor zenith angles were also masked during processing. The bathymetry of the northern and central GBR seldom exceeds 30 m and approximately 50% of the entire GBR is 30 m or less in depth (Wolanski 1994; Lewis 2001). The SeaDAS L2 shallow water mask flags pixels with a bathymetry less than 30 m and excludes them from data processing. Thus, the shallow water mask was deactivated.

3.2.5 Classification Algorithm

A simple, binary classification scheme was developed to identify the presence or absence of dense *Trichodesmium* surface aggregations based upon a set of selection criteria. The hyperspectral L_w data indicated that dense concentrations of *Trichodesmium* exhibit the red-edge reflectance feature described by Borstad et al. (1992). For this reason the first classification criteria was based on the difference in magnitude between L_w at about 680 nm and wavelengths longer than 700 nm. On investigating MODIS bands, it was found that normalised water-leaving radiance for 859 nm nLw(859), exhibited a strong signal for regions of dense *Trichodesmium* and the magnitude of the nLw(675) band was small and often near zero. The relative magnitudes between nLw(859) and nLw(678) MODIS wavebands were thus used as the first criteria in the algorithm.

$$\text{Criteria 1:} \quad nLw(859) > nLw(678). \qquad [3.4]$$

The hyperspectral radiometric data over *Trichodesmium* surface aggregations showed L_w was greater in magnitude at 555 nm (green) and 645 nm (orange/red) when compared with 678 nm. Consequently the second and third criteria used in the MODIS classification algorithm were:

$$\text{Criteria 2:} \quad nLw(645) > nLw(678), \text{ and} \qquad [3.5]$$

Criteria 3: nLw(555) > nLw(678). [3.6]

If criteria 1, 2 and 3 were all satisfied, a pixel was flagged as containing a surface aggregation of *Trichodesmium*. A fourth criterion was also introduced to discard pixels associated with negative nLw values.

Criteria 4: Disregard pixel if nLw(555), nLw (645), nLw (678) or nLw (859) < 0.

The influence of criteria 1, 2 and 3 on the final result was examined. Pixel flagging from criteria 1 alone and combinations of criteria 1 and 2, criteria 1 and 3 and 2 and 3 were considered. The results of this analysis are presented in Figure 4, based upon a MODIS Aqua image captured on 27 April 2007. The RGB true-colour image of the region shows a highly reflective vertical streak feature corresponding to dense *Trichodesmium* surface aggregations which were observed earlier that day whilst collecting hyperspectral radiometric data along the Cairns Transect (Figure 2b). The combined result of applying all three criteria in the classification scheme is presented in Figure 4b. The red pixels (Figure 4b) denote areas classified as containing dense *Trichodesmium* surface aggregations. It is evident that criteria 1, which is based upon the red-edge effect is the dominating component of the algorithm (Figure 4c). However, criteria 1 appears to flag pixels which are unlikely to be *Trichodesmium* located immediately adjacent to the coast and the fringing coral reef of Fitzroy Island (circled features Figure 4c). The combination of criteria 1 and 2 (Figure 4d) and criteria 1 and 3 (Figure 4 e) together appear to eliminate most of the near-shore, falsely flagged pixels. Therefore, both criteria 2 and 3 are deemed useful for removing near-shore, highly reflective pixels.

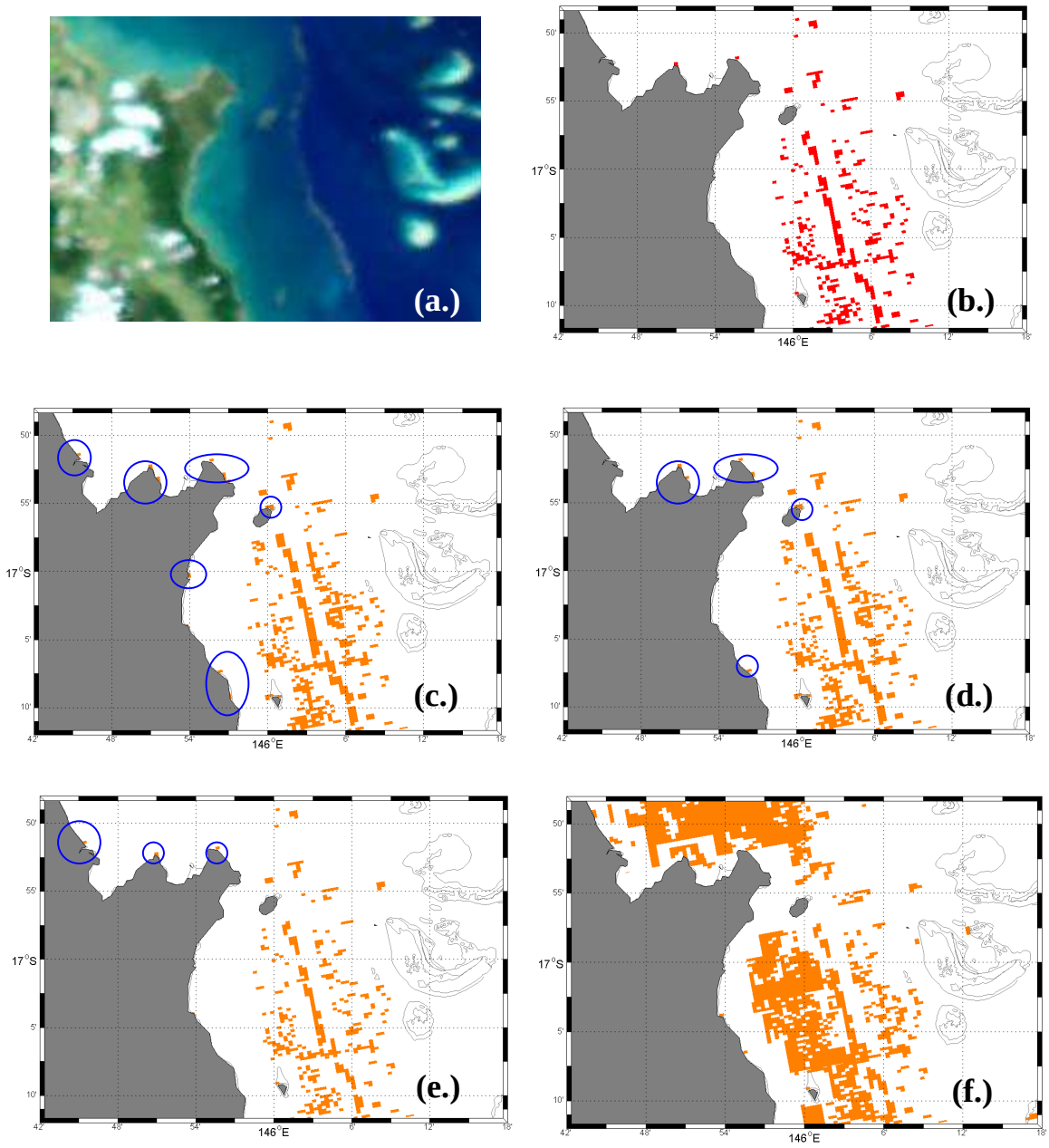

Figure 3.4: (a.) MODIS Aqua RGB true-colour image of the Cairns region captured on the 27 April, 2007. (b.) The result of the binary classification algorithm is plotted in red denoting regions of dense *Trichodesmium* surface aggregations. (c.) The result of criteria 1 alone (d.) The result of classification criteria 1 and 2, (e.) the result of classification criteria 1 and 3, and (f.) the result of classification criteria 2 and 3. Blue circles surround flagged pixels that are immediately adjacent to the coast.

3.2.6 Comparison of MODIS and Hyperspectral Rrs

In order to determine how well spectral features observed in the hyperspectral R_{rs} are represented in MODIS data a brief comparison between the two data sets was performed. For illustrative purposes four points along the Cairns Transect were examined. The four points α, β, γ and δ identified in Figure 5a correspond with the following: (α) no *Trichodesmium* evident, (β) very dense *Trichodesmium* surface aggregation with complete surface cover, (γ) moderate patches of *Trichodesmium* on the surface and, (δ) patchy, disperse surface aggregations of *Trichodesmium*. Unfortunately no chlorophyll or cell count data was available to normalise these observations to give a quantitative measure.

The comparison in Figure 5 shows that for the dense surface aggregations at location β, MODIS data (Figure 5b) exhibits a distinct NIR reflectance similar to that of the hyperspectral data (Figure 5c). The MODIS NIR reflectance is however, almost an order of magnitude less than that of the hyperspectral NIR reflectance. This is likely a consequence of the low signal-to-noise ratio exhibited by the 859 nm MODIS band. Nonetheless, for the moderate surface aggregations at location γ an increase in the magnitude of the MODIS NIR reflectance is evident. Although the shape and magnitude of the MODIS and hyperspectral R_{rs} spectra are similar, it is clear that MODIS underestimates the reflectance over extremely dense surface aggregations of *Trichodesmium*. This may partly be caused by spatial patchiness of the *Trichodesmium* within the MODIS pixel. It is also evident the degree of spectral information is not captured by MODIS. Worthy of note are the negative water-leaving radiance values at location γ. This effect is likely to be a consequence of an inappropriate atmospheric correction for this pixel.

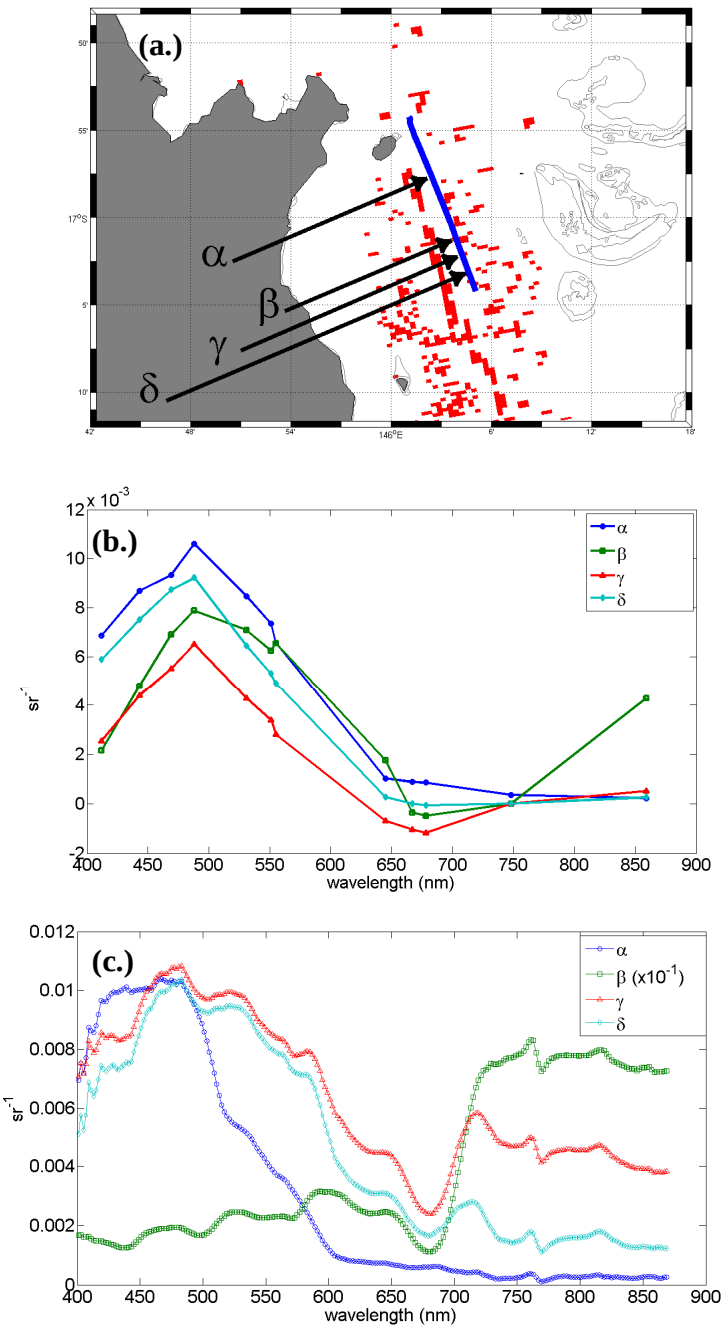

Figure 3.5: (a.) Four points α, β, γ and δ along the Cairns Transect were used to compare (b.) MODIS R_{rs} with (c.) hyperspectral above-water radiometer R_{rs}. Note that in (C.) the R_{rs} spectra for location β has been scaled by 10^{-1}.

3.3 Model Assessment

3.3.1 Validation of Algorithm

Algorithm performance was evaluated by sea-truthing the MODIS results with ships-of-opportunity sightings of dense *Trichodesmium* surface aggregations substantial in spatial extent, preferably in the order of ~10-100 m. Sparse, patchy observations of *Trichodesmium* were discarded from the match-up dataset. Observations with accompanying cloud cover and those which were within 1km of shoreline, islands or coral reefs and risked spectral contamination were also discarded. Table 3.2 details dates, times and geographic co-ordinates of 13 reported cases used in the algorithm validation. The sampling strategies for ocean colour validation match-up require sampling to occur within a few hours of overpass (Mueller 2003). However, because the *Trichodesmium* sightings recorded were not done for algorithm validation purposes, the observation times were often not within a few hours of MODIS overpass. Thus, the definition of a match-up between the MODIS algorithm and a *Trichodesmium* observation was relaxed as follows: Regardless of the sea-truth observation time, the MODIS Aqua image for that day was utilised. A generous match-up radius of 10 km (approximately 40 pixel radius) from the point of observation was used. The 10 km match-up radius was deemed broad enough to factor in wind and surface current movement of a surface aggregation between the time of observation and MODIS flyover time. In the event that no MODIS Aqua imagery was available for a given date due to lack of flyover or cloud cover, a suitable image ±1 day either side of a sea-truth observation was used.

For algorithm validation purposes of this study, a positive match-up (+) was defined as when the algorithm detected *Trichodesmium* and the result was consistent with sea-surface observations. Conversely, a negative match-up (-) occurred where a *Trichodesmium* sea-truth was observed and the algorithm failed to identify it. The resulting number of positive match-ups from a possible of 13 was 11, yielding an 85% correct classification (Table 3.2). The number of negative match-ups was 2 from 13 indicating the algorithm failed on 15% of cases. The two negative match-up observations 8 and 11 (see Table 2) were recorded as “patchy, medium dustings of *Trichodesmium*”.

For observations 8 and 11, it is possible the *Trichodesmium* surface patches were of sub-pixel spatial scales (< 250 m). Therefore, the water-leaving radiances were likely a spectral average of *Trichodesmium* and adjacent water. Thus for observations 8 and 11, the spectral characteristics of a *Trichodesmium* surface aggregation such as the red-edge may not have been detectable using the MODIS 250m resolution data.

When inspecting the validation imagery, the suitability of applying the high total radiance mask across all bands was considered. Of concern was the mask potentially removing pixels containing dense *Trichodesmium* surface aggregations. However, when examining the validation images the activation of the mask appeared only to eliminate highly reflective features such as islands, beaches and some coral reef structures.

3.3.2 Sensitivity Analysis

The sensitivity of criteria 1 of the binary classification algorithm was examined using a modified version of criteria 1:

$$\mathrm{nLw}(859) > c_1\,\mathrm{nLw}(678) \qquad [3.7]$$

where the parameter c_1 represents the magnitude of the reflectance peak of the 859 nm waveband relative to the minimum at the 678 nm waveband. Within the binary classification algorithm c_1 has a typical value of to 1 (equation 3.4). Generally for waters with a near-zero NIR reflectance contribution, c_1 is very small (<< 0.01). Figure 3.6 represents the response of criteria 1 as the value of c_1 is varied scene-wide from 0.01 – 10. As the value of c_1, increases from 0.01 towards 1, the total number of pixels flagged decreases. However once c_1 is greater than 1 the number of pixels flagged remains almost constant. The analysis therefore shows that criteria 1 are quite robust to variations in the parameter c_1 provided that c_1 is greater than 1.

Table 3.2: Time, dates and coordinates of *Trichodesmium* surface aggregations observed within the Great Barrier Reef for which the binary classification algorithm was applied. A positive match-up is denoted with a "+" and a negative match-up is denoted with "-" for each location.

Observation Number	**Date**	**Time**	**Latitude**	**Longitude**	**MODIS Date**	**Algorithm Match-up**
1	27/01/2005	NA	20°43.066'S	149°00.36'E	27/01/2005	+
2	27/04/2007	0940	16°12.720'S	145°37.494'E	27/04/2007	+
3	27/04/2007	1100	16°23.688'S	145°40.626'E	27/04/2007	+
4	27/04/2007	1500	16°54.312'S	146°01.116'E	27/04/2007	+
5	04/10/2007	0950	23°13.218'S	150°56.3400'E	03/10/2007	+
6	31/07/2008	1140	20°55.962'S	149°18.834'E	31/07/2008	+
7	30/09/2008	1215	16°47.100'S	145°50.640'E	30/09/2008	+
8	06/10/2008	0720	22°39.038'S	150°59.119'E	06/10/2008	-
9	14/11/2008	1415	18°33.644'S	146°30.082'E	15/11/2007	+
10	16/02/2009	1220	22°02.810'S	150°29.759'E	15/02/2009	+
11	18/02/2009	1503	21°39.720'S	151°04.514'E	18/02/2009	-
12	11/06/2009	1430	19°39.677'S	148°00.979'E	11/06/2009	+
13	30/06/2009	NA	19°52.752'S	148°09.540'E	30/06/2009	+

Positive Match-up = 85%, Negative Match-up = 15%

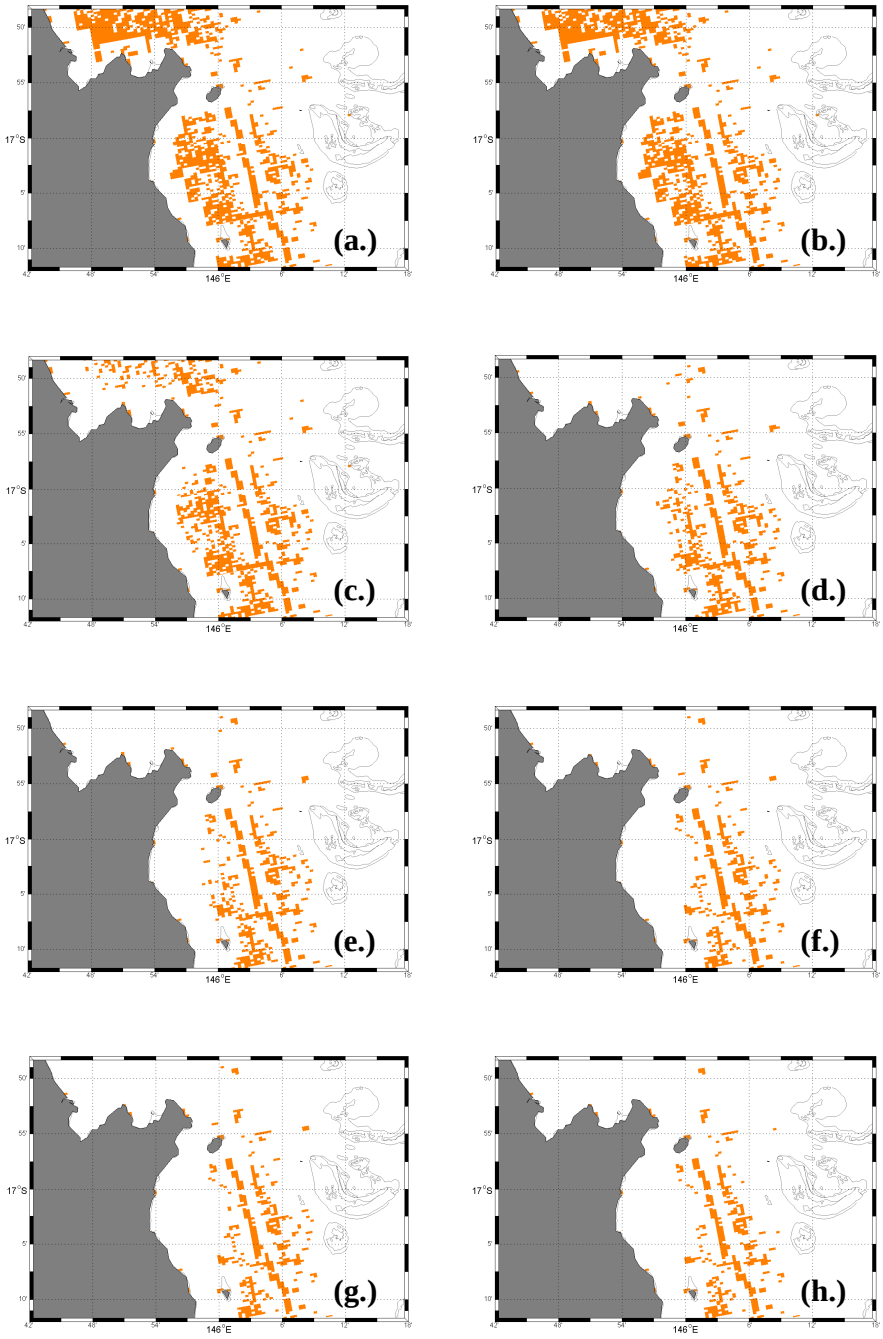

Figure 3.6: Sensitivity analysis of the classification criteria nLw(859) > c_1 nLw(678), where c_1 = 0.001, 0.01, 0.1, 0.5,1, 5, 10, and 100 corresponding to (a.), (b.), (c.), (d.), (e.), (f.), (g.) and (h.).

3.3.3 Confounding Effects

The binary classification algorithm was tested alongside the potential confounding effects discussed by Subramaniam et al (2002). A MODIS Aqua scene was selected that contained *Trichodesmium* in the presence of shallow bathymetry, high suspended sediments, high CDM, coral reefs and other phytoplankton.

The selected MODIS test image was from 28 January 2005 and is shown in Figure 3.7a. Several days prior to this date, a series of high rainfall events caused river flood plumes from the Proserpine [20°29'S, 148°43'E] and O'Connell [20°34'S, 148°40'E] river mouths to extend into the Whitsunday/Mackay region of the GBR (Rohde et al. 2006). Sampling of the flood plume event was conducted by the Australian Centre for Tropical Freshwater Research (ACTFR) on 27 January 2005. Extremely dense surface aggregations of *Trichodesmium* were reported during ACTFR sampling. A single surface sample collected at 20°43.062'S, 149°00.360'E yielded extremely high Chl-a concentrations due to *Trichodesmium* of 2300 mg Chla m^{-3} (Rohde et al. 2006). After running the binary classification algorithm on the MODIS image, the result was plotted in red over the RGB true-colour image (Figure 3.7b). The streaky spatial patterns exhibited in Fig 7B are consistent with the observations of Rohde et al. (2006) within the sampling site. It is interesting to note that the pixels classified as *Trichodesmium* were in highest concentration at the boundary zones of the river plume fronts.

Pixels in the region of potential confounding effects including: coral reefs, other phytoplankton, high suspended sediment and high levels of CDM were not misclassified as *Trichodesmium*. Regions of shallow bathymetry adjacent to the coastal zone, islands and coral reefs contained approximately 5% of the all pixels identified as surface aggregations of *Trichodesmium* by the algorithm. Of the 5 % of pixels flagged in regions of shallow bathymetry, the coastal region contained 0.2 %, the coral reefs contained 0.5 % and regions surrounding the islands where *Trichodesmium* was observed (Rohde et al. 2006) contained 4.3 %. However, of the 0.7 % of pixels flagged in the shallow coastal zone and in the vicinity of offshore coral reefs, there were no corresponding sea-truth observations. Thus, we cannot conclusively say that flagged pixels in those regions were truly false-positives. These results indicate the algorithm is suitable for use within the

GBR with minimal risk of being contaminated by the confounding effects discussed by Subramaniam et al. (2002). One potential confounding effect which was not tested was mass coral spawning. Surface slicks of coral spawn typically occur within the GBR during October-November and consist primarily of coral eggs and larvae (Oliver and Willis 1987). Coral spawn appears as white/pink surface streaks that are up to 5 km in length and 10m in width (Oliver and Willis 1987). However, coral spawn lacks strongly absorbing photosynthetic pigments. The large absorption due to Chl-a absorption at 678 nm should not be as pronounced within coral spawn as with *Trichodesmium*. Mass coral spawning events within the GBR occur during the night over a two month period late in the year (October-November). The events are sporadic, occurring for different times for different locations along the GBR (Negri, pers comm.). Surface aggregations of coral spawn are typically visible for around 24-36 hours after which time the larvae lose their buoyancy and descend (Negri, pers comm.). The remaining surface aggregates are then dispersed by predator feeding activity and physical processes (Negri, pers comm.). Events are generally geographically localised within the coral reefs and there is no literature to suggest that mass coral spawning could occur with the same spatial extent as massive *Trichodesmium* surface aggregations such as those described within the Capricorn Channel by Kuchler and Jupp (1988). Therefore, if the time scale and geographical localisation of mass coral spawning are considered, false-positive retrievals may be manageable with some degree of confidence, although this warrants further investigation.

It is also conceivable that other types of phytoplankton could potentially cause the algorithm to flag a pixel as containing *Trichodesmium*. For example cyanobacteria or dinoflagellate aggregations such as those forming red-tides in other parts of the world may be flagged by the classification algorithm described in this paper. However, phytoplankton surveys conducted within the GBR region have not identified the existence of other surface aggregation-forming phytoplankton in significant quantities (Revelante and Gilmartin 1982). This is thought to be a consequence of the relatively nutrient poor conditions within the GBR which are not suitable for the growth of large populations of phytoplankton other than *Trichodesmium*. Thus, based upon this knowledge of phytoplankton abundance and variability within the GBR, a false-positive retrieval due to

other phytoplankton seems unlikely. However, caution must be taken if attempting to apply this method for *Trichodesmium* detection in other regions of the world which contain surface aggregation forming phytoplankton with a L_w red-edge such as those discussed by authors such as Dierssen et al. (2006) and Kutser (2004).

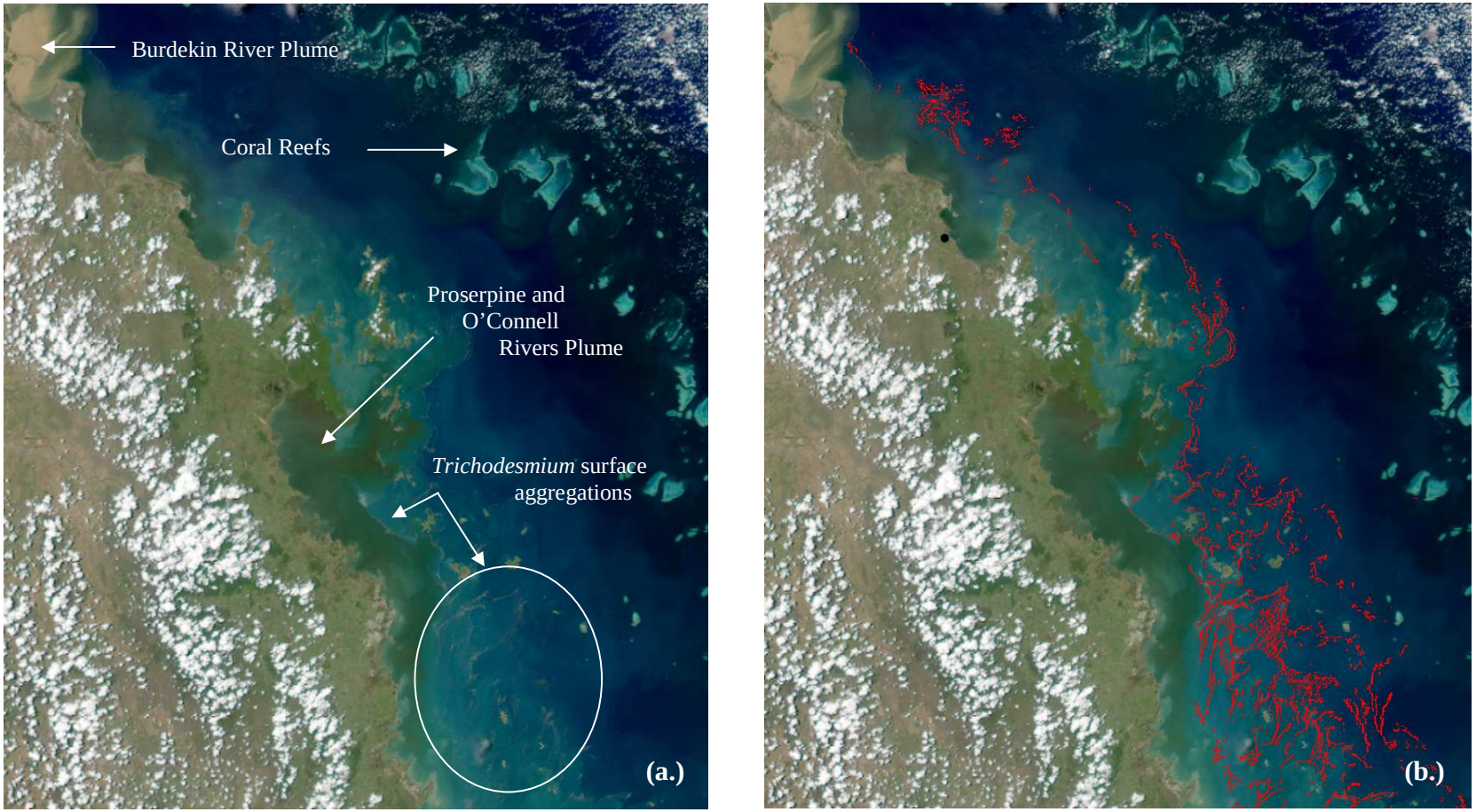

Figure 3.7: (a.) A true-colour RGB MODIS-Aqua image of the Whitsunday/Mackay region of the Great Barrier Reef from 27 January 2005. At the centre of the image is a river plume from the Pioneer and O'Connell Rivers and toward the top of the image is a high suspended sediment plume from the Burdekin River. Brown-red streaks are evident at the edge of the Pioneer/O'Connell River Plume and were identified as *Trichodesmium* spp. by Rohde et al. (2006). (b.) Results of the *Trichodesmium* binary classification algorithm plotted in red over the original true-colour RGB image.

3.3.4 Application: The Capricorn Channel and Southern Great Barrier Reef

The Capricorn Channel (22°30'S, 152°30'E), in the Southern GBR is a region where photography from NASA's Space Shuttle and the International Space Station have recorded large surface aggregations of plankton, which were later inferred to be *Trichodesmium* (Kuchler and Jupp 1988; Image Science and Analysis Laboratory 2002). As an application of the binary classification algorithm, a MODIS Aqua image from the Capricorn Channel on 17 October 2007 was selected. *Trichodesmium* surface aggregations are known to manifest in eddy swirls, parallel wind rows and convergence zones. The unprojected, true-colour MODIS Aqua image (Figure 3.8a) exhibited orange/brown spatial features consistent with those of *Trichodesmium*. The binary classification scheme was applied to the data and the results were plotted in red over the RGB true-colour image as shown in Figure 3.8b. The algorithm result indicated an extremely large surface distribution of *Trichodesmium* in the Capricorn Channel and the Northern section of Shoalwater Bay (21°30'S, 149°30'E) spanning a region in the order of 100,000 km^2. Unfortunately, due to a lack of sea truth data, this result was not definitive. However, it was reasonable to infer that the algorithm is identifying *Trichodesmium* when examining the fine spatial structures such as swirls and parallel lines which were mapped in the result (see Figure 3.8b).

Figure 3.8: (a.) A true-colour RGB MODIS-Aqua image of the Capricorn Channel region of the GBR captured on 17 October 2007. (b.) Results of the *Trichodesmium* binary classification algorithm plotted in red over the original true-colour RGB image.

3.4 Discussion

In this paper a simple method for detecting the presence or absence of *Trichodesmium* surface aggregations within the GBR region using MODIS imagery has been developed. This is an important contribution to a series of scientific works required to map *Trichodesmium* abundance on a global scale.

The binary classification algorithm correctly matched 11 out of 13 sea-truth observations thereby yielding an 85 % accuracy. Spatial features corresponding to distributions of *Trichodesmium* surface aggregations were also well represented due to the 250x250m spatial resolution of the MODIS data. This result indicates the algorithm performed well when detecting dense patches of *Trichodesmium* that dominated the water-leaving radiance of a pixel. However, sparse, patchy surface distributions of *Trichodesmium* that had sub-pixel spatial scales (< 250 m) were unlikely to be detected by the algorithm. It should however, be noted that of the four MODIS nLw bands used in the algorithm, only the two centred on 645 and 859 nm had a true spatial resolution of 250 m. The MODIS nLw bands centred on 555 and 678 nm have spatial resolutions of 500 m and 1 km respectively. Thus, bilinear interpolation was performed using SeaDAS processing to derive a set of co-registered bands with quasi 250 m pixel resolution. This effect may limit the robustness of the binary classification scheme described in this article. We would expect the binary classification scheme to perform well on sensors such the Ocean Colour Monitor (OCM-2) and MERIS which have local area coverage (LAC) pixel resolutions of 360 m and 300 m respectively across all bands.

The algorithm was found to be robust in the presence of potentially confounding effects such as shallow bathymetry, coral reefs, other phytoplankton, high CDM and high suspended sediment. However, annual mass coral spawning which manifests on the surface in a similar manner to *Trichodesmium* may yield false positives. Bio-optical and radiometric characterisations of coral spawn aggregations are required to further investigate this issue. However, it is likely that the absence of strongly absorbing chlorophyll pigments within the coral spawn mean that there will be no red-edge effect as seen in the water-leaving radiance of *Trichodesmium*. Much effort has also been placed upon identifying surface aggregations of *Trichodesmium* for the purpose of algorithm validation. However, further work is required to identify

situations in which false-positive retrievals occur. This will require a comprehensive library of non-*Trichodesmium* pixels to be compiled. Such analysis will allow for further improvement of the binary classification algorithm and increased confidence in MODIS-derived abundance maps of *Trichodesmium*.

The lack of other large-scale, surface aggregation forming phytoplankton in the GBR means that pixels identified using this algorithm will typically be *Trichodesmium*. It is therefore important to note that the algorithm described in this paper may be unsuitable for regions outside the GBR where it may be confounded by other red-tide forming phytoplankton. However, this may not necessarily be viewed as a negative outcome. It is conceivable that with further work the classification algorithm could be used for the detection and monitoring of red tides and harmful algal blooms (HABs) which manifest in a similar fashion to *Trichodesmium* and have similar optical properties.

Having established the potential to clearly define dense surface slicks using MODIS imagery the next challenge is to determine the algorithm's lower limit of detectability and attempt to provide quantitative data regarding abundance. However, adequate *in situ* measurements of cell counts and corresponding chlorophyll-a concentration is required. With a substantial quantitative *in situ* data set, an assessment of the algorithms accuracy can be performed. A suitable procedure is outlined by Tomlinson et al (2004) whereby *in situ* data and algorithm results are compared giving the percentage of confirmed positive, confirmed negative, false-positive and false-negative retrievals. First however, strategies for sampling dense surface aggregations of *Trichodesmium* must be carefully considered.

Contemporary *in situ* sampling methods must be carried out with careful measurements to ensure the fine surface layer structure is not overly disturbed. Conversely, the use of flow-through chlorophyll fluorometers can provide fine spatial resolution of chlorophyll-a concentration along transects. However, flow-through systems remain problematic with relatively clean water pumped from intakes often 1-2m beneath the surface inadequately representing the surface skin layer. Such difficulties in quantitatively sampling surface aggregations of cyanobacteria have also been identified as an issue within the Baltic Sea (Kutser 2009). Kutser et al (2009) states that acquiring a representative, quantitative sample from a dense surface aggregation of cyanobacteria is "nearly impossible." This is due to a combination of uncertainties introduced during sampling. Ship and instrument disturbances destroy

the surface layer and there are inherent difficulties in capturing buoyant cyanobacteria using Niskin bottles and/or buckets (Kutser 2009). Drawing sub-samples for filtration purposes also introduces uncertainties due to a portion of the cyanobacteria being sticky and remaining within the Niskin bottle/bucket (Kutser 2009). Thus, sampling strategies are required which can accurately quantify *Trichodesmium* aggregation on the surface, with an appropriate dynamic range right down to very fine dustings. Such work is currently underway within the GBR, however this task still remains an intractable problem.

Further quantification of the vertical distribution of *Trichodesmium* beneath dense surface aggregations is also warranted to provide a scaling factor which would allow the binary classification algorithm to yield some quantitative results regarding abundance. Surrounding dense surface aggregations a "halo" of dispersed *Trichodesmium* typically exists. Thus, it may be possible to quantify *Trichodesmium* in pixels adjacent to those identified by the binary classification scheme using the Westberry et al. (2005) semi-analytical inversion algorithm where concentrations exceed 3200 trichomes L^{-1}. It is important to note that surface aggregations only represent a fraction of *Trichodesmium* biomass. Therefore a quantitatively complete assessment of *Trichodesmium* abundance requires a synthesis of *in situ* data and information gathered from remote sensing algorithms, both binary classification methods and previous algorithms developed for lower abundances (Westberry et al. 2005; Dupouy et al. 2008b).

In conclusion, the application of the binary classification algorithm described in this paper will be beneficial for quantifying the spatial extent and duration of *Trichodesmium* surface aggregations within the GBR which are poorly documented. Such information will improve *Trichodesmium* N-fixation estimates within the GBR region. The hyperspectral, radiometric features of *Trichodesmium* described in this paper may also be useful for the future development of *Trichodesmium*-specific ocean colour inversion algorithms to be used on a global scale.

This page intentionally left blank.

4 Inversion of hyperspectral remote sensing reflectance for quantitative detection of *Trichodesmium* spp. within the Great Barrier Reef

Abstract

Trichodesmium spp. is a diazotrophic, marine cyanobacterium commonly found within tropical and sub-tropical waters (Capone et al. 1997). *Trichodesmium* is known to contribute significant quantities of new-nitrogen to the World's oceans (Mahaffey et al. 2005; Mulholland 2007) and as such much effort has been placed on quantifying its abundance using ocean colour remote sensing. This study examined the quasi-analytical algorithm (QAA) for inverting hyperspectral remote sensing reflectance, $R_{rs}(\lambda)$, to derive quantitative estimates of *Trichodesmium* abundance within the Great Barrier Reef (GBR), Australia. Both modelled and directly measured values of $R_{rs}(\lambda)$ were considered within this research. Modelling was performed with Hydrolight radiative transfer software using *Trichodesmium* chlorophyll-a (Chla) specific inherent optical properties (IOPs). The QAA was used to invert simulated $R_{rs}(\lambda)$ to derive the spectral phytoplankton absorption coefficient, $a_{\phi}^{QAA}(\lambda)$. To ascertain the presence of *Trichodesmium*, a similarity index measure (SIM) was computed. The SIM provided an indication of the level similarity of between the QAA derived $a_{\phi}^{QAA}(\lambda)$ with a reference *Trichodesmium* absorption spectra, $a_{Tri}^{ref}(\lambda)$. To benchmark the capabilities of the approach, SIM values were also computed for six other non-*Trichodesmium* phytoplankton. Upon examining the simulated data, it was found that the SIM could discriminate *Trichodesmium* from the six other phytoplankton above threshold Chla values of 0.2 mg Chla m^{-3} for Case 1 waters, and 3 mg Chla m^{-3} for Case 2 waters. The QAA-SIM method was applied to $R_{rs}(\lambda)$ data collected along a transect within the GBR on 3 October 2010 where *Trichodesmium* was known to be present. The QAA-SIM method positively identified the presence of

Trichodesmium during this transect. Furthermore, *Trichodesmium*-specific Chla concentrations were predicted from the magnitude of $a_{\phi}^{QAA}(\lambda)$ using an empirical relationship between Chla concentration and the magnitude of $a_{tri}(\lambda)$. The derived Chla values were compared with along-transect measurements made using a WETLabs Chla fluorometer housed within a ship-board, flow-through system. A good linear relationship was obtained between the measured and radiometrically derived Chla concentrations with an R^2 value of 0.81. Finally, total N-fixation during the trasect was considered. It was estimated that in 1.8 hours, *Trichodesmium* fixed 2 g of N within a 30 km^2 area. Estimated values were extrapolated and an annual areal *Trichodesmium*-specific N-fixation rate of 0.7 tonnes N m^{-2} yr^{-1} was derived

4.1 Introduction

Trichodesmium spp. is a pelagic cyanobacterium common to warm, oligotrophic waters (Capone et al. 1997). *Trichodesmium* has the ability to fix atmospheric Nitrogen and as such, is of great biogeochemical interest (Mahaffey et al. 2005). Within the Great Barrier Reef (GBR), Australia, *Trichodesmium* is likely to input quantities of new-N of similar magnitude to rivers (Furnas et al. 1995; Bell et al. 1999). However, uncertainties regarding *Trichodesmium*-specific N-fixation within the GBR currently exist due to a poor understanding of its abundance. In order to improve N-fixation estimates within the GBR, better techniques for detection and quantification of *Trichodesmium* are required.

Discrimination of near-surface *Trichodesmium* of varying concentration using space-borne remote sensing has been explored by several authors (Dupouy et al. 1988; Borstad et al. 1992; Dupouy 1992; Subramaniam and Carpenter 1994; Tassan 1994; Subramaniam et al. 1999b; Dupouy et al. 2000; Subramaniam et al. 2002; Westberry et al. 2005; Dupouy et al. 2008b; Hu et al. 2010). The detection of dense surface aggregations of *Trichodesmium* and other cyanobacteria has been shown to be relatively straight forward (Hu et al. 2010). Such surface aggregations exhibit a red-edge reflectance feature similar to terrestrial vegetation and this has been exploited by several authors for mapping spatial distributions using remote sensing (Kutser 2004; Gower et al. 2006; Hu et al. 2010). Westberry et al. (2005) developed a method for detecting *Trichodesmium* using an adapted version of the GSM01 semi-analytical ocean colour algorithm (Maritorena et al. 2002) in an attempt to detect global abundance of *Trichodesmium* at "sub-bloom" concentrations. However the adapted GSM01 method was limited in its ability to resolve *Trichodesmium* abundance. On a regional-scale, scant research has been conducted into developing methods for detecting *Trichodesmium* at "sub-bloom" concentrations within the GBR.

Several researchers have modelled or directly measured hyperspectral remote sensing reflectance, $R_{rs}(\lambda)$, spectra of *Trichodesmium* (Borstad et al. 1992; Subramaniam et al. 1999b; Dupouy et al. 2008a; Hu et al. 2010). The information from such $R_{rs}(\lambda)$ data has proved useful when developing *Trichodesmium*-specific algorithms for multi-band ocean colour sensors such as the Coastal Zone Colour Scanner (CZCS), the Sea-viewing Wide Field-of-view Sensor (SeaWiFS) and the Moderate Resolution Imaging Spectroradiometer (MODIS) (Subramaniam and

Carpenter 1994; Subramaniam et al. 2002; Westberry et al. 2005; Dupouy et al. 2008b; Hu et al. 2010). However, there is presently no literature which examines direct inversion of hyperspectral $R_{rs}(\lambda)$ as a means of detection and quantification of *Trichodesmium*. This may be, in part, because of the present lack of satellite borne, hyperspectral ocean colour sensors. However, there are currently several airborne hyperspectral sensors such as the Airborne Visible Infrared Spectrometer (AVIRIS) (Vane et al. 1993) and newly emerging technologies such as the Hyperspectral Imager for Coastal Oceans (HICO) (Corson et al. 2008). Ship-board measurements of hyperspectral $R_{rs}(\lambda)$ using above-water, and/or profiling radiometers are becoming more commonplace for algorithm development and validation purposes. Such hyperspectral data has the benefit of being able to resolve subtle spectral signatures not well resolved using multi-spectral sensors.

Lee and Carder (2004) examined the inversion of hyperspectral $R_{rs}(\lambda)$ using the quasi-analytical algorithm (QAA) (Lee et al. 2002) for the retrieval of spectral phytoplankton absorption coefficients, $a_{\phi}(\lambda)$. The results of Lee and Carder (2004) indicated that the QAA derived phytoplankton absorption coefficient, $a_{\phi}^{QAA}(\lambda)$, had an average difference of 21 % when compared to *in situ* measurements of $a_{\phi}(\lambda)$. The QAA also has the benefit of not requiring any priori information about the spectral shape of $a_{\phi}(\lambda)$ and is thus unlike ocean colour algorithms such as the GSM01 algorithm (Maritorena et al. 2002; Lee and Carder 2004). Lee and Carder (2004) also demonstrated that the QAA algorithm performed well in the optically complex coastal waters of the study. In another study, Craig et al. (2006) explored the QAA as a method for detecting the harmful alga *Karenia brevis* off the coast of Tampa Bay, Florida. Craig et al. (2006) collected hyperspectral $R_{rs}(\lambda)$ with accompanying *in situ* measurement of $a_{\phi}(\lambda)$. The study found that derived values of $a_{\phi}^{QAA}(\lambda)$ when compared with the *in situ* measurements of $a_{\phi}(\lambda)$ had an average difference of 23 % (Craig et al. 2006). Craig et al. (2006) used a similarity index measure (SIM) (Millie et al. 1997; Kirkpatrick et al. 2000) to compare $a_{\phi}^{QAA}(\lambda)$ values with a reference absorption coefficient measured from a mono-specific culture of *K. brevis*, $a_{brev}^{ref}(\lambda)$. The results found that the SIM had a linear relationship with

the log of *K. brevis* cell counts (Craig et al. 2006). Thus, the QAA and SIM methods in combination have the potential to discriminate a particular phytoplankton type from hyperspectral $R_{rs}(\lambda)$ observations.

The spectral absorption, $a_{tri}(\lambda)$, and scattering, $b_{tri}(\lambda)$, coefficients of *Trichodesmium* make its $R_{rs}(\lambda)$ spectrally distinct (Borstad et al. 1992; Dupouy et al. 2008a; Hu et al. 2010). Within this study, a method to invert hyperspectral $R_{rs}(\lambda)$ for the purposes of quantitatively detecting *Trichodesmium* is proposed. Firstly, we establish proof-of-concept that the combined QAA-SIM method can be used for discriminating *Trichodesmium* from other phytoplankton. This will be achieved using $R_{rs}(\lambda)$ values simulated for examples of Case 1 and Case 2 waters containing *Trichodesmium*. Secondly, we test the combined QAA-SIM method in an attempt to discriminate and quantify Chla-specific *Trichodesmium* abundance from transect $R_{rs}(\lambda)$ data collected within the GBR. Previous work has indicated the magnitude of $a_{\phi}(\lambda)$ can be used to estimate chlorophyll-a (Chla) specific phytoplankton abundance using ocean colour remote sensing (Bricaud et al. 1995; Carder et al. 1999). Thus, within this study, we aim to establish an empirical relationship between the *Trichodesmium*-specific absorption coefficient, $a_{tri}(\lambda)$, and Chla concentration. This relationship can then be used in combination with the QAA-SIM to retrieve *Trichodesmium* specific Chla concentration. In addition, we explore the potential use of this methodology for studying *Trichodesmium* specific N-fixation rates.

4.2 Data

4.2.1 Discrete Water Samples

Discrete seawater samples (n = 19) were collected from within the GBR during two research cruises aboard the RV Cape Ferguson during February and October 2009. The water column at each site was dominated by *Trichodesmium* and samples were gathered using either a clean bucket or Niskin bottle. Sub-samples were then immediately analysed using a dual beam Shimadzu UV-1600 spectrophotometer to determine coloured dissolved organic matter (CDOM) and particulate absorption coefficients. Following spectrophotometric analysis, particulate samples were frozen (- 20 °C) for later determination of Chla pigment concentration. Sample preparation, analysis and preservation followed the methods outlined in the Ocean Optics Protocols for Ocean Color Satellite Validation (Mitchell et al. 2003).

4.2.1.1 Particulate Absorption

Bulk samples of 100 - 250 mL containing *Trichodesmium* were filtered onto pre-combusted Whatman GF/F filters (Ø 25 mm) and rinsed using filtered seawater in order to determine the particulate absorption coefficients, $a_p(\lambda)$. The spectrophotometer baseline was determined using two blank Whatman GF/F filters. A Milli-Q dampened filter was used as the reference blank and a filter dampened with 0.22 μm filtered seawater as the sample blank. The optical density, OD, of a sample was measured from 250 - 800 nm with 0.5 nm resolution. The particulate absorption coefficient, $a_p(\lambda)$, was then calculated according to Mitchell et al. (2003),

$$a_p(\lambda) = \frac{2.303 A_f}{\beta V_f}\left(OD(\lambda) - OD_{NULL}\right) \qquad [4.1]$$

where, V_f was the volume filtered in cubic metres, A_f was the area of the filter in square metres, and β was the pathlength amplification correction coefficient for *Trichodesmium* taken to be 0.326 from Dupouy et al. (2008a). The value of OD_{NULL} was taken to be average *OD* over the spectral range 780 – 800 nm for which absorption by particulate matter was deemed negligible (Mitchell et al. 2003). Due to

low total suspended minerals in the mid-shelf and offshore waters of the GBR where samples were obtained, $a_p(\lambda)$ was deemed to approximate $a_{tri}(\lambda)$ reasonably well.

4.2.1.2 CDOM Absorption

For CDOM coefficient analysis, the spectrophotometer baseline was determined using a Milli-Q blank in the reference cuvette and a 0.22 μm filtered Milli-Q blank in the sample cuvette. Care was taken to let Milli-Q drawn from the purification system stand before use in order to reduce chances of micro-bubbles. CDOM samples were prepared first by pre-filtering solutions through pre-combusted Whatman GF/F filters under low vacuum in order to remove large colonies. The filtrate was then passed through 0.22 μm polycarbonate filters and placed into a clean 10 cm quartz cuvette. The CDOM absorption coefficient $a_g(\lambda)$ was determined from 250 – 800 nm at 0.5 nm resolution using the following equation (Mitchell et al. 2003)

$$a_g(\lambda) = \frac{2.303}{l}\left(OD(\lambda) - OD_{NULL}\right) \qquad [4.2]$$

where l is the pathlength in metres and OD_{NULL} was taken to be the OD at 680 nm at which absorption by CDOM is deemed negligible (Oubelkheir et al. 2006).

4.2.1.3 Chlorophyll-a Pigment Analysis

Concentrations of Chla pigment were determined either fluorometerically using a Turner Designs 10AU fluorometer (Parsons et al. 1984), or spectrophometrically with a Shimadzu UV-1600 spectrophometer using wavelengths specified by Jeffrey and Humphrey (1975). Extraction was performed by grinding filters in 90 % acetone followed by centrifuging at 500 rpm. Combined chlorophyll-a and phaeophytin (Chla + Pa) pigment concentration was determined first, following this, samples were acidified using 0.1 *N* HCl to break down any remaining Chla. Samples were then re-analysed to determine phaeophytin, Pa, concentration, this value was then subtracted from the combined Chla + Pa pigment concentration to give Chla concentration.

4.2.2 Above-water Hyperspectral Radiometry

Hyperspectral radiometric measurements of *Trichodesmium* were made aboard the RV Cape Ferguson in the southern GBR on 3 October 2009. Data were collected along a 33 km, northward running transect in the Southern GBR (21° 56' S, 151° 04' E) – (21° 40' S, 151° 04') as shown in Figure 4.2b. A custom built, three-channel radiometer simultaneously collected downwelling irradiance $E_d(\lambda)$, total upwelling radiance $L_t(\lambda)$ and sky radiance $L_{sky}(\lambda)$ along the transect. The radiometer comprised three NIST-traceable calibrated spectrometers with a spectral range of 400 – 860 nm and resolution of 3 nm. Values of $R_{rs}(\lambda)$ were derived using Mobley's ad hoc formula,

$$R_{rs}(\lambda) = \left[L_t(\lambda) - \rho L_{sky}(\lambda) \right] / E_d(\lambda), \qquad [4.3]$$

where ρ was the correction coefficient for sky radiance (Mobley 1999).

The instrument was boom mounted from the bow of the vessel such that observations of disturbances from the ship's wake were minimised. The viewing geometry of the $L_t(\lambda)$ and $L_{sky}(\lambda)$ radiometers was set to 40° off nadir and 40° off zenith respectively according to the Ocean Optics Protocols for Satellite Ocean Color Sensor Validation (Mueller et al. 2003). The azimuthal viewing angle of the radiometer relative to the sun was kept close to 135° by adjusting the orientation of the instrument as ship heading and/or solar angle changed. The value of ρ is dependent upon wind speed, solar zenith angle, and instrument viewing geometry (Mobley 1999). Thus, an appropriate value of ρ was determined from a look-up-table generated in Hydrolight (Slivkoff et al. 2006). A photograph of surface conditions during the transect is shown in Figure 4.1.

4.2.3 Flow-through Chlorophyll-a Fluorometry

A WETLabs combination Chla fluorescence and nephelometric turbidity meter (FLNTU) was used to measure along-transect Chla concentrations on 3 October 2010. Data was logged at ten second intervals. Water was pumped from 2 m below the surface into a debubbling chamber which housed the FLNTU meter. The debubbling chamber was used to remove unwanted bubbles generated by the pump by

allowing them to travel upward away from the FLNTU meter. The Chla fluorometer factory calibration coefficients were adjusted using offsets detailed in Appendix 2. A median average filter with a window with of 15 was applied upon Chla time series data to smooth out high frequency fluctuations and noisy data points.

Figure 4.1: Photograph of floating *Trichodesmium* surface aggregations (brown discolourations) observed during the radiometric transect. Image capture at: 1440 hours, 3 October 2010. Location: 22°39’46’’S, 151°04’21’ E.

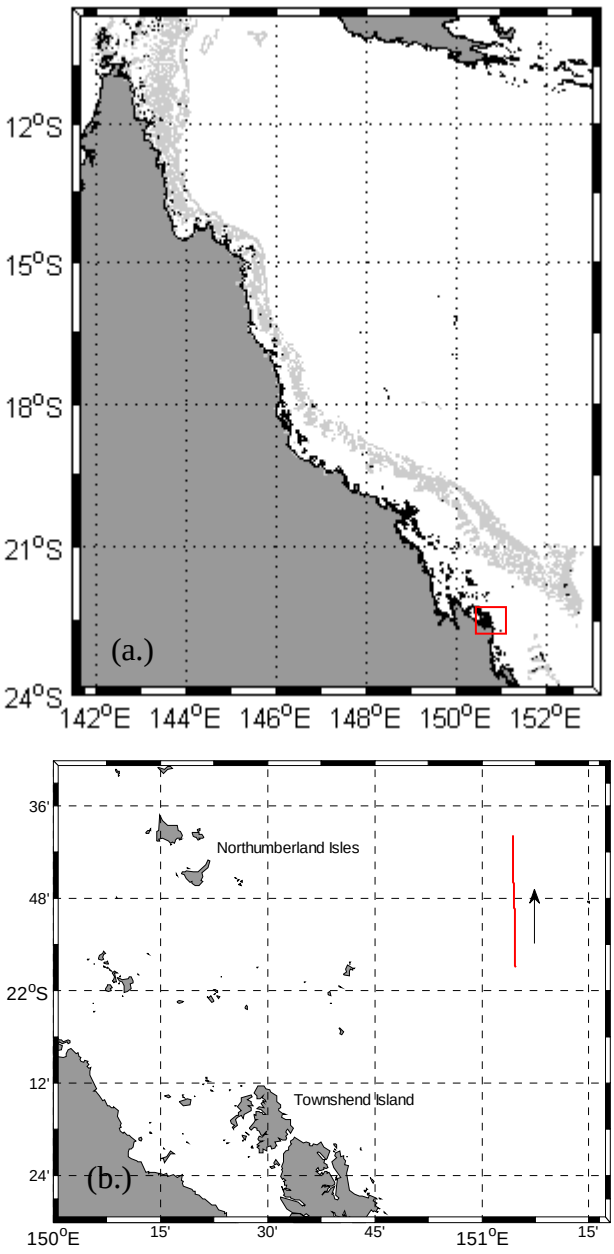

Figure 4.2: (a.) The Great Barrier Reef, Australia. The red square indicates the domain containing the transect. (b.) Zoom map of the transect location for which $R_{rs}(\lambda)$ and FLNTU Chla data were collected.

4.3 Methods

4.3.1 Hydrolight Modelling

Hyperspectral $R_{rs}(\lambda)$ was simulated using Hydrolight radiative transfer simulation software (Mobley and Sundman 2001a; Mobley and Sundman 2001b). $R_{rs}(\lambda)$ spectra were simulated for example Case 1 and Case 2 scenarios. For both Case 1 and 2 simulations, near surface *Trichodesmium*-specific concentrations ranged from 0.1 – 100 mg Chla m^{-3}. Case 1 simulations were deemed representative of offshore, reefal waters within the GBR. Conversely, Case 2 simulations were deemed to represent mid-shelf/near-shore waters of the GBR.

The *Trichodesmium* Chla specific CDOM and particulate absorption coefficients, denoted as $a^*_{g\,tri}(\lambda)$ and $a^*_{tri}(\lambda)$ respectively, were used as Hydrolight inputs. These coefficients were determined by normalising suitable $a_{g\,tri}(\lambda)$ and $a_{tri}(\lambda)$ spectra by their respective Chla concentration. The Chla specific backscattering coefficient of *Trichodesmium*, $b^*_{b\,tri}(\lambda)$, was characterized by Dupouy et al. (2008a) using a HOBI Labs HydroScat-6 (H6) instrument. The backscattering ratio, $\tilde{b}_b$, of *Trichodesmium* was estimated by Dupouy et al. (2008a) to range from 0.017 – 0.027. Within this chapter, the value of $\tilde{b}_b$ for *Trichodesmium* was chosen to be 0.02. To convert $b^*_{btri}(\lambda)$ values measured by Dupouy et al. (2008a) into Chla specific *Trichodesmium* scattering coefficients, $b^*_{tri}(\lambda)$, the following expression was used,

$$b^*_{tri}(\lambda) = \frac{1}{\tilde{b}_b}\; b^*_{btri}(\lambda). \qquad [4.5]$$

Dupouy et al. (2008a) showed that $b^*_{btri}(\lambda)$ could be fitted using a power law. As such, $b_{tri}(\lambda)$ was modelled within Hydrolight using the Gordon-Morel power law (Gordon and Morel 1983),

$$b_{tri}(\lambda) = b^*_{tri}(\lambda_0)\ \mathrm{Chla}^n \left(\frac{\lambda_0}{\lambda}\right)^{\gamma} \qquad [4.6]$$

where, $b^*_{tri}(\lambda_0)$ was the magnitude of $b^*_{tri}(\lambda)$ at a reference wavelength λ_0 = 550 nm, n= 0.62 and the spectral slope coefficient, γ =1.2, was taken from Dupouy et al. (2008a). The value of $b^*_{tri}(550)$ used was taken from Dupouy et al. (2008a) to be 0.475 m^2 mg^{-1}. Within Hydrolight, a Fournier-Forand scattering phase function, $\tilde{\beta}$, with $\tilde{b}_b$ = 0.02 was used for *Trichodesmium*.

The Case 1 Hydrolight model included the inherent optical properties (IOPs) of pure water (Pope and Fry 1997), *Trichodesmium* and CDOM covarying with Chla concentration. A low background concentration (0.1 gm m^{-3}) of calcareous sand was also included within the Case 1 model. Case 2 simulations included the IOPs of pure water, *Trichodesmium*, CDOM and brown sediment held at a constant concentration of 0.5 gm m^{-3}. The CDOM absorption coefficient, $a_g(\lambda)$, used within the Case 2 simulation was modelled according to Bricaud et al. (1981),

$$a_g(\lambda) = a(\lambda_0)e^{-S(\lambda-\lambda_0)}, \qquad [4.4]$$

where, the slope parameter, *S*, was set to 0.017 nm^{-1}, the reference wavelength, λ_0, was set to 440 nm, and absorption at the reference wavelength, $a(\lambda_0)$, was set to 0.2 m^{-1}. The Petzold average particle size scattering phase function, $\tilde{\beta}$, was selected for both brown sediment and calcareous sand.

All Hydrolight simulations were carried out for an infinitely deep water body, clear sky was assumed, solar zenith angle was set to 10°, and wind speed was set to 1 knot. Internal sources such as Raman scattering, Chla fluorescence and CDOM fluorescence were included. Values of $R_{rs}(\lambda)$ were simulated over the spectral range 400 – 700 nm with a 3 nm resolution.

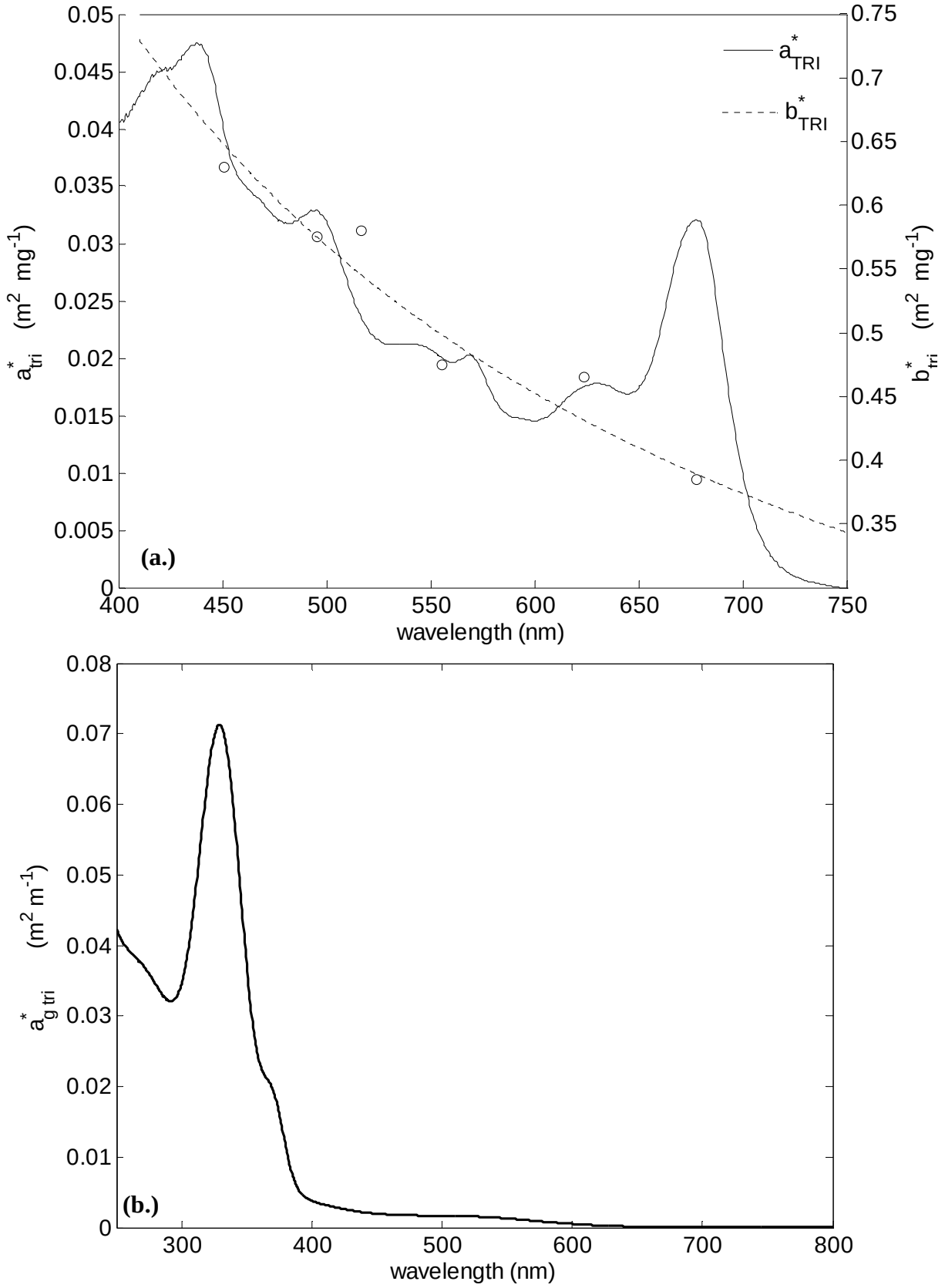

Figure 4.3: (a.) *Trichodesmium* Chla specific absorption, $a^*_{tri}(\lambda)$, and scattering, $b^*_{tri}(\lambda)$, coefficients used within Hydrolight simulations. Open circles represent

Hydroscat 6 measurements of $b^*_{tri}(\lambda)$ made by Dupouy et al. (2008a). (b.) *Trichodesmium* Chla specific CDOM absorption coefficient (McKinna, unpublished data).

4.3.2 The Quasi-Analytical Algorithm

The Quasi-Analytical Algorithm, QAA, is a physics-based inversion algorithm that derives IOPs from the sub-surface remote sensing reflectance, $r_{rs}(\lambda)$, by solving the quadratic expression of Gordon et al. (1988),

$$r_{rs}(\lambda) = g_1 u(\lambda) + g_2 \left[u(\lambda) \right]^2, \qquad [4.7]$$

where, g_1 and g_2 are scalar constants (Lee et al. 2002). The spectral parameter, $u(\lambda)$, is defined as,

$$u(\lambda) = \frac{b_b(\lambda)}{a(\lambda) + b_b(\lambda)}, \qquad [4.8]$$

where, $a(\lambda)$ and $b_b(\lambda)$ are the total absorption and backscattering coefficients respectively. The coefficients $a(\lambda)$ and $b_b(\lambda)$ are the sum of the absorption and backscattering coefficients of constituent matter within the water column and can be expressed as

$$a(\lambda) = a_w(\lambda) + a_\phi(\lambda) + a_{dg}(\lambda) \qquad [4.9]$$

$$b_b(\lambda) = b_{bw}(\lambda) + b_{bp}(\lambda) \qquad [4.10]$$

where, the subscripts w, ϕ, dg, and p correspond to pure water, phytoplankton, coloured dissolved and detrital matter, and particulate matter respectively.

Unlike other physics-based inversion algorithms such as the linear matrix inversion method (Hoge and Lyon 1996) and GSM01 algorithm (Maritorena et al. 2002), the QAA does solve for IOPs and constituent matter concentrations simultaneously (Lee et al. 2002). Conversely, the QAA uses a level-by-level approach. Level 0 to level 1 processing derives $a(\lambda)$ and $b_{bp}(\lambda)$ from $r_{rs}(\lambda)$. Then, level 1 to level 2 processing deconvolves $a(\lambda)$ into the absorption coefficients: $a_{dg}(\lambda)$ and $a_\phi(\lambda)$. Lee et al. (2002) stated that level 3 products such as pigment concentration may then be derived using pre-established relationships such as those of Carder et al. (1999). The benefit

of having a level-by-level approach is that products derived at lower levels have little or no influence upon those derived at the higher levels.

In addition, the QAA requires no prior information regarding the spectral shape of $a_\phi(\lambda)$. Thus, the QAA independently derives $a_\phi(\lambda)$ and thereby reduces potential errors and uncertainties associated with spectral models or inappropriate fixed spectral shapes of $a_\phi(\lambda)$ from propagating (Lee et al. 2002).

In the context of this investigation, the major limitation of the QAA is its inability to resolve $a_\phi(\lambda)$ accurately at wavelengths longer than 580 nm (Lee and Carder 2004). This is because $a(\lambda)$ is dominated by pure water at wavelengths longer than 580 nm. As such, the $R_{rs}(\lambda)$ at wavelengths longer than 580 nm contain very little information about $a_\phi(\lambda)$ (Lee and Carder 2004). Therefore, our derivation of $a_\phi(\lambda)$ has been limited to the spectral range of 400 – 580 nm.

The current version of the QAA v5 was used in this investigation, details of which can be found at: http://www.ioccg.org/groups/Software_OCA/QAA_v5.pdf. The complete details of the QAA algorithm are also given in Appendix 3 of this thesis.

4.3.3 Similarity Index Measure

The similarity index measure (SIM) used in this investigation was determined according to Mille et al. (1997). The fourth derivative spectrum of $a_\phi^{QAA}(\lambda)$ and a reference phytoplankton absorption spectrum, $a_\phi^{ref}(\lambda)$, were computed forming the vectors $\mathbf{A}_\varphi$ and $\mathbf{A}_{\mathbf{ref}}$ respectively. The SIM was then defined as

$$SIM = 1 - \left(\frac{2 \times \arccos(Q)}{\pi} \right). \qquad [4.11]$$

where,

$$Q = \frac{\left(\mathbf{A}_\varphi \bullet \mathbf{A}_{\mathbf{ref}} \right)}{\left(\left| \mathbf{A}_\varphi \right| \times \left| \mathbf{A}_{\mathbf{ref}} \right| \right)} \qquad [4.12]$$

Values of the SIM lay between zero and one. A SIM value close to 1 represented a small angle between $\mathbf{A}_\varphi$ and $\mathbf{A}_{\mathbf{ref}}$ in vector space, and indicated

$a_\phi^{QAA}(\lambda)$ and $a_\phi^{ref}(\lambda)$ were similar. Conversely, a small SIM value indicated $a_\phi^{QAA}(\lambda)$ and $a_\phi^{ref}(\lambda)$ were dissimilar.

In an attempt to evaluate the performance of the SIM method at discriminating *Trichodesmium*, a spectral library of seven different absorption spectra was collated. These reference absorption spectra, $a_\phi^{ref}(\lambda)$, are detailed in Table 4.1 and represented: *Trichodesmium* (Tri), generic green phytoplankton (PS), mixed picoplankton (Pico), mixed microplankton (Micro), *Prochlorococcus* (Pro), *Synechococcus* (Syn) and diatoms (Dia). Thus, for each QAA derived value of $a_\phi^{QAA}(\lambda)$, seven SIM values were computed, one for each phytoplankton reference. The seven SIM values were denoted SIM_{TRI}, SIM_{PS}, SIM_{MICRO}, SIM_{PICO}, SIM_{PRO}, SIM_{SYN} and SIM_{DIA}. The spectral library of absorption coefficients need not be chlorophyll-specific, as the SIM indicates how similar two absorption coefficients are with respect to shape. The absolute magnitude of two absorption coefficients is thus, relegated within the SIM calculation.

The absorption spectra of Tri was sampled from the GBR during this study. Whereas, the absorption spectra of Pro, Syn and Dia were collected within the GBR by Slivkoff, (unpublished data). The absorption spectra PS (Prieur and Sathyendranath 1981) was chosen as it has been used within several bio-optical studies including remote sensing algorithm development and modelling (Mobley and Sundman 2001a; Maritorena et al. 2002). The absorption spectra for Micro and Pico were taken from Ciotti et al. (2002) and deemed to approximate mixed populations of these particular phytoplankton size fractions.

The SIM values of the seven $a_\phi^{ref}(\lambda)$ spectra were first computed relative to one another over the spectral range 400 – 580 nm (Table 4.2). The resulting SIM_{TRI} values of *Trichodesmium* relative to the other six phytoplankton types ranged between 0.38 – 0.53 (see Table 4.2). It was thought these SIM_{TRI} values would have been smaller to indicate good separation in vector space between the fourth derivative spectra of $a_{tri}^{ref}(\lambda)$ and the other phytoplankton.

It was deemed that constraining the spectral range over which SIM values were computed may maximise the separation between $a_{tri}^{ref}(\lambda)$ and the other phytoplankton reference spectra. Thus, the normalised absorption spectra of PS, Micro, Pico, Dia,

Pro and Syn were plotted against the absorption spectra of *Trichodesmium* (see Figure 4.4). Figure 4.4 indicated that the greatest differences between *Trichodesmium* and other six phytoplankton $a_{\phi}^{ref}(\lambda)$ spectra occurred between 520 – 580 nm (shaded boxes). This observation was confirmed by examining the spectral covariance matrix of the seven phytoplankton $a_{\phi}^{ref}(\lambda)$ spectra (Figure 4.5). The spectral covariance matrix plot indicated that the high variances occurred between 520 - 580 nm.

The SIM values between each of the seven $a_{\phi}^{ref}(\lambda)$ spectra were again calculated, this time over the limited spectral range 520 -580 nm. The resulting SIM_{TRI} values of *Trichodesmium* relative to the other six phytoplankton types ranged between 0.07 – 0.38. This result indicated that using a spectral range of 520 – 580 nm maximises the ability of the SIM to discriminate between *Trichodesmium* and the reference phytoplankton. Thus SIM values for discriminating *Trichodesmium* within this study were computed from 520 - 580 nm.

Table 4.1: Details of phytoplankton spectral absorption coefficient data used as reference spectra $a_{\phi}^{ref}(\lambda)$ for determination of similarity index measures SIM.

Name	**Abbreviation**	**Data Source**	**GBR-Specific***
Trichodesmium	Tri	McKinna (unpublished data)	Yes
Phytoplankton	PS	Prieur and Sathyendranath (1981)	No
Microplankton	Micro	Ciotti et al. (2002)	No
Picoplankton	Pico	Ciotti et al. (2002)	No
Diatom	Dia	Slivkoff (unpublished data)	Yes
Prochlorococcus	Pro	Slivkoff (unpublished data)	Yes
Synechococcus	Syn	Slivkoff (unpublished data)	Yes

*GBR Specific: Yes = samples sourced from waters of the Great Barrier Reef, Australia, No = otherwise.

Table 4.2: Similarity index measures (SIM) calculated over the spectral range 400 – 580 nm for seven difference reference phytoplankton absorption spectra $a_{\phi}^{ref}(\lambda)$.

	Tri	**PS**	**Micro**	**Pic**	**Dia**	**Pro**	**Syn**
Tri	1	***0.38***	***0.48***	***0.48***	***0.53***	***0.51***	***0.52***
PS	-	1	0.65	0.64	0.71	0.66	0.33
Micro	-	-	1	0.57	0.70	0.86	0.40
Pico	-	-	-	1	0.62	0.64	0.46
Dia	-	-	-	-	1	0.71	0.5
Pro	-	-	-	-	-	1	0.42
Syn	-	-	-	-	-	-	1

Tri = *Trichodesmium*, PS = Green Phytoplankton, Micro = Microplankton, Pico = Picoplankton, Dia = Diatoms, Pro = *Prochlorococcus*, Syn = *Synechococcus*.

Table 4.3: Similarity index measures (SIM) calculated over the spectral range 520 – 580 nm for seven difference reference phytoplankton absorption spectra $a_{\phi}^{ref}(\lambda)$.

	Tricho	**PS**	**Pico**	**Micro**	**Dia**	**Pro**	**Syn**
Tricho	1	***0.09***	***0.07***	***0.23***	***0.17***	***0.38***	***0.20***
PS	-	1	0.69	0.70	0.57	0.70	0.05
Micro	-	-	1	0.57	0.75	0.43	0.03
Pico	-	-	-	1	0.70	0.68	0.30
Dia	-	-	-	-	1	0.49	0.11
Pro	-	-	-	-	-	1	0.37
Syn	-	-	-	-	-	-	1

Tri = *Trichodesmium*, PS = Green Phytoplankton, Micro = Microplankton, Pico = Picoplankton, Dia = 70Diatoms, Pro = *Prochlorococcus*, Syn = *Synechococcus*.

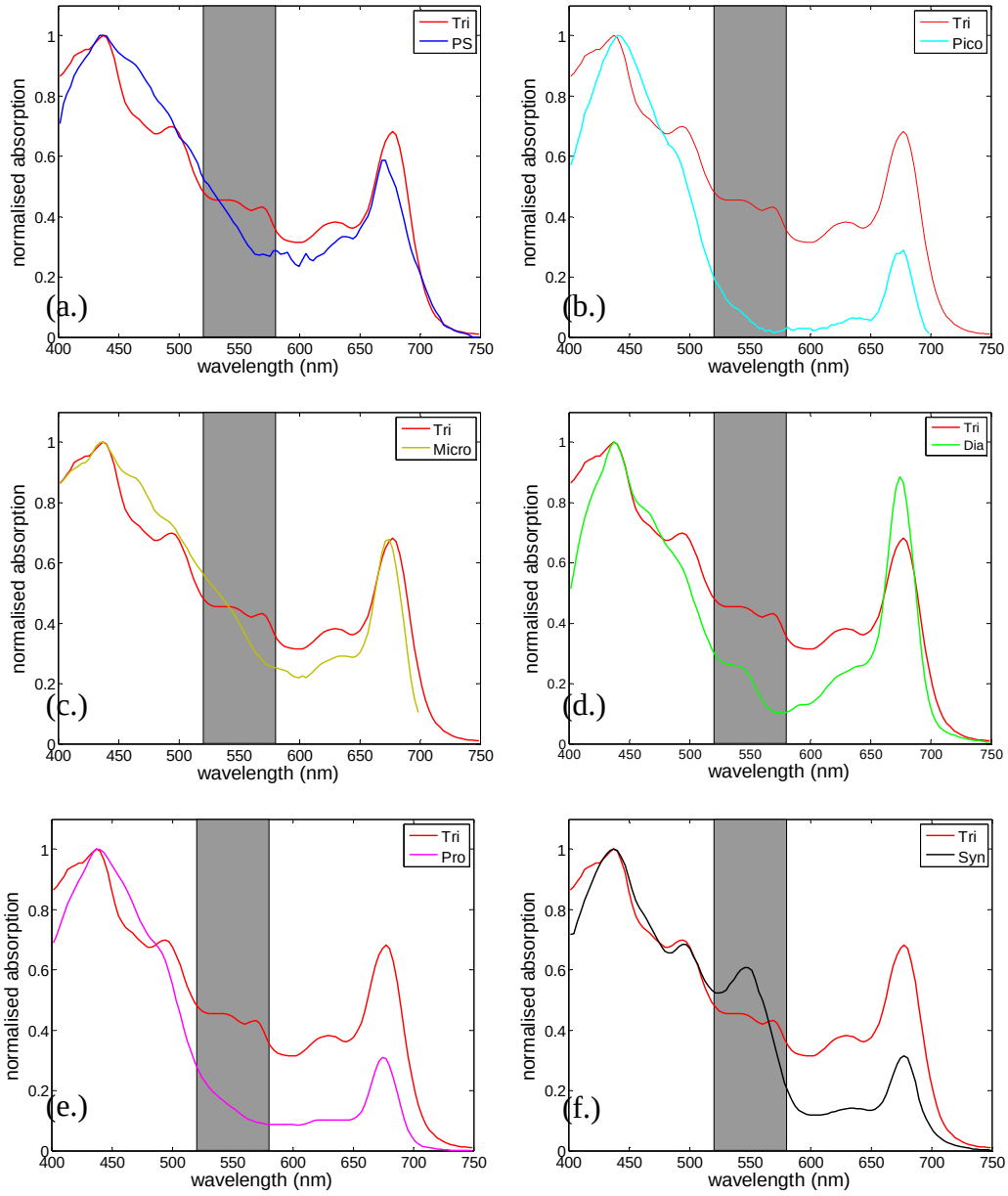

Figure 4.4: Comparison of the normalised *Trichodesmium* (Tri) absorption coefficient with normalised absorption coefficients of (a.) Green Phytoplankton (PS), (b.) Generic Picoplankton, (c.) Generic Microplankton, (d.) Diatoms, (e.) *Prochlorococcus*, and (f.) *Synechococcus*. The shaded rectangle represents the spectral range of 520 – 580 nm.

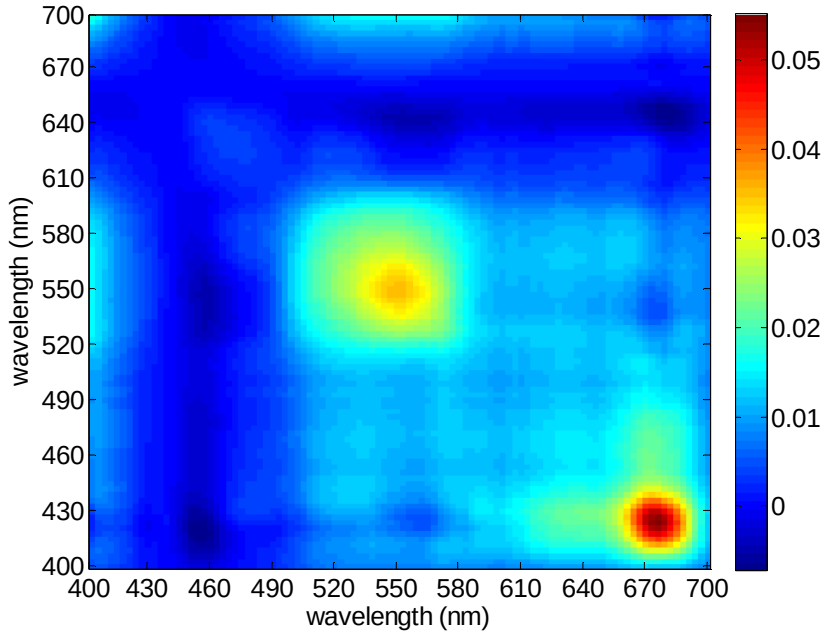

Figure 4.5: Spectral covariance matrix plot showing the spectral variability between the seven phytoplankton absorption spectra detailed in Table 4.1. Regions of highest variability occur between 520 – 580 nm and 660 – 680 nm.

4.4 Results and Discussion

4.4.1 Relationship between Chlorophyll-a Concentration and Absorption Coefficient Magnitude

The spectral shape of $a_{tri}(\lambda)$ exhibited peaks at 466, 495, 545, 575, and 620 nm respectively due to carotenoids, phycourobilin (PUB), phycoerythrobilin (PEB), phycoeryrthocyanin (PEC) and phycocyanin (PC) respectively (see Figure 4.3a). Absorption peaks at 435 and 620 nm are due to chlorophyll a (Chla). These values are consistent with those of literature (Subramaniam et al. 1999a; Dupouy et al. 2008a). The CDOM absorption coefficient of seawater surrounding *Trichodesmium* exhibited a strong peak at 330 nm and a shoulder at 368 nm (see Figure 4.3b) due to the presence of the ultra-violet (UV) absorbing microsporine-like amino acids (MAAs) (Steinberg et al. 2004). However, because Hydrolight modelling was

performed over the spectral range of 400 – 700 nm, the UV-absorbing MAAs had no effect upon the spectral shape of $R_{rs}(\lambda)$.

Research by Carder et al. (1999) revealed that Chla concentration could be related to the $a_{\phi}(\lambda)$ at 675 nm using the following relationship

$$Chla = 56.8\left[a_{\phi}(675)\right]^{1.03} \qquad [4.13]$$

Carder et al. (1999) postulated this relationship would be robust for estimating Chla concentration because absorption at 675 nm is relatively uncontaminated by accessory pigment absorption.

However within this study, the QAA did not derive $a_{\phi}(\lambda)$ at wavelengths beyond 580 nm. Thus, we have examined the relationship between Chla concentration and *Trichodesmium* absorption, $a_{tri}(\lambda)$, at 443 nm. A total of nineteen (n = 19) samples of *Trichodesmium* were analysed to derive absorption coefficients and corresponding Chla concentrations. The following curve was fit to the data

$$Chla = 257.5\left[a_{tri}(443)\right]^{1.929} \qquad [4.14]$$

The relationship between measured *Trichodesmium* Chla concentration and fitted Chla is shown in Figure 4.6. This relationship had an R-squared value of 0.98 and thus was assumed to be a reasonably good fit. However, it should be noted that the robustness of this relationship could be improved with an increased number of data points. Furthermore, $a_{tri}(\lambda)$ for *Trichodesmium* concentrations between 200 – 900 mg Chla m^{-3} should be measured to verify Equation 4.14 holds over the entire Chla range.

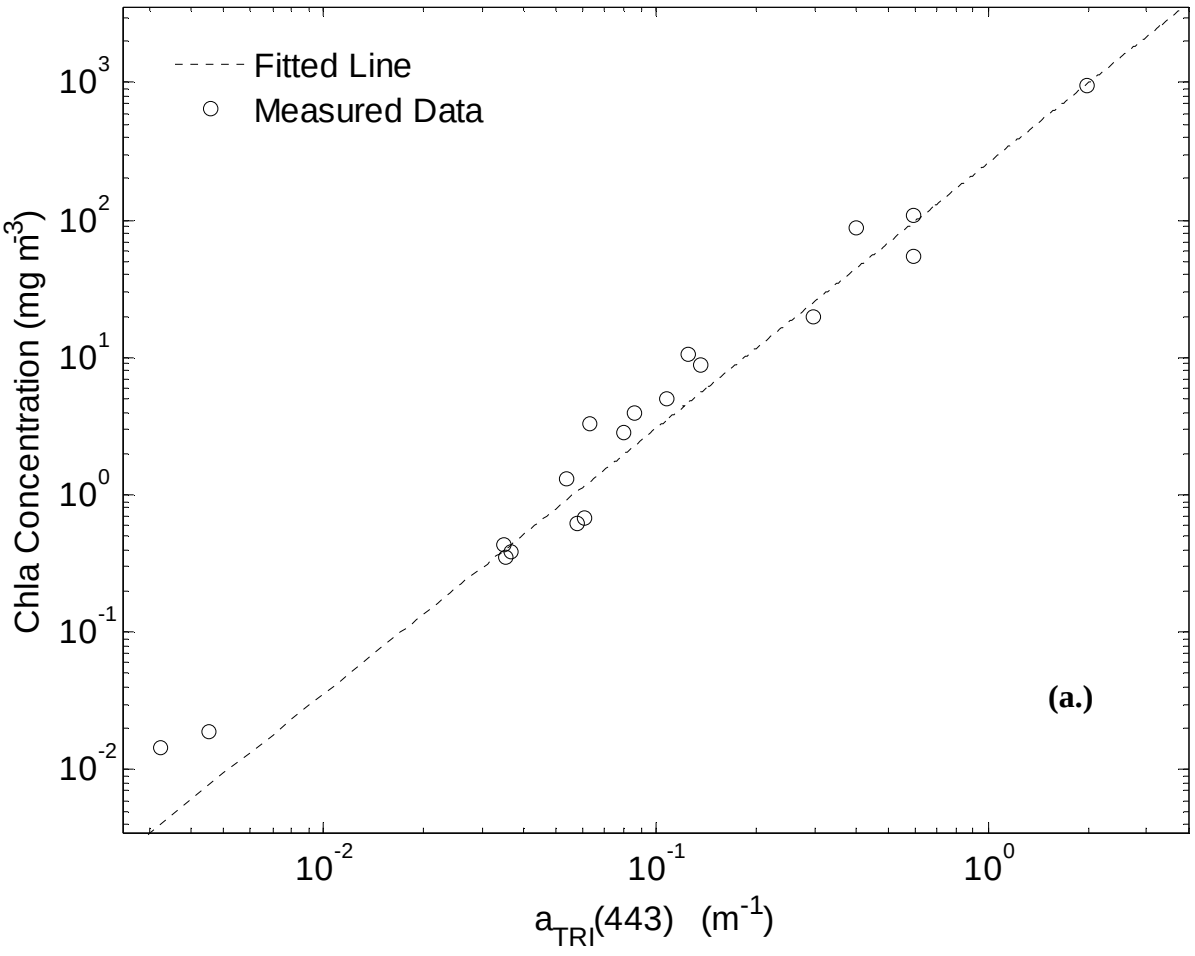

Figure 4.6: (a.) Log-log plot of Chla concentration of *Trichodesmium* varying with absorption coefficient at 443 nm.

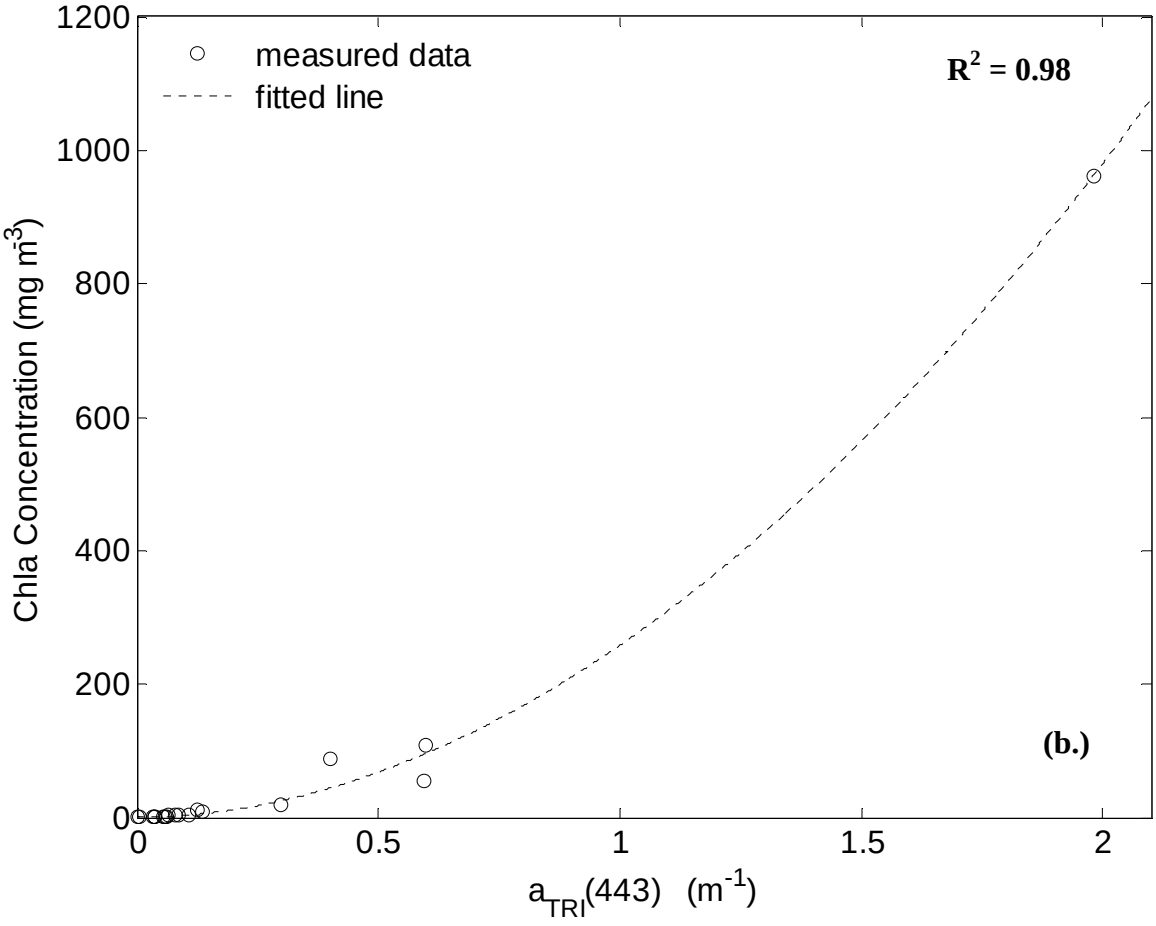

Figure 4.6: (b.) Unscaled plot of Chla concentration of *Trichodesmium* varying with absorption coefficient at 443 nm. The dashed line fitted according to Equation 4.4.

4.4.2 Modelled R_{rs}

Hydrolight modelled $R_{rs}(\lambda)$ for scenarios of Case 1 and 2 waters are presented in Figures 4.7a and 4.8a respectively. We hereby refer to the $R_{rs}(\lambda)$ for the Case 1 and Case 2 scenarios as $R_{rs}^{case1}(\lambda)$ and $R_{rs}^{case2}(\lambda)$ respectively. The results showed that the magnitude $R_{rs}^{case1}(\lambda)$ from about 400 – 500 nm decreased with increasing Chla concentration and subsequently *Trichodesmium* specific absorption features became more obvious. This observation was credited to increased absorption across all wavelengths with increased concentration of *Trichodesmium*. Conversely, the magnitude of $R_{rs}^{case2}(\lambda)$ became larger as the concentration of *Trichodesmium* increased. This was attributed to an increase in backscattering associated with increasing *Trichodesmium* concentration against a background dominated by constant CDOM and brown sediment absorption.

The characteristics of $R_{rs}^{case1}(\lambda)$ and $R_{rs}^{case2}(\lambda)$ at Chla concentrations exceeding 50 mg Chla m^{-3} were similar to previously measured and modelled values (Subramaniam et al. 1999b; Dupouy et al. 2008a; Hu et al. 2010). Within this study, a maximum reflectance peak was centred at 584 nm with lesser peaks evident at 560 and 527 nm. A broad peak was also evident between 458 and 480 nm as was a shoulder at 647 nm. For $R_{rs}^{case1}(\lambda)$, a blue peak occurred at 415 nm corresponding to pure water which was present until concentrations of *Trichodesmium* exceeded 10 mg Chla m^{-3}. Conversely, $R_{rs}^{case2}(\lambda)$ did not exhibit a spectral peak in the blue region, this was attributed to absorption by CDOM and brown sediments.

Absorption features of *Trichodesmium* were evident within both $R_{rs}^{case1}(\lambda)$ and $R_{rs}^{case2}(\lambda)$ spectra. These appeared as dips/troughs at 497, 545 and 569 nm due to the pigments PUB, PEB and PEC respectively. Reduced reflectance near 437 nm was attributed to absorption by Chla. Both $R_{rs}^{case1}(\lambda)$ and $R_{rs}^{case2}(\lambda)$ exhibited a peak at 690 nm corresponding to Chla fluorescence at *Trichodesmium* concentrations greater than 1 mg Chla m^{-3}.

4.4.3 QAA Derived Phytoplankton Absorption Coefficient.

Values of $a_{\phi}^{QAA}(\lambda)$ were derived from $R_{rs}^{case1}(\lambda)$ and $R_{rs}^{case2}(\lambda)$ over the spectral range 400 – 580 nm and are shown in Figures 4.7b and 4.8b. The shape of $a_{\phi}^{QAA}(\lambda)$ spectra derived from simulated $R_{rs}(\lambda)$ data contained features consistent with *Trichodesmium*. These features comprised absorption peaks at 437, 495, 536, 566 nm corresponding to the pigments: Chla, PUB, PEB and PEC respectively. The absorption peaks in $a_{\phi}^{QAA}(\lambda)$ were usually well defined when Chla concentration exceeded 1 mg Chla m^{-3}, particularly for the Case 2 scenario. In addition, for $a_{\phi}^{QAA}(\lambda)$ derived from $R_{rs}^{case2}(\lambda)$ at Chla concentrations below 1 mg Chla m^{-3}, the peak at 569 nm was not well resolved.

The magnitudes of $a_{\phi}^{QAA}(\lambda)$ values derived for the Case 1 water scenario were similar in magnitude to $a_{\phi}^{QAA}(\lambda)$ values derived for the Case 2 water scenario. Overall, these results indicated the QAA performed reasonably well at deriving $a_{\phi}^{QAA}(\lambda)$ for both the Case 1 and Case 2 simulated $R_{rs}(\lambda)$ data. However, should the concentration of CDOM have been higher, $a_{\phi}^{QAA}(\lambda)$ would have been increasingly difficult to resolve in the blue region. This shortcoming of the QAA was noted by Lee et al. (2010) in an investigation into error propagation within the algorithm. Unfortunately, as the $a_{\phi}^{QAA}(\lambda)$ is the last parameter to be derived using the QAA, errors sourced from estimations of $a(\lambda)$, $a_{dg}(\lambda)$ and $b_{bp}(\lambda)$ filter down into its derivation (Lee et al. 2010). In particular, Lee et al. (2010) acknowledged that for high values of $a_{dg}(\lambda)$, the algorithm can yield near-zero and even negative $a_{\phi}^{QAA}(\lambda)$ spectra.

4.4.4 Discrimination using SIM values

The SIM values computed for $a_{\phi}^{QAA}(\lambda)$ derived from simulated Case 1 $R_{rs}(\lambda)$ are shown in Figure 4.7c. The SIM_{TRI} value was zero for a *Trichodesmium* concentration of 0.1 mg Chla m^{-1}, indicating that *Trichodesmium* could not be discriminated. The value of SIM_{TRI} reached 0.48 at a *Trichodesmium* concentration

of 0.3 mg Chla m^{-1} from which point, SIM_{TRI} broke clear of the *SIM* values computed for other plankton. For concentrations between 1 – 10 mg Chla m^{-1}, SIM_{TRI} steadily increased and approached 0.6, whilst the SIM values of other phytoplankton remained less than 0.5 The SIM_{TRI} for concentrations greater than 20 mg Chla m^{-1} increased steadily and reached a value of 0.9 at 100 mg Chla m^{-1}. This result suggests that it may be possible to discriminate *Trichodesmium* from other plankton above a threshold of 0.3 mg Chla m^{-1} in Case 1 waters, and with more confidence for concentrations exceeding 1 mg Chla m^{-1}.

The SIM values computed for $a_{\phi}^{QAA}(\lambda)$ derived from simulated Case 2 $R_{rs}(\lambda)$ are shown in Figure 4.8c. The SIM_{TRI} values of *Trichodesmium* remained below 0.55 for concentrations less than 3 mg Chla m^{-1}. Within this concentration range, values of SIM_{MICRO} were greater than those of SIM_{TRI}, indicting that *Trichodesmium* could not be discriminated positively from mixed microplankton. For concentrations of *Trichodesmium* exceeding 3 mg Chla m^{-1}, the value of SIM_{TRI} was greater than 0.55 and became well separated from the *SIM* values for other plankton. This result showed that the limit of detectability of *Trichodesmium* within Case 2 water scenario was much higher than for the Case 1 water scenario.

These results indicated it was easier to discriminate *Trichodesmium* within Case 1 waters as opposed to Case 2 waters using the QAA-SIM approach. By examining the *SIM* plots (Figures 4.7c and 4.8c), it was evident that microplankton and *Synechococcus* are potential confounding effects and could yield false-positive retrievals at concentrations less than 0.2 mg Chla m^{-3} and 3 mg Chla m^{-3} for Case 1 and Case 2 waters respectively. For these Chla concentrations the SIM_{TRI} value was approximately 0.6 or higher. Thus, a SIM_{TRI} threshold value of 0.6, was determined to be appropriate for discriminating *Trichodesmium* effectively.

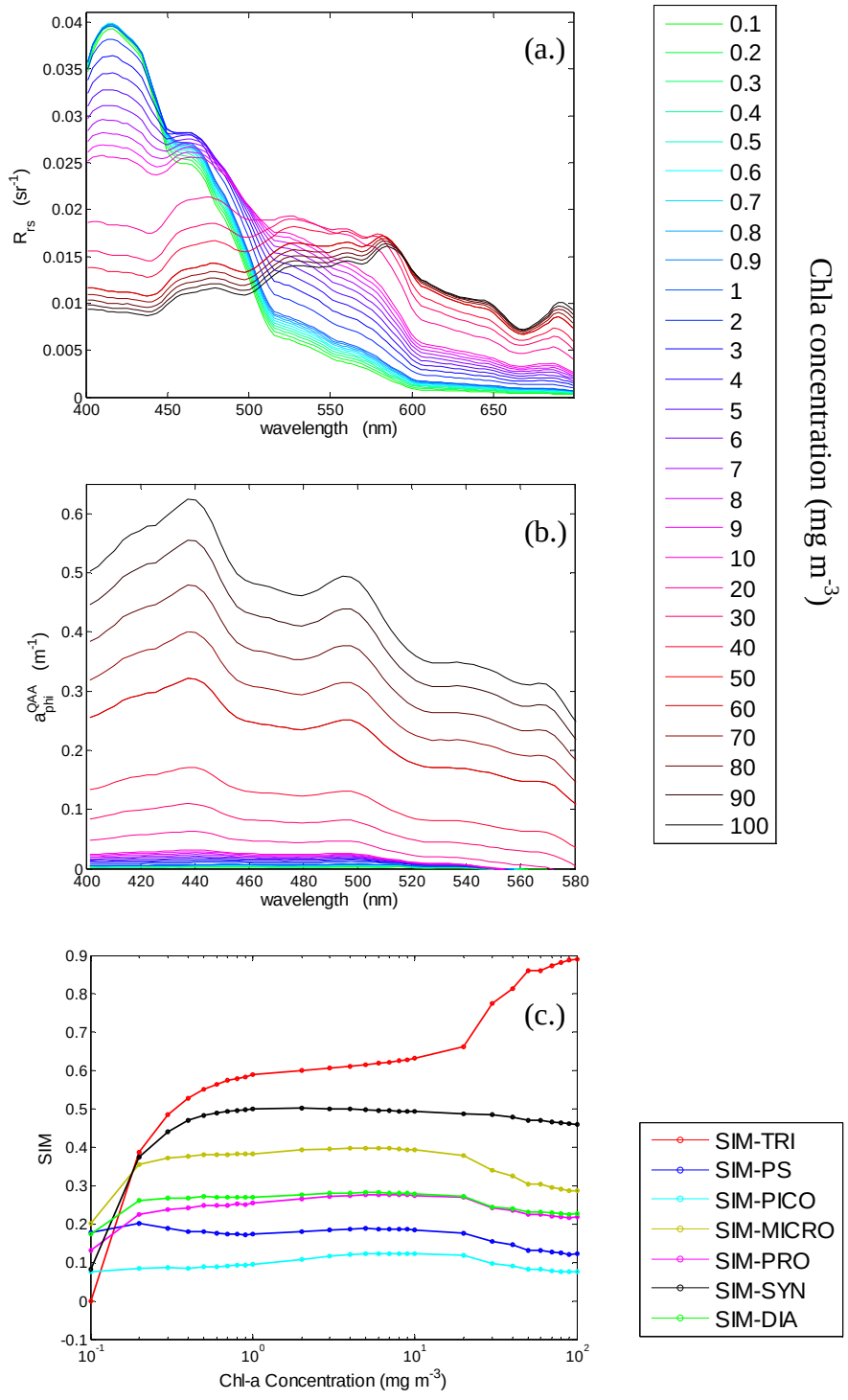

Figure 4.7: (a.) Modelled hyperspectral remote sensing reflectance for *Trichodesmium* in the Case 1 water scenario for Chla concentration increasing logarithmically from 0 – 100 mg m^{-3}. (b.) QAA-derived phytoplankton absorption coefficient $a_{\phi}^{QAA}(\lambda)$. (c.) Similarity index measures (SIM) computed using reference absorption spectra from the spectral library.

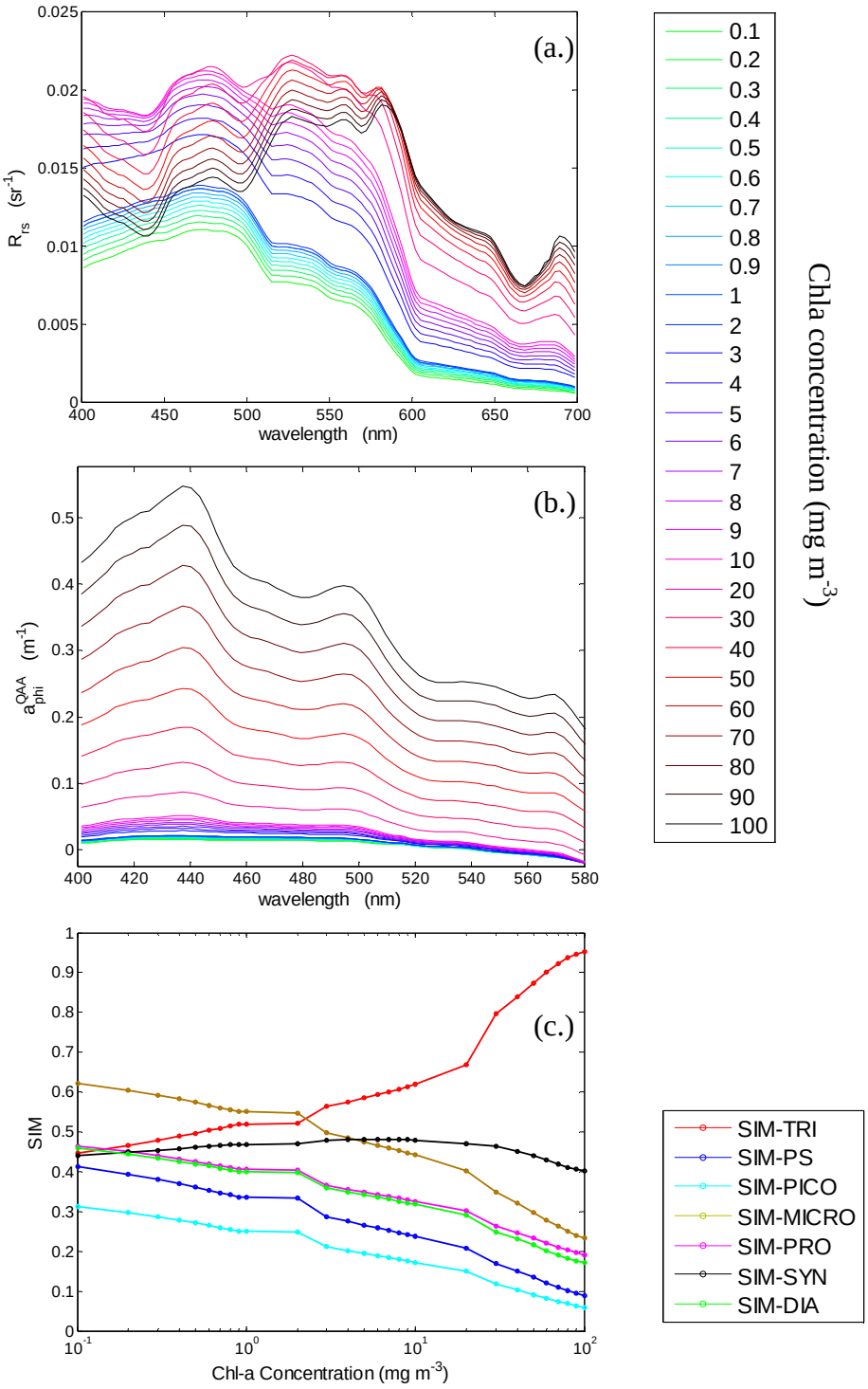

Figure 4.8: (a.) Modelled hyperspectral remote sensing reflectance for *Trichodesmium* in the Case 2 water scenario with Chla concentration increasing logarithmically from 0 – 100 mg m^{-3}. (b.) QAA-derived phytoplankton absorption coefficient $a_{\phi}^{QAA}(\lambda)$. (c.) Similarity index measures (SIM) computed using reference absorption spectra from the spectral library

4.4.5 Sensitivity of QAA-SIM to false-positive *Trichodesmium* detection

Using the Hydrolight Case 1 model, hyperspectral remote sensing reflectance spectra were simulated for non-*Trichodesmium*, oceanic, green phytoplankton ranging in concentration from 0.1 – 100 mg Cla m^{-3} (Figure 4.9a). The combined QAA-SIM method was then applied to the simulated remote sensing reflectance dataset. The motivation for this analysis was to determine if the QAA-SIM was robust against false-positive detection of *Trichodesmium*.

In section 4.4.4, a SIM_{TRI} threshold value of 0.6 was determined to be sufficient for discriminating the presence of *Trichodesmium* using the QAA-SIM method. However, the resulting SIM_{TRI} values (Figure 4.9c) remained below 0.4 for most Chla concentrations. The SIM_{TRI} only exceeded 0.4 on three occasions. For Chla concentrations of 10, 15 and 20 mg m^{-3} the values of SIM_{TRI} where 0.43, 0.45, 0.43 respectively. The SIM_{SYN} value also remained below 0.4 except for Chla concentrations 50 and 100 mg m^{-3}. Notably, after Chla concentration exceeded 0.3 mg m-3, SIM_{PS}, SIM_{PICO}, SIM_{MICRO}, SIM_{PRO}, and SIM_{DIA} began to distinctly separate from SIM_{TRI}.

The results from this sensitivity analysis suggest the QAA-SIM method is capable indicating the non-presence of *Trichodesmium*. Furthermore, these results indicate the method is somewhat robust to false-positive *Trichodesmium* retrievals.

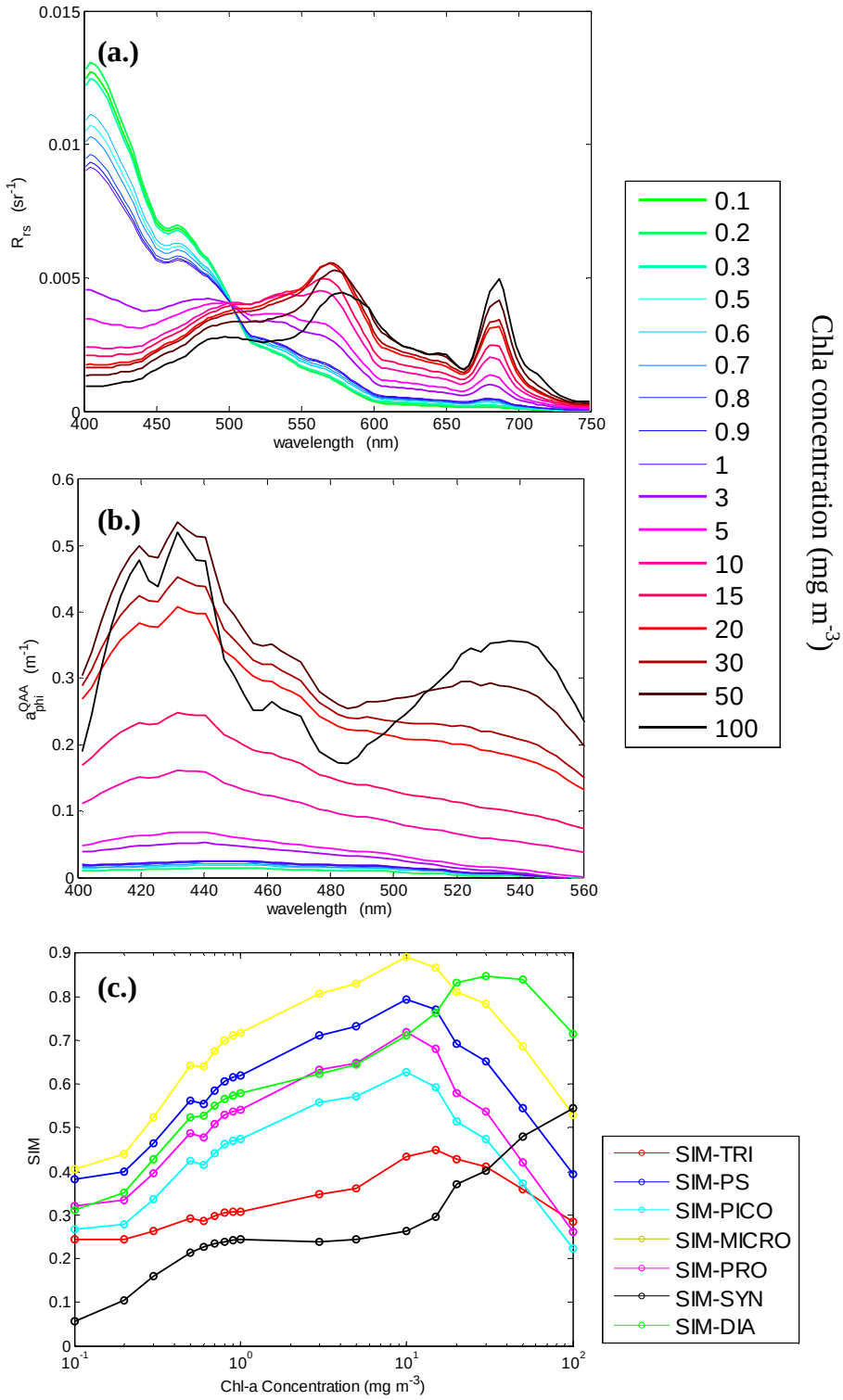

Figure 4.9: (a.) (a.) Modelled hyperspectral remote sensing reflectance using Hydrolight Case 1 model with Chla concentration ranging from 0.1 – 100 mg m^{-3}. (b.) QAA-derived phytoplankton absorption coefficient $a_{\phi}^{QAA}(\lambda)$. (c.) Similarity index measures (SIM) computed using reference absorption spectra from the spectral library.

4.4.6 Inversion of Transect Rrs

The $R_{rs}(\lambda)$ data collected on 3 October 2010 and the subsequently derived $a_{\phi}^{QAA}(\lambda)$ spectra are presented in Figure 4.10a and 4.10b respectively. Upon close inspection most $a_{\phi}^{QAA}(\lambda)$ spectra exhibited absorption features consistent with *Trichodesmium*, however some instrumental noise was evident. Values of SIM_{TRI} shown in Figure 4.10 are consistently greater than the threshold value of 0.6 and well separated from the *SIM* values of other plankton. Thus, based upon the *SIM* analysis, it was concluded that *Trichodesmium* was present for all 665 transect data points. This agreed with ship-board observations made at the time describing the presence of light surface dustings of *Trichodesmium* (see Figure 4.1).

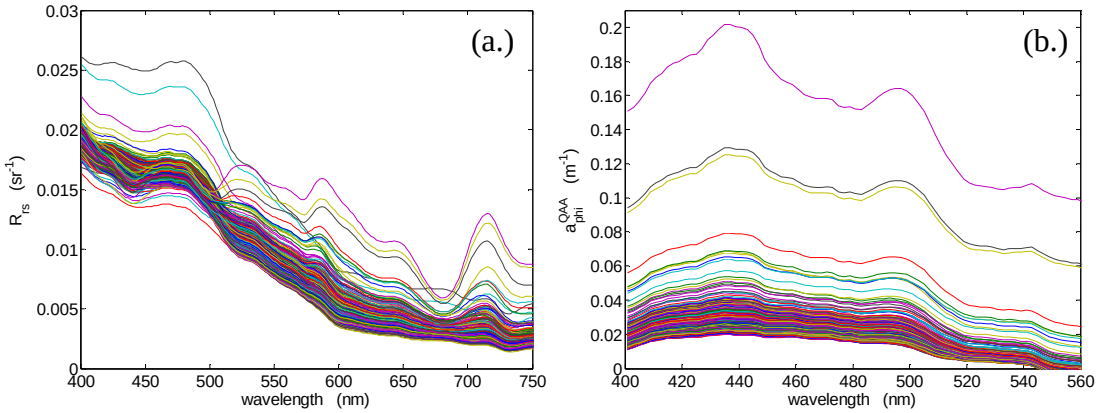

Figure 4.10: (a.) Along-transect remote sensing reflectance spectra $R_{rs}(\lambda)$ collected within the Great Barrier Reef on 3 October 2010. (b.) QAA-derived phytoplankton absorption coefficients [$a_{\phi}^{QAA}(\lambda)$ obtained by inverting each $R_{rs}(\lambda)$ spectra].

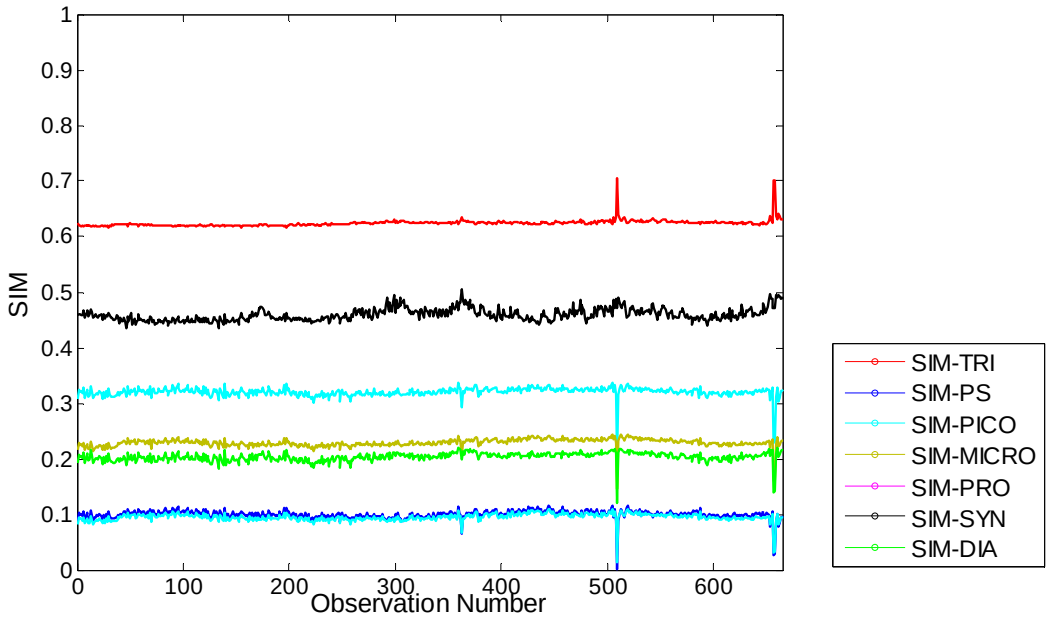

Figure 4.11: Along-transect similarity index measures (SIM) computed for each QAA derived $a_{\phi}^{QAA}(\lambda)$ spectra on 3 October 2010.

The empirical relationship between $a_{tri}(443)$ and Chla (Equation 4.14) was used to predict along-transect *Trichodesmium*–specific Chla concentration. Predicted Chla values were compared with FLNTU-measured Chla values to assess predictive skill of the method. Data were median filtered to remove noisy data points and lag-corrected by peak matching. It was found that FLNTU Chla values lagged R_{rs}-derived Chla values by 6 data points, which was equivalent to approximately 60 seconds. This lag time was deemed to represent the time taken for a particle to enter the intake manifold, pass through plumbing, enter the debubbling chamber and reach the FLNTU.

A sequence plot is shown in Figure 4.12 and reveals temporal similarities between predicted (red line) and measured Chla concentrations (green line). However, peaks in the predicted Chla sequence plot appeared much sharper than those of measured Chla sequence plot. This may have been a consequence of the residence time of the debubling chamber. A faster flow-rate and hence, lower residence time within the debubbling chamber, may have improved the measured Chla resolution. However, this would likely cause detrimental effects, including bubble formation and

cavitation which risk FLNTU data quality. Alternatively, the differences between the DALEC-retrieved and FLNTU-measured Chla time series plots may be due to fluorescence or absorption by non-*Trichodesmium* materials such as CDOM, detritus, or phytoplankton.

Sequence plots of along-transect Chla concentration derived using the standard NASA OC3 (Borstad et al. 1992; O'reilly 2002) and OC4 (O'reilly et al. 1998) algorithms were also plotted on Figure 4.11 (blue and black lines respectively). Both OC3 and OC4 resolved the temporal variability in the Chla signal with almost identical resolution to QAA predicted Chla values. However, when applied to the transect $R_{rs}(\lambda)$ spectra, the OC3 and OC4 algorithms consistently over-estimated the Chla concentration by approximately 0.2 mg Chla m^{-3} which agrees with the findings of Chauhan et al. (2002). Chauhan et al. (2002), using Ocean Colour Monitor (OCM) imagery, found that the standard NASA Chla algorithms consistently over-estimated Chla values for *Trichodesmium*. This may be because the OC3 and OC4 algorithms were developed using a global bio-optical database which contained very few *Trichodesmium* datapoints (O'reilly et al. 1998; O'reilly 2002; Westberry et al. 2005). Alternatively, CDOM absorption is known to cause band ratio Chla algorithms to over-estimate concentrations. The extent to which CDOM interfered with the OC3 and OC4 retrievals may have been quantifiable if measurements of CDOM absorption had been made.

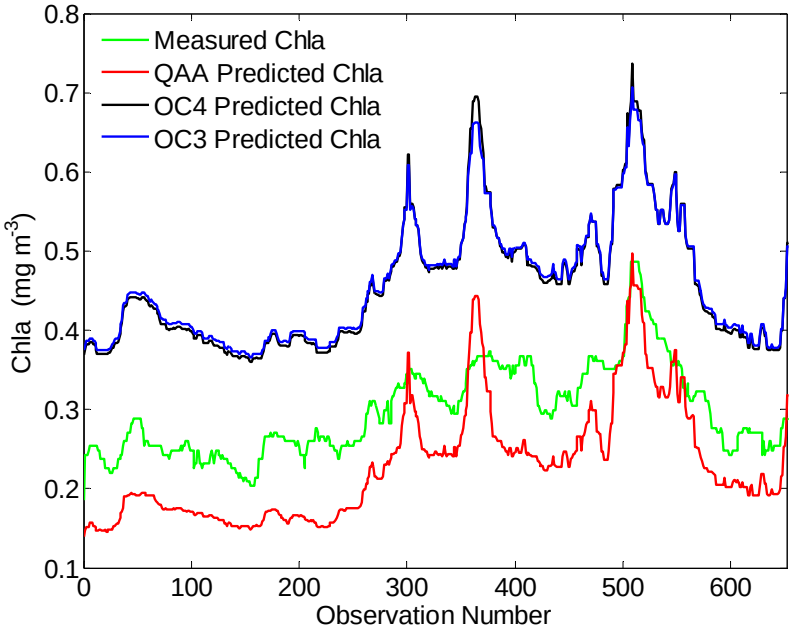

Figure 4.12: Sequence plot of Chla values measured using fluorometer in a flow-through system (green line), QAA derived Chla values (red line), NASA OC3 Chla algorithm (blue line) and NASA OC4 Chla algorithm (black line).

A scatter plot of measured versus predicted Chla is shown in Figure 4.13 revealing an almost one-to-one relationship with an R-squared value of 0.81. This result indicates that *Trichodesmium*-specific Chla was predicted reasonably well using Equation 4.14 over a Chla range of 0.2 – 0.5 mg Chla m^{-3}. However, the method appeared to slightly underestimate Chla concentration by approximately 0.05 mg Chl m^{-3}. It is almost certain that other phytoplankton were present in the upper two metres of the water column alongside *Trichodesmium*. This is may explain, in part, the discrepancy between the flow-through Chla values and those derived from the radiometric data. In addition, *Trichodesmium* often occurs in higher Chla concentrations than those observed during the transect on 3 October 2010. Therefore, it would be useful to study the performance of the described method over a wider range of Chla concentrations. However, the range of the FLNTU instrument used within this study was 0 – 50 mg Chla m^{-3}. Thus, a different approach is needed for *in situ* validation of this method where *Trichodesmium* concentrations exceed 50 mg Chla m^{-3}.

Also worthy of mention is that the flow-through system used within this study was not optimised for sampling dense surface aggregations of *Trichodesmium*. This is because the intake manifold was 2 m below the surface. The water 1 – 2 m beneath a *Trichodesmium* surface aggregation can have much lower Chla concentrations than at the surface (see Figure 5.2, Chapter 5). Thus, Chla concentrations estimated from $R_{rs}(\lambda)$ above a dense surface aggregation may be much higher than those measured by a flow-through fluorometer which samples seawater from 2 m below the surface.

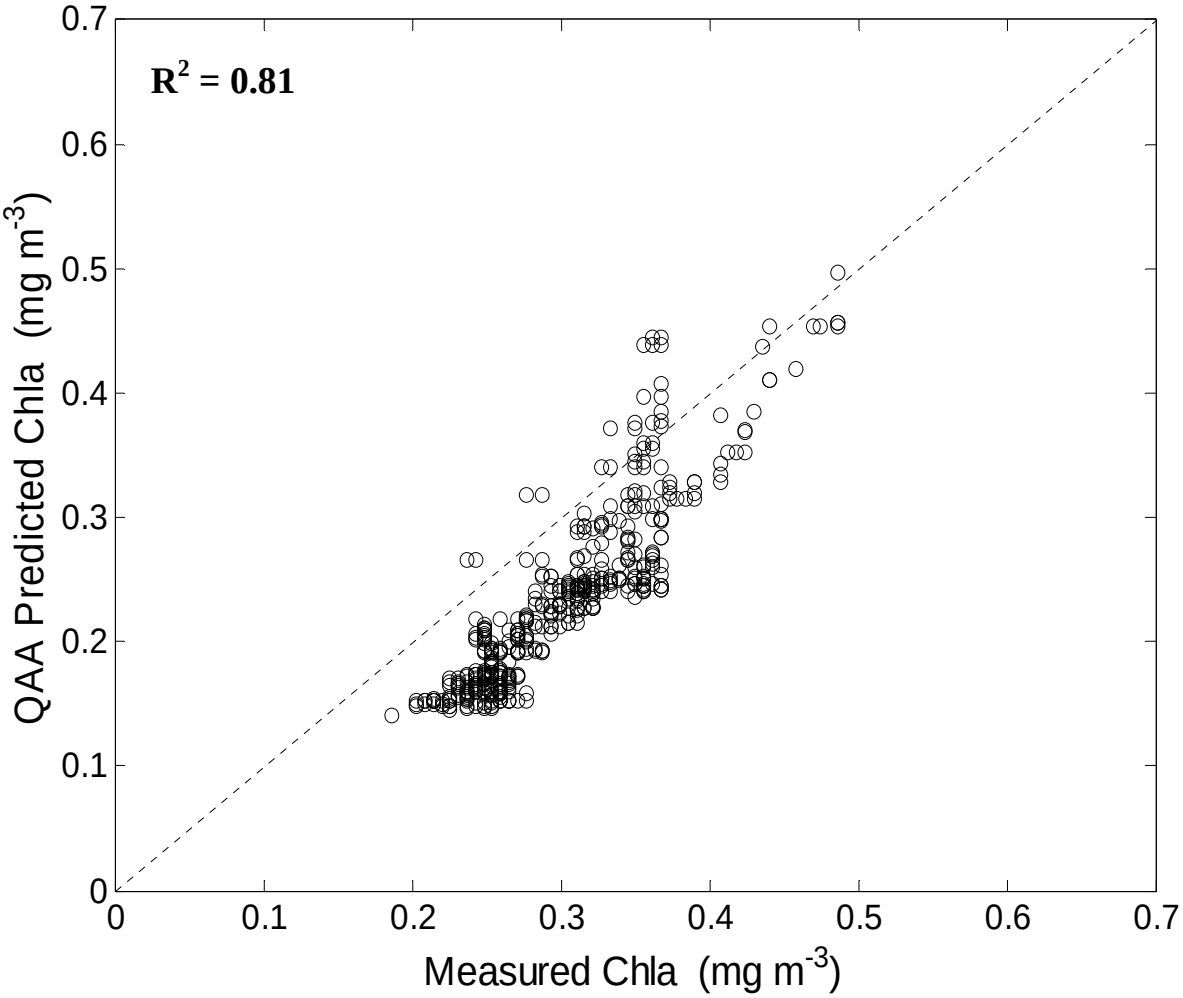

Figure 4.13: Scatter plot of measured versus radiometrically predicted Chla concentration for the 3 October 2010 transect.

4.5 Conclusion

Within this chapter, a method for discrimination and quantification of *Trichodesmium* using hyperspectral $R_{rs}(\lambda)$ data has been presented. Firstly, a proof-of-concept was established using Hydrolight simulated $R_{rs}(\lambda)$ spectra for examples of Case 1 and Case 2 waters. The QAA then inverted $R_{rs}(\lambda)$ to yield $a_{\phi}^{QAA}(\lambda)$ values which were compared using a SIM to an $a_{\phi}^{ref}(\lambda)$ spectrum of *Trichodesmium* and six other phytoplankton types. The results indicated that the combined QAA-SIM method could discriminate *Trichodesmium* from other plankton at concentrations greater than 0.3 mg Chla m^{-3} within Case 1 waters. Whereas, the combined QAA-SIM method could only discriminate *Trichodesmium* at concentrations greater than 3 mg Chla m^{-3} for Case 2 waters.

Following successful proof-of-concept, the QAA-SIM method was trialled upon transect $R_{rs}(\lambda)$ values. Transect data were collected within the GBR with accompanying high frequency Chla data measured using a flow-through fluorometer system. The magnitude of $a_{\phi}^{QAA}(\lambda)$ was then used to predict Chla concentration using a newly established empirical relationship. Values of *Trichodesmium* specific Chla were well predicted, yielding a near one-one relationship with an $R^2 = 0.81$, however, values were underestimated by approximately 0.05 mg Chl m^{-3}. Due to the consistency of this discrepancy, it was thought to have been sourced from the empirical relationship between $a_{tri}(443)$ and Chla concentration (Equation 4.14) which was derived using only 19 data points. Furthermore, it was assumed that samples of *Trichodesmium* were collected in clear waters with low NAP concentration. However, it is likely that minor contributions of NAP may have caused a slight over-estimation of $a_{tri}(\lambda)$. Thus, further investigation into the Chla-specific absorption coefficient of *Trichodesmium* is justified over a wider range of Chla values whilst measures are taken to eliminate contributions from NAP.

An aspect worthy of further investigation is self-shading of *Trichodesmium*. This is particularly pertinent in the case were surface aggregations are present. Subramaniam et al. (1999b) suggested self shading would cause SeaWiFS Chla

retrievals to be underestimated by a factor of four. However, within this chapter, the standard NASA band ratio-type Chla algorithms were found to over-estimate Chla abundance by a factor of two, complementing research of Chauhan et al. (2002). This may be a consequence of elevated CDOM absorption. To confirm this hypothesis, further measurements of IOPs are required alongside radiometric measurements during a *Trichodesmium* event. The effect of vertical distribution upon the QAA-SIM method may be studied further using Hydrolight simulations. This could be achieved by modelling varying vertical distributions of *Trichodesmium* in a similar fashion to Kutser et al. (2008) who modelled the influence of varying vertical distributions of cyanobacteria upon $R_{rs}(\lambda)$ within the Baltic Sea.

Further validation and development of the QAA-SIM approach would be possible using a suite of Hydrolight-simulated $R_{rs}(\lambda)$. A spectral library of $R_{rs}(\lambda)$ derived for varying concentrations of *Trichodesmium*, CDOM and sediments would be useful for both further validation and refinement of the QAA-SIM method. In addition, Hydrolight simulations of mixed phytoplankton assemblages were not considered in this chapter and warrant further study. Furthermore, improved Hydrolight simulations most likely require a better parameterisation of $b^*_{tri}(\lambda)$. Within this study, $b^*_{tri}(\lambda)$ of *Trichodesmium* was approximated using a spectral model (Gordon and Morel 1983). However, direct measurements by Subramaniam et al. (1999b) and Dupouy et al. (2008a) suggested the scattering coefficient of *Trichodesmium* exhibits wavelength dependence. As such, the power law used to model $b^*_{tri}(\lambda)$ may have introduced some uncertainties to $R_{rs}(\lambda)$. In addition, there are presently no directly measured values of $\tilde{b}_b$ reported for *Trichodesmium* and a value of 0.02 was used within this investigation. This highlights the need for further research into the scattering properties of *Trichodesmium*.

As an application of the SIM-QAA method, along-transect volumetric N-fixation rates were estimated (see Appendix 4). As a result, high resolution volumetric N-fixation rates were derived along transect from *Trichodesmium* specific Chla concentration. Furthermore, the along-transect areal N-fixation rate was estimated. With further refinement, this method would be extremely useful. By collecting multiple transect $R_{rs}(\lambda)$ data within the GBR, regional and seasonal

variability in *Trichodesmium* abundance may be resolved. Using such information, uncertainty regarding N-fixation loads within the GBR would be considerably reduced. To enhance this method, improved data regarding region-specific, local data regarding *Trichodesmium* physiology, Chla content, and N-fixation rates are essential.

The QAA-SIM method could conceivably be applied to other regions such as waters surrounding New Caledonia, the west Coast of India, the Gulf of Mexico and western Australia where *Trichodesmium* is known to be abundant (Devassy et al. 1978; Dupouy 1992; Subramaniam and Carpenter 1994; Subramaniam et al. 2002). Such information would provide a greater degree of information regarding global variability of *Trichodesmium* and hence contribute to understanding global N-budgets.

This page intentionally left blank.

5 Modelling the hyperspectral remote sensing reflectance signal of senescing *Trichodesmium* spp.

This chapter has been submitted to the journal: Estuarine, Coastal and Shelf Science.

Abstract

During a field survey within the Great Barrier Reef (GBR), Australia, on the 16 January 2009, large surface aggregations of the cyanobacterium *Trichodesmium* spp. were observed. The *Trichodesmium* manifested in two distinct colour modes: orange/brown (OB) and bright green (BG). Both colour modes were sampled and separate spectrophotometric measurements of the particulate and coloured dissolved organic matter (CDOM) absorption coefficients were made. The spectral absorption properties of the OB *Trichodesmium* were consistent with literature measurements. However, absorption measurements revealed the BG *Trichodesmium* had leached its water soluble phycobilipigments into the surrounding seawater. This observation strongly suggested that the BG *Trichodesmium* was undergoing cell lysis. The remote sensing reflectance spectra, $R_{rs}(\lambda)$, of OB and BG *Trichodesmium* were simulated using Hydrolight and denoted as $R_{rsOB}(\lambda)$ and $R_{rsBG}(\lambda)$ respectively. $R_{rsOB}(\lambda)$ exhibited a distinct peak at 582 nm which was not present in $R_{rs}(\lambda)$ of the BG *Trichodesmium*. In contrast, $R_{rsBG}(\lambda)$ exhibited a dominant peak at 560 nm. The issue of spatial patchiness was also explored to determine how differing proportions of OB and BG *Trichodesmium* affected the total $R_{rs}(\lambda)$ of a satellite observed pixel. This research demonstrated the potential to discriminate *Trichodesmium* physiological state using ocean colour remote sensing.

5.1 Introduction

Trichodesmium spp. is a colonial, marine cyanobacterium and is common throughout tropical and sub-tropical oligotrophic waters (Capone et al. 1997). *Trichodesmium* is ecologically significant in nutrient limited oceanic regions because of its ability to fix atmospheric Nitrogen (Capone et al. 2005). *Trichodesmium* often appears on the surface in large, floating aggregations commonly referred to as blooms or surface slicks (Capone et al. 1997). Such surface aggregations have the potential to influence physical, chemical and optical properties of surrounding water (Capone et al. 1997). Physical parameters influenced by dense surface aggregations of *Trichodesmium* include light penetration and ocean-atmosphere heat and gas exchanges (Capone et al. 1998).

Remote sensing has become a useful tool for monitoring cyanobacterial surface aggregations on large spatial scales (Kutser 2009). The optical properties of dense surface aggregations strongly influence the water-leaving radiance, L_w, signal making them optically conspicuous by producing a red-edge reflectance similar to terrestrial vegetation (Borstad et al. 1992; Kutser 2009). The red-edge reflectance feature is characterised by a L_w signal in the near infrared (NIR) (> 700 nm) which is greater in magnitude than L_w in the visible region (400 – 700 nm). In aquatic systems, where phytoplankton are dispersed, NIR photons are strongly absorbed by water molecules (Dierssen et al. 2006). Under such circumstances, small L_w peaks in the NIR region are attributed to chlorophyll-a (Chla) fluorescence (Dierssen et al. 2006). However, for high concentrations of phytoplankton, NIR light is scattered with higher efficiency than visible light which is usually absorbed by photopigments (Dierssen et al. 2006). Where dense concentrations of phytoplankton accumulate on the sea surface, the scattered NIR light is absorbed by seawater with lower efficiency. This results in the strong NIR reflectance (red-edge) which is characteristic of cyanobacterial surface aggregations (Kahru 1997; Dierssen et al. 2006; Kutser 2009).

The red-edge reflectance feature has been used to map phytoplankton surface blooms using various remote sensing platforms including: Landsat, the Advanced Very High Resolution Radiometer (AVHRR), the Medium Resolution Imaging Spectroradiometer (MERIS), and the Moderate Resolution Imaging

Spectroradiometer (MODIS) (Galat and Verdin 1989; Kahru 1997; Kutser 2004; Gower et al. 2005; Hu et al. 2010).

Recent algorithms such as the Maximum Chlorophyll Index (MCI) developed for MERIS (Gower et al. 2005) and the Floating Algae Index (FAI) developed for MODIS (Hu 2009) rely upon the red-edge reflectance feature. These algorithms are useful for mapping the spatial structure of large, dense surface aggregations of cyanobacteria, phytoplankton and floating vegetation such as *Sargassum* (Gower et al. 2006; Gower et al. 2008; Hu 2009). The FAI has been used to detect *Trichodesmium* surface aggregations on the west Florida Shelf (WFS) (Hu et al. 2010). Pixels with high FAI values are selected and the spectral shape of the multi-band remote sensing reflectance, $R_{rs}(\lambda)$, is examined (Hu et al. 2010). Hu et al. (2010) compared these MODIS multi-band $R_{rs}(\lambda)$ spectra with directly measured hyperspectral $R_{rs}(\lambda)$ values of *Trichodesmium* from the WFS and waters off Puerto Rico. Hu et al. (2010) found that *Trichodesmium* could be distinguished from other floating vegetation such as *Sargassum* based upon the unique reflectance characteristics of the cyanobacteria. However, the spectral shape and magnitude of the $R_{rs}(\lambda)$ is known to vary with the concentration and vertical distribution of *Trichodesmium* (Subramaniam et al. 1999b). Thus, the method of Hu et al. (2010) could benefit from a comprehensive knowledge of the $R_{rs}(\lambda)$ as *Trichodesmium* abundance varies. Variability in $R_{rs}(\lambda)$ can either be directly measured or otherwise modelled using radiative transfer simulation code such as Hydrolight (Mobley and Sundman 2001a; Mobley and Sundman 2001b). However, Hydrolight simulations require an appropriate set of the optical properties as user inputs.

The bio-optical backscattering and absorption coefficients of *Trichodesmium* have been studied by several authors (Subramaniam et al. 1999a; Subramaniam et al. 1999b; Dupouy et al. 2008a). These data have proved to be useful for the development of *Trichodesmium*-specific ocean colour algorithms (Subramaniam et al. 2002; Westberry et al. 2005). However, studies of bio-optical properties have been carried out for fresh samples of *Trichodesmium* collected from the field or laboratory cultures. At present there currently exists scant literature discussing the bio-optical properties of *Trichodesmium* at varying states of physiological health. Devassy et al (1978) studied *Trichodesmium* off the western coast of India and noted that the colour

of a dense surface aggregation changed over time. At the peak of growth, the *Trichodesmium* surface aggregation was noted to be distinctly reddish-brown and went on to become greyish-brown over time (Devassy et al. 1978). Devassy et al. (1978) also noted that the filtrate of samples collected within dense patches of *Trichodesmium* was often pink in colour. The pink discolouration of seawater associated with *Trichodesmium* has also been noted by others (Jones et al. 1986; Rueter et al. 1992). Literature discussing the pink solution leached from *Trichodesmium* is scant; however, it is likely to consist of the water soluble phycobilipigments which are present within *Trichodesmium* (Rueter et al. 1992). Furthermore, ultraviolet (UV) -absorbing, microsporine-like amino acids (MAAs) are exuded from *Trichodesmium* and have been shown to contribute to the coloured dissolved organic matter (CDOM) absorption coefficient, $a_g(\lambda)$ (Steinberg et al. 2004; Oubelkheir et al. 2006; Dupouy et al. 2008a).

Thus, there is anecdotal evidence that infers the optical properties of both *Trichodesmium* and the surrounding seawater vary with the physiological state of a high concentration, surface aggregation. It may therefore be possible to detect degradation of a *Trichodesmium* aggregation using ocean colour remote sensing. Previous research has shown that the bio-optical properties of cyanobacteria can change during mass cell lysis (Simis et al. 2005b; Zhang et al. 2009). Simis et al. (2005) cultured filamentous cyanobacteria collected from Lake Loosdrecht, the Netherlands, and measured changes to the optical properties and pigment concentration as the growth experiment progressed. The results of Simis et al. (2005) showed that as viral-induced mass cell lysis set in and the community of cyanobacteria collapsed, the magnitude of optical scattering and absorption were reduced by up to 80 % of original values measured at the beginning of the experiment (Simis et al. 2005b).

In this study we examined two distinct colour modes of *Trichodesmium* spp. sampled from an extremely dense surface aggregation within the Southern Great Barrier Reef (GBR), Australia. The difference in colour was inferred to be due to physiological state and pigment leaching. To confirm this, the spectral particulate and soluble absorption coefficients of the two colour modes of *Trichodesmium* were measured to ascertain the extent of pigment leaching from the cyanobacteria. Simulations of hyperspectral remote sensing reflectance $R_{rs}(\lambda)$ spectra using the

radiative transfer simulation software Hydrolight were conducted. The modelled $R_{rs}(\lambda)$ was then examined in order to identify spectral features that may allow the two colour modes to be discriminated using ocean colour sensors. This research presents for the first time bio-optical properties of senescing *Trichodesmium*. Such information may be useful for the development of optical remote sensing algorithms to monitor the physiological state of *Trichodesmium* surface aggregations.

5.2 Data and Methods

During a research cruise aboard the RV Cape Ferguson on 16 February 2009, dense surface patches (> 100 m across) of *Trichodesmium* were encountered in the Southern Great Barrier Reef (GBR). A single site located at 22° 02.810' S, 150° 29.759' E was sampled at 12:20 hrs Australian Eastern Standard Time (AEST, +10hrs UTC). Within the study site, *Trichodesmium* exhibited two distinct colour modes which are hereby referred to as: (i) orange/brown (OB) and (ii) bright green (BG) as shown in Figure 5.1. A vertical conductivity-temperature-depth (CTD) profile was measured using a SeaBird Electronics 19plus instrument accompanied by a WETLabs ECO Chla Fluorometer, a WETLabs c-star beam attenuation transmissometer and a D & A optical backscatter sensor. Secchi disk depth was also recorded. Discrete surface samples of the two colour modes of *Trichodesmium* were collected using a clean bucket. These were immediately transferred into separate, clean Niskin bottles in an attempt to keep the samples cool and dark. Subsamples were then drawn from the Niskin bottles to determine Chla and phaeophytin (Pa) concentrations, and the particulate and soluble absorption coefficients.

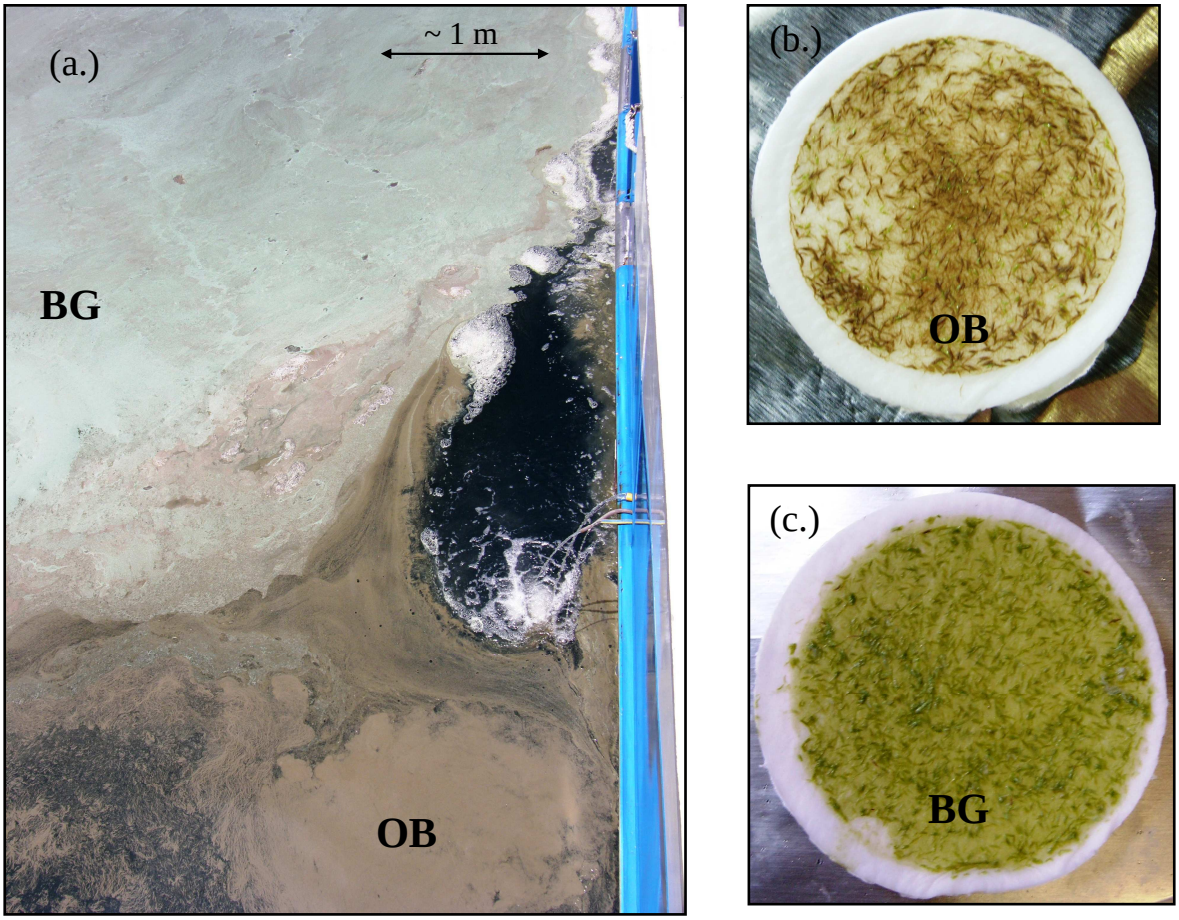

Figure 5.1: (a.) A dense surface aggregation of *Trichodesmium* spp. encountered on 16 February 2009 within the Southern Great Barrier Reef, Australia. The photograph is looking in the aft direction over the starboard side of the RV Cape Ferguson. Two distinct colour modes of *Trichodesmium* were observed: orange/brown (OB) and bright green (BG). Concentrations of OB and BG *Trichodesmium* colonies upon Whatman GF/F filters (Ø 25 mm) are shown in (b.) and (c.) respectively. [Image credit (a.): I. Zagorskis, Australian Institute of Marine Science (2009).]

5.3 Pigment Analysis

Duplicate 100 mL subsamples were drawn from each Niskin bottle. These were then filtered under low vacuum onto pre-combusted Whatman GF/F filters (Ø 25 mm). After filtration was complete, the filters were folded and wrapped separately in pre-combusted aluminium foil sheets and immediately frozen (-20 °C) for later analysis. Samples were extracted by grinding the filters in 90 % acetone. The combined chlorophyll-a and phaeophytin (Chla + Pa) concentration was then quantified using a Shimadzu UV-1600 spectrophotometer following Jeffrey and Humphrey (1975). The concentration of Pa was quantified spectrophotometrically after addition of 1 *N* HCl to break down remaining Chla. After determination of Pa concentration, this value was subtracted from the Chla + Pa value to yield the Chla concentration.

5.3.1 Absorption Coefficients

The spectral absorption coefficients for CDOM and total particulate matter were measured aboard the RV Cape Ferguson soon after sample collection. The methods for determining spectral absorption coefficients outlined by the Ocean Optics Protocols for Satellite Ocean Color Validation (Mitchell et al. 2003) were followed. CDOM samples were prepared by pre-filtering each sample through a pre-combusted Whatman GF/F filter (Ø 25 mm) under low vacuum to remove *Trichodesmium* colonies from solution. The filtrate was further filtered through a 0.22 μm pore polycarbonate filter into a 10 cm quartz cuvette for analysis with a dual-beam Shimaduz UV-1600 spectrophotometer. The spectrophotometer baseline was obtained using freshly prepared, Milli-Q water as a reference and Milli-Q water passed through a 0.22 μm polycarbonate filter as the sample. For each CDOM sample the optical density (OD) was measured over a spectral range of 250 – 800 nm with 0.5 nm resolution. The spectral CDOM absorption coefficient $a_g(\lambda)$ was determined from the OD using the following equation (Mitchell et al. 2003)

$$a_g(\lambda) = \frac{2.303}{l}\left(OD(\lambda) - OD_{NULL}\right) \qquad [5.1]$$

where *l* was the cuvette pathelength in metres (0.1 m) and OD_{NULL} was an offset value taken to be the OD value at 680nm where absorption due to CDOM was assumed to be zero (Oubelkheir et al. 2006).

Particulate absorption coefficients, $a_p(\lambda)$, were derived using the quantitative filter technique (QFT) (Mitchell et al. 2003). Samples of *Trichodesmium* and any other particulates were filtered onto pre-combusted Whatman GF/F filters (Ø 25 mm). The Shimadzu UV-1600 spectrophotometer baseline was determined using two clean filter blanks: a Milli-Q dampened filter as the reference and a filter dampened with 0.22 μm filtered seawater as the sample. The OD of a sample was measured from 250 - 800 nm with 0.5 nm resolution. The particulate absorption coefficient $a_p(\lambda)$ was then calculated using

$$a_p(\lambda) = \frac{2.303 A_f}{\beta V_f}\left(OD(\lambda) - OD_{NULL}\right) \qquad [5.2]$$

where A_f was the area of the filter in square metres, V_f was the volume filtered in cubic metres and β was the pathlength amplification correction coefficient for *Trichodesmium* taken to be 0.326 from Dupouy et al. (2008a). The value of OD_{NULL} was chosen to be the *OD* at 800 nm where absorption by particulate matter was deemed to be negligible (Mitchell et al. 2003). It was assumed that the particulate absorption coefficient was dominated by *Trichodesmium* and the influence of non-algal particulate matter (NAP) was negligible. Thus, $a_p(\lambda)$ was used to approximate the absorption coefficient of *Trichodesmium* $a_{tri}(\lambda)$.

5.3.2 Radiative Transfer Modelling

Hydrolight 5 radiative transfer software was used to simulate $R_{rs}(\lambda)$ for each colour mode of *Trichodesmium* sampled. Hydrolight numerically solves the equation of radiative transfer, however, requires the inherent optical properties (IOPs) of scattering and absorption coefficients for all constituents within the water column to be input. With Hydrolight, we modelled *Trichodesmium* for idealised offshore, blue water conditions with no sediments. Thus, the IOPs supplied to Hydrolight were the IOPs of pure water, *Trichodesmium* and CDOM. Absorption and scattering

coefficients for pure water are assumed constants and were taken from Pope and Fry (1997). The measured *Trichodesmium* absorption coefficients were normalised by their respective Chla concentrations to yield Cha specific particulate absorption coefficients for OB and BG *Trichodesmium* samples and are denoted as $a^*_{triOB}(\lambda)$ and $a^*_{triBG}(\lambda)$ respectively.

The spectral Chla specific scattering coefficient of *Trichodesmium*, $b^*_{tri}(\lambda)$, was not measured during this investigation. However, we have used values of the *Trichodesmium* Chla specific backscattering coefficient, $b^*_{b\,tri}(\lambda)$, to derive $b^*_{tri}(\lambda)$. The values of $b^*_{b\,tri}(\lambda)$ used within this investigation were measured by Dupouy et al. (2008a) using a HobiLabs Hydroscat 6 instrument. The backscattering ratio $\tilde{b}_b$ for *Trichodesmium* was also estimated by Dupouy et al. (2008a) to be between 0.017 and 0.027. Following this, we set $\tilde{b}_b$ = 0.02 and estimated $b^*_{tri}(\lambda)$ as follows

$$b^*_{tri}(\lambda) = \left(1/\tilde{b}_b\right) b^*_{b\,tri}(\lambda)\,. \qquad [5.3]$$

Within Hydrolight, a power law with Gordon-Morel values (Gordon et al. 1988) was used to model the spectral *Trichodesmium* scattering coefficient $b_{tri}(\lambda)$

$$b_{tri}(\lambda) = b^*_{tri}(\lambda_0)\ \mathrm{Chla}^n \left(\frac{\lambda_0}{\lambda}\right)^{\gamma} \qquad [5.4]$$

where, $b^*_{tri}(\lambda_0)$ was the magnitude of $b^*_{tri}(\lambda)$ at a reference wavelength λ_0 = 550 nm, and n= 0.62. The spectral slope coefficient was taken to be γ =1.2 according to Dupouy et al. (2008a). The value of $b^*_{tri}(550)$ was 0.475 $m^2\ mg^{-1}$, also taken from Dupouy et al. (2008a).

For modelling purposes, *Trichodesmium* was assumed to be amassed in the top 2 m of the water column which agreed with vertical profile data (see section 5.4.1). Thus, within Hydrolight the vertical Chla distribution was fixed to 100 mg Chla m^{-3} in the top 2 m, monotonically decreasing to 0.1 mg Chla m^{-3} at a depth of 10 m. R_{rs} spectra were modelled for both OB and BG *Trichodesmium* over a spectral range of 400 – 750 nm with 5 nm resolution.

Hydrolight also required environmental parameters such as solar zenith angle, wind conditions, cloud cover and optical depth to be input. Within this study we used

a solar zenith angle of 10° and assumed clear skies and an infinitely deep bottom. Wind speed was set to 1 knot which was consistent with field observations. Raman scattering, Chla fluorescence and CDOM fluorescence were also included in the model.

5.4 Results and Discussion

5.4.1 Oceanographic Conditions

Sea conditions during field sampling were glass-like, with a wind speed of 1 - 2 knots. These wind speeds are consistent with the concept of *Trichodesmium* surface aggregation formation during periods of relaxed wind stress (Capone et al. 1998). The CTD profile (Figure 5.2a) revealed the surface temperature and salinity were 29.5°C and 35.28 PSU respectively. Temperature reduced to 27.6 °C at the bottom depth of 38 m, whereas salinity remained constant throughout the water column. A small reduction in salinity of about 0.125 PSU was observed about 2 m beneath the thick surface layer of *Trichodesmium*. This was thought to be a sampling artefact caused by a high volume of *Trichodesmium* passing through the CTD flow cell slightly reducing the conductivity. The thickness of the *Trichodesmium* surface layer was approximately 1 - 2 m as indicated by high optical backscattering (Figure 5.2b), high Chla fluorescence (Figure 5.2c), and optical attenuation (Figure 5.2d) within this layer. Unfortunately the dynamic range of the Chla fluorometer was not large enough for a quantitative assessment of Chla concentrations within the surface layer. As an alternative, discrete Chla sampling provided these values. A Secchi disk depth, Z_d, of 5.5 m was recorded after breaking the dense surface layer. The diffuse attenuation coefficient, K_d, was approximated from Z_d according to Kirk (1994),

$$K_d = 1.7/Z_d \; . \qquad [5.5]$$

Consequently, a resulting K_d value of 0.31 m^{-1} was estimated beneath the *Trichodesmium*. Values of K_d were derived from average Secchi depths (De'ath and Fabricius 2008) within coastal, inner shelf and offshore waters of the GBR. These values were found to be 0.31 m^{-1} , 0.17 m^{-1} and 0.09 m^{-1} respectively. Thus, light attenuation beneath the *Trichodesmium* surface aggregation was of a similar magnitude to those expected for coastal waters within the GBR.

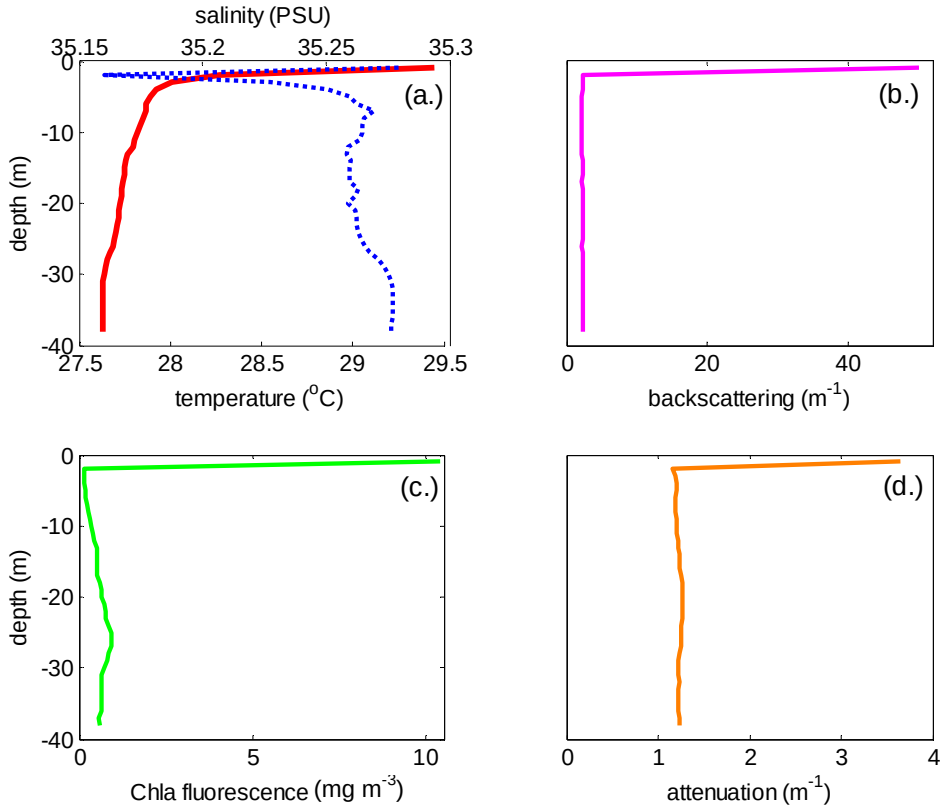

Figure 5.2: Vertical profile data collected using a SeaBird Electronics CTD instrument. (a.) Temperature (red) and salinity (dotted blue), (b.) optical backscattering (c.) Chla fluorescence, (d.) optical attenuation collected during a vertical profile beneath the *Trichodesmium* surface aggregation.

5.4.2 Discrete Pigment Samples

The mean Chla concentration for the OB and BG *Trichodesmium* samples was 57 ± 3.5 mg Chla m^{-3} and 315 ± 39 mg Chla m^{-3}, respectively. The Pa concentrations of the OB and BG samples were 9 ± 0.3 mg Pa m^{-3} and 77 ± 10 mg Pa m^{-3}, respectively. Because Pa is a degradation product of Chla, the ratio of Pa : Chla can act as a measure of physiological health. The ratio of Pa : Chla for the OB *Trichodesmium* sample was 0.17 and 0.25 for the BG sample. Previous experimental studies of freshwater cyanobacteria indicated that the Pa : Chla ratio remains low (< 0.3) during initial growth stages and increases sharply (> 1) corresponding to Chla breakdown at the onset of population collapse (Simis et al. 2005b; Zhang et al. 2009). In this study, the Pa : Chla ratios of both the OB and BG samples were low,

suggesting *Trichodesmium* was in good physiological condition. This result is reasonable for the OB sample; however, the BG sample was expected to show a significantly higher Pa : Chla ratio due to a increased level of Chla breakdown.

The difference in Chla concentration between the BG and OB samples was considered to be a sampling artefact. These discrepancies are likely due to immersion of the sampling bucket, which disturbed the structure of the surface aggregation. This problem was alluded to by Kutser et al. (2009) who indicated that accurate quantification of dense surface aggregations of cyanobacteria is an intractable problem. Unfortunately, it is likely that this artefact also carried through to absorption coefficient measurements also.

5.4.3 Particulate Pigment Absorption

To compare the spectral shapes of the absorption coefficients of the OB and BG *Trichodesmium* samples, each spectra was normalised to their respective values at 437 nm. The normalised absorption spectra are presented in Figure 5.3. The absorption spectra of the OB sample exhibited absorption peaks at 466, 495, 545, 575 and 620 nm assumed to be due to carotenoids, phycourobilin (PUB), phycoerythrobilin (PEB), phycoeryrthocyanin (PEC) and phycocyanin (PC) respectively. Chlorophyll-a absorption peaks were also evident at 437 and 675 nm. This observation was consistent with data reported in the literature for *Trichodesmium* (Subramaniam et al. 1999a; Dupouy et al. 2008a).

In contrast, the absorption spectra of the BG T*richodesmium* sample showed distinctly reduced absorption between 450 and 640 nm when compared with the absorption spectra of OB *Trichodesmium*. However, there appeared to be little difference in the spectral shape within the region of Chla absorption peaks at 437 and 675 nm. The BG sample exhibited a notable reduction in absorption around 495, 575 and 620 nm. Furthermore, the absorption peak at 545 nm appeared to be completely diminished. This spectral absorption data indicated that BG relative to OB *Trichodesmium* contained reduced concentrations of phycobilipigments PUB, PEB, PEC and PC, whist the Chla pigment was relatively intact.

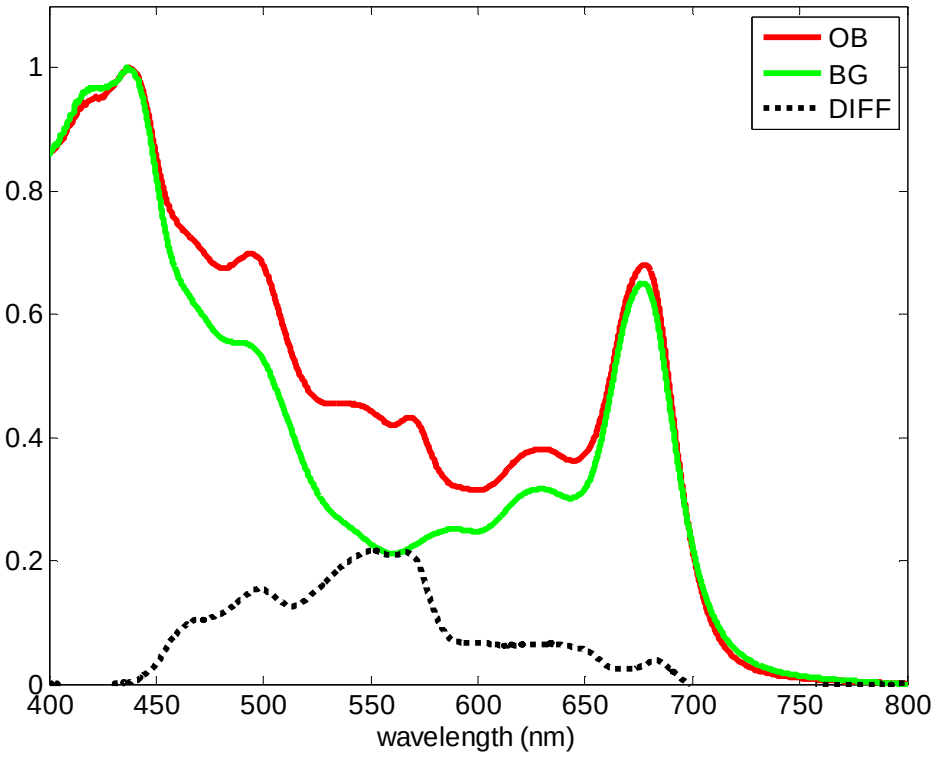

Figure 5.3: The normalised particulate absorption coefficient spectra for the OB and BG colour modes of *Trichodesmium*. The difference (DIFF) between the normalised OB and BG absorption spectra is plotted also.

5.4.4 Dissolved Pigment Absorption

The spectra of $a_g(\lambda)$ for seawater surrounding the OB and BG *Trichodesmium* samples differed greatly in both shape and magnitude. When analysing the dissolved pigments of the BG sample, a strong odour was noted and the seawater was tinted with a pink/rose colouration which complemented observations by Devassy et al. (1978). The $a_g(\lambda)$ spectra of both the OB and BG *Trichodesmium* samples revealed strong absorption in the UV with a peak centred at 330 nm and a shoulder at 368 nm attributed to the presence of MAAs concurrent with findings of Dupouy et al. (2008a). Maximum absorption occurred at 330 nm with a magnitude of 6.3 m^{-1} for the OB sample and exceeding 90 m^{-1} for the BG sample (see Figure 5.4).

The absorption coefficient, $a_{gOB}(\lambda)$, of CDOM surounding the OB *Trichodesmium* exhibited a broad absorption feature centred about 510 nm which is likely indicative of some minor leaching of phycobilipigments (Figure 5.5). The spectral absorption coefficient, $a_{gBG}(\lambda)$, of CDOM surrounding the BG *Trichodesmium* exhibited a distinct spectral shape when compared to that of the OB sample (Figure 5.5). Absorption peaks occurred at 496 and 541 nm with magnitudes of 3.9 and 3.5 m^{-1} respectively. These features corresponded to the phycobilipigments PUB and PEB whose absorption peaks within intact *Trichodesmium* occur around 495 and 545 nm (Subramaniam et al. 1999a). A lesser absorption peak within $a_{gBG}(\lambda)$ occurred around 630 nm and was likely to be associated with pigment leaching from PC. Two small shoulders were present within the $a_{gBG}(\lambda)$ spectra at 468 and 565 nm and were deemed to be associated with leaching of carotenoids and PEC respectively.

The particulate and dissolved spectral absorption coefficients indicated that the BG *Trichodesmium* had indeed leached phycobilipigments resulting in the sample's green appearance. Furthermore, these observations support the hypothesis that the BG *Trichodesmium* was undergoing cell lysis.

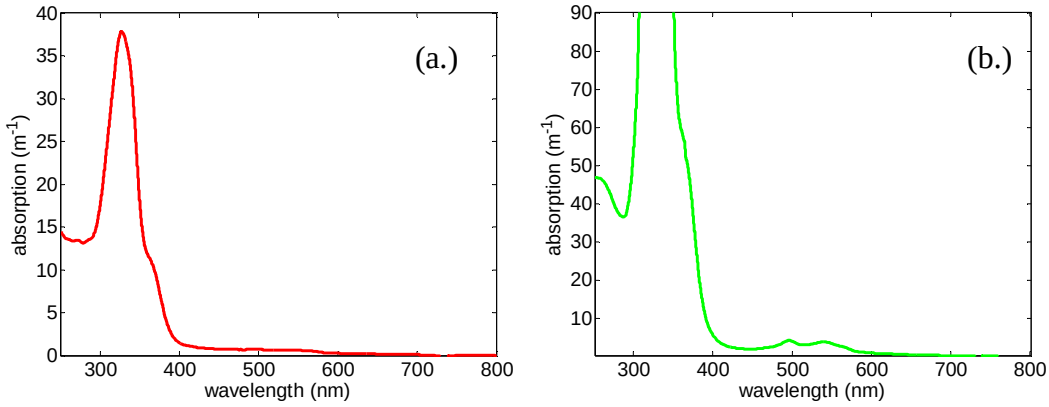

Figure 5.4: (a.) Measured CDOM spectral absorption coefficient for the OB *Trichodesmium* sample. (b.) Measured CDOM spectral absorption coefficient for the BG *Trichodesmium* sample. Note the scale of the y-axes on these plots differs.

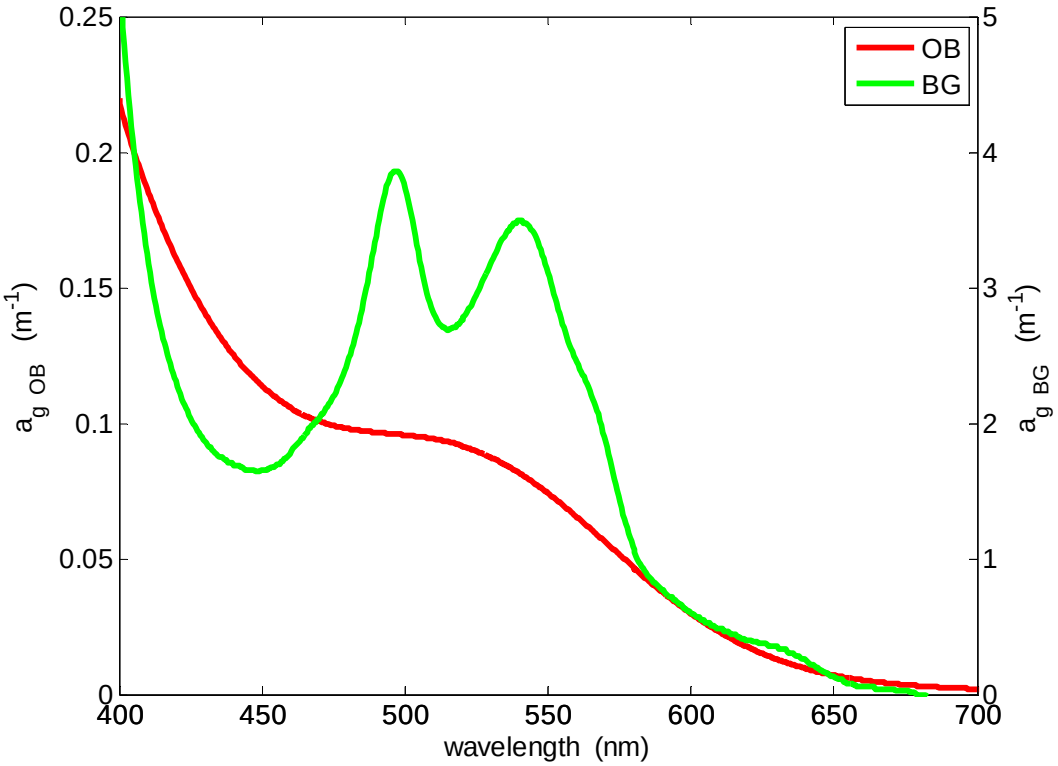

Figure 5.5: Spectra CDOM absorption coefficients $a_{gOB}(\lambda)$ and $a_{gBG}(\lambda)$ for the orange/brown (OB) and bright green (BG) colour modes of *Trichodesmium* respectively over the spectral range 400 – 700 nm.

5.4.5 Modelled Remote Sensing Reflectance

Modelled hyperspectral $R_{rs}(\lambda)$ spectra for the OB and BG *Trichodesmium* samples are presented in Figure 5.6 and hereby referred to as $R_{rsOB}(\lambda)$ and $R_{rsBG}(\lambda)$ respectively. The $R_{rs}(\lambda)$ spectra of both colour modes of *Trichodesmium* exhibited a peak at about 475 nm and troughs at 497 nm and 650 nm respectively. A red-edge peak was present at 690 nm. The $R_{rsOB}(\lambda)$ spectra contained spectral features consistent with reported hyperspectral measurements and modelled spectra of *Trichodesmium* (Borstad et al. 1992; Subramaniam et al. 1999b; Dupouy et al. 2008a; Hu et al. 2010). In particular, the $R_{rsOB}(\lambda)$ spectra exhibited distinct peaks at 527, 560 and 582 nm, a broad peak from 455 – 477 nm, and a shoulder at 642 nm. In contrast, the $R_{rsBG}(\lambda)$ spectra was dominated by a distinct peak at 560 nm and lacked dips/troughs at 547 and 567 nm exhibited in the $R_{rsOB}(\lambda)$ spectra. In addition, the $R_{rsBG}(\lambda)$ spectra exhibited no peak at 582 nm whilst the reflectance peak at 527 nm was greatly reduced in magnitude.

These results showed that $R_{rsOB}(\lambda)$ was spectrally distinct from $R_{rsBG}(\lambda)$, particularly due to the presence/absence of a peak at 582 nm. Unfortunately, there is no ocean colour band present in MODIS or MERIS centred on, or near, 582 nm that could be used to discriminate between OB and BG *Trichodesmium* (see Figure 5.6). However, MODIS has a band centred on 531 nm which may be useful for examining the reflectance peak at 527 nm which was distinct for $R_{rsOB}(\lambda)$ and diminished for $R_{rsBG}(\lambda)$. In addition, the gradient between 490 and 550 nm was found to be 4 x 10^{-5} and 8 x 10^{-5} sr^{-1} nm^{-1} for $R_{rsOB}(\lambda)$ and $R_{rsBG}(\lambda)$ respectively. As MODIS and MERIS both have bands in the vicinity of 490 and 550 nm, this gradient may be useful for discriminating OB from BG *Trichodesmium*. However, the gradient between 490 and 550 nm is likely to vary with Chla concentration. Therefore, discriminating OB from BG *Trichodesmium* using this approach requires further consideration.

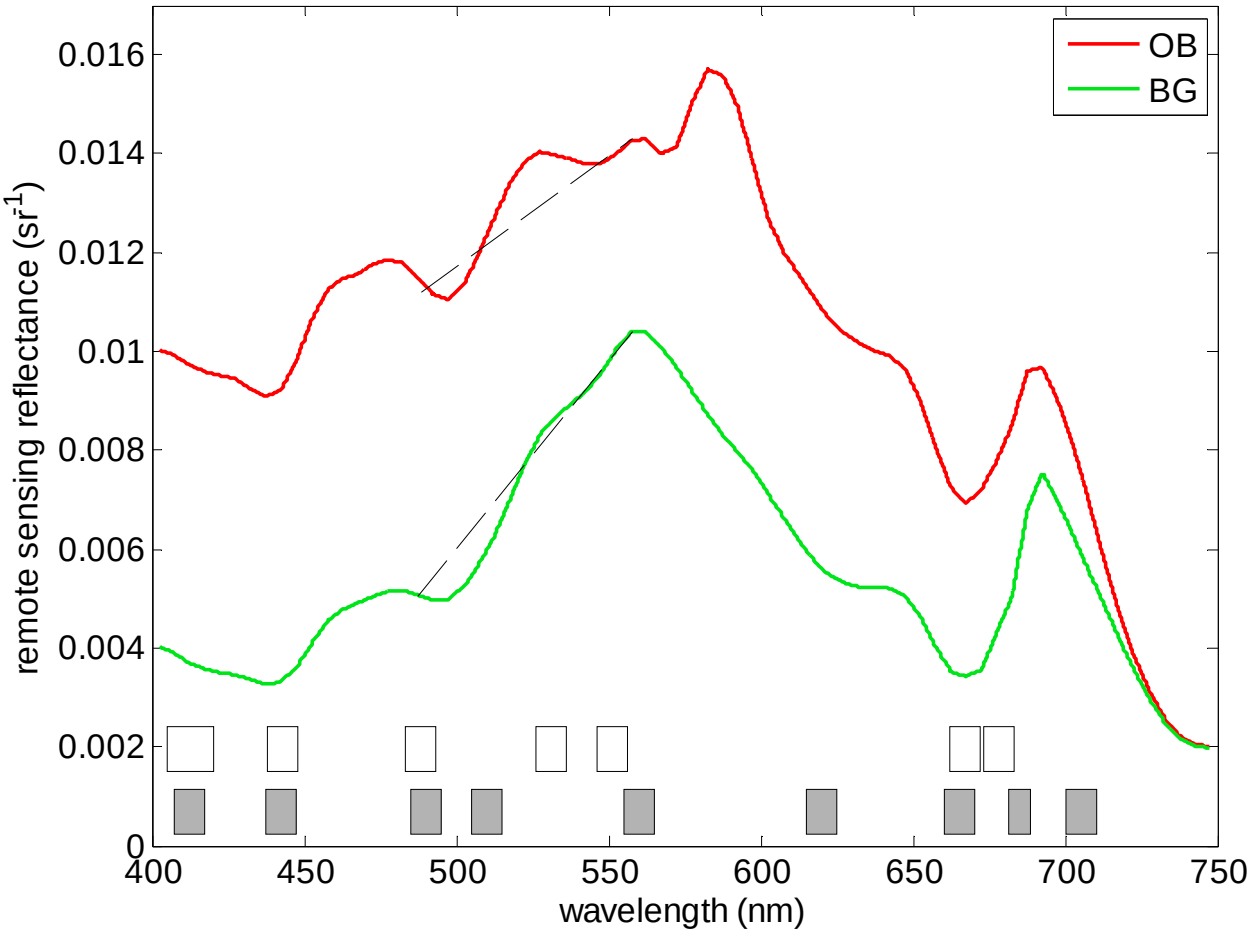

Figure 5.6: Hydrolight simulated remote sensing reflectance R_{rs} spectra for bright green (BG) and orange/brown (OB) colour modes of *Trichodesmium*. The grey and white boxes indicate the positions of the spectral bands of the MERIS and MODIS ocean colour sensors respectively. Dashed lines represent gradient between 490nm and 550 nm.

5.5 Discussion

This research has shown that the bio-optical characteristics of *Trichodesmium* may be linked to physiological state. This work validates the observations by Devassy et al. (1978) who reported colour changes of a *Trichodesmium* as it progressed from low to high concentration and eventual collapse. We have also shown that the pinkish-red colour imparted to seawater by decaying *Trichodesmium* may be attributed to cell lysis and release of water soluble phycobilipigments. The brilliant green colour of *Trichodesmium* colonies which had lost phycobilipigments indicated that the thylakoid membranes containing Chla probably remained intact for some period after cell lysis began. To determine the exact timescales of these breakdown processes requires further investigation. Nevertheless, these results indicate that it should be possible to discriminate bloom health from bio-optical properties.

An attempt was made to use the Pa : Chla ratios of the BG and OB *Trichodesmium* samples as a measure of physiological state. The BG sample was expected to have a high Pa : Chla ratio (> 1); however, the observed value of 0.25 was lower than expected. This discrepancy may be explained by a lag between leaching of the phycobilipigments and substantial Chla breakdown. Another method for determining *Trichodesmium* breakdown may be to use the ratio of phycobilipigments : Chla. Our results indicate that when *Trichodesmium* underwent cell lysis, the water soluble phycobilipigments were leached before Chla. This agrees with research by Simis et al. (2005) who showed that the PC : Chla ratio provided a good index for the progress of mass lysis within a cultured freshwater cyanobacterial community. The spectral features observed suggested significant leaching of phycobilipigments from *Trichodesmium* was observed in this study and therefore quantification of these solubilised pigments may assist in assessing physiological state. Appropriate metrics for *Trichodesmium* breakdown may be PEB : Chla or PUB : Chla ratios. To this end, previous work by Carpenter et al. (1993) may be useful where ratios of : phycoerythrin : Chla of 3.2 and 1.2 were established for fresh samples of *T. thiebautti* and *T. erythraeum* respectively.

The leaching of phycobilipigments from dense *Trichodesmium* has strong relevance to the field of bio-optics and ocean colour remote sensing. Physics-based

ocean colour inversion algorithms (Hoge and Lyon 1996; Carder et al. 1999; Lee et al. 2002; Maritorena et al. 2002) typically model $a_g(\lambda)$ using an exponential function defined by Bricaud et al. (1981)

$$a_g(\lambda) = a_g(\lambda_0)e^{-S(\lambda-\lambda_0)} \quad [5.5]$$

where λ_0 is a reference wavelength typically chosen to be 412 or 440 nm and *S* is a spectral slope coefficient which typically ranges between 0.010 – 0.020 nm^{-1} (Kirk 1994). However, this spectral model is not wavelength dependent and is thus not adequate for seawater containing considerable quantities of leached phycobilipigments.

The question now becomes: what method should be used to model $a_g(\lambda)$ for dense concentrations of *Trichodesmium* where pigment leaching is likely to have occurred? We briefly investigated the use of Gaussian curves alongside a single exponential function to approximate $a_{gBG}(\lambda)$ using non-linear least squares fitting (Figure 5.7). The Gaussian curves were centred on 473, 496, 540, 598, and 633 nm to approximate absorption peaks of carontenoids, PUB, PEB, PEC and PC pigments respectively. The optimally fitted exponential curve passed through 510 nm and had a spectral slope coefficient *S* of 0.0521 nm^{-1}, values that are not consistent with those typically used for modelling $a_g(\lambda)$. This exercise illustrated that the observed $a_g(\lambda)$ for BG *Trichodesmium* can be fitted reasonably well. However, this non-linear least squares fit is not as elegant as the contemporary model for $a_g(\lambda)$ of Bricaud et al. (1981) and would be difficult to implement into operational remote sensing algorithms.

In order to provide a truly robust model of $a_g(\lambda)$ for leached *Trichodesmium* pigments, further work is required to optically describe the process of pigment release as a surface aggregation decays. Furthermore, previous studies of seawater collected from within *Trichodesmium* aggregations found the pink colouration imparted by phycobilipigments fades and eventually disappear after 24 – 36 hours when exposed to natural or UV light (Jones et al. 1986). These observations suggest photodegradation of the phycobilipigments leached into the water column however, bacterial consumption (Steinberg et al. 2004) could also be a potential decay

mechanism. The degradation processes of leached pigments warrants further investigation.

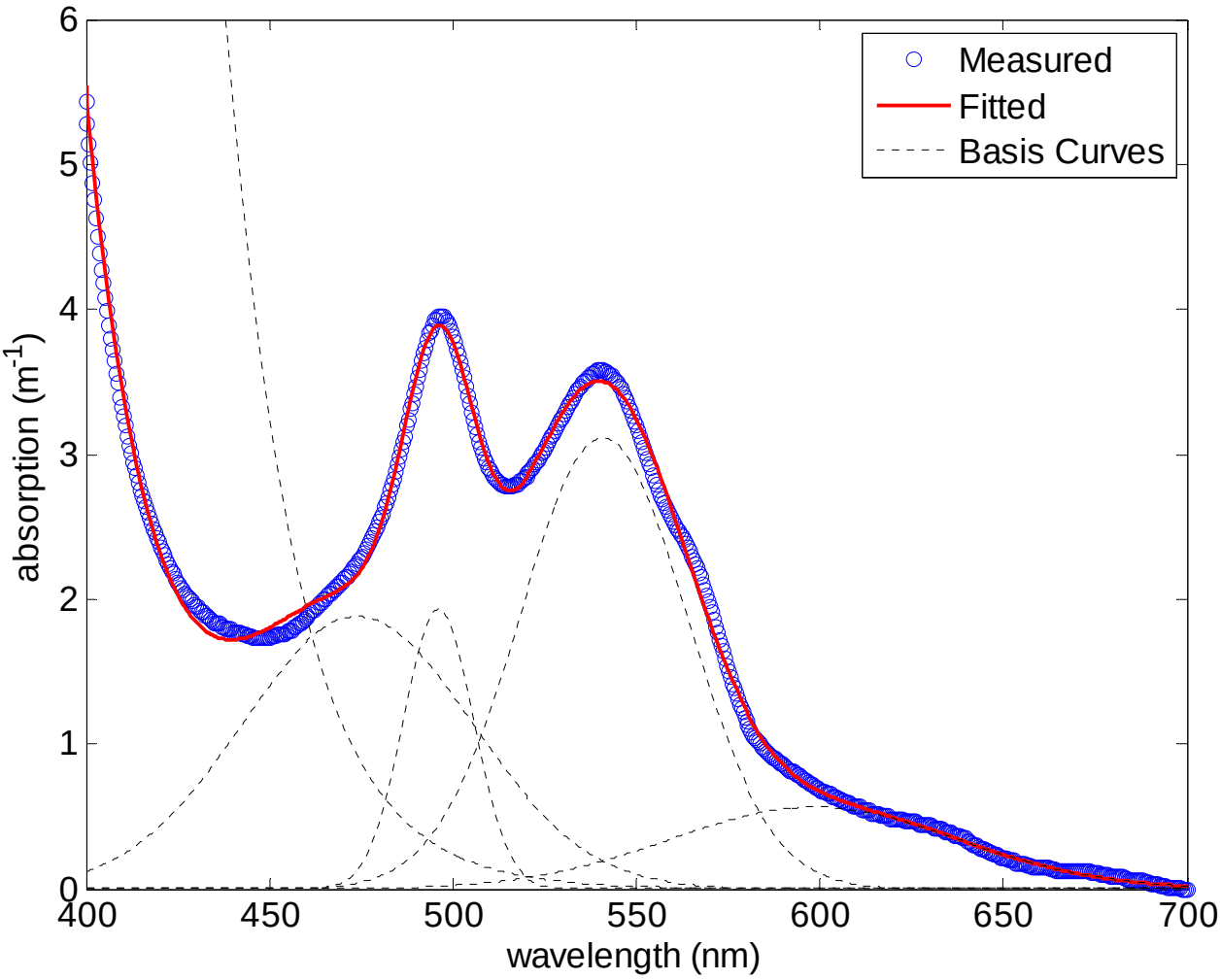

Figure 5.7: The measured absorption coefficient of dissolved pigments sampled from beneath the BG colour mode of *Trichodesmium* is represented as blue circles. A fitted line created using a series of Gaussian basis functions is shown as a red line. The dashed lines represent the individual basis curves used to fit the data.

Within this research, Hydrolight used a power law to estimate $b_{tri}(\lambda)$. However, previous investigations have identified wavelength dependence within $b_{b\,tri}(\lambda)$ due to reabsorption and fluorescence by the phycobilipigments (Subramaniam et al. 1999b; Dupouy et al. 2008a). Therefore, the power law approximation of $b_{tri}(\lambda)$ may have introduced some uncertainty to the magnitude of spectral peaks within the modelled R_{rs} spectra. For example, the magnitude of the modelled R_{rs} peak at 582 nm for OB *Trichodesmium* appeared to be slightly underestimated when compared with that of the literature (Borstad et al. 1992; Subramaniam et al. 1999b; Dupouy et al. 2008a; Hu et al. 2010). Furthermore, within Hydrolight it was assumed that $\tilde{b}_b$ had a constant value of 0.02 across all wavelengths. It is important to use appropriate $\tilde{b}_b$ within Hydrolight in order for the model to select an appropriate scattering phase function, $\tilde{\beta}$ (Mobley et al. 2002). Often $\tilde{b}_b$ can be treated as spectrally flat however, for pigment-containing particles $\tilde{b}_b$ can exhibit spectral dependence (Huot et al. 2007). Thus, using a constant value of $\tilde{b}_b$ across all wavelengths may be inappropriate. Therefore, the spectral characteristics of $\tilde{b}_b$ for *Trichodesmium* require further investigation.

Furthermore, the spectral absorption measurements of *Trichodesmium* from this investigation suggested that the BG *Trichodesmium* had lost much of its phycobilipigments, leading to its green appearance. This reduction in phycobilipigments may change the fluorescence and reabsorption properties within the BG sample. Therefore, the spectral shape and magnitude of $b_{tri}(\lambda)$ for lysing *Trichodesmium* is likely to be different to that of *Trichodesmium* with intact pigments. Research of freshwater cyanobacteria has shown the magnitude of optical scattering is reduced during bloom collapse (Simis et al. 2005b). The backscattering properties of *Trichodesmium* have been studied in detail by a small number of researchers (Subramaniam et al. 1999b; Dupouy et al. 2008a). However, there are presently no studies that have examinined the scattering properties of *Trichodesmium* at varying physiological states. Thus, there is a need for further investigation of the scattering properties of *Trichodesmium* populations during mass cell lysis.

Spatial patchiness and within-bloom optical variability presents an immense challenge for the optical discrimination of *Trichodesmium* physiological state. Current ocean colour sensors such as MERIS, SeaWiFS and MODIS have local area coverage (LAC) pixel resolutions of approximately 300 m, 1 km and 1 km respectively. The issue of spatial patchiness was discussed by Subramaniam et al. (2002) who developed a method for detection of *Trichodesmium* using SeaWiFS imagery. Subramaniam et al. (2002) suggested that due to the spatial patchiness of a *Trichodesmium*, the L_w signal measured within a SeaWiFS pixel of 1 x 1 km resolution would be the spectral combination of *Trichodesmium* patches and intermittent patches of clear waters. Field observations from this research indicated that the patches of different colour within the *Trichodesmium* surface bloom were in the order of 10 m across and thus of sub-pixel scale. Therefore, the sub-pixel patches of OB and BG *Trichodesmium* would most likely be unresolvable with current ocean colour sensors. However, the relative contribution of OB and BG patches within a pixel may be quantifiable.

To illustrate the effect of sub-pixel patchiness, we have treated the modelled $R_{rsOB}(\lambda)$ and $R_{rsBG}(\lambda)$ of OB and BG *Trichodesmium* surface aggregations as "basis vectors". The observed $R_{rs}(\lambda)$ for a given field-of-view was then assumed to be a linear combination of $R_{rsOB}(\lambda)$ and $R_{rsBG}(\lambda)$. This effect was simulated using the following relationship

$$R_{rs}(\lambda) = c\,R_{rsOB}(\lambda) + (1-c)\,R_{rsBG}(\lambda) \qquad [5.6]$$

where, c was the mixing ratio which ranged from 0 – 1. The results of this exercise are shown in Figure 5.8 and illustrates how the total $R_{rs}(\lambda)$ reflectance changes from a pixel initially dominated by OB *Trichodesmium* (c = 1) towards one which is dominated by BG *Trichodesmium* (c = 0). It is useful to note that this analysis only considers a pixel completely covered by a *Trichodesmium* surface aggregation. In reality, a surface distribution at the MODIS or MERIS pixel scales is likely to be patchy, with intermittent clear water features.

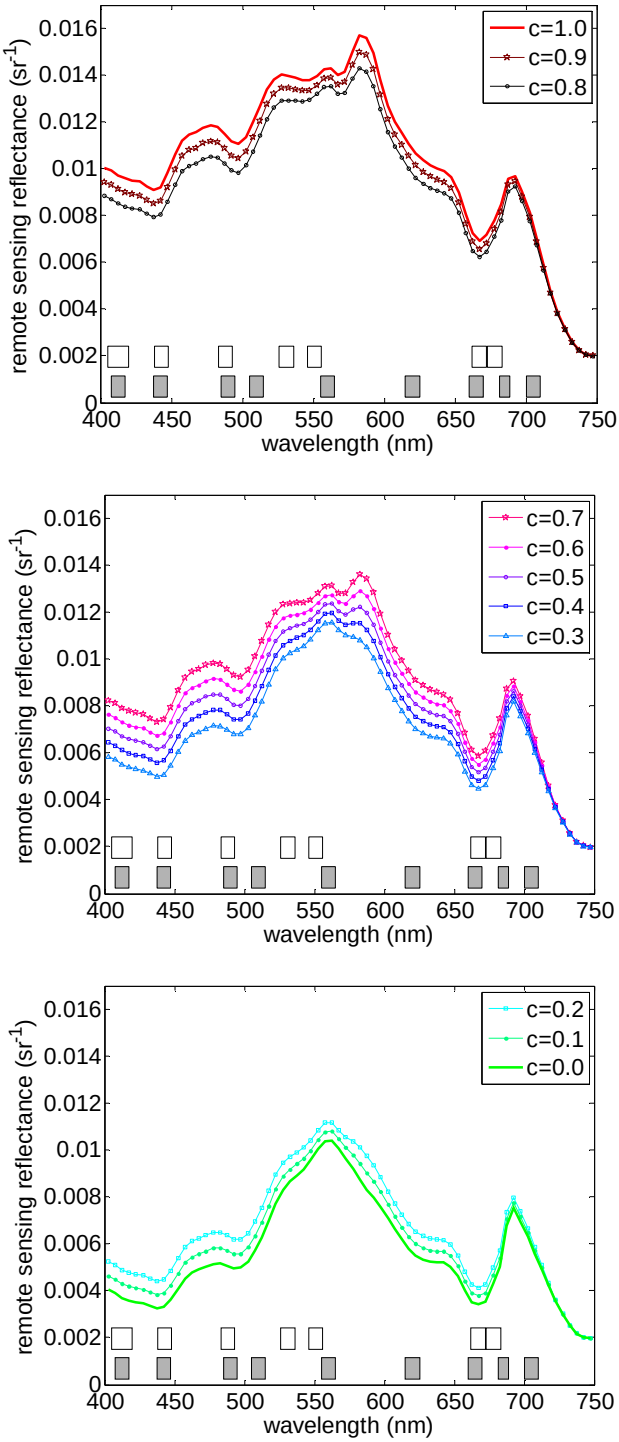

Figure 5.8: Estimated total R_{rs} spectra for a pixel containing varying proportions of OB and BG *Trichodesmium* dictated by the mixing ratio, *c*, as defined in Equation 5.6. The grey and white boxes indicate the positions of the spectral bands of the MERIS and MODIS ocean colour sensors respectively.

From Figure 5.8 it is clear that as the mixing ratio, *c*, decreased from unity toward zero, the total $R_{rs}(\lambda)$ spectra shifted from being dominated by OB *Trichodesmium* towards being dominated by BG *Trichodesmium*. The distinct peaks at 527 and 582 nm of the OB *Trichodesmium* became less prominent after $c = 0.7$. This observation suggests that after a field-of-view is covered by greater than 70 % BG *Trichodesmium*, the spectral characteristics of OB *Trichodesmium* become less distinct and the peak at 560 nm becomes the dominant feature.

5.6 Conclusion

This chapter has examined two distinct colour modes of *Trichodesmium* sampled within the Great Barrier Reef from a large surface aggregation. The absorption properties of the OB colour mode were consistent with previously reported literature values. However, the BG colour mode exhibited reduced absorption by phycobilipigments which were shown to have leached into the surrounding seawater upon examining the corresponding CDOM absorption coefficient. Thus, the BG *Trichodesmium* was assumed to be undergoing cell lysis.

Although the BG colonies of *Trichodesmium* sampled within this study were deemed to be undergoing cell lysis, others have found green *Trichodesmium* present at depth. During the *Diapalis Cruise*, Neveux et al. (2006) discovered green colonies of filamentous cyanobacteria in low concentrations at depths of 50 – 120 m within the Coral Sea. The green filaments were hypothesised to be a photoacclimated ecotype of *T. thiebautti*. However, Orcutt et al. (2008) who participated in the same research cruise refuted these claims. Instead, Orcutt et al. (2008) suggested the green colonies were *T. thiebautti* in senescence based upon an apparent lack of nitrogenase activity and degenerate DNA in comparison to healthy *T. thiebautti*. Further discussion of the green filaments was presented by Neveux et al. (2008) in which pulse amplitude modulation (PAM) fluorometry data was used to show the green filaments were photosynthetically well adapted to lower light levels than brown *Trichodesmium* colonies found in the upper water column.

Unfortunately the bio-optical properties of the green filamentous cyanobacteria sampled by Neveux et al. (2008) were not measured. Thus, a direct comparison to data presented within this thesis cannot be made. Furthermore, the

green *Trichodesmium* sampled within this study were buoyant and collected from within an extremely dense surface aggregation. In addition, the pink discolouration in the surrounding water indicated leaching of the phycobilipigments and senescence. As such, no comparisons have been drawn between the green *Trichodesmium* sampled within this chapter and those collected by Neveux et al. (2006) at depth. However, it is important to acknowledge that green *Trichodesmium* may be encountered in other circumstances other than during cell lysis.

Hyperspectral modelling using Hydrolight showed the R_{rs} of OB and BG *Trichodesmium* to be spectrally different. The effect of spatial patchiness was examined with results showing the distinct peaks exhibited by OB *Trichodesmium* became negligible after 70 % of a pixel was covered by BG *Trichodesmium*. It is likely that OB and BG *Trichodesmium* could be spectrally discriminated using MODIS and/or MERIS, however both satellites lack a spectral band near 580 nm which would be ideal for this purpose.

The results of this work are directly applicable to biological oceanographers and ocean colour scientists who wish to study the spatial and temporal resolution of *Trichodesmium* abundance using satellite remote sensing. This work may assist in optically determining the physiological state of a surface aggregation of *Trichodesmium* which is of significance ecologically and biogeochemically. This research has also mentioned and discussed the necessity of improved measurements of the scattering properties of *Trichodesmium* and in particular, studies into the spectral properties of the backscattering ratio.

Finally, it should be noted that the findings of this chapter were based upon only two samples collected from within a single *Trichodesmium* event. As such, the results should be interpreted with caution. In order to provide a complete and robust understanding, it is recommended that additional investigations of the optical properties of senescing *Trichodesmum* be conducted. Further work is also required to determine what contribution that other phytoplankton may have to the spectral reflectance characteristics of a complex mixed surface aggregation of *Trichodesmium*.

This page intentionally left blank

6 Thesis Conclusions and Future Work

Trichodesmium is a biogeochemically important diazotrophic, marine cyanobacterium. Not only is *Trichodesmium* estimated to be responsible for a large proportion of biogeochemically inferred nitrogen, it can also influence heat exchanges across the air-sea interface. Within the GBR, Australia, inputs of new-N due to *Trichodesmium* are likely to have order of magnitude uncertainties. This is associated with limited knowledge of spatial and temporal abundances of *Trichodesmium* within the GBR. Thus, an improved parameterisation of *Trichodesmium* variability is essential to enhance regional N-budgets. This PhD thesis was therefore concerned with the development of new methods for the detection and quantification of *Trichodesmium* within the GBR for application to ocean colour remote sensing.

An extensive review of contemporary remote sensing methods (**Chapter 2**) revealed that there were no methods specifically developed for, and validated within, the GBR. Thus, this PhD thesis examined the bio-optical and radiometric properties of *Trichodesmium* within the GBR. This research has resulted in two new methods being developed:

(i) A MODIS binary flag for detection of dense surface aggregations of *Trichodesmium* within the GBR (**Chapter 3**) and

(ii) A hyperspectral inversion method which discriminates and quantifies *Trichodesmium* abundance (**Chapter 4**).

In addition,

(iii) A brief investigation into the bio-optical properties of senescing *Trichodesmium* was conducted (**Chapter 5**).

6.1.1 A Binary Classification Algorithm

Within **Chapter 3**, surface aggregations of *Trichodesmium* were shown to exhibit a strong NIR reflectance feature when observed using above-water radiometry. Typically, water-leaving NIR radiances are negligible due to strong absorption of NIR photons by pure water. When examining the 859 nm band of MODIS, *Trichodesmium* surface aggregations were found to be distinct, highly reflective features against a background of low reflectance. Furthermore, *Trichodesmium* exhibited reduced reflectance within the 678 nm MODIS band due to strong Chla

absorption. Thus, a nLw(859) value larger than nLw(678), formed the primary detection criteria for the presence of a *Trichodesmium* surface aggregation. Two additional criteria which compared nLw(687) to the magnitudes of nLw(675) and nLw(555) respectively were used to remove potential confounding effects.

The binary classification algorithm was validated using *in situ* observations of *Trichodesmium* surface aggregations. The method was found to have an 85 % accuracy. Further tests of the algorithm found it robust against false-positive retrievals in the presence of potentially confounding effects such as highly reflective coral reefs and riverine plumes containing high CDOM and suspended sediment concentration. The method was found to resolve spatial features such as eddy swirls and windrow well. However, each pixel had a quasi-250 m resolution. Thus, small *Trichodesmium* surface aggregations of sub-pixel scale were likely to have difficulty in being detected. Nonetheless, this method provides a regionally validated method for detection of surface aggregations of *Trichodesmium* which may be applicable to optically similar regions such as the southwestern Pacific Ocean in the vicinity of New Caledonia.

6.1.2 Hyperspectral Inversion Algorithm

Within **Chapter 4** a method was developed which combined the QAA and a SIM for the purposes of discriminating *Trichodesmium* from hyperspectral $R_{rs}(\lambda)$ data. Initially, $R_{rs}(\lambda)$ were simulated with Hydrolight using *Trichodesmium* specific IOPs for examples of Case 1 and Case 2 waters. The $R_{rs}(\lambda)$ data were inverted using the QAA to derive $a_{\phi}^{QAA}(\lambda)$ which was compared with a reference absorption of *Trichodesmium* $a_{tri}^{ref}(\lambda)$ and six other phytoplankton. The results indicated that *Trichodesmium* could be discriminated from six other phytoplankton types at threshold concentrations of 0.2 and 1 mg Chla m^{-3} for the Case 1 and 2 waters considered. A SIM_{TRI} threshold of 0.6 was established, below which there was less confidence that *Trichodesmium* was well discriminated.

The combined QAA-SIM method was tested upon transect $R_{rs}(\lambda)$ data collected within the GBR for which *Trichodesmium* was known to be present. A flow-through system housing a Chla fluorometer was used to directly measure along-

transect Chla concentration. Once an along-transect data point was identified as containing *Trichodesmium* using the QAA-SIM method, Chla concentration was estimated based upon the magnitude of $a_{\phi}^{QAA}(\lambda)$ at 443 nm using a newly established empirical relationship. The radiometrically derived Chla, when compared with the fluorometer-measured Chla values, had strong linearity with an R-squared value of 0.81. However, Chla concentration was underestimated by approximately 0.05 mg Chla m^{-3}. Nonetheless, this was better than the standard NASA OC3 and OC4 algorithms which overestimated Chla concentration by 0.2 mg Chla m^{-3}.

The ability to discriminate and quantify *Trichodesmium* abundance with the QAA-SIM method has direct implications for resolving N-fixation rates with a high spatial and temporal resolution. For the single transect examined in **Chapter 4**, it was estimated that during 1.8 hours, approximately 2 grams of nitrogen was fixed within a 30 km^2 area. This value was extrapolated and a crude estimate of the annual areal N-fixation rate was determined to be 0.7 tonnes N km^{-2} yr^{-1} which was within the range of previous estimates within literature.

6.1.3 Bio-optical Properties of Senescing Trichodesmium

The bio-optical properties of two colour modes of *Trichodesmium* sampled within the GBR were examined in **Chapter 5**. *Trichodesmium* within a dense surface aggregation presented in two distinct colour modes denoted as orange/brown (OB) and bright-green (BG). Particulate and CDOM absorption coefficients revealed that the BG *Trichodesmium* had leached a large proportion of its water soluble phycobilipigments into the surrounding seawater. However, the spectral shape of the OB particulate absorption coefficient was as expected. This suggested that the BG *Trichodesmium* were undergoing cell lysis, whilst the OB *Trichodesmium* remained relatively intact. This was not clearly reflected in Pa:Chla ratios which were lower than expected. This suggested a lag between phycobilipigments leaching and Chla breakdown.

Modelling of hyperspectral $R_{rs}(\lambda)$ revealed both colour modes were spectrally distinct. In particular, the $R_{rs}(\lambda)$ of OB *Trichodesmium* exhibited a peak at 582 nm that was not present within the $R_{rs}(\lambda)$ of BG *Trichodesmium*. Thus, it was established that the two colours may be distinguishable using MERIS, as there is no

band on or near 582 nm for MODIS. However, future sensors would benefit from a spectral band centred on or near 580 nm to aid not only in discriminating different colour modes of *Trichodesmium* but also in discriminating *Trichodesmium* from other green phytoplankton. The $R_{rs}(\lambda)$ properties of a field-of-view containing varying concentrations of OB and BG *Trichodesmium* were also examined. This investigation found the dominant peak at 852 nm of OB *Trichodesmium* became less distinct when the field-of-view contained 70% or more BG *Trichodesmium*.

6.2 Overview and Implications

The newly developed methods within this PhD research project were shown to be suitable for the detection of *Trichodesmium* and were specifically designed for waters of the GBR, Australia. The methods were able to detect *Trichodesmium* in both dense surface aggregations and dispersed abundance. Thus, by combining radiometric data from ships of opportunity and satellite ocean colour sensors it should be possible to resolve spatial and temporal variations in *Trichodesmium* abundance. Furthermore, the bio-optical properties of *Trichodesmium* during cell lysis were examined. Thus, the potential to remotely sense *Trichodesmium* physiological state was established.

These results have implications for ecosystem health and bio-geochemistry studies within the GBR. As established within the literature, *Trichodesmium* is known to contribute significant quantities of new-N to the GBR. However, order of magnitude uncertainties are associated with estimates of N-fixation due to limited understanding of variability in *Trichodesmium* abundance. Heat exchanges across the air-sea interface are also known to be influenced by the presence of dense cyanobacterial surface aggregations. Furthermore, *Trichodesmium* surface aggregations have caused fouling and subsequent closure of beaches within the GBR. The new methods developed within this PhD thesis have the potential to address these scientific and management issues.

The QAA-SIM method discussed in **Chapter 4** was able to resolve information regarding *Trichodesmium* abundance with high temporal and spatial resolution. Furthermore, the ability to resolve along-transect N-fixation rates using derived abundance data was demonstrated. In addition, the binary classification algorithm

discussed in **Chapter 3** was found to be a robust method for the detection of *Trichodesmium* surface aggregations within the GBR. Thus, by collecting further along-transect hyperspectral radiometry and examining MODIS imagery, it should be possible to significantly enhance present understanding of *Trichodesmium* abundance and variability within the GBR.

Information detailed in **Chapter 5** regarding the bio-optical properties of senescing *Trichodesmium* in combination with the binary detection algorithm developed in **Chapter 3** could have the potential application to near-real time monitoring of *Trichodesmium* surface aggregations. Thus, the size, physiological state and movement of a *Trichodesmium* surface aggregation could be mapped using ocean colour satellites. This has direct implications for management, and response decisions regarding closure and/or cleanup of popular swimming beaches within the GBR should a large-scale *Trichodesmium* event occur.

Although the methods outlined within the thesis have been developed and validated specifically for the GBR, they may be applicable to other regions. For example, waters of the south-western tropical Pacific Ocean (SWTP) are likely to be optically similar to the GBR. Thus, the methods developed within this thesis may be directly applicable to the SWTP. Conversely, in regions such as the Gulf of Mexico and the west coast of India, the phytoplankton community is much more complex than within the GBR. Thus, application of GBR-specific algorithms may be more challenging for these regions and as such region-specific validation of algorithms is recommended.

6.3 Future Work

6.3.1 Sampling Strategies and Bio-optical Properties

For the purposes of determining the predictive skill of ocean colour algorithms, *in situ* validation points are essential. Large data sets such as SeaBAM have been essential to the development and tuning of global ocean colour algorithms. However, within this PhD project only a small number of *in situ Trichodesmium* bio-optical data points were collected. Thus, ongoing collection of *in situ* bio-optical, radiometric and Chla concentration data within the GBR is recommended. Such a dataset is not only useful for further development and validation of *Trichodesmium*

specific algorithms, but has applications for future development of region-specific ocean colour algorithms.

The quantification of dense surface aggregations of *Trichodesmium* has been identified as an intractable problem. Attempts to sample using buckets and Niskin bottles are fraught with difficulty. In particular, the immersion of instruments, buckets or Niskin bottles disperses the surface layer and as such it is difficult to get a representative sample. However, it was established that the boom-mounted hyperspectral radiometer was useful for monitoring dense surface aggregations remotely without disturbing the surface layer. Unfortunately, due to exceptional self-shading, it is extremely difficult to draw conclusions regarding *Trichodesmium* abundance beneath a dense surface aggregation using radiometry. Thus, further work is required to establish an understanding of *Trichodesmium* vertical distribution in these situations.

The vertical distribution of *Trichodesmium* also has implications upon Chla estimates derived from the flow-through fluorometer system. For example, the intake manifold for the flow-through system aboard the RV Cape Ferguson was 2 m below the surface. When the water column is well mixed, the flow-through system is likely to give a good approximation of Chla concentration in the upper few metres. However, in the situation where a dense surface aggregation of *Trichodesmium* is present, water sampled at 2 m may not be representative of the *Trichodesmium* abundance at the surface.

Within this PhD thesis, various shortcomings regarding the sampling of bio-optical properties were identified. In particular, it was assumed *Trichodesmium* had a spectrally flat backscattering ratio of 0.02. This value was used within Hydrolight for the purpose of modelling the $R_{rs}(\lambda)$ of *Trichodesmium*. However, the backscattering ratio of *Trichodesmium* may exhibit spectral dependencies. Therefore to improve radiative transfer modelling using Hydrolight, further studies of the scattering and backscattering coefficients of *Trichodesmium* are warranted.

Another potentially useful parameter to quantify in future studies of *Trichodesmium* bio-optical properties is phycobilipigment concentration. Within this PhD thesis, Chla concentration was routinely collected, however, there were no means established for quantification of phycobilipigment concentration. Phycobilipigments concentration is necessary for development and validation of phycobilipigment-

specfic retrieval algorithms. Furthermore, phycobilipigments : Chla ratios have been identified in literature as useful methods for assessing cyanobacterial physiological state.

The influence of spatial patchiness was briefly addressed within Chapter 5, by examining the effect of varying proportions of OB and BG *Trichodesmium* upon the $R_{rs}(\lambda)$ for a given field-of-view. However, further studies regarding the effect of sub-pixel patchiness upon the $R_{rs}(\lambda)$ spectra would be insightful. In addition, the effect of vertical variability of *Trichodesmium* abundance upon $R_{rs}(\lambda)$ warrants further investigation.

Thesis Appendices

Appendix 1: Look-up-table, LUT, of sky reflectance coefficients ρ……163

Appendix 2: FLNTU Linear Offsets……...251

Appendix 3: The Quasi-Analytical Algorithm……...253

Appendix 4: N-fixation Estimates from Derived *Trichodesmium* abundance....257

Appendix 1: Look-up-table, LUT, of sky reflectance coefficients ρ

The following pages contain the look-up-table (LUT) of sky reflectance coefficients, ρ, used for deriving above-water remote sensing reflectance according to Mobley (1999)

$$R_{rs} = \frac{L_u - \rho L_{sky}}{E_d} \qquad \text{[A1.1]}$$

where, the parameters L_u, L_{sky} and E_d are the total upwelling radiance, sky radiance and downwelling irradiance respectively. The coefficient ρ is dependent upon wind speed, solar zenith angle and sensor viewing geometry.

rho = L(surface reflected)/L(sky) (non-dimen) as in Mobley, 1999, Appl Opt 38, page 7445, Eq. 4

[(Theta,Phi) are the directions of photon travel.

Theta is measured from 0 at the zenith.

Solar photons travel in the Phi = 180 direction (the sun is located at Phi = 0).

(Thus Phi = 45 represents the 135 degree viewing angle for minimizing sun glitter.)]

These values are for 550 nm (see RhoNotes.pdf for discussion)

rho for WIND SPEED = 0.0 m/s THETA_SUN = 0.0 deg

I	J	Theta (zenith)	Phi	Phi-view	rho (Lrefl/Lsky)
10	1	0.0	0.0	0.0	0.0211
9	1	10.0	0.0	180.0	0.0211
9	2	10.0	15.0	165.0	0.0211
9	3	10.0	30.0	150.0	0.0211
9	4	10.0	45.0	135.0	0.0211
9	5	10.0	60.0	120.0	0.0211
9	6	10.0	75.0	105.0	0.0211
9	7	10.0	90.0	90.0	0.0211
9	8	10.0	105.0	75.0	0.0211
9	9	10.0	120.0	60.0	0.0211
9	10	10.0	135.0	45.0	0.0211
9	11	10.0	150.0	30.0	0.0211
9	12	10.0	165.0	15.0	0.0211
9	13	10.0	180.0	0.0	0.0211
8	1	20.0	0.0	180.0	0.0213
8	2	20.0	15.0	165.0	0.0213
8	3	20.0	30.0	150.0	0.0213
8	4	20.0	45.0	135.0	0.0213
8	5	20.0	60.0	120.0	0.0213
8	6	20.0	75.0	105.0	0.0213
8	7	20.0	90.0	90.0	0.0213
8	8	20.0	105.0	75.0	0.0213
8	9	20.0	120.0	60.0	0.0213
8	10	20.0	135.0	45.0	0.0213
8	11	20.0	150.0	30.0	0.0213
8	12	20.0	165.0	15.0	0.0213
8	13	20.0	180.0	0.0	0.0213
7	1	30.0	0.0	180.0	0.0223
7	2	30.0	15.0	165.0	0.0223
7	3	30.0	30.0	150.0	0.0223
7	4	30.0	45.0	135.0	0.0223
7	5	30.0	60.0	120.0	0.0223
7	6	30.0	75.0	105.0	0.0223
7	7	30.0	90.0	90.0	0.0223
7	8	30.0	105.0	75.0	0.0223
7	9	30.0	120.0	60.0	0.0223
7	10	30.0	135.0	45.0	0.0223
7	11	30.0	150.0	30.0	0.0223
7	12	30.0	165.0	15.0	0.0223
7	13	30.0	180.0	0.0	0.0223
6	1	40.0	0.0	180.0	0.0256
6	2	40.0	15.0	165.0	0.0256
6	3	40.0	30.0	150.0	0.0256
6	4	40.0	45.0	135.0	0.0256
6	5	40.0	60.0	120.0	0.0257
6	6	40.0	75.0	105.0	0.0257
6	7	40.0	90.0	90.0	0.0256
6	8	40.0	105.0	75.0	0.0257
6	9	40.0	120.0	60.0	0.0257
6	10	40.0	135.0	45.0	0.0256
6	11	40.0	150.0	30.0	0.0256
6	12	40.0	165.0	15.0	0.0256
6	13	40.0	180.0	0.0	0.0256
5	1	50.0	0.0	180.0	0.0355
5	2	50.0	15.0	165.0	0.0354
5	3	50.0	30.0	150.0	0.0357
5	4	50.0	45.0	135.0	0.0356
5	5	50.0	60.0	120.0	0.0355
5	6	50.0	75.0	105.0	0.0355
5	7	50.0	90.0	90.0	0.0355
5	8	50.0	105.0	75.0	0.0355
5	9	50.0	120.0	60.0	0.0355
5	10	50.0	135.0	45.0	0.0356
5	11	50.0	150.0	30.0	0.0357
5	12	50.0	165.0	15.0	0.0354
5	13	50.0	180.0	0.0	0.0355
4	1	60.0	0.0	180.0	0.0637
4	2	60.0	15.0	165.0	0.0633
4	3	60.0	30.0	150.0	0.0631
4	4	60.0	45.0	135.0	0.0630
4	5	60.0	60.0	120.0	0.0633
4	6	60.0	75.0	105.0	0.0633
4	7	60.0	90.0	90.0	0.0636
4	8	60.0	105.0	75.0	0.0633
4	9	60.0	120.0	60.0	0.0633
4	10	60.0	135.0	45.0	0.0630
4	11	60.0	150.0	30.0	0.0631
4	12	60.0	165.0	15.0	0.0633
4	13	60.0	180.0	0.0	0.0637
3	1	70.0	0.0	180.0	0.1425
3	2	70.0	15.0	165.0	0.1425
3	3	70.0	30.0	150.0	0.1410
3	4	70.0	45.0	135.0	0.1405

3	5	70.0	60.0	120.0	0.1404
3	6	70.0	75.0	105.0	0.1421
3	7	70.0	90.0	90.0	0.1408
3	8	70.0	105.0	75.0	0.1421
3	9	70.0	120.0	60.0	0.1404
3	10	70.0	135.0	45.0	0.1405
3	11	70.0	150.0	30.0	0.1410
3	12	70.0	165.0	15.0	0.1425
3	13	70.0	180.0	0.0	0.1425
2	1	80.0	0.0	180.0	0.3680
2	2	80.0	15.0	165.0	0.3677
2	3	80.0	30.0	150.0	0.3646
2	4	80.0	45.0	135.0	0.3686
2	5	80.0	60.0	120.0	0.3617
2	6	80.0	75.0	105.0	0.3656
2	7	80.0	90.0	90.0	0.3727
2	8	80.0	105.0	75.0	0.3656
2	9	80.0	120.0	60.0	0.3617
2	10	80.0	135.0	45.0	0.3686
2	11	80.0	150.0	30.0	0.3646
2	12	80.0	165.0	15.0	0.3677
2	13	80.0	180.0	0.0	0.3680
1	1	87.5	0.0	180.0	0.7714
1	2	87.5	15.0	165.0	0.7771
1	3	87.5	30.0	150.0	0.7745
1	4	87.5	45.0	135.0	0.7663
1	5	87.5	60.0	120.0	0.7766
1	6	87.5	75.0	105.0	0.7729
1	7	87.5	90.0	90.0	0.7732
1	8	87.5	105.0	75.0	0.7729
1	9	87.5	120.0	60.0	0.7766
1	10	87.5	135.0	45.0	0.7664
1	11	87.5	150.0	30.0	0.7745
1	12	87.5	165.0	15.0	0.7771
1	13	87.5	180.0	0.0	0.7714

rho for WIND SPEED = 0.0 m/s THETA_SUN = 10.0 deg

10	1	0.0	0.0	0.0	0.0211
9	1	10.0	0.0	180.0	0.0211
9	2	10.0	15.0	165.0	0.0211
9	3	10.0	30.0	150.0	0.0211
9	4	10.0	45.0	135.0	0.0211
9	5	10.0	60.0	120.0	0.0211
9	6	10.0	75.0	105.0	0.0211
9	7	10.0	90.0	90.0	0.0211
9	8	10.0	105.0	75.0	0.0211
9	9	10.0	120.0	60.0	0.0211
9	10	10.0	135.0	45.0	0.0211
9	11	10.0	150.0	30.0	0.0211
9	12	10.0	165.0	15.0	0.0211
9	13	10.0	180.0	0.0	0.0211
8	1	20.0	0.0	180.0	0.0213
8	2	20.0	15.0	165.0	0.0213
8	3	20.0	30.0	150.0	0.0213
8	4	20.0	45.0	135.0	0.0213
8	5	20.0	60.0	120.0	0.0213
8	6	20.0	75.0	105.0	0.0213
8	7	20.0	90.0	90.0	0.0213
8	8	20.0	105.0	75.0	0.0213
8	9	20.0	120.0	60.0	0.0213
8	10	20.0	135.0	45.0	0.0213
8	11	20.0	150.0	30.0	0.0213
8	12	20.0	165.0	15.0	0.0213
8	13	20.0	180.0	0.0	0.0213
7	1	30.0	0.0	180.0	0.0223
7	2	30.0	15.0	165.0	0.0223
7	3	30.0	30.0	150.0	0.0223
7	4	30.0	45.0	135.0	0.0223
7	5	30.0	60.0	120.0	0.0223
7	6	30.0	75.0	105.0	0.0223
7	7	30.0	90.0	90.0	0.0223
7	8	30.0	105.0	75.0	0.0223
7	9	30.0	120.0	60.0	0.0223
7	10	30.0	135.0	45.0	0.0223
7	11	30.0	150.0	30.0	0.0223
7	12	30.0	165.0	15.0	0.0223
7	13	30.0	180.0	0.0	0.0223
6	1	40.0	0.0	180.0	0.0256
6	2	40.0	15.0	165.0	0.0256
6	3	40.0	30.0	150.0	0.0256
6	4	40.0	45.0	135.0	0.0256
6	5	40.0	60.0	120.0	0.0257
6	6	40.0	75.0	105.0	0.0257
6	7	40.0	90.0	90.0	0.0256
6	8	40.0	105.0	75.0	0.0257
6	9	40.0	120.0	60.0	0.0257
6	10	40.0	135.0	45.0	0.0256
6	11	40.0	150.0	30.0	0.0256
6	12	40.0	165.0	15.0	0.0256
6	13	40.0	180.0	0.0	0.0256
5	1	50.0	0.0	180.0	0.0355
5	2	50.0	15.0	165.0	0.0354
5	3	50.0	30.0	150.0	0.0357
5	4	50.0	45.0	135.0	0.0356
5	5	50.0	60.0	120.0	0.0355
5	6	50.0	75.0	105.0	0.0355
5	7	50.0	90.0	90.0	0.0355
5	8	50.0	105.0	75.0	0.0355
5	9	50.0	120.0	60.0	0.0355
5	10	50.0	135.0	45.0	0.0356

5 11 50.0 150.0 30.0 0.0357
5 12 50.0 165.0 15.0 0.0354
5 13 50.0 180.0 0.0 0.0355
4 1 60.0 0.0 180.0 0.0637
4 2 60.0 15.0 165.0 0.0633
4 3 60.0 30.0 150.0 0.0631
4 4 60.0 45.0 135.0 0.0630
4 5 60.0 60.0 120.0 0.0633
4 6 60.0 75.0 105.0 0.0633
4 7 60.0 90.0 90.0 0.0636
4 8 60.0 105.0 75.0 0.0633
4 9 60.0 120.0 60.0 0.0633
4 10 60.0 135.0 45.0 0.0630
4 11 60.0 150.0 30.0 0.0631
4 12 60.0 165.0 15.0 0.0633
4 13 60.0 180.0 0.0 0.0637
3 1 70.0 0.0 180.0 0.1425
3 2 70.0 15.0 165.0 0.1425
3 3 70.0 30.0 150.0 0.1410
3 4 70.0 45.0 135.0 0.1405
3 5 70.0 60.0 120.0 0.1404
3 6 70.0 75.0 105.0 0.1421
3 7 70.0 90.0 90.0 0.1408
3 8 70.0 105.0 75.0 0.1421
3 9 70.0 120.0 60.0 0.1404
3 10 70.0 135.0 45.0 0.1405
3 11 70.0 150.0 30.0 0.1410
3 12 70.0 165.0 15.0 0.1425
3 13 70.0 180.0 0.0 0.1425
2 1 80.0 0.0 180.0 0.3680
2 2 80.0 15.0 165.0 0.3677
2 3 80.0 30.0 150.0 0.3646
2 4 80.0 45.0 135.0 0.3686
2 5 80.0 60.0 120.0 0.3617
2 6 80.0 75.0 105.0 0.3656
2 7 80.0 90.0 90.0 0.3727
2 8 80.0 105.0 75.0 0.3656
2 9 80.0 120.0 60.0 0.3617
2 10 80.0 135.0 45.0 0.3686
2 11 80.0 150.0 30.0 0.3646
2 12 80.0 165.0 15.0 0.3677
2 13 80.0 180.0 0.0 0.3680
1 1 87.5 0.0 180.0 0.7714
1 2 87.5 15.0 165.0 0.7771
1 3 87.5 30.0 150.0 0.7745
1 4 87.5 45.0 135.0 0.7664
1 5 87.5 60.0 120.0 0.7766
1 6 87.5 75.0 105.0 0.7729
1 7 87.5 90.0 90.0 0.7732
1 8 87.5 105.0 75.0 0.7729
1 9 87.5 120.0 60.0 0.7766
1 10 87.5 135.0 45.0 0.7664
1 11 87.5 150.0 30.0 0.7745
1 12 87.5 165.0 15.0 0.7771
1 13 87.5 180.0 0.0 0.7714
rho for WIND SPEED = 0.0 m/s THETA_SUN = 20.0 deg
10 1 0.0 0.0 0.0 0.0211
9 1 10.0 0.0 180.0 0.0211
9 2 10.0 15.0 165.0 0.0211
9 3 10.0 30.0 150.0 0.0211
9 4 10.0 45.0 135.0 0.0211
9 5 10.0 60.0 120.0 0.0211
9 6 10.0 75.0 105.0 0.0211
9 7 10.0 90.0 90.0 0.0211
9 8 10.0 105.0 75.0 0.0211
9 9 10.0 120.0 60.0 0.0211
9 10 10.0 135.0 45.0 0.0211
9 11 10.0 150.0 30.0 0.0211
9 12 10.0 165.0 15.0 0.0211
9 13 10.0 180.0 0.0 0.0211
8 1 20.0 0.0 180.0 0.0214
8 2 20.0 15.0 165.0 0.0213
8 3 20.0 30.0 150.0 0.0213
8 4 20.0 45.0 135.0 0.0213
8 5 20.0 60.0 120.0 0.0214
8 6 20.0 75.0 105.0 0.0213
8 7 20.0 90.0 90.0 0.0213
8 8 20.0 105.0 75.0 0.0213
8 9 20.0 120.0 60.0 0.0213
8 10 20.0 135.0 45.0 0.0213
8 11 20.0 150.0 30.0 0.0213
8 12 20.0 165.0 15.0 0.0213
8 13 20.0 180.0 0.0 0.0213
7 1 30.0 0.0 180.0 0.0223
7 2 30.0 15.0 165.0 0.0223
7 3 30.0 30.0 150.0 0.0223
7 4 30.0 45.0 135.0 0.0223
7 5 30.0 60.0 120.0 0.0223
7 6 30.0 75.0 105.0 0.0223
7 7 30.0 90.0 90.0 0.0223
7 8 30.0 105.0 75.0 0.0223
7 9 30.0 120.0 60.0 0.0223
7 10 30.0 135.0 45.0 0.0223
7 11 30.0 150.0 30.0 0.0223
7 12 30.0 165.0 15.0 0.0223
7 13 30.0 180.0 0.0 0.0223
6 1 40.0 0.0 180.0 0.0256
6 2 40.0 15.0 165.0 0.0256
6 3 40.0 30.0 150.0 0.0256

6	4	40.0	45.0	135.0	0.0256
6	5	40.0	60.0	120.0	0.0257
6	6	40.0	75.0	105.0	0.0257
6	7	40.0	90.0	90.0	0.0256
6	8	40.0	105.0	75.0	0.0257
6	9	40.0	120.0	60.0	0.0257
6	10	40.0	135.0	45.0	0.0256
6	11	40.0	150.0	30.0	0.0256
6	12	40.0	165.0	15.0	0.0256
6	13	40.0	180.0	0.0	0.0256
5	1	50.0	0.0	180.0	0.0355
5	2	50.0	15.0	165.0	0.0354
5	3	50.0	30.0	150.0	0.0357
5	4	50.0	45.0	135.0	0.0356
5	5	50.0	60.0	120.0	0.0355
5	6	50.0	75.0	105.0	0.0355
5	7	50.0	90.0	90.0	0.0355
5	8	50.0	105.0	75.0	0.0355
5	9	50.0	120.0	60.0	0.0355
5	10	50.0	135.0	45.0	0.0356
5	11	50.0	150.0	30.0	0.0357
5	12	50.0	165.0	15.0	0.0354
5	13	50.0	180.0	0.0	0.0355
4	1	60.0	0.0	180.0	0.0637
4	2	60.0	15.0	165.0	0.0633
4	3	60.0	30.0	150.0	0.0631
4	4	60.0	45.0	135.0	0.0630
4	5	60.0	60.0	120.0	0.0633
4	6	60.0	75.0	105.0	0.0633
4	7	60.0	90.0	90.0	0.0636
4	8	60.0	105.0	75.0	0.0633
4	9	60.0	120.0	60.0	0.0633
4	10	60.0	135.0	45.0	0.0630
4	11	60.0	150.0	30.0	0.0631
4	12	60.0	165.0	15.0	0.0633
4	13	60.0	180.0	0.0	0.0637
3	1	70.0	0.0	180.0	0.1425
3	2	70.0	15.0	165.0	0.1425
3	3	70.0	30.0	150.0	0.1410
3	4	70.0	45.0	135.0	0.1405
3	5	70.0	60.0	120.0	0.1404
3	6	70.0	75.0	105.0	0.1421
3	7	70.0	90.0	90.0	0.1408
3	8	70.0	105.0	75.0	0.1421
3	9	70.0	120.0	60.0	0.1404
3	10	70.0	135.0	45.0	0.1405
3	11	70.0	150.0	30.0	0.1410
3	12	70.0	165.0	15.0	0.1425
3	13	70.0	180.0	0.0	0.1425
2	1	80.0	0.0	180.0	0.3680
2	2	80.0	15.0	165.0	0.3677
2	3	80.0	30.0	150.0	0.3646
2	4	80.0	45.0	135.0	0.3686
2	5	80.0	60.0	120.0	0.3617
2	6	80.0	75.0	105.0	0.3656
2	7	80.0	90.0	90.0	0.3727
2	8	80.0	105.0	75.0	0.3656
2	9	80.0	120.0	60.0	0.3617
2	10	80.0	135.0	45.0	0.3686
2	11	80.0	150.0	30.0	0.3646
2	12	80.0	165.0	15.0	0.3677
2	13	80.0	180.0	0.0	0.3680
1	1	87.5	0.0	180.0	0.7714
1	2	87.5	15.0	165.0	0.7771
1	3	87.5	30.0	150.0	0.7745
1	4	87.5	45.0	135.0	0.7664
1	5	87.5	60.0	120.0	0.7766
1	6	87.5	75.0	105.0	0.7729
1	7	87.5	90.0	90.0	0.7732
1	8	87.5	105.0	75.0	0.7729
1	9	87.5	120.0	60.0	0.7766
1	10	87.5	135.0	45.0	0.7664
1	11	87.5	150.0	30.0	0.7745
1	12	87.5	165.0	15.0	0.7771
1	13	87.5	180.0	0.0	0.7714

rho for WIND SPEED = 0.0 m/s THETA_SUN = 30.0 deg

10	1	0.0	0.0	0.0	0.0211
9	1	10.0	0.0	180.0	0.0211
9	2	10.0	15.0	165.0	0.0211
9	3	10.0	30.0	150.0	0.0211
9	4	10.0	45.0	135.0	0.0211
9	5	10.0	60.0	120.0	0.0211
9	6	10.0	75.0	105.0	0.0211
9	7	10.0	90.0	90.0	0.0211
9	8	10.0	105.0	75.0	0.0211
9	9	10.0	120.0	60.0	0.0211
9	10	10.0	135.0	45.0	0.0211
9	11	10.0	150.0	30.0	0.0211
9	12	10.0	165.0	15.0	0.0211
9	13	10.0	180.0	0.0	0.0211
8	1	20.0	0.0	180.0	0.0213
8	2	20.0	15.0	165.0	0.0213
8	3	20.0	30.0	150.0	0.0213
8	4	20.0	45.0	135.0	0.0213
8	5	20.0	60.0	120.0	0.0213
8	6	20.0	75.0	105.0	0.0213
8	7	20.0	90.0	90.0	0.0213
8	8	20.0	105.0	75.0	0.0213
8	9	20.0	120.0	60.0	0.0213

8 10 20.0 135.0 45.0 0.0213
8 11 20.0 150.0 30.0 0.0213
8 12 20.0 165.0 15.0 0.0213
8 13 20.0 180.0 0.0 0.0213
7 1 30.0 0.0 180.0 0.0223
7 2 30.0 15.0 165.0 0.0223
7 3 30.0 30.0 150.0 0.0223
7 4 30.0 45.0 135.0 0.0223
7 5 30.0 60.0 120.0 0.0223
7 6 30.0 75.0 105.0 0.0223
7 7 30.0 90.0 90.0 0.0223
7 8 30.0 105.0 75.0 0.0223
7 9 30.0 120.0 60.0 0.0223
7 10 30.0 135.0 45.0 0.0223
7 11 30.0 150.0 30.0 0.0223
7 12 30.0 165.0 15.0 0.0223
7 13 30.0 180.0 0.0 0.0223
6 1 40.0 0.0 180.0 0.0256
6 2 40.0 15.0 165.0 0.0256
6 3 40.0 30.0 150.0 0.0256
6 4 40.0 45.0 135.0 0.0256
6 5 40.0 60.0 120.0 0.0257
6 6 40.0 75.0 105.0 0.0257
6 7 40.0 90.0 90.0 0.0256
6 8 40.0 105.0 75.0 0.0257
6 9 40.0 120.0 60.0 0.0257
6 10 40.0 135.0 45.0 0.0256
6 11 40.0 150.0 30.0 0.0256
6 12 40.0 165.0 15.0 0.0256
6 13 40.0 180.0 0.0 0.0256
5 1 50.0 0.0 180.0 0.0355
5 2 50.0 15.0 165.0 0.0354
5 3 50.0 30.0 150.0 0.0357
5 4 50.0 45.0 135.0 0.0356
5 5 50.0 60.0 120.0 0.0355
5 6 50.0 75.0 105.0 0.0355
5 7 50.0 90.0 90.0 0.0355
5 8 50.0 105.0 75.0 0.0355
5 9 50.0 120.0 60.0 0.0355
5 10 50.0 135.0 45.0 0.0356
5 11 50.0 150.0 30.0 0.0357
5 12 50.0 165.0 15.0 0.0354
5 13 50.0 180.0 0.0 0.0355
4 1 60.0 0.0 180.0 0.0637
4 2 60.0 15.0 165.0 0.0633
4 3 60.0 30.0 150.0 0.0631
4 4 60.0 45.0 135.0 0.0630
4 5 60.0 60.0 120.0 0.0633
4 6 60.0 75.0 105.0 0.0633
4 7 60.0 90.0 90.0 0.0636
4 8 60.0 105.0 75.0 0.0633
4 9 60.0 120.0 60.0 0.0633
4 10 60.0 135.0 45.0 0.0630
4 11 60.0 150.0 30.0 0.0631
4 12 60.0 165.0 15.0 0.0633
4 13 60.0 180.0 0.0 0.0637
3 1 70.0 0.0 180.0 0.1425
3 2 70.0 15.0 165.0 0.1425
3 3 70.0 30.0 150.0 0.1410
3 4 70.0 45.0 135.0 0.1405
3 5 70.0 60.0 120.0 0.1404
3 6 70.0 75.0 105.0 0.1421
3 7 70.0 90.0 90.0 0.1408
3 8 70.0 105.0 75.0 0.1421
3 9 70.0 120.0 60.0 0.1404
3 10 70.0 135.0 45.0 0.1405
3 11 70.0 150.0 30.0 0.1410
3 12 70.0 165.0 15.0 0.1425
3 13 70.0 180.0 0.0 0.1425
2 1 80.0 0.0 180.0 0.3680
2 2 80.0 15.0 165.0 0.3677
2 3 80.0 30.0 150.0 0.3646
2 4 80.0 45.0 135.0 0.3686
2 5 80.0 60.0 120.0 0.3617
2 6 80.0 75.0 105.0 0.3656
2 7 80.0 90.0 90.0 0.3727
2 8 80.0 105.0 75.0 0.3656
2 9 80.0 120.0 60.0 0.3617
2 10 80.0 135.0 45.0 0.3686
2 11 80.0 150.0 30.0 0.3646
2 12 80.0 165.0 15.0 0.3677
2 13 80.0 180.0 0.0 0.3680
1 1 87.5 0.0 180.0 0.7714
1 2 87.5 15.0 165.0 0.7771
1 3 87.5 30.0 150.0 0.7745
1 4 87.5 45.0 135.0 0.7664
1 5 87.5 60.0 120.0 0.7766
1 6 87.5 75.0 105.0 0.7729
1 7 87.5 90.0 90.0 0.7732
1 8 87.5 105.0 75.0 0.7729
1 9 87.5 120.0 60.0 0.7766
1 10 87.5 135.0 45.0 0.7664
1 11 87.5 150.0 30.0 0.7745
1 12 87.5 165.0 15.0 0.7771
1 13 87.5 180.0 0.0 0.7714
rho for WIND SPEED = 0.0 m/s THETA_SUN = 40.0
deg
10 1 0.0 0.0 0.0 0.0211
9 1 10.0 0.0 180.0 0.0211
9 2 10.0 15.0 165.0 0.0211

9	3	10.0	30.0	150.0	0.0211
9	4	10.0	45.0	135.0	0.0211
9	5	10.0	60.0	120.0	0.0211
9	6	10.0	75.0	105.0	0.0211
9	7	10.0	90.0	90.0	0.0211
9	8	10.0	105.0	75.0	0.0211
9	9	10.0	120.0	60.0	0.0211
9	10	10.0	135.0	45.0	0.0211
9	11	10.0	150.0	30.0	0.0211
9	12	10.0	165.0	15.0	0.0211
9	13	10.0	180.0	0.0	0.0211
8	1	20.0	0.0	180.0	0.0213
8	2	20.0	15.0	165.0	0.0213
8	3	20.0	30.0	150.0	0.0213
8	4	20.0	45.0	135.0	0.0213
8	5	20.0	60.0	120.0	0.0213
8	6	20.0	75.0	105.0	0.0213
8	7	20.0	90.0	90.0	0.0213
8	8	20.0	105.0	75.0	0.0213
8	9	20.0	120.0	60.0	0.0213
8	10	20.0	135.0	45.0	0.0213
8	11	20.0	150.0	30.0	0.0213
8	12	20.0	165.0	15.0	0.0213
8	13	20.0	180.0	0.0	0.0213
7	1	30.0	0.0	180.0	0.0223
7	2	30.0	15.0	165.0	0.0223
7	3	30.0	30.0	150.0	0.0223
7	4	30.0	45.0	135.0	0.0223
7	5	30.0	60.0	120.0	0.0223
7	6	30.0	75.0	105.0	0.0223
7	7	30.0	90.0	90.0	0.0223
7	8	30.0	105.0	75.0	0.0223
7	9	30.0	120.0	60.0	0.0223
7	10	30.0	135.0	45.0	0.0223
7	11	30.0	150.0	30.0	0.0223
7	12	30.0	165.0	15.0	0.0223
7	13	30.0	180.0	0.0	0.0223
6	1	40.0	0.0	180.0	0.0257
6	2	40.0	15.0	165.0	0.0256
6	3	40.0	30.0	150.0	0.0256
6	4	40.0	45.0	135.0	0.0256
6	5	40.0	60.0	120.0	0.0257
6	6	40.0	75.0	105.0	0.0257
6	7	40.0	90.0	90.0	0.0256
6	8	40.0	105.0	75.0	0.0257
6	9	40.0	120.0	60.0	0.0257
6	10	40.0	135.0	45.0	0.0256
6	11	40.0	150.0	30.0	0.0256
6	12	40.0	165.0	15.0	0.0256
6	13	40.0	180.0	0.0	0.0256
5	1	50.0	0.0	180.0	0.0355
5	2	50.0	15.0	165.0	0.0354
5	3	50.0	30.0	150.0	0.0357
5	4	50.0	45.0	135.0	0.0356
5	5	50.0	60.0	120.0	0.0355
5	6	50.0	75.0	105.0	0.0355
5	7	50.0	90.0	90.0	0.0355
5	8	50.0	105.0	75.0	0.0355
5	9	50.0	120.0	60.0	0.0355
5	10	50.0	135.0	45.0	0.0356
5	11	50.0	150.0	30.0	0.0357
5	12	50.0	165.0	15.0	0.0354
5	13	50.0	180.0	0.0	0.0355
4	1	60.0	0.0	180.0	0.0637
4	2	60.0	15.0	165.0	0.0633
4	3	60.0	30.0	150.0	0.0631
4	4	60.0	45.0	135.0	0.0630
4	5	60.0	60.0	120.0	0.0633
4	6	60.0	75.0	105.0	0.0633
4	7	60.0	90.0	90.0	0.0636
4	8	60.0	105.0	75.0	0.0633
4	9	60.0	120.0	60.0	0.0633
4	10	60.0	135.0	45.0	0.0630
4	11	60.0	150.0	30.0	0.0631
4	12	60.0	165.0	15.0	0.0633
4	13	60.0	180.0	0.0	0.0637
3	1	70.0	0.0	180.0	0.1425
3	2	70.0	15.0	165.0	0.1425
3	3	70.0	30.0	150.0	0.1410
3	4	70.0	45.0	135.0	0.1405
3	5	70.0	60.0	120.0	0.1404
3	6	70.0	75.0	105.0	0.1421
3	7	70.0	90.0	90.0	0.1408
3	8	70.0	105.0	75.0	0.1421
3	9	70.0	120.0	60.0	0.1404
3	10	70.0	135.0	45.0	0.1405
3	11	70.0	150.0	30.0	0.1410
3	12	70.0	165.0	15.0	0.1425
3	13	70.0	180.0	0.0	0.1425
2	1	80.0	0.0	180.0	0.3680
2	2	80.0	15.0	165.0	0.3677
2	3	80.0	30.0	150.0	0.3646
2	4	80.0	45.0	135.0	0.3686
2	5	80.0	60.0	120.0	0.3617
2	6	80.0	75.0	105.0	0.3656
2	7	80.0	90.0	90.0	0.3727
2	8	80.0	105.0	75.0	0.3656
2	9	80.0	120.0	60.0	0.3617
2	10	80.0	135.0	45.0	0.3686
2	11	80.0	150.0	30.0	0.3646

2 12 80.0 165.0 15.0 0.3677
2 13 80.0 180.0 0.0 0.3680
1 1 87.5 0.0 180.0 0.7714
1 2 87.5 15.0 165.0 0.7771
1 3 87.5 30.0 150.0 0.7745
1 4 87.5 45.0 135.0 0.7664
1 5 87.5 60.0 120.0 0.7766
1 6 87.5 75.0 105.0 0.7729
1 7 87.5 90.0 90.0 0.7732
1 8 87.5 105.0 75.0 0.7729
1 9 87.5 120.0 60.0 0.7766
1 10 87.5 135.0 45.0 0.7664
1 11 87.5 150.0 30.0 0.7745
1 12 87.5 165.0 15.0 0.7771
1 13 87.5 180.0 0.0 0.7714
rho for WIND SPEED = 0.0 m/s THETA_SUN = 50.0 deg
10 1 0.0 0.0 0.0 0.0211
9 1 10.0 0.0 180.0 0.0211
9 2 10.0 15.0 165.0 0.0211
9 3 10.0 30.0 150.0 0.0211
9 4 10.0 45.0 135.0 0.0211
9 5 10.0 60.0 120.0 0.0211
9 6 10.0 75.0 105.0 0.0211
9 7 10.0 90.0 90.0 0.0211
9 8 10.0 105.0 75.0 0.0211
9 9 10.0 120.0 60.0 0.0211
9 10 10.0 135.0 45.0 0.0211
9 11 10.0 150.0 30.0 0.0211
9 12 10.0 165.0 15.0 0.0211
9 13 10.0 180.0 0.0 0.0211
8 1 20.0 0.0 180.0 0.0213
8 2 20.0 15.0 165.0 0.0213
8 3 20.0 30.0 150.0 0.0213
8 4 20.0 45.0 135.0 0.0213
8 5 20.0 60.0 120.0 0.0213
8 6 20.0 75.0 105.0 0.0213
8 7 20.0 90.0 90.0 0.0213
8 8 20.0 105.0 75.0 0.0213
8 9 20.0 120.0 60.0 0.0213
8 10 20.0 135.0 45.0 0.0213
8 11 20.0 150.0 30.0 0.0213
8 12 20.0 165.0 15.0 0.0213
8 13 20.0 180.0 0.0 0.0213
7 1 30.0 0.0 180.0 0.0223
7 2 30.0 15.0 165.0 0.0223
7 3 30.0 30.0 150.0 0.0223
7 4 30.0 45.0 135.0 0.0223
7 5 30.0 60.0 120.0 0.0223
7 6 30.0 75.0 105.0 0.0223
7 7 30.0 90.0 90.0 0.0223
7 8 30.0 105.0 75.0 0.0223
7 9 30.0 120.0 60.0 0.0223
7 10 30.0 135.0 45.0 0.0223
7 11 30.0 150.0 30.0 0.0223
7 12 30.0 165.0 15.0 0.0223
7 13 30.0 180.0 0.0 0.0223
6 1 40.0 0.0 180.0 0.0256
6 2 40.0 15.0 165.0 0.0256
6 3 40.0 30.0 150.0 0.0256
6 4 40.0 45.0 135.0 0.0256
6 5 40.0 60.0 120.0 0.0257
6 6 40.0 75.0 105.0 0.0257
6 7 40.0 90.0 90.0 0.0256
6 8 40.0 105.0 75.0 0.0257
6 9 40.0 120.0 60.0 0.0257
6 10 40.0 135.0 45.0 0.0256
6 11 40.0 150.0 30.0 0.0256
6 12 40.0 165.0 15.0 0.0256
6 13 40.0 180.0 0.0 0.0256
5 1 50.0 0.0 180.0 0.0355
5 2 50.0 15.0 165.0 0.0354
5 3 50.0 30.0 150.0 0.0357
5 4 50.0 45.0 135.0 0.0356
5 5 50.0 60.0 120.0 0.0355
5 6 50.0 75.0 105.0 0.0355
5 7 50.0 90.0 90.0 0.0355
5 8 50.0 105.0 75.0 0.0355
5 9 50.0 120.0 60.0 0.0355
5 10 50.0 135.0 45.0 0.0356
5 11 50.0 150.0 30.0 0.0357
5 12 50.0 165.0 15.0 0.0354
5 13 50.0 180.0 0.0 0.0355
4 1 60.0 0.0 180.0 0.0637
4 2 60.0 15.0 165.0 0.0633
4 3 60.0 30.0 150.0 0.0631
4 4 60.0 45.0 135.0 0.0630
4 5 60.0 60.0 120.0 0.0633
4 6 60.0 75.0 105.0 0.0633
4 7 60.0 90.0 90.0 0.0636
4 8 60.0 105.0 75.0 0.0633
4 9 60.0 120.0 60.0 0.0633
4 10 60.0 135.0 45.0 0.0630
4 11 60.0 150.0 30.0 0.0631
4 12 60.0 165.0 15.0 0.0633
4 13 60.0 180.0 0.0 0.0637
3 1 70.0 0.0 180.0 0.1425
3 2 70.0 15.0 165.0 0.1425
3 3 70.0 30.0 150.0 0.1410
3 4 70.0 45.0 135.0 0.1405

3	5	70.0	60.0	120.0	0.1404
3	6	70.0	75.0	105.0	0.1421
3	7	70.0	90.0	90.0	0.1408
3	8	70.0	105.0	75.0	0.1421
3	9	70.0	120.0	60.0	0.1404
3	10	70.0	135.0	45.0	0.1405
3	11	70.0	150.0	30.0	0.1410
3	12	70.0	165.0	15.0	0.1425
3	13	70.0	180.0	0.0	0.1425
2	1	80.0	0.0	180.0	0.3680
2	2	80.0	15.0	165.0	0.3677
2	3	80.0	30.0	150.0	0.3646
2	4	80.0	45.0	135.0	0.3686
2	5	80.0	60.0	120.0	0.3617
2	6	80.0	75.0	105.0	0.3656
2	7	80.0	90.0	90.0	0.3727
2	8	80.0	105.0	75.0	0.3656
2	9	80.0	120.0	60.0	0.3617
2	10	80.0	135.0	45.0	0.3686
2	11	80.0	150.0	30.0	0.3646
2	12	80.0	165.0	15.0	0.3677
2	13	80.0	180.0	0.0	0.3680
1	1	87.5	0.0	180.0	0.7714
1	2	87.5	15.0	165.0	0.7771
1	3	87.5	30.0	150.0	0.7745
1	4	87.5	45.0	135.0	0.7664
1	5	87.5	60.0	120.0	0.7766
1	6	87.5	75.0	105.0	0.7729
1	7	87.5	90.0	90.0	0.7732
1	8	87.5	105.0	75.0	0.7729
1	9	87.5	120.0	60.0	0.7766
1	10	87.5	135.0	45.0	0.7664
1	11	87.5	150.0	30.0	0.7745
1	12	87.5	165.0	15.0	0.7771
1	13	87.5	180.0	0.0	0.7714

rho for WIND SPEED = 0.0 m/s THETA_SUN = 60.0 deg

10	1	0.0	0.0	0.0	0.0211
9	1	10.0	0.0	180.0	0.0211
9	2	10.0	15.0	165.0	0.0211
9	3	10.0	30.0	150.0	0.0211
9	4	10.0	45.0	135.0	0.0211
9	5	10.0	60.0	120.0	0.0211
9	6	10.0	75.0	105.0	0.0211
9	7	10.0	90.0	90.0	0.0211
9	8	10.0	105.0	75.0	0.0211
9	9	10.0	120.0	60.0	0.0211
9	10	10.0	135.0	45.0	0.0211
9	11	10.0	150.0	30.0	0.0211
9	12	10.0	165.0	15.0	0.0211
9	13	10.0	180.0	0.0	0.0211
8	1	20.0	0.0	180.0	0.0213
8	2	20.0	15.0	165.0	0.0213
8	3	20.0	30.0	150.0	0.0213
8	4	20.0	45.0	135.0	0.0213
8	5	20.0	60.0	120.0	0.0213
8	6	20.0	75.0	105.0	0.0213
8	7	20.0	90.0	90.0	0.0213
8	8	20.0	105.0	75.0	0.0213
8	9	20.0	120.0	60.0	0.0213
8	10	20.0	135.0	45.0	0.0213
8	11	20.0	150.0	30.0	0.0213
8	12	20.0	165.0	15.0	0.0213
8	13	20.0	180.0	0.0	0.0213
7	1	30.0	0.0	180.0	0.0223
7	2	30.0	15.0	165.0	0.0223
7	3	30.0	30.0	150.0	0.0223
7	4	30.0	45.0	135.0	0.0223
7	5	30.0	60.0	120.0	0.0223
7	6	30.0	75.0	105.0	0.0223
7	7	30.0	90.0	90.0	0.0223
7	8	30.0	105.0	75.0	0.0223
7	9	30.0	120.0	60.0	0.0223
7	10	30.0	135.0	45.0	0.0223
7	11	30.0	150.0	30.0	0.0223
7	12	30.0	165.0	15.0	0.0223
7	13	30.0	180.0	0.0	0.0223
6	1	40.0	0.0	180.0	0.0256
6	2	40.0	15.0	165.0	0.0256
6	3	40.0	30.0	150.0	0.0256
6	4	40.0	45.0	135.0	0.0256
6	5	40.0	60.0	120.0	0.0257
6	6	40.0	75.0	105.0	0.0257
6	7	40.0	90.0	90.0	0.0256
6	8	40.0	105.0	75.0	0.0257
6	9	40.0	120.0	60.0	0.0257
6	10	40.0	135.0	45.0	0.0256
6	11	40.0	150.0	30.0	0.0256
6	12	40.0	165.0	15.0	0.0256
6	13	40.0	180.0	0.0	0.0256
5	1	50.0	0.0	180.0	0.0355
5	2	50.0	15.0	165.0	0.0354
5	3	50.0	30.0	150.0	0.0357
5	4	50.0	45.0	135.0	0.0356
5	5	50.0	60.0	120.0	0.0355
5	6	50.0	75.0	105.0	0.0355
5	7	50.0	90.0	90.0	0.0355
5	8	50.0	105.0	75.0	0.0355
5	9	50.0	120.0	60.0	0.0355
5	10	50.0	135.0	45.0	0.0356

5 11 50.0 150.0 30.0 0.0357
5 12 50.0 165.0 15.0 0.0354
5 13 50.0 180.0 0.0 0.0355
4 1 60.0 0.0 180.0 0.0637
4 2 60.0 15.0 165.0 0.0633
4 3 60.0 30.0 150.0 0.0631
4 4 60.0 45.0 135.0 0.0630
4 5 60.0 60.0 120.0 0.0633
4 6 60.0 75.0 105.0 0.0633
4 7 60.0 90.0 90.0 0.0636
4 8 60.0 105.0 75.0 0.0633
4 9 60.0 120.0 60.0 0.0633
4 10 60.0 135.0 45.0 0.0630
4 11 60.0 150.0 30.0 0.0631
4 12 60.0 165.0 15.0 0.0633
4 13 60.0 180.0 0.0 0.0637
3 1 70.0 0.0 180.0 0.1425
3 2 70.0 15.0 165.0 0.1425
3 3 70.0 30.0 150.0 0.1410
3 4 70.0 45.0 135.0 0.1405
3 5 70.0 60.0 120.0 0.1404
3 6 70.0 75.0 105.0 0.1421
3 7 70.0 90.0 90.0 0.1408
3 8 70.0 105.0 75.0 0.1421
3 9 70.0 120.0 60.0 0.1404
3 10 70.0 135.0 45.0 0.1405
3 11 70.0 150.0 30.0 0.1410
3 12 70.0 165.0 15.0 0.1425
3 13 70.0 180.0 0.0 0.1425
2 1 80.0 0.0 180.0 0.3680
2 2 80.0 15.0 165.0 0.3677
2 3 80.0 30.0 150.0 0.3646
2 4 80.0 45.0 135.0 0.3686
2 5 80.0 60.0 120.0 0.3617
2 6 80.0 75.0 105.0 0.3656
2 7 80.0 90.0 90.0 0.3727
2 8 80.0 105.0 75.0 0.3656
2 9 80.0 120.0 60.0 0.3617
2 10 80.0 135.0 45.0 0.3686
2 11 80.0 150.0 30.0 0.3646
2 12 80.0 165.0 15.0 0.3677
2 13 80.0 180.0 0.0 0.3680
1 1 87.5 0.0 180.0 0.7714
1 2 87.5 15.0 165.0 0.7771
1 3 87.5 30.0 150.0 0.7745
1 4 87.5 45.0 135.0 0.7664
1 5 87.5 60.0 120.0 0.7766
1 6 87.5 75.0 105.0 0.7729
1 7 87.5 90.0 90.0 0.7732
1 8 87.5 105.0 75.0 0.7729
1 9 87.5 120.0 60.0 0.7766
1 10 87.5 135.0 45.0 0.7663
1 11 87.5 150.0 30.0 0.7745
1 12 87.5 165.0 15.0 0.7771
1 13 87.5 180.0 0.0 0.7714
rho for WIND SPEED = 0.0 m/s THETA_SUN = 70.0 deg
10 1 0.0 0.0 0.0 0.0211
9 1 10.0 0.0 180.0 0.0211
9 2 10.0 15.0 165.0 0.0211
9 3 10.0 30.0 150.0 0.0211
9 4 10.0 45.0 135.0 0.0211
9 5 10.0 60.0 120.0 0.0211
9 6 10.0 75.0 105.0 0.0211
9 7 10.0 90.0 90.0 0.0211
9 8 10.0 105.0 75.0 0.0211
9 9 10.0 120.0 60.0 0.0211
9 10 10.0 135.0 45.0 0.0211
9 11 10.0 150.0 30.0 0.0211
9 12 10.0 165.0 15.0 0.0211
9 13 10.0 180.0 0.0 0.0211
8 1 20.0 0.0 180.0 0.0213
8 2 20.0 15.0 165.0 0.0213
8 3 20.0 30.0 150.0 0.0213
8 4 20.0 45.0 135.0 0.0213
8 5 20.0 60.0 120.0 0.0213
8 6 20.0 75.0 105.0 0.0213
8 7 20.0 90.0 90.0 0.0213
8 8 20.0 105.0 75.0 0.0213
8 9 20.0 120.0 60.0 0.0213
8 10 20.0 135.0 45.0 0.0213
8 11 20.0 150.0 30.0 0.0213
8 12 20.0 165.0 15.0 0.0213
8 13 20.0 180.0 0.0 0.0213
7 1 30.0 0.0 180.0 0.0223
7 2 30.0 15.0 165.0 0.0223
7 3 30.0 30.0 150.0 0.0223
7 4 30.0 45.0 135.0 0.0223
7 5 30.0 60.0 120.0 0.0223
7 6 30.0 75.0 105.0 0.0223
7 7 30.0 90.0 90.0 0.0223
7 8 30.0 105.0 75.0 0.0223
7 9 30.0 120.0 60.0 0.0223
7 10 30.0 135.0 45.0 0.0223
7 11 30.0 150.0 30.0 0.0223
7 12 30.0 165.0 15.0 0.0223
7 13 30.0 180.0 0.0 0.0223
6 1 40.0 0.0 180.0 0.0256
6 2 40.0 15.0 165.0 0.0256
6 3 40.0 30.0 150.0 0.0256

6 4 40.0 45.0 135.0 0.0256
6 5 40.0 60.0 120.0 0.0257
6 6 40.0 75.0 105.0 0.0257
6 7 40.0 90.0 90.0 0.0256
6 8 40.0 105.0 75.0 0.0257
6 9 40.0 120.0 60.0 0.0257
6 10 40.0 135.0 45.0 0.0256
6 11 40.0 150.0 30.0 0.0256
6 12 40.0 165.0 15.0 0.0256
6 13 40.0 180.0 0.0 0.0256
5 1 50.0 0.0 180.0 0.0355
5 2 50.0 15.0 165.0 0.0354
5 3 50.0 30.0 150.0 0.0357
5 4 50.0 45.0 135.0 0.0356
5 5 50.0 60.0 120.0 0.0355
5 6 50.0 75.0 105.0 0.0355
5 7 50.0 90.0 90.0 0.0355
5 8 50.0 105.0 75.0 0.0355
5 9 50.0 120.0 60.0 0.0355
5 10 50.0 135.0 45.0 0.0356
5 11 50.0 150.0 30.0 0.0357
5 12 50.0 165.0 15.0 0.0354
5 13 50.0 180.0 0.0 0.0355
4 1 60.0 0.0 180.0 0.0637
4 2 60.0 15.0 165.0 0.0633
4 3 60.0 30.0 150.0 0.0631
4 4 60.0 45.0 135.0 0.0630
4 5 60.0 60.0 120.0 0.0633
4 6 60.0 75.0 105.0 0.0633
4 7 60.0 90.0 90.0 0.0636
4 8 60.0 105.0 75.0 0.0633
4 9 60.0 120.0 60.0 0.0633
4 10 60.0 135.0 45.0 0.0630
4 11 60.0 150.0 30.0 0.0631
4 12 60.0 165.0 15.0 0.0633
4 13 60.0 180.0 0.0 0.0637
3 1 70.0 0.0 180.0 0.1425
3 2 70.0 15.0 165.0 0.1425
3 3 70.0 30.0 150.0 0.1410
3 4 70.0 45.0 135.0 0.1405
3 5 70.0 60.0 120.0 0.1404
3 6 70.0 75.0 105.0 0.1421
3 7 70.0 90.0 90.0 0.1409
3 8 70.0 105.0 75.0 0.1421
3 9 70.0 120.0 60.0 0.1404
3 10 70.0 135.0 45.0 0.1405
3 11 70.0 150.0 30.0 0.1410
3 12 70.0 165.0 15.0 0.1425
3 13 70.0 180.0 0.0 0.1425
2 1 80.0 0.0 180.0 0.3680
2 2 80.0 15.0 165.0 0.3677
2 3 80.0 30.0 150.0 0.3646
2 4 80.0 45.0 135.0 0.3686
2 5 80.0 60.0 120.0 0.3617
2 6 80.0 75.0 105.0 0.3656
2 7 80.0 90.0 90.0 0.3727
2 8 80.0 105.0 75.0 0.3656
2 9 80.0 120.0 60.0 0.3617
2 10 80.0 135.0 45.0 0.3686
2 11 80.0 150.0 30.0 0.3646
2 12 80.0 165.0 15.0 0.3677
2 13 80.0 180.0 0.0 0.3680
1 1 87.5 0.0 180.0 0.7714
1 2 87.5 15.0 165.0 0.7771
1 3 87.5 30.0 150.0 0.7745
1 4 87.5 45.0 135.0 0.7664
1 5 87.5 60.0 120.0 0.7766
1 6 87.5 75.0 105.0 0.7729
1 7 87.5 90.0 90.0 0.7732
1 8 87.5 105.0 75.0 0.7729
1 9 87.5 120.0 60.0 0.7766
1 10 87.5 135.0 45.0 0.7663
1 11 87.5 150.0 30.0 0.7745
1 12 87.5 165.0 15.0 0.7771
1 13 87.5 180.0 0.0 0.7714
rho for WIND SPEED = 0.0 m/s THETA_SUN = 80.0 deg
10 1 0.0 0.0 0.0 0.0211
9 1 10.0 0.0 180.0 0.0211
9 2 10.0 15.0 165.0 0.0211
9 3 10.0 30.0 150.0 0.0211
9 4 10.0 45.0 135.0 0.0211
9 5 10.0 60.0 120.0 0.0211
9 6 10.0 75.0 105.0 0.0211
9 7 10.0 90.0 90.0 0.0211
9 8 10.0 105.0 75.0 0.0211
9 9 10.0 120.0 60.0 0.0211
9 10 10.0 135.0 45.0 0.0211
9 11 10.0 150.0 30.0 0.0211
9 12 10.0 165.0 15.0 0.0211
9 13 10.0 180.0 0.0 0.0211
8 1 20.0 0.0 180.0 0.0213
8 2 20.0 15.0 165.0 0.0213
8 3 20.0 30.0 150.0 0.0213
8 4 20.0 45.0 135.0 0.0213
8 5 20.0 60.0 120.0 0.0213
8 6 20.0 75.0 105.0 0.0213
8 7 20.0 90.0 90.0 0.0213
8 8 20.0 105.0 75.0 0.0213
8 9 20.0 120.0 60.0 0.0213

8 10 20.0 135.0 45.0 0.0213
8 11 20.0 150.0 30.0 0.0213
8 12 20.0 165.0 15.0 0.0213
8 13 20.0 180.0 0.0 0.0213
7 1 30.0 0.0 180.0 0.0223
7 2 30.0 15.0 165.0 0.0223
7 3 30.0 30.0 150.0 0.0223
7 4 30.0 45.0 135.0 0.0223
7 5 30.0 60.0 120.0 0.0223
7 6 30.0 75.0 105.0 0.0223
7 7 30.0 90.0 90.0 0.0223
7 8 30.0 105.0 75.0 0.0223
7 9 30.0 120.0 60.0 0.0223
7 10 30.0 135.0 45.0 0.0223
7 11 30.0 150.0 30.0 0.0223
7 12 30.0 165.0 15.0 0.0223
7 13 30.0 180.0 0.0 0.0223
6 1 40.0 0.0 180.0 0.0256
6 2 40.0 15.0 165.0 0.0256
6 3 40.0 30.0 150.0 0.0256
6 4 40.0 45.0 135.0 0.0256
6 5 40.0 60.0 120.0 0.0257
6 6 40.0 75.0 105.0 0.0257
6 7 40.0 90.0 90.0 0.0256
6 8 40.0 105.0 75.0 0.0257
6 9 40.0 120.0 60.0 0.0257
6 10 40.0 135.0 45.0 0.0256
6 11 40.0 150.0 30.0 0.0256
6 12 40.0 165.0 15.0 0.0256
6 13 40.0 180.0 0.0 0.0256
5 1 50.0 0.0 180.0 0.0355
5 2 50.0 15.0 165.0 0.0354
5 3 50.0 30.0 150.0 0.0357
5 4 50.0 45.0 135.0 0.0356
5 5 50.0 60.0 120.0 0.0355
5 6 50.0 75.0 105.0 0.0355
5 7 50.0 90.0 90.0 0.0355
5 8 50.0 105.0 75.0 0.0355
5 9 50.0 120.0 60.0 0.0355
5 10 50.0 135.0 45.0 0.0356
5 11 50.0 150.0 30.0 0.0357
5 12 50.0 165.0 15.0 0.0354
5 13 50.0 180.0 0.0 0.0355
4 1 60.0 0.0 180.0 0.0637
4 2 60.0 15.0 165.0 0.0633
4 3 60.0 30.0 150.0 0.0631
4 4 60.0 45.0 135.0 0.0630
4 5 60.0 60.0 120.0 0.0633
4 6 60.0 75.0 105.0 0.0633
4 7 60.0 90.0 90.0 0.0636
4 8 60.0 105.0 75.0 0.0633
4 9 60.0 120.0 60.0 0.0633
4 10 60.0 135.0 45.0 0.0630
4 11 60.0 150.0 30.0 0.0631
4 12 60.0 165.0 15.0 0.0633
4 13 60.0 180.0 0.0 0.0637
3 1 70.0 0.0 180.0 0.1425
3 2 70.0 15.0 165.0 0.1425
3 3 70.0 30.0 150.0 0.1410
3 4 70.0 45.0 135.0 0.1405
3 5 70.0 60.0 120.0 0.1404
3 6 70.0 75.0 105.0 0.1421
3 7 70.0 90.0 90.0 0.1408
3 8 70.0 105.0 75.0 0.1421
3 9 70.0 120.0 60.0 0.1404
3 10 70.0 135.0 45.0 0.1405
3 11 70.0 150.0 30.0 0.1410
3 12 70.0 165.0 15.0 0.1425
3 13 70.0 180.0 0.0 0.1425
2 1 80.0 0.0 180.0 0.3680
2 2 80.0 15.0 165.0 0.3677
2 3 80.0 30.0 150.0 0.3646
2 4 80.0 45.0 135.0 0.3686
2 5 80.0 60.0 120.0 0.3617
2 6 80.0 75.0 105.0 0.3656
2 7 80.0 90.0 90.0 0.3727
2 8 80.0 105.0 75.0 0.3656
2 9 80.0 120.0 60.0 0.3617
2 10 80.0 135.0 45.0 0.3686
2 11 80.0 150.0 30.0 0.3646
2 12 80.0 165.0 15.0 0.3677
2 13 80.0 180.0 0.0 0.3680
1 1 87.5 0.0 180.0 0.7714
1 2 87.5 15.0 165.0 0.7771
1 3 87.5 30.0 150.0 0.7745
1 4 87.5 45.0 135.0 0.7664
1 5 87.5 60.0 120.0 0.7766
1 6 87.5 75.0 105.0 0.7729
1 7 87.5 90.0 90.0 0.7732
1 8 87.5 105.0 75.0 0.7729
1 9 87.5 120.0 60.0 0.7766
1 10 87.5 135.0 45.0 0.7663
1 11 87.5 150.0 30.0 0.7745
1 12 87.5 165.0 15.0 0.7771
1 13 87.5 180.0 0.0 0.7714
rho for WIND SPEED = 2.0 m/s THETA_SUN = 0.0 deg
10 1 0.0 0.0 0.0 0.0034
9 1 10.0 0.0 180.0 0.2472
9 2 10.0 15.0 165.0 0.2365

9	3	10.0	30.0	150.0	0.2530
9	4	10.0	45.0	135.0	0.2544
9	5	10.0	60.0	120.0	0.2439
9	6	10.0	75.0	105.0	0.2408
9	7	10.0	90.0	90.0	0.2563
9	8	10.0	105.0	75.0	0.2408
9	9	10.0	120.0	60.0	0.2439
9	10	10.0	135.0	45.0	0.2544
9	11	10.0	150.0	30.0	0.2530
9	12	10.0	165.0	15.0	0.2365
9	13	10.0	180.0	0.0	0.2472
8	1	20.0	0.0	180.0	0.0909
8	2	20.0	15.0	165.0	0.0993
8	3	20.0	30.0	150.0	0.0977
8	4	20.0	45.0	135.0	0.0956
8	5	20.0	60.0	120.0	0.0984
8	6	20.0	75.0	105.0	0.0938
8	7	20.0	90.0	90.0	0.0919
8	8	20.0	105.0	75.0	0.0938
8	9	20.0	120.0	60.0	0.0984
8	10	20.0	135.0	45.0	0.0956
8	11	20.0	150.0	30.0	0.0977
8	12	20.0	165.0	15.0	0.0993
8	13	20.0	180.0	0.0	0.0909
7	1	30.0	0.0	180.0	0.0285
7	2	30.0	15.0	165.0	0.0316
7	3	30.0	30.0	150.0	0.0302
7	4	30.0	45.0	135.0	0.0299
7	5	30.0	60.0	120.0	0.0309
7	6	30.0	75.0	105.0	0.0301
7	7	30.0	90.0	90.0	0.0285
7	8	30.0	105.0	75.0	0.0301
7	9	30.0	120.0	60.0	0.0309
7	10	30.0	135.0	45.0	0.0299
7	11	30.0	150.0	30.0	0.0302
7	12	30.0	165.0	15.0	0.0316
7	13	30.0	180.0	0.0	0.0285
6	1	40.0	0.0	180.0	0.0271
6	2	40.0	15.0	165.0	0.0277
6	3	40.0	30.0	150.0	0.0277
6	4	40.0	45.0	135.0	0.0274
6	5	40.0	60.0	120.0	0.0273
6	6	40.0	75.0	105.0	0.0273
6	7	40.0	90.0	90.0	0.0274
6	8	40.0	105.0	75.0	0.0273
6	9	40.0	120.0	60.0	0.0273
6	10	40.0	135.0	45.0	0.0274
6	11	40.0	150.0	30.0	0.0277
6	12	40.0	165.0	15.0	0.0277
6	13	40.0	180.0	0.0	0.0271
5	1	50.0	0.0	180.0	0.0365
5	2	50.0	15.0	165.0	0.0372
5	3	50.0	30.0	150.0	0.0366
5	4	50.0	45.0	135.0	0.0368
5	5	50.0	60.0	120.0	0.0366
5	6	50.0	75.0	105.0	0.0367
5	7	50.0	90.0	90.0	0.0367
5	8	50.0	105.0	75.0	0.0367
5	9	50.0	120.0	60.0	0.0366
5	10	50.0	135.0	45.0	0.0368
5	11	50.0	150.0	30.0	0.0366
5	12	50.0	165.0	15.0	0.0372
5	13	50.0	180.0	0.0	0.0365
4	1	60.0	0.0	180.0	0.0652
4	2	60.0	15.0	165.0	0.0652
4	3	60.0	30.0	150.0	0.0659
4	4	60.0	45.0	135.0	0.0650
4	5	60.0	60.0	120.0	0.0654
4	6	60.0	75.0	105.0	0.0656
4	7	60.0	90.0	90.0	0.0653
4	8	60.0	105.0	75.0	0.0656
4	9	60.0	120.0	60.0	0.0654
4	10	60.0	135.0	45.0	0.0650
4	11	60.0	150.0	30.0	0.0659
4	12	60.0	165.0	15.0	0.0652
4	13	60.0	180.0	0.0	0.0652
3	1	70.0	0.0	180.0	0.1540
3	2	70.0	15.0	165.0	0.1529
3	3	70.0	30.0	150.0	0.1518
3	4	70.0	45.0	135.0	0.1520
3	5	70.0	60.0	120.0	0.1519
3	6	70.0	75.0	105.0	0.1503
3	7	70.0	90.0	90.0	0.1520
3	8	70.0	105.0	75.0	0.1503
3	9	70.0	120.0	60.0	0.1519
3	10	70.0	135.0	45.0	0.1520
3	11	70.0	150.0	30.0	0.1518
3	12	70.0	165.0	15.0	0.1529
3	13	70.0	180.0	0.0	0.1540
2	1	80.0	0.0	180.0	0.3331
2	2	80.0	15.0	165.0	0.3318
2	3	80.0	30.0	150.0	0.3356
2	4	80.0	45.0	135.0	0.3357
2	5	80.0	60.0	120.0	0.3370
2	6	80.0	75.0	105.0	0.3395
2	7	80.0	90.0	90.0	0.3391
2	8	80.0	105.0	75.0	0.3395
2	9	80.0	120.0	60.0	0.3370
2	10	80.0	135.0	45.0	0.3357
2	11	80.0	150.0	30.0	0.3356

2	12	80.0	165.0	15.0	0.3318
2	13	80.0	180.0	0.0	0.3331
1	1	87.5	0.0	180.0	0.4979
1	2	87.5	15.0	165.0	0.4953
1	3	87.5	30.0	150.0	0.5201
1	4	87.5	45.0	135.0	0.5082
1	5	87.5	60.0	120.0	0.4909
1	6	87.5	75.0	105.0	0.5068
1	7	87.5	90.0	90.0	0.4994
1	8	87.5	105.0	75.0	0.5068
1	9	87.5	120.0	60.0	0.4909
1	10	87.5	135.0	45.0	0.5082
1	11	87.5	150.0	30.0	0.5201
1	12	87.5	165.0	15.0	0.4953
1	13	87.5	180.0	0.0	0.4979

rho for WIND SPEED = 2.0 m/s THETA_SUN = 10.0 deg

10	1	0.0	0.0	0.0	0.2239
9	1	10.0	0.0	180.0	0.0824
9	2	10.0	15.0	165.0	0.0816
9	3	10.0	30.0	150.0	0.0829
9	4	10.0	45.0	135.0	0.0970
9	5	10.0	60.0	120.0	0.1145
9	6	10.0	75.0	105.0	0.1229
9	7	10.0	90.0	90.0	0.1637
9	8	10.0	105.0	75.0	0.1888
9	9	10.0	120.0	60.0	0.2382
9	10	10.0	135.0	45.0	0.2458
9	11	10.0	150.0	30.0	0.2528
9	12	10.0	165.0	15.0	0.2401
9	13	10.0	180.0	0.0	0.0012
8	1	20.0	0.0	180.0	0.0257
8	2	20.0	15.0	165.0	0.0282
8	3	20.0	30.0	150.0	0.0277
8	4	20.0	45.0	135.0	0.0289
8	5	20.0	60.0	120.0	0.0343
8	6	20.0	75.0	105.0	0.0434
8	7	20.0	90.0	90.0	0.0551
8	8	20.0	105.0	75.0	0.0787
8	9	20.0	120.0	60.0	0.1180
8	10	20.0	135.0	45.0	0.1626
8	11	20.0	150.0	30.0	0.2266
8	12	20.0	165.0	15.0	0.2763
8	13	20.0	180.0	0.0	0.2895
7	1	30.0	0.0	180.0	0.0246
7	2	30.0	15.0	165.0	0.0239
7	3	30.0	30.0	150.0	0.0243
7	4	30.0	45.0	135.0	0.0242
7	5	30.0	60.0	120.0	0.0242
7	6	30.0	75.0	105.0	0.0251
7	7	30.0	90.0	90.0	0.0254
7	8	30.0	105.0	75.0	0.0290
7	9	30.0	120.0	60.0	0.0324
7	10	30.0	135.0	45.0	0.0534
7	11	30.0	150.0	30.0	0.0795
7	12	30.0	165.0	15.0	0.1106
7	13	30.0	180.0	0.0	0.1315
6	1	40.0	0.0	180.0	0.0264
6	2	40.0	15.0	165.0	0.0271
6	3	40.0	30.0	150.0	0.0269
6	4	40.0	45.0	135.0	0.0268
6	5	40.0	60.0	120.0	0.0269
6	6	40.0	75.0	105.0	0.0270
6	7	40.0	90.0	90.0	0.0273
6	8	40.0	105.0	75.0	0.0274
6	9	40.0	120.0	60.0	0.0276
6	10	40.0	135.0	45.0	0.0297
6	11	40.0	150.0	30.0	0.0315
6	12	40.0	165.0	15.0	0.0342
6	13	40.0	180.0	0.0	0.0327
5	1	50.0	0.0	180.0	0.0363
5	2	50.0	15.0	165.0	0.0370
5	3	50.0	30.0	150.0	0.0364
5	4	50.0	45.0	135.0	0.0366
5	5	50.0	60.0	120.0	0.0364
5	6	50.0	75.0	105.0	0.0366
5	7	50.0	90.0	90.0	0.0367
5	8	50.0	105.0	75.0	0.0368
5	9	50.0	120.0	60.0	0.0368
5	10	50.0	135.0	45.0	0.0373
5	11	50.0	150.0	30.0	0.0374
5	12	50.0	165.0	15.0	0.0378
5	13	50.0	180.0	0.0	0.0372
4	1	60.0	0.0	180.0	0.0660
4	2	60.0	15.0	165.0	0.0660
4	3	60.0	30.0	150.0	0.0666
4	4	60.0	45.0	135.0	0.0655
4	5	60.0	60.0	120.0	0.0657
4	6	60.0	75.0	105.0	0.0658
4	7	60.0	90.0	90.0	0.0653
4	8	60.0	105.0	75.0	0.0656
4	9	60.0	120.0	60.0	0.0653
4	10	60.0	135.0	45.0	0.0649
4	11	60.0	150.0	30.0	0.0659
4	12	60.0	165.0	15.0	0.0652
4	13	60.0	180.0	0.0	0.0653
3	1	70.0	0.0	180.0	0.1572
3	2	70.0	15.0	165.0	0.1560
3	3	70.0	30.0	150.0	0.1546
3	4	70.0	45.0	135.0	0.1541

3	5	70.0	60.0	120.0	0.1535
3	6	70.0	75.0	105.0	0.1510
3	7	70.0	90.0	90.0	0.1521
3	8	70.0	105.0	75.0	0.1498
3	9	70.0	120.0	60.0	0.1509
3	10	70.0	135.0	45.0	0.1506
3	11	70.0	150.0	30.0	0.1501
3	12	70.0	165.0	15.0	0.1511
3	13	70.0	180.0	0.0	0.1521
2	1	80.0	0.0	180.0	0.3302
2	2	80.0	15.0	165.0	0.3291
2	3	80.0	30.0	150.0	0.3331
2	4	80.0	45.0	135.0	0.3337
2	5	80.0	60.0	120.0	0.3354
2	6	80.0	75.0	105.0	0.3385
2	7	80.0	90.0	90.0	0.3389
2	8	80.0	105.0	75.0	0.3399
2	9	80.0	120.0	60.0	0.3379
2	10	80.0	135.0	45.0	0.3371
2	11	80.0	150.0	30.0	0.3375
2	12	80.0	165.0	15.0	0.3339
2	13	80.0	180.0	0.0	0.3353
1	1	87.5	0.0	180.0	0.4712
1	2	87.5	15.0	165.0	0.4703
1	3	87.5	30.0	150.0	0.4968
1	4	87.5	45.0	135.0	0.4892
1	5	87.5	60.0	120.0	0.4775
1	6	87.5	75.0	105.0	0.4992
1	7	87.5	90.0	90.0	0.4985
1	8	87.5	105.0	75.0	0.5125
1	9	87.5	120.0	60.0	0.5026
1	10	87.5	135.0	45.0	0.5254
1	11	87.5	150.0	30.0	0.5416
1	12	87.5	165.0	15.0	0.5184
1	13	87.5	180.0	0.0	0.5228

rho for WIND SPEED = 2.0 m/s THETA_SUN = 20.0 deg

10	1	0.0	0.0	0.0	0.0865
9	1	10.0	0.0	180.0	0.0282
9	2	10.0	15.0	165.0	0.0249
9	3	10.0	30.0	150.0	0.0303
9	4	10.0	45.0	135.0	0.0315
9	5	10.0	60.0	120.0	0.0328
9	6	10.0	75.0	105.0	0.0401
9	7	10.0	90.0	90.0	0.0511
9	8	10.0	105.0	75.0	0.0752
9	9	10.0	120.0	60.0	0.1025
9	10	10.0	135.0	45.0	0.1631
9	11	10.0	150.0	30.0	0.2068
9	12	10.0	165.0	15.0	0.2326
9	13	10.0	180.0	0.0	0.2449
8	1	20.0	0.0	180.0	0.0227
8	2	20.0	15.0	165.0	0.0229
8	3	20.0	30.0	150.0	0.0236
8	4	20.0	45.0	135.0	0.0236
8	5	20.0	60.0	120.0	0.0236
8	6	20.0	75.0	105.0	0.0253
8	7	20.0	90.0	90.0	0.0283
8	8	20.0	105.0	75.0	0.0395
8	9	20.0	120.0	60.0	0.0740
8	10	20.0	135.0	45.0	0.1343
8	11	20.0	150.0	30.0	0.2155
8	12	20.0	165.0	15.0	0.2477
8	13	20.0	180.0	0.0	0.0024
7	1	30.0	0.0	180.0	0.0231
7	2	30.0	15.0	165.0	0.0233
7	3	30.0	30.0	150.0	0.0233
7	4	30.0	45.0	135.0	0.0236
7	5	30.0	60.0	120.0	0.0236
7	6	30.0	75.0	105.0	0.0239
7	7	30.0	90.0	90.0	0.0241
7	8	30.0	105.0	75.0	0.0254
7	9	30.0	120.0	60.0	0.0331
7	10	30.0	135.0	45.0	0.0580
7	11	30.0	150.0	30.0	0.1379
7	12	30.0	165.0	15.0	0.2359
7	13	30.0	180.0	0.0	0.2853
6	1	40.0	0.0	180.0	0.0262
6	2	40.0	15.0	165.0	0.0268
6	3	40.0	30.0	150.0	0.0266
6	4	40.0	45.0	135.0	0.0265
6	5	40.0	60.0	120.0	0.0265
6	6	40.0	75.0	105.0	0.0266
6	7	40.0	90.0	90.0	0.0270
6	8	40.0	105.0	75.0	0.0272
6	9	40.0	120.0	60.0	0.0277
6	10	40.0	135.0	45.0	0.0327
6	11	40.0	150.0	30.0	0.0479
6	12	40.0	165.0	15.0	0.0984
6	13	40.0	180.0	0.0	0.1297
5	1	50.0	0.0	180.0	0.0365
5	2	50.0	15.0	165.0	0.0372
5	3	50.0	30.0	150.0	0.0365
5	4	50.0	45.0	135.0	0.0367
5	5	50.0	60.0	120.0	0.0364
5	6	50.0	75.0	105.0	0.0365
5	7	50.0	90.0	90.0	0.0366
5	8	50.0	105.0	75.0	0.0368
5	9	50.0	120.0	60.0	0.0369
5	10	50.0	135.0	45.0	0.0376

5 11 50.0 150.0 30.0 0.0386
5 12 50.0 165.0 15.0 0.0430
5 13 50.0 180.0 0.0 0.0446
4 1 60.0 0.0 180.0 0.0673
4 2 60.0 15.0 165.0 0.0673
4 3 60.0 30.0 150.0 0.0677
4 4 60.0 45.0 135.0 0.0664
4 5 60.0 60.0 120.0 0.0663
4 6 60.0 75.0 105.0 0.0662
4 7 60.0 90.0 90.0 0.0655
4 8 60.0 105.0 75.0 0.0656
4 9 60.0 120.0 60.0 0.0654
4 10 60.0 135.0 45.0 0.0651
4 11 60.0 150.0 30.0 0.0663
4 12 60.0 165.0 15.0 0.0657
4 13 60.0 180.0 0.0 0.0661
3 1 70.0 0.0 180.0 0.1606
3 2 70.0 15.0 165.0 0.1592
3 3 70.0 30.0 150.0 0.1575
3 4 70.0 45.0 135.0 0.1565
3 5 70.0 60.0 120.0 0.1552
3 6 70.0 75.0 105.0 0.1520
3 7 70.0 90.0 90.0 0.1524
3 8 70.0 105.0 75.0 0.1496
3 9 70.0 120.0 60.0 0.1504
3 10 70.0 135.0 45.0 0.1502
3 11 70.0 150.0 30.0 0.1497
3 12 70.0 165.0 15.0 0.1509
3 13 70.0 180.0 0.0 0.1519
2 1 80.0 0.0 180.0 0.3269
2 2 80.0 15.0 165.0 0.3259
2 3 80.0 30.0 150.0 0.3302
2 4 80.0 45.0 135.0 0.3312
2 5 80.0 60.0 120.0 0.3335
2 6 80.0 75.0 105.0 0.3371
2 7 80.0 90.0 90.0 0.3381
2 8 80.0 105.0 75.0 0.3396
2 9 80.0 120.0 60.0 0.3383
2 10 80.0 135.0 45.0 0.3382
2 11 80.0 150.0 30.0 0.3396
2 12 80.0 165.0 15.0 0.3368
2 13 80.0 180.0 0.0 0.3386
1 1 87.5 0.0 180.0 0.4505
1 2 87.5 15.0 165.0 0.4507
1 3 87.5 30.0 150.0 0.4779
1 4 87.5 45.0 135.0 0.4730
1 5 87.5 60.0 120.0 0.4652
1 6 87.5 75.0 105.0 0.4914
1 7 87.5 90.0 90.0 0.4961
1 8 87.5 105.0 75.0 0.5153
1 9 87.5 120.0 60.0 0.5102
1 10 87.5 135.0 45.0 0.5376
1 11 87.5 150.0 30.0 0.5580
1 12 87.5 165.0 15.0 0.5370
1 13 87.5 180.0 0.0 0.5433
rho for WIND SPEED = 2.0 m/s THETA_SUN = 30.0 deg
10 1 0.0 0.0 0.0 0.0277
9 1 10.0 0.0 180.0 0.0229
9 2 10.0 15.0 165.0 0.0238
9 3 10.0 30.0 150.0 0.0231
9 4 10.0 45.0 135.0 0.0227
9 5 10.0 60.0 120.0 0.0229
9 6 10.0 75.0 105.0 0.0232
9 7 10.0 90.0 90.0 0.0233
9 8 10.0 105.0 75.0 0.0280
9 9 10.0 120.0 60.0 0.0321
9 10 10.0 135.0 45.0 0.0461
9 11 10.0 150.0 30.0 0.0628
9 12 10.0 165.0 15.0 0.0866
9 13 10.0 180.0 0.0 0.1117
8 1 20.0 0.0 180.0 0.0221
8 2 20.0 15.0 165.0 0.0223
8 3 20.0 30.0 150.0 0.0224
8 4 20.0 45.0 135.0 0.0225
8 5 20.0 60.0 120.0 0.0226
8 6 20.0 75.0 105.0 0.0228
8 7 20.0 90.0 90.0 0.0233
8 8 20.0 105.0 75.0 0.0259
8 9 20.0 120.0 60.0 0.0277
8 10 20.0 135.0 45.0 0.0604
8 11 20.0 150.0 30.0 0.1262
8 12 20.0 165.0 15.0 0.2114
8 13 20.0 180.0 0.0 0.2325
7 1 30.0 0.0 180.0 0.0228
7 2 30.0 15.0 165.0 0.0229
7 3 30.0 30.0 150.0 0.0230
7 4 30.0 45.0 135.0 0.0232
7 5 30.0 60.0 120.0 0.0232
7 6 30.0 75.0 105.0 0.0234
7 7 30.0 90.0 90.0 0.0238
7 8 30.0 105.0 75.0 0.0239
7 9 30.0 120.0 60.0 0.0254
7 10 30.0 135.0 45.0 0.0420
7 11 30.0 150.0 30.0 0.1234
7 12 30.0 165.0 15.0 0.2343
7 13 30.0 180.0 0.0 0.0039
6 1 40.0 0.0 180.0 0.0262
6 2 40.0 15.0 165.0 0.0268
6 3 40.0 30.0 150.0 0.0266

6	4	40.0	45.0	135.0	0.0264
6	5	40.0	60.0	120.0	0.0263
6	6	40.0	75.0	105.0	0.0264
6	7	40.0	90.0	90.0	0.0267
6	8	40.0	105.0	75.0	0.0270
6	9	40.0	120.0	60.0	0.0277
6	10	40.0	135.0	45.0	0.0298
6	11	40.0	150.0	30.0	0.0699
6	12	40.0	165.0	15.0	0.2077
6	13	40.0	180.0	0.0	0.2927
5	1	50.0	0.0	180.0	0.0369
5	2	50.0	15.0	165.0	0.0376
5	3	50.0	30.0	150.0	0.0369
5	4	50.0	45.0	135.0	0.0370
5	5	50.0	60.0	120.0	0.0366
5	6	50.0	75.0	105.0	0.0365
5	7	50.0	90.0	90.0	0.0366
5	8	50.0	105.0	75.0	0.0367
5	9	50.0	120.0	60.0	0.0369
5	10	50.0	135.0	45.0	0.0376
5	11	50.0	150.0	30.0	0.0449
5	12	50.0	165.0	15.0	0.0882
5	13	50.0	180.0	0.0	0.1432
4	1	60.0	0.0	180.0	0.0685
4	2	60.0	15.0	165.0	0.0686
4	3	60.0	30.0	150.0	0.0689
4	4	60.0	45.0	135.0	0.0674
4	5	60.0	60.0	120.0	0.0670
4	6	60.0	75.0	105.0	0.0667
4	7	60.0	90.0	90.0	0.0657
4	8	60.0	105.0	75.0	0.0658
4	9	60.0	120.0	60.0	0.0656
4	10	60.0	135.0	45.0	0.0653
4	11	60.0	150.0	30.0	0.0670
4	12	60.0	165.0	15.0	0.0691
4	13	60.0	180.0	0.0	0.0771
3	1	70.0	0.0	180.0	0.1627
3	2	70.0	15.0	165.0	0.1613
3	3	70.0	30.0	150.0	0.1595
3	4	70.0	45.0	135.0	0.1582
3	5	70.0	60.0	120.0	0.1567
3	6	70.0	75.0	105.0	0.1529
3	7	70.0	90.0	90.0	0.1529
3	8	70.0	105.0	75.0	0.1498
3	9	70.0	120.0	60.0	0.1505
3	10	70.0	135.0	45.0	0.1504
3	11	70.0	150.0	30.0	0.1501
3	12	70.0	165.0	15.0	0.1518
3	13	70.0	180.0	0.0	0.1530
2	1	80.0	0.0	180.0	0.3241
2	2	80.0	15.0	165.0	0.3232
2	3	80.0	30.0	150.0	0.3275
2	4	80.0	45.0	135.0	0.3288
2	5	80.0	60.0	120.0	0.3315
2	6	80.0	75.0	105.0	0.3355
2	7	80.0	90.0	90.0	0.3369
2	8	80.0	105.0	75.0	0.3387
2	9	80.0	120.0	60.0	0.3380
2	10	80.0	135.0	45.0	0.3392
2	11	80.0	150.0	30.0	0.3431
2	12	80.0	165.0	15.0	0.3428
2	13	80.0	180.0	0.0	0.3458
1	1	87.5	0.0	180.0	0.4400
1	2	87.5	15.0	165.0	0.4405
1	3	87.5	30.0	150.0	0.4675
1	4	87.5	45.0	135.0	0.4631
1	5	87.5	60.0	120.0	0.4567
1	6	87.5	75.0	105.0	0.4848
1	7	87.5	90.0	90.0	0.4925
1	8	87.5	105.0	75.0	0.5147
1	9	87.5	120.0	60.0	0.5128
1	10	87.5	135.0	45.0	0.5448
1	11	87.5	150.0	30.0	0.5719
1	12	87.5	165.0	15.0	0.5573
1	13	87.5	180.0	0.0	0.5679

rho for WIND SPEED = 2.0 m/s THETA_SUN = 40.0 deg

10	1	0.0	0.0	0.0	0.0231
9	1	10.0	0.0	180.0	0.0222
9	2	10.0	15.0	165.0	0.0220
9	3	10.0	30.0	150.0	0.0224
9	4	10.0	45.0	135.0	0.0220
9	5	10.0	60.0	120.0	0.0223
9	6	10.0	75.0	105.0	0.0225
9	7	10.0	90.0	90.0	0.0229
9	8	10.0	105.0	75.0	0.0231
9	9	10.0	120.0	60.0	0.0240
9	10	10.0	135.0	45.0	0.0232
9	11	10.0	150.0	30.0	0.0247
9	12	10.0	165.0	15.0	0.0286
9	13	10.0	180.0	0.0	0.0338
8	1	20.0	0.0	180.0	0.0218
8	2	20.0	15.0	165.0	0.0220
8	3	20.0	30.0	150.0	0.0221
8	4	20.0	45.0	135.0	0.0221
8	5	20.0	60.0	120.0	0.0222
8	6	20.0	75.0	105.0	0.0223
8	7	20.0	90.0	90.0	0.0223
8	8	20.0	105.0	75.0	0.0230
8	9	20.0	120.0	60.0	0.0245

8 10 20.0 135.0 45.0 0.0278
8 11 20.0 150.0 30.0 0.0398
8 12 20.0 165.0 15.0 0.0726
8 13 20.0 180.0 0.0 0.0970
7 1 30.0 0.0 180.0 0.0228
7 2 30.0 15.0 165.0 0.0229
7 3 30.0 30.0 150.0 0.0228
7 4 30.0 45.0 135.0 0.0231
7 5 30.0 60.0 120.0 0.0229
7 6 30.0 75.0 105.0 0.0232
7 7 30.0 90.0 90.0 0.0233
7 8 30.0 105.0 75.0 0.0236
7 9 30.0 120.0 60.0 0.0239
7 10 30.0 135.0 45.0 0.0260
7 11 30.0 150.0 30.0 0.0617
7 12 30.0 165.0 15.0 0.1705
7 13 30.0 180.0 0.0 0.2367
6 1 40.0 0.0 180.0 0.0263
6 2 40.0 15.0 165.0 0.0269
6 3 40.0 30.0 150.0 0.0267
6 4 40.0 45.0 135.0 0.0264
6 5 40.0 60.0 120.0 0.0264
6 6 40.0 75.0 105.0 0.0263
6 7 40.0 90.0 90.0 0.0266
6 8 40.0 105.0 75.0 0.0267
6 9 40.0 120.0 60.0 0.0272
6 10 40.0 135.0 45.0 0.0281
6 11 40.0 150.0 30.0 0.0607
6 12 40.0 165.0 15.0 0.2138
6 13 40.0 180.0 0.0 0.0058
5 1 50.0 0.0 180.0 0.0372
5 2 50.0 15.0 165.0 0.0379
5 3 50.0 30.0 150.0 0.0372
5 4 50.0 45.0 135.0 0.0373
5 5 50.0 60.0 120.0 0.0368
5 6 50.0 75.0 105.0 0.0367
5 7 50.0 90.0 90.0 0.0366
5 8 50.0 105.0 75.0 0.0367
5 9 50.0 120.0 60.0 0.0370
5 10 50.0 135.0 45.0 0.0375
5 11 50.0 150.0 30.0 0.0462
5 12 50.0 165.0 15.0 0.1859
5 13 50.0 180.0 0.0 0.3397
4 1 60.0 0.0 180.0 0.0691
4 2 60.0 15.0 165.0 0.0692
4 3 60.0 30.0 150.0 0.0695
4 4 60.0 45.0 135.0 0.0680
4 5 60.0 60.0 120.0 0.0676
4 6 60.0 75.0 105.0 0.0671
4 7 60.0 90.0 90.0 0.0661
4 8 60.0 105.0 75.0 0.0661
4 9 60.0 120.0 60.0 0.0659
4 10 60.0 135.0 45.0 0.0655
4 11 60.0 150.0 30.0 0.0670
4 12 60.0 165.0 15.0 0.1124
4 13 60.0 180.0 0.0 0.2022
3 1 70.0 0.0 180.0 0.1629
3 2 70.0 15.0 165.0 0.1616
3 3 70.0 30.0 150.0 0.1600
3 4 70.0 45.0 135.0 0.1588
3 5 70.0 60.0 120.0 0.1575
3 6 70.0 75.0 105.0 0.1536
3 7 70.0 90.0 90.0 0.1535
3 8 70.0 105.0 75.0 0.1503
3 9 70.0 120.0 60.0 0.1509
3 10 70.0 135.0 45.0 0.1509
3 11 70.0 150.0 30.0 0.1501
3 12 70.0 165.0 15.0 0.1562
3 13 70.0 180.0 0.0 0.1669
2 1 80.0 0.0 180.0 0.3222
2 2 80.0 15.0 165.0 0.3213
2 3 80.0 30.0 150.0 0.3257
2 4 80.0 45.0 135.0 0.3270
2 5 80.0 60.0 120.0 0.3299
2 6 80.0 75.0 105.0 0.3340
2 7 80.0 90.0 90.0 0.3356
2 8 80.0 105.0 75.0 0.3375
2 9 80.0 120.0 60.0 0.3373
2 10 80.0 135.0 45.0 0.3400
2 11 80.0 150.0 30.0 0.3481
2 12 80.0 165.0 15.0 0.3536
2 13 80.0 180.0 0.0 0.3600
1 1 87.5 0.0 180.0 0.4385
1 2 87.5 15.0 165.0 0.4389
1 3 87.5 30.0 150.0 0.4652
1 4 87.5 45.0 135.0 0.4600
1 5 87.5 60.0 120.0 0.4529
1 6 87.5 75.0 105.0 0.4805
1 7 87.5 90.0 90.0 0.4885
1 8 87.5 105.0 75.0 0.5109
1 9 87.5 120.0 60.0 0.5108
1 10 87.5 135.0 45.0 0.5483
1 11 87.5 150.0 30.0 0.5888
1 12 87.5 165.0 15.0 0.5919
1 13 87.5 180.0 0.0 0.6147
rho for WIND SPEED = 2.0 m/s THETA_SUN = 50.0 deg
10 1 0.0 0.0 0.0 0.0224
9 1 10.0 0.0 180.0 0.0218
9 2 10.0 15.0 165.0 0.0216

9	3	10.0	30.0	150.0	0.0219
9	4	10.0	45.0	135.0	0.0216
9	5	10.0	60.0	120.0	0.0218
9	6	10.0	75.0	105.0	0.0220
9	7	10.0	90.0	90.0	0.0223
9	8	10.0	105.0	75.0	0.0224
9	9	10.0	120.0	60.0	0.0225
9	10	10.0	135.0	45.0	0.0226
9	11	10.0	150.0	30.0	0.0234
9	12	10.0	165.0	15.0	0.0232
9	13	10.0	180.0	0.0	0.0239
8	1	20.0	0.0	180.0	0.0217
8	2	20.0	15.0	165.0	0.0219
8	3	20.0	30.0	150.0	0.0219
8	4	20.0	45.0	135.0	0.0219
8	5	20.0	60.0	120.0	0.0219
8	6	20.0	75.0	105.0	0.0220
8	7	20.0	90.0	90.0	0.0219
8	8	20.0	105.0	75.0	0.0226
8	9	20.0	120.0	60.0	0.0230
8	10	20.0	135.0	45.0	0.0237
8	11	20.0	150.0	30.0	0.0251
8	12	20.0	165.0	15.0	0.0274
8	13	20.0	180.0	0.0	0.0305
7	1	30.0	0.0	180.0	0.0228
7	2	30.0	15.0	165.0	0.0229
7	3	30.0	30.0	150.0	0.0228
7	4	30.0	45.0	135.0	0.0230
7	5	30.0	60.0	120.0	0.0229
7	6	30.0	75.0	105.0	0.0230
7	7	30.0	90.0	90.0	0.0231
7	8	30.0	105.0	75.0	0.0234
7	9	30.0	120.0	60.0	0.0238
7	10	30.0	135.0	45.0	0.0249
7	11	30.0	150.0	30.0	0.0283
7	12	30.0	165.0	15.0	0.0626
7	13	30.0	180.0	0.0	0.0982
6	1	40.0	0.0	180.0	0.0264
6	2	40.0	15.0	165.0	0.0269
6	3	40.0	30.0	150.0	0.0267
6	4	40.0	45.0	135.0	0.0265
6	5	40.0	60.0	120.0	0.0263
6	6	40.0	75.0	105.0	0.0263
6	7	40.0	90.0	90.0	0.0264
6	8	40.0	105.0	75.0	0.0266
6	9	40.0	120.0	60.0	0.0270
6	10	40.0	135.0	45.0	0.0276
6	11	40.0	150.0	30.0	0.0338
6	12	40.0	165.0	15.0	0.1468
6	13	40.0	180.0	0.0	0.2595
5	1	50.0	0.0	180.0	0.0373
5	2	50.0	15.0	165.0	0.0380
5	3	50.0	30.0	150.0	0.0373
5	4	50.0	45.0	135.0	0.0374
5	5	50.0	60.0	120.0	0.0370
5	6	50.0	75.0	105.0	0.0367
5	7	50.0	90.0	90.0	0.0368
5	8	50.0	105.0	75.0	0.0367
5	9	50.0	120.0	60.0	0.0372
5	10	50.0	135.0	45.0	0.0378
5	11	50.0	150.0	30.0	0.0429
5	12	50.0	165.0	15.0	0.2010
5	13	50.0	180.0	0.0	0.0099
4	1	60.0	0.0	180.0	0.0689
4	2	60.0	15.0	165.0	0.0691
4	3	60.0	30.0	150.0	0.0695
4	4	60.0	45.0	135.0	0.0682
4	5	60.0	60.0	120.0	0.0678
4	6	60.0	75.0	105.0	0.0675
4	7	60.0	90.0	90.0	0.0665
4	8	60.0	105.0	75.0	0.0665
4	9	60.0	120.0	60.0	0.0663
4	10	60.0	135.0	45.0	0.0659
4	11	60.0	150.0	30.0	0.0666
4	12	60.0	165.0	15.0	0.1954
4	13	60.0	180.0	0.0	0.4727
3	1	70.0	0.0	180.0	0.1618
3	2	70.0	15.0	165.0	0.1606
3	3	70.0	30.0	150.0	0.1592
3	4	70.0	45.0	135.0	0.1584
3	5	70.0	60.0	120.0	0.1574
3	6	70.0	75.0	105.0	0.1538
3	7	70.0	90.0	90.0	0.1540
3	8	70.0	105.0	75.0	0.1510
3	9	70.0	120.0	60.0	0.1518
3	10	70.0	135.0	45.0	0.1515
3	11	70.0	150.0	30.0	0.1490
3	12	70.0	165.0	15.0	0.1925
3	13	70.0	180.0	0.0	0.3722
2	1	80.0	0.0	180.0	0.3215
2	2	80.0	15.0	165.0	0.3205
2	3	80.0	30.0	150.0	0.3248
2	4	80.0	45.0	135.0	0.3260
2	5	80.0	60.0	120.0	0.3288
2	6	80.0	75.0	105.0	0.3328
2	7	80.0	90.0	90.0	0.3342
2	8	80.0	105.0	75.0	0.3359
2	9	80.0	120.0	60.0	0.3360
2	10	80.0	135.0	45.0	0.3400
2	11	80.0	150.0	30.0	0.3524

2 12 80.0 165.0 15.0 0.3680
2 13 80.0 180.0 0.0 0.4076
1 1 87.5 0.0 180.0 0.4430
1 2 87.5 15.0 165.0 0.4430
1 3 87.5 30.0 150.0 0.4689
1 4 87.5 45.0 135.0 0.4623
1 5 87.5 60.0 120.0 0.4534
1 6 87.5 75.0 105.0 0.4789
1 7 87.5 90.0 90.0 0.4847
1 8 87.5 105.0 75.0 0.5050
1 9 87.5 120.0 60.0 0.5050
1 10 87.5 135.0 45.0 0.5483
1 11 87.5 150.0 30.0 0.6096
1 12 87.5 165.0 15.0 0.6487
1 13 87.5 180.0 0.0 0.7020
rho for WIND SPEED = 2.0 m/s THETA_SUN = 60.0 deg
10 1 0.0 0.0 0.0 0.0219
9 1 10.0 0.0 180.0 0.0217
9 2 10.0 15.0 165.0 0.0214
9 3 10.0 30.0 150.0 0.0217
9 4 10.0 45.0 135.0 0.0213
9 5 10.0 60.0 120.0 0.0215
9 6 10.0 75.0 105.0 0.0217
9 7 10.0 90.0 90.0 0.0220
9 8 10.0 105.0 75.0 0.0219
9 9 10.0 120.0 60.0 0.0220
9 10 10.0 135.0 45.0 0.0220
9 11 10.0 150.0 30.0 0.0226
9 12 10.0 165.0 15.0 0.0224
9 13 10.0 180.0 0.0 0.0229
8 1 20.0 0.0 180.0 0.0217
8 2 20.0 15.0 165.0 0.0218
8 3 20.0 30.0 150.0 0.0219
8 4 20.0 45.0 135.0 0.0218
8 5 20.0 60.0 120.0 0.0218
8 6 20.0 75.0 105.0 0.0219
8 7 20.0 90.0 90.0 0.0217
8 8 20.0 105.0 75.0 0.0222
8 9 20.0 120.0 60.0 0.0225
8 10 20.0 135.0 45.0 0.0231
8 11 20.0 150.0 30.0 0.0237
8 12 20.0 165.0 15.0 0.0240
8 13 20.0 180.0 0.0 0.0242
7 1 30.0 0.0 180.0 0.0227
7 2 30.0 15.0 165.0 0.0228
7 3 30.0 30.0 150.0 0.0228
7 4 30.0 45.0 135.0 0.0230
7 5 30.0 60.0 120.0 0.0228
7 6 30.0 75.0 105.0 0.0229
7 7 30.0 90.0 90.0 0.0230
7 8 30.0 105.0 75.0 0.0231
7 9 30.0 120.0 60.0 0.0235
7 10 30.0 135.0 45.0 0.0245
7 11 30.0 150.0 30.0 0.0254
7 12 30.0 165.0 15.0 0.0288
7 13 30.0 180.0 0.0 0.0323
6 1 40.0 0.0 180.0 0.0263
6 2 40.0 15.0 165.0 0.0268
6 3 40.0 30.0 150.0 0.0267
6 4 40.0 45.0 135.0 0.0265
6 5 40.0 60.0 120.0 0.0263
6 6 40.0 75.0 105.0 0.0263
6 7 40.0 90.0 90.0 0.0264
6 8 40.0 105.0 75.0 0.0265
6 9 40.0 120.0 60.0 0.0269
6 10 40.0 135.0 45.0 0.0278
6 11 40.0 150.0 30.0 0.0306
6 12 40.0 165.0 15.0 0.0551
6 13 40.0 180.0 0.0 0.1131
5 1 50.0 0.0 180.0 0.0371
5 2 50.0 15.0 165.0 0.0378
5 3 50.0 30.0 150.0 0.0371
5 4 50.0 45.0 135.0 0.0373
5 5 50.0 60.0 120.0 0.0369
5 6 50.0 75.0 105.0 0.0369
5 7 50.0 90.0 90.0 0.0368
5 8 50.0 105.0 75.0 0.0369
5 9 50.0 120.0 60.0 0.0373
5 10 50.0 135.0 45.0 0.0385
5 11 50.0 150.0 30.0 0.0395
5 12 50.0 165.0 15.0 0.1363
5 13 50.0 180.0 0.0 0.3135
4 1 60.0 0.0 180.0 0.0683
4 2 60.0 15.0 165.0 0.0685
4 3 60.0 30.0 150.0 0.0690
4 4 60.0 45.0 135.0 0.0678
4 5 60.0 60.0 120.0 0.0677
4 6 60.0 75.0 105.0 0.0675
4 7 60.0 90.0 90.0 0.0668
4 8 60.0 105.0 75.0 0.0668
4 9 60.0 120.0 60.0 0.0670
4 10 60.0 135.0 45.0 0.0671
4 11 60.0 150.0 30.0 0.0678
4 12 60.0 165.0 15.0 0.2135
4 13 60.0 180.0 0.0 0.0212
3 1 70.0 0.0 180.0 0.1602
3 2 70.0 15.0 165.0 0.1589
3 3 70.0 30.0 150.0 0.1577
3 4 70.0 45.0 135.0 0.1572

3	5	70.0	60.0	120.0	0.1567
3	6	70.0	75.0	105.0	0.1537
3	7	70.0	90.0	90.0	0.1544
3	8	70.0	105.0	75.0	0.1518
3	9	70.0	120.0	60.0	0.1530
3	10	70.0	135.0	45.0	0.1529
3	11	70.0	150.0	30.0	0.1485
3	12	70.0	165.0	15.0	0.2822
3	13	70.0	180.0	0.0	0.8044
2	1	80.0	0.0	180.0	0.3215
2	2	80.0	15.0	165.0	0.3205
2	3	80.0	30.0	150.0	0.3247
2	4	80.0	45.0	135.0	0.3258
2	5	80.0	60.0	120.0	0.3283
2	6	80.0	75.0	105.0	0.3319
2	7	80.0	90.0	90.0	0.3331
2	8	80.0	105.0	75.0	0.3344
2	9	80.0	120.0	60.0	0.3344
2	10	80.0	135.0	45.0	0.3383
2	11	80.0	150.0	30.0	0.3510
2	12	80.0	165.0	15.0	0.4172
2	13	80.0	180.0	0.0	0.8426
1	1	87.5	0.0	180.0	0.4507
1	2	87.5	15.0	165.0	0.4504
1	3	87.5	30.0	150.0	0.4759
1	4	87.5	45.0	135.0	0.4681
1	5	87.5	60.0	120.0	0.4570
1	6	87.5	75.0	105.0	0.4795
1	7	87.5	90.0	90.0	0.4816
1	8	87.5	105.0	75.0	0.4982
1	9	87.5	120.0	60.0	0.4963
1	10	87.5	135.0	45.0	0.5422
1	11	87.5	150.0	30.0	0.6210
1	12	87.5	165.0	15.0	0.7136
1	13	87.5	180.0	0.0	1.0019

rho for WIND SPEED = 2.0 m/s THETA_SUN = 70.0 deg

10	1	0.0	0.0	0.0	0.0216
9	1	10.0	0.0	180.0	0.0215
9	2	10.0	15.0	165.0	0.0212
9	3	10.0	30.0	150.0	0.0216
9	4	10.0	45.0	135.0	0.0212
9	5	10.0	60.0	120.0	0.0214
9	6	10.0	75.0	105.0	0.0215
9	7	10.0	90.0	90.0	0.0217
9	8	10.0	105.0	75.0	0.0216
9	9	10.0	120.0	60.0	0.0216
9	10	10.0	135.0	45.0	0.0215
9	11	10.0	150.0	30.0	0.0220
9	12	10.0	165.0	15.0	0.0218
9	13	10.0	180.0	0.0	0.0222
8	1	20.0	0.0	180.0	0.0216
8	2	20.0	15.0	165.0	0.0217
8	3	20.0	30.0	150.0	0.0218
8	4	20.0	45.0	135.0	0.0217
8	5	20.0	60.0	120.0	0.0217
8	6	20.0	75.0	105.0	0.0217
8	7	20.0	90.0	90.0	0.0215
8	8	20.0	105.0	75.0	0.0219
8	9	20.0	120.0	60.0	0.0221
8	10	20.0	135.0	45.0	0.0225
8	11	20.0	150.0	30.0	0.0229
8	12	20.0	165.0	15.0	0.0231
8	13	20.0	180.0	0.0	0.0231
7	1	30.0	0.0	180.0	0.0226
7	2	30.0	15.0	165.0	0.0227
7	3	30.0	30.0	150.0	0.0227
7	4	30.0	45.0	135.0	0.0229
7	5	30.0	60.0	120.0	0.0227
7	6	30.0	75.0	105.0	0.0228
7	7	30.0	90.0	90.0	0.0228
7	8	30.0	105.0	75.0	0.0230
7	9	30.0	120.0	60.0	0.0232
7	10	30.0	135.0	45.0	0.0240
7	11	30.0	150.0	30.0	0.0245
7	12	30.0	165.0	15.0	0.0257
7	13	30.0	180.0	0.0	0.0263
6	1	40.0	0.0	180.0	0.0261
6	2	40.0	15.0	165.0	0.0267
6	3	40.0	30.0	150.0	0.0265
6	4	40.0	45.0	135.0	0.0263
6	5	40.0	60.0	120.0	0.0262
6	6	40.0	75.0	105.0	0.0262
6	7	40.0	90.0	90.0	0.0263
6	8	40.0	105.0	75.0	0.0264
6	9	40.0	120.0	60.0	0.0268
6	10	40.0	135.0	45.0	0.0277
6	11	40.0	150.0	30.0	0.0296
6	12	40.0	165.0	15.0	0.0340
6	13	40.0	180.0	0.0	0.0383
5	1	50.0	0.0	180.0	0.0368
5	2	50.0	15.0	165.0	0.0375
5	3	50.0	30.0	150.0	0.0369
5	4	50.0	45.0	135.0	0.0371
5	5	50.0	60.0	120.0	0.0368
5	6	50.0	75.0	105.0	0.0368
5	7	50.0	90.0	90.0	0.0368
5	8	50.0	105.0	75.0	0.0369
5	9	50.0	120.0	60.0	0.0374
5	10	50.0	135.0	45.0	0.0389

5 11 50.0 150.0 30.0 0.0411
5 12 50.0 165.0 15.0 0.0629
5 13 50.0 180.0 0.0 0.1305
4 1 60.0 0.0 180.0 0.0676
4 2 60.0 15.0 165.0 0.0678
4 3 60.0 30.0 150.0 0.0683
4 4 60.0 45.0 135.0 0.0673
4 5 60.0 60.0 120.0 0.0673
4 6 60.0 75.0 105.0 0.0675
4 7 60.0 90.0 90.0 0.0669
4 8 60.0 105.0 75.0 0.0673
4 9 60.0 120.0 60.0 0.0675
4 10 60.0 135.0 45.0 0.0688
4 11 60.0 150.0 30.0 0.0720
4 12 60.0 165.0 15.0 0.1515
4 13 60.0 180.0 0.0 0.4276
3 1 70.0 0.0 180.0 0.1584
3 2 70.0 15.0 165.0 0.1572
3 3 70.0 30.0 150.0 0.1562
3 4 70.0 45.0 135.0 0.1558
3 5 70.0 60.0 120.0 0.1558
3 6 70.0 75.0 105.0 0.1531
3 7 70.0 90.0 90.0 0.1547
3 8 70.0 105.0 75.0 0.1523
3 9 70.0 120.0 60.0 0.1547
3 10 70.0 135.0 45.0 0.1558
3 11 70.0 150.0 30.0 0.1531
3 12 70.0 165.0 15.0 0.2853
3 13 70.0 180.0 0.0 0.0554
2 1 80.0 0.0 180.0 0.3222
2 2 80.0 15.0 165.0 0.3212
2 3 80.0 30.0 150.0 0.3253
2 4 80.0 45.0 135.0 0.3261
2 5 80.0 60.0 120.0 0.3282
2 6 80.0 75.0 105.0 0.3315
2 7 80.0 90.0 90.0 0.3322
2 8 80.0 105.0 75.0 0.3332
2 9 80.0 120.0 60.0 0.3327
2 10 80.0 135.0 45.0 0.3354
2 11 80.0 150.0 30.0 0.3429
2 12 80.0 165.0 15.0 0.4732
2 13 80.0 180.0 0.0 1.6187
1 1 87.5 0.0 180.0 0.4598
1 2 87.5 15.0 165.0 0.4591
1 3 87.5 30.0 150.0 0.4844
1 4 87.5 45.0 135.0 0.4753
1 5 87.5 60.0 120.0 0.4621
1 6 87.5 75.0 105.0 0.4814
1 7 87.5 90.0 90.0 0.4794
1 8 87.5 105.0 75.0 0.4918
1 9 87.5 120.0 60.0 0.4860
1 10 87.5 135.0 45.0 0.5272
1 11 87.5 150.0 30.0 0.5994
1 12 87.5 165.0 15.0 0.7959
1 13 87.5 180.0 0.0 2.8758
rho for WIND SPEED = 2.0 m/s THETA_SUN = 80.0 deg
10 1 0.0 0.0 0.0 0.0214
9 1 10.0 0.0 180.0 0.0214
9 2 10.0 15.0 165.0 0.0211
9 3 10.0 30.0 150.0 0.0214
9 4 10.0 45.0 135.0 0.0210
9 5 10.0 60.0 120.0 0.0212
9 6 10.0 75.0 105.0 0.0214
9 7 10.0 90.0 90.0 0.0216
9 8 10.0 105.0 75.0 0.0214
9 9 10.0 120.0 60.0 0.0213
9 10 10.0 135.0 45.0 0.0212
9 11 10.0 150.0 30.0 0.0217
9 12 10.0 165.0 15.0 0.0214
9 13 10.0 180.0 0.0 0.0217
8 1 20.0 0.0 180.0 0.0215
8 2 20.0 15.0 165.0 0.0216
8 3 20.0 30.0 150.0 0.0217
8 4 20.0 45.0 135.0 0.0216
8 5 20.0 60.0 120.0 0.0216
8 6 20.0 75.0 105.0 0.0216
8 7 20.0 90.0 90.0 0.0214
8 8 20.0 105.0 75.0 0.0217
8 9 20.0 120.0 60.0 0.0218
8 10 20.0 135.0 45.0 0.0220
8 11 20.0 150.0 30.0 0.0223
8 12 20.0 165.0 15.0 0.0223
8 13 20.0 180.0 0.0 0.0223
7 1 30.0 0.0 180.0 0.0225
7 2 30.0 15.0 165.0 0.0225
7 3 30.0 30.0 150.0 0.0225
7 4 30.0 45.0 135.0 0.0228
7 5 30.0 60.0 120.0 0.0226
7 6 30.0 75.0 105.0 0.0227
7 7 30.0 90.0 90.0 0.0227
7 8 30.0 105.0 75.0 0.0228
7 9 30.0 120.0 60.0 0.0229
7 10 30.0 135.0 45.0 0.0235
7 11 30.0 150.0 30.0 0.0237
7 12 30.0 165.0 15.0 0.0243
7 13 30.0 180.0 0.0 0.0245
6 1 40.0 0.0 180.0 0.0260
6 2 40.0 15.0 165.0 0.0265
6 3 40.0 30.0 150.0 0.0264

6 4 40.0 45.0 135.0 0.0262
6 5 40.0 60.0 120.0 0.0261
6 6 40.0 75.0 105.0 0.0261
6 7 40.0 90.0 90.0 0.0262
6 8 40.0 105.0 75.0 0.0263
6 9 40.0 120.0 60.0 0.0266
6 10 40.0 135.0 45.0 0.0273
6 11 40.0 150.0 30.0 0.0289
6 12 40.0 165.0 15.0 0.0307
6 13 40.0 180.0 0.0 0.0313
5 1 50.0 0.0 180.0 0.0365
5 2 50.0 15.0 165.0 0.0372
5 3 50.0 30.0 150.0 0.0366
5 4 50.0 45.0 135.0 0.0369
5 5 50.0 60.0 120.0 0.0366
5 6 50.0 75.0 105.0 0.0367
5 7 50.0 90.0 90.0 0.0367
5 8 50.0 105.0 75.0 0.0368
5 9 50.0 120.0 60.0 0.0373
5 10 50.0 135.0 45.0 0.0389
5 11 50.0 150.0 30.0 0.0416
5 12 50.0 165.0 15.0 0.0480
5 13 50.0 180.0 0.0 0.0544
4 1 60.0 0.0 180.0 0.0669
4 2 60.0 15.0 165.0 0.0671
4 3 60.0 30.0 150.0 0.0677
4 4 60.0 45.0 135.0 0.0667
4 5 60.0 60.0 120.0 0.0669
4 6 60.0 75.0 105.0 0.0672
4 7 60.0 90.0 90.0 0.0668
4 8 60.0 105.0 75.0 0.0674
4 9 60.0 120.0 60.0 0.0679
4 10 60.0 135.0 45.0 0.0702
4 11 60.0 150.0 30.0 0.0769
4 12 60.0 165.0 15.0 0.0950
4 13 60.0 180.0 0.0 0.1893
3 1 70.0 0.0 180.0 0.1570
3 2 70.0 15.0 165.0 0.1558
3 3 70.0 30.0 150.0 0.1548
3 4 70.0 45.0 135.0 0.1547
3 5 70.0 60.0 120.0 0.1548
3 6 70.0 75.0 105.0 0.1527
3 7 70.0 90.0 90.0 0.1544
3 8 70.0 105.0 75.0 0.1528
3 9 70.0 120.0 60.0 0.1558
3 10 70.0 135.0 45.0 0.1593
3 11 70.0 150.0 30.0 0.1641
3 12 70.0 165.0 15.0 0.2152
3 13 70.0 180.0 0.0 0.5927
2 1 80.0 0.0 180.0 0.3233
2 2 80.0 15.0 165.0 0.3222
2 3 80.0 30.0 150.0 0.3262
2 4 80.0 45.0 135.0 0.3267
2 5 80.0 60.0 120.0 0.3284
2 6 80.0 75.0 105.0 0.3311
2 7 80.0 90.0 90.0 0.3316
2 8 80.0 105.0 75.0 0.3321
2 9 80.0 120.0 60.0 0.3314
2 10 80.0 135.0 45.0 0.3324
2 11 80.0 150.0 30.0 0.3345
2 12 80.0 165.0 15.0 0.3951
2 13 80.0 180.0 0.0 0.1895
1 1 87.5 0.0 180.0 0.4686
1 2 87.5 15.0 165.0 0.4674
1 3 87.5 30.0 150.0 0.4924
1 4 87.5 45.0 135.0 0.4820
1 5 87.5 60.0 120.0 0.4666
1 6 87.5 75.0 105.0 0.4834
1 7 87.5 90.0 90.0 0.4781
1 8 87.5 105.0 75.0 0.4870
1 9 87.5 120.0 60.0 0.4760
1 10 87.5 135.0 45.0 0.5044
1 11 87.5 150.0 30.0 0.5396
1 12 87.5 165.0 15.0 0.6137
1 13 87.5 180.0 0.0 2.4486
rho for WIND SPEED = 4.0 m/s THETA_SUN = 0.0 deg
10 1 0.0 0.0 0.0 0.0018
9 1 10.0 0.0 180.0 0.1795
9 2 10.0 15.0 165.0 0.1802
9 3 10.0 30.0 150.0 0.1812
9 4 10.0 45.0 135.0 0.1874
9 5 10.0 60.0 120.0 0.1789
9 6 10.0 75.0 105.0 0.1725
9 7 10.0 90.0 90.0 0.1807
9 8 10.0 105.0 75.0 0.1725
9 9 10.0 120.0 60.0 0.1789
9 10 10.0 135.0 45.0 0.1874
9 11 10.0 150.0 30.0 0.1812
9 12 10.0 165.0 15.0 0.1802
9 13 10.0 180.0 0.0 0.1795
8 1 20.0 0.0 180.0 0.1465
8 2 20.0 15.0 165.0 0.1447
8 3 20.0 30.0 150.0 0.1463
8 4 20.0 45.0 135.0 0.1490
8 5 20.0 60.0 120.0 0.1457
8 6 20.0 75.0 105.0 0.1488
8 7 20.0 90.0 90.0 0.1441
8 8 20.0 105.0 75.0 0.1488
8 9 20.0 120.0 60.0 0.1457

8 10 20.0 135.0 45.0 0.1490
8 11 20.0 150.0 30.0 0.1463
8 12 20.0 165.0 15.0 0.1447
8 13 20.0 180.0 0.0 0.1465
7 1 30.0 0.0 180.0 0.0614
7 2 30.0 15.0 165.0 0.0669
7 3 30.0 30.0 150.0 0.0638
7 4 30.0 45.0 135.0 0.0648
7 5 30.0 60.0 120.0 0.0692
7 6 30.0 75.0 105.0 0.0651
7 7 30.0 90.0 90.0 0.0584
7 8 30.0 105.0 75.0 0.0652
7 9 30.0 120.0 60.0 0.0692
7 10 30.0 135.0 45.0 0.0648
7 11 30.0 150.0 30.0 0.0638
7 12 30.0 165.0 15.0 0.0669
7 13 30.0 180.0 0.0 0.0614
6 1 40.0 0.0 180.0 0.0333
6 2 40.0 15.0 165.0 0.0348
6 3 40.0 30.0 150.0 0.0330
6 4 40.0 45.0 135.0 0.0352
6 5 40.0 60.0 120.0 0.0343
6 6 40.0 75.0 105.0 0.0342
6 7 40.0 90.0 90.0 0.0332
6 8 40.0 105.0 75.0 0.0342
6 9 40.0 120.0 60.0 0.0343
6 10 40.0 135.0 45.0 0.0352
6 11 40.0 150.0 30.0 0.0330
6 12 40.0 165.0 15.0 0.0348
6 13 40.0 180.0 0.0 0.0333
5 1 50.0 0.0 180.0 0.0390
5 2 50.0 15.0 165.0 0.0395
5 3 50.0 30.0 150.0 0.0395
5 4 50.0 45.0 135.0 0.0389
5 5 50.0 60.0 120.0 0.0389
5 6 50.0 75.0 105.0 0.0392
5 7 50.0 90.0 90.0 0.0395
5 8 50.0 105.0 75.0 0.0392
5 9 50.0 120.0 60.0 0.0389
5 10 50.0 135.0 45.0 0.0389
5 11 50.0 150.0 30.0 0.0395
5 12 50.0 165.0 15.0 0.0395
5 13 50.0 180.0 0.0 0.0390
4 1 60.0 0.0 180.0 0.0717
4 2 60.0 15.0 165.0 0.0719
4 3 60.0 30.0 150.0 0.0723
4 4 60.0 45.0 135.0 0.0719
4 5 60.0 60.0 120.0 0.0715
4 6 60.0 75.0 105.0 0.0716
4 7 60.0 90.0 90.0 0.0720
4 8 60.0 105.0 75.0 0.0716
4 9 60.0 120.0 60.0 0.0715
4 10 60.0 135.0 45.0 0.0719
4 11 60.0 150.0 30.0 0.0723
4 12 60.0 165.0 15.0 0.0719
4 13 60.0 180.0 0.0 0.0717
3 1 70.0 0.0 180.0 0.1585
3 2 70.0 15.0 165.0 0.1578
3 3 70.0 30.0 150.0 0.1567
3 4 70.0 45.0 135.0 0.1586
3 5 70.0 60.0 120.0 0.1579
3 6 70.0 75.0 105.0 0.1580
3 7 70.0 90.0 90.0 0.1602
3 8 70.0 105.0 75.0 0.1580
3 9 70.0 120.0 60.0 0.1579
3 10 70.0 135.0 45.0 0.1586
3 11 70.0 150.0 30.0 0.1567
3 12 70.0 165.0 15.0 0.1578
3 13 70.0 180.0 0.0 0.1585
2 1 80.0 0.0 180.0 0.2830
2 2 80.0 15.0 165.0 0.2841
2 3 80.0 30.0 150.0 0.2893
2 4 80.0 45.0 135.0 0.2857
2 5 80.0 60.0 120.0 0.2824
2 6 80.0 75.0 105.0 0.2926
2 7 80.0 90.0 90.0 0.2895
2 8 80.0 105.0 75.0 0.2926
2 9 80.0 120.0 60.0 0.2824
2 10 80.0 135.0 45.0 0.2857
2 11 80.0 150.0 30.0 0.2893
2 12 80.0 165.0 15.0 0.2841
2 13 80.0 180.0 0.0 0.2830
1 1 87.5 0.0 180.0 0.3568
1 2 87.5 15.0 165.0 0.3619
1 3 87.5 30.0 150.0 0.3895
1 4 87.5 45.0 135.0 0.3797
1 5 87.5 60.0 120.0 0.3704
1 6 87.5 75.0 105.0 0.3680
1 7 87.5 90.0 90.0 0.3721
1 8 87.5 105.0 75.0 0.3680
1 9 87.5 120.0 60.0 0.3704
1 10 87.5 135.0 45.0 0.3797
1 11 87.5 150.0 30.0 0.3895
1 12 87.5 165.0 15.0 0.3619
1 13 87.5 180.0 0.0 0.3568
rho for WIND SPEED = 4.0 m/s THETA_SUN = 10.0
deg
10 1 0.0 0.0 0.0 0.1667
9 1 10.0 0.0 180.0 0.1292
9 2 10.0 15.0 165.0 0.1159

9	3	10.0	30.0	150.0	0.1441
9	4	10.0	45.0	135.0	0.1332
9	5	10.0	60.0	120.0	0.1513
9	6	10.0	75.0	105.0	0.1620
9	7	10.0	90.0	90.0	0.1717
9	8	10.0	105.0	75.0	0.1798
9	9	10.0	120.0	60.0	0.1752
9	10	10.0	135.0	45.0	0.1591
9	11	10.0	150.0	30.0	0.1478
9	12	10.0	165.0	15.0	0.1293
9	13	10.0	180.0	0.0	0.0006
8	1	20.0	0.0	180.0	0.0614
8	2	20.0	15.0	165.0	0.0582
8	3	20.0	30.0	150.0	0.0604
8	4	20.0	45.0	135.0	0.0672
8	5	20.0	60.0	120.0	0.0756
8	6	20.0	75.0	105.0	0.0948
8	7	20.0	90.0	90.0	0.1229
8	8	20.0	105.0	75.0	0.1341
8	9	20.0	120.0	60.0	0.1549
8	10	20.0	135.0	45.0	0.1677
8	11	20.0	150.0	30.0	0.1859
8	12	20.0	165.0	15.0	0.1973
8	13	20.0	180.0	0.0	0.1875
7	1	30.0	0.0	180.0	0.0267
7	2	30.0	15.0	165.0	0.0287
7	3	30.0	30.0	150.0	0.0306
7	4	30.0	45.0	135.0	0.0301
7	5	30.0	60.0	120.0	0.0362
7	6	30.0	75.0	105.0	0.0419
7	7	30.0	90.0	90.0	0.0498
7	8	30.0	105.0	75.0	0.0629
7	9	30.0	120.0	60.0	0.0766
7	10	30.0	135.0	45.0	0.1188
7	11	30.0	150.0	30.0	0.1421
7	12	30.0	165.0	15.0	0.1630
7	13	30.0	180.0	0.0	0.1872
6	1	40.0	0.0	180.0	0.0288
6	2	40.0	15.0	165.0	0.0287
6	3	40.0	30.0	150.0	0.0284
6	4	40.0	45.0	135.0	0.0284
6	5	40.0	60.0	120.0	0.0282
6	6	40.0	75.0	105.0	0.0297
6	7	40.0	90.0	90.0	0.0308
6	8	40.0	105.0	75.0	0.0338
6	9	40.0	120.0	60.0	0.0399
6	10	40.0	135.0	45.0	0.0508
6	11	40.0	150.0	30.0	0.0629
6	12	40.0	165.0	15.0	0.0808
6	13	40.0	180.0	0.0	0.0819
5	1	50.0	0.0	180.0	0.0387
5	2	50.0	15.0	165.0	0.0392
5	3	50.0	30.0	150.0	0.0389
5	4	50.0	45.0	135.0	0.0386
5	5	50.0	60.0	120.0	0.0386
5	6	50.0	75.0	105.0	0.0388
5	7	50.0	90.0	90.0	0.0394
5	8	50.0	105.0	75.0	0.0391
5	9	50.0	120.0	60.0	0.0396
5	10	50.0	135.0	45.0	0.0424
5	11	50.0	150.0	30.0	0.0431
5	12	50.0	165.0	15.0	0.0455
5	13	50.0	180.0	0.0	0.0454
4	1	60.0	0.0	180.0	0.0735
4	2	60.0	15.0	165.0	0.0737
4	3	60.0	30.0	150.0	0.0738
4	4	60.0	45.0	135.0	0.0731
4	5	60.0	60.0	120.0	0.0723
4	6	60.0	75.0	105.0	0.0720
4	7	60.0	90.0	90.0	0.0722
4	8	60.0	105.0	75.0	0.0714
4	9	60.0	120.0	60.0	0.0712
4	10	60.0	135.0	45.0	0.0716
4	11	60.0	150.0	30.0	0.0723
4	12	60.0	165.0	15.0	0.0716
4	13	60.0	180.0	0.0	0.0715
3	1	70.0	0.0	180.0	0.1624
3	2	70.0	15.0	165.0	0.1616
3	3	70.0	30.0	150.0	0.1600
3	4	70.0	45.0	135.0	0.1612
3	5	70.0	60.0	120.0	0.1597
3	6	70.0	75.0	105.0	0.1589
3	7	70.0	90.0	90.0	0.1603
3	8	70.0	105.0	75.0	0.1574
3	9	70.0	120.0	60.0	0.1568
3	10	70.0	135.0	45.0	0.1570
3	11	70.0	150.0	30.0	0.1549
3	12	70.0	165.0	15.0	0.1559
3	13	70.0	180.0	0.0	0.1566
2	1	80.0	0.0	180.0	0.2772
2	2	80.0	15.0	165.0	0.2786
2	3	80.0	30.0	150.0	0.2843
2	4	80.0	45.0	135.0	0.2816
2	5	80.0	60.0	120.0	0.2793
2	6	80.0	75.0	105.0	0.2907
2	7	80.0	90.0	90.0	0.2890
2	8	80.0	105.0	75.0	0.2935
2	9	80.0	120.0	60.0	0.2845
2	10	80.0	135.0	45.0	0.2889
2	11	80.0	150.0	30.0	0.2934

2 12 80.0 165.0 15.0 0.2888
2 13 80.0 180.0 0.0 0.2881
1 1 87.5 0.0 180.0 0.3325
1 2 87.5 15.0 165.0 0.3376
1 3 87.5 30.0 150.0 0.3667
1 4 87.5 45.0 135.0 0.3609
1 5 87.5 60.0 120.0 0.3570
1 6 87.5 75.0 105.0 0.3607
1 7 87.5 90.0 90.0 0.3711
1 8 87.5 105.0 75.0 0.3732
1 9 87.5 120.0 60.0 0.3818
1 10 87.5 135.0 45.0 0.3964
1 11 87.5 150.0 30.0 0.4105
1 12 87.5 165.0 15.0 0.3844
1 13 87.5 180.0 0.0 0.3796
rho for WIND SPEED = 4.0 m/s THETA_SUN = 20.0 deg
10 1 0.0 0.0 0.0 0.1316
9 1 10.0 0.0 180.0 0.0647
9 2 10.0 15.0 165.0 0.0587
9 3 10.0 30.0 150.0 0.0616
9 4 10.0 45.0 135.0 0.0735
9 5 10.0 60.0 120.0 0.0699
9 6 10.0 75.0 105.0 0.0836
9 7 10.0 90.0 90.0 0.1017
9 8 10.0 105.0 75.0 0.1296
9 9 10.0 120.0 60.0 0.1518
9 10 10.0 135.0 45.0 0.1695
9 11 10.0 150.0 30.0 0.1597
9 12 10.0 165.0 15.0 0.1663
9 13 10.0 180.0 0.0 0.1567
8 1 20.0 0.0 180.0 0.0279
8 2 20.0 15.0 165.0 0.0285
8 3 20.0 30.0 150.0 0.0297
8 4 20.0 45.0 135.0 0.0304
8 5 20.0 60.0 120.0 0.0393
8 6 20.0 75.0 105.0 0.0448
8 7 20.0 90.0 90.0 0.0697
8 8 20.0 105.0 75.0 0.0924
8 9 20.0 120.0 60.0 0.1232
8 10 20.0 135.0 45.0 0.1550
8 11 20.0 150.0 30.0 0.1671
8 12 20.0 165.0 15.0 0.1446
8 13 20.0 180.0 0.0 0.0013
7 1 30.0 0.0 180.0 0.0241
7 2 30.0 15.0 165.0 0.0244
7 3 30.0 30.0 150.0 0.0255
7 4 30.0 45.0 135.0 0.0252
7 5 30.0 60.0 120.0 0.0261
7 6 30.0 75.0 105.0 0.0292
7 7 30.0 90.0 90.0 0.0314
7 8 30.0 105.0 75.0 0.0477
7 9 30.0 120.0 60.0 0.0766
7 10 30.0 135.0 45.0 0.1205
7 11 30.0 150.0 30.0 0.1612
7 12 30.0 165.0 15.0 0.1871
7 13 30.0 180.0 0.0 0.1939
6 1 40.0 0.0 180.0 0.0274
6 2 40.0 15.0 165.0 0.0277
6 3 40.0 30.0 150.0 0.0274
6 4 40.0 45.0 135.0 0.0278
6 5 40.0 60.0 120.0 0.0276
6 6 40.0 75.0 105.0 0.0280
6 7 40.0 90.0 90.0 0.0290
6 8 40.0 105.0 75.0 0.0325
6 9 40.0 120.0 60.0 0.0366
6 10 40.0 135.0 45.0 0.0599
6 11 40.0 150.0 30.0 0.1075
6 12 40.0 165.0 15.0 0.1604
6 13 40.0 180.0 0.0 0.1850
5 1 50.0 0.0 180.0 0.0392
5 2 50.0 15.0 165.0 0.0397
5 3 50.0 30.0 150.0 0.0393
5 4 50.0 45.0 135.0 0.0389
5 5 50.0 60.0 120.0 0.0387
5 6 50.0 75.0 105.0 0.0387
5 7 50.0 90.0 90.0 0.0392
5 8 50.0 105.0 75.0 0.0391
5 9 50.0 120.0 60.0 0.0403
5 10 50.0 135.0 45.0 0.0464
5 11 50.0 150.0 30.0 0.0572
5 12 50.0 165.0 15.0 0.0849
5 13 50.0 180.0 0.0 0.0996
4 1 60.0 0.0 180.0 0.0764
4 2 60.0 15.0 165.0 0.0765
4 3 60.0 30.0 150.0 0.0764
4 4 60.0 45.0 135.0 0.0750
4 5 60.0 60.0 120.0 0.0736
4 6 60.0 75.0 105.0 0.0727
4 7 60.0 90.0 90.0 0.0725
4 8 60.0 105.0 75.0 0.0714
4 9 60.0 120.0 60.0 0.0712
4 10 60.0 135.0 45.0 0.0718
4 11 60.0 150.0 30.0 0.0746
4 12 60.0 165.0 15.0 0.0765
4 13 60.0 180.0 0.0 0.0789
3 1 70.0 0.0 180.0 0.1664
3 2 70.0 15.0 165.0 0.1656
3 3 70.0 30.0 150.0 0.1636
3 4 70.0 45.0 135.0 0.1642

3	5	70.0	60.0	120.0	0.1618
3	6	70.0	75.0	105.0	0.1600
3	7	70.0	90.0	90.0	0.1607
3	8	70.0	105.0	75.0	0.1572
3	9	70.0	120.0	60.0	0.1563
3	10	70.0	135.0	45.0	0.1566
3	11	70.0	150.0	30.0	0.1550
3	12	70.0	165.0	15.0	0.1565
3	13	70.0	180.0	0.0	0.1574
2	1	80.0	0.0	180.0	0.2711
2	2	80.0	15.0	165.0	0.2729
2	3	80.0	30.0	150.0	0.2791
2	4	80.0	45.0	135.0	0.2771
2	5	80.0	60.0	120.0	0.2758
2	6	80.0	75.0	105.0	0.2882
2	7	80.0	90.0	90.0	0.2877
2	8	80.0	105.0	75.0	0.2933
2	9	80.0	120.0	60.0	0.2854
2	10	80.0	135.0	45.0	0.2914
2	11	80.0	150.0	30.0	0.2976
2	12	80.0	165.0	15.0	0.2947
2	13	80.0	180.0	0.0	0.2947
1	1	87.5	0.0	180.0	0.3133
1	2	87.5	15.0	165.0	0.3182
1	3	87.5	30.0	150.0	0.3480
1	4	87.5	45.0	135.0	0.3447
1	5	87.5	60.0	120.0	0.3444
1	6	87.5	75.0	105.0	0.3529
1	7	87.5	90.0	90.0	0.3683
1	8	87.5	105.0	75.0	0.3754
1	9	87.5	120.0	60.0	0.3890
1	10	87.5	135.0	45.0	0.4083
1	11	87.5	150.0	30.0	0.4273
1	12	87.5	165.0	15.0	0.4039
1	13	87.5	180.0	0.0	0.3997

rho for WIND SPEED = 4.0 m/s THETA_SUN = 30.0 deg

10	1	0.0	0.0	0.0	0.0625
9	1	10.0	0.0	180.0	0.0248
9	2	10.0	15.0	165.0	0.0257
9	3	10.0	30.0	150.0	0.0318
9	4	10.0	45.0	135.0	0.0328
9	5	10.0	60.0	120.0	0.0357
9	6	10.0	75.0	105.0	0.0354
9	7	10.0	90.0	90.0	0.0451
9	8	10.0	105.0	75.0	0.0542
9	9	10.0	120.0	60.0	0.0667
9	10	10.0	135.0	45.0	0.0856
9	11	10.0	150.0	30.0	0.1111
9	12	10.0	165.0	15.0	0.1365
9	13	10.0	180.0	0.0	0.1417
8	1	20.0	0.0	180.0	0.0234
8	2	20.0	15.0	165.0	0.0242
8	3	20.0	30.0	150.0	0.0232
8	4	20.0	45.0	135.0	0.0233
8	5	20.0	60.0	120.0	0.0256
8	6	20.0	75.0	105.0	0.0265
8	7	20.0	90.0	90.0	0.0307
8	8	20.0	105.0	75.0	0.0393
8	9	20.0	120.0	60.0	0.0717
8	10	20.0	135.0	45.0	0.1040
8	11	20.0	150.0	30.0	0.1532
8	12	20.0	165.0	15.0	0.1668
8	13	20.0	180.0	0.0	0.1516
7	1	30.0	0.0	180.0	0.0235
7	2	30.0	15.0	165.0	0.0237
7	3	30.0	30.0	150.0	0.0238
7	4	30.0	45.0	135.0	0.0240
7	5	30.0	60.0	120.0	0.0241
7	6	30.0	75.0	105.0	0.0244
7	7	30.0	90.0	90.0	0.0263
7	8	30.0	105.0	75.0	0.0287
7	9	30.0	120.0	60.0	0.0475
7	10	30.0	135.0	45.0	0.0932
7	11	30.0	150.0	30.0	0.1438
7	12	30.0	165.0	15.0	0.1581
7	13	30.0	180.0	0.0	0.0021
6	1	40.0	0.0	180.0	0.0274
6	2	40.0	15.0	165.0	0.0278
6	3	40.0	30.0	150.0	0.0273
6	4	40.0	45.0	135.0	0.0276
6	5	40.0	60.0	120.0	0.0273
6	6	40.0	75.0	105.0	0.0275
6	7	40.0	90.0	90.0	0.0278
6	8	40.0	105.0	75.0	0.0287
6	9	40.0	120.0	60.0	0.0331
6	10	40.0	135.0	45.0	0.0581
6	11	40.0	150.0	30.0	0.1179
6	12	40.0	165.0	15.0	0.1902
6	13	40.0	180.0	0.0	0.2051
5	1	50.0	0.0	180.0	0.0402
5	2	50.0	15.0	165.0	0.0407
5	3	50.0	30.0	150.0	0.0401
5	4	50.0	45.0	135.0	0.0395
5	5	50.0	60.0	120.0	0.0390
5	6	50.0	75.0	105.0	0.0388
5	7	50.0	90.0	90.0	0.0391
5	8	50.0	105.0	75.0	0.0389
5	9	50.0	120.0	60.0	0.0395
5	10	50.0	135.0	45.0	0.0459

5 11 50.0 150.0 30.0 0.0814
5 12 50.0 165.0 15.0 0.1600
5 13 50.0 180.0 0.0 0.2187
4 1 60.0 0.0 180.0 0.0791
4 2 60.0 15.0 165.0 0.0792
4 3 60.0 30.0 150.0 0.0788
4 4 60.0 45.0 135.0 0.0771
4 5 60.0 60.0 120.0 0.0751
4 6 60.0 75.0 105.0 0.0737
4 7 60.0 90.0 90.0 0.0731
4 8 60.0 105.0 75.0 0.0717
4 9 60.0 120.0 60.0 0.0714
4 10 60.0 135.0 45.0 0.0725
4 11 60.0 150.0 30.0 0.0801
4 12 60.0 165.0 15.0 0.1117
4 13 60.0 180.0 0.0 0.1414
3 1 70.0 0.0 180.0 0.1688
3 2 70.0 15.0 165.0 0.1681
3 3 70.0 30.0 150.0 0.1660
3 4 70.0 45.0 135.0 0.1664
3 5 70.0 60.0 120.0 0.1635
3 6 70.0 75.0 105.0 0.1611
3 7 70.0 90.0 90.0 0.1612
3 8 70.0 105.0 75.0 0.1573
3 9 70.0 120.0 60.0 0.1563
3 10 70.0 135.0 45.0 0.1570
3 11 70.0 150.0 30.0 0.1565
3 12 70.0 165.0 15.0 0.1643
3 13 70.0 180.0 0.0 0.1706
2 1 80.0 0.0 180.0 0.2663
2 2 80.0 15.0 165.0 0.2683
2 3 80.0 30.0 150.0 0.2747
2 4 80.0 45.0 135.0 0.2731
2 5 80.0 60.0 120.0 0.2724
2 6 80.0 75.0 105.0 0.2855
2 7 80.0 90.0 90.0 0.2858
2 8 80.0 105.0 75.0 0.2921
2 9 80.0 120.0 60.0 0.2852
2 10 80.0 135.0 45.0 0.2936
2 11 80.0 150.0 30.0 0.3037
2 12 80.0 165.0 15.0 0.3054
2 13 80.0 180.0 0.0 0.3077
1 1 87.5 0.0 180.0 0.3030
1 2 87.5 15.0 165.0 0.3075
1 3 87.5 30.0 150.0 0.3371
1 4 87.5 45.0 135.0 0.3342
1 5 87.5 60.0 120.0 0.3353
1 6 87.5 75.0 105.0 0.3460
1 7 87.5 90.0 90.0 0.3643
1 8 87.5 105.0 75.0 0.3741
1 9 87.5 120.0 60.0 0.3911
1 10 87.5 135.0 45.0 0.4155
1 11 87.5 150.0 30.0 0.4430
1 12 87.5 165.0 15.0 0.4279
1 13 87.5 180.0 0.0 0.4266
rho for WIND SPEED = 4.0 m/s THETA_SUN = 40.0 deg
10 1 0.0 0.0 0.0 0.0278
9 1 10.0 0.0 180.0 0.0235
9 2 10.0 15.0 165.0 0.0247
9 3 10.0 30.0 150.0 0.0235
9 4 10.0 45.0 135.0 0.0238
9 5 10.0 60.0 120.0 0.0238
9 6 10.0 75.0 105.0 0.0238
9 7 10.0 90.0 90.0 0.0262
9 8 10.0 105.0 75.0 0.0286
9 9 10.0 120.0 60.0 0.0298
9 10 10.0 135.0 45.0 0.0450
9 11 10.0 150.0 30.0 0.0529
9 12 10.0 165.0 15.0 0.0604
9 13 10.0 180.0 0.0 0.0581
8 1 20.0 0.0 180.0 0.0228
8 2 20.0 15.0 165.0 0.0228
8 3 20.0 30.0 150.0 0.0224
8 4 20.0 45.0 135.0 0.0226
8 5 20.0 60.0 120.0 0.0229
8 6 20.0 75.0 105.0 0.0247
8 7 20.0 90.0 90.0 0.0246
8 8 20.0 105.0 75.0 0.0258
8 9 20.0 120.0 60.0 0.0342
8 10 20.0 135.0 45.0 0.0487
8 11 20.0 150.0 30.0 0.0810
8 12 20.0 165.0 15.0 0.1192
8 13 20.0 180.0 0.0 0.1348
7 1 30.0 0.0 180.0 0.0234
7 2 30.0 15.0 165.0 0.0236
7 3 30.0 30.0 150.0 0.0235
7 4 30.0 45.0 135.0 0.0236
7 5 30.0 60.0 120.0 0.0236
7 6 30.0 75.0 105.0 0.0239
7 7 30.0 90.0 90.0 0.0241
7 8 30.0 105.0 75.0 0.0259
7 9 30.0 120.0 60.0 0.0274
7 10 30.0 135.0 45.0 0.0483
7 11 30.0 150.0 30.0 0.1055
7 12 30.0 165.0 15.0 0.1603
7 13 30.0 180.0 0.0 0.1626
6 1 40.0 0.0 180.0 0.0276
6 2 40.0 15.0 165.0 0.0280
6 3 40.0 30.0 150.0 0.0275

6	4	40.0	45.0	135.0	0.0277
6	5	40.0	60.0	120.0	0.0273
6	6	40.0	75.0	105.0	0.0272
6	7	40.0	90.0	90.0	0.0275
6	8	40.0	105.0	75.0	0.0279
6	9	40.0	120.0	60.0	0.0297
6	10	40.0	135.0	45.0	0.0421
6	11	40.0	150.0	30.0	0.0991
6	12	40.0	165.0	15.0	0.1641
6	13	40.0	180.0	0.0	0.0034
5	1	50.0	0.0	180.0	0.0409
5	2	50.0	15.0	165.0	0.0414
5	3	50.0	30.0	150.0	0.0409
5	4	50.0	45.0	135.0	0.0401
5	5	50.0	60.0	120.0	0.0395
5	6	50.0	75.0	105.0	0.0391
5	7	50.0	90.0	90.0	0.0392
5	8	50.0	105.0	75.0	0.0389
5	9	50.0	120.0	60.0	0.0392
5	10	50.0	135.0	45.0	0.0422
5	11	50.0	150.0	30.0	0.0815
5	12	50.0	165.0	15.0	0.1978
5	13	50.0	180.0	0.0	0.2483
4	1	60.0	0.0	180.0	0.0804
4	2	60.0	15.0	165.0	0.0806
4	3	60.0	30.0	150.0	0.0803
4	4	60.0	45.0	135.0	0.0785
4	5	60.0	60.0	120.0	0.0763
4	6	60.0	75.0	105.0	0.0747
4	7	60.0	90.0	90.0	0.0739
4	8	60.0	105.0	75.0	0.0723
4	9	60.0	120.0	60.0	0.0718
4	10	60.0	135.0	45.0	0.0723
4	11	60.0	150.0	30.0	0.0862
4	12	60.0	165.0	15.0	0.1855
4	13	60.0	180.0	0.0	0.3081
3	1	70.0	0.0	180.0	0.1690
3	2	70.0	15.0	165.0	0.1683
3	3	70.0	30.0	150.0	0.1664
3	4	70.0	45.0	135.0	0.1670
3	5	70.0	60.0	120.0	0.1644
3	6	70.0	75.0	105.0	0.1619
3	7	70.0	90.0	90.0	0.1618
3	8	70.0	105.0	75.0	0.1578
3	9	70.0	120.0	60.0	0.1567
3	10	70.0	135.0	45.0	0.1573
3	11	70.0	150.0	30.0	0.1576
3	12	70.0	165.0	15.0	0.2076
3	13	70.0	180.0	0.0	0.2794
2	1	80.0	0.0	180.0	0.2637
2	2	80.0	15.0	165.0	0.2657
2	3	80.0	30.0	150.0	0.2721
2	4	80.0	45.0	135.0	0.2705
2	5	80.0	60.0	120.0	0.2699
2	6	80.0	75.0	105.0	0.2830
2	7	80.0	90.0	90.0	0.2836
2	8	80.0	105.0	75.0	0.2900
2	9	80.0	120.0	60.0	0.2839
2	10	80.0	135.0	45.0	0.2950
2	11	80.0	150.0	30.0	0.3117
2	12	80.0	165.0	15.0	0.3312
2	13	80.0	180.0	0.0	0.3532
1	1	87.5	0.0	180.0	0.3008
1	2	87.5	15.0	165.0	0.3049
1	3	87.5	30.0	150.0	0.3340
1	4	87.5	45.0	135.0	0.3302
1	5	87.5	60.0	120.0	0.3307
1	6	87.5	75.0	105.0	0.3413
1	7	87.5	90.0	90.0	0.3598
1	8	87.5	105.0	75.0	0.3697
1	9	87.5	120.0	60.0	0.3885
1	10	87.5	135.0	45.0	0.4189
1	11	87.5	150.0	30.0	0.4626
1	12	87.5	165.0	15.0	0.4695
1	13	87.5	180.0	0.0	0.4792

rho for WIND SPEED = 4.0 m/s THETA_SUN = 50.0 deg

10	1	0.0	0.0	0.0	0.0236
9	1	10.0	0.0	180.0	0.0226
9	2	10.0	15.0	165.0	0.0226
9	3	10.0	30.0	150.0	0.0226
9	4	10.0	45.0	135.0	0.0229
9	5	10.0	60.0	120.0	0.0228
9	6	10.0	75.0	105.0	0.0228
9	7	10.0	90.0	90.0	0.0232
9	8	10.0	105.0	75.0	0.0253
9	9	10.0	120.0	60.0	0.0242
9	10	10.0	135.0	45.0	0.0264
9	11	10.0	150.0	30.0	0.0250
9	12	10.0	165.0	15.0	0.0286
9	13	10.0	180.0	0.0	0.0279
8	1	20.0	0.0	180.0	0.0225
8	2	20.0	15.0	165.0	0.0224
8	3	20.0	30.0	150.0	0.0221
8	4	20.0	45.0	135.0	0.0222
8	5	20.0	60.0	120.0	0.0224
8	6	20.0	75.0	105.0	0.0228
8	7	20.0	90.0	90.0	0.0233
8	8	20.0	105.0	75.0	0.0237
8	9	20.0	120.0	60.0	0.0245

8 10 20.0 135.0 45.0 0.0269
8 11 20.0 150.0 30.0 0.0386
8 12 20.0 165.0 15.0 0.0527
8 13 20.0 180.0 0.0 0.0635
7 1 30.0 0.0 180.0 0.0233
7 2 30.0 15.0 165.0 0.0235
7 3 30.0 30.0 150.0 0.0234
7 4 30.0 45.0 135.0 0.0235
7 5 30.0 60.0 120.0 0.0233
7 6 30.0 75.0 105.0 0.0235
7 7 30.0 90.0 90.0 0.0236
7 8 30.0 105.0 75.0 0.0243
7 9 30.0 120.0 60.0 0.0256
7 10 30.0 135.0 45.0 0.0291
7 11 30.0 150.0 30.0 0.0539
7 12 30.0 165.0 15.0 0.1058
7 13 30.0 180.0 0.0 0.1361
6 1 40.0 0.0 180.0 0.0276
6 2 40.0 15.0 165.0 0.0281
6 3 40.0 30.0 150.0 0.0275
6 4 40.0 45.0 135.0 0.0278
6 5 40.0 60.0 120.0 0.0273
6 6 40.0 75.0 105.0 0.0272
6 7 40.0 90.0 90.0 0.0272
6 8 40.0 105.0 75.0 0.0277
6 9 40.0 120.0 60.0 0.0285
6 10 40.0 135.0 45.0 0.0302
6 11 40.0 150.0 30.0 0.0641
6 12 40.0 165.0 15.0 0.1571
6 13 40.0 180.0 0.0 0.1884
5 1 50.0 0.0 180.0 0.0411
5 2 50.0 15.0 165.0 0.0416
5 3 50.0 30.0 150.0 0.0412
5 4 50.0 45.0 135.0 0.0404
5 5 50.0 60.0 120.0 0.0399
5 6 50.0 75.0 105.0 0.0394
5 7 50.0 90.0 90.0 0.0396
5 8 50.0 105.0 75.0 0.0390
5 9 50.0 120.0 60.0 0.0396
5 10 50.0 135.0 45.0 0.0403
5 11 50.0 150.0 30.0 0.0661
5 12 50.0 165.0 15.0 0.1790
5 13 50.0 180.0 0.0 0.0062
4 1 60.0 0.0 180.0 0.0801
4 2 60.0 15.0 165.0 0.0804
4 3 60.0 30.0 150.0 0.0803
4 4 60.0 45.0 135.0 0.0788
4 5 60.0 60.0 120.0 0.0768
4 6 60.0 75.0 105.0 0.0754
4 7 60.0 90.0 90.0 0.0748
4 8 60.0 105.0 75.0 0.0731
4 9 60.0 120.0 60.0 0.0726
4 10 60.0 135.0 45.0 0.0723
4 11 60.0 150.0 30.0 0.0792
4 12 60.0 165.0 15.0 0.2213
4 13 60.0 180.0 0.0 0.3727
3 1 70.0 0.0 180.0 0.1674
3 2 70.0 15.0 165.0 0.1669
3 3 70.0 30.0 150.0 0.1653
3 4 70.0 45.0 135.0 0.1663
3 5 70.0 60.0 120.0 0.1642
3 6 70.0 75.0 105.0 0.1622
3 7 70.0 90.0 90.0 0.1624
3 8 70.0 105.0 75.0 0.1586
3 9 70.0 120.0 60.0 0.1575
3 10 70.0 135.0 45.0 0.1576
3 11 70.0 150.0 30.0 0.1560
3 12 70.0 165.0 15.0 0.2938
3 13 70.0 180.0 0.0 0.5607
2 1 80.0 0.0 180.0 0.2629
2 2 80.0 15.0 165.0 0.2649
2 3 80.0 30.0 150.0 0.2711
2 4 80.0 45.0 135.0 0.2693
2 5 80.0 60.0 120.0 0.2684
2 6 80.0 75.0 105.0 0.2812
2 7 80.0 90.0 90.0 0.2815
2 8 80.0 105.0 75.0 0.2874
2 9 80.0 120.0 60.0 0.2815
2 10 80.0 135.0 45.0 0.2945
2 11 80.0 150.0 30.0 0.3173
2 12 80.0 165.0 15.0 0.3898
2 13 80.0 180.0 0.0 0.6182
1 1 87.5 0.0 180.0 0.3041
1 2 87.5 15.0 165.0 0.3080
1 3 87.5 30.0 150.0 0.3368
1 4 87.5 45.0 135.0 0.3317
1 5 87.5 60.0 120.0 0.3305
1 6 87.5 75.0 105.0 0.3390
1 7 87.5 90.0 90.0 0.3555
1 8 87.5 105.0 75.0 0.3634
1 9 87.5 120.0 60.0 0.3818
1 10 87.5 135.0 45.0 0.4180
1 11 87.5 150.0 30.0 0.4844
1 12 87.5 165.0 15.0 0.5387
1 13 87.5 180.0 0.0 0.6809
rho for WIND SPEED = 4.0 m/s THETA_SUN = 60.0
deg
10 1 0.0 0.0 0.0 0.0226
9 1 10.0 0.0 180.0 0.0220
9 2 10.0 15.0 165.0 0.0221

9	3	10.0	30.0	150.0	0.0222
9	4	10.0	45.0	135.0	0.0223
9	5	10.0	60.0	120.0	0.0223
9	6	10.0	75.0	105.0	0.0221
9	7	10.0	90.0	90.0	0.0224
9	8	10.0	105.0	75.0	0.0224
9	9	10.0	120.0	60.0	0.0232
9	10	10.0	135.0	45.0	0.0235
9	11	10.0	150.0	30.0	0.0237
9	12	10.0	165.0	15.0	0.0250
9	13	10.0	180.0	0.0	0.0236
8	1	20.0	0.0	180.0	0.0223
8	2	20.0	15.0	165.0	0.0222
8	3	20.0	30.0	150.0	0.0219
8	4	20.0	45.0	135.0	0.0220
8	5	20.0	60.0	120.0	0.0221
8	6	20.0	75.0	105.0	0.0224
8	7	20.0	90.0	90.0	0.0227
8	8	20.0	105.0	75.0	0.0230
8	9	20.0	120.0	60.0	0.0235
8	10	20.0	135.0	45.0	0.0241
8	11	20.0	150.0	30.0	0.0254
8	12	20.0	165.0	15.0	0.0290
8	13	20.0	180.0	0.0	0.0305
7	1	30.0	0.0	180.0	0.0232
7	2	30.0	15.0	165.0	0.0234
7	3	30.0	30.0	150.0	0.0233
7	4	30.0	45.0	135.0	0.0234
7	5	30.0	60.0	120.0	0.0232
7	6	30.0	75.0	105.0	0.0233
7	7	30.0	90.0	90.0	0.0233
7	8	30.0	105.0	75.0	0.0239
7	9	30.0	120.0	60.0	0.0248
7	10	30.0	135.0	45.0	0.0265
7	11	30.0	150.0	30.0	0.0311
7	12	30.0	165.0	15.0	0.0519
7	13	30.0	180.0	0.0	0.0691
6	1	40.0	0.0	180.0	0.0275
6	2	40.0	15.0	165.0	0.0279
6	3	40.0	30.0	150.0	0.0274
6	4	40.0	45.0	135.0	0.0277
6	5	40.0	60.0	120.0	0.0273
6	6	40.0	75.0	105.0	0.0272
6	7	40.0	90.0	90.0	0.0272
6	8	40.0	105.0	75.0	0.0275
6	9	40.0	120.0	60.0	0.0284
6	10	40.0	135.0	45.0	0.0302
6	11	40.0	150.0	30.0	0.0406
6	12	40.0	165.0	15.0	0.1001
6	13	40.0	180.0	0.0	0.1519
5	1	50.0	0.0	180.0	0.0407
5	2	50.0	15.0	165.0	0.0413
5	3	50.0	30.0	150.0	0.0409
5	4	50.0	45.0	135.0	0.0402
5	5	50.0	60.0	120.0	0.0399
5	6	50.0	75.0	105.0	0.0396
5	7	50.0	90.0	90.0	0.0397
5	8	50.0	105.0	75.0	0.0393
5	9	50.0	120.0	60.0	0.0400
5	10	50.0	135.0	45.0	0.0410
5	11	50.0	150.0	30.0	0.0509
5	12	50.0	165.0	15.0	0.1628
5	13	50.0	180.0	0.0	0.2501
4	1	60.0	0.0	180.0	0.0789
4	2	60.0	15.0	165.0	0.0792
4	3	60.0	30.0	150.0	0.0794
4	4	60.0	45.0	135.0	0.0782
4	5	60.0	60.0	120.0	0.0767
4	6	60.0	75.0	105.0	0.0755
4	7	60.0	90.0	90.0	0.0756
4	8	60.0	105.0	75.0	0.0739
4	9	60.0	120.0	60.0	0.0742
4	10	60.0	135.0	45.0	0.0745
4	11	60.0	150.0	30.0	0.0768
4	12	60.0	165.0	15.0	0.2094
4	13	60.0	180.0	0.0	0.0142
3	1	70.0	0.0	180.0	0.1652
3	2	70.0	15.0	165.0	0.1648
3	3	70.0	30.0	150.0	0.1633
3	4	70.0	45.0	135.0	0.1648
3	5	70.0	60.0	120.0	0.1632
3	6	70.0	75.0	105.0	0.1619
3	7	70.0	90.0	90.0	0.1628
3	8	70.0	105.0	75.0	0.1596
3	9	70.0	120.0	60.0	0.1589
3	10	70.0	135.0	45.0	0.1590
3	11	70.0	150.0	30.0	0.1544
3	12	70.0	165.0	15.0	0.3178
3	13	70.0	180.0	0.0	0.6639
2	1	80.0	0.0	180.0	0.2636
2	2	80.0	15.0	165.0	0.2654
2	3	80.0	30.0	150.0	0.2715
2	4	80.0	45.0	135.0	0.2693
2	5	80.0	60.0	120.0	0.2679
2	6	80.0	75.0	105.0	0.2801
2	7	80.0	90.0	90.0	0.2797
2	8	80.0	105.0	75.0	0.2848
2	9	80.0	120.0	60.0	0.2785
2	10	80.0	135.0	45.0	0.2912
2	11	80.0	150.0	30.0	0.3134

2	12	80.0	165.0	15.0	0.5150
2	13	80.0	180.0	0.0	1.2860
1	1	87.5	0.0	180.0	0.3106
1	2	87.5	15.0	165.0	0.3145
1	3	87.5	30.0	150.0	0.3430
1	4	87.5	45.0	135.0	0.3367
1	5	87.5	60.0	120.0	0.3334
1	6	87.5	75.0	105.0	0.3389
1	7	87.5	90.0	90.0	0.3521
1	8	87.5	105.0	75.0	0.3564
1	9	87.5	120.0	60.0	0.3723
1	10	87.5	135.0	45.0	0.4101
1	11	87.5	150.0	30.0	0.4916
1	12	87.5	165.0	15.0	0.7140
1	13	87.5	180.0	0.0	1.6658

rho for WIND SPEED = 4.0 m/s THETA_SUN = 70.0 deg

10	1	0.0	0.0	0.0	0.0220
9	1	10.0	0.0	180.0	0.0217
9	2	10.0	15.0	165.0	0.0218
9	3	10.0	30.0	150.0	0.0218
9	4	10.0	45.0	135.0	0.0219
9	5	10.0	60.0	120.0	0.0219
9	6	10.0	75.0	105.0	0.0217
9	7	10.0	90.0	90.0	0.0219
9	8	10.0	105.0	75.0	0.0218
9	9	10.0	120.0	60.0	0.0224
9	10	10.0	135.0	45.0	0.0225
9	11	10.0	150.0	30.0	0.0227
9	12	10.0	165.0	15.0	0.0229
9	13	10.0	180.0	0.0	0.0225
8	1	20.0	0.0	180.0	0.0221
8	2	20.0	15.0	165.0	0.0220
8	3	20.0	30.0	150.0	0.0216
8	4	20.0	45.0	135.0	0.0218
8	5	20.0	60.0	120.0	0.0219
8	6	20.0	75.0	105.0	0.0221
8	7	20.0	90.0	90.0	0.0223
8	8	20.0	105.0	75.0	0.0225
8	9	20.0	120.0	60.0	0.0227
8	10	20.0	135.0	45.0	0.0231
8	11	20.0	150.0	30.0	0.0237
8	12	20.0	165.0	15.0	0.0253
8	13	20.0	180.0	0.0	0.0253
7	1	30.0	0.0	180.0	0.0230
7	2	30.0	15.0	165.0	0.0232
7	3	30.0	30.0	150.0	0.0231
7	4	30.0	45.0	135.0	0.0232
7	5	30.0	60.0	120.0	0.0230
7	6	30.0	75.0	105.0	0.0232
7	7	30.0	90.0	90.0	0.0230
7	8	30.0	105.0	75.0	0.0235
7	9	30.0	120.0	60.0	0.0239
7	10	30.0	135.0	45.0	0.0252
7	11	30.0	150.0	30.0	0.0268
7	12	30.0	165.0	15.0	0.0323
7	13	30.0	180.0	0.0	0.0324
6	1	40.0	0.0	180.0	0.0272
6	2	40.0	15.0	165.0	0.0276
6	3	40.0	30.0	150.0	0.0271
6	4	40.0	45.0	135.0	0.0275
6	5	40.0	60.0	120.0	0.0271
6	6	40.0	75.0	105.0	0.0271
6	7	40.0	90.0	90.0	0.0271
6	8	40.0	105.0	75.0	0.0274
6	9	40.0	120.0	60.0	0.0281
6	10	40.0	135.0	45.0	0.0301
6	11	40.0	150.0	30.0	0.0331
6	12	40.0	165.0	15.0	0.0544
6	13	40.0	180.0	0.0	0.0796
5	1	50.0	0.0	180.0	0.0401
5	2	50.0	15.0	165.0	0.0406
5	3	50.0	30.0	150.0	0.0403
5	4	50.0	45.0	135.0	0.0398
5	5	50.0	60.0	120.0	0.0397
5	6	50.0	75.0	105.0	0.0395
5	7	50.0	90.0	90.0	0.0398
5	8	50.0	105.0	75.0	0.0395
5	9	50.0	120.0	60.0	0.0405
5	10	50.0	135.0	45.0	0.0425
5	11	50.0	150.0	30.0	0.0493
5	12	50.0	165.0	15.0	0.1115
5	13	50.0	180.0	0.0	0.2183
4	1	60.0	0.0	180.0	0.0773
4	2	60.0	15.0	165.0	0.0777
4	3	60.0	30.0	150.0	0.0779
4	4	60.0	45.0	135.0	0.0771
4	5	60.0	60.0	120.0	0.0760
4	6	60.0	75.0	105.0	0.0754
4	7	60.0	90.0	90.0	0.0758
4	8	60.0	105.0	75.0	0.0749
4	9	60.0	120.0	60.0	0.0755
4	10	60.0	135.0	45.0	0.0781
4	11	60.0	150.0	30.0	0.0819
4	12	60.0	165.0	15.0	0.1909
4	13	60.0	180.0	0.0	0.3839
3	1	70.0	0.0	180.0	0.1630
3	2	70.0	15.0	165.0	0.1625
3	3	70.0	30.0	150.0	0.1613
3	4	70.0	45.0	135.0	0.1629

3	5	70.0	60.0	120.0	0.1619
3	6	70.0	75.0	105.0	0.1612
3	7	70.0	90.0	90.0	0.1630
3	8	70.0	105.0	75.0	0.1602
3	9	70.0	120.0	60.0	0.1609
3	10	70.0	135.0	45.0	0.1626
3	11	70.0	150.0	30.0	0.1582
3	12	70.0	165.0	15.0	0.2925
3	13	70.0	180.0	0.0	0.0422
2	1	80.0	0.0	180.0	0.2652
2	2	80.0	15.0	165.0	0.2669
2	3	80.0	30.0	150.0	0.2727
2	4	80.0	45.0	135.0	0.2702
2	5	80.0	60.0	120.0	0.2682
2	6	80.0	75.0	105.0	0.2795
2	7	80.0	90.0	90.0	0.2783
2	8	80.0	105.0	75.0	0.2825
2	9	80.0	120.0	60.0	0.2752
2	10	80.0	135.0	45.0	0.2856
2	11	80.0	150.0	30.0	0.3001
2	12	80.0	165.0	15.0	0.4748
2	13	80.0	180.0	0.0	1.4078
1	1	87.5	0.0	180.0	0.3185
1	2	87.5	15.0	165.0	0.3225
1	3	87.5	30.0	150.0	0.3509
1	4	87.5	45.0	135.0	0.3434
1	5	87.5	60.0	120.0	0.3379
1	6	87.5	75.0	105.0	0.3403
1	7	87.5	90.0	90.0	0.3497
1	8	87.5	105.0	75.0	0.3500
1	9	87.5	120.0	60.0	0.3615
1	10	87.5	135.0	45.0	0.3929
1	11	87.5	150.0	30.0	0.4623
1	12	87.5	165.0	15.0	0.7383
1	13	87.5	180.0	0.0	2.9140

rho for WIND SPEED = 4.0 m/s THETA_SUN = 80.0 deg

10	1	0.0	0.0	0.0	0.0216
9	1	10.0	0.0	180.0	0.0213
9	2	10.0	15.0	165.0	0.0215
9	3	10.0	30.0	150.0	0.0215
9	4	10.0	45.0	135.0	0.0216
9	5	10.0	60.0	120.0	0.0216
9	6	10.0	75.0	105.0	0.0213
9	7	10.0	90.0	90.0	0.0216
9	8	10.0	105.0	75.0	0.0214
9	9	10.0	120.0	60.0	0.0218
9	10	10.0	135.0	45.0	0.0219
9	11	10.0	150.0	30.0	0.0220
9	12	10.0	165.0	15.0	0.0221
9	13	10.0	180.0	0.0	0.0218
8	1	20.0	0.0	180.0	0.0219
8	2	20.0	15.0	165.0	0.0217
8	3	20.0	30.0	150.0	0.0214
8	4	20.0	45.0	135.0	0.0215
8	5	20.0	60.0	120.0	0.0217
8	6	20.0	75.0	105.0	0.0219
8	7	20.0	90.0	90.0	0.0220
8	8	20.0	105.0	75.0	0.0220
8	9	20.0	120.0	60.0	0.0221
8	10	20.0	135.0	45.0	0.0223
8	11	20.0	150.0	30.0	0.0225
8	12	20.0	165.0	15.0	0.0232
8	13	20.0	180.0	0.0	0.0236
7	1	30.0	0.0	180.0	0.0228
7	2	30.0	15.0	165.0	0.0229
7	3	30.0	30.0	150.0	0.0228
7	4	30.0	45.0	135.0	0.0230
7	5	30.0	60.0	120.0	0.0228
7	6	30.0	75.0	105.0	0.0230
7	7	30.0	90.0	90.0	0.0228
7	8	30.0	105.0	75.0	0.0232
7	9	30.0	120.0	60.0	0.0234
7	10	30.0	135.0	45.0	0.0243
7	11	30.0	150.0	30.0	0.0254
7	12	30.0	165.0	15.0	0.0268
7	13	30.0	180.0	0.0	0.0272
6	1	40.0	0.0	180.0	0.0268
6	2	40.0	15.0	165.0	0.0273
6	3	40.0	30.0	150.0	0.0268
6	4	40.0	45.0	135.0	0.0272
6	5	40.0	60.0	120.0	0.0269
6	6	40.0	75.0	105.0	0.0269
6	7	40.0	90.0	90.0	0.0269
6	8	40.0	105.0	75.0	0.0272
6	9	40.0	120.0	60.0	0.0277
6	10	40.0	135.0	45.0	0.0295
6	11	40.0	150.0	30.0	0.0318
6	12	40.0	165.0	15.0	0.0389
6	13	40.0	180.0	0.0	0.0427
5	1	50.0	0.0	180.0	0.0394
5	2	50.0	15.0	165.0	0.0400
5	3	50.0	30.0	150.0	0.0397
5	4	50.0	45.0	135.0	0.0393
5	5	50.0	60.0	120.0	0.0393
5	6	50.0	75.0	105.0	0.0393
5	7	50.0	90.0	90.0	0.0398
5	8	50.0	105.0	75.0	0.0395
5	9	50.0	120.0	60.0	0.0405
5	10	50.0	135.0	45.0	0.0431

5 11 50.0 150.0 30.0 0.0505
5 12 50.0 165.0 15.0 0.0733
5 13 50.0 180.0 0.0 0.1253
4 1 60.0 0.0 180.0 0.0759
4 2 60.0 15.0 165.0 0.0762
4 3 60.0 30.0 150.0 0.0766
4 4 60.0 45.0 135.0 0.0759
4 5 60.0 60.0 120.0 0.0752
4 6 60.0 75.0 105.0 0.0750
4 7 60.0 90.0 90.0 0.0758
4 8 60.0 105.0 75.0 0.0752
4 9 60.0 120.0 60.0 0.0766
4 10 60.0 135.0 45.0 0.0816
4 11 60.0 150.0 30.0 0.0933
4 12 60.0 165.0 15.0 0.1522
4 13 60.0 180.0 0.0 0.3550
3 1 70.0 0.0 180.0 0.1613
3 2 70.0 15.0 165.0 0.1608
3 3 70.0 30.0 150.0 0.1596
3 4 70.0 45.0 135.0 0.1614
3 5 70.0 60.0 120.0 0.1606
3 6 70.0 75.0 105.0 0.1605
3 7 70.0 90.0 90.0 0.1627
3 8 70.0 105.0 75.0 0.1608
3 9 70.0 120.0 60.0 0.1622
3 10 70.0 135.0 45.0 0.1675
3 11 70.0 150.0 30.0 0.1728
3 12 70.0 165.0 15.0 0.2531
3 13 70.0 180.0 0.0 0.6043
2 1 80.0 0.0 180.0 0.2674
2 2 80.0 15.0 165.0 0.2689
2 3 80.0 30.0 150.0 0.2745
2 4 80.0 45.0 135.0 0.2714
2 5 80.0 60.0 120.0 0.2689
2 6 80.0 75.0 105.0 0.2793
2 7 80.0 90.0 90.0 0.2775
2 8 80.0 105.0 75.0 0.2808
2 9 80.0 120.0 60.0 0.2727
2 10 80.0 135.0 45.0 0.2798
2 11 80.0 150.0 30.0 0.2860
2 12 80.0 165.0 15.0 0.3451
2 13 80.0 180.0 0.0 0.1383
1 1 87.5 0.0 180.0 0.3265
1 2 87.5 15.0 165.0 0.3305
1 3 87.5 30.0 150.0 0.3585
1 4 87.5 45.0 135.0 0.3499
1 5 87.5 60.0 120.0 0.3422
1 6 87.5 75.0 105.0 0.3419
1 7 87.5 90.0 90.0 0.3483
1 8 87.5 105.0 75.0 0.3453
1 9 87.5 120.0 60.0 0.3514
1 10 87.5 135.0 45.0 0.3694
1 11 87.5 150.0 30.0 0.3998
1 12 87.5 165.0 15.0 0.4359
1 13 87.5 180.0 0.0 1.4882
rho for WIND SPEED = 6.0 m/s THETA_SUN = 0.0 deg
10 1 0.0 0.0 0.0 0.0012
9 1 10.0 0.0 180.0 0.1449
9 2 10.0 15.0 165.0 0.1372
9 3 10.0 30.0 150.0 0.1394
9 4 10.0 45.0 135.0 0.1456
9 5 10.0 60.0 120.0 0.1394
9 6 10.0 75.0 105.0 0.1355
9 7 10.0 90.0 90.0 0.1384
9 8 10.0 105.0 75.0 0.1355
9 9 10.0 120.0 60.0 0.1394
9 10 10.0 135.0 45.0 0.1456
9 11 10.0 150.0 30.0 0.1394
9 12 10.0 165.0 15.0 0.1372
9 13 10.0 180.0 0.0 0.1449
8 1 20.0 0.0 180.0 0.1508
8 2 20.0 15.0 165.0 0.1525
8 3 20.0 30.0 150.0 0.1562
8 4 20.0 45.0 135.0 0.1574
8 5 20.0 60.0 120.0 0.1536
8 6 20.0 75.0 105.0 0.1555
8 7 20.0 90.0 90.0 0.1484
8 8 20.0 105.0 75.0 0.1555
8 9 20.0 120.0 60.0 0.1536
8 10 20.0 135.0 45.0 0.1574
8 11 20.0 150.0 30.0 0.1562
8 12 20.0 165.0 15.0 0.1525
8 13 20.0 180.0 0.0 0.1508
7 1 30.0 0.0 180.0 0.1000
7 2 30.0 15.0 165.0 0.1027
7 3 30.0 30.0 150.0 0.1011
7 4 30.0 45.0 135.0 0.0989
7 5 30.0 60.0 120.0 0.1015
7 6 30.0 75.0 105.0 0.1003
7 7 30.0 90.0 90.0 0.0964
7 8 30.0 105.0 75.0 0.1003
7 9 30.0 120.0 60.0 0.1015
7 10 30.0 135.0 45.0 0.0989
7 11 30.0 150.0 30.0 0.1011
7 12 30.0 165.0 15.0 0.1027
7 13 30.0 180.0 0.0 0.1000
6 1 40.0 0.0 180.0 0.0485
6 2 40.0 15.0 165.0 0.0532
6 3 40.0 30.0 150.0 0.0486

6	4	40.0	45.0	135.0	0.0511
6	5	40.0	60.0	120.0	0.0526
6	6	40.0	75.0	105.0	0.0513
6	7	40.0	90.0	90.0	0.0489
6	8	40.0	105.0	75.0	0.0513
6	9	40.0	120.0	60.0	0.0526
6	10	40.0	135.0	45.0	0.0511
6	11	40.0	150.0	30.0	0.0486
6	12	40.0	165.0	15.0	0.0532
6	13	40.0	180.0	0.0	0.0485
5	1	50.0	0.0	180.0	0.0446
5	2	50.0	15.0	165.0	0.0452
5	3	50.0	30.0	150.0	0.0439
5	4	50.0	45.0	135.0	0.0436
5	5	50.0	60.0	120.0	0.0445
5	6	50.0	75.0	105.0	0.0451
5	7	50.0	90.0	90.0	0.0452
5	8	50.0	105.0	75.0	0.0451
5	9	50.0	120.0	60.0	0.0445
5	10	50.0	135.0	45.0	0.0436
5	11	50.0	150.0	30.0	0.0439
5	12	50.0	165.0	15.0	0.0452
5	13	50.0	180.0	0.0	0.0446
4	1	60.0	0.0	180.0	0.0759
4	2	60.0	15.0	165.0	0.0767
4	3	60.0	30.0	150.0	0.0774
4	4	60.0	45.0	135.0	0.0768
4	5	60.0	60.0	120.0	0.0762
4	6	60.0	75.0	105.0	0.0768
4	7	60.0	90.0	90.0	0.0768
4	8	60.0	105.0	75.0	0.0768
4	9	60.0	120.0	60.0	0.0762
4	10	60.0	135.0	45.0	0.0768
4	11	60.0	150.0	30.0	0.0774
4	12	60.0	165.0	15.0	0.0767
4	13	60.0	180.0	0.0	0.0759
3	1	70.0	0.0	180.0	0.1552
3	2	70.0	15.0	165.0	0.1550
3	3	70.0	30.0	150.0	0.1546
3	4	70.0	45.0	135.0	0.1558
3	5	70.0	60.0	120.0	0.1541
3	6	70.0	75.0	105.0	0.1557
3	7	70.0	90.0	90.0	0.1582
3	8	70.0	105.0	75.0	0.1557
3	9	70.0	120.0	60.0	0.1541
3	10	70.0	135.0	45.0	0.1558
3	11	70.0	150.0	30.0	0.1546
3	12	70.0	165.0	15.0	0.1550
3	13	70.0	180.0	0.0	0.1552
2	1	80.0	0.0	180.0	0.2425
2	2	80.0	15.0	165.0	0.2483
2	3	80.0	30.0	150.0	0.2543
2	4	80.0	45.0	135.0	0.2487
2	5	80.0	60.0	120.0	0.2441
2	6	80.0	75.0	105.0	0.2554
2	7	80.0	90.0	90.0	0.2535
2	8	80.0	105.0	75.0	0.2554
2	9	80.0	120.0	60.0	0.2441
2	10	80.0	135.0	45.0	0.2487
2	11	80.0	150.0	30.0	0.2543
2	12	80.0	165.0	15.0	0.2483
2	13	80.0	180.0	0.0	0.2425
1	1	87.5	0.0	180.0	0.2953
1	2	87.5	15.0	165.0	0.2931
1	3	87.5	30.0	150.0	0.3229
1	4	87.5	45.0	135.0	0.3183
1	5	87.5	60.0	120.0	0.3009
1	6	87.5	75.0	105.0	0.3067
1	7	87.5	90.0	90.0	0.3136
1	8	87.5	105.0	75.0	0.3067
1	9	87.5	120.0	60.0	0.3009
1	10	87.5	135.0	45.0	0.3183
1	11	87.5	150.0	30.0	0.3229
1	12	87.5	165.0	15.0	0.2931
1	13	87.5	180.0	0.0	0.2953

rho for WIND SPEED = 6.0 m/s THETA_SUN = 10.0 deg

10	1	0.0	0.0	0.0	0.1259
9	1	10.0	0.0	180.0	0.1330
9	2	10.0	15.0	165.0	0.1407
9	3	10.0	30.0	150.0	0.1435
9	4	10.0	45.0	135.0	0.1508
9	5	10.0	60.0	120.0	0.1504
9	6	10.0	75.0	105.0	0.1552
9	7	10.0	90.0	90.0	0.1537
9	8	10.0	105.0	75.0	0.1501
9	9	10.0	120.0	60.0	0.1286
9	10	10.0	135.0	45.0	0.1173
9	11	10.0	150.0	30.0	0.1060
9	12	10.0	165.0	15.0	0.0895
9	13	10.0	180.0	0.0	0.0004
8	1	20.0	0.0	180.0	0.0939
8	2	20.0	15.0	165.0	0.0837
8	3	20.0	30.0	150.0	0.0948
8	4	20.0	45.0	135.0	0.0984
8	5	20.0	60.0	120.0	0.1055
8	6	20.0	75.0	105.0	0.1288
8	7	20.0	90.0	90.0	0.1410
8	8	20.0	105.0	75.0	0.1409
8	9	20.0	120.0	60.0	0.1493

8 10 20.0 135.0 45.0 0.1567
8 11 20.0 150.0 30.0 0.1545
8 12 20.0 165.0 15.0 0.1535
8 13 20.0 180.0 0.0 0.1418
7 1 30.0 0.0 180.0 0.0440
7 2 30.0 15.0 165.0 0.0466
7 3 30.0 30.0 150.0 0.0464
7 4 30.0 45.0 135.0 0.0482
7 5 30.0 60.0 120.0 0.0555
7 6 30.0 75.0 105.0 0.0711
7 7 30.0 90.0 90.0 0.0809
7 8 30.0 105.0 75.0 0.1079
7 9 30.0 120.0 60.0 0.1170
7 10 30.0 135.0 45.0 0.1426
7 11 30.0 150.0 30.0 0.1563
7 12 30.0 165.0 15.0 0.1736
7 13 30.0 180.0 0.0 0.1794
6 1 40.0 0.0 180.0 0.0294
6 2 40.0 15.0 165.0 0.0321
6 3 40.0 30.0 150.0 0.0322
6 4 40.0 45.0 135.0 0.0337
6 5 40.0 60.0 120.0 0.0341
6 6 40.0 75.0 105.0 0.0370
6 7 40.0 90.0 90.0 0.0441
6 8 40.0 105.0 75.0 0.0477
6 9 40.0 120.0 60.0 0.0624
6 10 40.0 135.0 45.0 0.0811
6 11 40.0 150.0 30.0 0.1008
6 12 40.0 165.0 15.0 0.1167
6 13 40.0 180.0 0.0 0.1290
5 1 50.0 0.0 180.0 0.0431
5 2 50.0 15.0 165.0 0.0424
5 3 50.0 30.0 150.0 0.0426
5 4 50.0 45.0 135.0 0.0414
5 5 50.0 60.0 120.0 0.0416
5 6 50.0 75.0 105.0 0.0428
5 7 50.0 90.0 90.0 0.0440
5 8 50.0 105.0 75.0 0.0452
5 9 50.0 120.0 60.0 0.0487
5 10 50.0 135.0 45.0 0.0556
5 11 50.0 150.0 30.0 0.0586
5 12 50.0 165.0 15.0 0.0673
5 13 50.0 180.0 0.0 0.0706
4 1 60.0 0.0 180.0 0.0781
4 2 60.0 15.0 165.0 0.0789
4 3 60.0 30.0 150.0 0.0790
4 4 60.0 45.0 135.0 0.0783
4 5 60.0 60.0 120.0 0.0772
4 6 60.0 75.0 105.0 0.0773
4 7 60.0 90.0 90.0 0.0769
4 8 60.0 105.0 75.0 0.0766
4 9 60.0 120.0 60.0 0.0758
4 10 60.0 135.0 45.0 0.0785
4 11 60.0 150.0 30.0 0.0774
4 12 60.0 165.0 15.0 0.0791
4 13 60.0 180.0 0.0 0.0795
3 1 70.0 0.0 180.0 0.1585
3 2 70.0 15.0 165.0 0.1583
3 3 70.0 30.0 150.0 0.1574
3 4 70.0 45.0 135.0 0.1581
3 5 70.0 60.0 120.0 0.1555
3 6 70.0 75.0 105.0 0.1564
3 7 70.0 90.0 90.0 0.1582
3 8 70.0 105.0 75.0 0.1552
3 9 70.0 120.0 60.0 0.1534
3 10 70.0 135.0 45.0 0.1548
3 11 70.0 150.0 30.0 0.1539
3 12 70.0 165.0 15.0 0.1538
3 13 70.0 180.0 0.0 0.1542
2 1 80.0 0.0 180.0 0.2352
2 2 80.0 15.0 165.0 0.2414
2 3 80.0 30.0 150.0 0.2480
2 4 80.0 45.0 135.0 0.2435
2 5 80.0 60.0 120.0 0.2402
2 6 80.0 75.0 105.0 0.2530
2 7 80.0 90.0 90.0 0.2529
2 8 80.0 105.0 75.0 0.2566
2 9 80.0 120.0 60.0 0.2469
2 10 80.0 135.0 45.0 0.2528
2 11 80.0 150.0 30.0 0.2598
2 12 80.0 165.0 15.0 0.2546
2 13 80.0 180.0 0.0 0.2492
1 1 87.5 0.0 180.0 0.2714
1 2 87.5 15.0 165.0 0.2703
1 3 87.5 30.0 150.0 0.3009
1 4 87.5 45.0 135.0 0.3000
1 5 87.5 60.0 120.0 0.2882
1 6 87.5 75.0 105.0 0.2996
1 7 87.5 90.0 90.0 0.3125
1 8 87.5 105.0 75.0 0.3117
1 9 87.5 120.0 60.0 0.3115
1 10 87.5 135.0 45.0 0.3348
1 11 87.5 150.0 30.0 0.3432
1 12 87.5 165.0 15.0 0.3147
1 13 87.5 180.0 0.0 0.3178
rho for WIND SPEED = 6.0 m/s THETA_SUN = 20.0
deg
10 1 0.0 0.0 0.0 0.1388
9 1 10.0 0.0 180.0 0.1136
9 2 10.0 15.0 165.0 0.0767

9	3	10.0	30.0	150.0	0.0901
9	4	10.0	45.0	135.0	0.0959
9	5	10.0	60.0	120.0	0.0989
9	6	10.0	75.0	105.0	0.1188
9	7	10.0	90.0	90.0	0.1272
9	8	10.0	105.0	75.0	0.1415
9	9	10.0	120.0	60.0	0.1556
9	10	10.0	135.0	45.0	0.1381
9	11	10.0	150.0	30.0	0.1331
9	12	10.0	165.0	15.0	0.1304
9	13	10.0	180.0	0.0	0.1155
8	1	20.0	0.0	180.0	0.0458
8	2	20.0	15.0	165.0	0.0463
8	3	20.0	30.0	150.0	0.0468
8	4	20.0	45.0	135.0	0.0541
8	5	20.0	60.0	120.0	0.0592
8	6	20.0	75.0	105.0	0.0767
8	7	20.0	90.0	90.0	0.0923
8	8	20.0	105.0	75.0	0.1175
8	9	20.0	120.0	60.0	0.1377
8	10	20.0	135.0	45.0	0.1462
8	11	20.0	150.0	30.0	0.1305
8	12	20.0	165.0	15.0	0.1051
8	13	20.0	180.0	0.0	0.0009
7	1	30.0	0.0	180.0	0.0277
7	2	30.0	15.0	165.0	0.0271
7	3	30.0	30.0	150.0	0.0271
7	4	30.0	45.0	135.0	0.0293
7	5	30.0	60.0	120.0	0.0321
7	6	30.0	75.0	105.0	0.0400
7	7	30.0	90.0	90.0	0.0565
7	8	30.0	105.0	75.0	0.0785
7	9	30.0	120.0	60.0	0.1098
7	10	30.0	135.0	45.0	0.1373
7	11	30.0	150.0	30.0	0.1513
7	12	30.0	165.0	15.0	0.1495
7	13	30.0	180.0	0.0	0.1457
6	1	40.0	0.0	180.0	0.0287
6	2	40.0	15.0	165.0	0.0298
6	3	40.0	30.0	150.0	0.0294
6	4	40.0	45.0	135.0	0.0297
6	5	40.0	60.0	120.0	0.0294
6	6	40.0	75.0	105.0	0.0316
6	7	40.0	90.0	90.0	0.0339
6	8	40.0	105.0	75.0	0.0439
6	9	40.0	120.0	60.0	0.0614
6	10	40.0	135.0	45.0	0.1002
6	11	40.0	150.0	30.0	0.1293
6	12	40.0	165.0	15.0	0.1773
6	13	40.0	180.0	0.0	0.1899
5	1	50.0	0.0	180.0	0.0432
5	2	50.0	15.0	165.0	0.0434
5	3	50.0	30.0	150.0	0.0429
5	4	50.0	45.0	135.0	0.0419
5	5	50.0	60.0	120.0	0.0417
5	6	50.0	75.0	105.0	0.0419
5	7	50.0	90.0	90.0	0.0427
5	8	50.0	105.0	75.0	0.0446
5	9	50.0	120.0	60.0	0.0472
5	10	50.0	135.0	45.0	0.0643
5	11	50.0	150.0	30.0	0.0937
5	12	50.0	165.0	15.0	0.1290
5	13	50.0	180.0	0.0	0.1431
4	1	60.0	0.0	180.0	0.0819
4	2	60.0	15.0	165.0	0.0826
4	3	60.0	30.0	150.0	0.0822
4	4	60.0	45.0	135.0	0.0808
4	5	60.0	60.0	120.0	0.0789
4	6	60.0	75.0	105.0	0.0782
4	7	60.0	90.0	90.0	0.0772
4	8	60.0	105.0	75.0	0.0766
4	9	60.0	120.0	60.0	0.0761
4	10	60.0	135.0	45.0	0.0809
4	11	60.0	150.0	30.0	0.0877
4	12	60.0	165.0	15.0	0.1035
4	13	60.0	180.0	0.0	0.1125
3	1	70.0	0.0	180.0	0.1620
3	2	70.0	15.0	165.0	0.1619
3	3	70.0	30.0	150.0	0.1606
3	4	70.0	45.0	135.0	0.1606
3	5	70.0	60.0	120.0	0.1572
3	6	70.0	75.0	105.0	0.1572
3	7	70.0	90.0	90.0	0.1584
3	8	70.0	105.0	75.0	0.1549
3	9	70.0	120.0	60.0	0.1531
3	10	70.0	135.0	45.0	0.1549
3	11	70.0	150.0	30.0	0.1562
3	12	70.0	165.0	15.0	0.1575
3	13	70.0	180.0	0.0	0.1611
2	1	80.0	0.0	180.0	0.2278
2	2	80.0	15.0	165.0	0.2344
2	3	80.0	30.0	150.0	0.2415
2	4	80.0	45.0	135.0	0.2380
2	5	80.0	60.0	120.0	0.2358
2	6	80.0	75.0	105.0	0.2499
2	7	80.0	90.0	90.0	0.2513
2	8	80.0	105.0	75.0	0.2564
2	9	80.0	120.0	60.0	0.2482
2	10	80.0	135.0	45.0	0.2562
2	11	80.0	150.0	30.0	0.2657

2 12 80.0 165.0 15.0 0.2625
2 13 80.0 180.0 0.0 0.2582
1 1 87.5 0.0 180.0 0.2523
1 2 87.5 15.0 165.0 0.2518
1 3 87.5 30.0 150.0 0.2825
1 4 87.5 45.0 135.0 0.2838
1 5 87.5 60.0 120.0 0.2761
1 6 87.5 75.0 105.0 0.2918
1 7 87.5 90.0 90.0 0.3094
1 8 87.5 105.0 75.0 0.3135
1 9 87.5 120.0 60.0 0.3181
1 10 87.5 135.0 45.0 0.3467
1 11 87.5 150.0 30.0 0.3600
1 12 87.5 165.0 15.0 0.3345
1 13 87.5 180.0 0.0 0.3392
rho for WIND SPEED = 6.0 m/s THETA_SUN = 30.0 deg
10 1 0.0 0.0 0.0 0.0891
9 1 10.0 0.0 180.0 0.0478
9 2 10.0 15.0 165.0 0.0457
9 3 10.0 30.0 150.0 0.0468
9 4 10.0 45.0 135.0 0.0420
9 5 10.0 60.0 120.0 0.0607
9 6 10.0 75.0 105.0 0.0535
9 7 10.0 90.0 90.0 0.0669
9 8 10.0 105.0 75.0 0.0884
9 9 10.0 120.0 60.0 0.0955
9 10 10.0 135.0 45.0 0.1053
9 11 10.0 150.0 30.0 0.1348
9 12 10.0 165.0 15.0 0.1351
9 13 10.0 180.0 0.0 0.1386
8 1 20.0 0.0 180.0 0.0250
8 2 20.0 15.0 165.0 0.0261
8 3 20.0 30.0 150.0 0.0285
8 4 20.0 45.0 135.0 0.0306
8 5 20.0 60.0 120.0 0.0315
8 6 20.0 75.0 105.0 0.0375
8 7 20.0 90.0 90.0 0.0427
8 8 20.0 105.0 75.0 0.0709
8 9 20.0 120.0 60.0 0.0986
8 10 20.0 135.0 45.0 0.1270
8 11 20.0 150.0 30.0 0.1412
8 12 20.0 165.0 15.0 0.1329
8 13 20.0 180.0 0.0 0.1168
7 1 30.0 0.0 180.0 0.0259
7 2 30.0 15.0 165.0 0.0246
7 3 30.0 30.0 150.0 0.0247
7 4 30.0 45.0 135.0 0.0249
7 5 30.0 60.0 120.0 0.0269
7 6 30.0 75.0 105.0 0.0286
7 7 30.0 90.0 90.0 0.0312
7 8 30.0 105.0 75.0 0.0480
7 9 30.0 120.0 60.0 0.0715
7 10 30.0 135.0 45.0 0.1118
7 11 30.0 150.0 30.0 0.1394
7 12 30.0 165.0 15.0 0.1172
7 13 30.0 180.0 0.0 0.0015
6 1 40.0 0.0 180.0 0.0288
6 2 40.0 15.0 165.0 0.0293
6 3 40.0 30.0 150.0 0.0289
6 4 40.0 45.0 135.0 0.0290
6 5 40.0 60.0 120.0 0.0285
6 6 40.0 75.0 105.0 0.0290
6 7 40.0 90.0 90.0 0.0293
6 8 40.0 105.0 75.0 0.0350
6 9 40.0 120.0 60.0 0.0507
6 10 40.0 135.0 45.0 0.0891
6 11 40.0 150.0 30.0 0.1333
6 12 40.0 165.0 15.0 0.1620
6 13 40.0 180.0 0.0 0.1578
5 1 50.0 0.0 180.0 0.0449
5 2 50.0 15.0 165.0 0.0450
5 3 50.0 30.0 150.0 0.0443
5 4 50.0 45.0 135.0 0.0429
5 5 50.0 60.0 120.0 0.0424
5 6 50.0 75.0 105.0 0.0421
5 7 50.0 90.0 90.0 0.0423
5 8 50.0 105.0 75.0 0.0427
5 9 50.0 120.0 60.0 0.0448
5 10 50.0 135.0 45.0 0.0586
5 11 50.0 150.0 30.0 0.1208
5 12 50.0 165.0 15.0 0.1901
5 13 50.0 180.0 0.0 0.2232
4 1 60.0 0.0 180.0 0.0854
4 2 60.0 15.0 165.0 0.0861
4 3 60.0 30.0 150.0 0.0855
4 4 60.0 45.0 135.0 0.0834
4 5 60.0 60.0 120.0 0.0809
4 6 60.0 75.0 105.0 0.0795
4 7 60.0 90.0 90.0 0.0779
4 8 60.0 105.0 75.0 0.0770
4 9 60.0 120.0 60.0 0.0758
4 10 60.0 135.0 45.0 0.0826
4 11 60.0 150.0 30.0 0.1026
4 12 60.0 165.0 15.0 0.1644
4 13 60.0 180.0 0.0 0.2089
3 1 70.0 0.0 180.0 0.1639
3 2 70.0 15.0 165.0 0.1639
3 3 70.0 30.0 150.0 0.1626
3 4 70.0 45.0 135.0 0.1624

3	5	70.0	60.0	120.0	0.1585
3	6	70.0	75.0	105.0	0.1580
3	7	70.0	90.0	90.0	0.1586
3	8	70.0	105.0	75.0	0.1549
3	9	70.0	120.0	60.0	0.1531
3	10	70.0	135.0	45.0	0.1560
3	11	70.0	150.0	30.0	0.1631
3	12	70.0	165.0	15.0	0.1879
3	13	70.0	180.0	0.0	0.2110
2	1	80.0	0.0	180.0	0.2221
2	2	80.0	15.0	165.0	0.2289
2	3	80.0	30.0	150.0	0.2362
2	4	80.0	45.0	135.0	0.2333
2	5	80.0	60.0	120.0	0.2318
2	6	80.0	75.0	105.0	0.2466
2	7	80.0	90.0	90.0	0.2489
2	8	80.0	105.0	75.0	0.2548
2	9	80.0	120.0	60.0	0.2480
2	10	80.0	135.0	45.0	0.2588
2	11	80.0	150.0	30.0	0.2737
2	12	80.0	165.0	15.0	0.2822
2	13	80.0	180.0	0.0	0.2811
1	1	87.5	0.0	180.0	0.2417
1	2	87.5	15.0	165.0	0.2413
1	3	87.5	30.0	150.0	0.2715
1	4	87.5	45.0	135.0	0.2731
1	5	87.5	60.0	120.0	0.2671
1	6	87.5	75.0	105.0	0.2849
1	7	87.5	90.0	90.0	0.3050
1	8	87.5	105.0	75.0	0.3118
1	9	87.5	120.0	60.0	0.3197
1	10	87.5	135.0	45.0	0.3542
1	11	87.5	150.0	30.0	0.3767
1	12	87.5	165.0	15.0	0.3609
1	13	87.5	180.0	0.0	0.3705

rho for WIND SPEED = 6.0 m/s THETA_SUN = 40.0 deg

10	1	0.0	0.0	0.0	0.0438
9	1	10.0	0.0	180.0	0.0249
9	2	10.0	15.0	165.0	0.0244
9	3	10.0	30.0	150.0	0.0250
9	4	10.0	45.0	135.0	0.0288
9	5	10.0	60.0	120.0	0.0280
9	6	10.0	75.0	105.0	0.0284
9	7	10.0	90.0	90.0	0.0373
9	8	10.0	105.0	75.0	0.0440
9	9	10.0	120.0	60.0	0.0486
9	10	10.0	135.0	45.0	0.0638
9	11	10.0	150.0	30.0	0.0765
9	12	10.0	165.0	15.0	0.0806
9	13	10.0	180.0	0.0	0.0878
8	1	20.0	0.0	180.0	0.0255
8	2	20.0	15.0	165.0	0.0236
8	3	20.0	30.0	150.0	0.0233
8	4	20.0	45.0	135.0	0.0236
8	5	20.0	60.0	120.0	0.0259
8	6	20.0	75.0	105.0	0.0267
8	7	20.0	90.0	90.0	0.0297
8	8	20.0	105.0	75.0	0.0379
8	9	20.0	120.0	60.0	0.0501
8	10	20.0	135.0	45.0	0.0738
8	11	20.0	150.0	30.0	0.1093
8	12	20.0	165.0	15.0	0.1278
8	13	20.0	180.0	0.0	0.1438
7	1	30.0	0.0	180.0	0.0243
7	2	30.0	15.0	165.0	0.0243
7	3	30.0	30.0	150.0	0.0242
7	4	30.0	45.0	135.0	0.0243
7	5	30.0	60.0	120.0	0.0246
7	6	30.0	75.0	105.0	0.0246
7	7	30.0	90.0	90.0	0.0265
7	8	30.0	105.0	75.0	0.0288
7	9	30.0	120.0	60.0	0.0415
7	10	30.0	135.0	45.0	0.0748
7	11	30.0	150.0	30.0	0.1175
7	12	30.0	165.0	15.0	0.1374
7	13	30.0	180.0	0.0	0.1257
6	1	40.0	0.0	180.0	0.0291
6	2	40.0	15.0	165.0	0.0297
6	3	40.0	30.0	150.0	0.0292
6	4	40.0	45.0	135.0	0.0291
6	5	40.0	60.0	120.0	0.0285
6	6	40.0	75.0	105.0	0.0287
6	7	40.0	90.0	90.0	0.0288
6	8	40.0	105.0	75.0	0.0298
6	9	40.0	120.0	60.0	0.0362
6	10	40.0	135.0	45.0	0.0652
6	11	40.0	150.0	30.0	0.1151
6	12	40.0	165.0	15.0	0.1312
6	13	40.0	180.0	0.0	0.0025
5	1	50.0	0.0	180.0	0.0463
5	2	50.0	15.0	165.0	0.0463
5	3	50.0	30.0	150.0	0.0455
5	4	50.0	45.0	135.0	0.0440
5	5	50.0	60.0	120.0	0.0432
5	6	50.0	75.0	105.0	0.0426
5	7	50.0	90.0	90.0	0.0426
5	8	50.0	105.0	75.0	0.0423
5	9	50.0	120.0	60.0	0.0428
5	10	50.0	135.0	45.0	0.0538

5 11 50.0 150.0 30.0 0.1129
5 12 50.0 165.0 15.0 0.1872
5 13 50.0 180.0 0.0 0.1916
4 1 60.0 0.0 180.0 0.0871
4 2 60.0 15.0 165.0 0.0879
4 3 60.0 30.0 150.0 0.0874
4 4 60.0 45.0 135.0 0.0852
4 5 60.0 60.0 120.0 0.0825
4 6 60.0 75.0 105.0 0.0808
4 7 60.0 90.0 90.0 0.0789
4 8 60.0 105.0 75.0 0.0777
4 9 60.0 120.0 60.0 0.0761
4 10 60.0 135.0 45.0 0.0782
4 11 60.0 150.0 30.0 0.1153
4 12 60.0 165.0 15.0 0.2302
4 13 60.0 180.0 0.0 0.3317
3 1 70.0 0.0 180.0 0.1636
3 2 70.0 15.0 165.0 0.1638
3 3 70.0 30.0 150.0 0.1627
3 4 70.0 45.0 135.0 0.1628
3 5 70.0 60.0 120.0 0.1590
3 6 70.0 75.0 105.0 0.1586
3 7 70.0 90.0 90.0 0.1590
3 8 70.0 105.0 75.0 0.1551
3 9 70.0 120.0 60.0 0.1532
3 10 70.0 135.0 45.0 0.1557
3 11 70.0 150.0 30.0 0.1693
3 12 70.0 165.0 15.0 0.2718
3 13 70.0 180.0 0.0 0.3683
2 1 80.0 0.0 180.0 0.2191
2 2 80.0 15.0 165.0 0.2258
2 3 80.0 30.0 150.0 0.2331
2 4 80.0 45.0 135.0 0.2301
2 5 80.0 60.0 120.0 0.2287
2 6 80.0 75.0 105.0 0.2437
2 7 80.0 90.0 90.0 0.2462
2 8 80.0 105.0 75.0 0.2521
2 9 80.0 120.0 60.0 0.2462
2 10 80.0 135.0 45.0 0.2602
2 11 80.0 150.0 30.0 0.2832
2 12 80.0 165.0 15.0 0.3403
2 13 80.0 180.0 0.0 0.4239
1 1 87.5 0.0 180.0 0.2389
1 2 87.5 15.0 165.0 0.2383
1 3 87.5 30.0 150.0 0.2680
1 4 87.5 45.0 135.0 0.2687
1 5 87.5 60.0 120.0 0.2623
1 6 87.5 75.0 105.0 0.2799
1 7 87.5 90.0 90.0 0.3001
1 8 87.5 105.0 75.0 0.3072
1 9 87.5 120.0 60.0 0.3167
1 10 87.5 135.0 45.0 0.3579
1 11 87.5 150.0 30.0 0.3977
1 12 87.5 165.0 15.0 0.4063
1 13 87.5 180.0 0.0 0.4609
rho for WIND SPEED = 6.0 m/s THETA_SUN = 50.0 deg
10 1 0.0 0.0 0.0 0.0246
9 1 10.0 0.0 180.0 0.0235
9 2 10.0 15.0 165.0 0.0232
9 3 10.0 30.0 150.0 0.0250
9 4 10.0 45.0 135.0 0.0239
9 5 10.0 60.0 120.0 0.0245
9 6 10.0 75.0 105.0 0.0239
9 7 10.0 90.0 90.0 0.0246
9 8 10.0 105.0 75.0 0.0268
9 9 10.0 120.0 60.0 0.0288
9 10 10.0 135.0 45.0 0.0370
9 11 10.0 150.0 30.0 0.0350
9 12 10.0 165.0 15.0 0.0421
9 13 10.0 180.0 0.0 0.0531
8 1 20.0 0.0 180.0 0.0234
8 2 20.0 15.0 165.0 0.0230
8 3 20.0 30.0 150.0 0.0227
8 4 20.0 45.0 135.0 0.0229
8 5 20.0 60.0 120.0 0.0231
8 6 20.0 75.0 105.0 0.0238
8 7 20.0 90.0 90.0 0.0238
8 8 20.0 105.0 75.0 0.0267
8 9 20.0 120.0 60.0 0.0280
8 10 20.0 135.0 45.0 0.0357
8 11 20.0 150.0 30.0 0.0631
8 12 20.0 165.0 15.0 0.0744
8 13 20.0 180.0 0.0 0.1001
7 1 30.0 0.0 180.0 0.0242
7 2 30.0 15.0 165.0 0.0242
7 3 30.0 30.0 150.0 0.0241
7 4 30.0 45.0 135.0 0.0241
7 5 30.0 60.0 120.0 0.0242
7 6 30.0 75.0 105.0 0.0241
7 7 30.0 90.0 90.0 0.0245
7 8 30.0 105.0 75.0 0.0260
7 9 30.0 120.0 60.0 0.0293
7 10 30.0 135.0 45.0 0.0427
7 11 30.0 150.0 30.0 0.0741
7 12 30.0 165.0 15.0 0.1252
7 13 30.0 180.0 0.0 0.1422
6 1 40.0 0.0 180.0 0.0293
6 2 40.0 15.0 165.0 0.0299
6 3 40.0 30.0 150.0 0.0294

6 4 40.0 45.0 135.0 0.0293
6 5 40.0 60.0 120.0 0.0286
6 6 40.0 75.0 105.0 0.0287
6 7 40.0 90.0 90.0 0.0285
6 8 40.0 105.0 75.0 0.0293
6 9 40.0 120.0 60.0 0.0307
6 10 40.0 135.0 45.0 0.0395
6 11 40.0 150.0 30.0 0.0903
6 12 40.0 165.0 15.0 0.1477
6 13 40.0 180.0 0.0 0.1448
5 1 50.0 0.0 180.0 0.0466
5 2 50.0 15.0 165.0 0.0466
5 3 50.0 30.0 150.0 0.0460
5 4 50.0 45.0 135.0 0.0445
5 5 50.0 60.0 120.0 0.0439
5 6 50.0 75.0 105.0 0.0430
5 7 50.0 90.0 90.0 0.0431
5 8 50.0 105.0 75.0 0.0422
5 9 50.0 120.0 60.0 0.0427
5 10 50.0 135.0 45.0 0.0482
5 11 50.0 150.0 30.0 0.0854
5 12 50.0 165.0 15.0 0.1600
5 13 50.0 180.0 0.0 0.0045
4 1 60.0 0.0 180.0 0.0867
4 2 60.0 15.0 165.0 0.0876
4 3 60.0 30.0 150.0 0.0874
4 4 60.0 45.0 135.0 0.0856
4 5 60.0 60.0 120.0 0.0832
4 6 60.0 75.0 105.0 0.0818
4 7 60.0 90.0 90.0 0.0799
4 8 60.0 105.0 75.0 0.0787
4 9 60.0 120.0 60.0 0.0772
4 10 60.0 135.0 45.0 0.0765
4 11 60.0 150.0 30.0 0.0997
4 12 60.0 165.0 15.0 0.2277
4 13 60.0 180.0 0.0 0.3056
3 1 70.0 0.0 180.0 0.1619
3 2 70.0 15.0 165.0 0.1622
3 3 70.0 30.0 150.0 0.1613
3 4 70.0 45.0 135.0 0.1619
3 5 70.0 60.0 120.0 0.1586
3 6 70.0 75.0 105.0 0.1586
3 7 70.0 90.0 90.0 0.1593
3 8 70.0 105.0 75.0 0.1556
3 9 70.0 120.0 60.0 0.1535
3 10 70.0 135.0 45.0 0.1555
3 11 70.0 150.0 30.0 0.1629
3 12 70.0 165.0 15.0 0.3508
3 13 70.0 180.0 0.0 0.6211
2 1 80.0 0.0 180.0 0.2183
2 2 80.0 15.0 165.0 0.2250
2 3 80.0 30.0 150.0 0.2320
2 4 80.0 45.0 135.0 0.2288
2 5 80.0 60.0 120.0 0.2270
2 6 80.0 75.0 105.0 0.2415
2 7 80.0 90.0 90.0 0.2436
2 8 80.0 105.0 75.0 0.2490
2 9 80.0 120.0 60.0 0.2432
2 10 80.0 135.0 45.0 0.2590
2 11 80.0 150.0 30.0 0.2920
2 12 80.0 165.0 15.0 0.4734
2 13 80.0 180.0 0.0 0.8324
1 1 87.5 0.0 180.0 0.2416
1 2 87.5 15.0 165.0 0.2406
1 3 87.5 30.0 150.0 0.2701
1 4 87.5 45.0 135.0 0.2695
1 5 87.5 60.0 120.0 0.2615
1 6 87.5 75.0 105.0 0.2772
1 7 87.5 90.0 90.0 0.2954
1 8 87.5 105.0 75.0 0.3006
1 9 87.5 120.0 60.0 0.3098
1 10 87.5 135.0 45.0 0.3566
1 11 87.5 150.0 30.0 0.4193
1 12 87.5 165.0 15.0 0.5693
1 13 87.5 180.0 0.0 0.9319
rho for WIND SPEED = 6.0 m/s THETA_SUN = 60.0 deg
10 1 0.0 0.0 0.0 0.0232
9 1 10.0 0.0 180.0 0.0227
9 2 10.0 15.0 165.0 0.0225
9 3 10.0 30.0 150.0 0.0230
9 4 10.0 45.0 135.0 0.0229
9 5 10.0 60.0 120.0 0.0225
9 6 10.0 75.0 105.0 0.0229
9 7 10.0 90.0 90.0 0.0234
9 8 10.0 105.0 75.0 0.0235
9 9 10.0 120.0 60.0 0.0237
9 10 10.0 135.0 45.0 0.0253
9 11 10.0 150.0 30.0 0.0263
9 12 10.0 165.0 15.0 0.0253
9 13 10.0 180.0 0.0 0.0261
8 1 20.0 0.0 180.0 0.0230
8 2 20.0 15.0 165.0 0.0227
8 3 20.0 30.0 150.0 0.0223
8 4 20.0 45.0 135.0 0.0225
8 5 20.0 60.0 120.0 0.0226
8 6 20.0 75.0 105.0 0.0232
8 7 20.0 90.0 90.0 0.0230
8 8 20.0 105.0 75.0 0.0241
8 9 20.0 120.0 60.0 0.0251

8 10 20.0 135.0 45.0 0.0268
8 11 20.0 150.0 30.0 0.0351
8 12 20.0 165.0 15.0 0.0424
8 13 20.0 180.0 0.0 0.0493
7 1 30.0 0.0 180.0 0.0240
7 2 30.0 15.0 165.0 0.0240
7 3 30.0 30.0 150.0 0.0239
7 4 30.0 45.0 135.0 0.0239
7 5 30.0 60.0 120.0 0.0239
7 6 30.0 75.0 105.0 0.0238
7 7 30.0 90.0 90.0 0.0240
7 8 30.0 105.0 75.0 0.0250
7 9 30.0 120.0 60.0 0.0259
7 10 30.0 135.0 45.0 0.0303
7 11 30.0 150.0 30.0 0.0424
7 12 30.0 165.0 15.0 0.0804
7 13 30.0 180.0 0.0 0.0944
6 1 40.0 0.0 180.0 0.0291
6 2 40.0 15.0 165.0 0.0297
6 3 40.0 30.0 150.0 0.0292
6 4 40.0 45.0 135.0 0.0292
6 5 40.0 60.0 120.0 0.0286
6 6 40.0 75.0 105.0 0.0287
6 7 40.0 90.0 90.0 0.0284
6 8 40.0 105.0 75.0 0.0291
6 9 40.0 120.0 60.0 0.0301
6 10 40.0 135.0 45.0 0.0344
6 11 40.0 150.0 30.0 0.0580
6 12 40.0 165.0 15.0 0.1260
6 13 40.0 180.0 0.0 0.1641
5 1 50.0 0.0 180.0 0.0460
5 2 50.0 15.0 165.0 0.0461
5 3 50.0 30.0 150.0 0.0455
5 4 50.0 45.0 135.0 0.0443
5 5 50.0 60.0 120.0 0.0439
5 6 50.0 75.0 105.0 0.0434
5 7 50.0 90.0 90.0 0.0435
5 8 50.0 105.0 75.0 0.0428
5 9 50.0 120.0 60.0 0.0435
5 10 50.0 135.0 45.0 0.0455
5 11 50.0 150.0 30.0 0.0659
5 12 50.0 165.0 15.0 0.1706
5 13 50.0 180.0 0.0 0.2097
4 1 60.0 0.0 180.0 0.0851
4 2 60.0 15.0 165.0 0.0861
4 3 60.0 30.0 150.0 0.0861
4 4 60.0 45.0 135.0 0.0847
4 5 60.0 60.0 120.0 0.0830
4 6 60.0 75.0 105.0 0.0820
4 7 60.0 90.0 90.0 0.0810
4 8 60.0 105.0 75.0 0.0799
4 9 60.0 120.0 60.0 0.0793
4 10 60.0 135.0 45.0 0.0793
4 11 60.0 150.0 30.0 0.0906
4 12 60.0 165.0 15.0 0.2050
4 13 60.0 180.0 0.0 0.0109
3 1 70.0 0.0 180.0 0.1597
3 2 70.0 15.0 165.0 0.1600
3 3 70.0 30.0 150.0 0.1593
3 4 70.0 45.0 135.0 0.1602
3 5 70.0 60.0 120.0 0.1574
3 6 70.0 75.0 105.0 0.1582
3 7 70.0 90.0 90.0 0.1595
3 8 70.0 105.0 75.0 0.1562
3 9 70.0 120.0 60.0 0.1544
3 10 70.0 135.0 45.0 0.1563
3 11 70.0 150.0 30.0 0.1565
3 12 70.0 165.0 15.0 0.3389
3 13 70.0 180.0 0.0 0.5779
2 1 80.0 0.0 180.0 0.2192
2 2 80.0 15.0 165.0 0.2258
2 3 80.0 30.0 150.0 0.2326
2 4 80.0 45.0 135.0 0.2289
2 5 80.0 60.0 120.0 0.2265
2 6 80.0 75.0 105.0 0.2402
2 7 80.0 90.0 90.0 0.2414
2 8 80.0 105.0 75.0 0.2458
2 9 80.0 120.0 60.0 0.2393
2 10 80.0 135.0 45.0 0.2544
2 11 80.0 150.0 30.0 0.2834
2 12 80.0 165.0 15.0 0.5779
2 13 80.0 180.0 0.0 1.3930
1 1 87.5 0.0 180.0 0.2474
1 2 87.5 15.0 165.0 0.2462
1 3 87.5 30.0 150.0 0.2757
1 4 87.5 45.0 135.0 0.2740
1 5 87.5 60.0 120.0 0.2638
1 6 87.5 75.0 105.0 0.2768
1 7 87.5 90.0 90.0 0.2916
1 8 87.5 105.0 75.0 0.2935
1 9 87.5 120.0 60.0 0.3003
1 10 87.5 135.0 45.0 0.3476
1 11 87.5 150.0 30.0 0.4231
1 12 87.5 165.0 15.0 0.7594
1 13 87.5 180.0 0.0 2.3879
rho for WIND SPEED = 6.0 m/s THETA_SUN = 70.0
deg
10 1 0.0 0.0 0.0 0.0223
9 1 10.0 0.0 180.0 0.0221
9 2 10.0 15.0 165.0 0.0220

9	3	10.0	30.0	150.0	0.0224
9	4	10.0	45.0	135.0	0.0223
9	5	10.0	60.0	120.0	0.0219
9	6	10.0	75.0	105.0	0.0222
9	7	10.0	90.0	90.0	0.0225
9	8	10.0	105.0	75.0	0.0225
9	9	10.0	120.0	60.0	0.0226
9	10	10.0	135.0	45.0	0.0231
9	11	10.0	150.0	30.0	0.0239
9	12	10.0	165.0	15.0	0.0243
9	13	10.0	180.0	0.0	0.0241
8	1	20.0	0.0	180.0	0.0227
8	2	20.0	15.0	165.0	0.0223
8	3	20.0	30.0	150.0	0.0220
8	4	20.0	45.0	135.0	0.0221
8	5	20.0	60.0	120.0	0.0222
8	6	20.0	75.0	105.0	0.0227
8	7	20.0	90.0	90.0	0.0224
8	8	20.0	105.0	75.0	0.0233
8	9	20.0	120.0	60.0	0.0235
8	10	20.0	135.0	45.0	0.0242
8	11	20.0	150.0	30.0	0.0260
8	12	20.0	165.0	15.0	0.0278
8	13	20.0	180.0	0.0	0.0311
7	1	30.0	0.0	180.0	0.0237
7	2	30.0	15.0	165.0	0.0237
7	3	30.0	30.0	150.0	0.0236
7	4	30.0	45.0	135.0	0.0236
7	5	30.0	60.0	120.0	0.0237
7	6	30.0	75.0	105.0	0.0235
7	7	30.0	90.0	90.0	0.0237
7	8	30.0	105.0	75.0	0.0241
7	9	30.0	120.0	60.0	0.0251
7	10	30.0	135.0	45.0	0.0268
7	11	30.0	150.0	30.0	0.0329
7	12	30.0	165.0	15.0	0.0465
7	13	30.0	180.0	0.0	0.0511
6	1	40.0	0.0	180.0	0.0286
6	2	40.0	15.0	165.0	0.0292
6	3	40.0	30.0	150.0	0.0288
6	4	40.0	45.0	135.0	0.0289
6	5	40.0	60.0	120.0	0.0284
6	6	40.0	75.0	105.0	0.0285
6	7	40.0	90.0	90.0	0.0283
6	8	40.0	105.0	75.0	0.0290
6	9	40.0	120.0	60.0	0.0298
6	10	40.0	135.0	45.0	0.0328
6	11	40.0	150.0	30.0	0.0423
6	12	40.0	165.0	15.0	0.0899
6	13	40.0	180.0	0.0	0.1254
5	1	50.0	0.0	180.0	0.0449
5	2	50.0	15.0	165.0	0.0450
5	3	50.0	30.0	150.0	0.0446
5	4	50.0	45.0	135.0	0.0437
5	5	50.0	60.0	120.0	0.0435
5	6	50.0	75.0	105.0	0.0433
5	7	50.0	90.0	90.0	0.0437
5	8	50.0	105.0	75.0	0.0433
5	9	50.0	120.0	60.0	0.0444
5	10	50.0	135.0	45.0	0.0474
5	11	50.0	150.0	30.0	0.0608
5	12	50.0	165.0	15.0	0.1542
5	13	50.0	180.0	0.0	0.2745
4	1	60.0	0.0	180.0	0.0830
4	2	60.0	15.0	165.0	0.0840
4	3	60.0	30.0	150.0	0.0842
4	4	60.0	45.0	135.0	0.0832
4	5	60.0	60.0	120.0	0.0820
4	6	60.0	75.0	105.0	0.0819
4	7	60.0	90.0	90.0	0.0813
4	8	60.0	105.0	75.0	0.0811
4	9	60.0	120.0	60.0	0.0812
4	10	60.0	135.0	45.0	0.0843
4	11	60.0	150.0	30.0	0.0932
4	12	60.0	165.0	15.0	0.2159
4	13	60.0	180.0	0.0	0.3496
3	1	70.0	0.0	180.0	0.1575
3	2	70.0	15.0	165.0	0.1578
3	3	70.0	30.0	150.0	0.1572
3	4	70.0	45.0	135.0	0.1583
3	5	70.0	60.0	120.0	0.1561
3	6	70.0	75.0	105.0	0.1573
3	7	70.0	90.0	90.0	0.1595
3	8	70.0	105.0	75.0	0.1567
3	9	70.0	120.0	60.0	0.1559
3	10	70.0	135.0	45.0	0.1595
3	11	70.0	150.0	30.0	0.1566
3	12	70.0	165.0	15.0	0.3011
3	13	70.0	180.0	0.0	0.0357
2	1	80.0	0.0	180.0	0.2211
2	2	80.0	15.0	165.0	0.2276
2	3	80.0	30.0	150.0	0.2342
2	4	80.0	45.0	135.0	0.2300
2	5	80.0	60.0	120.0	0.2269
2	6	80.0	75.0	105.0	0.2396
2	7	80.0	90.0	90.0	0.2398
2	8	80.0	105.0	75.0	0.2431
2	9	80.0	120.0	60.0	0.2353
2	10	80.0	135.0	45.0	0.2473
2	11	80.0	150.0	30.0	0.2660

2	12	80.0	165.0	15.0	0.4592
2	13	80.0	180.0	0.0	1.1522
1	1	87.5	0.0	180.0	0.2548
1	2	87.5	15.0	165.0	0.2534
1	3	87.5	30.0	150.0	0.2829
1	4	87.5	45.0	135.0	0.2802
1	5	87.5	60.0	120.0	0.2677
1	6	87.5	75.0	105.0	0.2779
1	7	87.5	90.0	90.0	0.2889
1	8	87.5	105.0	75.0	0.2872
1	9	87.5	120.0	60.0	0.2897
1	10	87.5	135.0	45.0	0.3295
1	11	87.5	150.0	30.0	0.3890
1	12	87.5	165.0	15.0	0.7150
1	13	87.5	180.0	0.0	2.7706

rho for WIND SPEED = 6.0 m/s THETA_SUN = 80.0 deg

10	1	0.0	0.0	0.0	0.0217
9	1	10.0	0.0	180.0	0.0217
9	2	10.0	15.0	165.0	0.0216
9	3	10.0	30.0	150.0	0.0219
9	4	10.0	45.0	135.0	0.0218
9	5	10.0	60.0	120.0	0.0215
9	6	10.0	75.0	105.0	0.0217
9	7	10.0	90.0	90.0	0.0219
9	8	10.0	105.0	75.0	0.0218
9	9	10.0	120.0	60.0	0.0218
9	10	10.0	135.0	45.0	0.0222
9	11	10.0	150.0	30.0	0.0227
9	12	10.0	165.0	15.0	0.0225
9	13	10.0	180.0	0.0	0.0227
8	1	20.0	0.0	180.0	0.0223
8	2	20.0	15.0	165.0	0.0220
8	3	20.0	30.0	150.0	0.0216
8	4	20.0	45.0	135.0	0.0218
8	5	20.0	60.0	120.0	0.0219
8	6	20.0	75.0	105.0	0.0223
8	7	20.0	90.0	90.0	0.0219
8	8	20.0	105.0	75.0	0.0226
8	9	20.0	120.0	60.0	0.0226
8	10	20.0	135.0	45.0	0.0230
8	11	20.0	150.0	30.0	0.0236
8	12	20.0	165.0	15.0	0.0246
8	13	20.0	180.0	0.0	0.0254
7	1	30.0	0.0	180.0	0.0233
7	2	30.0	15.0	165.0	0.0233
7	3	30.0	30.0	150.0	0.0232
7	4	30.0	45.0	135.0	0.0233
7	5	30.0	60.0	120.0	0.0233
7	6	30.0	75.0	105.0	0.0232
7	7	30.0	90.0	90.0	0.0233
7	8	30.0	105.0	75.0	0.0236
7	9	30.0	120.0	60.0	0.0243
7	10	30.0	135.0	45.0	0.0255
7	11	30.0	150.0	30.0	0.0282
7	12	30.0	165.0	15.0	0.0307
7	13	30.0	180.0	0.0	0.0322
6	1	40.0	0.0	180.0	0.0280
6	2	40.0	15.0	165.0	0.0287
6	3	40.0	30.0	150.0	0.0283
6	4	40.0	45.0	135.0	0.0284
6	5	40.0	60.0	120.0	0.0280
6	6	40.0	75.0	105.0	0.0283
6	7	40.0	90.0	90.0	0.0280
6	8	40.0	105.0	75.0	0.0287
6	9	40.0	120.0	60.0	0.0293
6	10	40.0	135.0	45.0	0.0322
6	11	40.0	150.0	30.0	0.0379
6	12	40.0	165.0	15.0	0.0549
6	13	40.0	180.0	0.0	0.0740
5	1	50.0	0.0	180.0	0.0438
5	2	50.0	15.0	165.0	0.0439
5	3	50.0	30.0	150.0	0.0436
5	4	50.0	45.0	135.0	0.0429
5	5	50.0	60.0	120.0	0.0429
5	6	50.0	75.0	105.0	0.0430
5	7	50.0	90.0	90.0	0.0436
5	8	50.0	105.0	75.0	0.0433
5	9	50.0	120.0	60.0	0.0447
5	10	50.0	135.0	45.0	0.0488
5	11	50.0	150.0	30.0	0.0607
5	12	50.0	165.0	15.0	0.1137
5	13	50.0	180.0	0.0	0.2218
4	1	60.0	0.0	180.0	0.0810
4	2	60.0	15.0	165.0	0.0820
4	3	60.0	30.0	150.0	0.0823
4	4	60.0	45.0	135.0	0.0817
4	5	60.0	60.0	120.0	0.0809
4	6	60.0	75.0	105.0	0.0813
4	7	60.0	90.0	90.0	0.0813
4	8	60.0	105.0	75.0	0.0816
4	9	60.0	120.0	60.0	0.0828
4	10	60.0	135.0	45.0	0.0892
4	11	60.0	150.0	30.0	0.1052
4	12	60.0	165.0	15.0	0.1980
4	13	60.0	180.0	0.0	0.4368
3	1	70.0	0.0	180.0	0.1559
3	2	70.0	15.0	165.0	0.1561
3	3	70.0	30.0	150.0	0.1556
3	4	70.0	45.0	135.0	0.1568

3	5	70.0	60.0	120.0	0.1548
3	6	70.0	75.0	105.0	0.1565
3	7	70.0	90.0	90.0	0.1590
3	8	70.0	105.0	75.0	0.1571
3	9	70.0	120.0	60.0	0.1570
3	10	70.0	135.0	45.0	0.1643
3	11	70.0	150.0	30.0	0.1716
3	12	70.0	165.0	15.0	0.2650
3	13	70.0	180.0	0.0	0.5586
2	1	80.0	0.0	180.0	0.2237
2	2	80.0	15.0	165.0	0.2300
2	3	80.0	30.0	150.0	0.2363
2	4	80.0	45.0	135.0	0.2315
2	5	80.0	60.0	120.0	0.2277
2	6	80.0	75.0	105.0	0.2394
2	7	80.0	90.0	90.0	0.2389
2	8	80.0	105.0	75.0	0.2410
2	9	80.0	120.0	60.0	0.2321
2	10	80.0	135.0	45.0	0.2403
2	11	80.0	150.0	30.0	0.2490
2	12	80.0	165.0	15.0	0.3021
2	13	80.0	180.0	0.0	0.1067
1	1	87.5	0.0	180.0	0.2625
1	2	87.5	15.0	165.0	0.2608
1	3	87.5	30.0	150.0	0.2902
1	4	87.5	45.0	135.0	0.2863
1	5	87.5	60.0	120.0	0.2716
1	6	87.5	75.0	105.0	0.2793
1	7	87.5	90.0	90.0	0.2874
1	8	87.5	105.0	75.0	0.2826
1	9	87.5	120.0	60.0	0.2802
1	10	87.5	135.0	45.0	0.3058
1	11	87.5	150.0	30.0	0.3264
1	12	87.5	165.0	15.0	0.3598
1	13	87.5	180.0	0.0	1.0583

rho for WIND SPEED = 8.0 m/s THETA_SUN = 0.0 deg

10	1	0.0	0.0	0.0	0.0010
9	1	10.0	0.0	180.0	0.1184
9	2	10.0	15.0	165.0	0.1129
9	3	10.0	30.0	150.0	0.1169
9	4	10.0	45.0	135.0	0.1191
9	5	10.0	60.0	120.0	0.1150
9	6	10.0	75.0	105.0	0.1129
9	7	10.0	90.0	90.0	0.1188
9	8	10.0	105.0	75.0	0.1129
9	9	10.0	120.0	60.0	0.1150
9	10	10.0	135.0	45.0	0.1191
9	11	10.0	150.0	30.0	0.1169
9	12	10.0	165.0	15.0	0.1129
9	13	10.0	180.0	0.0	0.1184
8	1	20.0	0.0	180.0	0.1503
8	2	20.0	15.0	165.0	0.1443
8	3	20.0	30.0	150.0	0.1490
8	4	20.0	45.0	135.0	0.1507
8	5	20.0	60.0	120.0	0.1469
8	6	20.0	75.0	105.0	0.1474
8	7	20.0	90.0	90.0	0.1432
8	8	20.0	105.0	75.0	0.1474
8	9	20.0	120.0	60.0	0.1469
8	10	20.0	135.0	45.0	0.1507
8	11	20.0	150.0	30.0	0.1490
8	12	20.0	165.0	15.0	0.1443
8	13	20.0	180.0	0.0	0.1503
7	1	30.0	0.0	180.0	0.1170
7	2	30.0	15.0	165.0	0.1223
7	3	30.0	30.0	150.0	0.1182
7	4	30.0	45.0	135.0	0.1175
7	5	30.0	60.0	120.0	0.1215
7	6	30.0	75.0	105.0	0.1203
7	7	30.0	90.0	90.0	0.1093
7	8	30.0	105.0	75.0	0.1203
7	9	30.0	120.0	60.0	0.1215
7	10	30.0	135.0	45.0	0.1175
7	11	30.0	150.0	30.0	0.1182
7	12	30.0	165.0	15.0	0.1223
7	13	30.0	180.0	0.0	0.1170
6	1	40.0	0.0	180.0	0.0723
6	2	40.0	15.0	165.0	0.0731
6	3	40.0	30.0	150.0	0.0699
6	4	40.0	45.0	135.0	0.0710
6	5	40.0	60.0	120.0	0.0733
6	6	40.0	75.0	105.0	0.0730
6	7	40.0	90.0	90.0	0.0702
6	8	40.0	105.0	75.0	0.0730
6	9	40.0	120.0	60.0	0.0733
6	10	40.0	135.0	45.0	0.0710
6	11	40.0	150.0	30.0	0.0699
6	12	40.0	165.0	15.0	0.0731
6	13	40.0	180.0	0.0	0.0723
5	1	50.0	0.0	180.0	0.0541
5	2	50.0	15.0	165.0	0.0567
5	3	50.0	30.0	150.0	0.0537
5	4	50.0	45.0	135.0	0.0554
5	5	50.0	60.0	120.0	0.0550
5	6	50.0	75.0	105.0	0.0557
5	7	50.0	90.0	90.0	0.0529
5	8	50.0	105.0	75.0	0.0557
5	9	50.0	120.0	60.0	0.0550
5	10	50.0	135.0	45.0	0.0554

5 11 50.0 150.0 30.0 0.0537
5 12 50.0 165.0 15.0 0.0567
5 13 50.0 180.0 0.0 0.0541
4 1 60.0 0.0 180.0 0.0801
4 2 60.0 15.0 165.0 0.0809
4 3 60.0 30.0 150.0 0.0815
4 4 60.0 45.0 135.0 0.0803
4 5 60.0 60.0 120.0 0.0797
4 6 60.0 75.0 105.0 0.0807
4 7 60.0 90.0 90.0 0.0816
4 8 60.0 105.0 75.0 0.0807
4 9 60.0 120.0 60.0 0.0797
4 10 60.0 135.0 45.0 0.0803
4 11 60.0 150.0 30.0 0.0815
4 12 60.0 165.0 15.0 0.0809
4 13 60.0 180.0 0.0 0.0801
3 1 70.0 0.0 180.0 0.1469
3 2 70.0 15.0 165.0 0.1479
3 3 70.0 30.0 150.0 0.1495
3 4 70.0 45.0 135.0 0.1497
3 5 70.0 60.0 120.0 0.1472
3 6 70.0 75.0 105.0 0.1503
3 7 70.0 90.0 90.0 0.1526
3 8 70.0 105.0 75.0 0.1503
3 9 70.0 120.0 60.0 0.1472
3 10 70.0 135.0 45.0 0.1497
3 11 70.0 150.0 30.0 0.1495
3 12 70.0 165.0 15.0 0.1479
3 13 70.0 180.0 0.0 0.1469
2 1 80.0 0.0 180.0 0.2166
2 2 80.0 15.0 165.0 0.2243
2 3 80.0 30.0 150.0 0.2285
2 4 80.0 45.0 135.0 0.2242
2 5 80.0 60.0 120.0 0.2183
2 6 80.0 75.0 105.0 0.2301
2 7 80.0 90.0 90.0 0.2306
2 8 80.0 105.0 75.0 0.2301
2 9 80.0 120.0 60.0 0.2183
2 10 80.0 135.0 45.0 0.2242
2 11 80.0 150.0 30.0 0.2285
2 12 80.0 165.0 15.0 0.2243
2 13 80.0 180.0 0.0 0.2166
1 1 87.5 0.0 180.0 0.2560
1 2 87.5 15.0 165.0 0.2609
1 3 87.5 30.0 150.0 0.2898
1 4 87.5 45.0 135.0 0.2766
1 5 87.5 60.0 120.0 0.2670
1 6 87.5 75.0 105.0 0.2667
1 7 87.5 90.0 90.0 0.2721
1 8 87.5 105.0 75.0 0.2667
1 9 87.5 120.0 60.0 0.2670
1 10 87.5 135.0 45.0 0.2766
1 11 87.5 150.0 30.0 0.2898
1 12 87.5 165.0 15.0 0.2609
1 13 87.5 180.0 0.0 0.2560
rho for WIND SPEED = 8.0 m/s THETA_SUN = 10.0 deg
10 1 0.0 0.0 0.0 0.1049
9 1 10.0 0.0 180.0 0.1331
9 2 10.0 15.0 165.0 0.1377
9 3 10.0 30.0 150.0 0.1328
9 4 10.0 45.0 135.0 0.1432
9 5 10.0 60.0 120.0 0.1380
9 6 10.0 75.0 105.0 0.1445
9 7 10.0 90.0 90.0 0.1316
9 8 10.0 105.0 75.0 0.1242
9 9 10.0 120.0 60.0 0.1049
9 10 10.0 135.0 45.0 0.0944
9 11 10.0 150.0 30.0 0.0832
9 12 10.0 165.0 15.0 0.0704
9 13 10.0 180.0 0.0 0.0004
8 1 20.0 0.0 180.0 0.1103
8 2 20.0 15.0 165.0 0.1042
8 3 20.0 30.0 150.0 0.1118
8 4 20.0 45.0 135.0 0.1170
8 5 20.0 60.0 120.0 0.1207
8 6 20.0 75.0 105.0 0.1386
8 7 20.0 90.0 90.0 0.1388
8 8 20.0 105.0 75.0 0.1443
8 9 20.0 120.0 60.0 0.1381
8 10 20.0 135.0 45.0 0.1367
8 11 20.0 150.0 30.0 0.1295
8 12 20.0 165.0 15.0 0.1277
8 13 20.0 180.0 0.0 0.1127
7 1 30.0 0.0 180.0 0.0630
7 2 30.0 15.0 165.0 0.0622
7 3 30.0 30.0 150.0 0.0627
7 4 30.0 45.0 135.0 0.0678
7 5 30.0 60.0 120.0 0.0781
7 6 30.0 75.0 105.0 0.0986
7 7 30.0 90.0 90.0 0.1024
7 8 30.0 105.0 75.0 0.1198
7 9 30.0 120.0 60.0 0.1298
7 10 30.0 135.0 45.0 0.1476
7 11 30.0 150.0 30.0 0.1535
7 12 30.0 165.0 15.0 0.1655
7 13 30.0 180.0 0.0 0.1703
6 1 40.0 0.0 180.0 0.0397
6 2 40.0 15.0 165.0 0.0399
6 3 40.0 30.0 150.0 0.0418

6	4	40.0	45.0	135.0	0.0430
6	5	40.0	60.0	120.0	0.0459
6	6	40.0	75.0	105.0	0.0528
6	7	40.0	90.0	90.0	0.0617
6	8	40.0	105.0	75.0	0.0715
6	9	40.0	120.0	60.0	0.0893
6	10	40.0	135.0	45.0	0.1103
6	11	40.0	150.0	30.0	0.1256
6	12	40.0	165.0	15.0	0.1400
6	13	40.0	180.0	0.0	0.1484
5	1	50.0	0.0	180.0	0.0453
5	2	50.0	15.0	165.0	0.0461
5	3	50.0	30.0	150.0	0.0468
5	4	50.0	45.0	135.0	0.0461
5	5	50.0	60.0	120.0	0.0461
5	6	50.0	75.0	105.0	0.0484
5	7	50.0	90.0	90.0	0.0515
5	8	50.0	105.0	75.0	0.0535
5	9	50.0	120.0	60.0	0.0634
5	10	50.0	135.0	45.0	0.0722
5	11	50.0	150.0	30.0	0.0843
5	12	50.0	165.0	15.0	0.0938
5	13	50.0	180.0	0.0	0.1023
4	1	60.0	0.0	180.0	0.0822
4	2	60.0	15.0	165.0	0.0820
4	3	60.0	30.0	150.0	0.0823
4	4	60.0	45.0	135.0	0.0809
4	5	60.0	60.0	120.0	0.0795
4	6	60.0	75.0	105.0	0.0801
4	7	60.0	90.0	90.0	0.0817
4	8	60.0	105.0	75.0	0.0801
4	9	60.0	120.0	60.0	0.0815
4	10	60.0	135.0	45.0	0.0870
4	11	60.0	150.0	30.0	0.0887
4	12	60.0	165.0	15.0	0.0916
4	13	60.0	180.0	0.0	0.0919
3	1	70.0	0.0	180.0	0.1490
3	2	70.0	15.0	165.0	0.1502
3	3	70.0	30.0	150.0	0.1514
3	4	70.0	45.0	135.0	0.1514
3	5	70.0	60.0	120.0	0.1481
3	6	70.0	75.0	105.0	0.1506
3	7	70.0	90.0	90.0	0.1525
3	8	70.0	105.0	75.0	0.1499
3	9	70.0	120.0	60.0	0.1472
3	10	70.0	135.0	45.0	0.1507
3	11	70.0	150.0	30.0	0.1495
3	12	70.0	165.0	15.0	0.1492
3	13	70.0	180.0	0.0	0.1486
2	1	80.0	0.0	180.0	0.2085
2	2	80.0	15.0	165.0	0.2165
2	3	80.0	30.0	150.0	0.2215
2	4	80.0	45.0	135.0	0.2184
2	5	80.0	60.0	120.0	0.2139
2	6	80.0	75.0	105.0	0.2274
2	7	80.0	90.0	90.0	0.2300
2	8	80.0	105.0	75.0	0.2314
2	9	80.0	120.0	60.0	0.2215
2	10	80.0	135.0	45.0	0.2292
2	11	80.0	150.0	30.0	0.2352
2	12	80.0	165.0	15.0	0.2316
2	13	80.0	180.0	0.0	0.2244
1	1	87.5	0.0	180.0	0.2331
1	2	87.5	15.0	165.0	0.2388
1	3	87.5	30.0	150.0	0.2678
1	4	87.5	45.0	135.0	0.2592
1	5	87.5	60.0	120.0	0.2545
1	6	87.5	75.0	105.0	0.2597
1	7	87.5	90.0	90.0	0.2710
1	8	87.5	105.0	75.0	0.2714
1	9	87.5	120.0	60.0	0.2774
1	10	87.5	135.0	45.0	0.2922
1	11	87.5	150.0	30.0	0.3102
1	12	87.5	165.0	15.0	0.2821
1	13	87.5	180.0	0.0	0.2783

rho for WIND SPEED = 8.0 m/s THETA_SUN = 20.0 deg

10	1	0.0	0.0	0.0	0.1276
9	1	10.0	0.0	180.0	0.1237
9	2	10.0	15.0	165.0	0.0994
9	3	10.0	30.0	150.0	0.1100
9	4	10.0	45.0	135.0	0.1122
9	5	10.0	60.0	120.0	0.1172
9	6	10.0	75.0	105.0	0.1307
9	7	10.0	90.0	90.0	0.1388
9	8	10.0	105.0	75.0	0.1423
9	9	10.0	120.0	60.0	0.1324
9	10	10.0	135.0	45.0	0.1188
9	11	10.0	150.0	30.0	0.1148
9	12	10.0	165.0	15.0	0.1102
9	13	10.0	180.0	0.0	0.0936
8	1	20.0	0.0	180.0	0.0642
8	2	20.0	15.0	165.0	0.0607
8	3	20.0	30.0	150.0	0.0667
8	4	20.0	45.0	135.0	0.0674
8	5	20.0	60.0	120.0	0.0771
8	6	20.0	75.0	105.0	0.0974
8	7	20.0	90.0	90.0	0.1138
8	8	20.0	105.0	75.0	0.1228
8	9	20.0	120.0	60.0	0.1343

8	10	20.0	135.0	45.0	0.1313
8	11	20.0	150.0	30.0	0.1072
8	12	20.0	165.0	15.0	0.0846
8	13	20.0	180.0	0.0	0.0007
7	1	30.0	0.0	180.0	0.0330
7	2	30.0	15.0	165.0	0.0361
7	3	30.0	30.0	150.0	0.0385
7	4	30.0	45.0	135.0	0.0425
7	5	30.0	60.0	120.0	0.0464
7	6	30.0	75.0	105.0	0.0568
7	7	30.0	90.0	90.0	0.0769
7	8	30.0	105.0	75.0	0.1005
7	9	30.0	120.0	60.0	0.1215
7	10	30.0	135.0	45.0	0.1378
7	11	30.0	150.0	30.0	0.1370
7	12	30.0	165.0	15.0	0.1249
7	13	30.0	180.0	0.0	0.1186
6	1	40.0	0.0	180.0	0.0322
6	2	40.0	15.0	165.0	0.0324
6	3	40.0	30.0	150.0	0.0319
6	4	40.0	45.0	135.0	0.0335
6	5	40.0	60.0	120.0	0.0336
6	6	40.0	75.0	105.0	0.0401
6	7	40.0	90.0	90.0	0.0448
6	8	40.0	105.0	75.0	0.0619
6	9	40.0	120.0	60.0	0.0864
6	10	40.0	135.0	45.0	0.1186
6	11	40.0	150.0	30.0	0.1439
6	12	40.0	165.0	15.0	0.1714
6	13	40.0	180.0	0.0	0.1808
5	1	50.0	0.0	180.0	0.0467
5	2	50.0	15.0	165.0	0.0465
5	3	50.0	30.0	150.0	0.0461
5	4	50.0	45.0	135.0	0.0452
5	5	50.0	60.0	120.0	0.0451
5	6	50.0	75.0	105.0	0.0458
5	7	50.0	90.0	90.0	0.0472
5	8	50.0	105.0	75.0	0.0518
5	9	50.0	120.0	60.0	0.0597
5	10	50.0	135.0	45.0	0.0897
5	11	50.0	150.0	30.0	0.1181
5	12	50.0	165.0	15.0	0.1593
5	13	50.0	180.0	0.0	0.1698
4	1	60.0	0.0	180.0	0.0852
4	2	60.0	15.0	165.0	0.0858
4	3	60.0	30.0	150.0	0.0856
4	4	60.0	45.0	135.0	0.0835
4	5	60.0	60.0	120.0	0.0810
4	6	60.0	75.0	105.0	0.0805
4	7	60.0	90.0	90.0	0.0813
4	8	60.0	105.0	75.0	0.0802
4	9	60.0	120.0	60.0	0.0815
4	10	60.0	135.0	45.0	0.0932
4	11	60.0	150.0	30.0	0.1079
4	12	60.0	165.0	15.0	0.1355
4	13	60.0	180.0	0.0	0.1448
3	1	70.0	0.0	180.0	0.1516
3	2	70.0	15.0	165.0	0.1530
3	3	70.0	30.0	150.0	0.1539
3	4	70.0	45.0	135.0	0.1534
3	5	70.0	60.0	120.0	0.1492
3	6	70.0	75.0	105.0	0.1511
3	7	70.0	90.0	90.0	0.1524
3	8	70.0	105.0	75.0	0.1495
3	9	70.0	120.0	60.0	0.1471
3	10	70.0	135.0	45.0	0.1520
3	11	70.0	150.0	30.0	0.1578
3	12	70.0	165.0	15.0	0.1657
3	13	70.0	180.0	0.0	0.1704
2	1	80.0	0.0	180.0	0.2005
2	2	80.0	15.0	165.0	0.2087
2	3	80.0	30.0	150.0	0.2143
2	4	80.0	45.0	135.0	0.2122
2	5	80.0	60.0	120.0	0.2090
2	6	80.0	75.0	105.0	0.2239
2	7	80.0	90.0	90.0	0.2281
2	8	80.0	105.0	75.0	0.2311
2	9	80.0	120.0	60.0	0.2231
2	10	80.0	135.0	45.0	0.2332
2	11	80.0	150.0	30.0	0.2430
2	12	80.0	165.0	15.0	0.2424
2	13	80.0	180.0	0.0	0.2386
1	1	87.5	0.0	180.0	0.2146
1	2	87.5	15.0	165.0	0.2207
1	3	87.5	30.0	150.0	0.2495
1	4	87.5	45.0	135.0	0.2439
1	5	87.5	60.0	120.0	0.2427
1	6	87.5	75.0	105.0	0.2521
1	7	87.5	90.0	90.0	0.2678
1	8	87.5	105.0	75.0	0.2729
1	9	87.5	120.0	60.0	0.2837
1	10	87.5	135.0	45.0	0.3037
1	11	87.5	150.0	30.0	0.3277
1	12	87.5	165.0	15.0	0.3028
1	13	87.5	180.0	0.0	0.3012

rho for WIND SPEED = 8.0 m/s THETA_SUN = 30.0 deg

10	1	0.0	0.0	0.0	0.1088
9	1	10.0	0.0	180.0	0.0584
9	2	10.0	15.0	165.0	0.0624

9	3	10.0	30.0	150.0	0.0627
9	4	10.0	45.0	135.0	0.0615
9	5	10.0	60.0	120.0	0.0726
9	6	10.0	75.0	105.0	0.0763
9	7	10.0	90.0	90.0	0.0923
9	8	10.0	105.0	75.0	0.0919
9	9	10.0	120.0	60.0	0.1083
9	10	10.0	135.0	45.0	0.1158
9	11	10.0	150.0	30.0	0.1337
9	12	10.0	165.0	15.0	0.1260
9	13	10.0	180.0	0.0	0.1293
8	1	20.0	0.0	180.0	0.0351
8	2	20.0	15.0	165.0	0.0352
8	3	20.0	30.0	150.0	0.0365
8	4	20.0	45.0	135.0	0.0409
8	5	20.0	60.0	120.0	0.0396
8	6	20.0	75.0	105.0	0.0510
8	7	20.0	90.0	90.0	0.0609
8	8	20.0	105.0	75.0	0.0875
8	9	20.0	120.0	60.0	0.1103
8	10	20.0	135.0	45.0	0.1305
8	11	20.0	150.0	30.0	0.1259
8	12	20.0	165.0	15.0	0.1105
8	13	20.0	180.0	0.0	0.1002
7	1	30.0	0.0	180.0	0.0267
7	2	30.0	15.0	165.0	0.0269
7	3	30.0	30.0	150.0	0.0277
7	4	30.0	45.0	135.0	0.0287
7	5	30.0	60.0	120.0	0.0308
7	6	30.0	75.0	105.0	0.0323
7	7	30.0	90.0	90.0	0.0466
7	8	30.0	105.0	75.0	0.0669
7	9	30.0	120.0	60.0	0.0927
7	10	30.0	135.0	45.0	0.1189
7	11	30.0	150.0	30.0	0.1226
7	12	30.0	165.0	15.0	0.0947
7	13	30.0	180.0	0.0	0.0012
6	1	40.0	0.0	180.0	0.0313
6	2	40.0	15.0	165.0	0.0314
6	3	40.0	30.0	150.0	0.0309
6	4	40.0	45.0	135.0	0.0311
6	5	40.0	60.0	120.0	0.0309
6	6	40.0	75.0	105.0	0.0331
6	7	40.0	90.0	90.0	0.0361
6	8	40.0	105.0	75.0	0.0442
6	9	40.0	120.0	60.0	0.0713
6	10	40.0	135.0	45.0	0.1019
6	11	40.0	150.0	30.0	0.1346
6	12	40.0	165.0	15.0	0.1434
6	13	40.0	180.0	0.0	0.1292
5	1	50.0	0.0	180.0	0.0486
5	2	50.0	15.0	165.0	0.0485
5	3	50.0	30.0	150.0	0.0478
5	4	50.0	45.0	135.0	0.0464
5	5	50.0	60.0	120.0	0.0454
5	6	50.0	75.0	105.0	0.0451
5	7	50.0	90.0	90.0	0.0451
5	8	50.0	105.0	75.0	0.0482
5	9	50.0	120.0	60.0	0.0560
5	10	50.0	135.0	45.0	0.0825
5	11	50.0	150.0	30.0	0.1398
5	12	50.0	165.0	15.0	0.1931
5	13	50.0	180.0	0.0	0.2111
4	1	60.0	0.0	180.0	0.0891
4	2	60.0	15.0	165.0	0.0896
4	3	60.0	30.0	150.0	0.0892
4	4	60.0	45.0	135.0	0.0864
4	5	60.0	60.0	120.0	0.0831
4	6	60.0	75.0	105.0	0.0817
4	7	60.0	90.0	90.0	0.0815
4	8	60.0	105.0	75.0	0.0795
4	9	60.0	120.0	60.0	0.0796
4	10	60.0	135.0	45.0	0.0926
4	11	60.0	150.0	30.0	0.1360
4	12	60.0	165.0	15.0	0.2030
4	13	60.0	180.0	0.0	0.2408
3	1	70.0	0.0	180.0	0.1528
3	2	70.0	15.0	165.0	0.1543
3	3	70.0	30.0	150.0	0.1553
3	4	70.0	45.0	135.0	0.1546
3	5	70.0	60.0	120.0	0.1500
3	6	70.0	75.0	105.0	0.1515
3	7	70.0	90.0	90.0	0.1523
3	8	70.0	105.0	75.0	0.1492
3	9	70.0	120.0	60.0	0.1468
3	10	70.0	135.0	45.0	0.1552
3	11	70.0	150.0	30.0	0.1725
3	12	70.0	165.0	15.0	0.2191
3	13	70.0	180.0	0.0	0.2549
2	1	80.0	0.0	180.0	0.1944
2	2	80.0	15.0	165.0	0.2027
2	3	80.0	30.0	150.0	0.2086
2	4	80.0	45.0	135.0	0.2070
2	5	80.0	60.0	120.0	0.2046
2	6	80.0	75.0	105.0	0.2202
2	7	80.0	90.0	90.0	0.2254
2	8	80.0	105.0	75.0	0.2293
2	9	80.0	120.0	60.0	0.2228
2	10	80.0	135.0	45.0	0.2365
2	11	80.0	150.0	30.0	0.2551

2	12	80.0	165.0	15.0	0.2822
2	13	80.0	180.0	0.0	0.2910
1	1	87.5	0.0	180.0	0.2040
1	2	87.5	15.0	165.0	0.2103
1	3	87.5	30.0	150.0	0.2382
1	4	87.5	45.0	135.0	0.2335
1	5	87.5	60.0	120.0	0.2337
1	6	87.5	75.0	105.0	0.2451
1	7	87.5	90.0	90.0	0.2633
1	8	87.5	105.0	75.0	0.2709
1	9	87.5	120.0	60.0	0.2851
1	10	87.5	135.0	45.0	0.3110
1	11	87.5	150.0	30.0	0.3474
1	12	87.5	165.0	15.0	0.3416
1	13	87.5	180.0	0.0	0.3534

rho for WIND SPEED = 8.0 m/s THETA_SUN = 40.0 deg

10	1	0.0	0.0	0.0	0.0581
9	1	10.0	0.0	180.0	0.0335
9	2	10.0	15.0	165.0	0.0326
9	3	10.0	30.0	150.0	0.0348
9	4	10.0	45.0	135.0	0.0379
9	5	10.0	60.0	120.0	0.0360
9	6	10.0	75.0	105.0	0.0475
9	7	10.0	90.0	90.0	0.0492
9	8	10.0	105.0	75.0	0.0528
9	9	10.0	120.0	60.0	0.0675
9	10	10.0	135.0	45.0	0.0787
9	11	10.0	150.0	30.0	0.0916
9	12	10.0	165.0	15.0	0.1086
9	13	10.0	180.0	0.0	0.1006
8	1	20.0	0.0	180.0	0.0263
8	2	20.0	15.0	165.0	0.0245
8	3	20.0	30.0	150.0	0.0257
8	4	20.0	45.0	135.0	0.0260
8	5	20.0	60.0	120.0	0.0285
8	6	20.0	75.0	105.0	0.0312
8	7	20.0	90.0	90.0	0.0364
8	8	20.0	105.0	75.0	0.0466
8	9	20.0	120.0	60.0	0.0684
8	10	20.0	135.0	45.0	0.0921
8	11	20.0	150.0	30.0	0.1124
8	12	20.0	165.0	15.0	0.1244
8	13	20.0	180.0	0.0	0.1359
7	1	30.0	0.0	180.0	0.0258
7	2	30.0	15.0	165.0	0.0254
7	3	30.0	30.0	150.0	0.0254
7	4	30.0	45.0	135.0	0.0258
7	5	30.0	60.0	120.0	0.0268
7	6	30.0	75.0	105.0	0.0270
7	7	30.0	90.0	90.0	0.0308
7	8	30.0	105.0	75.0	0.0371
7	9	30.0	120.0	60.0	0.0602
7	10	30.0	135.0	45.0	0.0910
7	11	30.0	150.0	30.0	0.1215
7	12	30.0	165.0	15.0	0.1180
7	13	30.0	180.0	0.0	0.1040
6	1	40.0	0.0	180.0	0.0315
6	2	40.0	15.0	165.0	0.0320
6	3	40.0	30.0	150.0	0.0314
6	4	40.0	45.0	135.0	0.0310
6	5	40.0	60.0	120.0	0.0304
6	6	40.0	75.0	105.0	0.0307
6	7	40.0	90.0	90.0	0.0314
6	8	40.0	105.0	75.0	0.0348
6	9	40.0	120.0	60.0	0.0454
6	10	40.0	135.0	45.0	0.0814
6	11	40.0	150.0	30.0	0.1180
6	12	40.0	165.0	15.0	0.1112
6	13	40.0	180.0	0.0	0.0020
5	1	50.0	0.0	180.0	0.0504
5	2	50.0	15.0	165.0	0.0502
5	3	50.0	30.0	150.0	0.0495
5	4	50.0	45.0	135.0	0.0477
5	5	50.0	60.0	120.0	0.0464
5	6	50.0	75.0	105.0	0.0457
5	7	50.0	90.0	90.0	0.0451
5	8	50.0	105.0	75.0	0.0457
5	9	50.0	120.0	60.0	0.0498
5	10	50.0	135.0	45.0	0.0699
5	11	50.0	150.0	30.0	0.1264
5	12	50.0	165.0	15.0	0.1668
5	13	50.0	180.0	0.0	0.1618
4	1	60.0	0.0	180.0	0.0909
4	2	60.0	15.0	165.0	0.0915
4	3	60.0	30.0	150.0	0.0912
4	4	60.0	45.0	135.0	0.0883
4	5	60.0	60.0	120.0	0.0848
4	6	60.0	75.0	105.0	0.0831
4	7	60.0	90.0	90.0	0.0825
4	8	60.0	105.0	75.0	0.0799
4	9	60.0	120.0	60.0	0.0789
4	10	60.0	135.0	45.0	0.0883
4	11	60.0	150.0	30.0	0.1405
4	12	60.0	165.0	15.0	0.2450
4	13	60.0	180.0	0.0	0.3188
3	1	70.0	0.0	180.0	0.1521
3	2	70.0	15.0	165.0	0.1538
3	3	70.0	30.0	150.0	0.1551
3	4	70.0	45.0	135.0	0.1547

3	5	70.0	60.0	120.0	0.1502
3	6	70.0	75.0	105.0	0.1517
3	7	70.0	90.0	90.0	0.1523
3	8	70.0	105.0	75.0	0.1490
3	9	70.0	120.0	60.0	0.1464
3	10	70.0	135.0	45.0	0.1525
3	11	70.0	150.0	30.0	0.1848
3	12	70.0	165.0	15.0	0.3191
3	13	70.0	180.0	0.0	0.4388
2	1	80.0	0.0	180.0	0.1911
2	2	80.0	15.0	165.0	0.1994
2	3	80.0	30.0	150.0	0.2053
2	4	80.0	45.0	135.0	0.2036
2	5	80.0	60.0	120.0	0.2012
2	6	80.0	75.0	105.0	0.2169
2	7	80.0	90.0	90.0	0.2223
2	8	80.0	105.0	75.0	0.2263
2	9	80.0	120.0	60.0	0.2207
2	10	80.0	135.0	45.0	0.2376
2	11	80.0	150.0	30.0	0.2712
2	12	80.0	165.0	15.0	0.3894
2	13	80.0	180.0	0.0	0.4899
1	1	87.5	0.0	180.0	0.2008
1	2	87.5	15.0	165.0	0.2070
1	3	87.5	30.0	150.0	0.2342
1	4	87.5	45.0	135.0	0.2290
1	5	87.5	60.0	120.0	0.2287
1	6	87.5	75.0	105.0	0.2400
1	7	87.5	90.0	90.0	0.2582
1	8	87.5	105.0	75.0	0.2660
1	9	87.5	120.0	60.0	0.2819
1	10	87.5	135.0	45.0	0.3143
1	11	87.5	150.0	30.0	0.3688
1	12	87.5	165.0	15.0	0.4496
1	13	87.5	180.0	0.0	0.5285

rho for WIND SPEED = 8.0 m/s THETA_SUN = 50.0 deg

10	1	0.0	0.0	0.0	0.0330
9	1	10.0	0.0	180.0	0.0252
9	2	10.0	15.0	165.0	0.0244
9	3	10.0	30.0	150.0	0.0260
9	4	10.0	45.0	135.0	0.0242
9	5	10.0	60.0	120.0	0.0264
9	6	10.0	75.0	105.0	0.0272
9	7	10.0	90.0	90.0	0.0312
9	8	10.0	105.0	75.0	0.0335
9	9	10.0	120.0	60.0	0.0397
9	10	10.0	135.0	45.0	0.0455
9	11	10.0	150.0	30.0	0.0479
9	12	10.0	165.0	15.0	0.0632
9	13	10.0	180.0	0.0	0.0598
8	1	20.0	0.0	180.0	0.0239
8	2	20.0	15.0	165.0	0.0239
8	3	20.0	30.0	150.0	0.0235
8	4	20.0	45.0	135.0	0.0240
8	5	20.0	60.0	120.0	0.0243
8	6	20.0	75.0	105.0	0.0257
8	7	20.0	90.0	90.0	0.0267
8	8	20.0	105.0	75.0	0.0299
8	9	20.0	120.0	60.0	0.0368
8	10	20.0	135.0	45.0	0.0544
8	11	20.0	150.0	30.0	0.0766
8	12	20.0	165.0	15.0	0.0933
8	13	20.0	180.0	0.0	0.1139
7	1	30.0	0.0	180.0	0.0253
7	2	30.0	15.0	165.0	0.0252
7	3	30.0	30.0	150.0	0.0252
7	4	30.0	45.0	135.0	0.0249
7	5	30.0	60.0	120.0	0.0251
7	6	30.0	75.0	105.0	0.0253
7	7	30.0	90.0	90.0	0.0261
7	8	30.0	105.0	75.0	0.0293
7	9	30.0	120.0	60.0	0.0376
7	10	30.0	135.0	45.0	0.0552
7	11	30.0	150.0	30.0	0.0899
7	12	30.0	165.0	15.0	0.1289
7	13	30.0	180.0	0.0	0.1341
6	1	40.0	0.0	180.0	0.0318
6	2	40.0	15.0	165.0	0.0323
6	3	40.0	30.0	150.0	0.0317
6	4	40.0	45.0	135.0	0.0312
6	5	40.0	60.0	120.0	0.0306
6	6	40.0	75.0	105.0	0.0303
6	7	40.0	90.0	90.0	0.0308
6	8	40.0	105.0	75.0	0.0311
6	9	40.0	120.0	60.0	0.0340
6	10	40.0	135.0	45.0	0.0527
6	11	40.0	150.0	30.0	0.1026
6	12	40.0	165.0	15.0	0.1350
6	13	40.0	180.0	0.0	0.1214
5	1	50.0	0.0	180.0	0.0508
5	2	50.0	15.0	165.0	0.0507
5	3	50.0	30.0	150.0	0.0501
5	4	50.0	45.0	135.0	0.0484
5	5	50.0	60.0	120.0	0.0472
5	6	50.0	75.0	105.0	0.0464
5	7	50.0	90.0	90.0	0.0458
5	8	50.0	105.0	75.0	0.0453
5	9	50.0	120.0	60.0	0.0466
5	10	50.0	135.0	45.0	0.0582

5 11 50.0 150.0 30.0 0.0983
5 12 50.0 165.0 15.0 0.1433
5 13 50.0 180.0 0.0 0.0037
4 1 60.0 0.0 180.0 0.0905
4 2 60.0 15.0 165.0 0.0912
4 3 60.0 30.0 150.0 0.0912
4 4 60.0 45.0 135.0 0.0886
4 5 60.0 60.0 120.0 0.0855
4 6 60.0 75.0 105.0 0.0841
4 7 60.0 90.0 90.0 0.0837
4 8 60.0 105.0 75.0 0.0808
4 9 60.0 120.0 60.0 0.0795
4 10 60.0 135.0 45.0 0.0825
4 11 60.0 150.0 30.0 0.1196
4 12 60.0 165.0 15.0 0.2238
4 13 60.0 180.0 0.0 0.2630
3 1 70.0 0.0 180.0 0.1503
3 2 70.0 15.0 165.0 0.1521
3 3 70.0 30.0 150.0 0.1536
3 4 70.0 45.0 135.0 0.1536
3 5 70.0 60.0 120.0 0.1495
3 6 70.0 75.0 105.0 0.1515
3 7 70.0 90.0 90.0 0.1524
3 8 70.0 105.0 75.0 0.1491
3 9 70.0 120.0 60.0 0.1462
3 10 70.0 135.0 45.0 0.1503
3 11 70.0 150.0 30.0 0.1738
3 12 70.0 165.0 15.0 0.3745
3 13 70.0 180.0 0.0 0.6047
2 1 80.0 0.0 180.0 0.1902
2 2 80.0 15.0 165.0 0.1985
2 3 80.0 30.0 150.0 0.2041
2 4 80.0 45.0 135.0 0.2021
2 5 80.0 60.0 120.0 0.1993
2 6 80.0 75.0 105.0 0.2145
2 7 80.0 90.0 90.0 0.2195
2 8 80.0 105.0 75.0 0.2227
2 9 80.0 120.0 60.0 0.2171
2 10 80.0 135.0 45.0 0.2358
2 11 80.0 150.0 30.0 0.2780
2 12 80.0 165.0 15.0 0.5476
2 13 80.0 180.0 0.0 0.9824
1 1 87.5 0.0 180.0 0.2029
1 2 87.5 15.0 165.0 0.2090
1 3 87.5 30.0 150.0 0.2358
1 4 87.5 45.0 135.0 0.2294
1 5 87.5 60.0 120.0 0.2276
1 6 87.5 75.0 105.0 0.2372
1 7 87.5 90.0 90.0 0.2535
1 8 87.5 105.0 75.0 0.2593
1 9 87.5 120.0 60.0 0.2747
1 10 87.5 135.0 45.0 0.3122
1 11 87.5 150.0 30.0 0.3873
1 12 87.5 165.0 15.0 0.6380
1 13 87.5 180.0 0.0 1.3532
rho for WIND SPEED = 8.0 m/s THETA_SUN = 60.0 deg
10 1 0.0 0.0 0.0 0.0251
9 1 10.0 0.0 180.0 0.0232
9 2 10.0 15.0 165.0 0.0233
9 3 10.0 30.0 150.0 0.0239
9 4 10.0 45.0 135.0 0.0231
9 5 10.0 60.0 120.0 0.0239
9 6 10.0 75.0 105.0 0.0239
9 7 10.0 90.0 90.0 0.0240
9 8 10.0 105.0 75.0 0.0251
9 9 10.0 120.0 60.0 0.0274
9 10 10.0 135.0 45.0 0.0288
9 11 10.0 150.0 30.0 0.0326
9 12 10.0 165.0 15.0 0.0327
9 13 10.0 180.0 0.0 0.0366
8 1 20.0 0.0 180.0 0.0235
8 2 20.0 15.0 165.0 0.0232
8 3 20.0 30.0 150.0 0.0230
8 4 20.0 45.0 135.0 0.0232
8 5 20.0 60.0 120.0 0.0231
8 6 20.0 75.0 105.0 0.0240
8 7 20.0 90.0 90.0 0.0237
8 8 20.0 105.0 75.0 0.0266
8 9 20.0 120.0 60.0 0.0272
8 10 20.0 135.0 45.0 0.0341
8 11 20.0 150.0 30.0 0.0458
8 12 20.0 165.0 15.0 0.0600
8 13 20.0 180.0 0.0 0.0625
7 1 30.0 0.0 180.0 0.0250
7 2 30.0 15.0 165.0 0.0249
7 3 30.0 30.0 150.0 0.0249
7 4 30.0 45.0 135.0 0.0247
7 5 30.0 60.0 120.0 0.0248
7 6 30.0 75.0 105.0 0.0249
7 7 30.0 90.0 90.0 0.0252
7 8 30.0 105.0 75.0 0.0264
7 9 30.0 120.0 60.0 0.0296
7 10 30.0 135.0 45.0 0.0372
7 11 30.0 150.0 30.0 0.0613
7 12 30.0 165.0 15.0 0.0952
7 13 30.0 180.0 0.0 0.1116
6 1 40.0 0.0 180.0 0.0315
6 2 40.0 15.0 165.0 0.0320
6 3 40.0 30.0 150.0 0.0315

6	4	40.0	45.0	135.0	0.0311
6	5	40.0	60.0	120.0	0.0306
6	6	40.0	75.0	105.0	0.0303
6	7	40.0	90.0	90.0	0.0306
6	8	40.0	105.0	75.0	0.0310
6	9	40.0	120.0	60.0	0.0329
6	10	40.0	135.0	45.0	0.0414
6	11	40.0	150.0	30.0	0.0751
6	12	40.0	165.0	15.0	0.1409
6	13	40.0	180.0	0.0	0.1667
5	1	50.0	0.0	180.0	0.0500
5	2	50.0	15.0	165.0	0.0499
5	3	50.0	30.0	150.0	0.0495
5	4	50.0	45.0	135.0	0.0481
5	5	50.0	60.0	120.0	0.0473
5	6	50.0	75.0	105.0	0.0468
5	7	50.0	90.0	90.0	0.0463
5	8	50.0	105.0	75.0	0.0461
5	9	50.0	120.0	60.0	0.0470
5	10	50.0	135.0	45.0	0.0517
5	11	50.0	150.0	30.0	0.0844
5	12	50.0	165.0	15.0	0.1667
5	13	50.0	180.0	0.0	0.1822
4	1	60.0	0.0	180.0	0.0886
4	2	60.0	15.0	165.0	0.0894
4	3	60.0	30.0	150.0	0.0897
4	4	60.0	45.0	135.0	0.0876
4	5	60.0	60.0	120.0	0.0852
4	6	60.0	75.0	105.0	0.0843
4	7	60.0	90.0	90.0	0.0848
4	8	60.0	105.0	75.0	0.0820
4	9	60.0	120.0	60.0	0.0814
4	10	60.0	135.0	45.0	0.0830
4	11	60.0	150.0	30.0	0.1053
4	12	60.0	165.0	15.0	0.2001
4	13	60.0	180.0	0.0	0.0094
3	1	70.0	0.0	180.0	0.1482
3	2	70.0	15.0	165.0	0.1499
3	3	70.0	30.0	150.0	0.1516
3	4	70.0	45.0	135.0	0.1519
3	5	70.0	60.0	120.0	0.1483
3	6	70.0	75.0	105.0	0.1508
3	7	70.0	90.0	90.0	0.1523
3	8	70.0	105.0	75.0	0.1494
3	9	70.0	120.0	60.0	0.1466
3	10	70.0	135.0	45.0	0.1502
3	11	70.0	150.0	30.0	0.1585
3	12	70.0	165.0	15.0	0.3424
3	13	70.0	180.0	0.0	0.5062
2	1	80.0	0.0	180.0	0.1911
2	2	80.0	15.0	165.0	0.1993
2	3	80.0	30.0	150.0	0.2047
2	4	80.0	45.0	135.0	0.2022
2	5	80.0	60.0	120.0	0.1988
2	6	80.0	75.0	105.0	0.2131
2	7	80.0	90.0	90.0	0.2170
2	8	80.0	105.0	75.0	0.2192
2	9	80.0	120.0	60.0	0.2126
2	10	80.0	135.0	45.0	0.2302
2	11	80.0	150.0	30.0	0.2630
2	12	80.0	165.0	15.0	0.6068
2	13	80.0	180.0	0.0	1.3228
1	1	87.5	0.0	180.0	0.2080
1	2	87.5	15.0	165.0	0.2140
1	3	87.5	30.0	150.0	0.2409
1	4	87.5	45.0	135.0	0.2333
1	5	87.5	60.0	120.0	0.2295
1	6	87.5	75.0	105.0	0.2365
1	7	87.5	90.0	90.0	0.2496
1	8	87.5	105.0	75.0	0.2523
1	9	87.5	120.0	60.0	0.2649
1	10	87.5	135.0	45.0	0.3022
1	11	87.5	150.0	30.0	0.3825
1	12	87.5	165.0	15.0	0.8565
1	13	87.5	180.0	0.0	2.5976

rho for WIND SPEED = 8.0 m/s THETA_SUN = 70.0 deg

10	1	0.0	0.0	0.0	0.0233
9	1	10.0	0.0	180.0	0.0225
9	2	10.0	15.0	165.0	0.0226
9	3	10.0	30.0	150.0	0.0227
9	4	10.0	45.0	135.0	0.0224
9	5	10.0	60.0	120.0	0.0226
9	6	10.0	75.0	105.0	0.0229
9	7	10.0	90.0	90.0	0.0229
9	8	10.0	105.0	75.0	0.0237
9	9	10.0	120.0	60.0	0.0237
9	10	10.0	135.0	45.0	0.0245
9	11	10.0	150.0	30.0	0.0257
9	12	10.0	165.0	15.0	0.0264
9	13	10.0	180.0	0.0	0.0271
8	1	20.0	0.0	180.0	0.0230
8	2	20.0	15.0	165.0	0.0227
8	3	20.0	30.0	150.0	0.0225
8	4	20.0	45.0	135.0	0.0227
8	5	20.0	60.0	120.0	0.0226
8	6	20.0	75.0	105.0	0.0231
8	7	20.0	90.0	90.0	0.0228
8	8	20.0	105.0	75.0	0.0240
8	9	20.0	120.0	60.0	0.0245

8	10	20.0	135.0	45.0	0.0271
8	11	20.0	150.0	30.0	0.0318
8	12	20.0	165.0	15.0	0.0352
8	13	20.0	180.0	0.0	0.0377
7	1	30.0	0.0	180.0	0.0245
7	2	30.0	15.0	165.0	0.0245
7	3	30.0	30.0	150.0	0.0245
7	4	30.0	45.0	135.0	0.0243
7	5	30.0	60.0	120.0	0.0244
7	6	30.0	75.0	105.0	0.0244
7	7	30.0	90.0	90.0	0.0248
7	8	30.0	105.0	75.0	0.0252
7	9	30.0	120.0	60.0	0.0266
7	10	30.0	135.0	45.0	0.0314
7	11	30.0	150.0	30.0	0.0424
7	12	30.0	165.0	15.0	0.0664
7	13	30.0	180.0	0.0	0.0797
6	1	40.0	0.0	180.0	0.0308
6	2	40.0	15.0	165.0	0.0313
6	3	40.0	30.0	150.0	0.0309
6	4	40.0	45.0	135.0	0.0307
6	5	40.0	60.0	120.0	0.0303
6	6	40.0	75.0	105.0	0.0301
6	7	40.0	90.0	90.0	0.0305
6	8	40.0	105.0	75.0	0.0307
6	9	40.0	120.0	60.0	0.0323
6	10	40.0	135.0	45.0	0.0370
6	11	40.0	150.0	30.0	0.0570
6	12	40.0	165.0	15.0	0.1254
6	13	40.0	180.0	0.0	0.1642
5	1	50.0	0.0	180.0	0.0486
5	2	50.0	15.0	165.0	0.0485
5	3	50.0	30.0	150.0	0.0483
5	4	50.0	45.0	135.0	0.0472
5	5	50.0	60.0	120.0	0.0468
5	6	50.0	75.0	105.0	0.0467
5	7	50.0	90.0	90.0	0.0466
5	8	50.0	105.0	75.0	0.0467
5	9	50.0	120.0	60.0	0.0479
5	10	50.0	135.0	45.0	0.0525
5	11	50.0	150.0	30.0	0.0763
5	12	50.0	165.0	15.0	0.1841
5	13	50.0	180.0	0.0	0.2892
4	1	60.0	0.0	180.0	0.0862
4	2	60.0	15.0	165.0	0.0870
4	3	60.0	30.0	150.0	0.0875
4	4	60.0	45.0	135.0	0.0859
4	5	60.0	60.0	120.0	0.0841
4	6	60.0	75.0	105.0	0.0841
4	7	60.0	90.0	90.0	0.0851
4	8	60.0	105.0	75.0	0.0833
4	9	60.0	120.0	60.0	0.0835
4	10	60.0	135.0	45.0	0.0876
4	11	60.0	150.0	30.0	0.1043
4	12	60.0	165.0	15.0	0.2309
4	13	60.0	180.0	0.0	0.3230
3	1	70.0	0.0	180.0	0.1463
3	2	70.0	15.0	165.0	0.1479
3	3	70.0	30.0	150.0	0.1496
3	4	70.0	45.0	135.0	0.1501
3	5	70.0	60.0	120.0	0.1470
3	6	70.0	75.0	105.0	0.1499
3	7	70.0	90.0	90.0	0.1521
3	8	70.0	105.0	75.0	0.1496
3	9	70.0	120.0	60.0	0.1477
3	10	70.0	135.0	45.0	0.1528
3	11	70.0	150.0	30.0	0.1535
3	12	70.0	165.0	15.0	0.2936
3	13	70.0	180.0	0.0	0.0310
2	1	80.0	0.0	180.0	0.1932
2	2	80.0	15.0	165.0	0.2012
2	3	80.0	30.0	150.0	0.2064
2	4	80.0	45.0	135.0	0.2034
2	5	80.0	60.0	120.0	0.1992
2	6	80.0	75.0	105.0	0.2124
2	7	80.0	90.0	90.0	0.2153
2	8	80.0	105.0	75.0	0.2162
2	9	80.0	120.0	60.0	0.2081
2	10	80.0	135.0	45.0	0.2222
2	11	80.0	150.0	30.0	0.2407
2	12	80.0	165.0	15.0	0.4454
2	13	80.0	180.0	0.0	0.9883
1	1	87.5	0.0	180.0	0.2149
1	2	87.5	15.0	165.0	0.2208
1	3	87.5	30.0	150.0	0.2479
1	4	87.5	45.0	135.0	0.2389
1	5	87.5	60.0	120.0	0.2331
1	6	87.5	75.0	105.0	0.2373
1	7	87.5	90.0	90.0	0.2470
1	8	87.5	105.0	75.0	0.2461
1	9	87.5	120.0	60.0	0.2542
1	10	87.5	135.0	45.0	0.2839
1	11	87.5	150.0	30.0	0.3445
1	12	87.5	165.0	15.0	0.6786
1	13	87.5	180.0	0.0	2.2662

rho for WIND SPEED = 8.0 m/s THETA_SUN = 80.0 deg

10	1	0.0	0.0	0.0	0.0222
9	1	10.0	0.0	180.0	0.0218
9	2	10.0	15.0	165.0	0.0220

9	3	10.0	30.0	150.0	0.0221
9	4	10.0	45.0	135.0	0.0218
9	5	10.0	60.0	120.0	0.0219
9	6	10.0	75.0	105.0	0.0222
9	7	10.0	90.0	90.0	0.0221
9	8	10.0	105.0	75.0	0.0225
9	9	10.0	120.0	60.0	0.0224
9	10	10.0	135.0	45.0	0.0227
9	11	10.0	150.0	30.0	0.0233
9	12	10.0	165.0	15.0	0.0234
9	13	10.0	180.0	0.0	0.0238
8	1	20.0	0.0	180.0	0.0225
8	2	20.0	15.0	165.0	0.0222
8	3	20.0	30.0	150.0	0.0220
8	4	20.0	45.0	135.0	0.0222
8	5	20.0	60.0	120.0	0.0221
8	6	20.0	75.0	105.0	0.0226
8	7	20.0	90.0	90.0	0.0222
8	8	20.0	105.0	75.0	0.0231
8	9	20.0	120.0	60.0	0.0232
8	10	20.0	135.0	45.0	0.0243
8	11	20.0	150.0	30.0	0.0255
8	12	20.0	165.0	15.0	0.0269
8	13	20.0	180.0	0.0	0.0284
7	1	30.0	0.0	180.0	0.0240
7	2	30.0	15.0	165.0	0.0239
7	3	30.0	30.0	150.0	0.0240
7	4	30.0	45.0	135.0	0.0238
7	5	30.0	60.0	120.0	0.0240
7	6	30.0	75.0	105.0	0.0240
7	7	30.0	90.0	90.0	0.0243
7	8	30.0	105.0	75.0	0.0245
7	9	30.0	120.0	60.0	0.0255
7	10	30.0	135.0	45.0	0.0274
7	11	30.0	150.0	30.0	0.0322
7	12	30.0	165.0	15.0	0.0409
7	13	30.0	180.0	0.0	0.0469
6	1	40.0	0.0	180.0	0.0300
6	2	40.0	15.0	165.0	0.0305
6	3	40.0	30.0	150.0	0.0302
6	4	40.0	45.0	135.0	0.0300
6	5	40.0	60.0	120.0	0.0298
6	6	40.0	75.0	105.0	0.0297
6	7	40.0	90.0	90.0	0.0302
6	8	40.0	105.0	75.0	0.0303
6	9	40.0	120.0	60.0	0.0317
6	10	40.0	135.0	45.0	0.0357
6	11	40.0	150.0	30.0	0.0472
6	12	40.0	165.0	15.0	0.0802
6	13	40.0	180.0	0.0	0.1150
5	1	50.0	0.0	180.0	0.0471
5	2	50.0	15.0	165.0	0.0471
5	3	50.0	30.0	150.0	0.0469
5	4	50.0	45.0	135.0	0.0461
5	5	50.0	60.0	120.0	0.0460
5	6	50.0	75.0	105.0	0.0463
5	7	50.0	90.0	90.0	0.0465
5	8	50.0	105.0	75.0	0.0468
5	9	50.0	120.0	60.0	0.0483
5	10	50.0	135.0	45.0	0.0541
5	11	50.0	150.0	30.0	0.0720
5	12	50.0	165.0	15.0	0.1568
5	13	50.0	180.0	0.0	0.2784
4	1	60.0	0.0	180.0	0.0840
4	2	60.0	15.0	165.0	0.0848
4	3	60.0	30.0	150.0	0.0854
4	4	60.0	45.0	135.0	0.0842
4	5	60.0	60.0	120.0	0.0828
4	6	60.0	75.0	105.0	0.0834
4	7	60.0	90.0	90.0	0.0850
4	8	60.0	105.0	75.0	0.0838
4	9	60.0	120.0	60.0	0.0851
4	10	60.0	135.0	45.0	0.0933
4	11	60.0	150.0	30.0	0.1136
4	12	60.0	165.0	15.0	0.2297
4	13	60.0	180.0	0.0	0.4627
3	1	70.0	0.0	180.0	0.1450
3	2	70.0	15.0	165.0	0.1465
3	3	70.0	30.0	150.0	0.1482
3	4	70.0	45.0	135.0	0.1488
3	5	70.0	60.0	120.0	0.1458
3	6	70.0	75.0	105.0	0.1491
3	7	70.0	90.0	90.0	0.1515
3	8	70.0	105.0	75.0	0.1498
3	9	70.0	120.0	60.0	0.1484
3	10	70.0	135.0	45.0	0.1570
3	11	70.0	150.0	30.0	0.1661
3	12	70.0	165.0	15.0	0.2595
3	13	70.0	180.0	0.0	0.4917
2	1	80.0	0.0	180.0	0.1959
2	2	80.0	15.0	165.0	0.2038
2	3	80.0	30.0	150.0	0.2087
2	4	80.0	45.0	135.0	0.2051
2	5	80.0	60.0	120.0	0.2001
2	6	80.0	75.0	105.0	0.2122
2	7	80.0	90.0	90.0	0.2142
2	8	80.0	105.0	75.0	0.2139
2	9	80.0	120.0	60.0	0.2046
2	10	80.0	135.0	45.0	0.2143
2	11	80.0	150.0	30.0	0.2215

2 12 80.0 165.0 15.0 0.2725
2 13 80.0 180.0 0.0 0.0882
1 1 87.5 0.0 180.0 0.2221
1 2 87.5 15.0 165.0 0.2278
1 3 87.5 30.0 150.0 0.2550
1 4 87.5 45.0 135.0 0.2446
1 5 87.5 60.0 120.0 0.2368
1 6 87.5 75.0 105.0 0.2385
1 7 87.5 90.0 90.0 0.2454
1 8 87.5 105.0 75.0 0.2416
1 9 87.5 120.0 60.0 0.2449
1 10 87.5 135.0 45.0 0.2615
1 11 87.5 150.0 30.0 0.2842
1 12 87.5 165.0 15.0 0.3235
1 13 87.5 180.0 0.0 0.8327
rho for WIND SPEED = 10.0 m/s THETA_SUN = 0.0 deg
10 1 0.0 0.0 0.0 0.0008
9 1 10.0 0.0 180.0 0.0998
9 2 10.0 15.0 165.0 0.0919
9 3 10.0 30.0 150.0 0.0977
9 4 10.0 45.0 135.0 0.1020
9 5 10.0 60.0 120.0 0.0959
9 6 10.0 75.0 105.0 0.0917
9 7 10.0 90.0 90.0 0.0985
9 8 10.0 105.0 75.0 0.0917
9 9 10.0 120.0 60.0 0.0959
9 10 10.0 135.0 45.0 0.1020
9 11 10.0 150.0 30.0 0.0977
9 12 10.0 165.0 15.0 0.0919
9 13 10.0 180.0 0.0 0.0998
8 1 20.0 0.0 180.0 0.1435
8 2 20.0 15.0 165.0 0.1380
8 3 20.0 30.0 150.0 0.1361
8 4 20.0 45.0 135.0 0.1406
8 5 20.0 60.0 120.0 0.1356
8 6 20.0 75.0 105.0 0.1361
8 7 20.0 90.0 90.0 0.1366
8 8 20.0 105.0 75.0 0.1361
8 9 20.0 120.0 60.0 0.1356
8 10 20.0 135.0 45.0 0.1406
8 11 20.0 150.0 30.0 0.1361
8 12 20.0 165.0 15.0 0.1380
8 13 20.0 180.0 0.0 0.1435
7 1 30.0 0.0 180.0 0.1321
7 2 30.0 15.0 165.0 0.1298
7 3 30.0 30.0 150.0 0.1335
7 4 30.0 45.0 135.0 0.1326
7 5 30.0 60.0 120.0 0.1363
7 6 30.0 75.0 105.0 0.1357
7 7 30.0 90.0 90.0 0.1231
7 8 30.0 105.0 75.0 0.1357
7 9 30.0 120.0 60.0 0.1363
7 10 30.0 135.0 45.0 0.1326
7 11 30.0 150.0 30.0 0.1335
7 12 30.0 165.0 15.0 0.1298
7 13 30.0 180.0 0.0 0.1321
6 1 40.0 0.0 180.0 0.0941
6 2 40.0 15.0 165.0 0.0943
6 3 40.0 30.0 150.0 0.0915
6 4 40.0 45.0 135.0 0.0931
6 5 40.0 60.0 120.0 0.0932
6 6 40.0 75.0 105.0 0.0971
6 7 40.0 90.0 90.0 0.0902
6 8 40.0 105.0 75.0 0.0971
6 9 40.0 120.0 60.0 0.0932
6 10 40.0 135.0 45.0 0.0931
6 11 40.0 150.0 30.0 0.0915
6 12 40.0 165.0 15.0 0.0943
6 13 40.0 180.0 0.0 0.0942
5 1 50.0 0.0 180.0 0.0654
5 2 50.0 15.0 165.0 0.0686
5 3 50.0 30.0 150.0 0.0654
5 4 50.0 45.0 135.0 0.0659
5 5 50.0 60.0 120.0 0.0675
5 6 50.0 75.0 105.0 0.0672
5 7 50.0 90.0 90.0 0.0613
5 8 50.0 105.0 75.0 0.0672
5 9 50.0 120.0 60.0 0.0675
5 10 50.0 135.0 45.0 0.0659
5 11 50.0 150.0 30.0 0.0654
5 12 50.0 165.0 15.0 0.0686
5 13 50.0 180.0 0.0 0.0654
4 1 60.0 0.0 180.0 0.0831
4 2 60.0 15.0 165.0 0.0852
4 3 60.0 30.0 150.0 0.0851
4 4 60.0 45.0 135.0 0.0840
4 5 60.0 60.0 120.0 0.0838
4 6 60.0 75.0 105.0 0.0846
4 7 60.0 90.0 90.0 0.0861
4 8 60.0 105.0 75.0 0.0846
4 9 60.0 120.0 60.0 0.0838
4 10 60.0 135.0 45.0 0.0840
4 11 60.0 150.0 30.0 0.0851
4 12 60.0 165.0 15.0 0.0852
4 13 60.0 180.0 0.0 0.0831
3 1 70.0 0.0 180.0 0.1389
3 2 70.0 15.0 165.0 0.1409
3 3 70.0 30.0 150.0 0.1442
3 4 70.0 45.0 135.0 0.1427

3	5	70.0	60.0	120.0	0.1401
3	6	70.0	75.0	105.0	0.1441
3	7	70.0	90.0	90.0	0.1471
3	8	70.0	105.0	75.0	0.1441
3	9	70.0	120.0	60.0	0.1401
3	10	70.0	135.0	45.0	0.1427
3	11	70.0	150.0	30.0	0.1442
3	12	70.0	165.0	15.0	0.1409
3	13	70.0	180.0	0.0	0.1389
2	1	80.0	0.0	180.0	0.1962
2	2	80.0	15.0	165.0	0.2030
2	3	80.0	30.0	150.0	0.2072
2	4	80.0	45.0	135.0	0.2046
2	5	80.0	60.0	120.0	0.1959
2	6	80.0	75.0	105.0	0.2095
2	7	80.0	90.0	90.0	0.2099
2	8	80.0	105.0	75.0	0.2095
2	9	80.0	120.0	60.0	0.1959
2	10	80.0	135.0	45.0	0.2046
2	11	80.0	150.0	30.0	0.2072
2	12	80.0	165.0	15.0	0.2030
2	13	80.0	180.0	0.0	0.1962
1	1	87.5	0.0	180.0	0.2224
1	2	87.5	15.0	165.0	0.2338
1	3	87.5	30.0	150.0	0.2585
1	4	87.5	45.0	135.0	0.2440
1	5	87.5	60.0	120.0	0.2365
1	6	87.5	75.0	105.0	0.2380
1	7	87.5	90.0	90.0	0.2356
1	8	87.5	105.0	75.0	0.2380
1	9	87.5	120.0	60.0	0.2365
1	10	87.5	135.0	45.0	0.2440
1	11	87.5	150.0	30.0	0.2585
1	12	87.5	165.0	15.0	0.2338
1	13	87.5	180.0	0.0	0.2224

rho for WIND SPEED = 10.0 m/s THETA_SUN = 10.0 deg

10	1	0.0	0.0	0.0	0.0883
9	1	10.0	0.0	180.0	0.1331
9	2	10.0	15.0	165.0	0.1410
9	3	10.0	30.0	150.0	0.1277
9	4	10.0	45.0	135.0	0.1287
9	5	10.0	60.0	120.0	0.1246
9	6	10.0	75.0	105.0	0.1226
9	7	10.0	90.0	90.0	0.1184
9	8	10.0	105.0	75.0	0.1018
9	9	10.0	120.0	60.0	0.0859
9	10	10.0	135.0	45.0	0.0736
9	11	10.0	150.0	30.0	0.0685
9	12	10.0	165.0	15.0	0.0567
9	13	10.0	180.0	0.0	0.0003
8	1	20.0	0.0	180.0	0.1168
8	2	20.0	15.0	165.0	0.1142
8	3	20.0	30.0	150.0	0.1183
8	4	20.0	45.0	135.0	0.1327
8	5	20.0	60.0	120.0	0.1324
8	6	20.0	75.0	105.0	0.1450
8	7	20.0	90.0	90.0	0.1405
8	8	20.0	105.0	75.0	0.1402
8	9	20.0	120.0	60.0	0.1222
8	10	20.0	135.0	45.0	0.1211
8	11	20.0	150.0	30.0	0.1095
8	12	20.0	165.0	15.0	0.1069
8	13	20.0	180.0	0.0	0.0927
7	1	30.0	0.0	180.0	0.0833
7	2	30.0	15.0	165.0	0.0787
7	3	30.0	30.0	150.0	0.0818
7	4	30.0	45.0	135.0	0.0830
7	5	30.0	60.0	120.0	0.0997
7	6	30.0	75.0	105.0	0.1168
7	7	30.0	90.0	90.0	0.1161
7	8	30.0	105.0	75.0	0.1330
7	9	30.0	120.0	60.0	0.1355
7	10	30.0	135.0	45.0	0.1503
7	11	30.0	150.0	30.0	0.1461
7	12	30.0	165.0	15.0	0.1512
7	13	30.0	180.0	0.0	0.1555
6	1	40.0	0.0	180.0	0.0529
6	2	40.0	15.0	165.0	0.0517
6	3	40.0	30.0	150.0	0.0531
6	4	40.0	45.0	135.0	0.0543
6	5	40.0	60.0	120.0	0.0591
6	6	40.0	75.0	105.0	0.0728
6	7	40.0	90.0	90.0	0.0810
6	8	40.0	105.0	75.0	0.0925
6	9	40.0	120.0	60.0	0.1115
6	10	40.0	135.0	45.0	0.1288
6	11	40.0	150.0	30.0	0.1449
6	12	40.0	165.0	15.0	0.1572
6	13	40.0	180.0	0.0	0.1596
5	1	50.0	0.0	180.0	0.0483
5	2	50.0	15.0	165.0	0.0489
5	3	50.0	30.0	150.0	0.0523
5	4	50.0	45.0	135.0	0.0525
5	5	50.0	60.0	120.0	0.0521
5	6	50.0	75.0	105.0	0.0541
5	7	50.0	90.0	90.0	0.0619
5	8	50.0	105.0	75.0	0.0618
5	9	50.0	120.0	60.0	0.0800
5	10	50.0	135.0	45.0	0.0908

5 11 50.0 150.0 30.0 0.1087
5 12 50.0 165.0 15.0 0.1216
5 13 50.0 180.0 0.0 0.1304
4 1 60.0 0.0 180.0 0.0836
4 2 60.0 15.0 165.0 0.0839
4 3 60.0 30.0 150.0 0.0843
4 4 60.0 45.0 135.0 0.0824
4 5 60.0 60.0 120.0 0.0810
4 6 60.0 75.0 105.0 0.0824
4 7 60.0 90.0 90.0 0.0861
4 8 60.0 105.0 75.0 0.0840
4 9 60.0 120.0 60.0 0.0888
4 10 60.0 135.0 45.0 0.0948
4 11 60.0 150.0 30.0 0.1018
4 12 60.0 165.0 15.0 0.1056
4 13 60.0 180.0 0.0 0.1059
3 1 70.0 0.0 180.0 0.1397
3 2 70.0 15.0 165.0 0.1423
3 3 70.0 30.0 150.0 0.1450
3 4 70.0 45.0 135.0 0.1437
3 5 70.0 60.0 120.0 0.1404
3 6 70.0 75.0 105.0 0.1439
3 7 70.0 90.0 90.0 0.1469
3 8 70.0 105.0 75.0 0.1437
3 9 70.0 120.0 60.0 0.1412
3 10 70.0 135.0 45.0 0.1472
3 11 70.0 150.0 30.0 0.1447
3 12 70.0 165.0 15.0 0.1461
3 13 70.0 180.0 0.0 0.1448
2 1 80.0 0.0 180.0 0.1873
2 2 80.0 15.0 165.0 0.1945
2 3 80.0 30.0 150.0 0.1996
2 4 80.0 45.0 135.0 0.1981
2 5 80.0 60.0 120.0 0.1912
2 6 80.0 75.0 105.0 0.2066
2 7 80.0 90.0 90.0 0.2091
2 8 80.0 105.0 75.0 0.2110
2 9 80.0 120.0 60.0 0.1995
2 10 80.0 135.0 45.0 0.2103
2 11 80.0 150.0 30.0 0.2153
2 12 80.0 165.0 15.0 0.2114
2 13 80.0 180.0 0.0 0.2051
1 1 87.5 0.0 180.0 0.2005
1 2 87.5 15.0 165.0 0.2122
1 3 87.5 30.0 150.0 0.2371
1 4 87.5 45.0 135.0 0.2272
1 5 87.5 60.0 120.0 0.2244
1 6 87.5 75.0 105.0 0.2311
1 7 87.5 90.0 90.0 0.2345
1 8 87.5 105.0 75.0 0.2427
1 9 87.5 120.0 60.0 0.2466
1 10 87.5 135.0 45.0 0.2591
1 11 87.5 150.0 30.0 0.2787
1 12 87.5 165.0 15.0 0.2549
1 13 87.5 180.0 0.0 0.2442
rho for WIND SPEED = 10.0 m/s THETA_SUN = 20.0 deg
10 1 0.0 0.0 0.0 0.1233
9 1 10.0 0.0 180.0 0.1352
9 2 10.0 15.0 165.0 0.1131
9 3 10.0 30.0 150.0 0.1238
9 4 10.0 45.0 135.0 0.1164
9 5 10.0 60.0 120.0 0.1330
9 6 10.0 75.0 105.0 0.1360
9 7 10.0 90.0 90.0 0.1331
9 8 10.0 105.0 75.0 0.1355
9 9 10.0 120.0 60.0 0.1169
9 10 10.0 135.0 45.0 0.1047
9 11 10.0 150.0 30.0 0.0989
9 12 10.0 165.0 15.0 0.0898
9 13 10.0 180.0 0.0 0.0754
8 1 20.0 0.0 180.0 0.0817
8 2 20.0 15.0 165.0 0.0693
8 3 20.0 30.0 150.0 0.0854
8 4 20.0 45.0 135.0 0.0846
8 5 20.0 60.0 120.0 0.1002
8 6 20.0 75.0 105.0 0.1101
8 7 20.0 90.0 90.0 0.1248
8 8 20.0 105.0 75.0 0.1275
8 9 20.0 120.0 60.0 0.1319
8 10 20.0 135.0 45.0 0.1162
8 11 20.0 150.0 30.0 0.0879
8 12 20.0 165.0 15.0 0.0693
8 13 20.0 180.0 0.0 0.0006
7 1 30.0 0.0 180.0 0.0421
7 2 30.0 15.0 165.0 0.0475
7 3 30.0 30.0 150.0 0.0497
7 4 30.0 45.0 135.0 0.0527
7 5 30.0 60.0 120.0 0.0617
7 6 30.0 75.0 105.0 0.0732
7 7 30.0 90.0 90.0 0.0969
7 8 30.0 105.0 75.0 0.1142
7 9 30.0 120.0 60.0 0.1278
7 10 30.0 135.0 45.0 0.1344
7 11 30.0 150.0 30.0 0.1207
7 12 30.0 165.0 15.0 0.1062
7 13 30.0 180.0 0.0 0.0966
6 1 40.0 0.0 180.0 0.0351
6 2 40.0 15.0 165.0 0.0359
6 3 40.0 30.0 150.0 0.0349

6 4 40.0 45.0 135.0 0.0376
6 5 40.0 60.0 120.0 0.0372
6 6 40.0 75.0 105.0 0.0508
6 7 40.0 90.0 90.0 0.0601
6 8 40.0 105.0 75.0 0.0867
6 9 40.0 120.0 60.0 0.1063
6 10 40.0 135.0 45.0 0.1284
6 11 40.0 150.0 30.0 0.1516
6 12 40.0 165.0 15.0 0.1634
6 13 40.0 180.0 0.0 0.1721
5 1 50.0 0.0 180.0 0.0501
5 2 50.0 15.0 165.0 0.0495
5 3 50.0 30.0 150.0 0.0495
5 4 50.0 45.0 135.0 0.0488
5 5 50.0 60.0 120.0 0.0485
5 6 50.0 75.0 105.0 0.0504
5 7 50.0 90.0 90.0 0.0516
5 8 50.0 105.0 75.0 0.0603
5 9 50.0 120.0 60.0 0.0769
5 10 50.0 135.0 45.0 0.1144
5 11 50.0 150.0 30.0 0.1409
5 12 50.0 165.0 15.0 0.1791
5 13 50.0 180.0 0.0 0.1902
4 1 60.0 0.0 180.0 0.0866
4 2 60.0 15.0 165.0 0.0874
4 3 60.0 30.0 150.0 0.0873
4 4 60.0 45.0 135.0 0.0850
4 5 60.0 60.0 120.0 0.0821
4 6 60.0 75.0 105.0 0.0818
4 7 60.0 90.0 90.0 0.0845
4 8 60.0 105.0 75.0 0.0842
4 9 60.0 120.0 60.0 0.0861
4 10 60.0 135.0 45.0 0.1054
4 11 60.0 150.0 30.0 0.1300
4 12 60.0 165.0 15.0 0.1656
4 13 60.0 180.0 0.0 0.1719
3 1 70.0 0.0 180.0 0.1415
3 2 70.0 15.0 165.0 0.1442
3 3 70.0 30.0 150.0 0.1469
3 4 70.0 45.0 135.0 0.1450
3 5 70.0 60.0 120.0 0.1409
3 6 70.0 75.0 105.0 0.1439
3 7 70.0 90.0 90.0 0.1465
3 8 70.0 105.0 75.0 0.1432
3 9 70.0 120.0 60.0 0.1412
3 10 70.0 135.0 45.0 0.1503
3 11 70.0 150.0 30.0 0.1604
3 12 70.0 165.0 15.0 0.1777
3 13 70.0 180.0 0.0 0.1838
2 1 80.0 0.0 180.0 0.1787
2 2 80.0 15.0 165.0 0.1862
2 3 80.0 30.0 150.0 0.1920
2 4 80.0 45.0 135.0 0.1914
2 5 80.0 60.0 120.0 0.1859
2 6 80.0 75.0 105.0 0.2027
2 7 80.0 90.0 90.0 0.2070
2 8 80.0 105.0 75.0 0.2107
2 9 80.0 120.0 60.0 0.2012
2 10 80.0 135.0 45.0 0.2150
2 11 80.0 150.0 30.0 0.2256
2 12 80.0 165.0 15.0 0.2259
2 13 80.0 180.0 0.0 0.2276
1 1 87.5 0.0 180.0 0.1828
1 2 87.5 15.0 165.0 0.1944
1 3 87.5 30.0 150.0 0.2191
1 4 87.5 45.0 135.0 0.2122
1 5 87.5 60.0 120.0 0.2127
1 6 87.5 75.0 105.0 0.2233
1 7 87.5 90.0 90.0 0.2315
1 8 87.5 105.0 75.0 0.2439
1 9 87.5 120.0 60.0 0.2526
1 10 87.5 135.0 45.0 0.2703
1 11 87.5 150.0 30.0 0.2966
1 12 87.5 165.0 15.0 0.2763
1 13 87.5 180.0 0.0 0.2678
rho for WIND SPEED = 10.0 m/s THETA_SUN = 30.0 deg
10 1 0.0 0.0 0.0 0.1143
9 1 10.0 0.0 180.0 0.0700
9 2 10.0 15.0 165.0 0.0795
9 3 10.0 30.0 150.0 0.0788
9 4 10.0 45.0 135.0 0.0777
9 5 10.0 60.0 120.0 0.1056
9 6 10.0 75.0 105.0 0.0859
9 7 10.0 90.0 90.0 0.0904
9 8 10.0 105.0 75.0 0.1122
9 9 10.0 120.0 60.0 0.1178
9 10 10.0 135.0 45.0 0.1173
9 11 10.0 150.0 30.0 0.1287
9 12 10.0 165.0 15.0 0.1181
9 13 10.0 180.0 0.0 0.1173
8 1 20.0 0.0 180.0 0.0514
8 2 20.0 15.0 165.0 0.0423
8 3 20.0 30.0 150.0 0.0452
8 4 20.0 45.0 135.0 0.0497
8 5 20.0 60.0 120.0 0.0509
8 6 20.0 75.0 105.0 0.0656
8 7 20.0 90.0 90.0 0.0842
8 8 20.0 105.0 75.0 0.0993
8 9 20.0 120.0 60.0 0.1194

8 10 20.0 135.0 45.0 0.1268
8 11 20.0 150.0 30.0 0.1143
8 12 20.0 165.0 15.0 0.0909
8 13 20.0 180.0 0.0 0.0847
7 1 30.0 0.0 180.0 0.0271
7 2 30.0 15.0 165.0 0.0304
7 3 30.0 30.0 150.0 0.0326
7 4 30.0 45.0 135.0 0.0322
7 5 30.0 60.0 120.0 0.0355
7 6 30.0 75.0 105.0 0.0383
7 7 30.0 90.0 90.0 0.0646
7 8 30.0 105.0 75.0 0.0841
7 9 30.0 120.0 60.0 0.1094
7 10 30.0 135.0 45.0 0.1198
7 11 30.0 150.0 30.0 0.1106
7 12 30.0 165.0 15.0 0.0789
7 13 30.0 180.0 0.0 0.0010
6 1 40.0 0.0 180.0 0.0343
6 2 40.0 15.0 165.0 0.0336
6 3 40.0 30.0 150.0 0.0330
6 4 40.0 45.0 135.0 0.0336
6 5 40.0 60.0 120.0 0.0337
6 6 40.0 75.0 105.0 0.0365
6 7 40.0 90.0 90.0 0.0437
6 8 40.0 105.0 75.0 0.0568
6 9 40.0 120.0 60.0 0.0881
6 10 40.0 135.0 45.0 0.1106
6 11 40.0 150.0 30.0 0.1314
6 12 40.0 165.0 15.0 0.1231
6 13 40.0 180.0 0.0 0.1082
5 1 50.0 0.0 180.0 0.0517
5 2 50.0 15.0 165.0 0.0515
5 3 50.0 30.0 150.0 0.0512
5 4 50.0 45.0 135.0 0.0499
5 5 50.0 60.0 120.0 0.0480
5 6 50.0 75.0 105.0 0.0477
5 7 50.0 90.0 90.0 0.0484
5 8 50.0 105.0 75.0 0.0533
5 9 50.0 120.0 60.0 0.0705
5 10 50.0 135.0 45.0 0.1049
5 11 50.0 150.0 30.0 0.1542
5 12 50.0 165.0 15.0 0.1889
5 13 50.0 180.0 0.0 0.2004
4 1 60.0 0.0 180.0 0.0905
4 2 60.0 15.0 165.0 0.0913
4 3 60.0 30.0 150.0 0.0909
4 4 60.0 45.0 135.0 0.0879
4 5 60.0 60.0 120.0 0.0841
4 6 60.0 75.0 105.0 0.0829
4 7 60.0 90.0 90.0 0.0837
4 8 60.0 105.0 75.0 0.0818
4 9 60.0 120.0 60.0 0.0836
4 10 60.0 135.0 45.0 0.1027
4 11 60.0 150.0 30.0 0.1641
4 12 60.0 165.0 15.0 0.2392
4 13 60.0 180.0 0.0 0.2606
3 1 70.0 0.0 180.0 0.1420
3 2 70.0 15.0 165.0 0.1449
3 3 70.0 30.0 150.0 0.1477
3 4 70.0 45.0 135.0 0.1458
3 5 70.0 60.0 120.0 0.1413
3 6 70.0 75.0 105.0 0.1439
3 7 70.0 90.0 90.0 0.1461
3 8 70.0 105.0 75.0 0.1426
3 9 70.0 120.0 60.0 0.1404
3 10 70.0 135.0 45.0 0.1564
3 11 70.0 150.0 30.0 0.1836
3 12 70.0 165.0 15.0 0.2477
3 13 70.0 180.0 0.0 0.2988
2 1 80.0 0.0 180.0 0.1721
2 2 80.0 15.0 165.0 0.1798
2 3 80.0 30.0 150.0 0.1859
2 4 80.0 45.0 135.0 0.1857
2 5 80.0 60.0 120.0 0.1812
2 6 80.0 75.0 105.0 0.1987
2 7 80.0 90.0 90.0 0.2039
2 8 80.0 105.0 75.0 0.2086
2 9 80.0 120.0 60.0 0.2009
2 10 80.0 135.0 45.0 0.2193
2 11 80.0 150.0 30.0 0.2429
2 12 80.0 165.0 15.0 0.2928
2 13 80.0 180.0 0.0 0.3105
1 1 87.5 0.0 180.0 0.1724
1 2 87.5 15.0 165.0 0.1839
1 3 87.5 30.0 150.0 0.2079
1 4 87.5 45.0 135.0 0.2019
1 5 87.5 60.0 120.0 0.2037
1 6 87.5 75.0 105.0 0.2161
1 7 87.5 90.0 90.0 0.2271
1 8 87.5 105.0 75.0 0.2417
1 9 87.5 120.0 60.0 0.2536
1 10 87.5 135.0 45.0 0.2773
1 11 87.5 150.0 30.0 0.3210
1 12 87.5 165.0 15.0 0.3267
1 13 87.5 180.0 0.0 0.3556
rho for WIND SPEED = 10.0 m/s THETA_SUN = 40.0
deg
10 1 0.0 0.0 0.0 0.0689
9 1 10.0 0.0 180.0 0.0391
9 2 10.0 15.0 165.0 0.0447

9	3	10.0	30.0	150.0	0.0480
9	4	10.0	45.0	135.0	0.0445
9	5	10.0	60.0	120.0	0.0499
9	6	10.0	75.0	105.0	0.0607
9	7	10.0	90.0	90.0	0.0606
9	8	10.0	105.0	75.0	0.0624
9	9	10.0	120.0	60.0	0.0847
9	10	10.0	135.0	45.0	0.0996
9	11	10.0	150.0	30.0	0.1089
9	12	10.0	165.0	15.0	0.1140
9	13	10.0	180.0	0.0	0.1181
8	1	20.0	0.0	180.0	0.0272
8	2	20.0	15.0	165.0	0.0253
8	3	20.0	30.0	150.0	0.0291
8	4	20.0	45.0	135.0	0.0294
8	5	20.0	60.0	120.0	0.0328
8	6	20.0	75.0	105.0	0.0379
8	7	20.0	90.0	90.0	0.0460
8	8	20.0	105.0	75.0	0.0603
8	9	20.0	120.0	60.0	0.0847
8	10	20.0	135.0	45.0	0.1002
8	11	20.0	150.0	30.0	0.1170
8	12	20.0	165.0	15.0	0.1211
8	13	20.0	180.0	0.0	0.1205
7	1	30.0	0.0	180.0	0.0278
7	2	30.0	15.0	165.0	0.0268
7	3	30.0	30.0	150.0	0.0267
7	4	30.0	45.0	135.0	0.0282
7	5	30.0	60.0	120.0	0.0284
7	6	30.0	75.0	105.0	0.0294
7	7	30.0	90.0	90.0	0.0363
7	8	30.0	105.0	75.0	0.0467
7	9	30.0	120.0	60.0	0.0737
7	10	30.0	135.0	45.0	0.1035
7	11	30.0	150.0	30.0	0.1213
7	12	30.0	165.0	15.0	0.1009
7	13	30.0	180.0	0.0	0.0882
6	1	40.0	0.0	180.0	0.0339
6	2	40.0	15.0	165.0	0.0344
6	3	40.0	30.0	150.0	0.0337
6	4	40.0	45.0	135.0	0.0329
6	5	40.0	60.0	120.0	0.0323
6	6	40.0	75.0	105.0	0.0335
6	7	40.0	90.0	90.0	0.0343
6	8	40.0	105.0	75.0	0.0415
6	9	40.0	120.0	60.0	0.0572
6	10	40.0	135.0	45.0	0.0936
6	11	40.0	150.0	30.0	0.1183
6	12	40.0	165.0	15.0	0.0960
6	13	40.0	180.0	0.0	0.0016
5	1	50.0	0.0	180.0	0.0537
5	2	50.0	15.0	165.0	0.0536
5	3	50.0	30.0	150.0	0.0532
5	4	50.0	45.0	135.0	0.0515
5	5	50.0	60.0	120.0	0.0492
5	6	50.0	75.0	105.0	0.0484
5	7	50.0	90.0	90.0	0.0479
5	8	50.0	105.0	75.0	0.0494
5	9	50.0	120.0	60.0	0.0575
5	10	50.0	135.0	45.0	0.0862
5	11	50.0	150.0	30.0	0.1350
5	12	50.0	165.0	15.0	0.1486
5	13	50.0	180.0	0.0	0.1344
4	1	60.0	0.0	180.0	0.0924
4	2	60.0	15.0	165.0	0.0933
4	3	60.0	30.0	150.0	0.0930
4	4	60.0	45.0	135.0	0.0899
4	5	60.0	60.0	120.0	0.0858
4	6	60.0	75.0	105.0	0.0843
4	7	60.0	90.0	90.0	0.0846
4	8	60.0	105.0	75.0	0.0814
4	9	60.0	120.0	60.0	0.0815
4	10	60.0	135.0	45.0	0.0984
4	11	60.0	150.0	30.0	0.1614
4	12	60.0	165.0	15.0	0.2556
4	13	60.0	180.0	0.0	0.3054
3	1	70.0	0.0	180.0	0.1410
3	2	70.0	15.0	165.0	0.1441
3	3	70.0	30.0	150.0	0.1472
3	4	70.0	45.0	135.0	0.1455
3	5	70.0	60.0	120.0	0.1411
3	6	70.0	75.0	105.0	0.1438
3	7	70.0	90.0	90.0	0.1457
3	8	70.0	105.0	75.0	0.1421
3	9	70.0	120.0	60.0	0.1393
3	10	70.0	135.0	45.0	0.1499
3	11	70.0	150.0	30.0	0.2032
3	12	70.0	165.0	15.0	0.3582
3	13	70.0	180.0	0.0	0.4911
2	1	80.0	0.0	180.0	0.1686
2	2	80.0	15.0	165.0	0.1763
2	3	80.0	30.0	150.0	0.1823
2	4	80.0	45.0	135.0	0.1821
2	5	80.0	60.0	120.0	0.1777
2	6	80.0	75.0	105.0	0.1952
2	7	80.0	90.0	90.0	0.2006
2	8	80.0	105.0	75.0	0.2053
2	9	80.0	120.0	60.0	0.1985
2	10	80.0	135.0	45.0	0.2199
2	11	80.0	150.0	30.0	0.2639

2 12 80.0 165.0 15.0 0.4428
2 13 80.0 180.0 0.0 0.5554
1 1 87.5 0.0 180.0 0.1690
1 2 87.5 15.0 165.0 0.1804
1 3 87.5 30.0 150.0 0.2036
1 4 87.5 45.0 135.0 0.1972
1 5 87.5 60.0 120.0 0.1985
1 6 87.5 75.0 105.0 0.2108
1 7 87.5 90.0 90.0 0.2223
1 8 87.5 105.0 75.0 0.2365
1 9 87.5 120.0 60.0 0.2500
1 10 87.5 135.0 45.0 0.2799
1 11 87.5 150.0 30.0 0.3432
1 12 87.5 165.0 15.0 0.4625
1 13 87.5 180.0 0.0 0.5895
rho for WIND SPEED = 10.0 m/s THETA_SUN = 50.0 deg
10 1 0.0 0.0 0.0 0.0442
9 1 10.0 0.0 180.0 0.0275
9 2 10.0 15.0 165.0 0.0254
9 3 10.0 30.0 150.0 0.0268
9 4 10.0 45.0 135.0 0.0253
9 5 10.0 60.0 120.0 0.0306
9 6 10.0 75.0 105.0 0.0318
9 7 10.0 90.0 90.0 0.0393
9 8 10.0 105.0 75.0 0.0411
9 9 10.0 120.0 60.0 0.0452
9 10 10.0 135.0 45.0 0.0660
9 11 10.0 150.0 30.0 0.0584
9 12 10.0 165.0 15.0 0.0799
9 13 10.0 180.0 0.0 0.0692
8 1 20.0 0.0 180.0 0.0247
8 2 20.0 15.0 165.0 0.0250
8 3 20.0 30.0 150.0 0.0243
8 4 20.0 45.0 135.0 0.0254
8 5 20.0 60.0 120.0 0.0247
8 6 20.0 75.0 105.0 0.0287
8 7 20.0 90.0 90.0 0.0284
8 8 20.0 105.0 75.0 0.0362
8 9 20.0 120.0 60.0 0.0462
8 10 20.0 135.0 45.0 0.0713
8 11 20.0 150.0 30.0 0.0916
8 12 20.0 165.0 15.0 0.1095
8 13 20.0 180.0 0.0 0.1153
7 1 30.0 0.0 180.0 0.0263
7 2 30.0 15.0 165.0 0.0265
7 3 30.0 30.0 150.0 0.0264
7 4 30.0 45.0 135.0 0.0261
7 5 30.0 60.0 120.0 0.0262
7 6 30.0 75.0 105.0 0.0267
7 7 30.0 90.0 90.0 0.0282
7 8 30.0 105.0 75.0 0.0337
7 9 30.0 120.0 60.0 0.0451
7 10 30.0 135.0 45.0 0.0678
7 11 30.0 150.0 30.0 0.1028
7 12 30.0 165.0 15.0 0.1307
7 13 30.0 180.0 0.0 0.1258
6 1 40.0 0.0 180.0 0.0343
6 2 40.0 15.0 165.0 0.0348
6 3 40.0 30.0 150.0 0.0341
6 4 40.0 45.0 135.0 0.0333
6 5 40.0 60.0 120.0 0.0325
6 6 40.0 75.0 105.0 0.0322
6 7 40.0 90.0 90.0 0.0332
6 8 40.0 105.0 75.0 0.0334
6 9 40.0 120.0 60.0 0.0395
6 10 40.0 135.0 45.0 0.0673
6 11 40.0 150.0 30.0 0.1095
6 12 40.0 165.0 15.0 0.1211
6 13 40.0 180.0 0.0 0.1015
5 1 50.0 0.0 180.0 0.0542
5 2 50.0 15.0 165.0 0.0541
5 3 50.0 30.0 150.0 0.0539
5 4 50.0 45.0 135.0 0.0523
5 5 50.0 60.0 120.0 0.0501
5 6 50.0 75.0 105.0 0.0492
5 7 50.0 90.0 90.0 0.0487
5 8 50.0 105.0 75.0 0.0479
5 9 50.0 120.0 60.0 0.0504
5 10 50.0 135.0 45.0 0.0702
5 11 50.0 150.0 30.0 0.1120
5 12 50.0 165.0 15.0 0.1273
5 13 50.0 180.0 0.0 0.0031
4 1 60.0 0.0 180.0 0.0918
4 2 60.0 15.0 165.0 0.0928
4 3 60.0 30.0 150.0 0.0929
4 4 60.0 45.0 135.0 0.0901
4 5 60.0 60.0 120.0 0.0864
4 6 60.0 75.0 105.0 0.0853
4 7 60.0 90.0 90.0 0.0857
4 8 60.0 105.0 75.0 0.0821
4 9 60.0 120.0 60.0 0.0811
4 10 60.0 135.0 45.0 0.0878
4 11 60.0 150.0 30.0 0.1386
4 12 60.0 165.0 15.0 0.2160
4 13 60.0 180.0 0.0 0.2264
3 1 70.0 0.0 180.0 0.1391
3 2 70.0 15.0 165.0 0.1422
3 3 70.0 30.0 150.0 0.1455
3 4 70.0 45.0 135.0 0.1442

3	5	70.0	60.0	120.0	0.1402
3	6	70.0	75.0	105.0	0.1433
3	7	70.0	90.0	90.0	0.1454
3	8	70.0	105.0	75.0	0.1418
3	9	70.0	120.0	60.0	0.1387
3	10	70.0	135.0	45.0	0.1446
3	11	70.0	150.0	30.0	0.1873
3	12	70.0	165.0	15.0	0.3980
3	13	70.0	180.0	0.0	0.5695
2	1	80.0	0.0	180.0	0.1676
2	2	80.0	15.0	165.0	0.1753
2	3	80.0	30.0	150.0	0.1812
2	4	80.0	45.0	135.0	0.1805
2	5	80.0	60.0	120.0	0.1757
2	6	80.0	75.0	105.0	0.1926
2	7	80.0	90.0	90.0	0.1974
2	8	80.0	105.0	75.0	0.2013
2	9	80.0	120.0	60.0	0.1945
2	10	80.0	135.0	45.0	0.2174
2	11	80.0	150.0	30.0	0.2661
2	12	80.0	165.0	15.0	0.6031
2	13	80.0	180.0	0.0	1.1372
1	1	87.5	0.0	180.0	0.1705
1	2	87.5	15.0	165.0	0.1819
1	3	87.5	30.0	150.0	0.2048
1	4	87.5	45.0	135.0	0.1972
1	5	87.5	60.0	120.0	0.1971
1	6	87.5	75.0	105.0	0.2078
1	7	87.5	90.0	90.0	0.2177
1	8	87.5	105.0	75.0	0.2296
1	9	87.5	120.0	60.0	0.2424
1	10	87.5	135.0	45.0	0.2767
1	11	87.5	150.0	30.0	0.3609
1	12	87.5	165.0	15.0	0.7200
1	13	87.5	180.0	0.0	1.4475

rho for WIND SPEED = 10.0 m/s THETA_SUN = 60.0 deg

10	1	0.0	0.0	0.0	0.0267
9	1	10.0	0.0	180.0	0.0236
9	2	10.0	15.0	165.0	0.0239
9	3	10.0	30.0	150.0	0.0252
9	4	10.0	45.0	135.0	0.0239
9	5	10.0	60.0	120.0	0.0253
9	6	10.0	75.0	105.0	0.0246
9	7	10.0	90.0	90.0	0.0250
9	8	10.0	105.0	75.0	0.0267
9	9	10.0	120.0	60.0	0.0335
9	10	10.0	135.0	45.0	0.0343
9	11	10.0	150.0	30.0	0.0406
9	12	10.0	165.0	15.0	0.0431
9	13	10.0	180.0	0.0	0.0463
8	1	20.0	0.0	180.0	0.0240
8	2	20.0	15.0	165.0	0.0237
8	3	20.0	30.0	150.0	0.0236
8	4	20.0	45.0	135.0	0.0240
8	5	20.0	60.0	120.0	0.0238
8	6	20.0	75.0	105.0	0.0251
8	7	20.0	90.0	90.0	0.0248
8	8	20.0	105.0	75.0	0.0296
8	9	20.0	120.0	60.0	0.0313
8	10	20.0	135.0	45.0	0.0408
8	11	20.0	150.0	30.0	0.0591
8	12	20.0	165.0	15.0	0.0755
8	13	20.0	180.0	0.0	0.0829
7	1	30.0	0.0	180.0	0.0260
7	2	30.0	15.0	165.0	0.0262
7	3	30.0	30.0	150.0	0.0261
7	4	30.0	45.0	135.0	0.0258
7	5	30.0	60.0	120.0	0.0257
7	6	30.0	75.0	105.0	0.0261
7	7	30.0	90.0	90.0	0.0266
7	8	30.0	105.0	75.0	0.0280
7	9	30.0	120.0	60.0	0.0333
7	10	30.0	135.0	45.0	0.0459
7	11	30.0	150.0	30.0	0.0791
7	12	30.0	165.0	15.0	0.1090
7	13	30.0	180.0	0.0	0.1247
6	1	40.0	0.0	180.0	0.0339
6	2	40.0	15.0	165.0	0.0344
6	3	40.0	30.0	150.0	0.0339
6	4	40.0	45.0	135.0	0.0332
6	5	40.0	60.0	120.0	0.0325
6	6	40.0	75.0	105.0	0.0322
6	7	40.0	90.0	90.0	0.0329
6	8	40.0	105.0	75.0	0.0336
6	9	40.0	120.0	60.0	0.0365
6	10	40.0	135.0	45.0	0.0509
6	11	40.0	150.0	30.0	0.0936
6	12	40.0	165.0	15.0	0.1474
6	13	40.0	180.0	0.0	0.1699
5	1	50.0	0.0	180.0	0.0533
5	2	50.0	15.0	165.0	0.0532
5	3	50.0	30.0	150.0	0.0532
5	4	50.0	45.0	135.0	0.0520
5	5	50.0	60.0	120.0	0.0502
5	6	50.0	75.0	105.0	0.0497
5	7	50.0	90.0	90.0	0.0493
5	8	50.0	105.0	75.0	0.0489
5	9	50.0	120.0	60.0	0.0503
5	10	50.0	135.0	45.0	0.0595

5 11 50.0 150.0 30.0 0.1026
5 12 50.0 165.0 15.0 0.1608
5 13 50.0 180.0 0.0 0.1598
4 1 60.0 0.0 180.0 0.0898
4 2 60.0 15.0 165.0 0.0908
4 3 60.0 30.0 150.0 0.0912
4 4 60.0 45.0 135.0 0.0890
4 5 60.0 60.0 120.0 0.0861
4 6 60.0 75.0 105.0 0.0855
4 7 60.0 90.0 90.0 0.0868
4 8 60.0 105.0 75.0 0.0832
4 9 60.0 120.0 60.0 0.0826
4 10 60.0 135.0 45.0 0.0865
4 11 60.0 150.0 30.0 0.1186
4 12 60.0 165.0 15.0 0.1951
4 13 60.0 180.0 0.0 0.0081
3 1 70.0 0.0 180.0 0.1371
3 2 70.0 15.0 165.0 0.1402
3 3 70.0 30.0 150.0 0.1435
3 4 70.0 45.0 135.0 0.1425
3 5 70.0 60.0 120.0 0.1390
3 6 70.0 75.0 105.0 0.1425
3 7 70.0 90.0 90.0 0.1451
3 8 70.0 105.0 75.0 0.1417
3 9 70.0 120.0 60.0 0.1386
3 10 70.0 135.0 45.0 0.1433
3 11 70.0 150.0 30.0 0.1628
3 12 70.0 165.0 15.0 0.3419
3 13 70.0 180.0 0.0 0.4450
2 1 80.0 0.0 180.0 0.1686
2 2 80.0 15.0 165.0 0.1761
2 3 80.0 30.0 150.0 0.1818
2 4 80.0 45.0 135.0 0.1806
2 5 80.0 60.0 120.0 0.1751
2 6 80.0 75.0 105.0 0.1910
2 7 80.0 90.0 90.0 0.1947
2 8 80.0 105.0 75.0 0.1975
2 9 80.0 120.0 60.0 0.1895
2 10 80.0 135.0 45.0 0.2109
2 11 80.0 150.0 30.0 0.2451
2 12 80.0 165.0 15.0 0.6269
2 13 80.0 180.0 0.0 1.2356
1 1 87.5 0.0 180.0 0.1751
1 2 87.5 15.0 165.0 0.1866
1 3 87.5 30.0 150.0 0.2094
1 4 87.5 45.0 135.0 0.2006
1 5 87.5 60.0 120.0 0.1987
1 6 87.5 75.0 105.0 0.2069
1 7 87.5 90.0 90.0 0.2140
1 8 87.5 105.0 75.0 0.2224
1 9 87.5 120.0 60.0 0.2324
1 10 87.5 135.0 45.0 0.2656
1 11 87.5 150.0 30.0 0.3483
1 12 87.5 165.0 15.0 0.9341
1 13 87.5 180.0 0.0 2.5427
rho for WIND SPEED = 10.0 m/s THETA_SUN = 70.0 deg
10 1 0.0 0.0 0.0 0.0246
9 1 10.0 0.0 180.0 0.0227
9 2 10.0 15.0 165.0 0.0229
9 3 10.0 30.0 150.0 0.0231
9 4 10.0 45.0 135.0 0.0229
9 5 10.0 60.0 120.0 0.0230
9 6 10.0 75.0 105.0 0.0233
9 7 10.0 90.0 90.0 0.0236
9 8 10.0 105.0 75.0 0.0248
9 9 10.0 120.0 60.0 0.0250
9 10 10.0 135.0 45.0 0.0251
9 11 10.0 150.0 30.0 0.0272
9 12 10.0 165.0 15.0 0.0299
9 13 10.0 180.0 0.0 0.0265
8 1 20.0 0.0 180.0 0.0234
8 2 20.0 15.0 165.0 0.0231
8 3 20.0 30.0 150.0 0.0229
8 4 20.0 45.0 135.0 0.0233
8 5 20.0 60.0 120.0 0.0231
8 6 20.0 75.0 105.0 0.0237
8 7 20.0 90.0 90.0 0.0236
8 8 20.0 105.0 75.0 0.0249
8 9 20.0 120.0 60.0 0.0260
8 10 20.0 135.0 45.0 0.0312
8 11 20.0 150.0 30.0 0.0391
8 12 20.0 165.0 15.0 0.0455
8 13 20.0 180.0 0.0 0.0501
7 1 30.0 0.0 180.0 0.0253
7 2 30.0 15.0 165.0 0.0256
7 3 30.0 30.0 150.0 0.0256
7 4 30.0 45.0 135.0 0.0253
7 5 30.0 60.0 120.0 0.0252
7 6 30.0 75.0 105.0 0.0253
7 7 30.0 90.0 90.0 0.0260
7 8 30.0 105.0 75.0 0.0264
7 9 30.0 120.0 60.0 0.0282
7 10 30.0 135.0 45.0 0.0373
7 11 30.0 150.0 30.0 0.0519
7 12 30.0 165.0 15.0 0.0863
7 13 30.0 180.0 0.0 0.1047
6 1 40.0 0.0 180.0 0.0329
6 2 40.0 15.0 165.0 0.0335
6 3 40.0 30.0 150.0 0.0331

6 4 40.0 45.0 135.0 0.0326
6 5 40.0 60.0 120.0 0.0322
6 6 40.0 75.0 105.0 0.0320
6 7 40.0 90.0 90.0 0.0327
6 8 40.0 105.0 75.0 0.0328
6 9 40.0 120.0 60.0 0.0350
6 10 40.0 135.0 45.0 0.0424
6 11 40.0 150.0 30.0 0.0747
6 12 40.0 165.0 15.0 0.1555
6 13 40.0 180.0 0.0 0.1941
5 1 50.0 0.0 180.0 0.0515
5 2 50.0 15.0 165.0 0.0515
5 3 50.0 30.0 150.0 0.0517
5 4 50.0 45.0 135.0 0.0509
5 5 50.0 60.0 120.0 0.0496
5 6 50.0 75.0 105.0 0.0496
5 7 50.0 90.0 90.0 0.0496
5 8 50.0 105.0 75.0 0.0496
5 9 50.0 120.0 60.0 0.0511
5 10 50.0 135.0 45.0 0.0583
5 11 50.0 150.0 30.0 0.0933
5 12 50.0 165.0 15.0 0.2094
5 13 50.0 180.0 0.0 0.3003
4 1 60.0 0.0 180.0 0.0872
4 2 60.0 15.0 165.0 0.0882
4 3 60.0 30.0 150.0 0.0888
4 4 60.0 45.0 135.0 0.0871
4 5 60.0 60.0 120.0 0.0848
4 6 60.0 75.0 105.0 0.0852
4 7 60.0 90.0 90.0 0.0871
4 8 60.0 105.0 75.0 0.0845
4 9 60.0 120.0 60.0 0.0847
4 10 60.0 135.0 45.0 0.0898
4 11 60.0 150.0 30.0 0.1158
4 12 60.0 165.0 15.0 0.2410
4 13 60.0 180.0 0.0 0.2976
3 1 70.0 0.0 180.0 0.1354
3 2 70.0 15.0 165.0 0.1384
3 3 70.0 30.0 150.0 0.1418
3 4 70.0 45.0 135.0 0.1408
3 5 70.0 60.0 120.0 0.1377
3 6 70.0 75.0 105.0 0.1415
3 7 70.0 90.0 90.0 0.1448
3 8 70.0 105.0 75.0 0.1416
3 9 70.0 120.0 60.0 0.1391
3 10 70.0 135.0 45.0 0.1454
3 11 70.0 150.0 30.0 0.1512
3 12 70.0 165.0 15.0 0.2840
3 13 70.0 180.0 0.0 0.0266
2 1 80.0 0.0 180.0 0.1707
2 2 80.0 15.0 165.0 0.1782
2 3 80.0 30.0 150.0 0.1835
2 4 80.0 45.0 135.0 0.1819
2 5 80.0 60.0 120.0 0.1755
2 6 80.0 75.0 105.0 0.1904
2 7 80.0 90.0 90.0 0.1928
2 8 80.0 105.0 75.0 0.1943
2 9 80.0 120.0 60.0 0.1847
2 10 80.0 135.0 45.0 0.2019
2 11 80.0 150.0 30.0 0.2194
2 12 80.0 165.0 15.0 0.4343
2 13 80.0 180.0 0.0 0.8512
1 1 87.5 0.0 180.0 0.1814
1 2 87.5 15.0 165.0 0.1929
1 3 87.5 30.0 150.0 0.2159
1 4 87.5 45.0 135.0 0.2058
1 5 87.5 60.0 120.0 0.2019
1 6 87.5 75.0 105.0 0.2074
1 7 87.5 90.0 90.0 0.2115
1 8 87.5 105.0 75.0 0.2162
1 9 87.5 120.0 60.0 0.2218
1 10 87.5 135.0 45.0 0.2471
1 11 87.5 150.0 30.0 0.3076
1 12 87.5 165.0 15.0 0.6319
1 13 87.5 180.0 0.0 1.8849
rho for WIND SPEED = 10.0 m/s THETA_SUN = 80.0 deg
10 1 0.0 0.0 0.0 0.0228
9 1 10.0 0.0 180.0 0.0220
9 2 10.0 15.0 165.0 0.0221
9 3 10.0 30.0 150.0 0.0222
9 4 10.0 45.0 135.0 0.0222
9 5 10.0 60.0 120.0 0.0221
9 6 10.0 75.0 105.0 0.0223
9 7 10.0 90.0 90.0 0.0226
9 8 10.0 105.0 75.0 0.0228
9 9 10.0 120.0 60.0 0.0229
9 10 10.0 135.0 45.0 0.0234
9 11 10.0 150.0 30.0 0.0239
9 12 10.0 165.0 15.0 0.0242
9 13 10.0 180.0 0.0 0.0249
8 1 20.0 0.0 180.0 0.0228
8 2 20.0 15.0 165.0 0.0224
8 3 20.0 30.0 150.0 0.0223
8 4 20.0 45.0 135.0 0.0227
8 5 20.0 60.0 120.0 0.0224
8 6 20.0 75.0 105.0 0.0230
8 7 20.0 90.0 90.0 0.0227
8 8 20.0 105.0 75.0 0.0236
8 9 20.0 120.0 60.0 0.0241

8 10 20.0 135.0 45.0 0.0258
8 11 20.0 150.0 30.0 0.0278
8 12 20.0 165.0 15.0 0.0303
8 13 20.0 180.0 0.0 0.0324
7 1 30.0 0.0 180.0 0.0246
7 2 30.0 15.0 165.0 0.0249
7 3 30.0 30.0 150.0 0.0249
7 4 30.0 45.0 135.0 0.0247
7 5 30.0 60.0 120.0 0.0247
7 6 30.0 75.0 105.0 0.0247
7 7 30.0 90.0 90.0 0.0254
7 8 30.0 105.0 75.0 0.0256
7 9 30.0 120.0 60.0 0.0267
7 10 30.0 135.0 45.0 0.0300
7 11 30.0 150.0 30.0 0.0374
7 12 30.0 165.0 15.0 0.0530
7 13 30.0 180.0 0.0 0.0648
6 1 40.0 0.0 180.0 0.0319
6 2 40.0 15.0 165.0 0.0324
6 3 40.0 30.0 150.0 0.0321
6 4 40.0 45.0 135.0 0.0318
6 5 40.0 60.0 120.0 0.0316
6 6 40.0 75.0 105.0 0.0316
6 7 40.0 90.0 90.0 0.0324
6 8 40.0 105.0 75.0 0.0324
6 9 40.0 120.0 60.0 0.0342
6 10 40.0 135.0 45.0 0.0397
6 11 40.0 150.0 30.0 0.0565
6 12 40.0 165.0 15.0 0.1093
6 13 40.0 180.0 0.0 0.1570
5 1 50.0 0.0 180.0 0.0497
5 2 50.0 15.0 165.0 0.0497
5 3 50.0 30.0 150.0 0.0500
5 4 50.0 45.0 135.0 0.0496
5 5 50.0 60.0 120.0 0.0486
5 6 50.0 75.0 105.0 0.0490
5 7 50.0 90.0 90.0 0.0495
5 8 50.0 105.0 75.0 0.0497
5 9 50.0 120.0 60.0 0.0516
5 10 50.0 135.0 45.0 0.0598
5 11 50.0 150.0 30.0 0.0844
5 12 50.0 165.0 15.0 0.1950
5 13 50.0 180.0 0.0 0.3232
4 1 60.0 0.0 180.0 0.0849
4 2 60.0 15.0 165.0 0.0859
4 3 60.0 30.0 150.0 0.0866
4 4 60.0 45.0 135.0 0.0853
4 5 60.0 60.0 120.0 0.0835
4 6 60.0 75.0 105.0 0.0844
4 7 60.0 90.0 90.0 0.0869
4 8 60.0 105.0 75.0 0.0850
4 9 60.0 120.0 60.0 0.0863
4 10 60.0 135.0 45.0 0.0958
4 11 60.0 150.0 30.0 0.1204
4 12 60.0 165.0 15.0 0.2536
4 13 60.0 180.0 0.0 0.4663
3 1 70.0 0.0 180.0 0.1343
3 2 70.0 15.0 165.0 0.1372
3 3 70.0 30.0 150.0 0.1405
3 4 70.0 45.0 135.0 0.1397
3 5 70.0 60.0 120.0 0.1366
3 6 70.0 75.0 105.0 0.1407
3 7 70.0 90.0 90.0 0.1440
3 8 70.0 105.0 75.0 0.1415
3 9 70.0 120.0 60.0 0.1395
3 10 70.0 135.0 45.0 0.1489
3 11 70.0 150.0 30.0 0.1601
3 12 70.0 165.0 15.0 0.2499
3 13 70.0 180.0 0.0 0.4327
2 1 80.0 0.0 180.0 0.1736
2 2 80.0 15.0 165.0 0.1809
2 3 80.0 30.0 150.0 0.1859
2 4 80.0 45.0 135.0 0.1837
2 5 80.0 60.0 120.0 0.1764
2 6 80.0 75.0 105.0 0.1901
2 7 80.0 90.0 90.0 0.1917
2 8 80.0 105.0 75.0 0.1919
2 9 80.0 120.0 60.0 0.1810
2 10 80.0 135.0 45.0 0.1934
2 11 80.0 150.0 30.0 0.1983
2 12 80.0 165.0 15.0 0.2476
2 13 80.0 180.0 0.0 0.0736
1 1 87.5 0.0 180.0 0.1881
1 2 87.5 15.0 165.0 0.1997
1 3 87.5 30.0 150.0 0.2227
1 4 87.5 45.0 135.0 0.2112
1 5 87.5 60.0 120.0 0.2054
1 6 87.5 75.0 105.0 0.2085
1 7 87.5 90.0 90.0 0.2100
1 8 87.5 105.0 75.0 0.2117
1 9 87.5 120.0 60.0 0.2128
1 10 87.5 135.0 45.0 0.2258
1 11 87.5 150.0 30.0 0.2490
1 12 87.5 165.0 15.0 0.2775
1 13 87.5 180.0 0.0 0.6464
rho for WIND SPEED = 12.0 m/s THETA_SUN = 0.0
deg
10 1 0.0 0.0 0.0 0.0007
9 1 10.0 0.0 180.0 0.0870
9 2 10.0 15.0 165.0 0.0810

9	3	10.0	30.0	150.0	0.0870
9	4	10.0	45.0	135.0	0.0895
9	5	10.0	60.0	120.0	0.0873
9	6	10.0	75.0	105.0	0.0812
9	7	10.0	90.0	90.0	0.0882
9	8	10.0	105.0	75.0	0.0812
9	9	10.0	120.0	60.0	0.0873
9	10	10.0	135.0	45.0	0.0895
9	11	10.0	150.0	30.0	0.0870
9	12	10.0	165.0	15.0	0.0810
9	13	10.0	180.0	0.0	0.0870
8	1	20.0	0.0	180.0	0.1362
8	2	20.0	15.0	165.0	0.1277
8	3	20.0	30.0	150.0	0.1254
8	4	20.0	45.0	135.0	0.1317
8	5	20.0	60.0	120.0	0.1257
8	6	20.0	75.0	105.0	0.1245
8	7	20.0	90.0	90.0	0.1263
8	8	20.0	105.0	75.0	0.1245
8	9	20.0	120.0	60.0	0.1257
8	10	20.0	135.0	45.0	0.1317
8	11	20.0	150.0	30.0	0.1254
8	12	20.0	165.0	15.0	0.1277
8	13	20.0	180.0	0.0	0.1362
7	1	30.0	0.0	180.0	0.1355
7	2	30.0	15.0	165.0	0.1317
7	3	30.0	30.0	150.0	0.1380
7	4	30.0	45.0	135.0	0.1374
7	5	30.0	60.0	120.0	0.1401
7	6	30.0	75.0	105.0	0.1389
7	7	30.0	90.0	90.0	0.1303
7	8	30.0	105.0	75.0	0.1389
7	9	30.0	120.0	60.0	0.1401
7	10	30.0	135.0	45.0	0.1374
7	11	30.0	150.0	30.0	0.1380
7	12	30.0	165.0	15.0	0.1317
7	13	30.0	180.0	0.0	0.1355
6	1	40.0	0.0	180.0	0.1086
6	2	40.0	15.0	165.0	0.1091
6	3	40.0	30.0	150.0	0.1049
6	4	40.0	45.0	135.0	0.1044
6	5	40.0	60.0	120.0	0.1059
6	6	40.0	75.0	105.0	0.1086
6	7	40.0	90.0	90.0	0.1014
6	8	40.0	105.0	75.0	0.1086
6	9	40.0	120.0	60.0	0.1059
6	10	40.0	135.0	45.0	0.1044
6	11	40.0	150.0	30.0	0.1049
6	12	40.0	165.0	15.0	0.1091
6	13	40.0	180.0	0.0	0.1086
5	1	50.0	0.0	180.0	0.0791
5	2	50.0	15.0	165.0	0.0804
5	3	50.0	30.0	150.0	0.0793
5	4	50.0	45.0	135.0	0.0815
5	5	50.0	60.0	120.0	0.0811
5	6	50.0	75.0	105.0	0.0820
5	7	50.0	90.0	90.0	0.0760
5	8	50.0	105.0	75.0	0.0820
5	9	50.0	120.0	60.0	0.0811
5	10	50.0	135.0	45.0	0.0815
5	11	50.0	150.0	30.0	0.0793
5	12	50.0	165.0	15.0	0.0804
5	13	50.0	180.0	0.0	0.0791
4	1	60.0	0.0	180.0	0.0892
4	2	60.0	15.0	165.0	0.0918
4	3	60.0	30.0	150.0	0.0906
4	4	60.0	45.0	135.0	0.0894
4	5	60.0	60.0	120.0	0.0892
4	6	60.0	75.0	105.0	0.0912
4	7	60.0	90.0	90.0	0.0906
4	8	60.0	105.0	75.0	0.0912
4	9	60.0	120.0	60.0	0.0892
4	10	60.0	135.0	45.0	0.0894
4	11	60.0	150.0	30.0	0.0906
4	12	60.0	165.0	15.0	0.0918
4	13	60.0	180.0	0.0	0.0892
3	1	70.0	0.0	180.0	0.1342
3	2	70.0	15.0	165.0	0.1371
3	3	70.0	30.0	150.0	0.1404
3	4	70.0	45.0	135.0	0.1394
3	5	70.0	60.0	120.0	0.1358
3	6	70.0	75.0	105.0	0.1403
3	7	70.0	90.0	90.0	0.1433
3	8	70.0	105.0	75.0	0.1403
3	9	70.0	120.0	60.0	0.1358
3	10	70.0	135.0	45.0	0.1394
3	11	70.0	150.0	30.0	0.1404
3	12	70.0	165.0	15.0	0.1371
3	13	70.0	180.0	0.0	0.1342
2	1	80.0	0.0	180.0	0.1824
2	2	80.0	15.0	165.0	0.1897
2	3	80.0	30.0	150.0	0.1939
2	4	80.0	45.0	135.0	0.1906
2	5	80.0	60.0	120.0	0.1830
2	6	80.0	75.0	105.0	0.1956
2	7	80.0	90.0	90.0	0.1961
2	8	80.0	105.0	75.0	0.1956
2	9	80.0	120.0	60.0	0.1830
2	10	80.0	135.0	45.0	0.1906
2	11	80.0	150.0	30.0	0.1939

2 12 80.0 165.0 15.0 0.1897
2 13 80.0 180.0 0.0 0.1824
1 1 87.5 0.0 180.0 0.2036
1 2 87.5 15.0 165.0 0.2180
1 3 87.5 30.0 150.0 0.2352
1 4 87.5 45.0 135.0 0.2257
1 5 87.5 60.0 120.0 0.2170
1 6 87.5 75.0 105.0 0.2179
1 7 87.5 90.0 90.0 0.2181
1 8 87.5 105.0 75.0 0.2179
1 9 87.5 120.0 60.0 0.2170
1 10 87.5 135.0 45.0 0.2257
1 11 87.5 150.0 30.0 0.2352
1 12 87.5 165.0 15.0 0.2180
1 13 87.5 180.0 0.0 0.2036
rho for WIND SPEED = 12.0 m/s THETA_SUN = 10.0 deg
10 1 0.0 0.0 0.0 0.0777
9 1 10.0 0.0 180.0 0.1295
9 2 10.0 15.0 165.0 0.1306
9 3 10.0 30.0 150.0 0.1191
9 4 10.0 45.0 135.0 0.1192
9 5 10.0 60.0 120.0 0.1152
9 6 10.0 75.0 105.0 0.1134
9 7 10.0 90.0 90.0 0.1091
9 8 10.0 105.0 75.0 0.0886
9 9 10.0 120.0 60.0 0.0771
9 10 10.0 135.0 45.0 0.0683
9 11 10.0 150.0 30.0 0.0602
9 12 10.0 165.0 15.0 0.0495
9 13 10.0 180.0 0.0 0.0003
8 1 20.0 0.0 180.0 0.1154
8 2 20.0 15.0 165.0 0.1190
8 3 20.0 30.0 150.0 0.1218
8 4 20.0 45.0 135.0 0.1342
8 5 20.0 60.0 120.0 0.1322
8 6 20.0 75.0 105.0 0.1377
8 7 20.0 90.0 90.0 0.1337
8 8 20.0 105.0 75.0 0.1296
8 9 20.0 120.0 60.0 0.1134
8 10 20.0 135.0 45.0 0.1096
8 11 20.0 150.0 30.0 0.0988
8 12 20.0 165.0 15.0 0.0946
8 13 20.0 180.0 0.0 0.0820
7 1 30.0 0.0 180.0 0.0975
7 2 30.0 15.0 165.0 0.0936
7 3 30.0 30.0 150.0 0.0913
7 4 30.0 45.0 135.0 0.0976
7 5 30.0 60.0 120.0 0.1115
7 6 30.0 75.0 105.0 0.1227
7 7 30.0 90.0 90.0 0.1207
7 8 30.0 105.0 75.0 0.1330
7 9 30.0 120.0 60.0 0.1308
7 10 30.0 135.0 45.0 0.1423
7 11 30.0 150.0 30.0 0.1369
7 12 30.0 165.0 15.0 0.1438
7 13 30.0 180.0 0.0 0.1399
6 1 40.0 0.0 180.0 0.0625
6 2 40.0 15.0 165.0 0.0622
6 3 40.0 30.0 150.0 0.0632
6 4 40.0 45.0 135.0 0.0650
6 5 40.0 60.0 120.0 0.0737
6 6 40.0 75.0 105.0 0.0892
6 7 40.0 90.0 90.0 0.0964
6 8 40.0 105.0 75.0 0.1067
6 9 40.0 120.0 60.0 0.1222
6 10 40.0 135.0 45.0 0.1370
6 11 40.0 150.0 30.0 0.1498
6 12 40.0 165.0 15.0 0.1597
6 13 40.0 180.0 0.0 0.1634
5 1 50.0 0.0 180.0 0.0561
5 2 50.0 15.0 165.0 0.0568
5 3 50.0 30.0 150.0 0.0592
5 4 50.0 45.0 135.0 0.0589
5 5 50.0 60.0 120.0 0.0614
5 6 50.0 75.0 105.0 0.0654
5 7 50.0 90.0 90.0 0.0750
5 8 50.0 105.0 75.0 0.0791
5 9 50.0 120.0 60.0 0.0972
5 10 50.0 135.0 45.0 0.1071
5 11 50.0 150.0 30.0 0.1230
5 12 50.0 165.0 15.0 0.1356
5 13 50.0 180.0 0.0 0.1460
4 1 60.0 0.0 180.0 0.0831
4 2 60.0 15.0 165.0 0.0838
4 3 60.0 30.0 150.0 0.0861
4 4 60.0 45.0 135.0 0.0844
4 5 60.0 60.0 120.0 0.0828
4 6 60.0 75.0 105.0 0.0853
4 7 60.0 90.0 90.0 0.0908
4 8 60.0 105.0 75.0 0.0881
4 9 60.0 120.0 60.0 0.0969
4 10 60.0 135.0 45.0 0.1059
4 11 60.0 150.0 30.0 0.1168
4 12 60.0 165.0 15.0 0.1243
4 13 60.0 180.0 0.0 0.1257
3 1 70.0 0.0 180.0 0.1332
3 2 70.0 15.0 165.0 0.1364
3 3 70.0 30.0 150.0 0.1394
3 4 70.0 45.0 135.0 0.1380

3	5	70.0	60.0	120.0	0.1342
3	6	70.0	75.0	105.0	0.1387
3	7	70.0	90.0	90.0	0.1430
3	8	70.0	105.0	75.0	0.1404
3	9	70.0	120.0	60.0	0.1393
3	10	70.0	135.0	45.0	0.1475
3	11	70.0	150.0	30.0	0.1491
3	12	70.0	165.0	15.0	0.1486
3	13	70.0	180.0	0.0	0.1480
2	1	80.0	0.0	180.0	0.1735
2	2	80.0	15.0	165.0	0.1806
2	3	80.0	30.0	150.0	0.1857
2	4	80.0	45.0	135.0	0.1838
2	5	80.0	60.0	120.0	0.1780
2	6	80.0	75.0	105.0	0.1921
2	7	80.0	90.0	90.0	0.1952
2	8	80.0	105.0	75.0	0.1968
2	9	80.0	120.0	60.0	0.1875
2	10	80.0	135.0	45.0	0.1990
2	11	80.0	150.0	30.0	0.2020
2	12	80.0	165.0	15.0	0.2013
2	13	80.0	180.0	0.0	0.1944
1	1	87.5	0.0	180.0	0.1824
1	2	87.5	15.0	165.0	0.1966
1	3	87.5	30.0	150.0	0.2146
1	4	87.5	45.0	135.0	0.2092
1	5	87.5	60.0	120.0	0.2052
1	6	87.5	75.0	105.0	0.2111
1	7	87.5	90.0	90.0	0.2170
1	8	87.5	105.0	75.0	0.2223
1	9	87.5	120.0	60.0	0.2267
1	10	87.5	135.0	45.0	0.2407
1	11	87.5	150.0	30.0	0.2550
1	12	87.5	165.0	15.0	0.2393
1	13	87.5	180.0	0.0	0.2253

rho for WIND SPEED = 12.0 m/s THETA_SUN = 20.0 deg

10	1	0.0	0.0	0.0	0.1171
9	1	10.0	0.0	180.0	0.1356
9	2	10.0	15.0	165.0	0.1155
9	3	10.0	30.0	150.0	0.1225
9	4	10.0	45.0	135.0	0.1197
9	5	10.0	60.0	120.0	0.1248
9	6	10.0	75.0	105.0	0.1333
9	7	10.0	90.0	90.0	0.1263
9	8	10.0	105.0	75.0	0.1238
9	9	10.0	120.0	60.0	0.1078
9	10	10.0	135.0	45.0	0.0969
9	11	10.0	150.0	30.0	0.0880
9	12	10.0	165.0	15.0	0.0786
9	13	10.0	180.0	0.0	0.0650
8	1	20.0	0.0	180.0	0.0994
8	2	20.0	15.0	165.0	0.0814
8	3	20.0	30.0	150.0	0.0960
8	4	20.0	45.0	135.0	0.0944
8	5	20.0	60.0	120.0	0.1099
8	6	20.0	75.0	105.0	0.1169
8	7	20.0	90.0	90.0	0.1276
8	8	20.0	105.0	75.0	0.1247
8	9	20.0	120.0	60.0	0.1222
8	10	20.0	135.0	45.0	0.1036
8	11	20.0	150.0	30.0	0.0792
8	12	20.0	165.0	15.0	0.0606
8	13	20.0	180.0	0.0	0.0005
7	1	30.0	0.0	180.0	0.0528
7	2	30.0	15.0	165.0	0.0581
7	3	30.0	30.0	150.0	0.0577
7	4	30.0	45.0	135.0	0.0619
7	5	30.0	60.0	120.0	0.0760
7	6	30.0	75.0	105.0	0.0836
7	7	30.0	90.0	90.0	0.1051
7	8	30.0	105.0	75.0	0.1196
7	9	30.0	120.0	60.0	0.1276
7	10	30.0	135.0	45.0	0.1251
7	11	30.0	150.0	30.0	0.1116
7	12	30.0	165.0	15.0	0.0958
7	13	30.0	180.0	0.0	0.0854
6	1	40.0	0.0	180.0	0.0407
6	2	40.0	15.0	165.0	0.0437
6	3	40.0	30.0	150.0	0.0430
6	4	40.0	45.0	135.0	0.0455
6	5	40.0	60.0	120.0	0.0489
6	6	40.0	75.0	105.0	0.0632
6	7	40.0	90.0	90.0	0.0752
6	8	40.0	105.0	75.0	0.1009
6	9	40.0	120.0	60.0	0.1188
6	10	40.0	135.0	45.0	0.1309
6	11	40.0	150.0	30.0	0.1494
6	12	40.0	165.0	15.0	0.1523
6	13	40.0	180.0	0.0	0.1607
5	1	50.0	0.0	180.0	0.0522
5	2	50.0	15.0	165.0	0.0521
5	3	50.0	30.0	150.0	0.0520
5	4	50.0	45.0	135.0	0.0523
5	5	50.0	60.0	120.0	0.0519
5	6	50.0	75.0	105.0	0.0563
5	7	50.0	90.0	90.0	0.0642
5	8	50.0	105.0	75.0	0.0727
5	9	50.0	120.0	60.0	0.0915
5	10	50.0	135.0	45.0	0.1282

5 11 50.0 150.0 30.0 0.1503
5 12 50.0 165.0 15.0 0.1862
5 13 50.0 180.0 0.0 0.1907
4 1 60.0 0.0 180.0 0.0862
4 2 60.0 15.0 165.0 0.0870
4 3 60.0 30.0 150.0 0.0876
4 4 60.0 45.0 135.0 0.0848
4 5 60.0 60.0 120.0 0.0824
4 6 60.0 75.0 105.0 0.0828
4 7 60.0 90.0 90.0 0.0859
4 8 60.0 105.0 75.0 0.0888
4 9 60.0 120.0 60.0 0.0931
4 10 60.0 135.0 45.0 0.1214
4 11 60.0 150.0 30.0 0.1480
4 12 60.0 165.0 15.0 0.1844
4 13 60.0 180.0 0.0 0.1921
3 1 70.0 0.0 180.0 0.1342
3 2 70.0 15.0 165.0 0.1372
3 3 70.0 30.0 150.0 0.1404
3 4 70.0 45.0 135.0 0.1387
3 5 70.0 60.0 120.0 0.1341
3 6 70.0 75.0 105.0 0.1379
3 7 70.0 90.0 90.0 0.1415
3 8 70.0 105.0 75.0 0.1389
3 9 70.0 120.0 60.0 0.1400
3 10 70.0 135.0 45.0 0.1535
3 11 70.0 150.0 30.0 0.1726
3 12 70.0 165.0 15.0 0.1964
3 13 70.0 180.0 0.0 0.2040
2 1 80.0 0.0 180.0 0.1640
2 2 80.0 15.0 165.0 0.1721
2 3 80.0 30.0 150.0 0.1778
2 4 80.0 45.0 135.0 0.1770
2 5 80.0 60.0 120.0 0.1725
2 6 80.0 75.0 105.0 0.1881
2 7 80.0 90.0 90.0 0.1929
2 8 80.0 105.0 75.0 0.1964
2 9 80.0 120.0 60.0 0.1890
2 10 80.0 135.0 45.0 0.2036
2 11 80.0 150.0 30.0 0.2204
2 12 80.0 165.0 15.0 0.2277
2 13 80.0 180.0 0.0 0.2312
1 1 87.5 0.0 180.0 0.1652
1 2 87.5 15.0 165.0 0.1792
1 3 87.5 30.0 150.0 0.1972
1 4 87.5 45.0 135.0 0.1944
1 5 87.5 60.0 120.0 0.1938
1 6 87.5 75.0 105.0 0.2034
1 7 87.5 90.0 90.0 0.2138
1 8 87.5 105.0 75.0 0.2233
1 9 87.5 120.0 60.0 0.2325
1 10 87.5 135.0 45.0 0.2521
1 11 87.5 150.0 30.0 0.2780
1 12 87.5 165.0 15.0 0.2694
1 13 87.5 180.0 0.0 0.2595
rho for WIND SPEED = 12.0 m/s THETA_SUN = 30.0 deg
10 1 0.0 0.0 0.0 0.1164
9 1 10.0 0.0 180.0 0.0902
9 2 10.0 15.0 165.0 0.0900
9 3 10.0 30.0 150.0 0.0888
9 4 10.0 45.0 135.0 0.0909
9 5 10.0 60.0 120.0 0.1023
9 6 10.0 75.0 105.0 0.0946
9 7 10.0 90.0 90.0 0.1015
9 8 10.0 105.0 75.0 0.1146
9 9 10.0 120.0 60.0 0.1164
9 10 10.0 135.0 45.0 0.1182
9 11 10.0 150.0 30.0 0.1160
9 12 10.0 165.0 15.0 0.1072
9 13 10.0 180.0 0.0 0.1146
8 1 20.0 0.0 180.0 0.0567
8 2 20.0 15.0 165.0 0.0517
8 3 20.0 30.0 150.0 0.0522
8 4 20.0 45.0 135.0 0.0619
8 5 20.0 60.0 120.0 0.0619
8 6 20.0 75.0 105.0 0.0751
8 7 20.0 90.0 90.0 0.0939
8 8 20.0 105.0 75.0 0.1063
8 9 20.0 120.0 60.0 0.1204
8 10 20.0 135.0 45.0 0.1191
8 11 20.0 150.0 30.0 0.1046
8 12 20.0 165.0 15.0 0.0821
8 13 20.0 180.0 0.0 0.0739
7 1 30.0 0.0 180.0 0.0360
7 2 30.0 15.0 165.0 0.0359
7 3 30.0 30.0 150.0 0.0380
7 4 30.0 45.0 135.0 0.0380
7 5 30.0 60.0 120.0 0.0415
7 6 30.0 75.0 105.0 0.0528
7 7 30.0 90.0 90.0 0.0737
7 8 30.0 105.0 75.0 0.0947
7 9 30.0 120.0 60.0 0.1129
7 10 30.0 135.0 45.0 0.1181
7 11 30.0 150.0 30.0 0.1001
7 12 30.0 165.0 15.0 0.0700
7 13 30.0 180.0 0.0 0.0009
6 1 40.0 0.0 180.0 0.0359
6 2 40.0 15.0 165.0 0.0368
6 3 40.0 30.0 150.0 0.0371

6	4	40.0	45.0	135.0	0.0370
6	5	40.0	60.0	120.0	0.0385
6	6	40.0	75.0	105.0	0.0417
6	7	40.0	90.0	90.0	0.0533
6	8	40.0	105.0	75.0	0.0678
6	9	40.0	120.0	60.0	0.0988
6	10	40.0	135.0	45.0	0.1145
6	11	40.0	150.0	30.0	0.1245
6	12	40.0	165.0	15.0	0.1119
6	13	40.0	180.0	0.0	0.0968
5	1	50.0	0.0	180.0	0.0533
5	2	50.0	15.0	165.0	0.0536
5	3	50.0	30.0	150.0	0.0530
5	4	50.0	45.0	135.0	0.0525
5	5	50.0	60.0	120.0	0.0502
5	6	50.0	75.0	105.0	0.0509
5	7	50.0	90.0	90.0	0.0547
5	8	50.0	105.0	75.0	0.0618
5	9	50.0	120.0	60.0	0.0865
5	10	50.0	135.0	45.0	0.1149
5	11	50.0	150.0	30.0	0.1579
5	12	50.0	165.0	15.0	0.1808
5	13	50.0	180.0	0.0	0.1852
4	1	60.0	0.0	180.0	0.0899
4	2	60.0	15.0	165.0	0.0905
4	3	60.0	30.0	150.0	0.0906
4	4	60.0	45.0	135.0	0.0872
4	5	60.0	60.0	120.0	0.0832
4	6	60.0	75.0	105.0	0.0828
4	7	60.0	90.0	90.0	0.0841
4	8	60.0	105.0	75.0	0.0850
4	9	60.0	120.0	60.0	0.0883
4	10	60.0	135.0	45.0	0.1174
4	11	60.0	150.0	30.0	0.1802
4	12	60.0	165.0	15.0	0.2479
4	13	60.0	180.0	0.0	0.2701
3	1	70.0	0.0	180.0	0.1341
3	2	70.0	15.0	165.0	0.1374
3	3	70.0	30.0	150.0	0.1408
3	4	70.0	45.0	135.0	0.1391
3	5	70.0	60.0	120.0	0.1340
3	6	70.0	75.0	105.0	0.1373
3	7	70.0	90.0	90.0	0.1401
3	8	70.0	105.0	75.0	0.1374
3	9	70.0	120.0	60.0	0.1372
3	10	70.0	135.0	45.0	0.1587
3	11	70.0	150.0	30.0	0.2025
3	12	70.0	165.0	15.0	0.2767
3	13	70.0	180.0	0.0	0.3242
2	1	80.0	0.0	180.0	0.1574
2	2	80.0	15.0	165.0	0.1655
2	3	80.0	30.0	150.0	0.1716
2	4	80.0	45.0	135.0	0.1713
2	5	80.0	60.0	120.0	0.1676
2	6	80.0	75.0	105.0	0.1839
2	7	80.0	90.0	90.0	0.1897
2	8	80.0	105.0	75.0	0.1942
2	9	80.0	120.0	60.0	0.1885
2	10	80.0	135.0	45.0	0.2118
2	11	80.0	150.0	30.0	0.2473
2	12	80.0	165.0	15.0	0.3123
2	13	80.0	180.0	0.0	0.3450
1	1	87.5	0.0	180.0	0.1551
1	2	87.5	15.0	165.0	0.1687
1	3	87.5	30.0	150.0	0.1862
1	4	87.5	45.0	135.0	0.1843
1	5	87.5	60.0	120.0	0.1850
1	6	87.5	75.0	105.0	0.1965
1	7	87.5	90.0	90.0	0.2092
1	8	87.5	105.0	75.0	0.2209
1	9	87.5	120.0	60.0	0.2334
1	10	87.5	135.0	45.0	0.2593
1	11	87.5	150.0	30.0	0.3000
1	12	87.5	165.0	15.0	0.3485
1	13	87.5	180.0	0.0	0.3706

rho for WIND SPEED = 12.0 m/s THETA_SUN = 40.0 deg

10	1	0.0	0.0	0.0	0.0780
9	1	10.0	0.0	180.0	0.0505
9	2	10.0	15.0	165.0	0.0497
9	3	10.0	30.0	150.0	0.0547
9	4	10.0	45.0	135.0	0.0588
9	5	10.0	60.0	120.0	0.0564
9	6	10.0	75.0	105.0	0.0683
9	7	10.0	90.0	90.0	0.0736
9	8	10.0	105.0	75.0	0.0744
9	9	10.0	120.0	60.0	0.0937
9	10	10.0	135.0	45.0	0.1009
9	11	10.0	150.0	30.0	0.1066
9	12	10.0	165.0	15.0	0.1153
9	13	10.0	180.0	0.0	0.1233
8	1	20.0	0.0	180.0	0.0304
8	2	20.0	15.0	165.0	0.0331
8	3	20.0	30.0	150.0	0.0333
8	4	20.0	45.0	135.0	0.0359
8	5	20.0	60.0	120.0	0.0402
8	6	20.0	75.0	105.0	0.0463
8	7	20.0	90.0	90.0	0.0555
8	8	20.0	105.0	75.0	0.0718
8	9	20.0	120.0	60.0	0.0917

8 10 20.0 135.0 45.0 0.1060
8 11 20.0 150.0 30.0 0.1143
8 12 20.0 165.0 15.0 0.1147
8 13 20.0 180.0 0.0 0.1123
7 1 30.0 0.0 180.0 0.0294
7 2 30.0 15.0 165.0 0.0287
7 3 30.0 30.0 150.0 0.0294
7 4 30.0 45.0 135.0 0.0310
7 5 30.0 60.0 120.0 0.0315
7 6 30.0 75.0 105.0 0.0352
7 7 30.0 90.0 90.0 0.0438
7 8 30.0 105.0 75.0 0.0566
7 9 30.0 120.0 60.0 0.0818
7 10 30.0 135.0 45.0 0.1059
7 11 30.0 150.0 30.0 0.1153
7 12 30.0 165.0 15.0 0.0913
7 13 30.0 180.0 0.0 0.0792
6 1 40.0 0.0 180.0 0.0365
6 2 40.0 15.0 165.0 0.0363
6 3 40.0 30.0 150.0 0.0357
6 4 40.0 45.0 135.0 0.0355
6 5 40.0 60.0 120.0 0.0343
6 6 40.0 75.0 105.0 0.0368
6 7 40.0 90.0 90.0 0.0380
6 8 40.0 105.0 75.0 0.0508
6 9 40.0 120.0 60.0 0.0696
6 10 40.0 135.0 45.0 0.0999
6 11 40.0 150.0 30.0 0.1145
6 12 40.0 165.0 15.0 0.0862
6 13 40.0 180.0 0.0 0.0014
5 1 50.0 0.0 180.0 0.0554
5 2 50.0 15.0 165.0 0.0557
5 3 50.0 30.0 150.0 0.0550
5 4 50.0 45.0 135.0 0.0536
5 5 50.0 60.0 120.0 0.0511
5 6 50.0 75.0 105.0 0.0504
5 7 50.0 90.0 90.0 0.0508
5 8 50.0 105.0 75.0 0.0529
5 9 50.0 120.0 60.0 0.0683
5 10 50.0 135.0 45.0 0.0980
5 11 50.0 150.0 30.0 0.1352
5 12 50.0 165.0 15.0 0.1381
5 13 50.0 180.0 0.0 0.1210
4 1 60.0 0.0 180.0 0.0911
4 2 60.0 15.0 165.0 0.0922
4 3 60.0 30.0 150.0 0.0925
4 4 60.0 45.0 135.0 0.0890
4 5 60.0 60.0 120.0 0.0847
4 6 60.0 75.0 105.0 0.0839
4 7 60.0 90.0 90.0 0.0843
4 8 60.0 105.0 75.0 0.0822
4 9 60.0 120.0 60.0 0.0841
4 10 60.0 135.0 45.0 0.1092
4 11 60.0 150.0 30.0 0.1719
4 12 60.0 165.0 15.0 0.2530
4 13 60.0 180.0 0.0 0.2857
3 1 70.0 0.0 180.0 0.1328
3 2 70.0 15.0 165.0 0.1362
3 3 70.0 30.0 150.0 0.1399
3 4 70.0 45.0 135.0 0.1385
3 5 70.0 60.0 120.0 0.1335
3 6 70.0 75.0 105.0 0.1368
3 7 70.0 90.0 90.0 0.1394
3 8 70.0 105.0 75.0 0.1361
3 9 70.0 120.0 60.0 0.1340
3 10 70.0 135.0 45.0 0.1504
3 11 70.0 150.0 30.0 0.2241
3 12 70.0 165.0 15.0 0.3716
3 13 70.0 180.0 0.0 0.5019
2 1 80.0 0.0 180.0 0.1538
2 2 80.0 15.0 165.0 0.1619
2 3 80.0 30.0 150.0 0.1678
2 4 80.0 45.0 135.0 0.1675
2 5 80.0 60.0 120.0 0.1639
2 6 80.0 75.0 105.0 0.1802
2 7 80.0 90.0 90.0 0.1861
2 8 80.0 105.0 75.0 0.1906
2 9 80.0 120.0 60.0 0.1856
2 10 80.0 135.0 45.0 0.2095
2 11 80.0 150.0 30.0 0.2713
2 12 80.0 165.0 15.0 0.4772
2 13 80.0 180.0 0.0 0.6231
1 1 87.5 0.0 180.0 0.1516
1 2 87.5 15.0 165.0 0.1650
1 3 87.5 30.0 150.0 0.1819
1 4 87.5 45.0 135.0 0.1795
1 5 87.5 60.0 120.0 0.1799
1 6 87.5 75.0 105.0 0.1912
1 7 87.5 90.0 90.0 0.2042
1 8 87.5 105.0 75.0 0.2157
1 9 87.5 120.0 60.0 0.2295
1 10 87.5 135.0 45.0 0.2617
1 11 87.5 150.0 30.0 0.3270
1 12 87.5 165.0 15.0 0.5480
1 13 87.5 180.0 0.0 0.7328
rho for WIND SPEED = 12.0 m/s THETA_SUN = 50.0
deg
10 1 0.0 0.0 0.0 0.0506
9 1 10.0 0.0 180.0 0.0328
9 2 10.0 15.0 165.0 0.0311

9	3	10.0	30.0	150.0	0.0308
9	4	10.0	45.0	135.0	0.0299
9	5	10.0	60.0	120.0	0.0370
9	6	10.0	75.0	105.0	0.0381
9	7	10.0	90.0	90.0	0.0473
9	8	10.0	105.0	75.0	0.0497
9	9	10.0	120.0	60.0	0.0559
9	10	10.0	135.0	45.0	0.0705
9	11	10.0	150.0	30.0	0.0694
9	12	10.0	165.0	15.0	0.0912
9	13	10.0	180.0	0.0	0.0865
8	1	20.0	0.0	180.0	0.0264
8	2	20.0	15.0	165.0	0.0262
8	3	20.0	30.0	150.0	0.0254
8	4	20.0	45.0	135.0	0.0297
8	5	20.0	60.0	120.0	0.0285
8	6	20.0	75.0	105.0	0.0340
8	7	20.0	90.0	90.0	0.0325
8	8	20.0	105.0	75.0	0.0464
8	9	20.0	120.0	60.0	0.0577
8	10	20.0	135.0	45.0	0.0785
8	11	20.0	150.0	30.0	0.1014
8	12	20.0	165.0	15.0	0.1116
8	13	20.0	180.0	0.0	0.1119
7	1	30.0	0.0	180.0	0.0279
7	2	30.0	15.0	165.0	0.0282
7	3	30.0	30.0	150.0	0.0281
7	4	30.0	45.0	135.0	0.0275
7	5	30.0	60.0	120.0	0.0289
7	6	30.0	75.0	105.0	0.0288
7	7	30.0	90.0	90.0	0.0316
7	8	30.0	105.0	75.0	0.0396
7	9	30.0	120.0	60.0	0.0540
7	10	30.0	135.0	45.0	0.0782
7	11	30.0	150.0	30.0	0.1073
7	12	30.0	165.0	15.0	0.1259
7	13	30.0	180.0	0.0	0.1194
6	1	40.0	0.0	180.0	0.0365
6	2	40.0	15.0	165.0	0.0368
6	3	40.0	30.0	150.0	0.0362
6	4	40.0	45.0	135.0	0.0351
6	5	40.0	60.0	120.0	0.0345
6	6	40.0	75.0	105.0	0.0343
6	7	40.0	90.0	90.0	0.0362
6	8	40.0	105.0	75.0	0.0370
6	9	40.0	120.0	60.0	0.0500
6	10	40.0	135.0	45.0	0.0785
6	11	40.0	150.0	30.0	0.1115
6	12	40.0	165.0	15.0	0.1122
6	13	40.0	180.0	0.0	0.0919
5	1	50.0	0.0	180.0	0.0559
5	2	50.0	15.0	165.0	0.0562
5	3	50.0	30.0	150.0	0.0557
5	4	50.0	45.0	135.0	0.0544
5	5	50.0	60.0	120.0	0.0518
5	6	50.0	75.0	105.0	0.0508
5	7	50.0	90.0	90.0	0.0510
5	8	50.0	105.0	75.0	0.0507
5	9	50.0	120.0	60.0	0.0545
5	10	50.0	135.0	45.0	0.0796
5	11	50.0	150.0	30.0	0.1182
5	12	50.0	165.0	15.0	0.1187
5	13	50.0	180.0	0.0	0.0028
4	1	60.0	0.0	180.0	0.0904
4	2	60.0	15.0	165.0	0.0916
4	3	60.0	30.0	150.0	0.0923
4	4	60.0	45.0	135.0	0.0892
4	5	60.0	60.0	120.0	0.0852
4	6	60.0	75.0	105.0	0.0848
4	7	60.0	90.0	90.0	0.0851
4	8	60.0	105.0	75.0	0.0819
4	9	60.0	120.0	60.0	0.0823
4	10	60.0	135.0	45.0	0.0961
4	11	60.0	150.0	30.0	0.1500
4	12	60.0	165.0	15.0	0.2084
4	13	60.0	180.0	0.0	0.2047
3	1	70.0	0.0	180.0	0.1309
3	2	70.0	15.0	165.0	0.1343
3	3	70.0	30.0	150.0	0.1382
3	4	70.0	45.0	135.0	0.1371
3	5	70.0	60.0	120.0	0.1325
3	6	70.0	75.0	105.0	0.1361
3	7	70.0	90.0	90.0	0.1388
3	8	70.0	105.0	75.0	0.1352
3	9	70.0	120.0	60.0	0.1329
3	10	70.0	135.0	45.0	0.1430
3	11	70.0	150.0	30.0	0.1969
3	12	70.0	165.0	15.0	0.3946
3	13	70.0	180.0	0.0	0.5436
2	1	80.0	0.0	180.0	0.1528
2	2	80.0	15.0	165.0	0.1608
2	3	80.0	30.0	150.0	0.1666
2	4	80.0	45.0	135.0	0.1659
2	5	80.0	60.0	120.0	0.1619
2	6	80.0	75.0	105.0	0.1775
2	7	80.0	90.0	90.0	0.1828
2	8	80.0	105.0	75.0	0.1865
2	9	80.0	120.0	60.0	0.1812
2	10	80.0	135.0	45.0	0.2046
2	11	80.0	150.0	30.0	0.2716

2	12	80.0	165.0	15.0	0.6193
2	13	80.0	180.0	0.0	1.1251
1	1	87.5	0.0	180.0	0.1528
1	2	87.5	15.0	165.0	0.1662
1	3	87.5	30.0	150.0	0.1828
1	4	87.5	45.0	135.0	0.1793
1	5	87.5	60.0	120.0	0.1783
1	6	87.5	75.0	105.0	0.1881
1	7	87.5	90.0	90.0	0.1996
1	8	87.5	105.0	75.0	0.2088
1	9	87.5	120.0	60.0	0.2218
1	10	87.5	135.0	45.0	0.2578
1	11	87.5	150.0	30.0	0.3343
1	12	87.5	165.0	15.0	0.7923
1	13	87.5	180.0	0.0	1.6678

rho for WIND SPEED = 12.0 m/s THETA_SUN = 60.0 deg

10	1	0.0	0.0	0.0	0.0321
9	1	10.0	0.0	180.0	0.0247
9	2	10.0	15.0	165.0	0.0262
9	3	10.0	30.0	150.0	0.0264
9	4	10.0	45.0	135.0	0.0257
9	5	10.0	60.0	120.0	0.0265
9	6	10.0	75.0	105.0	0.0279
9	7	10.0	90.0	90.0	0.0309
9	8	10.0	105.0	75.0	0.0344
9	9	10.0	120.0	60.0	0.0427
9	10	10.0	135.0	45.0	0.0420
9	11	10.0	150.0	30.0	0.0524
9	12	10.0	165.0	15.0	0.0554
9	13	10.0	180.0	0.0	0.0535
8	1	20.0	0.0	180.0	0.0250
8	2	20.0	15.0	165.0	0.0249
8	3	20.0	30.0	150.0	0.0248
8	4	20.0	45.0	135.0	0.0250
8	5	20.0	60.0	120.0	0.0250
8	6	20.0	75.0	105.0	0.0272
8	7	20.0	90.0	90.0	0.0282
8	8	20.0	105.0	75.0	0.0332
8	9	20.0	120.0	60.0	0.0386
8	10	20.0	135.0	45.0	0.0520
8	11	20.0	150.0	30.0	0.0702
8	12	20.0	165.0	15.0	0.0852
8	13	20.0	180.0	0.0	0.0931
7	1	30.0	0.0	180.0	0.0274
7	2	30.0	15.0	165.0	0.0275
7	3	30.0	30.0	150.0	0.0275
7	4	30.0	45.0	135.0	0.0272
7	5	30.0	60.0	120.0	0.0272
7	6	30.0	75.0	105.0	0.0275
7	7	30.0	90.0	90.0	0.0284
7	8	30.0	105.0	75.0	0.0309
7	9	30.0	120.0	60.0	0.0392
7	10	30.0	135.0	45.0	0.0584
7	11	30.0	150.0	30.0	0.0911
7	12	30.0	165.0	15.0	0.1213
7	13	30.0	180.0	0.0	0.1319
6	1	40.0	0.0	180.0	0.0360
6	2	40.0	15.0	165.0	0.0363
6	3	40.0	30.0	150.0	0.0359
6	4	40.0	45.0	135.0	0.0350
6	5	40.0	60.0	120.0	0.0345
6	6	40.0	75.0	105.0	0.0341
6	7	40.0	90.0	90.0	0.0349
6	8	40.0	105.0	75.0	0.0363
6	9	40.0	120.0	60.0	0.0415
6	10	40.0	135.0	45.0	0.0619
6	11	40.0	150.0	30.0	0.1071
6	12	40.0	165.0	15.0	0.1491
6	13	40.0	180.0	0.0	0.1636
5	1	50.0	0.0	180.0	0.0547
5	2	50.0	15.0	165.0	0.0552
5	3	50.0	30.0	150.0	0.0549
5	4	50.0	45.0	135.0	0.0540
5	5	50.0	60.0	120.0	0.0518
5	6	50.0	75.0	105.0	0.0513
5	7	50.0	90.0	90.0	0.0516
5	8	50.0	105.0	75.0	0.0510
5	9	50.0	120.0	60.0	0.0536
5	10	50.0	135.0	45.0	0.0684
5	11	50.0	150.0	30.0	0.1134
5	12	50.0	165.0	15.0	0.1572
5	13	50.0	180.0	0.0	0.1463
4	1	60.0	0.0	180.0	0.0883
4	2	60.0	15.0	165.0	0.0895
4	3	60.0	30.0	150.0	0.0905
4	4	60.0	45.0	135.0	0.0879
4	5	60.0	60.0	120.0	0.0848
4	6	60.0	75.0	105.0	0.0849
4	7	60.0	90.0	90.0	0.0860
4	8	60.0	105.0	75.0	0.0829
4	9	60.0	120.0	60.0	0.0820
4	10	60.0	135.0	45.0	0.0901
4	11	60.0	150.0	30.0	0.1295
4	12	60.0	165.0	15.0	0.1884
4	13	60.0	180.0	0.0	0.0073
3	1	70.0	0.0	180.0	0.1290
3	2	70.0	15.0	165.0	0.1324
3	3	70.0	30.0	150.0	0.1363
3	4	70.0	45.0	135.0	0.1354

3	5	70.0	60.0	120.0	0.1312
3	6	70.0	75.0	105.0	0.1352
3	7	70.0	90.0	90.0	0.1383
3	8	70.0	105.0	75.0	0.1348
3	9	70.0	120.0	60.0	0.1319
3	10	70.0	135.0	45.0	0.1398
3	11	70.0	150.0	30.0	0.1719
3	12	70.0	165.0	15.0	0.3331
3	13	70.0	180.0	0.0	0.4119
2	1	80.0	0.0	180.0	0.1536
2	2	80.0	15.0	165.0	0.1616
2	3	80.0	30.0	150.0	0.1671
2	4	80.0	45.0	135.0	0.1660
2	5	80.0	60.0	120.0	0.1612
2	6	80.0	75.0	105.0	0.1759
2	7	80.0	90.0	90.0	0.1800
2	8	80.0	105.0	75.0	0.1825
2	9	80.0	120.0	60.0	0.1760
2	10	80.0	135.0	45.0	0.1969
2	11	80.0	150.0	30.0	0.2354
2	12	80.0	165.0	15.0	0.6150
2	13	80.0	180.0	0.0	1.1278
1	1	87.5	0.0	180.0	0.1569
1	2	87.5	15.0	165.0	0.1706
1	3	87.5	30.0	150.0	0.1870
1	4	87.5	45.0	135.0	0.1823
1	5	87.5	60.0	120.0	0.1796
1	6	87.5	75.0	105.0	0.1870
1	7	87.5	90.0	90.0	0.1958
1	8	87.5	105.0	75.0	0.2018
1	9	87.5	120.0	60.0	0.2117
1	10	87.5	135.0	45.0	0.2460
1	11	87.5	150.0	30.0	0.3260
1	12	87.5	165.0	15.0	0.9661
1	13	87.5	180.0	0.0	2.3219

rho for WIND SPEED = 12.0 m/s THETA_SUN = 70.0 deg

10	1	0.0	0.0	0.0	0.0259
9	1	10.0	0.0	180.0	0.0234
9	2	10.0	15.0	165.0	0.0236
9	3	10.0	30.0	150.0	0.0238
9	4	10.0	45.0	135.0	0.0242
9	5	10.0	60.0	120.0	0.0240
9	6	10.0	75.0	105.0	0.0243
9	7	10.0	90.0	90.0	0.0248
9	8	10.0	105.0	75.0	0.0271
9	9	10.0	120.0	60.0	0.0279
9	10	10.0	135.0	45.0	0.0316
9	11	10.0	150.0	30.0	0.0319
9	12	10.0	165.0	15.0	0.0351
9	13	10.0	180.0	0.0	0.0346
8	1	20.0	0.0	180.0	0.0244
8	2	20.0	15.0	165.0	0.0238
8	3	20.0	30.0	150.0	0.0238
8	4	20.0	45.0	135.0	0.0241
8	5	20.0	60.0	120.0	0.0240
8	6	20.0	75.0	105.0	0.0248
8	7	20.0	90.0	90.0	0.0256
8	8	20.0	105.0	75.0	0.0264
8	9	20.0	120.0	60.0	0.0301
8	10	20.0	135.0	45.0	0.0372
8	11	20.0	150.0	30.0	0.0486
8	12	20.0	165.0	15.0	0.0615
8	13	20.0	180.0	0.0	0.0626
7	1	30.0	0.0	180.0	0.0266
7	2	30.0	15.0	165.0	0.0268
7	3	30.0	30.0	150.0	0.0268
7	4	30.0	45.0	135.0	0.0265
7	5	30.0	60.0	120.0	0.0265
7	6	30.0	75.0	105.0	0.0266
7	7	30.0	90.0	90.0	0.0274
7	8	30.0	105.0	75.0	0.0285
7	9	30.0	120.0	60.0	0.0325
7	10	30.0	135.0	45.0	0.0444
7	11	30.0	150.0	30.0	0.0711
7	12	30.0	165.0	15.0	0.1050
7	13	30.0	180.0	0.0	0.1285
6	1	40.0	0.0	180.0	0.0348
6	2	40.0	15.0	165.0	0.0352
6	3	40.0	30.0	150.0	0.0349
6	4	40.0	45.0	135.0	0.0342
6	5	40.0	60.0	120.0	0.0340
6	6	40.0	75.0	105.0	0.0336
6	7	40.0	90.0	90.0	0.0345
6	8	40.0	105.0	75.0	0.0347
6	9	40.0	120.0	60.0	0.0380
6	10	40.0	135.0	45.0	0.0488
6	11	40.0	150.0	30.0	0.0927
6	12	40.0	165.0	15.0	0.1751
6	13	40.0	180.0	0.0	0.2110
5	1	50.0	0.0	180.0	0.0528
5	2	50.0	15.0	165.0	0.0533
5	3	50.0	30.0	150.0	0.0533
5	4	50.0	45.0	135.0	0.0527
5	5	50.0	60.0	120.0	0.0511
5	6	50.0	75.0	105.0	0.0511
5	7	50.0	90.0	90.0	0.0519
5	8	50.0	105.0	75.0	0.0513
5	9	50.0	120.0	60.0	0.0533
5	10	50.0	135.0	45.0	0.0639

5 11 50.0 150.0 30.0 0.1082
5 12 50.0 165.0 15.0 0.2174
5 13 50.0 180.0 0.0 0.2897
4 1 60.0 0.0 180.0 0.0857
4 2 60.0 15.0 165.0 0.0870
4 3 60.0 30.0 150.0 0.0881
4 4 60.0 45.0 135.0 0.0860
4 5 60.0 60.0 120.0 0.0834
4 6 60.0 75.0 105.0 0.0845
4 7 60.0 90.0 90.0 0.0862
4 8 60.0 105.0 75.0 0.0840
4 9 60.0 120.0 60.0 0.0839
4 10 60.0 135.0 45.0 0.0913
4 11 60.0 150.0 30.0 0.1238
4 12 60.0 165.0 15.0 0.2418
4 13 60.0 180.0 0.0 0.2775
3 1 70.0 0.0 180.0 0.1275
3 2 70.0 15.0 165.0 0.1307
3 3 70.0 30.0 150.0 0.1346
3 4 70.0 45.0 135.0 0.1338
3 5 70.0 60.0 120.0 0.1299
3 6 70.0 75.0 105.0 0.1342
3 7 70.0 90.0 90.0 0.1378
3 8 70.0 105.0 75.0 0.1344
3 9 70.0 120.0 60.0 0.1321
3 10 70.0 135.0 45.0 0.1403
3 11 70.0 150.0 30.0 0.1517
3 12 70.0 165.0 15.0 0.2769
3 13 70.0 180.0 0.0 0.0240
2 1 80.0 0.0 180.0 0.1557
2 2 80.0 15.0 165.0 0.1637
2 3 80.0 30.0 150.0 0.1689
2 4 80.0 45.0 135.0 0.1672
2 5 80.0 60.0 120.0 0.1616
2 6 80.0 75.0 105.0 0.1752
2 7 80.0 90.0 90.0 0.1780
2 8 80.0 105.0 75.0 0.1792
2 9 80.0 120.0 60.0 0.1710
2 10 80.0 135.0 45.0 0.1877
2 11 80.0 150.0 30.0 0.2057
2 12 80.0 165.0 15.0 0.4172
2 13 80.0 180.0 0.0 0.7564
1 1 87.5 0.0 180.0 0.1628
1 2 87.5 15.0 165.0 0.1766
1 3 87.5 30.0 150.0 0.1931
1 4 87.5 45.0 135.0 0.1872
1 5 87.5 60.0 120.0 0.1826
1 6 87.5 75.0 105.0 0.1875
1 7 87.5 90.0 90.0 0.1933
1 8 87.5 105.0 75.0 0.1957
1 9 87.5 120.0 60.0 0.2014
1 10 87.5 135.0 45.0 0.2273
1 11 87.5 150.0 30.0 0.2806
1 12 87.5 165.0 15.0 0.5980
1 13 87.5 180.0 0.0 1.6872
rho for WIND SPEED = 12.0 m/s THETA_SUN = 80.0 deg
10 1 0.0 0.0 0.0 0.0233
9 1 10.0 0.0 180.0 0.0224
9 2 10.0 15.0 165.0 0.0225
9 3 10.0 30.0 150.0 0.0225
9 4 10.0 45.0 135.0 0.0227
9 5 10.0 60.0 120.0 0.0228
9 6 10.0 75.0 105.0 0.0228
9 7 10.0 90.0 90.0 0.0231
9 8 10.0 105.0 75.0 0.0236
9 9 10.0 120.0 60.0 0.0244
9 10 10.0 135.0 45.0 0.0252
9 11 10.0 150.0 30.0 0.0255
9 12 10.0 165.0 15.0 0.0261
9 13 10.0 180.0 0.0 0.0276
8 1 20.0 0.0 180.0 0.0233
8 2 20.0 15.0 165.0 0.0230
8 3 20.0 30.0 150.0 0.0230
8 4 20.0 45.0 135.0 0.0233
8 5 20.0 60.0 120.0 0.0231
8 6 20.0 75.0 105.0 0.0236
8 7 20.0 90.0 90.0 0.0237
8 8 20.0 105.0 75.0 0.0245
8 9 20.0 120.0 60.0 0.0258
8 10 20.0 135.0 45.0 0.0282
8 11 20.0 150.0 30.0 0.0322
8 12 20.0 165.0 15.0 0.0374
8 13 20.0 180.0 0.0 0.0402
7 1 30.0 0.0 180.0 0.0257
7 2 30.0 15.0 165.0 0.0259
7 3 30.0 30.0 150.0 0.0260
7 4 30.0 45.0 135.0 0.0258
7 5 30.0 60.0 120.0 0.0258
7 6 30.0 75.0 105.0 0.0259
7 7 30.0 90.0 90.0 0.0266
7 8 30.0 105.0 75.0 0.0271
7 9 30.0 120.0 60.0 0.0289
7 10 30.0 135.0 45.0 0.0339
7 11 30.0 150.0 30.0 0.0462
7 12 30.0 165.0 15.0 0.0689
7 13 30.0 180.0 0.0 0.0819
6 1 40.0 0.0 180.0 0.0335
6 2 40.0 15.0 165.0 0.0339
6 3 40.0 30.0 150.0 0.0338

6 4 40.0 45.0 135.0 0.0333
6 5 40.0 60.0 120.0 0.0332
6 6 40.0 75.0 105.0 0.0331
6 7 40.0 90.0 90.0 0.0341
6 8 40.0 105.0 75.0 0.0341
6 9 40.0 120.0 60.0 0.0368
6 10 40.0 135.0 45.0 0.0438
6 11 40.0 150.0 30.0 0.0695
6 12 40.0 165.0 15.0 0.1347
6 13 40.0 180.0 0.0 0.1863
5 1 50.0 0.0 180.0 0.0509
5 2 50.0 15.0 165.0 0.0513
5 3 50.0 30.0 150.0 0.0514
5 4 50.0 45.0 135.0 0.0512
5 5 50.0 60.0 120.0 0.0500
5 6 50.0 75.0 105.0 0.0504
5 7 50.0 90.0 90.0 0.0517
5 8 50.0 105.0 75.0 0.0514
5 9 50.0 120.0 60.0 0.0538
5 10 50.0 135.0 45.0 0.0640
5 11 50.0 150.0 30.0 0.0947
5 12 50.0 165.0 15.0 0.2165
5 13 50.0 180.0 0.0 0.3378
4 1 60.0 0.0 180.0 0.0834
4 2 60.0 15.0 165.0 0.0847
4 3 60.0 30.0 150.0 0.0859
4 4 60.0 45.0 135.0 0.0842
4 5 60.0 60.0 120.0 0.0821
4 6 60.0 75.0 105.0 0.0836
4 7 60.0 90.0 90.0 0.0860
4 8 60.0 105.0 75.0 0.0844
4 9 60.0 120.0 60.0 0.0854
4 10 60.0 135.0 45.0 0.0961
4 11 60.0 150.0 30.0 0.1251
4 12 60.0 165.0 15.0 0.2606
4 13 60.0 180.0 0.0 0.4486
3 1 70.0 0.0 180.0 0.1266
3 2 70.0 15.0 165.0 0.1298
3 3 70.0 30.0 150.0 0.1335
3 4 70.0 45.0 135.0 0.1327
3 5 70.0 60.0 120.0 0.1289
3 6 70.0 75.0 105.0 0.1333
3 7 70.0 90.0 90.0 0.1370
3 8 70.0 105.0 75.0 0.1343
3 9 70.0 120.0 60.0 0.1321
3 10 70.0 135.0 45.0 0.1429
3 11 70.0 150.0 30.0 0.1548
3 12 70.0 165.0 15.0 0.2418
3 13 70.0 180.0 0.0 0.3923
2 1 80.0 0.0 180.0 0.1586
2 2 80.0 15.0 165.0 0.1664
2 3 80.0 30.0 150.0 0.1713
2 4 80.0 45.0 135.0 0.1690
2 5 80.0 60.0 120.0 0.1625
2 6 80.0 75.0 105.0 0.1749
2 7 80.0 90.0 90.0 0.1768
2 8 80.0 105.0 75.0 0.1767
2 9 80.0 120.0 60.0 0.1672
2 10 80.0 135.0 45.0 0.1790
2 11 80.0 150.0 30.0 0.1831
2 12 80.0 165.0 15.0 0.2315
2 13 80.0 180.0 0.0 0.0647
1 1 87.5 0.0 180.0 0.1691
1 2 87.5 15.0 165.0 0.1832
1 3 87.5 30.0 150.0 0.1995
1 4 87.5 45.0 135.0 0.1923
1 5 87.5 60.0 120.0 0.1858
1 6 87.5 75.0 105.0 0.1884
1 7 87.5 90.0 90.0 0.1917
1 8 87.5 105.0 75.0 0.1914
1 9 87.5 120.0 60.0 0.1927
1 10 87.5 135.0 45.0 0.2063
1 11 87.5 150.0 30.0 0.2240
1 12 87.5 165.0 15.0 0.2581
1 13 87.5 180.0 0.0 0.5576
rho for WIND SPEED = 14.0 m/s THETA_SUN = 0.0 deg
10 1 0.0 0.0 0.0 0.0006
9 1 10.0 0.0 180.0 0.0743
9 2 10.0 15.0 165.0 0.0701
9 3 10.0 30.0 150.0 0.0762
9 4 10.0 45.0 135.0 0.0770
9 5 10.0 60.0 120.0 0.0786
9 6 10.0 75.0 105.0 0.0707
9 7 10.0 90.0 90.0 0.0780
9 8 10.0 105.0 75.0 0.0707
9 9 10.0 120.0 60.0 0.0786
9 10 10.0 135.0 45.0 0.0770
9 11 10.0 150.0 30.0 0.0762
9 12 10.0 165.0 15.0 0.0701
9 13 10.0 180.0 0.0 0.0743
8 1 20.0 0.0 180.0 0.1289
8 2 20.0 15.0 165.0 0.1174
8 3 20.0 30.0 150.0 0.1146
8 4 20.0 45.0 135.0 0.1228
8 5 20.0 60.0 120.0 0.1158
8 6 20.0 75.0 105.0 0.1129
8 7 20.0 90.0 90.0 0.1161
8 8 20.0 105.0 75.0 0.1129
8 9 20.0 120.0 60.0 0.1158

8	10	20.0	135.0	45.0	0.1228
8	11	20.0	150.0	30.0	0.1146
8	12	20.0	165.0	15.0	0.1173
8	13	20.0	180.0	0.0	0.1289
7	1	30.0	0.0	180.0	0.1389
7	2	30.0	15.0	165.0	0.1337
7	3	30.0	30.0	150.0	0.1425
7	4	30.0	45.0	135.0	0.1422
7	5	30.0	60.0	120.0	0.1439
7	6	30.0	75.0	105.0	0.1422
7	7	30.0	90.0	90.0	0.1376
7	8	30.0	105.0	75.0	0.1422
7	9	30.0	120.0	60.0	0.1439
7	10	30.0	135.0	45.0	0.1422
7	11	30.0	150.0	30.0	0.1425
7	12	30.0	165.0	15.0	0.1337
7	13	30.0	180.0	0.0	0.1390
6	1	40.0	0.0	180.0	0.1230
6	2	40.0	15.0	165.0	0.1239
6	3	40.0	30.0	150.0	0.1184
6	4	40.0	45.0	135.0	0.1157
6	5	40.0	60.0	120.0	0.1186
6	6	40.0	75.0	105.0	0.1202
6	7	40.0	90.0	90.0	0.1127
6	8	40.0	105.0	75.0	0.1202
6	9	40.0	120.0	60.0	0.1186
6	10	40.0	135.0	45.0	0.1157
6	11	40.0	150.0	30.0	0.1184
6	12	40.0	165.0	15.0	0.1239
6	13	40.0	180.0	0.0	0.1230
5	1	50.0	0.0	180.0	0.0929
5	2	50.0	15.0	165.0	0.0922
5	3	50.0	30.0	150.0	0.0933
5	4	50.0	45.0	135.0	0.0970
5	5	50.0	60.0	120.0	0.0946
5	6	50.0	75.0	105.0	0.0969
5	7	50.0	90.0	90.0	0.0906
5	8	50.0	105.0	75.0	0.0969
5	9	50.0	120.0	60.0	0.0946
5	10	50.0	135.0	45.0	0.0970
5	11	50.0	150.0	30.0	0.0933
5	12	50.0	165.0	15.0	0.0922
5	13	50.0	180.0	0.0	0.0929
4	1	60.0	0.0	180.0	0.0953
4	2	60.0	15.0	165.0	0.0985
4	3	60.0	30.0	150.0	0.0961
4	4	60.0	45.0	135.0	0.0948
4	5	60.0	60.0	120.0	0.0946
4	6	60.0	75.0	105.0	0.0979
4	7	60.0	90.0	90.0	0.0951
4	8	60.0	105.0	75.0	0.0979
4	9	60.0	120.0	60.0	0.0946
4	10	60.0	135.0	45.0	0.0948
4	11	60.0	150.0	30.0	0.0962
4	12	60.0	165.0	15.0	0.0985
4	13	60.0	180.0	0.0	0.0953
3	1	70.0	0.0	180.0	0.1294
3	2	70.0	15.0	165.0	0.1332
3	3	70.0	30.0	150.0	0.1365
3	4	70.0	45.0	135.0	0.1361
3	5	70.0	60.0	120.0	0.1316
3	6	70.0	75.0	105.0	0.1365
3	7	70.0	90.0	90.0	0.1395
3	8	70.0	105.0	75.0	0.1365
3	9	70.0	120.0	60.0	0.1316
3	10	70.0	135.0	45.0	0.1361
3	11	70.0	150.0	30.0	0.1365
3	12	70.0	165.0	15.0	0.1332
3	13	70.0	180.0	0.0	0.1294
2	1	80.0	0.0	180.0	0.1686
2	2	80.0	15.0	165.0	0.1764
2	3	80.0	30.0	150.0	0.1806
2	4	80.0	45.0	135.0	0.1767
2	5	80.0	60.0	120.0	0.1701
2	6	80.0	75.0	105.0	0.1817
2	7	80.0	90.0	90.0	0.1823
2	8	80.0	105.0	75.0	0.1817
2	9	80.0	120.0	60.0	0.1701
2	10	80.0	135.0	45.0	0.1767
2	11	80.0	150.0	30.0	0.1806
2	12	80.0	165.0	15.0	0.1764
2	13	80.0	180.0	0.0	0.1686
1	1	87.5	0.0	180.0	0.1848
1	2	87.5	15.0	165.0	0.2022
1	3	87.5	30.0	150.0	0.2120
1	4	87.5	45.0	135.0	0.2074
1	5	87.5	60.0	120.0	0.1974
1	6	87.5	75.0	105.0	0.1977
1	7	87.5	90.0	90.0	0.2006
1	8	87.5	105.0	75.0	0.1977
1	9	87.5	120.0	60.0	0.1974
1	10	87.5	135.0	45.0	0.2074
1	11	87.5	150.0	30.0	0.2120
1	12	87.5	165.0	15.0	0.2022
1	13	87.5	180.0	0.0	0.1848

rho for WIND SPEED = 14.0 m/s THETA_SUN = 10.0 deg

10	1	0.0	0.0	0.0	0.0670
9	1	10.0	0.0	180.0	0.1260
9	2	10.0	15.0	165.0	0.1202

9	3	10.0	30.0	150.0	0.1104
9	4	10.0	45.0	135.0	0.1098
9	5	10.0	60.0	120.0	0.1058
9	6	10.0	75.0	105.0	0.1041
9	7	10.0	90.0	90.0	0.0999
9	8	10.0	105.0	75.0	0.0753
9	9	10.0	120.0	60.0	0.0683
9	10	10.0	135.0	45.0	0.0629
9	11	10.0	150.0	30.0	0.0519
9	12	10.0	165.0	15.0	0.0423
9	13	10.0	180.0	0.0	0.0002
8	1	20.0	0.0	180.0	0.1140
8	2	20.0	15.0	165.0	0.1238
8	3	20.0	30.0	150.0	0.1254
8	4	20.0	45.0	135.0	0.1357
8	5	20.0	60.0	120.0	0.1319
8	6	20.0	75.0	105.0	0.1304
8	7	20.0	90.0	90.0	0.1269
8	8	20.0	105.0	75.0	0.1190
8	9	20.0	120.0	60.0	0.1045
8	10	20.0	135.0	45.0	0.0982
8	11	20.0	150.0	30.0	0.0880
8	12	20.0	165.0	15.0	0.0822
8	13	20.0	180.0	0.0	0.0713
7	1	30.0	0.0	180.0	0.1117
7	2	30.0	15.0	165.0	0.1085
7	3	30.0	30.0	150.0	0.1009
7	4	30.0	45.0	135.0	0.1122
7	5	30.0	60.0	120.0	0.1234
7	6	30.0	75.0	105.0	0.1286
7	7	30.0	90.0	90.0	0.1253
7	8	30.0	105.0	75.0	0.1329
7	9	30.0	120.0	60.0	0.1261
7	10	30.0	135.0	45.0	0.1343
7	11	30.0	150.0	30.0	0.1277
7	12	30.0	165.0	15.0	0.1363
7	13	30.0	180.0	0.0	0.1242
6	1	40.0	0.0	180.0	0.0720
6	2	40.0	15.0	165.0	0.0727
6	3	40.0	30.0	150.0	0.0734
6	4	40.0	45.0	135.0	0.0757
6	5	40.0	60.0	120.0	0.0884
6	6	40.0	75.0	105.0	0.1056
6	7	40.0	90.0	90.0	0.1118
6	8	40.0	105.0	75.0	0.1209
6	9	40.0	120.0	60.0	0.1329
6	10	40.0	135.0	45.0	0.1453
6	11	40.0	150.0	30.0	0.1547
6	12	40.0	165.0	15.0	0.1621
6	13	40.0	180.0	0.0	0.1673
5	1	50.0	0.0	180.0	0.0638
5	2	50.0	15.0	165.0	0.0648
5	3	50.0	30.0	150.0	0.0661
5	4	50.0	45.0	135.0	0.0653
5	5	50.0	60.0	120.0	0.0706
5	6	50.0	75.0	105.0	0.0767
5	7	50.0	90.0	90.0	0.0880
5	8	50.0	105.0	75.0	0.0964
5	9	50.0	120.0	60.0	0.1144
5	10	50.0	135.0	45.0	0.1234
5	11	50.0	150.0	30.0	0.1373
5	12	50.0	165.0	15.0	0.1497
5	13	50.0	180.0	0.0	0.1615
4	1	60.0	0.0	180.0	0.0826
4	2	60.0	15.0	165.0	0.0837
4	3	60.0	30.0	150.0	0.0879
4	4	60.0	45.0	135.0	0.0865
4	5	60.0	60.0	120.0	0.0846
4	6	60.0	75.0	105.0	0.0881
4	7	60.0	90.0	90.0	0.0955
4	8	60.0	105.0	75.0	0.0921
4	9	60.0	120.0	60.0	0.1050
4	10	60.0	135.0	45.0	0.1171
4	11	60.0	150.0	30.0	0.1318
4	12	60.0	165.0	15.0	0.1430
4	13	60.0	180.0	0.0	0.1455
3	1	70.0	0.0	180.0	0.1266
3	2	70.0	15.0	165.0	0.1305
3	3	70.0	30.0	150.0	0.1339
3	4	70.0	45.0	135.0	0.1322
3	5	70.0	60.0	120.0	0.1280
3	6	70.0	75.0	105.0	0.1335
3	7	70.0	90.0	90.0	0.1391
3	8	70.0	105.0	75.0	0.1371
3	9	70.0	120.0	60.0	0.1374
3	10	70.0	135.0	45.0	0.1479
3	11	70.0	150.0	30.0	0.1535
3	12	70.0	165.0	15.0	0.1511
3	13	70.0	180.0	0.0	0.1511
2	1	80.0	0.0	180.0	0.1596
2	2	80.0	15.0	165.0	0.1668
2	3	80.0	30.0	150.0	0.1718
2	4	80.0	45.0	135.0	0.1696
2	5	80.0	60.0	120.0	0.1648
2	6	80.0	75.0	105.0	0.1777
2	7	80.0	90.0	90.0	0.1814
2	8	80.0	105.0	75.0	0.1826
2	9	80.0	120.0	60.0	0.1754
2	10	80.0	135.0	45.0	0.1878
2	11	80.0	150.0	30.0	0.1887

2 12 80.0 165.0 15.0 0.1913
2 13 80.0 180.0 0.0 0.1836
1 1 87.5 0.0 180.0 0.1642
1 2 87.5 15.0 165.0 0.1811
1 3 87.5 30.0 150.0 0.1921
1 4 87.5 45.0 135.0 0.1911
1 5 87.5 60.0 120.0 0.1860
1 6 87.5 75.0 105.0 0.1911
1 7 87.5 90.0 90.0 0.1994
1 8 87.5 105.0 75.0 0.2019
1 9 87.5 120.0 60.0 0.2069
1 10 87.5 135.0 45.0 0.2224
1 11 87.5 150.0 30.0 0.2313
1 12 87.5 165.0 15.0 0.2236
1 13 87.5 180.0 0.0 0.2063
rho for WIND SPEED = 14.0 m/s THETA_SUN = 20.0 deg
10 1 0.0 0.0 0.0 0.1108
9 1 10.0 0.0 180.0 0.1360
9 2 10.0 15.0 165.0 0.1178
9 3 10.0 30.0 150.0 0.1212
9 4 10.0 45.0 135.0 0.1230
9 5 10.0 60.0 120.0 0.1166
9 6 10.0 75.0 105.0 0.1307
9 7 10.0 90.0 90.0 0.1196
9 8 10.0 105.0 75.0 0.1122
9 9 10.0 120.0 60.0 0.0987
9 10 10.0 135.0 45.0 0.0891
9 11 10.0 150.0 30.0 0.0771
9 12 10.0 165.0 15.0 0.0674
9 13 10.0 180.0 0.0 0.0546
8 1 20.0 0.0 180.0 0.1170
8 2 20.0 15.0 165.0 0.0935
8 3 20.0 30.0 150.0 0.1067
8 4 20.0 45.0 135.0 0.1042
8 5 20.0 60.0 120.0 0.1197
8 6 20.0 75.0 105.0 0.1237
8 7 20.0 90.0 90.0 0.1303
8 8 20.0 105.0 75.0 0.1219
8 9 20.0 120.0 60.0 0.1125
8 10 20.0 135.0 45.0 0.0909
8 11 20.0 150.0 30.0 0.0706
8 12 20.0 165.0 15.0 0.0519
8 13 20.0 180.0 0.0 0.0004
7 1 30.0 0.0 180.0 0.0636
7 2 30.0 15.0 165.0 0.0687
7 3 30.0 30.0 150.0 0.0656
7 4 30.0 45.0 135.0 0.0711
7 5 30.0 60.0 120.0 0.0904
7 6 30.0 75.0 105.0 0.0939
7 7 30.0 90.0 90.0 0.1133
7 8 30.0 105.0 75.0 0.1250
7 9 30.0 120.0 60.0 0.1275
7 10 30.0 135.0 45.0 0.1158
7 11 30.0 150.0 30.0 0.1024
7 12 30.0 165.0 15.0 0.0854
7 13 30.0 180.0 0.0 0.0743
6 1 40.0 0.0 180.0 0.0464
6 2 40.0 15.0 165.0 0.0514
6 3 40.0 30.0 150.0 0.0510
6 4 40.0 45.0 135.0 0.0535
6 5 40.0 60.0 120.0 0.0606
6 6 40.0 75.0 105.0 0.0757
6 7 40.0 90.0 90.0 0.0902
6 8 40.0 105.0 75.0 0.1151
6 9 40.0 120.0 60.0 0.1313
6 10 40.0 135.0 45.0 0.1333
6 11 40.0 150.0 30.0 0.1473
6 12 40.0 165.0 15.0 0.1411
6 13 40.0 180.0 0.0 0.1493
5 1 50.0 0.0 180.0 0.0543
5 2 50.0 15.0 165.0 0.0547
5 3 50.0 30.0 150.0 0.0546
5 4 50.0 45.0 135.0 0.0558
5 5 50.0 60.0 120.0 0.0552
5 6 50.0 75.0 105.0 0.0622
5 7 50.0 90.0 90.0 0.0768
5 8 50.0 105.0 75.0 0.0851
5 9 50.0 120.0 60.0 0.1061
5 10 50.0 135.0 45.0 0.1420
5 11 50.0 150.0 30.0 0.1598
5 12 50.0 165.0 15.0 0.1934
5 13 50.0 180.0 0.0 0.1913
4 1 60.0 0.0 180.0 0.0858
4 2 60.0 15.0 165.0 0.0866
4 3 60.0 30.0 150.0 0.0879
4 4 60.0 45.0 135.0 0.0845
4 5 60.0 60.0 120.0 0.0828
4 6 60.0 75.0 105.0 0.0839
4 7 60.0 90.0 90.0 0.0874
4 8 60.0 105.0 75.0 0.0934
4 9 60.0 120.0 60.0 0.1000
4 10 60.0 135.0 45.0 0.1374
4 11 60.0 150.0 30.0 0.1661
4 12 60.0 165.0 15.0 0.2032
4 13 60.0 180.0 0.0 0.2122
3 1 70.0 0.0 180.0 0.1269
3 2 70.0 15.0 165.0 0.1301
3 3 70.0 30.0 150.0 0.1339
3 4 70.0 45.0 135.0 0.1325

3	5	70.0	60.0	120.0	0.1272
3	6	70.0	75.0	105.0	0.1318
3	7	70.0	90.0	90.0	0.1364
3	8	70.0	105.0	75.0	0.1346
3	9	70.0	120.0	60.0	0.1389
3	10	70.0	135.0	45.0	0.1568
3	11	70.0	150.0	30.0	0.1849
3	12	70.0	165.0	15.0	0.2150
3	13	70.0	180.0	0.0	0.2242
2	1	80.0	0.0	180.0	0.1494
2	2	80.0	15.0	165.0	0.1580
2	3	80.0	30.0	150.0	0.1636
2	4	80.0	45.0	135.0	0.1626
2	5	80.0	60.0	120.0	0.1591
2	6	80.0	75.0	105.0	0.1734
2	7	80.0	90.0	90.0	0.1789
2	8	80.0	105.0	75.0	0.1821
2	9	80.0	120.0	60.0	0.1767
2	10	80.0	135.0	45.0	0.1922
2	11	80.0	150.0	30.0	0.2153
2	12	80.0	165.0	15.0	0.2294
2	13	80.0	180.0	0.0	0.2347
1	1	87.5	0.0	180.0	0.1477
1	2	87.5	15.0	165.0	0.1639
1	3	87.5	30.0	150.0	0.1753
1	4	87.5	45.0	135.0	0.1767
1	5	87.5	60.0	120.0	0.1749
1	6	87.5	75.0	105.0	0.1836
1	7	87.5	90.0	90.0	0.1960
1	8	87.5	105.0	75.0	0.2028
1	9	87.5	120.0	60.0	0.2125
1	10	87.5	135.0	45.0	0.2340
1	11	87.5	150.0	30.0	0.2594
1	12	87.5	165.0	15.0	0.2626
1	13	87.5	180.0	0.0	0.2512

rho for WIND SPEED = 14.0 m/s THETA_SUN = 30.0 deg

10	1	0.0	0.0	0.0	0.1186
9	1	10.0	0.0	180.0	0.1105
9	2	10.0	15.0	165.0	0.1005
9	3	10.0	30.0	150.0	0.0989
9	4	10.0	45.0	135.0	0.1042
9	5	10.0	60.0	120.0	0.0991
9	6	10.0	75.0	105.0	0.1033
9	7	10.0	90.0	90.0	0.1126
9	8	10.0	105.0	75.0	0.1169
9	9	10.0	120.0	60.0	0.1150
9	10	10.0	135.0	45.0	0.1191
9	11	10.0	150.0	30.0	0.1033
9	12	10.0	165.0	15.0	0.0964
9	13	10.0	180.0	0.0	0.1119
8	1	20.0	0.0	180.0	0.0619
8	2	20.0	15.0	165.0	0.0610
8	3	20.0	30.0	150.0	0.0592
8	4	20.0	45.0	135.0	0.0742
8	5	20.0	60.0	120.0	0.0729
8	6	20.0	75.0	105.0	0.0847
8	7	20.0	90.0	90.0	0.1037
8	8	20.0	105.0	75.0	0.1133
8	9	20.0	120.0	60.0	0.1215
8	10	20.0	135.0	45.0	0.1114
8	11	20.0	150.0	30.0	0.0950
8	12	20.0	165.0	15.0	0.0733
8	13	20.0	180.0	0.0	0.0631
7	1	30.0	0.0	180.0	0.0449
7	2	30.0	15.0	165.0	0.0414
7	3	30.0	30.0	150.0	0.0434
7	4	30.0	45.0	135.0	0.0439
7	5	30.0	60.0	120.0	0.0475
7	6	30.0	75.0	105.0	0.0674
7	7	30.0	90.0	90.0	0.0827
7	8	30.0	105.0	75.0	0.1054
7	9	30.0	120.0	60.0	0.1165
7	10	30.0	135.0	45.0	0.1163
7	11	30.0	150.0	30.0	0.0896
7	12	30.0	165.0	15.0	0.0611
7	13	30.0	180.0	0.0	0.0007
6	1	40.0	0.0	180.0	0.0375
6	2	40.0	15.0	165.0	0.0400
6	3	40.0	30.0	150.0	0.0412
6	4	40.0	45.0	135.0	0.0404
6	5	40.0	60.0	120.0	0.0434
6	6	40.0	75.0	105.0	0.0468
6	7	40.0	90.0	90.0	0.0628
6	8	40.0	105.0	75.0	0.0787
6	9	40.0	120.0	60.0	0.1096
6	10	40.0	135.0	45.0	0.1184
6	11	40.0	150.0	30.0	0.1176
6	12	40.0	165.0	15.0	0.1006
6	13	40.0	180.0	0.0	0.0854
5	1	50.0	0.0	180.0	0.0550
5	2	50.0	15.0	165.0	0.0556
5	3	50.0	30.0	150.0	0.0548
5	4	50.0	45.0	135.0	0.0551
5	5	50.0	60.0	120.0	0.0524
5	6	50.0	75.0	105.0	0.0542
5	7	50.0	90.0	90.0	0.0609
5	8	50.0	105.0	75.0	0.0702
5	9	50.0	120.0	60.0	0.1025
5	10	50.0	135.0	45.0	0.1250

5 11 50.0 150.0 30.0 0.1617
5 12 50.0 165.0 15.0 0.1726
5 13 50.0 180.0 0.0 0.1700
4 1 60.0 0.0 180.0 0.0892
4 2 60.0 15.0 165.0 0.0896
4 3 60.0 30.0 150.0 0.0903
4 4 60.0 45.0 135.0 0.0865
4 5 60.0 60.0 120.0 0.0823
4 6 60.0 75.0 105.0 0.0827
4 7 60.0 90.0 90.0 0.0846
4 8 60.0 105.0 75.0 0.0883
4 9 60.0 120.0 60.0 0.0930
4 10 60.0 135.0 45.0 0.1321
4 11 60.0 150.0 30.0 0.1962
4 12 60.0 165.0 15.0 0.2566
4 13 60.0 180.0 0.0 0.2796
3 1 70.0 0.0 180.0 0.1263
3 2 70.0 15.0 165.0 0.1298
3 3 70.0 30.0 150.0 0.1338
3 4 70.0 45.0 135.0 0.1324
3 5 70.0 60.0 120.0 0.1267
3 6 70.0 75.0 105.0 0.1306
3 7 70.0 90.0 90.0 0.1341
3 8 70.0 105.0 75.0 0.1322
3 9 70.0 120.0 60.0 0.1340
3 10 70.0 135.0 45.0 0.1609
3 11 70.0 150.0 30.0 0.2213
3 12 70.0 165.0 15.0 0.3056
3 13 70.0 180.0 0.0 0.3496
2 1 80.0 0.0 180.0 0.1427
2 2 80.0 15.0 165.0 0.1513
2 3 80.0 30.0 150.0 0.1572
2 4 80.0 45.0 135.0 0.1568
2 5 80.0 60.0 120.0 0.1540
2 6 80.0 75.0 105.0 0.1691
2 7 80.0 90.0 90.0 0.1754
2 8 80.0 105.0 75.0 0.1797
2 9 80.0 120.0 60.0 0.1761
2 10 80.0 135.0 45.0 0.2042
2 11 80.0 150.0 30.0 0.2516
2 12 80.0 165.0 15.0 0.3319
2 13 80.0 180.0 0.0 0.3795
1 1 87.5 0.0 180.0 0.1378
1 2 87.5 15.0 165.0 0.1535
1 3 87.5 30.0 150.0 0.1646
1 4 87.5 45.0 135.0 0.1666
1 5 87.5 60.0 120.0 0.1664
1 6 87.5 75.0 105.0 0.1768
1 7 87.5 90.0 90.0 0.1913
1 8 87.5 105.0 75.0 0.2001
1 9 87.5 120.0 60.0 0.2132
1 10 87.5 135.0 45.0 0.2413
1 11 87.5 150.0 30.0 0.2790
1 12 87.5 165.0 15.0 0.3704
1 13 87.5 180.0 0.0 0.3855
rho for WIND SPEED = 14.0 m/s THETA_SUN = 40.0 deg
10 1 0.0 0.0 0.0 0.0872
9 1 10.0 0.0 180.0 0.0619
9 2 10.0 15.0 165.0 0.0546
9 3 10.0 30.0 150.0 0.0614
9 4 10.0 45.0 135.0 0.0730
9 5 10.0 60.0 120.0 0.0630
9 6 10.0 75.0 105.0 0.0759
9 7 10.0 90.0 90.0 0.0865
9 8 10.0 105.0 75.0 0.0864
9 9 10.0 120.0 60.0 0.1027
9 10 10.0 135.0 45.0 0.1021
9 11 10.0 150.0 30.0 0.1044
9 12 10.0 165.0 15.0 0.1166
9 13 10.0 180.0 0.0 0.1284
8 1 20.0 0.0 180.0 0.0336
8 2 20.0 15.0 165.0 0.0409
8 3 20.0 30.0 150.0 0.0375
8 4 20.0 45.0 135.0 0.0425
8 5 20.0 60.0 120.0 0.0477
8 6 20.0 75.0 105.0 0.0547
8 7 20.0 90.0 90.0 0.0650
8 8 20.0 105.0 75.0 0.0834
8 9 20.0 120.0 60.0 0.0988
8 10 20.0 135.0 45.0 0.1119
8 11 20.0 150.0 30.0 0.1116
8 12 20.0 165.0 15.0 0.1083
8 13 20.0 180.0 0.0 0.1040
7 1 30.0 0.0 180.0 0.0309
7 2 30.0 15.0 165.0 0.0306
7 3 30.0 30.0 150.0 0.0320
7 4 30.0 45.0 135.0 0.0338
7 5 30.0 60.0 120.0 0.0346
7 6 30.0 75.0 105.0 0.0410
7 7 30.0 90.0 90.0 0.0514
7 8 30.0 105.0 75.0 0.0666
7 9 30.0 120.0 60.0 0.0900
7 10 30.0 135.0 45.0 0.1084
7 11 30.0 150.0 30.0 0.1093
7 12 30.0 165.0 15.0 0.0817
7 13 30.0 180.0 0.0 0.0703
6 1 40.0 0.0 180.0 0.0391
6 2 40.0 15.0 165.0 0.0382
6 3 40.0 30.0 150.0 0.0377

6 4 40.0 45.0 135.0 0.0381
6 5 40.0 60.0 120.0 0.0362
6 6 40.0 75.0 105.0 0.0401
6 7 40.0 90.0 90.0 0.0417
6 8 40.0 105.0 75.0 0.0602
6 9 40.0 120.0 60.0 0.0820
6 10 40.0 135.0 45.0 0.1061
6 11 40.0 150.0 30.0 0.1107
6 12 40.0 165.0 15.0 0.0765
6 13 40.0 180.0 0.0 0.0012
5 1 50.0 0.0 180.0 0.0571
5 2 50.0 15.0 165.0 0.0579
5 3 50.0 30.0 150.0 0.0569
5 4 50.0 45.0 135.0 0.0556
5 5 50.0 60.0 120.0 0.0529
5 6 50.0 75.0 105.0 0.0523
5 7 50.0 90.0 90.0 0.0537
5 8 50.0 105.0 75.0 0.0563
5 9 50.0 120.0 60.0 0.0791
5 10 50.0 135.0 45.0 0.1098
5 11 50.0 150.0 30.0 0.1355
5 12 50.0 165.0 15.0 0.1276
5 13 50.0 180.0 0.0 0.1077
4 1 60.0 0.0 180.0 0.0897
4 2 60.0 15.0 165.0 0.0911
4 3 60.0 30.0 150.0 0.0921
4 4 60.0 45.0 135.0 0.0882
4 5 60.0 60.0 120.0 0.0836
4 6 60.0 75.0 105.0 0.0836
4 7 60.0 90.0 90.0 0.0841
4 8 60.0 105.0 75.0 0.0830
4 9 60.0 120.0 60.0 0.0867
4 10 60.0 135.0 45.0 0.1199
4 11 60.0 150.0 30.0 0.1825
4 12 60.0 165.0 15.0 0.2505
4 13 60.0 180.0 0.0 0.2659
3 1 70.0 0.0 180.0 0.1247
3 2 70.0 15.0 165.0 0.1284
3 3 70.0 30.0 150.0 0.1326
3 4 70.0 45.0 135.0 0.1315
3 5 70.0 60.0 120.0 0.1259
3 6 70.0 75.0 105.0 0.1299
3 7 70.0 90.0 90.0 0.1331
3 8 70.0 105.0 75.0 0.1301
3 9 70.0 120.0 60.0 0.1288
3 10 70.0 135.0 45.0 0.1509
3 11 70.0 150.0 30.0 0.2450
3 12 70.0 165.0 15.0 0.3849
3 13 70.0 180.0 0.0 0.5127
2 1 80.0 0.0 180.0 0.1389
2 2 80.0 15.0 165.0 0.1475
2 3 80.0 30.0 150.0 0.1533
2 4 80.0 45.0 135.0 0.1530
2 5 80.0 60.0 120.0 0.1502
2 6 80.0 75.0 105.0 0.1653
2 7 80.0 90.0 90.0 0.1716
2 8 80.0 105.0 75.0 0.1759
2 9 80.0 120.0 60.0 0.1726
2 10 80.0 135.0 45.0 0.1992
2 11 80.0 150.0 30.0 0.2786
2 12 80.0 165.0 15.0 0.5116
2 13 80.0 180.0 0.0 0.6908
1 1 87.5 0.0 180.0 0.1342
1 2 87.5 15.0 165.0 0.1497
1 3 87.5 30.0 150.0 0.1603
1 4 87.5 45.0 135.0 0.1617
1 5 87.5 60.0 120.0 0.1612
1 6 87.5 75.0 105.0 0.1715
1 7 87.5 90.0 90.0 0.1862
1 8 87.5 105.0 75.0 0.1948
1 9 87.5 120.0 60.0 0.2090
1 10 87.5 135.0 45.0 0.2434
1 11 87.5 150.0 30.0 0.3107
1 12 87.5 165.0 15.0 0.6334
1 13 87.5 180.0 0.0 0.8762
rho for WIND SPEED = 14.0 m/s THETA_SUN = 50.0 deg
10 1 0.0 0.0 0.0 0.0571
9 1 10.0 0.0 180.0 0.0382
9 2 10.0 15.0 165.0 0.0368
9 3 10.0 30.0 150.0 0.0347
9 4 10.0 45.0 135.0 0.0345
9 5 10.0 60.0 120.0 0.0434
9 6 10.0 75.0 105.0 0.0444
9 7 10.0 90.0 90.0 0.0554
9 8 10.0 105.0 75.0 0.0583
9 9 10.0 120.0 60.0 0.0666
9 10 10.0 135.0 45.0 0.0750
9 11 10.0 150.0 30.0 0.0804
9 12 10.0 165.0 15.0 0.1025
9 13 10.0 180.0 0.0 0.1037
8 1 20.0 0.0 180.0 0.0282
8 2 20.0 15.0 165.0 0.0274
8 3 20.0 30.0 150.0 0.0265
8 4 20.0 45.0 135.0 0.0340
8 5 20.0 60.0 120.0 0.0322
8 6 20.0 75.0 105.0 0.0392
8 7 20.0 90.0 90.0 0.0365
8 8 20.0 105.0 75.0 0.0566
8 9 20.0 120.0 60.0 0.0692

8 10 20.0 135.0 45.0 0.0857
8 11 20.0 150.0 30.0 0.1111
8 12 20.0 165.0 15.0 0.1138
8 13 20.0 180.0 0.0 0.1085
7 1 30.0 0.0 180.0 0.0294
7 2 30.0 15.0 165.0 0.0298
7 3 30.0 30.0 150.0 0.0297
7 4 30.0 45.0 135.0 0.0290
7 5 30.0 60.0 120.0 0.0317
7 6 30.0 75.0 105.0 0.0308
7 7 30.0 90.0 90.0 0.0349
7 8 30.0 105.0 75.0 0.0455
7 9 30.0 120.0 60.0 0.0629
7 10 30.0 135.0 45.0 0.0885
7 11 30.0 150.0 30.0 0.1119
7 12 30.0 165.0 15.0 0.1210
7 13 30.0 180.0 0.0 0.1129
6 1 40.0 0.0 180.0 0.0387
6 2 40.0 15.0 165.0 0.0388
6 3 40.0 30.0 150.0 0.0383
6 4 40.0 45.0 135.0 0.0369
6 5 40.0 60.0 120.0 0.0364
6 6 40.0 75.0 105.0 0.0363
6 7 40.0 90.0 90.0 0.0391
6 8 40.0 105.0 75.0 0.0407
6 9 40.0 120.0 60.0 0.0606
6 10 40.0 135.0 45.0 0.0897
6 11 40.0 150.0 30.0 0.1135
6 12 40.0 165.0 15.0 0.1033
6 13 40.0 180.0 0.0 0.0823
5 1 50.0 0.0 180.0 0.0575
5 2 50.0 15.0 165.0 0.0583
5 3 50.0 30.0 150.0 0.0576
5 4 50.0 45.0 135.0 0.0564
5 5 50.0 60.0 120.0 0.0535
5 6 50.0 75.0 105.0 0.0524
5 7 50.0 90.0 90.0 0.0533
5 8 50.0 105.0 75.0 0.0534
5 9 50.0 120.0 60.0 0.0587
5 10 50.0 135.0 45.0 0.0890
5 11 50.0 150.0 30.0 0.1244
5 12 50.0 165.0 15.0 0.1100
5 13 50.0 180.0 0.0 0.0025
4 1 60.0 0.0 180.0 0.0889
4 2 60.0 15.0 165.0 0.0904
4 3 60.0 30.0 150.0 0.0917
4 4 60.0 45.0 135.0 0.0882
4 5 60.0 60.0 120.0 0.0840
4 6 60.0 75.0 105.0 0.0843
4 7 60.0 90.0 90.0 0.0845
4 8 60.0 105.0 75.0 0.0818
4 9 60.0 120.0 60.0 0.0835
4 10 60.0 135.0 45.0 0.1045
4 11 60.0 150.0 30.0 0.1614
4 12 60.0 165.0 15.0 0.2008
4 13 60.0 180.0 0.0 0.1830
3 1 70.0 0.0 180.0 0.1227
3 2 70.0 15.0 165.0 0.1265
3 3 70.0 30.0 150.0 0.1308
3 4 70.0 45.0 135.0 0.1300
3 5 70.0 60.0 120.0 0.1247
3 6 70.0 75.0 105.0 0.1290
3 7 70.0 90.0 90.0 0.1323
3 8 70.0 105.0 75.0 0.1287
3 9 70.0 120.0 60.0 0.1270
3 10 70.0 135.0 45.0 0.1414
3 11 70.0 150.0 30.0 0.2066
3 12 70.0 165.0 15.0 0.3911
3 13 70.0 180.0 0.0 0.5177
2 1 80.0 0.0 180.0 0.1379
2 2 80.0 15.0 165.0 0.1464
2 3 80.0 30.0 150.0 0.1520
2 4 80.0 45.0 135.0 0.1513
2 5 80.0 60.0 120.0 0.1481
2 6 80.0 75.0 105.0 0.1625
2 7 80.0 90.0 90.0 0.1681
2 8 80.0 105.0 75.0 0.1716
2 9 80.0 120.0 60.0 0.1680
2 10 80.0 135.0 45.0 0.1918
2 11 80.0 150.0 30.0 0.2772
2 12 80.0 165.0 15.0 0.6355
2 13 80.0 180.0 0.0 1.1131
1 1 87.5 0.0 180.0 0.1350
1 2 87.5 15.0 165.0 0.1506
1 3 87.5 30.0 150.0 0.1608
1 4 87.5 45.0 135.0 0.1613
1 5 87.5 60.0 120.0 0.1595
1 6 87.5 75.0 105.0 0.1684
1 7 87.5 90.0 90.0 0.1814
1 8 87.5 105.0 75.0 0.1880
1 9 87.5 120.0 60.0 0.2011
1 10 87.5 135.0 45.0 0.2389
1 11 87.5 150.0 30.0 0.3077
1 12 87.5 165.0 15.0 0.8647
1 13 87.5 180.0 0.0 1.8881
rho for WIND SPEED = 14.0 m/s THETA_SUN = 60.0
deg
10 1 0.0 0.0 0.0 0.0376
9 1 10.0 0.0 180.0 0.0257
9 2 10.0 15.0 165.0 0.0285

9	3	10.0	30.0	150.0	0.0276
9	4	10.0	45.0	135.0	0.0276
9	5	10.0	60.0	120.0	0.0277
9	6	10.0	75.0	105.0	0.0312
9	7	10.0	90.0	90.0	0.0369
9	8	10.0	105.0	75.0	0.0422
9	9	10.0	120.0	60.0	0.0520
9	10	10.0	135.0	45.0	0.0497
9	11	10.0	150.0	30.0	0.0642
9	12	10.0	165.0	15.0	0.0677
9	13	10.0	180.0	0.0	0.0608
8	1	20.0	0.0	180.0	0.0259
8	2	20.0	15.0	165.0	0.0261
8	3	20.0	30.0	150.0	0.0260
8	4	20.0	45.0	135.0	0.0260
8	5	20.0	60.0	120.0	0.0262
8	6	20.0	75.0	105.0	0.0294
8	7	20.0	90.0	90.0	0.0316
8	8	20.0	105.0	75.0	0.0369
8	9	20.0	120.0	60.0	0.0459
8	10	20.0	135.0	45.0	0.0633
8	11	20.0	150.0	30.0	0.0814
8	12	20.0	165.0	15.0	0.0949
8	13	20.0	180.0	0.0	0.1034
7	1	30.0	0.0	180.0	0.0289
7	2	30.0	15.0	165.0	0.0289
7	3	30.0	30.0	150.0	0.0289
7	4	30.0	45.0	135.0	0.0285
7	5	30.0	60.0	120.0	0.0287
7	6	30.0	75.0	105.0	0.0290
7	7	30.0	90.0	90.0	0.0302
7	8	30.0	105.0	75.0	0.0338
7	9	30.0	120.0	60.0	0.0452
7	10	30.0	135.0	45.0	0.0709
7	11	30.0	150.0	30.0	0.1030
7	12	30.0	165.0	15.0	0.1336
7	13	30.0	180.0	0.0	0.1391
6	1	40.0	0.0	180.0	0.0381
6	2	40.0	15.0	165.0	0.0382
6	3	40.0	30.0	150.0	0.0379
6	4	40.0	45.0	135.0	0.0367
6	5	40.0	60.0	120.0	0.0364
6	6	40.0	75.0	105.0	0.0359
6	7	40.0	90.0	90.0	0.0370
6	8	40.0	105.0	75.0	0.0391
6	9	40.0	120.0	60.0	0.0465
6	10	40.0	135.0	45.0	0.0729
6	11	40.0	150.0	30.0	0.1206
6	12	40.0	165.0	15.0	0.1508
6	13	40.0	180.0	0.0	0.1573
5	1	50.0	0.0	180.0	0.0562
5	2	50.0	15.0	165.0	0.0571
5	3	50.0	30.0	150.0	0.0567
5	4	50.0	45.0	135.0	0.0560
5	5	50.0	60.0	120.0	0.0534
5	6	50.0	75.0	105.0	0.0528
5	7	50.0	90.0	90.0	0.0539
5	8	50.0	105.0	75.0	0.0531
5	9	50.0	120.0	60.0	0.0569
5	10	50.0	135.0	45.0	0.0773
5	11	50.0	150.0	30.0	0.1242
5	12	50.0	165.0	15.0	0.1536
5	13	50.0	180.0	0.0	0.1328
4	1	60.0	0.0	180.0	0.0867
4	2	60.0	15.0	165.0	0.0883
4	3	60.0	30.0	150.0	0.0899
4	4	60.0	45.0	135.0	0.0869
4	5	60.0	60.0	120.0	0.0834
4	6	60.0	75.0	105.0	0.0843
4	7	60.0	90.0	90.0	0.0853
4	8	60.0	105.0	75.0	0.0826
4	9	60.0	120.0	60.0	0.0814
4	10	60.0	135.0	45.0	0.0938
4	11	60.0	150.0	30.0	0.1404
4	12	60.0	165.0	15.0	0.1818
4	13	60.0	180.0	0.0	0.0066
3	1	70.0	0.0	180.0	0.1209
3	2	70.0	15.0	165.0	0.1246
3	3	70.0	30.0	150.0	0.1290
3	4	70.0	45.0	135.0	0.1283
3	5	70.0	60.0	120.0	0.1234
3	6	70.0	75.0	105.0	0.1279
3	7	70.0	90.0	90.0	0.1315
3	8	70.0	105.0	75.0	0.1280
3	9	70.0	120.0	60.0	0.1252
3	10	70.0	135.0	45.0	0.1362
3	11	70.0	150.0	30.0	0.1810
3	12	70.0	165.0	15.0	0.3244
3	13	70.0	180.0	0.0	0.3788
2	1	80.0	0.0	180.0	0.1387
2	2	80.0	15.0	165.0	0.1472
2	3	80.0	30.0	150.0	0.1525
2	4	80.0	45.0	135.0	0.1513
2	5	80.0	60.0	120.0	0.1474
2	6	80.0	75.0	105.0	0.1608
2	7	80.0	90.0	90.0	0.1653
2	8	80.0	105.0	75.0	0.1674
2	9	80.0	120.0	60.0	0.1625
2	10	80.0	135.0	45.0	0.1828
2	11	80.0	150.0	30.0	0.2256

2 12 80.0 165.0 15.0 0.6032
2 13 80.0 180.0 0.0 1.0202
1 1 87.5 0.0 180.0 0.1388
1 2 87.5 15.0 165.0 0.1546
1 3 87.5 30.0 150.0 0.1646
1 4 87.5 45.0 135.0 0.1640
1 5 87.5 60.0 120.0 0.1605
1 6 87.5 75.0 105.0 0.1672
1 7 87.5 90.0 90.0 0.1776
1 8 87.5 105.0 75.0 0.1811
1 9 87.5 120.0 60.0 0.1911
1 10 87.5 135.0 45.0 0.2263
1 11 87.5 150.0 30.0 0.3037
1 12 87.5 165.0 15.0 0.9981
1 13 87.5 180.0 0.0 2.1014
rho for WIND SPEED = 14.0 m/s THETA_SUN = 70.0
deg
10 1 0.0 0.0 0.0 0.0272
9 1 10.0 0.0 180.0 0.0241
9 2 10.0 15.0 165.0 0.0244
9 3 10.0 30.0 150.0 0.0246
9 4 10.0 45.0 135.0 0.0255
9 5 10.0 60.0 120.0 0.0250
9 6 10.0 75.0 105.0 0.0253
9 7 10.0 90.0 90.0 0.0260
9 8 10.0 105.0 75.0 0.0293
9 9 10.0 120.0 60.0 0.0308
9 10 10.0 135.0 45.0 0.0381
9 11 10.0 150.0 30.0 0.0365
9 12 10.0 165.0 15.0 0.0404
9 13 10.0 180.0 0.0 0.0428
8 1 20.0 0.0 180.0 0.0255
8 2 20.0 15.0 165.0 0.0246
8 3 20.0 30.0 150.0 0.0246
8 4 20.0 45.0 135.0 0.0249
8 5 20.0 60.0 120.0 0.0249
8 6 20.0 75.0 105.0 0.0260
8 7 20.0 90.0 90.0 0.0275
8 8 20.0 105.0 75.0 0.0280
8 9 20.0 120.0 60.0 0.0342
8 10 20.0 135.0 45.0 0.0432
8 11 20.0 150.0 30.0 0.0581
8 12 20.0 165.0 15.0 0.0776
8 13 20.0 180.0 0.0 0.0752
7 1 30.0 0.0 180.0 0.0279
7 2 30.0 15.0 165.0 0.0280
7 3 30.0 30.0 150.0 0.0280
7 4 30.0 45.0 135.0 0.0278
7 5 30.0 60.0 120.0 0.0277
7 6 30.0 75.0 105.0 0.0279
7 7 30.0 90.0 90.0 0.0287
7 8 30.0 105.0 75.0 0.0305
7 9 30.0 120.0 60.0 0.0367
7 10 30.0 135.0 45.0 0.0515
7 11 30.0 150.0 30.0 0.0903
7 12 30.0 165.0 15.0 0.1237
7 13 30.0 180.0 0.0 0.1522
6 1 40.0 0.0 180.0 0.0367
6 2 40.0 15.0 165.0 0.0369
6 3 40.0 30.0 150.0 0.0368
6 4 40.0 45.0 135.0 0.0359
6 5 40.0 60.0 120.0 0.0358
6 6 40.0 75.0 105.0 0.0352
6 7 40.0 90.0 90.0 0.0363
6 8 40.0 105.0 75.0 0.0366
6 9 40.0 120.0 60.0 0.0410
6 10 40.0 135.0 45.0 0.0553
6 11 40.0 150.0 30.0 0.1107
6 12 40.0 165.0 15.0 0.1948
6 13 40.0 180.0 0.0 0.2280
5 1 50.0 0.0 180.0 0.0541
5 2 50.0 15.0 165.0 0.0551
5 3 50.0 30.0 150.0 0.0548
5 4 50.0 45.0 135.0 0.0546
5 5 50.0 60.0 120.0 0.0526
5 6 50.0 75.0 105.0 0.0526
5 7 50.0 90.0 90.0 0.0542
5 8 50.0 105.0 75.0 0.0530
5 9 50.0 120.0 60.0 0.0556
5 10 50.0 135.0 45.0 0.0695
5 11 50.0 150.0 30.0 0.1231
5 12 50.0 165.0 15.0 0.2254
5 13 50.0 180.0 0.0 0.2791
4 1 60.0 0.0 180.0 0.0841
4 2 60.0 15.0 165.0 0.0857
4 3 60.0 30.0 150.0 0.0874
4 4 60.0 45.0 135.0 0.0849
4 5 60.0 60.0 120.0 0.0821
4 6 60.0 75.0 105.0 0.0838
4 7 60.0 90.0 90.0 0.0854
4 8 60.0 105.0 75.0 0.0836
4 9 60.0 120.0 60.0 0.0832
4 10 60.0 135.0 45.0 0.0928
4 11 60.0 150.0 30.0 0.1319
4 12 60.0 165.0 15.0 0.2426
4 13 60.0 180.0 0.0 0.2574
3 1 70.0 0.0 180.0 0.1195
3 2 70.0 15.0 165.0 0.1231
3 3 70.0 30.0 150.0 0.1274
3 4 70.0 45.0 135.0 0.1268

3	5	70.0	60.0	120.0	0.1222
3	6	70.0	75.0	105.0	0.1268
3	7	70.0	90.0	90.0	0.1309
3	8	70.0	105.0	75.0	0.1273
3	9	70.0	120.0	60.0	0.1250
3	10	70.0	135.0	45.0	0.1353
3	11	70.0	150.0	30.0	0.1522
3	12	70.0	165.0	15.0	0.2698
3	13	70.0	180.0	0.0	0.0214
2	1	80.0	0.0	180.0	0.1408
2	2	80.0	15.0	165.0	0.1492
2	3	80.0	30.0	150.0	0.1543
2	4	80.0	45.0	135.0	0.1525
2	5	80.0	60.0	120.0	0.1477
2	6	80.0	75.0	105.0	0.1600
2	7	80.0	90.0	90.0	0.1633
2	8	80.0	105.0	75.0	0.1640
2	9	80.0	120.0	60.0	0.1573
2	10	80.0	135.0	45.0	0.1734
2	11	80.0	150.0	30.0	0.1920
2	12	80.0	165.0	15.0	0.4001
2	13	80.0	180.0	0.0	0.6616
1	1	87.5	0.0	180.0	0.1442
1	2	87.5	15.0	165.0	0.1603
1	3	87.5	30.0	150.0	0.1702
1	4	87.5	45.0	135.0	0.1686
1	5	87.5	60.0	120.0	0.1632
1	6	87.5	75.0	105.0	0.1675
1	7	87.5	90.0	90.0	0.1750
1	8	87.5	105.0	75.0	0.1753
1	9	87.5	120.0	60.0	0.1810
1	10	87.5	135.0	45.0	0.2074
1	11	87.5	150.0	30.0	0.2535
1	12	87.5	165.0	15.0	0.5642
1	13	87.5	180.0	0.0	1.4897

rho for WIND SPEED = 14.0 m/s THETA_SUN = 80.0 deg

10	1	0.0	0.0	0.0	0.0238
9	1	10.0	0.0	180.0	0.0229
9	2	10.0	15.0	165.0	0.0230
9	3	10.0	30.0	150.0	0.0227
9	4	10.0	45.0	135.0	0.0232
9	5	10.0	60.0	120.0	0.0236
9	6	10.0	75.0	105.0	0.0233
9	7	10.0	90.0	90.0	0.0236
9	8	10.0	105.0	75.0	0.0243
9	9	10.0	120.0	60.0	0.0260
9	10	10.0	135.0	45.0	0.0271
9	11	10.0	150.0	30.0	0.0271
9	12	10.0	165.0	15.0	0.0281
9	13	10.0	180.0	0.0	0.0303
8	1	20.0	0.0	180.0	0.0239
8	2	20.0	15.0	165.0	0.0236
8	3	20.0	30.0	150.0	0.0236
8	4	20.0	45.0	135.0	0.0239
8	5	20.0	60.0	120.0	0.0237
8	6	20.0	75.0	105.0	0.0243
8	7	20.0	90.0	90.0	0.0247
8	8	20.0	105.0	75.0	0.0254
8	9	20.0	120.0	60.0	0.0275
8	10	20.0	135.0	45.0	0.0306
8	11	20.0	150.0	30.0	0.0366
8	12	20.0	165.0	15.0	0.0445
8	13	20.0	180.0	0.0	0.0480
7	1	30.0	0.0	180.0	0.0269
7	2	30.0	15.0	165.0	0.0269
7	3	30.0	30.0	150.0	0.0270
7	4	30.0	45.0	135.0	0.0268
7	5	30.0	60.0	120.0	0.0269
7	6	30.0	75.0	105.0	0.0271
7	7	30.0	90.0	90.0	0.0277
7	8	30.0	105.0	75.0	0.0285
7	9	30.0	120.0	60.0	0.0311
7	10	30.0	135.0	45.0	0.0379
7	11	30.0	150.0	30.0	0.0549
7	12	30.0	165.0	15.0	0.0847
7	13	30.0	180.0	0.0	0.0990
6	1	40.0	0.0	180.0	0.0352
6	2	40.0	15.0	165.0	0.0354
6	3	40.0	30.0	150.0	0.0354
6	4	40.0	45.0	135.0	0.0347
6	5	40.0	60.0	120.0	0.0349
6	6	40.0	75.0	105.0	0.0345
6	7	40.0	90.0	90.0	0.0357
6	8	40.0	105.0	75.0	0.0358
6	9	40.0	120.0	60.0	0.0393
6	10	40.0	135.0	45.0	0.0480
6	11	40.0	150.0	30.0	0.0825
6	12	40.0	165.0	15.0	0.1602
6	13	40.0	180.0	0.0	0.2157
5	1	50.0	0.0	180.0	0.0520
5	2	50.0	15.0	165.0	0.0529
5	3	50.0	30.0	150.0	0.0528
5	4	50.0	45.0	135.0	0.0529
5	5	50.0	60.0	120.0	0.0514
5	6	50.0	75.0	105.0	0.0519
5	7	50.0	90.0	90.0	0.0539
5	8	50.0	105.0	75.0	0.0530
5	9	50.0	120.0	60.0	0.0559
5	10	50.0	135.0	45.0	0.0682

5	11	50.0	150.0	30.0	0.1050
5	12	50.0	165.0	15.0	0.2380
5	13	50.0	180.0	0.0	0.3524
4	1	60.0	0.0	180.0	0.0819
4	2	60.0	15.0	165.0	0.0834
4	3	60.0	30.0	150.0	0.0852
4	4	60.0	45.0	135.0	0.0831
4	5	60.0	60.0	120.0	0.0807
4	6	60.0	75.0	105.0	0.0829
4	7	60.0	90.0	90.0	0.0850
4	8	60.0	105.0	75.0	0.0838
4	9	60.0	120.0	60.0	0.0844
4	10	60.0	135.0	45.0	0.0965
4	11	60.0	150.0	30.0	0.1297
4	12	60.0	165.0	15.0	0.2676
4	13	60.0	180.0	0.0	0.4310
3	1	70.0	0.0	180.0	0.1189
3	2	70.0	15.0	165.0	0.1223
3	3	70.0	30.0	150.0	0.1265
3	4	70.0	45.0	135.0	0.1258
3	5	70.0	60.0	120.0	0.1212
3	6	70.0	75.0	105.0	0.1259
3	7	70.0	90.0	90.0	0.1300
3	8	70.0	105.0	75.0	0.1270
3	9	70.0	120.0	60.0	0.1247
3	10	70.0	135.0	45.0	0.1368
3	11	70.0	150.0	30.0	0.1495
3	12	70.0	165.0	15.0	0.2337
3	13	70.0	180.0	0.0	0.3520
2	1	80.0	0.0	180.0	0.1436
2	2	80.0	15.0	165.0	0.1520
2	3	80.0	30.0	150.0	0.1567
2	4	80.0	45.0	135.0	0.1542
2	5	80.0	60.0	120.0	0.1486
2	6	80.0	75.0	105.0	0.1597
2	7	80.0	90.0	90.0	0.1620
2	8	80.0	105.0	75.0	0.1616
2	9	80.0	120.0	60.0	0.1534
2	10	80.0	135.0	45.0	0.1646
2	11	80.0	150.0	30.0	0.1679
2	12	80.0	165.0	15.0	0.2154
2	13	80.0	180.0	0.0	0.0558
1	1	87.5	0.0	180.0	0.1502
1	2	87.5	15.0	165.0	0.1666
1	3	87.5	30.0	150.0	0.1762
1	4	87.5	45.0	135.0	0.1734
1	5	87.5	60.0	120.0	0.1662
1	6	87.5	75.0	105.0	0.1683
1	7	87.5	90.0	90.0	0.1735
1	8	87.5	105.0	75.0	0.1711
1	9	87.5	120.0	60.0	0.1727
1	10	87.5	135.0	45.0	0.1869
1	11	87.5	150.0	30.0	0.1991
1	12	87.5	165.0	15.0	0.2386
1	13	87.5	180.0	0.0	0.4688

Appendix 2: FLNTU Linear Offsets

During seven separate research cruises within the Great Barrier Reef aboard the RV Cape Ferguson, a total of 103 *in situ* chlorophyll-a (Chla) samples were collected and later compared with Chla concentrations derived using a WETLabs combination Chla fluorometer and nephelometric turbidity sensor (FLNTU). *In situ* Chla samples were filtered onto Whatmann GF/F filters and then frozen (-20°). Upon return to shore, Chla concentration was determined fluorometrically using a Turner Designs 10AU fluorometer after grinding filters in 90 % acetone according to Parsons et al. (1984). Whereas, the FLNTU instrument was housed within a flow-through system and designed to measure along-transect Chla concentrations.

Figure A2.1 shows strong linearity ($R^2 = 0.86$) between *in situ* Chla values and those derived using the FLNTU. However, the FLNTU instrument appeared to slightly overestimate Chla concentration by approximately 0.05 mg m^{-3}. A line of best fit through the data was determined

$$\text{Chla}_{\text{in situ}} = 0.9289\left[\text{Chla}_{\text{FLNTU}}\right] - 0.0632 \qquad \text{[A1.1]}$$

where, $\text{Chla}_{\text{in situ}}$ and $\text{Chla}_{\text{FLNTU}}$ are *in situ* measured and FLNTU measured Chla respectively. This linear relationship was thus used to correct FLNTU values.

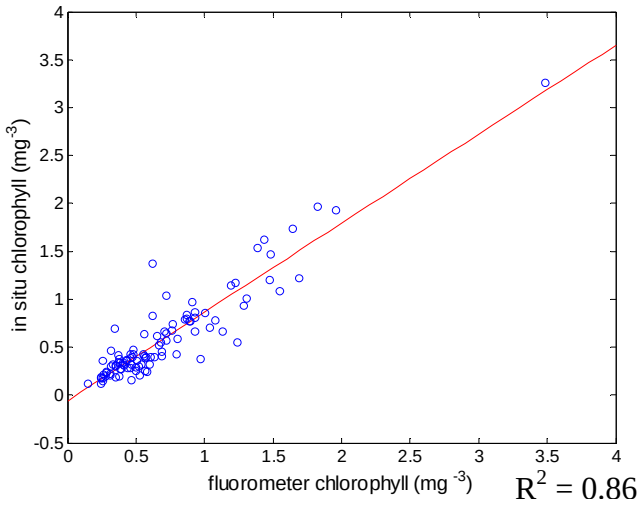

Figure A2.1: Values of Chla concentration derived using a WETLabs FLNTU instrument plotted against *in situ* measurements.

This page intentionally left blank

Appendix 3: The Quasi-Analytical Algorithm

The Quasi-analytical algorithm of Lee et al. (2002) derives the IOPs of absorption and backscattering coefficients from above-water remote sensing reflectance $R_{rs}(\lambda)$ by analytically solving the relationship of Gordon et al. (1988)

$$r_{rs}(\lambda) = \sum_{i=1}^{2} g_i \left[u(\lambda) \right]^i \qquad \text{[A3.1]}$$

where, g_1 and g_2 are pre-determined coefficients and $r_{rs}(\lambda)$ is the sub-surface remote sensing reflectance just beneath the surface. The parameter $u(\lambda)$ is defined

$$u(\lambda) = \frac{b_b(\lambda)}{a(\lambda) + b_b(\lambda)} \qquad \text{[A3.2]}$$

where, $a(\lambda)$ and $b_b(\lambda)$ are the total absorption and backscattering coefficients respectively. The following outlines the steps of the QAA v5 processing algorithm (http://www.ioccg.org/groups/Software_OCA/QAA_v5.pdf).

Processing Steps

1.) Semi-analytical Approach

First derive the sub-surface remote sensing $r_{rs}(\lambda)$ from above-water remote sensing

$$r_{rs}(\lambda) = \frac{R_{rs}(\lambda)}{\left(0.52 + 1.7\, R_{rs}(\lambda)\right)} \qquad \text{[A3.3]}$$

2.) Semi-analytical Approach

The quadratic expression A2.1 is solved to derive $u(\lambda)$

$$u(\lambda) = \frac{-g_0 + \sqrt{(g_0)^2 + 4 g_1 r_{rs}(\lambda)}}{2 g_1} \qquad \text{[A3.4]}$$

where, g_1 and g_2 are given values of 0.089 and 0.125 respectively.

3.) Empirical Approach

Total absorption $a(\lambda_0)$ is determined at a reference wavelength λ_0 = 550, 555, or 650 nm, where $R_{rs}(\lambda)$ can be accurately measured

$$a(\lambda_0) = a_w(\lambda_0) + 10^{-1.146-1.366\chi-0.469\chi^2} \quad \text{[A3.5]}$$

where, $a_w(\lambda_0)$ is the absorption coefficient of pure water at λ_0 (Pope and Fry 1997) is a constant and χ is determined by

$$\chi = \log\left(\frac{r_{rs}(443) + r_{rs}(490)}{r_{rs}(\lambda_0) + 5\left(\frac{r_{rs}(667)}{r_{rs}(443)}\right) r_{rs}(667)}\right) \quad \text{[A3.6]}$$

4.) Analytical Approach

Using $a_0(\lambda)$, a value of $b_b(\lambda_0)$ can be derived to solved for as follows

$$b_b(\lambda_0) = \frac{u(\lambda_0)a(\lambda_0)}{1-u(\lambda_0)} \quad \text{[A3.7]}$$

The particulate backscattering coefficient at λ_0 is denoted $b_{bp}(\lambda_0)$ is then determined by subtracting the backscattering coefficient of pure water at λ_0, $b_{bw}(\lambda_0)$ (Pope and Fry 1997) from $b_b(\lambda_0)$

$$b_{bp}(\lambda_0) = b_b(\lambda_0) - b_{bw}(\lambda_0)$$

5.) Empirical Approach

The spectral power coefficient γ of the particulate backscattering coefficient $b_{bp}(\lambda)$ is estimated using the following empirical relationship

$$\eta = 2.0\left(1 - 1.2e^{-0.9\left[r_{rs}(443)/r_{rs}(\lambda_0)\right]}\right) \quad \text{[A3.8]}$$

6.) Analytical Approach

The value of $b_{bp}(\lambda)$ is determined using the following equation

$$b_{bp}(\lambda) = b_{bp}(\lambda_0)\left(\frac{555}{\lambda}\right)^{\gamma} \quad [A3.9]$$

7.) Analytical Approach

Using $b_{bp}(\lambda)$, the spectral absorption coefficient $a(\lambda)$ is determined analytically by solving

$$a(\lambda) = \frac{\left[1-u(\lambda)\right]\left[b_{bw}(\lambda)+b_{bp}(\lambda)\right]}{u(\lambda)} \quad [A3.10]$$

8.) Empirical Approach

The QAA estimates the absorption coefficient of coloured dissolved and detrital matter at 440 nm denoted $a_{dg}(440)$. This first requires three parameters ξ and ζ and *S* to first be derived

$$\zeta = 0.74 + \frac{0.2}{0.8 + \left(r_{rs}(443)/r_{rs}(\lambda_0)\right)} \quad [A3.11]$$

$$S = 0.015 + \frac{0.002}{0.6 + r_{rs}(443)/r_{rs}(\lambda_0)} \quad [A3.12]$$

$$\xi = e^{S(443-431)}$$

9.) Semi-analytical Approach

The value of $a_{dg}(\lambda_0)$ is then determined using

$$a_{dg}(440) = \frac{\left[a(410)-a(440)\right]}{\xi-\zeta} - \frac{\left[a_w(410)-a_w(440)\right]}{\xi-\zeta} \quad [A3.13]$$

10.) Analytical Approach

The spectral absorption coefficient of coloured dissolved and detrital matter can then be determined by

$$a_{dg}(\lambda) = a_{dg}(440)e^{-S(\lambda-440)} \quad \text{[A3.14]}$$

11.) Analytical Approach

The spectral phytoplankton absorption coefficient $a_{\phi}(\lambda)$ can then be derived as follows

$$a_{\phi}(\lambda) = a(\lambda) - a_{dg}(\lambda) - a_{w}(\lambda) \quad \text{[A3.15]}$$

Quality Control Constraints

The following quality control constraints are placed upon the above-water remote sensing reflectance at 667 nm $R_{rs}(667)$ before being processed with the QAA.

Upper limit of $R_{rs}(667)$

$$R_{rs}(667) = 20\left[R_{rs}(667)\right]^{1.5} \quad \text{[A3.16]}$$

Lower limit of $R_{rs}(667)$

$$R_{rs}(667) = 0.9\left[R_{rs}(667)\right]^{1.7} \quad \text{[A3.17]}$$

If $R_{rs}(667)$ is outside of the defined limits an estimation of its value is made using the following

$$R_{rs}(667) = 1.27\left[R_{rs}(555)\right]^{1.47} + 0.00018\left[R_{rs}(490)/R_{rs}(555)\right]^{-3.19} \quad \text{[A3.18]}$$

Appendix 4: N-fixation Estimates from Derived *Trichodesmium* abundance

Several methods have been presented to estimate *Trichodesmium* specific N fixation using ocean colour remote sensing (Hood et al. 2002; Westberry and Siegel 2006). We present a simple estimate of along-transect N-fixation rates based on using *Trichodesmium*–specific Chla concentration derived from hyperspectral $R_{rs}(\lambda)$ data. This method allows localised estimates of N-fixation to be made using high-spatial resolution, hyperspectral data for a particular region of interest. The aim was to develop a method that is reproducible for other high spatial, hyperspectral sensors. Furthermore, N-fixation estimates may then be extrapolated to a larger region.

The method relies upon values of N-fixation rates per cell of *Trichodesmium* reported by Carpenter et al. (1983a). In addition, information regarding the Chla content per trichome and the number of cells per trichome was also required and sourced from Letelier and Karl (1996) and Capone et al. (2005) respectively (see Table A4.1). Using these data an estimate of the *Trichodesmium*-specific volumetricN-fixation rate, derived as a function of Chla concentration, was estimated to be 3×10^{-5} grams N $(\text{mg Chla})^{-1}$ m^{-3} hr^{-1}.

This Chlorophyll-a specific *Trichodesmium* N-fixation rate was multiplied by the derived Chla values at each data point to yield along-transect N-fixation per cubic metre per hour as shown in Figure A4.1. By integrating under the curve, the quantity of N-fixed per cubic meter over the duration of the transect was estimated to be 1×10^{-6} grams N m^{-3}. The N-fixation rate of *Trichodesmium* has been shown to decrease to 9 percent of surface values at a depth of 50 m (Carpenter and Price 1977). Assuming that N-fixation monotonically decreases with depth, the N-fixation rate, *Nrate*, at a given depth *z* can be expressed as

$$Nrate(z) = Nrate(0)e^{-\kappa z} \qquad \text{[A4.1]}$$

where, the decay constant κ is 0.0491. We integrated Eqauation 4.15 over a depths from 0 - 30 m to estimate the along-transect areal N-fixation to be 2×10^{-4} grams N m^{-2}. This calculation was performed under the assumption the average depth of the GBR is about 30 m (Wolanski 1994). The length of the transect was known to be 30 km and the width of the radiometer's field-of-view was

approximately 1 m. Thus, the total area viewed during the transect was approximately 3×10^{4} m^2. By multiplying areal N-fixation by the total area viewed, the total quantity of N-fixed during the transect was estimated to be 2 grams.

To determine if the volumetric N-fixation rate of 3×10^{-5} grams N^{-1} (mg Chla)$^{-1}$ m^{-3} hr^{-1} was reasonable, we derived a value for annual areal N-fixation. Firstly, the along-transect areal fixation rate was divided by the time duration of the transect (1.8 hours) to yield an areal fixation rate of 1×10^{-4} grams N m^{-2} hr^{-1}. It was next assumed N-fixation occurred for 10 hours a day, 365 days a year, which yielded an annual areal N-fixation rate of 0.7 grams N m^{-2} yr^{-1} which has equivalent units of tonnes N km^{-2} yr^{-1}. The value of 0.7 tonnes N km^{-2} yr^{-1} was similar magnitude to annual areal fixation rates reported by Furnas et al. (1996) and Bell et al. (1999).

We thus used the derived areal fixation rate to estimate annual N-inputs for the Far Northern, Northern, Central and Southern Great Barrier Reef due to *Trichodesmium*. Table A4.2 details the areas spanned by each region. Using this information, we estimate the total amount of N-fixed by *Trichodesmium* for each region. When considering the Northern GBR, the annual N-input due to *Trichodesmium* was estimated to be 10,000 tonnes N y^{-1}. This value is within the range of previous estimates (Furnas and Mitchell 1996; Bell et al. 1999). For comparative purposes, we compiled annual N-input estimated for rivers along each region of the GBR (see Table A4.2). The data suggests that N-inputs from *Trichodesmium* are of similar magnitude to N-inputs from from rivers, which complements previous studies (Furnas and Mitchell 1996; Bell et al. 1999).

Although, similar to results of others (Furnas and Mitchell 1996; Bell et al. 1999), these order of magnitude estimates are not definitive, and should be heeded with caution. For example, we assumed a steady standing crop of *Trichodesmium* between 0.2 – 0.5 mg Chla m^{-3} and have not considered periodic population fluctuations. Thus, more transect $R_{rs}(\lambda)$ data is necessary for determining temporal variability in *Trichodesmium* abundance within the GBR and hence improving N-load estimates. Furthermore, N-fixation rates of *Trichodesmium* have been shown to have dependence upon photosynthetically available radiation (PAR) and euphotic depth (Hood et al. 2002). Euphotic depth and diffuse attenuation coefficients can be determined using IOPs derived using the QAA (Lee et al. 2005; Lee et al. 2007). Thus, it may be possible to implement a more sophisticated model for estimating

Trichodesmium fixation such as that of Hood et al. (2002). This prospect is worthy of further investigation.

Table A4.1: Values used for estimation of Chla-specific *Trichodesmium* N-fixation rate

Parameter	Value	Units	Data Source
Average N-fixation rate	0.10	pg N cell^{-1} h^{-1}	Capone et al. (2005)
Chlorophyll-a concentration per trichome	0.3	ng Chla trichome^{-1}	Letelier and Karl (1996)
Average number of cells per trichome	100	cells trichome $^{-1}$	Carpenter (1983a)

Table A4.2: Nitrogen inputs from rivers and *Trichodesmium* to the Great Barrier Reef

Region	Latitude °S	Area km^2	River Inputs*	*Trichodesmium* Inputs*	Percentage Difference
Far Northern GBR	10-16	45,000	7,000	30,000	23 %
Northern GBR	16-18	15,000	4,000	10,000	40 %
Central GBR	18-21	65,000	16,000	40,000	40 %
Southern GBR	21-25	75,000	14,000	60,000	23 %
Total GBR	10-25	200,000	41,000	140,000	72 %

River input data sourced from Furnas (2002).

*Units: tonnes N yr^{-1}

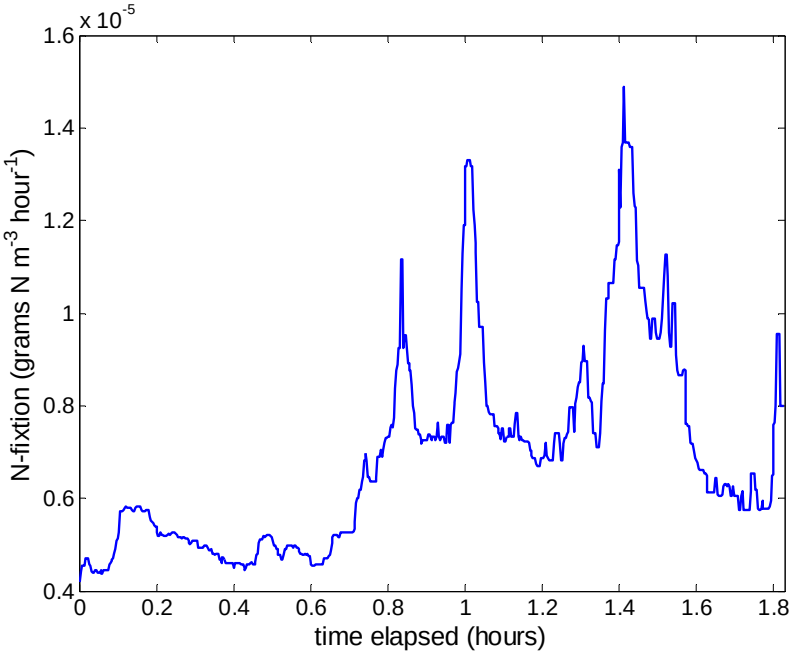

Figure A4.1: Plot of along-transect volumetric nitrogen fixation rate derived from *Trichodesmium* specific Chla concentration.

References

Alvain, S., C. Moulin, Y. Dandonneau, and F. M. Breon. 2005. Remote sensing of phytoplankton groups in case 1 waters from global SeaWiFS imagery. Deep Sea Research Part I **52:** 1989-2004.

Andruleit, H., S. Stager, U. Rogalla, and P. Cepek. 2003. Living coccolithophores in the northern Arabian Sea: ecological tolerances and environmental control. Marine Micropaleontology **49**.

Antoine, D., J.-M. André, and A. Morel. 1996. Oceanic primary production: 2. Estimation at global scale from satellite (Coastal Zone Color Scanner) chlorophyll. Global Biogeochem. Cycles **10:** 57-69.

Baith, K., R. Lindsay, G. Fu, and C. R. Mcclain. 2001. SeaDAS, a data analysis system for ocean-color satellite sensors. EOS Transactions of the American Geophysical Union **82:** 202.

Bell, P. R. F., I. Elmetri, and P. Uwins. 1999. Nitrogen fixation by *Trichodesmium* in the Central and Norhtern Great Barrier Reef Lagoon: relative importance of the fixed nitrogen load. Marine Ecology Progress Series **186:** 119-126.

Bellwood, D. R., T. P. Hughes, C. Folke, and M. Nystrom. 2004. Confronting the coral reef crisis. Nature **429:** 827-833.

Berkelmans, R., G. De'ath, S. Kininmonth, and W. Skirving. 2004. A comparison of the 1998 and 2002 coral bleaching events on the Great Barrier Reef: spatial correlation, patterns, and predictions. Coral Reefs **23:** 74-83.

Borstad, G. A., J. F. R. Gower, and E. J. Carpenter. 1992. Development of Algorithms for Remote Sensing of Trichodesmium Blooms, p. 193-210. *In* E. J. Carpenter, D. G. Capone and J. G. Reuter [eds.], Marine Pelagic Cyanobacteria: *Trichodesmium* and other Diazotrophs.

Brando, V. E., T. Schroeder, and A. G. Dekker. 2010. Reef Rescue Marine Monitoring Program: Using Remote Sensing for GBR-wide Water Quality.

Bricaud, A., A. Morel, and L. Prieur. 1981. Absorption by dissolved organic matter of the sea (yellow substance) n the UV and visible domains. Limnology and Oceanography **26:** 43-53.

Bricaud, A., M. Babin, A. Morel, and H. Claustre. 1995. Variability in the chlorophyll-specific absorption coefficients of natural phytoplankton: Analysis and parameterization Journal of Geophysical Research **100:** 13,321 - 331,332.

Brockmann, C. 2003. Demonstration of BEAM Software - A tutorial for making best use of VISAT. Proceedings of the MERIS User Workshop. ESA.

Brodie, J. and others 2008. Scientific Consensus Statement on Water Quality in the Great Barrier Reef.

---. 2010. Dispersal of suspended sediements and nutrients in the Great Barrier Reef lagoon during river-discharge events: conclusions from satellite remote sensing and concurrent flood-plume sampling. Marine and Freshwater Research **61:** 651-664.

Capone, D. G., J. P. Zehr, H. W. Paerl, B. Bergman, and E. J. Carpenter. 1997. Trichodesmium, a globally significant marine cyanobacterium. Science **276:** 1221.

Capone, D. G. and others 1998. An extensive bloom of the N 2-fixing cyanobacterium Trichodesmium erythraeum in the central Arabian Sea. MEPS **172:** 281-292.

---. 2005. Nitrogen fixation by Trichodesmium spp.: An important source of new nitrogen to the tropical and subtropical North Atlantic Ocean. Global Biogeochem. Cycles **19:** GB2024.

Carder, K. L., R. G. Steward, G. R. Harvey, and P. B. Ortner. 1989. Marine Humic and Fulvic Acids: Their Effects on Remote Sensing of Ocean Chlorophyll. Limnology and Oceanography **34:** 68-81.

Carder, K. L., F. R. Chen, Z. Lee, and S. K. Hawes. 1999. Semianalytical Moderate Resolution Imaging Spectroradiometer algorithms for chlorophyll *a* and absorption with bio-optical domains based on nitrate depletion. Journal of Geophysical Research **104:** 5403-5421.

Carpenter, E. J., and C. C. Price. 1977. Nitrogen fixation, distribution and production of *Oscillotoria (Trichodesmium)* spp. in the Western Sargasso and Caribbean Seas. Limnology and Oceanography **20:** 60-72.

Carpenter, E. J. 1983a. Nitrogen fixation by marine *Oscillatoria* (*Trichodesmium*) in the world's oceans, p. 65-103. *In* E. J. Carpenter and D. G. Capone [eds.], Nitrogen in the Marine Environment. Academic Press Inc.

Carpenter, E. J., and K. Romans. 1991. Major role of the Cyanobacterium *Trichodesmium* in Nutrient Cycling in the North Atlantic Ocean. Science **254:** 1356-1358.

Carpenter, E. J., and D. G. Capone. 1992. Nitrogen Fixation in *Trichodesmium* Blooms, p. 211-217. *In* E. J. Carpenter, D. G. Capone and J. G. Rueter [eds.], Marine Pelagic Cyanobacteria: *Trichodesmium* and other Diazotrophs. Kluwer Academic.

Carpenter, E. J. and others 1993. The tropical diazotrophic phytoplankter Trichodesmium: biological characteristics of two common species. Marine Ecology-Progress Series **95:** 295-295.

Chang, J. 2000. Precision of differenct methods used for estimating the abundance of the nitrogen fixing cyanobacterium, *Trichodesmium* Ehrenberg. Journal of Experimental Marine Biology and Ecology **245:** 245-224.

Chauhan, P., M. Mohan, S. R. Nayak, and R. R. Navalgund. 2002. Comparison of Ocean Color Chlorophyll Algorithms for the IRS-P4 Sensor Using in-situ Data. Journal of the Indian Society of Remote Sensing **30:** 87-94.

Committee, Q. H. S. 2004. Queensland Harmful Algal Blkoom Operational Procedures. *In* D. o. N. R. a. Mines [ed.]. Queensland Government.

Corson, M. R., D. R. Korwan, R. L. Lucke, W. A. Snyder, and C. Davis. 2008. The Hyperspectral Imager for the Coastal Ocean (HICO) on the International Space Station. IEEE Proceedings of the International Geosciences and Remote Sensing Symposium **IV:** 101-104.

Craig, S. E. and others 2006. Use of hyperspectral remote sensing reflectance for detection and assessment of the harful alga, *Karenia brevis*. Applied Optics **45:** 5414-5425.

De'ath, G., and K. Fabricius. 2008. Water Quality of the Great Barrier Reef: Distributions, Effects on Reef Biota and Trigger Values for the Protection of Ecosystem Health: Report to the Great Barrier Reef Marine Park Authority. Australian Insitute of Marine Science.

Desa, A. and others 2005. Detection of *Trichodesmium* bloom patches along the eastern Arabian Sea by IRS-P4/OCM ocean color sensor and by *in-situ* measurements. Indian Journal of Marine Sciences **34:** 374-386.

Devassy, V. P., P. M. A. Bhattathiri, and S. Z. Qasim. 1978. *Trichodesmium* Phenomenon. Indian Journal of Marine Sciences **7:** 168-186.

Devlin, M., and B. Schaffelke. 2009. Spatial extent of riverine flood plumes and exposure of marine ecosystems in the Tully coastal region, Great Barrier Reef. Marine and Freshwater Research **60:** 1109-1122.

Dierssen, H. M., R. M. Kudela, J. P. Ryan, and R. C. Zimmerman. 2006. Red and black tides: Quantitative analysis of water-leaving radiances and perceived color for phytoplankton, colored dissolved organic matter, and suspended sediments. Limnology and Oceanography **51:** 2646-2659.

Dupouy, C., M. Petit, and Y. Dandonneau. 1988. Satellite detected cyanobacteria bloom in the southwestern tropical Pacific: Implications for oceanic nitrogen fixations. International Journal of Remote Sensing **9:** 389-396.

Dupouy, C. 1992. Discoloured waters in the Melanesian Archipelago (New Caledonia and Vanuatu). The value of the Nimbus-7 Coastal Zone Colour Scanner obserevations, p. 177-191. *In* E. J. Carpenter, D. G. Capone and J. G. Rueter [eds.], Marine Pelgaic Cyanobacteria: *Trichodesmium* and other Diazotrophs. Kluwer Academic Publishers.

Dupouy, C. and others 2000. Satellite Captures *Trichodesmium* bloom in the Southwestern Pacific. EOS Transactions of the American Geophysical Union **81:** 13-16.

Dupouy, C., J. Neveux, G. Dirberg, R. Rottgers, M. M. B. Tenorio, and S. Ouillon. 2008a. Bio-optical properties of the marine cyanobacteria Trichodesmium spp. Journal of Applied Remote Sensing **2:** 023503-023517.

Dupouy, C., D. Benielli-Gary, Y. Dandonneau, J. Neveux, G. Dirberg, and T. Westberry. 2008b. On the feasibility of detecting Trichodesmium blooms with SeaWiFS in the southwestern tropical Pacific, p. 715010. *In* R. J. Frouin et al. [eds.], Remote Sensing of Inland, Coastal, and Oceanic Waters. SPIE.

Falconer, I. 2001. Toxic cyanobacterial bloom problems in Australian waters: risks and impacts on human health. Phycologia **40:** 228-233.

Franz, B. A. and others 2006. MODIS Land Bands for Ocean Remote Sensing Applications. *Proc.* Ocean Optics XVIII, Montreal, Canada, 19-13 October 2006.

Fujita, Y., and S. Shimura. 1974. Phycoerythrin of the marine blue-green alga *Trichodesmium thiebautti*. Plant and Cell Physiology **15:** 939-942.

Furnas, M. J. 1992. Pelagic *Trichodesmium* (=*Oscillatoria*) in the Great Barrier Reef Region, p. 265-272. *In* E. J. Carpenter, D. G. Capone and J. G. Reuter [eds.], Marine Pelagic Cayanobacteria: *Trichodesmium* and other Diazotrophs. Dordrecht, The Netherlands.

Furnas, M. J., A. W. Mitchell, and M. Skuza. 1995. Phosphorus and Nitrogen Budgets for the Central Great Barrier Reef shelf. Research Report 36. Great Barrier Reef Marine Park Authority.

Furnas, M. J., and A. W. Mitchell. 1996. Nutrient inputs into the central Great Barrier Reef (Australia) from sub-surface intrusions of Coral Sea waters: a two-dimensional displacement model. Continental Shelf Research **16:** 1127-1148.

Galat, D. L., and J. P. Verdin. 1989. Patchiness, collapse and sucession of a cyanobacterial bloom evaluated by synoptic sampling and remote sensing. Journal of Plankton Research **11:** 925-948.

Gbrmpa. 2005. Research Publication No. 84: Measuring the Economic Value of the Great Barrier Reef. Great Barrier Reef Marine Park Authority.

Gitelson, A. A., S. Laorawat, G. P. Keydan, and A. Vonshak. 1995. Optical properties of dense algal cultures outdoors and their application to remote estimation of biomass and pigment concentration in *Spirulina platensis* (cyanobacteria). Journal of Phycology **31:** 828-834.

Gons, H. J., H. Hakvoort, S. W. M. Peters, and S. G. H. Simis. 2005. Optical Detection of Cyanobacterial Blooms, p. 177-199. *In* J. Huisman, H. C. P. Matthijs and P. M. Visser [eds.], Harmful Cyanobacteria. Springer.

Gordon, H. R., and A. Morel. 1983. Remote Assesment of Ocean Color for Interpretation of Satellite Visible Imagery, a Review. Springer.

Gordon, H. R. and others 1988. A semianalytic radiance model of ocean color. Journal of Geophysical Research **93:** 10,909-910,924.

Gordon, H. R., and M. Wang. 1994. Retrieval of water-leaving radiance and aerosol optical thickness over oceans with SeaWiFS: a preliminary algorithm. Applied Optics **33:** 443-452.

Gower, J., R. Doerffer, and G. Borstad. 1999. Interpretation of the 685 nm peak in water-leaving radiance spectra in terms of fluorescence, absorption and scattering, and its observation by MERIS. International Journal of Remote Sensing **9** 1771-1786.

Gower, J., S. King, G. Borstad, and L. Brown. 2005. Detection of intense plankton blooms using the 709nm band of the MERIS imaging spectrometer. International Journal of Remote Sensing **26:** 2005-2012.

Gower, J., C. Hu, G. Borstad, and S. King. 2006. Ocean Color Satellite Show Extensive Lines of Floating *Sargassum* in the Gulf of Mexico. IEEE Transactions on Geoscience and Remote Sensing **44:** 3619-3625.

Gower, J., S. King, and P. Goncalves. 2008. Global monitoring of plankton blooms using MERIS MCI. International Journal of Remote Sensing **29:** 6209-6216.

Gumley, L., J. Descloitres, and J. Schmaltz. 2010. Creating Reprojected True-Color MODIS Images: A Tutorial. URL ftp://ftp.ssec.wisc.edu/pub/IMAPP/MODIS/TrueColor/MODIS_True_Color_v1.0.2.pdf.

Guptha, M. V. S., R. Mohan, and A. S. Muralinath. 1995. Living Coccolithophorids from the Arabian Sea. Riv. It. Paleont. Strat. **100:** 551-574.

Hedge, S., A. C. Anil, H. S. Patil, S. Mitbavkar, V. Krishnamurthy, and V. V. Gopalakrishna. 2008. Influence of environmental settings on the prevalence of *Trichodesmium* spp. in the Bay of Bengal. Marine Ecology Progress Series **356:** 93-101.

Hoge, F. E., and P. E. Lyon. 1996. Satellite retrieval of inherent optical properties by linear matrix inversion of oceanic radiance models: An analysis of model and radiance measurements. Journal of Geophysical Research **101:** 16,631-616,648.

Hood, R. R., A. Subramanium, L. R. May, E. J. Carpenter, and D. G. Capone. 2002. Remote estimation of nitrogen fixation by *Trichodesmium* Deep-Sea Research II **49:** 123-147.

Hood, R. R., V. J. Coles, and D. G. Capone. 2004. Modeling the distribution of Trichodesmium and nitrogen fixation in the Atlantic Ocean. Journal of Geophysical Research **109:** C06006.

Hovis, W. A. and others 1980. Nimbus-7 Coastal Zone Color Scanner: System Description and Initial Imagery. Science, New Series **210:** 60-63.

Hu, C. 2009. A novel ocean color index to detect floating algae in the global oceans. Remote Sensing of Environment **113:** 2118-2129.

Hu, C., J. Cannizzaro, K. L. Carder, F. E. Muller-Karger, and R. Hardy. 2010. Remote detection of Trichodesmium blooms in optically complex coastal waters: Examples with MODIS full-spectral data. Remote Sensing of Environment **114:** 2048-2058.

Hughes, T. P., and J. H. Connell. 1999. Multiple Stressors on Coral Reefs: A Long-Term Perspective. Limnology and Oceanography **44:** 932-940.

Huot, Y., A. Morel, M. S. Twardowski, D. Stramski, and R. A. Reynolds. 2007. Particle optical backscattering along a chlorophyll gradient in the upper layer of the eastern South Pacific Ocean. Biogeosciences Discuss **4:** 4571-4604.

Ibelings, B. W., M. Vonk, H. F. J. Los, D. T. Van Der Molen, and W. M. Mooij. 2003. Fuzzy Modeling of Cyanobacterial Surface Waterblooms: Validation with NOAA-AVHHR Satellite Images. Ecological Applications **13:** 1456-1472.

Image Science and Analysis Laboratory, Nasa-Johnson Space Center, "The Gateway to Astronaut Photography of Earth.". 2002. Plankton Bloom, Australia-Q. *In* ISS005-E-21571.JPG [ed.]. <http://eol.jsc.nasa.gov/sseop/images/ESC/small/ISS005/ISS005-E-21571.JPG> (13/08/2009 12:53:28).

Ioccg. 2000. Remote Sensing of Ocean Colour in Coastal and other Optically-Complex, Waters. *In* V. Stuart [ed.], Reports and Monographs of the International Ocean Colour Coordinating Group. IOCCG.

---. 2006. Remote Sensing of Inherent Optical Properties: Fundamentals, Tests of Algorithms, and Applications. *In* V. Stuart [ed.], Reports and Monographs of the International Ocean Colour Coordinating Group. IOCCG.

---. 2008. Why Ocean Colour? The Societal Benefits of Ocean-Colour Technology. *In* V. Stuart [ed.], Reports and Monographs of the International Ocean Colour Coordinating Group. IOCCG.

Janson, S., P. J. A. Siddiqui, A. E. Walsby, K. M. Romans, E. J. Carpenter, and B. Bergman. 1995. Cytomorphological Characterization of the Planktonic Diazotrophic Cyanobacteria *Trichodesmium* spp. from the Indian Ocean and Caribbean and Sargasso Seas. Journal of Phycology **31:** 463-477.

Jeffrey, S. W., and G. F. Humphrey. 1975. New spectrophotometric equations for determining chlorophylls a, b, b1 and c2 in higher plants, algae and natural phytoplankton. Biochemie und Physiolgie der Pflanzen **167:** 191-194.

Jones, G. B., F. G. Thomas, and C. Burdon-Jones. 1986. Influence of Trichodesmium blooms on cadmium and iron speciation in Great Barrier Reef lagoon waters. Estuarine, Coastal and Shelf Science **23:** 387-401.

Kahru, M. 1997. Using Satellites to Monitor Large-Scale Environmental Change: A Case Study of Cyanobacteria Blooms in the Baltic Sea, p. 43-61. *In* M. Kahru and C. W. Brown [eds.], Monitoring Algal Blooms: New Techniques for Detecting Large-Scale Environmental Change. Springer-Verlag.

Karl, D., R. Letelier, L. Tupas, J. Dore, J. Christian, and D. Hebel. 1997. The role of nitrogen fixation in biogeochemical cycling in the subtropical North Pacific Ocean. Nature **388:** 533-538.

Kirk, J. T. O. 1994. Light and Photosynthesis in Aquatic Ecosystems: 2nd Ed. Cambridege University Press.

Kirkpatrick, G. J., D. F. Millie, M. A. Moline, and O. M. Schofield. 2000. Optical Discrimination of a Phytoplankton Species in Natural Mixed Populations. Limnology and Oceanography **45:** 467-471.

Kuchler, D., and D. L. B. Jupp. 1988. Shuttle photograph captures massive phytoplankton bloom in the Great Barrier Reef. International Journal of Remote Sensing **9:** 1229-1301.

Kutser, T. 2004. Quantitative detection of chlorophyll in cyanobacterial blooms by satellite remote sensing. Limnology and Oceanography **49:** 2179-2189.

Kutser, T., L. Metsamaa, and A. G. Dekker. 2008. Influence of vertical distribution of cyanobacteria in the water column on remote sensing signal. Estuarine, Coastal and Shelf Science **78:** 649-654.

Kutser, T. 2009. Passive optical remote sensing of cyanobacteria and other intense phytoplankton blooms in coastal an inland waters. International Journal of Remote Sensing **30:** 4401-4425.

Laroche, J., and E. Brietbarth. 2005. Imporatance of the diazotrophs as a source of new nitrogen in the ocean. Journal of Sea Research **53:** 67-91.

Lee, Z., K. L. Carder, and R. A. Arnone. 2002. Deriving inherent optical properties from water color: a multiband quasi-analytical algorithm for optically deep waters. Applied Optics **41:** 5755-5722.

Lee, Z., and K. L. Carder. 2004. Absorption spectrum of phytoplankton pigments derived from hyperspectral remote -sensing reflectance. Remote Sensing of Environment **89:** 361-368.

Lee, Z., K. Du, and R. Arnone. 2005. A model for the diffuse attenuation coefficient of downwelling irradiance. Journal of Geophysical Research **110:** C02016.

Lee, Z., A. Weidemann, J. Kindle, R. Arnone, K. L. Carder, and C. Davis. 2007. Euphotic zone depth: Its derivation and implication to ocean-color remote sensing. Journal of Geophysical Research **112:** C03009.

Lee, Z., R. Arnone, C. Hu, J. Werdell, and B. Lubac. 2010. Uncertainties of optical parameters and their propogations in an analytical ocean colour inversion algorithm. Applied Optics **49:** 369-381.

Letelier, R., and D. Karl. 1996. Role of *Trichodesmium* spp. in the productivity of the subtropical North Pacific Ocean. Marine Ecology Progress Series **133:** 263-273.

Lewis, A. 2001. Great Barrier Reef Depth and Elevation Model: GBRDEM. CRC Reef Reef Research Centre Technical Report Number 33. CRC Reef Reef Research Centre.

Lewis, M., R, O. Ulloa, and T. Platt. 1988. Photosynthetic action, absorption, and quantum yield spectra for a natural population of *Oscillatoria* in the North Atlantic. Limnology and Oceanography **33:** 92-98.

Longhurst, A., S. Sathyendranath, T. Platt, and C. Caverhill. 1995. An estimate of global primary production in the ocean from satellite radiometer data. Journal of Plankton Research **17:** 1245-1271.

Mahaffey, C., A. F. Michaels, and D. G. Capone. 2005. The Conundrum of Marine N_2 Fixation. American Journal of Science **305:** 546-595.

Mancuso, R. 2003. Red tide chokes beaches. Townsville Bulletin, 25 September 2003. http://www.aims.gov.au/arnat/arnat-010-02-20000043.htm.

Maritorena, S., D. A. Siegel, and A. R. Peterson. 2002. Optimization of a semianalytical ocean color model for global-scale applications. Applied Optics **41**.

Marshall, S. M. 1933. The Production of mocroplankton in the Great Barrier Reef Region, p. 111-157. Scientific Report of the Great Barrier Reef Epedition 1928-1929.

Mccook, L. J. 1999. Macroalgae, nutrients and phase shifts on coral reefs: scientific issues and management consequences for the Great Barrier Reef. Coral Reefs **18:** 357-367.

Menon, H. B., A. Lotliker, and S. R. Nayak. 2005. Pre-monsoon bio-optical properties in estuarine, coastal and Lakshadweep waters. Estuarine, Coastal and Shelf Science **63:** 211-223.

Miller, R. L., and B. A. Mckee. 2004. Using MODIS Terra 250 m imagery to map concentrations of total suspended matter in coastal waters. Remote Sensing of Environment **93:** 259-266.

Millie, D. F., O. M. Schofield, G. J. Kirkpatrick, G. Johnsen, P. A. Tester, and B. T. Vinyard. 1997. Detection of harmful algal blooms using photopigments and absorption signatures: a case study of the florida red tide dinoflagellate, *Gymnodinium breve*. Limnology and Oceanography **42:** 1240-1251.

Mitchell, B. G. 1990. Algorithms for determining the absorption coefficient for aquatic particulates using the quantitative filter technique, p. 137-148. Ocean Optics X. SPIE.

Mitchell, B. G., M. Kahru, J. Wieland, and M. Stramska. 2003. Determination of spectral absortion coefficients of particles, dissolved material and phytoplankton for discrete water samples, p. 39-64. *In* J. L. Mueller, G. S. Fargion and C. McClain [eds.], Ocean Optics Protocols for Satellite Ocean Color Sensor Validation, Revision 4, Vol. IV.

Mobley, C. D. 1994. Light and Water: Radiative Transfer in Natural Waters. Academic Press.

---. 1999. Estimation of the Remote-Sensing Reflectance from Above-Surface Measurements. Applied Optics **38:** 7442-7455

Mobley, C. D., and L. K. Sundman. 2001a. HydroLight 4.2 User's Guide. Sequoia Scientific Inc.

---. 2001b. HydoLight 4.2 Technical Documentation. Sequoia Scientific Inc.

Mobley, C. D., L. K. Sundman, and E. Boss. 2002. Phase function effects on oceanic light field. Applied Optics **41:** 1035-1050.

Moss, A., J. Brodie, and M. Furnas. 2005. Water quality guidelines for the Great Barrier Reef World Heritage Area: a basis for development and preliminary values. Marine pollution bulletin **51:** 76-88.

Mueller, J. L. and others 2003. Above-Water Radiance and Remote Sensing Reflectance Measurement and Analysis Protocols, p. 21-31. Ocean Optics Protocols for Satellite Ocean Color Sensor Validation, Revision 4, Volume III. National Aeronautical and Space Administration.

Mueller, J. L. 2003. Field Measuremtents, Sampling Strategies, Ancillary Data, Metadata, Data Archival: General Protocols, p. 41-50. Ocean Optics Protocols for Satellite Ocean Color Sensor Validation, Revision 4, Volume I. National Aeronautical and Space Administration.

Mulholland, M., P. Bernhardt, C. Heil, D. Bronk, and J. O'neil. 2006. Nitrogen fixation and release of fixed nitrogen by Trichodesmium spp. in the Gulf of Mexico. Limnology and Oceanography **51:** 1762-1776.

Mulholland, M. R. 2007. The fate of nitrogen fixed by diazotrophs in the worlds oceans. Biogeosciences **4:** 37-51.

Navarro, R. 1998. Optical Properties of Photosynthetic Pigments and Abundance of the Cyanobacterium in the Eastern Caribbean Basin. Ph.D. Thesis. The University of Puerto Rico.

Neveux, J., M. M. B. Tenorio, C. Dupouy, and T. A. Villareal. 2006. Spectral diversity of phycoerythins and diazotroph abundance in tropical waters. Limnology and Oceanography **51:** 1689-1698.

Neveux, J., M. B. Tenorio, C. Dupouy, and T. A. Villareal. 2008. Response to "Another look at green *Trichodesmium* colonies". Limnology and Oceanography **53:** 2052-2055.

O' Neil, J. M., and M. Roman. 1992. Grazers and Associated Organisms of *Trichodesmium*, p. 61-74. *In* E. J. Carpenter, D. G. Capone and J. G. Rueter [eds.], Marine Pelagic Cyanobacteria: *Trichodesmium* and other Diazotrophs. Kluwer Academic.

O'reilly, J. E. and others 1998. Ocean color chlorophyll algorithms for SeaWiFS. J. Geophys. Res. **103:** 24937-24953.

O'reilly, J. E. 2002. SeaWiFS Postlaunch Calibration and Validation Analyses, Part 3. . *In* S. B. Hooker and E. R. Firestone [eds.], NASA Techinical Memo 2000-206892. NASA Goddard Space Flight Center.

Oliver, J. K., and B. L. Willis. 1987. Coral-spawn in the Great Barrier Reef: preliminary observations. Marine Biology **94:** 521-525.

Orcutt, K. M., K. Gunderson, and U. Rasmussen. 2008. Another look at green *Trichodesmium* colonies. Limnology and Oceanography **53:** 2049-2051.

Oubelkheir, K. and others 2006. Using inherent optical properties to investigate biogeochemical dynamics in a tropical macrotidal coastal system. J. Geophys. Res. **111:** C07021.

Parsons, T. R., Y. Maita, and C. M. Lalli. 1984. A Manual of Chemical and Biological Methods for Seawater Analysis. Pergamon Press.

Pope, R. M., and E. S. Fry. 1997. Absorption spectrum (380 - 700 nm) of pure water. II. Integrating cavity measurements. Applied Optics **36:** 8710-8723

Prieur, L., and S. Sathyendranath. 1981. An optical classification of coastal and oceanic waters based on specific spectral absorption curves of phytoplankton pigments, dissolved organic matter and particulate materials. Limnology and Oceanography **26:** 671-689.

Reinart, A., and T. Kutser. 2006. Comparison of different satellite sensors in detecting cyanobacterial bloom events in the Baltic Sea. Remote Sensing of Environment **102:** 74-85.

Revelante, N., and M. Gilmartin. 1982. Dynamics of a phytoplankton bloom in the Great Barrier Reef Lagoon. Journal of Plankton Research **4:** 47-76.

Rohde, K. and others 2006. Fresh and Marine Water quality in the Mackay Whitsunday Region, 2004/2005. Mackay Whitsunday Natural Resource Management Group, Mackay, Australia.

Rueter, J. G., D. A. Hutchins, R. W. Smith, and N. L. Unsworth. 1992. Iron Nutrition of *Trichodesmium*, p. 289-306. *In* E. J. Carpenter, D. G. Capone and J. G. Reuter [eds.], Marine Pelagic Cayanobacteria: *Trichodesmium* and other Diazotrophs. Kluwer Academic Publishers.

Sarangi, R. K., P. Chauhan, S. R. Nayak, and U. Shreedhar. 2005. Remote sensing of *Trichodesmium* blooms in the coastal waters off Gurjarat, India using IRS-P4 OCM. International Journal of Remote Sensing **26:** 1777-1780.

Sathyendranath, S., L. Prieur, and A. Morel. 1989. A three component model of ocean colour and its application to remote sensing of phytoplankton pigments in coastal waters. International Journal of Remote Sensing **10:** 1373-1394.

Simis, S. G. H., S. W. M. Peters, and H. J. Gons. 2005a. Remote Sensing of the Cyanobacterial Pigment Phycocyanin in Turbid Inland Water. Limnology and Oceanography **50:** 237-245.

Simis, S. G. H., M. Tijdens, H. L. Hoogveld, and H. J. Gons. 2005b. Optical changes associated with cyanobacterial bloom termination by viral lysis. J. Plankton Res. **27:** 937-949.

Simis, S. G. H., A. Ruiz-Verdu, J. A. Dominguez-Gomez, R. Pena-Martinez, S. W. M. Peters, and H. J. Gons. 2007. Influence of phytoplankton pigment compositions on remote sensing of cyanobacterial biomass. Remote Sensing of Environment **106:** 414-427.

Slivkoff, M. M., M. J. Furnas, and M. Lynch. 2006. Continual Transect Ocean Colour Remote Sensing Validation in the Great Barrier Reef Marine Park. *Proc.* Ocean Optics XVIII, Montreal, Canada, 9-13 October, 2006.

Smith, R. C., and E. T. Baker. 1981. Optical properties of the clearest natural waters. Applied Optics **20:** 177-184.

Steinberg, D. K., N. B. Nelson, C. A. Carlson, and A. C. Prusak. 2004. Production of chromophoric dissolved organic matter (CDOM) in the open ocean by zooplankton and the colonial cyanobacterium *Trichodesmium* spp. Marine Ecology Progress Series **267:** 45-56.

Stumpf, R. P., and M. C. Tomlinson. 2005. Remote Sensing Harmful Algal Blooms, p. 277-296. *In* R. L. Miller, C. E. Del Castillo and B. A. McKee [eds.], Remote Sensing of Coastal Aquatic Environments: Technologies, Techniques and Applications. Springer.

Subramaniam, A., and E. J. Carpenter. 1994. An empirically derived protocol for the detection of blooms of the marine cyanobacterium *Trichodesmium* using CZCS imagery. International Journal of Remote Sensing **15:** 1559-1569.

Subramaniam, A., E. J. Carpenter, D. Karentz, and P. G. Falkowski. 1999a. Bio-optical properties of the Marine Diazotrophic Cyanobacteria *Trichodesmium* spp. I. Absorption and Photosynthetic Action Spectra. Limnology and Oceanography **44:** 608-617.

Subramaniam, A., E. J. Carpenter, and P. G. Falkowski. 1999b. Bio-optical properties of the marine diazotrophic cyanobacteria *Trichodesmium* spp. II. A reflectance model for remote sensing. Limnology and Oceanography **44:** 618-627.

Subramaniam, A., C. W. Brown, R. R. Hood, E. J. Carpenter, and D. G. Capone. 2002. Detecting Trichodesmium blooms in SeaWiFS imagery. Deep Sea Research Part II: Topical Studies in Oceanography **49:** 107-121.

Suresh, T., E. Desa, A. Mascarenhas, P. Matondkar, P. Naik, and S. R. Nyak. 2006. Cross Calibration of IRS-P4 OCM Satellite Sensor *In* T. N. Krishnamurti, B. N. Goswami and I. T [eds.], Proc. of SPIE Vo. 6404, Remote Sensing of the Atmoshpere, Oceans, and Interactions.

Svejkovsky, J., and J. Shandley. 2001. Detection of offshore phytoplankton bloom with AVHRR and SAR imagery. International Journal of Remote Sensing **22:** 471-485.

Tassan, S. 1988. The effect of dissolved yellow substance on the quantitative retrieval of chlorophyll and total suspended sediment concentrations from remote measurements of water colour. International Journal of Remote Sensing **9:** 787 - 797.

---. 1994. SeaWiFS potential for remote sensing of marine *Trichodesmium* at sub-bloom concentrations. International Journal of Remote Sensing **16:** 3619-3627.

---. 1995. SeaWiFS potential for remote sensing of marine *Trichodesmium* at sub-bloom concentrations. International Journal of Remote Sensing **16:** 3619-3627.

Tomlinson, M. C. and others 2004. Evaluation of the use of SeaWiFS imagery or detection of *Karenia brevis* harmful algal blooms in the eastern Gulf of Mexico. Remote Sensing of Environment **91:** 293-303.

Vane, G., R. O. Green, T. G. Chrien, H. T. Enmark, E. G. Hansen, and W. M. Porter. 1993. The airborne visible/infrared imaging spectrometer (AVIRIS). Remote Sensing of Environment **44:** 127-143.

Villareal, T. A., and E. J. Carpenter. 1990. Diel buoyancy regulation in the marine diazotrophic cyanobacterium *Trichodesmium thiebautti*. Limnology and Oceanography **35:** 1832-1837.

Wang, M., and W. Shi. 2005. Estimation of ocean contributions at the MODIS near-infrared wavelengths along the east coast of the U.S.: Two case studies. Geophysical Research Letters **32:** L13606.

---. 2007. The NIR-SWIR combined atmospheric correction approach for MODIS ocean color data processing. Opt. Express **15:** 15722-15733.

Wang, M., S. Son, and W. Shi. 2009. Evalution of MODIS SWIR and NIR-SWIR atmospheric correction algorithms using SeaBASS data. Remote Sensing of Environment **113:** 635-644.

Wei, G., M. T. Mcculloch, G. Mortimer, W. Deng, and L. Xie. 2009. Evidence for ocean acidification in the Great Barrier Reef of Australia. Geochimica et Cosmochimica Acta **73:** 2332-2346.

Westberry, T. K., D. A. Siegel, and A. Subramaniam. 2005. An improved bio-optical model for the remote sensing of *Trichodesmium* spp. blooms. Journal of Geophysical Research **110:** C06012.

Westberry, T. K., and D. A. Siegel. 2006. Spatial and temporal distribution of *Trichodesmium* blooms in the world's oceans. Global Biogechemical Cycles **20**.

Wolanski, E. 1994. Physical Oceanographic Processes of the Great Barrier Reef. CRC Press.

Zhang, Y., M. A. Van Dijk, M. Liu, G. Zhu, and B. Qin. 2009. The contribution of phytoplankton degradation to chromophoric dissolved organic matter (CDOM) in eutrophic shallow lakes: Field and experimental evidence. Water Research **43:** 4685-4697.